ULTRASTRUCTURAL AND CYTOCHEMICAL STUDIES OF THE EXTRAEMBRYONIC MEMBRANES OF THE RAT

by

Reid Sandford Connell Jr., M.S.

Volume 1

A THESIS
Presented to the Department of Anatomy
and the Graduate Division of the University of Oregon Medical School
in partial fulfillment of
the requirements for the degree of
Doctor of Philosophy

June 1967

APP[redacted]

(Professor in Charge of Thesis)

[redacted]

(Chairman, Graduate Council)

ACKNOWLEDGMENTS

I gratefully acknowledge the guidance, instruction and encouragement given to me by Dr. Robert L. Bacon and Dr. David L. Gunberg.

I also wish to thank Mrs. Elaine Jendritza for her skillful typing of the final manuscript.

And, finally, I wish to express my fond appreciation for the patience, encouragement and understanding given to me by my loving wife, Marilyn, and family.

This investigation was supported by United States Public Health Service training grants from the National Institutes of Health, Division of General Medical Science (Anatomical Sciences GM-00445) and the National Institute of Neurological Disease and Blindness (GT-05025-12).

TABLE OF CONTENTS

PAGE

PAGE

PAGES

LIST OF ILLUSTRATIONS

12 Day Avascular Trophoblast Figures

12 Day Vascular Trophoblast

14 Day Placental Labyrinth

18 Day Placental Labyrinth

22 Day Placental Labyrinth

25 Day Placental Labyrinth

12 Day Visceral Yolk Sac

14 Day Visceral Yolk Sac

18 Day Visceral Yolk Sac

22 Day Visceral Yolk Sac

25 Day Visceral Yolk Sac

INTRODUCTION

"The first man knew her not perfectly, and in
like manner the last hath not traced her out"
---Ecclesiasticus

The placenta has long been one of the least understood organs. Views about its structure and function are still undergoing modifications, along with the application of more diversified methods of investigation. Many of the more recent studies of placental morphology have focused on histochemical and ultrastructural aspects. With the availability of methods for electron cytochemistry, it has become possible to depict the ultrastructural localization of certain enzyme activities with much greater precision than could be done formerly with the older methods of light microscopy.

The objectives of this investigation are:

1. to clarify certain discrepancies among the descriptions of the ultrastructure of the rat labyrinthine placenta and to ascertain the subcellular localization of adenosine mono-, di- and triphosphatase activities on the 12th, 14th, 18th and 22nd days of gestation.
2. to characterize the ultrastructure of the rat visceral yolk sac placenta and to ascertain the subcellular localization of adenosine mono-, di- and triphosphatase activities on the 12th, 14th, 18th and 22nd days of gestation.
3. to determine any alterations in both the ultrastructure and the pattern of the enzymic activities of the aforementioned membranes of the rat whose gestation has been prolonged three days beyond the time of normal parturition.

General Considerations

Grosser (1), observing that the degree of intimacy of contact between maternal and fetal blood varied greatly from species to species, arranged the chorio-allantoic placenta of mammals in an ascending order from the simplest to the more complex on the basis of the successive disappearance of intervening uterine tissues. In the simplest placental type, fetal and maternal blood streams are separated by six cell layers: uterine vascular endothelium, uterine connective tissue, uterine epithelium, fetal chorionic epithelium, fetal connective tissue and fetal capillary endothelium. In the more complex placentas, qualitative differences in the invasive and aggressive properties of the trophoblast cause successive erosion of the three maternal constituents until maternal blood directly bathes the fetal chorionic epithelium. By utilizing the names of the maternal and fetal tissues with the most intimate association at term, Grosser distinguishes the following four types of placentae: (1) The epitheliochorial, in which all maternal tissues are intact and in close apposition to the fetal chorionic epithelium. (2) The syndesmochorial, in which there exists only five cell layers. The uterine epithelium becomes eroded, leaving the chorion in contact with the uterine connective tissue. (3) The endotheliochorial, in which the uterine connective tissue is lost and the chorionic epithelium comes in contact with the endothelium of the maternal capillaries. (4) The hemochorial, in which the maternal endothelium also disappears and maternal blood comes into direct contact with the chorionic epithelium.

Subsequently, Mossman (2, 3) suggested that Grosser's classification be extended to include a fifth placental type, the hemoendothelialis, in which even the fetal chorion, to a large extent, disappears, leaving the

fetal vascular endothelium in direct contact with maternal blood. Since his observations of a gradual thinning of fetal tissue layers with an ultimate loss of trophoblast toward the end of gestation corroborated earlier studies (4, 5), he included in this group chorio-allantoic placentas of the "rabbit, probably the guinea pig and rat, and possibly most rodents". Mossman (2) also proposed that all placentae at the beginning of their development are of the epitheliochorial type, but, due to qualitative differences in the invasive and aggressive properties of their trophoblast, some come to have fewer cell layers separating maternal and fetal circulations. Furthermore, he suggested that probably all definitive placentae possess some areas of separating membrane similar to that of the less intimate types.

Such studies regarding placental morphology were described at a time when it was considered possible to explain all placental exchange on the basis of simple physical diffusion and filtration. Consequently, two general concepts developed which have, until recently, dominated the subject of placental physiology. The first of these held that all chorio-allantoic placentas of eutherian mammals could be arranged in a phylogenetic order from the most primitive six layered epitheliochorial placental, which is the least permeable, to the most advanced two layered hemoendothelial barrier in which transport is most rapid and complete. The second concept proposed that, as gestation advances in any given species of mammal, the remaining tissue layers of the placental barrier gradually diminish in width and become progressively more permeable.

During the 1940's, physiological studies, such as those by Flexner and Gellhorn (6, 7), indicated that metabolites were actively transported from one blood stream to the other, or at least underwent facilitated

diffusion (8). Therefore, the placenta could no longer be considered as a simple semipermeable membrane in which the efficiency of passage of metabolites was inversely proportional to the number of tissue layers present in that structure. The thickness of the placental barrier then appeared to be secondary to the vital capabilities of its tissue constituents and attention was focused upon its cytochemical qualities and cytological structure.

Since phosphatase enzymes were known to be involved in a wide variety of chemical reactions occurring in tissue functions such as metabolism and transport (9, 10, 11, 12, 13, 14, 15, 16), it was believed that histochemical studies of these enzymes would provide information regarding the functional capabilities of various constituents of the maternal-fetal complex and permit further definition and differentiation of placental types. Excellent reviews of the enzymatic capabilities of the placenta have been reported by Hafez (17), Hagerman (18), and Page and Glendening (19).

Histochemical Studies of Chorio-allantoic Placentas

Epitheliochorial placenta

One of the first histochemical studies of phosphatases in the placenta of any animal was the investigation by Wislocki and Dempsey (20) of the epitheliochorial placenta of the sow. In this animal, they found rather intense alkaline glycerophosphatase activity in the endothelium of the capillaries and the stroma of the luminal part of the uterine mucosa. Acid glycerophosphatase activity was as intense as alkaline glycerophosphatase, but exhibited a different distribution. Evidence of its activity was observed in the glandular epithelium and, to a much lesser extent, in the superficial stroma and epithelial cells

lining the surface of the endometrium. In the chorionic epithelium, alkaline glycerophosphatase was confined to the brush border and distal third of the columnar cells lining the chorionic fossae. Acid glycerophosphatase was found to have a similar localization, but, unlike alkaline glycerophosphatase, it also occurred in the epithelial cells lining the chorionic areolae.

In a succeeding study, Dempsey and Deane (21) found that histochemically demonstrable phosphatases could react with several different phosphorylated substrates other than glycerophosphate and that the histological localization of activity to one substrate did not always correspond to that obtained with another. This finding prompted Dempsey and Wislocki (22) to re-examine the localization of phosphatase in the sow placenta. When tested with adenylic acid, fructose diphosphate and nucleic acid at pH 9.0, the distribution of phosphatases was similar to that first described and utilizing glycerophosphate as substrate. However, at pH 7.0, only activity to adenylic acid could be demonstrated. In the chorion this activity was localized not only to the columnar cells of the chorionic fossae, but also to a greater extent in the apical portion of cells of the chorionic areolae. In the uterus a faint and diffuse reaction occurred in all of the tissues.

Syndesmochorial placenta

The distribution of phosphatases in the syndesmochorial placenta of ruminants has been localized to three main sites which are very similar to those described in the pig placenta. Wimsatt (23) first localized an alkaline phosphatase which was able to hydrolyze several monophosphoric acid esters in the cytoplasm of trophoblastic binucleate giant cells of both the cow and sheep. Although no differences were noted in the intra-

cytoplasmic distribution of activity when different substrates were employed, the most intense reactions were obtained with nucleic acid, and followed by hexose diphosphate, glycerophosphate and adenylic acid in descending order. Wimsatt also found that the giant cells displayed marked variations in phosphatase content in accordance with their location in the placenta. Enzymatic activity appeared highest in giant cells near the tips of the chorionic villi, although not all of the cells exhibited a reaction. Those on the sides and between the bases of the villi exhibited little to no enzyme activity. Subsequently, Weeth and Herman (24) described the presence of alkaline phosphatase in the cryptal epithelial lining of the uterus of the sow and sheep. More recently Foley et al. (25) and Bjorkman (26), in addition to describing phosphatase activity in binucleate giant cells, noted that activity in the cryptal epithelium was not only uneven but diffusely distributed, whereas activity in the walls of maternal blood vessels was quite intense.

The localization of acid phosphatase as shown by both Wimsatt and Bjorkman (23, 26) was much less distinct than alkaline phosphatase in that its activity was diffusely distributed over all cells. Reactions were identified, however, in the stroma and cryptal epithelium of the uterine mucosa and found to be distributed unevenly in the trophoblast. Acid phosphatase activity was most pronounced in the trophoblastic giant cells.

Endotheliochorial placenta

Accounts of the distribution of phosphatases in the endotheliochorial placenta of the cat (22) and shrew (27) with supplementary observations on the dog (28) have shown that as pregnancy advances the preponderance of activity to various monophosphorylated substrates shifts

from the uterine tissues to the trophoblast and fetal stroma of the placental labyrinth.

These investigators (22, 27, 28) reported dense accumulations of activity to alkaline phosphate and nucleic acid substrates on the surface epithelium of the uterus, throughout the uterine glands and stroma, and surrounding the maternal blood vessels during early pregnancy. However, following the erosion of the uterine epithelium, and the incorporation of maternal capillaries into the developing placental lamellae, the content of phosphatases in these tissues is seen to gradually diminish until acid and alkaline phosphatases are limited to the uterine glands. Even then activity is only obtained with glycerophosphate substrate.

The authors also reported little phosphatase activity in the trophoblast until the time that the placental labyrinth is essentially completed. Thereafter, enzyme activity increases with advancing gestational age. In the cat and dog placenta, Wislocki et al. (28) and Dempsey et al. (22) reported that following the use of glycerophosphate, nucleic acid, fructose diphosphate and adenylic acid at pH 9.0, there was an intense concentration of phosphatases, with exception of adenylic acid, which produced a weaker response in the trophoblast and fetal stroma of the placental labyrinth. On the other hand, the hypertrophied endothelium surrounding the maternal blood channels contained none. When the pH of the reaction mixture was adjusted to 7.0, only the substrate adenylic acid elicited a positive histochemical response. Wislocki and Wimsatt (27) described a similar distribution of glycerophosphatase activity in the shrew labyrinth. They also found a faint reaction in the hypertrophied endothelium when using glycerophosphate at pH 7.0 or nucleic acid at pH's 9.5 and 7.0. Both groups of investigators failed to demon-

strate acid phosphatase in the fetal portions of the placenta.

Hemochorial placenta

Of all the hemochorial placentas, that of the human has been most extensively investigated. In young placentae small amounts of alkaline phosphatase were found in the brush border and outer margin of the syncytial trophoblast (22, 29, 30, 31, 32, 33). As gestation proceeded, this activity increased steadily, spreading throughout the syncytial cytoplasm until the enzyme was distributed in an outer and inner lamina separated by a middle nuclear region in which less intense reaction occurred (22, 31, 32, 34, 35). All other fetal components of the placenta are essentially negative as is the decidua with exception of the well defined junctional zone in which interstitial deposits of phosphatases do occur.

The distribution of phosphatase reactions displayed with additional substrates at alkaline pHs are substantially similar and differs only in the time of appearance and degree of activity (22, 29, 30, 32, 35). The most intense enzymatic reaction is obtained following the use of fructose diphosphate and nucleic acid. Less activity is demonstrated with glycerophosphate and adenylic acid (22).

The distribution of acid phosphatase is reported to be limited to trace amounts located in the stroma of fetal villi during the early part of gestation, whereas later in pregnancy it is predominantly located on the maternal side of the syntrophoblast (22, 29, 30, 33, 36). Smaller amounts of activity are also reported to be localized in the nuclei of the cytotrophoblast and underlying stromal cells (32, 33, 34, 35).

"Hemoendothelial placenta"

The histochemical distribution of phosphatases in the various species of animals which supposedly possessed a hemoendothelial placenta have been

investigated at closely seriated stages. In the mouse, rabbit and hamster (37), rat (37, 38, 39), and guinea pig (22, 40, 41) phosphatase activity appears to be localized in many of the same structural sites as those described in the hemochorial placenta of man. During early gestation in these rodents, alkaline glycerophosphatase is present in both the cellular and syncytial trophoblast, but not in the underlying fetal stroma and fetal capillaries. Abundant activity is also found in the mononuclear trophoblastic giant cells. As the placental labyrinth continues to differentiate, phosphatases accumulate in increasing amounts in the syncytial trophoblast, whereas it decreases in the cellular trophoblast. At the same time the lamellae of the labyrinth become thinner. Therefore, toward the end of gestation, when every maternal blood channel is clearly defined by lines of intense staining, it could not be determined clearly if this phosphatase activity occurred in trophoblast.

In the maternal rodent placenta, with exception of the rat (38), small amounts of activity have been reported in the decidua basalis. On the other hand, greater accumulations of alkaline phosphatase are observed in the junctional zone between the decidua and fetal placenta where it is predominantly localized in the interstitial spaces.

Acid glycerophosphatase also occurs in the syncytial trophoblast of the mouse and rabbit placental labyrinth, but only in small amounts where it is confined to the nuclei (37). On the other hand, in the rat labyrinth, which has been more extensively investigated, low (38) to moderate (39) activity is observed in the cytoplasm of the syncytium during most of the gestation. Toward the end of pregnancy, however, this activity becomes very intense (37, 38, 39). At term, strong acid

glycerophosphatase activity also occurs in the cytotrophoblast of the spongy zone and in the giant trophoblastic cells of the junctional zone (38, 39). Activity in the endometrium of the rodent is confined to the decidua basalis (37, 38, 39). In addition to glycerophosphatase, enzymatic activity is demonstrable with the substrates adenylic acid, nucleic acid and fructose diphosphate at pH 9.0 in the guinea pig placenta (22), and with ATP at pH 9.4 in the rat placenta. Although the distribution of activity to these substrates is identical to that of glycerophosphata, a denser reaction occurred with fructose diphosphate and nucleic acid. Less activity is obtained with adenylic acid and glycerophosphate which in turn is slightly greater than that with ATP. At pH 7.0 fructose diphosphate elicits only a weak response whereas a moderately strong reaction occurs with adenylic acid.

Since the distribution of phosphatases in the rodent placenta corresponds closely to that of the hemochorial placenta, several investigators seriously questioned the validity of classifying those placentas under hemoendothelial (37, 41, 42). On the basis that fetal vessels were always negative and that phosphatases, which in early pregnancy had a marked predilection for the syncytium, constituted a continuous layer throughout pregnancy, Hard (41) felt that the trophoblast persisted as a lining of the maternal blood channels until birth. Wislocki et al. (37) agreed with Hard but concluded that the distribution of phosphatases could not answer the question as to whether the rodent placenta became partly or mainly hemoendothelial at term. Their conclusion was based on the possibility that the localization of phosphatases in the endothelial lining of the uterine capillaries in the epitheliochorial and syndesmochorial placentae suggested that the enzymes might have a marked predilection for the first cellular barrier inter-

vening between maternal and fetal circulation, rather than a fixed relationship to the trophoblastic syncytium. If this were the case, the fetal endothelium which becomes the limiting membrane between the maternal and fetal blood in the hemoendothelial placenta might then become the site of phosphatase concentration precisely as the syncytium had in earlier stages. Therefore, the question as to whether the ultimate labyrinth barrier in rodents consisted solely of endothelium or of epithelium and endothelium indistinguishably fused could not be resolved until more sophisticated techniques for cytological examination were developed.

Ultrastructural Studies of Chorio-allantoic Placentas

With the development of the electron microscope, a means to investigate further the detailed structure of the various placental types was made available. Even though embedding media and microtomy techniques were not as refined as they are presently, early cytological studies with this instrument quickly revealed that the placenta is often organized in a manner not discernable by light microscopy and that Grosser's system of placental classification frequently does not represent the true structural complexity of the placental barrier. Because of these findings, rather strenuous objections have been raised against the continued use of Grosser's classification (43, 44, 45).

Epitheliochorial placenta

In the epitheliochorial placenta the area of fetal maternal exchange as seen with the light microscope is represented by either closely apposed corrugated folds of maternal and fetal epithelium (sow) or by cotyledons where chorionic villi interlock with endometrial crypts (mare). Ultrastructural studies of this placental type have not only shown that there

is a far more intimate apposition between the chorionic and uterine epithelium than was previously realized, but have provided structural evidence for specialized areas of metabolic exchange (46, 47, 48, 49, 50).

In a fine structural study of the pig placenta, Dempsey, Wislocki and Amoroso (46) reported that the surface area of the chorionic ridges and fossae is greatly extended by numerous microvilli which mutually interdigitate with outward projections of the uterine epithelium to form an extremely tight zone of apposition, too tight according to these authors, to allow for absorption of uterine secretions through the chorionic ridges and fossae. On the basis of its structural characteristics, it was suggested that the absorption of uterine secretions takes place in the chorionic areolae which form cup-like, patent spaces between the chorionic and uterine epithelia at intervals where branched glands open into the uterine lumen. In addition to possessing irregularly shaped, often bulbous, projections, these cells were described as having complicated infoldings of the apical plasma membrane which communicate laterally with one another to form a network of channels continuous with the lumen of the areolae. These infoldings are thought to provide access for various materials to the interior of the cell. The epithelial plasma membranes of the chorionic fossae were also found to possess thread-like invaginations. These invaginations, however, do not communicate laterally with one another.

At the ultrastructural level, the placenta of the mare differs from the placenta of the pig in that the maternal and fetal zone of the mutually interdigitating microvilli is quite loose and forms small intervillous spaces (50). As opposed to complicated surface infoldings, the trophoblastic cytoplasm is provided with caveolae at the bases of some

microvilli and contains numerous vesicles with a content similar to that found in the intervillous spaces.

Although the chorionic epithelium of the pig and mare never become invasive or disappear, a close relationship develops between maternal and fetal capillary beds. By mid-gestation, fetal capillaries penetrate intimately between the cells of the trophoblast and form "intraepithelial plexuses". By full term the lamina of chorionic cytoplasm separating fetal capillaries from the endometrium becomes extremely thin. The maternal capillaries in a similar manner displace the uterine epithelial cells by compression until only thinned-out plates of cytoplasm separate them from the fetal trophoblast. At mid-gestation, electron micrographs of the chorionic epithelium exhibit cytoplasmic vacuoles located near the "intraepithelial vessels", but in no other locations. Dempsey, Wislocki and Amoroso (46) are of the opinion that the vacuoles create spaces into which the capillaries can burrow. Electron micrographs also show that two distinct basement membranes remain interposed between the fetal capillary endothelium and chorionic epithelium during gestation (46). Nevertheless, the distance separating the two sets of capillaries has been described as being only six or eight microns (48).

Syndesmochorial placenta

The region of intimate attachment between fetal and maternal tissues in the ruminant placenta generally consists of chorionic villi fitting into maternal crypts separated from each other by septa. In these placentomes two epithelial layers can usually be identified, the trophoblastic epithelium of the fetal villus and the epithelium lining the maternal crypts. Since the uterine endometrium has been described as being eroded in the syndesmochorial placenta (1), the nature and origin

of the epithelium investing the connective tissue of the maternal crypts has proved to be exceedingly difficult and controversial. Assheton (51) considered this layer to be a fetal plasmodium formed by the fusion of trophoblastic giant cells following the close of the attack upon the uterine epithelium by the trophoblast. In the past, this view has been supported by both Wimsatt (52, 53) and Amoroso (54). Presently, however, the opinion has gained ground that the epithelial lining of crypts in many ruminant species is of maternal origin.

Electron microscope studies of the fetal-maternaljunction in placentomes of the cow (55, 56, 57), deer (58), and sheep and goats (59, 60, 61, 62) have revealed the presence of numerous microvilli projecting from both sides of contact surfaces, thus creating an intimate apposition of interlocking microvilli, similar to that found between trophoblast and endometrium in the sows and mare placenta. In the sheep and goat, the cells of the cryptal lining are fused with each other to a greater extent than occur in the cow and deer, but occasionally single cryptal cells are found (59, 60, 61, 62). Sheep and goat placentomes also differ from that of cows and deer in that the cryptal cells do not rest on a continuous basement membrane and possess processes of varying sizes which protrude into the connective tissue and establish contact with fibroblasts or with capillary endothelium (59, 60, 61, 62).

Further evidence of the maternal origin of the cryptal lining has been presented by Bjorkman (61) who has shown that an intimate fetal-maternal apposition is established in the ovine placentome even before chorionic villi have formed and that, at this time and later on, an intact syncytial or partly cellular layer lines the uterine stroma. The results of these ultrastructural studies appear to confirm the hypothesis

that the cryptal lining is derived from maternal endometrial epithelium, a fact which would, according to the above mentioned authors, place the placentas of those ruminants thus far examined among placentae of an epitheliochorial type.

Endotheliochorial placenta

Basically, the area of fetal-maternal exchange in the placenta of most carnivores with exception of the hyena consists of a series of more or less parallel trophoblastic plates or lamellae which separate the endothelial lined blood vessels from the endothelium of the fetal capillaries located in the subjacent stroma. This type of placental relationship has been classified as endotheliochorial. Wislocki and Dempsey (28), however, after staining the endotheliochorial placenta of the cat with triacid connective tissue stains, detected an additional zone of amorphous substance intervening between the maternal endothelium and fetal trophoblast. Furthermore, they found decidual giant cells lodged in this zone and between the maternal capillaries. Wislocki and Dempsey considered these cells to be derived from fibroblasts of the original uterine mucosa which are transformed into giant cells during the invasion of the endometrium by the fetal trophoblast.

This intermediate zone of ill-defined, amorphous substance has been characterized with the electron microscope in the cat by Dempsey and Wislocki (63) and in the ferret by Lawn and Chiquoine (64). In both animals this layer has a fibrillar texture similar to that of basement membranes. In the cat it varies a good deal in thickness and may even be absent, so that in certain locations the plasma membrane of the endothelial cells and that of the syncytial trophoblast are directly contiguous. On the other hand, in the ferret the intermediate layer is more

uniform in thickness and is only perforated where small processes protrude from the maternal endothelium to penetrate between the folds of the syncytium. The rather smooth and regular maternal surface, in contrast to its scalloped and irregular fetal surface, suggests that the intermediate layer may be eroded by the trophoblast and constantly renewed. As there are no connective tissue cells present during its formation, Lawn and Chiquoine suggest the fibrous material must be the product of the maternal endothelial cells or of the chorionic syncytium or of both of them. On the basis of its fine structure, Dempsey and Wislocki (63) and Lawn and Chiquoine (64) have suggested that the maternal endothelium, which is characteristically thick and basophilic, is most active in this respect.

In electron micrographs, the cytoplasm of the thickened, hyperplastic endothelial cells has a spongy appearance, owing to the presence of numerous, irregular shaped vacuoles containing a flocculent precipitate. These vacuoles frequently communicate directly with the lumen of the maternal capillary. In addition to small canalicular spaces, the cytoplasm of the endothelial cells has an abundance of granular endoplasmic reticulum and Golgi elements which are characteristics currently believed to be associated with protein synthesis. The orientation of the endoplasmic reticulum suggests that the protein that is synthesized passes into the intermediate layer (63).

The cytoplasm of the syncytial trophoblast is considerably less dense than that of the maternal endothelial cells, and lacks the great concentration of granular endoplasmic reticulum found in the latter. A moderate number of granular cisterns are present, however, as well as Golgi elements, but these too are less abundant than those in the maternal

endothelium. Scattered throughout the cytoplasm are numerous smooth vesicles and tubules. These profiles are usually closely associated with the cell surfaces which are extensively folded. Here, transition stages are found which suggest that the vesicles or tubules either arise from or become continuous with the surface membrane.

Since a definite layer of connective tissue and decidual giant cells is found intervening between the maternal endothelium and syncytial trophoblast during pregnancy, Dempsey and Wislocki (63) and Lawn and Chiquoine (64) have suggested that in some carnivores the definitive placental labyrinth is syndesmochorial rather than endotheliochorial.

Hemochorial placenta

In the anthropoid hemochorial placenta, the trophoblast, which constitutes the principle component of the placental membrane, consists of an inner cytotrophoblast layer (the Langhans cells) adjacent to the fetal stroma and an outer multinucleate trophoblast layer (the syncytium) which is bathed by circulating maternal blood (47). In the past, there has been considerable controversy as to the origin and mode of proliferation of the multinucleate trophoblast layer and to the fate of the cytotrophoblast (54, 55). Due to the absence of more convincing evidence than that which is provided with the light microscope, many investigators have opinioned that the trophoblast is composed initially of cytotrophoblast which gradually becomes transformed into a multinucleate syncytium (66, 67).

Early studies of the human placenta with the electron microscope have yielded varying conclusions. Bargmann and Knoop (68), who were the first investigators to consider in any detail the origin of the multinucleate trophoblast, suggested that it is a plasmodium owing its origin

not to the coalescence of originally separate cells, but to the multiplication of the nuclei within a mass of cytoplasm which increases in amount by growth but which itself does not undergo division. Boyd and Hamilton (65) have pointed out that if the trophoblast consists of a plasmodium, then there should be persistent evidence of intercellular spaces resulting from the original separation of the cells. Bargmann and Knoop, however, found no such spaces in their study.

Dempsey and Wislocki (69), Boyd and Hughes (70), Wislocki and Dempsey (71), Sawasaki et al. (72), Terzakis and Rhodin (73), and Rhodin and Terazakis (74) were unable to find cell membranes extending between the two surfaces of the multinucleate trophoblast layer and, therefore, concluded that the trophoblast covering the vascular villi must be syncytial. These authors also demonstrated that individual Langhans' cells persist, although in greatly reduced numbers, until term. The presence of desmosomes at the borders between the cytotrophoblast and the syncytium was interpreted as evidence for a close relation between these two trophoblast layers, but no evidence of the formation of the syncytium from the cytotrophoblast was found.

In a subsequent fine structural study of the normal human first trimester placenta, Terzakis (75) described cells with cytoplasmic characteristics intermediate between those of the cytotrophoblast and the syncytial trophoblast. Carter (76, 77) recently reported the occurrence of remnants of sets of cell membranes with desmosomes in the syncytial cytoplasm and of discontinuities in the limiting plasma membranes between the cytotrophoblast and syncytium in both cell columns and tertiary villi. Carter also found that syncytial nuclei in these areas have a morphological picture very similar to the cytotrophoblastic

cell nuclei. On the other hand, Lister (78, 79, 80), who has examined extensively sections of chorionic villi from the first trimester placenta and from both the fetal and maternal surfaces of the term placenta, has found no break in the integrity of the cell membranes between the syncytium and cytotrophoblast.

Enders (81) has recently demonstrated a sequence in the formation of the syncytium from the cytotrophoblast in both the early and term placentae. More recently, Boyd and Hamilton (65) have reported similar findings. In both of these papers the authors have described the cytotrophoblast as first undergoing a cytoplasmic differentiation to become similar to the syncytium. This differentiation was reported as being followed by a disintegration of the cell membranes and the incorporation of the cytotrophoblast into the syncytium, leaving only remnants of cell membranes and desmosomes which persist for a short time and subsequently disappear. A similar sequence of events has also been reported as ocurring in the monkey placenta (82).

Evidence pointing in the same direction has been adduced by Midgley (83), Wynn (84), Pierce and Midgley (85) and Wynn and Davies (86), who examined the ultrastructure of choriocarcinomas transplanted into the cheek pouches of hamsters. These authors obtained evidence of morphological intermediates between cytotrophoblast and syncytial trophoblast. Since autoradiographic studies of the incorporation of tritiated thymidine into the immature monkey (87) and human placenta (88) have shown that deoxyribonucleic acid synthesis does not occur in the syncytial trophoblast, Pierce, Midgley and Beals (82) have concluded that cytotrophoblast is the only source for the growth of the syntrophoblast.

In addition to observations of the methods in which Langhans cells

contribute to the syncytium, many significant observations have been made on the cytology of the trophoblast at various stages of gestation (89, 90, 91, 92, 93, 94, 95).

"Hemoendothelial placenta"

The first ultrastructural studies of the labyrinth of rodents quickly established that the placenta of the rat, rabbit and guinea pig is hemochorial rather than hemoendothelial as had been previously proposed. Dempsey and Wislocki (96), who first examined the fine structure of the labyrinthine barrier of the rat on the 15th, 17th and 21st days of gestation, found that the maternal blood spaces and fetal capillaries of the labyrinth are separated, even in the thinnest parts, by a succession of three thin, widely overlapping and imbricated sheets of trophoblastic cytoplasm supported by a delicate, finely fibrillar basement membrane which is often double. The outer-most trophoblast layer, bordering the maternal blood space, was described as consisting of syncytially fused cells, whereas the trophoblast contiguous with the basement membrane was believed to consist of separate discrete cells. The syncytial or cellular nature of the middle trophoblastic layer was not described.

Upon re-examining the ultrastructure of the rat placenta in a more definitive study, which also included observations of the rabbit placenta on the 28th day of gestation, Wislocki and Dempsey (97) interpreted the labyrinth as consisting of 2 or 3 overlapping sheets of cytotrophoblastic cells rather than as an inner cellular layer and an outer syncytial layer as previously described. Wislocki and Dempsey also observed two distinct basement membranes in the labyrinth, one supporting the trophoblast and the other supporting the endothelial cells lining fetal capil-

laries. The narrow space between the two membranes was described as containing wisps of collagen. These observations were subsequently extended by Schiebler and Knoop (98, 99), who examined the fine structure of the rat placental labyrinth on the 20th and 21st days of gestation. These authors, however, did not observe two separate basement membranes and reported the occurrence of only a single basement membrane intervening between the trophoblast and fetal endothelium. In addition to describing the cellular nature of the labyrinth, Schiebler and Knoop observed wide spaces between the outer and middle layers of trophoblast which frequently communicated with maternal blood sinuses. On the other hand, trophoblast cells of the inner layer were always found to be closely apposed.

Owers and Mossman (100), utilizing the newer fixatives and embedding media for electron microscopy, have given an account of the rat placental labyrinth on the 15th and 16th days of gestation, which differs considerably from previous descriptions. In this study the placental barrier was found to consist of only two layers of trophoblast overlying fetal endothelium. The outer trophoblast adjacent to maternal blood was described as a relatively thick imbricated cellular layer, whereas the inner trophoblast was described as being an attenuated syncytial layer with widely scattered nuclei.

More recently, Jollie (101) has studied the fine structure of the rat placental labyrinth from the day of its establishment until term. At all stages the placental barrier was found to consist of three cytoplasmic layers which he individually named from the maternal blood space inward to the allantoic capillary endothelium as trophoblast I, trophoblast II and element III. Of these labyrinthine components, Jollie has

described element III as the only layer being syncytial. Enders (45) who has studied the fine structure of the hemochorial placenta in various species of mammals, has given a similar description for the labyrinth of the laboratory rat, laboratory mouse, hamster and deer mouse. In this study, however, Enders presented evidence which suggests that trophoblast II in the rat as well as in the other aforementioned rodents, is also syncytial in nature. The observations of the placental structure of the laboratory mouse have since been confirmed by Kirby and Bradbury (102).

In their report on the fine structure of the rat placenta, Wislocki and Dempsey (97) also included a brief account of the hemochorial nature of the rabbit placenta. In this report they suggested that the rabbit labyrinth consists of thin overlapping sheets of trophoblastic cells similar to those found in the rat placenta. Larsen (103) who recently examined the rabbit placenta on the 11th, 14th, 21st and 28th days of gestation, has described the trophoblast as consisting of an outer syncytial later (bordering maternal blood), separated from an inner cellular layer by large irregular spaces which are interrupted at intervals by desmosomal attachments. In addition to many short microvilli, the syncytial layer was found to contain a greater abundance of pinocytotic vesicles, large vacuoles, granular endoplasmic reticulum, golgi vesicles, mitochondria and fat inclusions than the inner cytotrophoblastic layer.

Wynn and Davies (104) have confirmed the presence of two trophoblastic layers in the rabbit labyrinth. These authors, however, described the outer trophoblast layer as a pseudosyncytium consisting of peculiar masses of syncytial elements, connected by desmosomes and separated by

plasma membranes from similar syncytial aggregates. They also described the inner layer of trophoblast as a discontinuous cellular layer interposed between the outer pseudosyncytial elements and fetal capillary. In a subsequent fine structural study of the rabbit labyrinth, Enders (45) was unable to demonstrate partitioning cytoplasmic membranes and thus considered this evidence that the trophoblast bordering the maternal blood space is a true syncytium. In addition to nests of individual cells in the inner layer of trophoblast, Enders also found flanges of cytoplasm which extended for considerable distances and on occasion between at least two nuclei. He interpreted this finding as indicating that the inner layer must be in the form of multinucleate cells or have syncytial regions.

Fine structural studies of the hemochorial placenta of the guinea pig, chipmunk and armadillo have also been reported. Davies, Dempsey and Amoroso (105) and Enders (45) have found that the term guinea pig labyrinth consists of a single continuous layer of syncytium varying in thickness and having micorvilli both on its free and basal surfaces. One of the most striking features of the guinea pig labyrinth is that it is probably the thinnest of all of the hemochorial placentas thus far examined. Enders has demonstrated that the trophoblast in some areas becomes as thin as the diameter of a single microvillus.

Observations on the placental labyrinth from the chipmunk show that the trophoblast in late pregnancy also forms a single syncytial layer enclosing the maternal blood spaces (45). Occasionally, however, individual trophoblast cells are found between the syncytium and the basement membrane. Also, the fetal vessels are not as closely associated with the trophoblast in the chipmunk placenta as they are in the guinea pig

placenta. Under the numerous microvilli of the free surface of the syncytial trophoblast of the chipmunk labyrinth, there are extensive subsurface spaces which communicate with the maternal blood sinuses. Evidence of pinocytosis is found at the margins of these spaces as well as between the surface microvilli.

The hemochorial villi of the armadillo placenta have also been described as being covered by a single layer of syncytial trophoblast. From the free surface of this layer extends long, complexly branched and anastomosing microvilli (45, 104, 106, 107). In the later stages of pregnancy, infoldings of the basal plasma membrane were observed to form branching channels of small diameter which extend into the trophoblast over its entire fetal surface. Evidence of pinocytotic activity was found on both surfaces of the syncytium. With exception of the tips of growing villi, cytotrophoblastic cells were completely absent at all stages of gestation.

On the basis of both his own comparative fine structural studies and those individual reports of other investigators (previously reviewed), Enders (45) has pointed out that both labyrinthine and villous hemochorial placentas can be grouped according to the number of layers of trophoblast present during the last third of gestation. In this manner, placentas of the rat, mouse, hamster, and deer mouse, which have three layers of trophoblast between the maternal blood space and fetal vessels, would be designated labyrinthine hemotrichorial. The rabbit with two layers of trophoblast would be labyrinthine hemodichorial, the guinea pig and chipmunk with one layer of trophoblast would be labyrinthine hemomonochorial, and the human and armadillo, also with one layer of trophoblast, would be villous hemomonochorial.

Ultrastructural examinations of the placental barrier of rodents and lagamorphs have thus revealed that the trophoblast persists throughout gestation. Its continued presence then would favor the supposition advanced through histochemical studies that phosphatases in the hemochorial placenta of these mammals are principally located in the trophoblastic layer rather than in the fetal endothelium (37, 41). However, since the trophoblast in the rat as revealed by the electron microscope consists of three discrete layers, histochemical studies of phosphatases with the light microscope give no clues as to which layers the activities are associated. Therefore, one of the objectives of this thesis is to describe the ultrastructural localization of several adenosine nucleoside phosphatases in the rat placental labyrinth at closely seriated stages of gestation.

Histochemical and Ultrastructural Studies of the Visceral Yolk Sac Placenta

In addition to the objections to Grosser's classification alluded to earlier in this review, a second objection stemmed from the fact that Grosser's classification is based on one region of the choric-allantoic placenta and tends to divert attention away from other equally important regions of the extraembryonic membranes which are physiologically active in the exchange between mother and fetus. These structures may function either successively or concurrently with the chorio-allantoic placenta during gestation. One such region is the yolk sac placenta which in vertebrates is probably the most primitive form of placentation (3, 44, 48, 54, 108, 109).

In viviparous forms of Elasmobranchii (110), teleostei (111, 112, 113, 114), amphibians and some reptiles (115), the yolk sac placenta,

in addition to absorbing endogenous yolk through its endoderm, is also involved in the physiological interchange of materials between maternal and fetal blood streams and is, therefore, functionally quite similar to the chorio-vitelline placenta of mammals (116). In marsupials thus far investigated, except for three species in which a chorio-allantoic placenta develops, the embryo and subsequent fetus is nourished exclusively through the trilaminar yolk sac placenta (vascular chorio-vitelline placenta) (48, 54, 117).

In addition to a well-developed chorio-allantoic placenta, Eutherian mammals also develop, at least temporarily, a yolk sac placenta which may occur as a primitive bilaminar omphalopleure consisting of ectoderm and entoderm with no intervening mesoderm, or as a vascular trilaminar omphalopleure with vascularized mesoderm interposed between ectoderm and entoderm (3, 44, 54, 109). Yolk sac placentation in some orders of mammals involves a very different and more complex structure. In such animals only that portion of the yolk sac endoderm at the embryonic hemisphere becomes vascularized. With subsequent growth of the embryo, this vascular trilaminar omphalopleure is gradually reflected towards the abembryonic hemisphere until it comes into close apposition with the avascular (bilaminar omphalopleure) portion of the yolk sac entoderm as is seen in figure 2. This "inverted" type of yolk sac placentation is characteristic not only of Rodentia (rat, mouse, guinea pig) and lagamorpha (rabbits), but also of many microchiroptera (bats), most Insectivora and the Dasypodidae (armadillos).

The bilaminar or parietal portion of the inverted yolk sac appears to be provisional or transient in nature and degenerates early in pregnancy, thus bringing the visceral entoderm into intimate contact

with the regenerated uterine epithelium. On the other hand, the basal surface of the trilaminar or visceral yolk sac increases in surface area through the formation of elaborate vascularized villi and persists throughout gestation.

The general morphology of the yolk sac and the method of its formation in different animals is well known (3, 44, 54, 109). There is no unanimous agreement, however, as to its function(s), nor is their agreement as to whether those that persist throughout gestation function successively or concurrently with the chorio-allantoic placenta. Therefore, it is necessary, for the sake of clarity, to present a brief chronological summary of pertinent cytological and histochemical studies which have led placentologists to ascribe placental functions to this structure.

The presence of various-sized granules in the apical cytoplasm of the visceral yolk sac epithelium of the rodent, bat and rabbit has been the subject of description, discussion and speculation by a number of investigators (37, 118, 119). Some have regarded them as being secretory granules which are destined to be discharged into the yolk sac cavity or uterine lumen, whereas others have maintained that they represent materials which have been absorbed from the yolk sac cavity or uterine lumen for subsequent transmission to the fetus. Bridgeman (119) has reported that these large supranuclear proteinaceous granules appear in endodermal cells destined to form the visceral yolk sac in the rodent as early as the sixth day of gestation and disappear by the ninth, possibly through their extrusion into the yolk sac cavity. She subsequently found that similar granules reappeared reaching a maximum size and number per cell on the day preceding the rupture of Reichert's membrane. The granules

then remained until the 20th day of pregnancy. Asai (120), a leading exponent of the secretory theory, claimed that these granules were proteolytic enzymes which were discharged at the appropriate time for the purpose of digesting the parietal yolk sac and its underlying structures. More recently, Ower (121), who has localized strong cathepsin activity in the visceral endoderm of the rat yolk sac, has suggested a similar hypothesis. Litwer (122), also an exponent of the secretory theory, claimed that the granules also released a lipase necessary for the absorption of fat by the endodermal cells. On the basis of absorption studies, Branca (123) and Gerard (124) disagreed with the secretory hypotheses and regarded the granules as albuminoid in nature arising as the result of the absorption of proteins from the yolk sac cavity and uterine lumen.

That the yolk sac is capable of absorbing exogeneous materials has been shown by Goldman (125), who first reported that the visceral endodermal cells of the mouse yolk sac are able to concentrate trypan blue. Wislocki (126, 127) and Wislocki, Dean and Dempsey (37) extended this observation to include the rat, rabbit and guinea pig. In these studies they observed that trypan blue appeared in the apical cytoplasm in the form of small droplets which resembled the normally occurring proteinaceous acidophilic granules described earlier.

In a subsequent study, Wislocki, Dean and Dempsey (37) noted a similarity between the tinctorial properties of the apical granules and the embryotrophic material in the adjoining yolk sac and uterine cavities. They considered further that some of the granules resembled fragments of extravasated maternal erythrocytes which were numerous in the embryotroph.

In additional absorption experiments, Everett (128) reported that vital dyes having a small molecular weight rapidly passed through Reichert's membrane and the parietal and visceral yolk sac to gain access to the fetal circulation. On the other hand, he found that azo dyes of larger molecular weight, presumably non-metabolizable, such as trypan blue, were concentrated in the visceral yolk sac epithelium inside the preformed granules which he considered to be Golgi elements. Bridgman confirmed part of this study and added that when injected prior to the eighth day, trypan blue seemed to be held by the apical granules, whereas later the dye appeared inside preformed apical vacuoles where it is found until the end of gestation.

In view of these observations, Everett and Wislocki contended that the visceral yolk sac functioned in the absorption of uterine secretions and exogenous materials from the maternal circulation and selectively transported them to the fetus. Wimsatt (118) agreed with this conclusion, but did not consider the apical granules as materials absorbed by the yolk sac entoderm. Instead, he considered the granules as non-usable metabolic by-products or non-metabolizable materials of which the endodermal cells have no means of disposing and hence store for the duration of pregnancy. This belief seems to be consistent with recent absorption studies of the yolk sac in which the localization of vital dyes was found to correspond to the area of lysosomes which are known to store metabolically inert materials (129). A final interpretation of the granules has recently been advanced by Stephens (130), who believes that their early disappearance and reappearance indicates that they are a complicated energy store which is built up and is later degraded and used by the embryo via the vitelline circulation.

Both in vitro and in vivo experiments have been designed to study absorption by visceral endoderm with the electron microscope. In organ cultures of the rat visceral yolk sac, Sorokin and Padykula (131) reported that the visceral endoderm avidly engulfed cholesterol which had been added to the culture medium and concentrated it as osmiophilic membrane bound droplets in the supranuclear cytoplasm.

Luse and her associates (132, 133) have studied absorption in third trimester rabbit and mouse yolk sacs following intrauterine injections of colloidal gold, saccharated iron, lipids, colloidal carbon, egg albumin, bovine gamma globulin, salivary gland virus and erythrocytes. All of these materials were found to be ingested into the apical cytoplasm of the visceral yolk sac cells as pinocytotic vesicles, which were often in close association with small saccular or canalicular infoldings of the surface membrane. In addition to entering the cytoplasm, iron, collodial carbon, gamma globulin, salivary gland virus and lipids also "penetrated" the endodermal nuclei. On the basis of further work, Luse, Davies and Clark (134) have suggested that these material enter the nuclei not only by way of electron microscopically demonstrated nuclear pores, but also by nuclear membrane pinocytosis. Of these injected materials, only colloidal gold is found within the mesenchymal cells underlying the visceral epithelium. However, the pathway by which this particulate material reached these cells is not observed.

In a sequential study of the yolk sac by electron microscopy (13th, 14th and 15th days of gestation), Carpenter and Ferm (135) demonstrated the progressive uptake of thorotrast particles by the visceral epithelial cells of the golden hamster. They described the particles as entering apical invaginations of the surface membrane which distally became con-

fluent with large membrane-limited vacuoles. There appeared to be no evidence of transfer of these particles to the subjacent connective tissue spaces or vitelline blood vessels.

Further information concerning the functional activities of the yolk sac has been obtained through histochemical studies of its lipid and glycogen content.

In addition to supranuclear granules, numerous fat droplets of variable size are found in the basal portion of the visceral yolk sac epithelium in both rodents and bats. These sudanophilic droplets have been described as first appearing apically (120, 122, 123) on the 9th day of gestation (119), reaching a maximum by the 15th day and then remaining until term (27, 136). Bridgman has found a close correlation of the appearance of fat with the formation of the brush border of the visceral epithelium. Wislocki, Dean and Dempsey (37) have examined frozen sections of the yolk sac epithelium under the polarizing microscope and have observed that birefringent fat droplets are also invariably present. Since these droplets coincide with those of lipid, the authors considered them one and the same. When examined by ultraviolet light these same sections of yolk sac epithelium revealed whitish-yellow dots of fluorescence. Although not convinced that the fluorescent dots were the birefringent fat droplets of previous examination, Wislocki, Deane and Dempsey cautiously suggested that they might be attributed to steroid substances or possibly lipochromes.

Glycogen has been reported as appearing in the inverted yolk sac as early as the 10th day of gestation (37, 136) and as late as the 14th day (27, 118, 119, 130, 131). In the visceral endoderm glycogen appeared to be most abundant during the period of 15 to 18 days where it was typically

found in the basal cytoplasm (119, 137, 138, 139). After the 18th day, glycogen was steadily depleted until term. Padykula and Richardson (139) have pointed out that although the visceral endodermal cells are the primary site of storage, the underlying mesenchymal cells are also capable of synthesizing glycogen. In fact, glycogen in the inverted yolk sac of the bat is most abundant in these cells (118).

In an early glycogen study of the human and monkey, Dempsey and Wislocki (140) developed the thesis that glycogen was deposited in the placenta, fetal membranes and fetus in regions which for various reasons were anoxic, ischaemic or poorly vascularized. On this assumption, Wislocki, Dean and Dempsey (37) suggested that the large quantities of glycogen in the rodent yolk sac, in contrast to the placental labyrinth which in early pregnancy contained none, provided an anaerobic source of energy for those tissues with a reduced circulatory efficiency.

McKay, Adams, Hertig and Danziger (29, 30) also observed large amounts of glycogen in the yolk sac of the 5, 6 and 7 mm human embryo and its absence from both the syncytial trophoblast and fetal liver cells. These authors proposed that this indicated that the yolk sac, in a manner similar to the rodent, supplied glucose to the embryo during the first weeks of gestation. This finding challenges the assumption that the human yolk sac, although present at term as a reduced vesicle, plays no role in metabolic exchange.

As a result of many of these histophysiological and histochemical studies, a concept developed that placental transfer was accomplished in rodents mainly by the yolk sac in early gestation and that the slower developing chorio-allantoic placenta assumed this function later in pregnancy. Padykula (38), however, has pointed out that if increased

enzymatic activity indicates greater functional activity, then it could be assumed that the visceral yolk sac performs a greater role in transfer upon its exposure to the uterine cavity.

In the rat, mouse, guinea pig, bat, and shrew, all of which have an inverted yolk sac placenta, alkaline glycerophosphatase has been reported as first appearing on the 13th day of gestation in both the brush border and apical cytoplasm of the visceral endoderm (27, 37, 38, 41, 42, 118, 130). This activity was found to rise sharply on or immediately after the 15th day, reaching a peak in the rat and mouse on the 16th through 19th days and thereafter becoming less intense and more diffuse (37, 38, 42). In the guinea pig, which has a 68 day gestation period, peak activity occurs around 45 to 50 days and by the 60th day completely disappears (41). Moderate alkaline glycerophosphatase activity is also found in the underlying mesenchymal cells and the endothelial lining of the vitelline capillaries (37, 118, 130). However, in the guinea pig the activity in these cells appears to be transient as it completely disappears by the 21st day of gestation (41).

When glycerophosphate is substituted with nuclei acid, fructose diphosphate, and adenylic acid substrates, at an alkaline pH (9.4), activity in the bat yolk sac is limited to the last third of gestation where it occurs in the visceral epithelium, mesenchymal cells and vitelline capillaries (118). When adenosine triphosphate is used as a substrate, hydrolytic activity in the rat visceral epithelium appears more intense than that observed with glycerophosphate, but the time of appearance and distribution follows a similar pattern (38).

In the rat, mouse and bat, acid glycerophosphatase activity is found on the 15th day of pregnancy in the supranuclear cytoplasm of the

endodermal cells (37, 118). This activity is found to increase with advancing gestation until the cytoplasm is completely stained (39). Intense acid phosphatase activity is also found with nucleic and adenylic acid (118). These substrates differ from glycerophosphate in that they also elicit a response in the mesenchymal cells and vitelline vessels.

Regardless of its functional capabilities, the surface area of the yolk sac relative to embryo size decreases with the establishment and subsequent growth of the labyrinthine placenta. Because of this, many investigators have maintained that the rodent yolk sac becomes less important with increasing gestational age. Wislocki, Deane and Dempsey (37), however, have suggested the possibility that the two types of placentas in rodents are complementary in nature. This suggestion was based on their observations that iron, as revealed by the Turnbull blue method, is secreted by the uterine glands and absorbed by the visceral yolk sac for fetal use, whereas the Bodian protargol reaction indicated that bound calcium is transmitted to the fetus through the allantoic placenta. Such evidence is in complete agreement with subsequent studies of Bridgman (119).

Further evidence that the inverted yolk sac of rodents and lagamorphs functions concurrently with the chorio-allantoic placenta has been presented by Brambell and his colleagues (141, 142, 143, 144, 145, 146). They have demonstrated experimentally that antibodies find their way from the maternal circulation into the embryo not by passage through the thin and supposedly more permeable layers of the chorio-allantoic placenta as previously thought, but exclusively by way of the yolk sac placenta.

By developing a procedure in which they could ligate the vitelline vessels of alternate fetuses without disturbing their visceral splanchno-

pleure, Brambell et al. (142) developed a means of experimentally studying the transmission of antibodies to the fetus with internal controls. Using such preparations in nonimmune rabbits 23-26 days pregnant and injecting immune serum prepared in other rabbits either into the uterine cavity or intravenously into the maternal circulation, they demonstrated that complete arrest of the vitelline circulation stopped the transmission of antibodies whether from the uterine cavity or maternal circulation. In subsequent experiments, however, Brambell and Halliday (145) found that surgical intervention with the vitelline vessels of fetal rats on the 19th day of gestation did not completely prevent immune rat serum from entering the fetal circulation. This, they proposed, indicated that antibodies absorbed by the visceral yolk sac in addition to being transmitted by the vitelline vessels is also routed through the exocoelom, amniotic cavity and fetal gut. To preclude the entry of antibodies by these routes, the authors removed the visceral yolk sac and ligated the mouth and nose of each fetus. Since absorption was even then taking place, Brambell and Halliday concluded that the endodermal sinus of Duval is capable of antibody absorption and that anastomosis of the vitelline vessels with the allantoic vessels might maintain a partial circulation which would account for the continued transmission of antibodies to the fetus.

Smith and Schechtman (147) have studied the transmission of antigenically labelled materials to the rabbit fetus before, during and after the degeneration of the parietal yolk sac. Their results indicate that the bilaminar wall acts as a barrier to macromolecules from the 9th through the 13th days of gestation. Therefore, during this period only those materials absorbed and stored by the visceral yolk sac prior to

the 9th day are transferred into the embryonic circulation.

Histological evidence in support of transport of antibodies and serum proteins by the yolk sac has been demonstrated through the use of autoradiographic and fluorescent dye techniques. On injecting I 131 labelled gamma globulins into pregnant rats on the 11th, 15th and 17th days, Anderson (148) produced autoradiographs which showed that gamma globulin entered the apical portions of the visceral endodermal cells in small amounts both before and after the rupture of the parietal wall. Although the gamma globulin gained access to the endodermal sinus of Duval, penetration into the apical cytoplasm of the cells in that area was not detectable. This finding would appear to be contrary to the postulate of Brambell and Halliday that this is a major site of antibody transfer. The autoradiographs agreed with seralogical evidence, indicating that the trophoblast of the labyrinth placenta probably acts as a barrier to gamma globulins.

Both Mayersbach (149) and Davies (150) have described the localization of serum protiens labelled with fluorescent dyes in the yolk sac. In the rat during the last third of pregnancy, Mayersbach found through the analysis of both tissue and fluid samples a transfer of proteins across the yolk sac cavity with uptake by the visceral endoderm and passage to the vitelline vessels. This study also ruled out the chorio-allantoic placenta as a route of transfer. Mayersbach, however, did consider the endodermal sinus of Duval as a possible route of transfer. In the rabbit, Davies (150) found that fluorescent labelled Bovine gamma globulin was rapidly taken up by the visceral endoderm in the form of droplets by a process of pinocytosis. Davies also emphasized the passage of these absorbed proteins into the exocoelomic and amniotic

cavities.

Since most of this information concerning prenatal transference of immunity was based on animals with relatively short gestation periods, Leissring and Anderson (151) undertook a study comparing the passive immunization of the fetal guinea pig which has a rather protracted gestation period as compared to that reported for rabbits. In this study seralogical titrations of maternal sera, fetal sera and fetal tissues were made after surgically intervening with the different possible routes of antibody transfer. The results indicated that the transfer of antibodies to the guinea pig fetus is primarily by way of the vitelline circulation until the 40th day, and that there is a gradual shift in this function until 50 days, after which the fetal gut is the predominant site of transfer. In a subsequent paper, Anderson and Leissring (152) attempted to correlate both the decline in alkaline phosphatase activity and senescent changes in the yolk sac with the shift in antibody transfer to the fetal gut. However, little attention was given to the fact that in order to reach the gut for absorption, antibodies must still cross the visceral yolk sac.

The role of the yolk sac in transmission of passive immunity to the young has been extensively reviewed by Brambell and Hemmings (153) and Davies (154).

As one can see from this brief review of the literature, the yolk sac is actively involved in absorptive, secretory, storage and transfer activities. Therefore, this membrane must have an extremely fascinating complex cytological structure, since these epithelial cells are capable of selectively transporting certain large molecules, as antibodies and serum proteins, and yet are also capable of withholding and segregating

other colloidal substances such as trypan blue. The use of the electron microscope has now made it possible to study more closely both the striking differentiation that the yolk sac placenta undergoes during its brief life history and the structures involved in the above mentioned activities.

Although fine structural studies of the yolk sac epithelium in the guinea pig (155), rat (48, 97, 139, 156, 157), human (90), and rabbit (108) have been reported, those other than for the rabbit have dealt with only a limited period of gestation and/or have been reported only as brief communications. Furthermore, apart from a brief description by Wislocki and Dempsey (97), the ultrastructure of the underlying mesenchymal cells, connective tissue elements, vitelline vessels, serosal basement membrane and mesothelial cells lining the exocoelomic cavity has not been described. These structures would appear to be of considerable importance since they also have been implicated in the active transport of macromolecules to the fetus. Since there has not been a closely seriated fine structural study of the rodent yolk sac including stages before and after the loss of Reichert's membrane, such a study seemed warranted. It was also felt that the fine structural localization of adenosine nucleoside phosphatase, which plays a role in general energy release, might provide additional information relating to the functional activities of the various structures of the rat visceral yolk sac at progressive stages of gestation.

MATERIALS AND METHODS

Animals:

Normally cycling primiparous female rats of the Sprague-Dawley strain exhibiting proestrous or early estrous lavages were allowed to mate at random for a period of two hours in an inverted light cycle room. From the examination of vaginal lavages for the presence of spermatozoa, it was possible to fix the time of mating to within ± one hour. The first day of gestation was designated as the twenty-four hour period following the observation of spermatozoa in the vagina. According to this method of timing, mothers normally deliver on the 22nd day post coitum.

Prolonged gestation to 25 days was achieved by intramuscular injections of 1 ug of estradiol (10 IU) in 0.3 cc of sesame oil, and 4 mg (4 IU) of progesterone in 0.4 cc of sesame oil, beginning on the morning of the 20th day and daily thereafter through the 25th day of gestation (158).

Handling of tissues:

Under Nembutal anesthesia (5-6 mg/100 g body weight), pregnant rats were autopsied on the 12th, 14th, 18th, 22nd and 25th days of gestation, five animals on each day. Each conceptus was surgically removed individually by making a small longitudinal incision on the antimesometrial surface of the uterus between adjacent implantation sites. This allowed the uterine musculature to retract, separating the uterine epithelium (decidua parietalis) from the implant to a point along the perimeter of the placenta. Then, with a concave spatula, the intact implant was easily shelled from the endometrial gland and transferred to a drop of ice-cold fixative. In this manner it was possible to prepare

tissues from an individual implant without mechanically disturbing the placental circulation of other fetuses.

Once submerged in fixing fluid, the accessory membranes enclosing the embryos were separated. In the 12 and 14 day fetuses, the decidua capsularis was grasped with fine forceps and pulled free. The parietal yolk sac and chorion laeve both adhere to its inner surface, thus leaving the visceral yolk sac exposed (Figure 2). On the 16th day of gestation, Reichert's membrane ruptures and recoils to the margin of the chorionic plate, taking with it the decidua capsularis, chorion laeve and parietal yolk sac. Therefore, the 18, 22 and 25 day implants separate from the uterus at the plane between the decidua parietalis and visceral yolk sac (Figure 3).

The visceral yolk sacs were then cut free from the chorionic plate of the labyrinthine placenta, pulled from the underlying amnion, and subdivided into several rectangular pieces. It was not necessary to cut the yolk sacs into small blocks since the total tissue thickness is less than one millimeter and is easily penetrated by fixing fluids.

Each of the chorio-allantoic placentae was hemisected and blocks approximately 1 x 1 x 3 mm in size were excised from the center of the labyrinth so that the long axis (across which sections were later cut) extended vertically between the maternal and fetal surfaces.

Fixation:

After excision, all of the tissues were transferred to one dram vials containing fresh 3% glutaraldehyde buffered to pH 7.4 with 0.1 M sodium cacodylate and allowed to fix for one hour at 3-4° C (159). Following fixation, the unbound glutaraldehyde was removed from the tissues in order to avoid interference with either the enzymatic reac-

tions or the post fixation with osmium tetroxide. This was accomplished by rinsing the tissues six times for 30 minutes each in cold 0.1 M cacodylate buffer pH 7.4 containing 0.22 M sucrose. The tissues were then left in the last change of buffer and allowed to wash for at least 24 hours at 3-4° C. Occasionally these tissues were kept in the buffer for periods up to one week with no evident loss of structural detail or enzymatic activity (159). Some of the tissues were then frozen in a mixture of isopentane super-cooled to -68° C with either absolute isopropyl alcohol and dry ice or liquid nitrogen. Thin (10 u) and thick (50 u) frozen sections were cut in a Pearse microtome and were transferred to cold 0.1 M cacodylate buffer containing 0.22 M sucrose before being placed in the various incubation media.

Histochemical procedures:

The demonstration of ATP-, ADP,- and AMPase activities was accomplished by employing a standard Wachstein-Meisel (160) medium containing one of the following substrates: Adenosine triphosphate (ATP), adenosine diphosphate (ADP) or adenylic acid (AMP).

1. Experimental:

Stock solutions were routinely prepared the day before the experiment and are as follows: (a) tris hydroxymethyl aminomethane-maleate (tris maleate buffer)[1] pH 7.2, 0.2 M; (b) lead nitrate, 2%; (c) magnesium sulphate, 0.1 M; (d) ATP (Sigma Chemical Company),

[1]The use of tris-maleate buffer considerably reduces the extraneous precipitate and nonspecific staining commonly encountered with other buffer systems. The maleic ions appear to play an important role in determining the concentration of lead ions in solution. Therefore, the purity of maleic acid is essential in this buffer. Lead precipitate free incubation media were consistently obtained when maleic acid supplied by Matheson, Coleman and Bell was used in making this buffer.

ADP (Calbiochem[2]) and ATP (Sigma Chemical Company), 125 mg percent solutions respectively. The final incubation mixture was prepared immediately before use in the following order, with thorough mixing after the addition of each component:

Tris maleate buffer 0.2 M, pH 7.2	20 ml
Phosphate ester substrate 125 mg/100 ml	20 ml
Lead nitrate 2%	3 ml
Magnesium sulphate 0.1 M	5 ml
Distilled water	2 ml

In addition to thick (50 u) sections, small blocks of unfrozen placental labyrinth and visceral yolk sac were incubated along with thin (10 u) frozen sections. In order to determine optimum lengths of time for incubation of tissues, the thin sections were periodically removed from the incubation media, washed briefly in several changes of cacodylate buffer, treated with dilute ammonium sulfide to develop a visible precipitate of lead sulfide from the final lead phosphate reaction product and mounted in glycerine jelly for examination with a light microscope. When the frozen sections first demonstrated a visible deposition of final reaction product, the 50 u sections and small unfrozen blocks were removed from the incubation medium. This degree of reaction was usually reached within 30 minutes. These tissues (destined for electron microscopy) were deliberately under-reacted, as judged by light microscopic standards, in order to obtain a more discrete localization of enzymatic activity with respect to fine structural detail.

[2]Incubation medium containing ADP from sources other than Calbiochem was found to be unstable and not applicable to this cytochemical reaction.

2. Controls:

For control experiments tissue sections and blocks were incubated either in media in which nucleotide phosphate esters were replaced with equimolar concentrations of B glycerophosphate, or in substrate-free media. Other control preparations were obtained by inactivating enzymes through pretreatment of specimens for one hour in buffered one percent osmium tetroxide prior to incubation in the substrate containing media.

No appreciable changes in pH occurred as a result of incubation, which, in all cases, was carried out at room temperature (22° C).

Post-fixation:

After incubations were completed, all thick sections and blocks of tissue were washed three times in cold 0.1 M cacodylate buffer pH 7.4 containing 0.22 M sucrose over a period of about 30 minutes. They were then refixed for one hour in 1-2 percent osmium tetroxide buffered to pH 7.4 containing 0.22 M sucrose, dehydrated and embedded in plastic as described below.

Dehydration and embedding:

The tissues were rapidly dehydrated through the following graded series of cold ethanol solutions: 50 percent for 10 minutes, 70 percent for 20 minutes, three changes of 95 percent for a total of 90 minutes. Occasionally the tissues were left in 95 percent ethanol overnight or until they could be infiltrated with plastic and embedded. Prior to infiltration the tissues were dehydrated further in three changes of absolute ethanol for a total of 60 minutes and then with two changes of propylene oxide for a total of 40 minutes. Following this dehydration, the tissues were infiltrated for at least three hours in a one-to-one

mixture of fresh propylene oxide and complete epoxy resin mixture. The epoxy embedding medium was made up by using Epon 812 (a Shell Chemical Company epoxy resin), dodecenyl succinic anhydride and methyl nadic anhydride (hardening agents) and 2, 4, 6, tri (dimethylaminomethyl) phenol (accelerator). These resin components were made up into two stock solutions, A and B as recommended by Luft (161). Most of the tissues were embedded in a mixture of the two in the proportion of six parts of A to 4 parts of B with 1.5 percent accelerator (v/v) added immediately before use. Each of the tissue blocks were transferred from the infiltration mixture, with a minimum of liquid, to size No. 00 gelatin capsules filled with the complete resin mixture. The plastic was then polymerized by heat as follows: 14 hours at 35° C., 10 hours at 45° C., and 16 hours at 60° C.

Staining and sectioning:

The polymerized blocks of tissue were sectioned on a Porter-Blum MTI microtome (Sorvall) with fractured glass knives and on an LKB ultrotome with a diamond knife (DuPont). Thick 1 u sections for orientation with the light microscope were treated with Richardson's stain (162) and mounted on glass slides. Thin sections about 500 to 700 Å thick were collected from a water bath on etched 200, 300 or 400-mesh copper grids, either naked or covered with a supporting carbonized collodion film, and examined without additional staining. It was subsequently found that the deposits of final reaction product (lead phosphate) could be differentiated with the electron microscope from the staining produced by the usual heavy metal "staining solutions" uranyl acetate, lead hydroxide and lead citrate. Therefore, the overall contrast of cell membranes, organelles and inclusions, examined

with the electron microscope, was increased by double staining the thin sections, first with 5% aqueous uranyl acetate for 10-30 minutes (161), and then with 0.1-0.2% lead citrate for 30 seconds (163). The thin sections were examined in an RCA, Model EMU 3F, electron microscope. Photographic negatives were taken at original magnifications of about 1,400 to 6,200 and were photographically enlarged to the desired size.

RESULTS

General Description

For the purpose of general orientation and convenience in interpreting the ultrastructural and cytochemical results to be presented in this thesis, a short description of the relationships existing between the extraembryonic membranes and the uterine structures from 12 days to term will be presented.

In the 12 day embryo the inverted yolk sac placenta is well developed, whereas the chorio-allantoic placenta has just been established through the contact of allantoic mesoderm with the base of the trophoblastic ectoplacental cone. By the 14th day post coitum, fetal blood vessels from the allantois have invaded the ectoplacental cone and formed well vascularized trophoblastic lamellae of the hemochorial labyrinthine type (Figure 1). At this time three general zones are recognizable in the fetal portion of the chorio-allantoic placenta (Figure 2). The innermost zone, the labyrinthine trophoblast, is composed of numerous branching and anastomosing trabecular cords of trophoblast which border maternal blood spaces and contain vascular cores of the peripheral allantoic circulation. Throughout gestation the trabecular cords of the placental labyrinth consist of at least four cytoplasmic elements which are interposed between maternal and fetal blood streams. These cell layers are, from the maternal blood sinus inward: trophoblast I, trophoblast II, trophoblast III and fetal endothelium (Figure 1). The middle zone of the chorio-allantoic placenta caps the mesometrial and lateral sides of the labyrinth and is called the spongiotrophoblast (Figures 2 and 3). This zone consists of a mass of cytotrophoblast cells which lack fetal blood vessels, but is extensively

perforated by maternal blood sinuses. The outer surface of the spongiotrophoblast is continuous with a loose meshwork of mutually interdigitating giant trophoblast cells which constitute the remaining portion of the ectoplacental cone and the third zone of the choric-allantoic placenta (Figures 2 and 3). Here, giant trophoblast cells form a continuous sheath around the margin of the fetal accessory membranes. They also maintain a close association with all surfaces of the uterine decidua. The interstices between these giant cells contain circulating maternal blood.

Growth of the choric-allantoic placenta is continuous through the 16th day of gestation. This is achieved both by cell division and by the invasion of the spongiotrophoblast by allantoic capillaries to form additional trabecular cords of labyrinthine trophoblast. Although growth occurs at the expense of the spongiotrophoblast, a small but distinct zone does persist throughout gestation. The labyrinthine growth is more lateral than mesometrial, therefore, the placenta becomes flattened or button shaped instead of conical.

The inverted yolk sac placenta of the rat is well developed by the 12th day post coitum and is divided into two distinct morphological zones (Figure 2): (1) an outer, non-vascular parietal wall, and (2) an inner, vascular, visceral wall. The parietal yolk sac consists of a single layer of cuboidal endodermal cells lining the inner surface of Reichert's membrane. This thick basement membrane and the parietal yolk sac are firmly attached to the fetal surface of the choric-allantoic placenta along a line encircling the entrance of the allantoic vessels into the chorionic plate (Figure 2). The parietal yolk sac is continuous with the visceral yolk sac at this point. Reichert's membrane

then extends over the entire maternal surface of the parietal yolk sac (Figure 2). The outer surface of this membrane is in close contact with the loose meshwork of interdigitating trophoblastic giant cells described earlier. Therefore, over much of its surface, it appears that Reichert's membrane is directly bathed by circulating maternal blood.

The visceral yolk sac, as can be seen in Figure 4, is composed of simple columnar endodermal cells resting on a highly vascularized layer of splanchnic mesoderm. The mesenchymal elements comprising this layer form a loose meshwork of connective tissue cells and fibers which surround and support the vitelline vessels, which have developed from this same mesenchyme. A somewhat thickened layer of extracellular material, the serosal basement membrane, separates the visceral yolk sac from the mesothelium, a simple squamous epithelium that lines the exocoelomic cavity. Near its attachment to the chorio-allantoic placenta, the yolk sac accompanies branching allantoic vessels into the placental labyrinth. Here the visceral endodermal cells become attached to the adventitia of the allantoic vessels while the parietal endodermal cells become adherent to Reichert's membrane. Such invaginations form perivascular recesses called endodermal sinuses which are best developed after the 16th day of gestation (Figure 3).

On the 16th day post coitum, the placenta seems to reach its greatest diameter. Late on this day Reichert's membrane, and with it the decidua capsularis, giant trophoblast cell layer and parietal yolk sac rupture at the antimesometrial pole and contracts by intrinsic elasticity to the perimeter of the placenta (Figure 3). The only parts of these transitory structures which persist after the 16th day are the reflected

portions of Reichert's membrane and the parietal yolk sac which are firmly attached to the fetal surface of the chorio-allantoic placenta (Figure 3). After these structural changes have taken place, the yolk sac cavity and uterine lumen become confluent (Figure 3). This places the visceral splanchnopleure in apposition to the decidua parietalis. As gestation proceeds the mesometrial portion of the visceral yolk sac becomes enlarged through the formation of ridges or villi (Figure 3). These villi are created by the proliferating pattern of the underlying vitelline vessels and overlying epithelium. Such a villous pattern gives the yolk sac a rugose appearance. There is always a capillary in the core of each villus. The antimesometrial portion of the visceral yolk sac is less vascular than its counterpart, and remains smooth throughout gestation (Figure 3).

More detailed histological and cytological descriptions of the developing components of the chorio-allantoic placenta and the inverted yolk sac placenta may be found in the following publications: Duval (4); Jenkinson (164); Huber (165); Everett (128); Keibel (166); Mossman (3); Bridgman (119, 167). In considering previous light microscopic descriptions of the developmental changes found in rat placental structures on a given day of gestation, one must bear in mind that methods by which a particular gestational age is determined are inconsistent. Many investigators have assigned the first day of pregnancy to the morning on which spermatozoa are found in the vagina. By such a method of dating, their developmental descriptions are 24 hours in advance of those presented in this thesis. The current method of determining gestational age of the developing conceptus is to consider the time at which spermatozoa are found in the vagina as day zero. Such

is the method of timing employed in this study.

Placental Labyrinth of the 12th Day

Ultrastructure

1. Avascular trophoblast

On the 12th day of gestation fetal vessels from the allantois have just made contact with the base of the ectoplacental cone. Therefore, most of the labyrinthine placenta appears as numerous branching cords of nonvascular epithelioid trophoblast separated from each other by maternal blood sinuses. These cords appear to consist of either two or four cellular layers (Figure 5), which may be interpreted as either two outer cell layers bordering maternal blood spaces and enclosing two inner cell layers or simply as two outer cell layers. For convenience of description, they will be referred to as inner and outer trophoblastic cell layers.

The cells forming the outer layer which encloses the maternal blood spaces are usually somewhat narrower than the inner cells and have their greatest depth across the site of their nucleus (Figures 6 and 9). Both the outer and inner surfaces of this layer have irregular microvilli and/or pesudopod-like projections of varying sizes. They are most numerous on the surface facing the maternal blood spaces. Some of these pleomorphic evaginations are tall and slender while others, on both surfaces of the outer layer, have terminal bulbous enlargements which contain rosettes of RNP granules and other cytoplasmic materials (Figures 10-12). Since the maternal blood spaces are pervaded with granular and fibrillar material and numerous free floating vesicular profiles with a content similar to the bulbous projections, it is presumed that the terminal bulbous

enlargements become pinched off from the cell surface (Figures 13-15). Another type of secretory evagination which resembles microapocrine secretions is also seen. Here, a solation of the outer plasma membrane presumably occurs with a resulting formation of blebs or blisters into which cytoplasmic components may enter and subsequently be expelled from the cell (Figure 7). Pinocytotic activities are rarely seen in this layer of trophoblast cells.

The limiting membranes of the inner and outer cell layers do not pursue parallel lines, but tortuously separate for considerable distances before again swinging into close apposition (Figures 6, 8, 13, 16 and 17). This arrangement frequently results in the formation of large oval or elongated intercellular spaces which are periodically interrupted by desmosomes (Figures 5, 8 and 12). Occasionally the intercellular spaces between the inner and outer cell layers are confluent with the maternal blood space (sinus) by way of large openings between cells of the outer layer. Such openings expose the inner cells which also have numerous surface evaginations, to circulating maternal plasma (Figures 13 and 17). The intercellular spaces exhibit granular material and vesicular profiles just as the maternal blood sinuses do (Figure 13). Again, evidence of pinocytotic activity is rarely seen in the inner layer of cells.

During this early stage of development, trophoblastic cells of the inner layer are actively multiplying as indicated by the presence of numerous mitotic figures (Figure 18). No such activity is seen in the outer layer of cells on this day, or in any trophoblast layer examined after the 12th day. One of the striking features of the cytoplasm encountered on the 12th day is the dominance of RNP granules

which gives the trophoblastic cells a marked granular appearance (Figures 6, 8, 12, 16, 17 and 19). These ribosomes, which are far more abundant in the inner layer of cells, occur primarily as free clusters (rosettes) (Figures 6, 8, 16 and 17).

The rough endoplasmic reticulum, although scarce, is more prominent in the outer cells which are most intimately associated with the maternal blood (Figures 9 and 20). Here the RER assumes the appearance of either parallel skeins of membranes or greatly dilated vesicular profiles. When it occurs as skeins, the cisternae are most commonly oriented with the long axis of the cells and their lumina contain a moderately dense granular substance (Figure 9). As irregular dilated vesicular profiles, the cisternae show no particular orientation, but are frequently closely associated with the limiting membrane of the cell (Figure 20). Also of particular interest is the fact that they contain a material which is distinctly fibrillar in nature. Some of the fibrils are quite elongated. The cells of the inner layer also have rough endoplasmic reticulum with vesicular profiles, but they are much less abundant than in the outer layer (Figures 8 and 16). Here the granular reticulum has no particular orientation and appears distributed at random throughout the cytoplasm. The cisternae, like those of the outer layer of cells, contain a moderately dense fibrillar material. Occasionally, in the inner layer of trophoblast, small dilatations and larger outpocketings in the RER, forming the outer layer of the nuclear envelope, are seen (Figures 7 and 8). Although golgi membranes and vesicles are not abundant, they are frequently found in both the inner and outer cell layers of the trophoblast. Here they are located in the perinuclear

region and are oriented parallel to the closest cell surface (Figures 8 and 20). The golgi complex, as seen in this material, consists of stacks of flattened cisternae which are associated with numerous vesicles and vacuoles. A few of the paired membranes have dilatations at their ends, while others are completely distended to form large vacuoles. Occasionally small vesicles are seen to coalesce (Figure 8). What little granular material that is found in their cisternae is only moderately electron dense.

Mitochondria of the trophoblast cells are usually large, round and have cristae which rarely are seen to reach across the mitochondrial matrix. Very frequently the inner membranes appear in progressive stages of degeneration. This process is evidenced by the disrupted nature of cristae and by the presence of vesicular profiles within the mitochondrial matrix (Figures 10, 12, 15, 16 and 20). The possibility exists that these observations are artifacts which have been introduced through poor fixation.

Contrary to what might be expected from the placental tissue which performs such a wide number of functions, a very limited number of lipid inclusions, vacuoles, myelin figures, lysosome-like and multivesicular bodies are found in the cytoplasm of the trophoblast cells. A few fine lipid droplets of a uniformly light intensity are found throughout the cytoplasm of both cell layers. However, clusters of the larger droplets occur specifically in the cells of the inner layer (Figure 6). Two types of vacuoles can be identified. The first consists of large spherical bodies which contain a uniformly granular material of either a light or medium electron density (Figure 13). A few of these bodies appear to have the same consis-

tency as that of the red blood cells seen in the maternal blood spaces (Figure 19). It might be suggested that these vacuoles contain phagocytized erythrocytes in various stages of disintegration. The second type of vacuole is much smaller and contains whorled myelin-like figures and/or small elements of varying electron density. (Figures 8, 16 and 20). These vacuoles may represent late stages in the degeneration of mitochondria. An occasional multivesicular body is seen in the cells of the outer layer. These complex bodies contain small vesicles of considerable electron density and may well represent lysosome-like bodies (Figures 11 and 20). Fine filaments are commonly found in the cells of both the inner and outer layers of trophoblast. Generally, those occurring at the cell periphery are in association with the intracellular surface of desmosomes and course at slight angles to the surface as long slender groups (Figures 12, 14 and 15). The filaments found deeper in the cytoplasm usually occur as bundles which follow no one specific course through the cell (Figure 11).

2. Vascular trophoblast

Only in one instance on the 12th day were fetal vessels from the allantois found to have penetrated the cords of epitheliod trophoblast. Here well vascularized trophoblastic lamellae of the hemochorial labyrinthine type are formed (Figure 21). Such trophoblastic lamellae are composed of at least four discrete cytoplasmic elements which are interposed between maternal and fetal blood spaces. Together they form the labyrinthine barrier. In order to distinguish these layers from those of the avascular cords of epithelioid trophoblast, they will be referred to, from maternal blood sinus inward, as trophoblast I (T I), trophoblast II (T II), trophoblast III (T III)

and fetal endothelium (endo). In addition, the limiting membranes of each cell layer will be divided into a fetal surface (that facing fetal blood) and a maternal surface (that facing maternal blood).

Trophoblast I is a relatively thin cellular layer which extends pleomorphic evaginations of its outer plasma membrane into the maternal blood sinuses. The cytoplasm of this layer is particularly rich in RNP granules and membrane bound vesicles containing various amounts of electron dense material. Occasionally these vesicles are seen either in a close relationship with surface membranes or passing from the cytoplasm into the bases of outer surface projections which have terminal bulbous enlargements. Whether these vesicles represent absorption or secretory vacuoles cannot be determined. The apposing surface membranes of T I and T II, which are relatively free of evaginations and infoldings, are usually nonparallel except at intercellular attachments where they become contiguous.

Trophoblast II is a much thicker layer and contains an abundance of vacuoles and vesicles. Although it is difficult to trace their origin, most of them represent endoplasmic reticulum, microvesicular profiles and/or micropinocytotic vesicles. The common border of T II and T III is markedly different from that seen between T I and T II in that an extremely close apposition exists between the two surfaces throughout their entire length. This apposition is characterized by small tight junctions (zonula occludens) and intermediate junctions (zonula adherens). These intercellular attachment devices are more distinguishable as gestation advances and, therefore, will be considered again at a later stage.

Trophoblast III, except for the occurrence of free lipid droplets, resembles T II. Other cytoplasmic components of this layer include

rosettes of RNP granules, golgi membranes and smooth surfaced vesicles. As in T II, these vesicles may represent smooth endoplasmic reticulum, golgi microvesicular profiles and/or evidence of micropinocytosis. Very little rough endoplasmic reticulum is evident in the three layers of trophoblast. The fetal limiting membrane of T III is frequently infolded and fronts on an often ill-defined basement membrane which separates this layer from fetal endothelium. The fetal capillary endothelium is a relatively thin layer except in regions of its nuclei. The inner surface of this layer bordering the fetal blood space also has pseudopod-like projections with terminal bulbous enlargements which contain small vesicles and granular material. The endothelial cytoplasm shows little evidence of micropinocytotic activity. On the other hand, rough endoplasmic reticulum is far more abundant than in the three layers of trophoblast.

Cytochemistry

1. Avascular trophoblast

Although the final reaction product resulting from the hydrolysis of ATP, ADP and AMP is all deposited at the same fine structural sites to be described, a more intense reaction is seen with ATP. After incubations with these substrates, small deposits of lead phosphate are seen on the outer surface membranes of both layers of trophoblast cells. In all cases, the final product appears most abundant on membranes bordering intercellular spaces.

In the instance where ATP is used as substrate, the precipitate occurs as either individual granules or clusters of granules which are irregularly spaced along the plasma membrane and its evaginations (Figures 5 and 10). Such activity is sparse on the surfaces bordering

the maternal blood spaces. On the other hand, the granular material and the membranes of the "free" floating vesicular profiles found within maternal blood sinuses and intercellular spaces show a considerable amount of final product (Figures 13 and 19). In instances where the granular material of the maternal blood sinus is in close contact with the bordering trophoblast cells, the final product is rarely found (Figure 15).

When ADP is used as substrate, less final product is deposited. That which does occur is found sparsely along the surface membrane bounding the intercellular spaces (Figures 16 and 17). As is the case with ATP, final product is also found associated with the intercellular contents (Figure 16). Activity is only sparingly found along the plasma membranes bordering the maternal blood sinuses (Figures 8, 16 and 17).

When AMP is used as substrate, considerably more activity occurs than with ADP, but less than with ATP. The final hydrolysis products of AMP occur in a beaded fashion along the surface membranes of the inner layer of trophoblast cells which border wide intercellular spaces (Figure 6). When the intercellular space between adjacent inner cells is extremely narrow, activity is sparse. (This phenomena may be due to diffusion problems which will be considered later in the discussion section.) Relatively little enzymatic activity occurs on the surfaces of the outer cell layer (Figures 6, 11 and 12).

In considering all three substrates, the only final product found within the cytoplasm is seen in an occasional caveola. This presents additional evidence for the small amount of pinocytotic activity observed on the 12th day of gestation. An additional

observation on the 12th day is that the limiting membranes of maternal blood cells are coated with the final reaction product resulting from the hydrolysis of all three substrates (Figures 10 and 14).

2. Vascular trophoblast

Unfortunately, tissue sections showing enzymatic activity in the 12 day placental labyrinth were not found.

Placental Labyrinth of the 14th Day

Ultrastructure

Although the constituents of the 14 day labyrinthine barrier are seen to be similar to their counterparts at 12 days, an increase in complexity of the three trophoblast layers is evident. Generally, the cytoplasm of trophoblast I appears more attenuated than in the previous stage, and shows for the first time distinct pores or fenestrations which are closed by a thin diaphragm of amorphous material (Figures 22 and 23). The outer plasma membrane of this layer is relatively smooth and has few cytoplasmic projections except in regions where cells bordering the maternal blood simuses are brought into close apposition (Figures 22 and 24). Here, the apposing surfaces extend numerous irregular microvilli which appear to interdigitate and thus break up maternal blood spaces into smaller channels (Figure 24). In addition to cytoplasmic extensions, the inner plasma membrane of trophoblast I has infoldings. These surface projections and infoldings loosely interdigitate with those of the outer surface of adjacent trophoblast II cells (Figure 25).

The cytoplasm of trophoblast II, which shows the greatest variation in thickness, is pervaded with numerous rosettes of RNP granules, mitochondria and smooth membrane bound vesicular profiles (Figure 22). Since most of these vesicles have a characteristically dense rim with an

electron transparent center, they are interpreted as caveolae, (Figure 25), pinocytotic vesicles and sections cut through tubular infoldings rather than golgi vesicular profiles. The common border between T II and T III exhibits little change over the preceding stage except that now the junction between the two layers forms an irregular series of undulations with secondary interdigitations superimposed (Figures 22 and 23). Attachments between these two layers still appear as small localized thickenings that lack the intercellular contact layer of typical desmosomes (Figure 22).

Trophoblast III closely resembles T II in thickness, but has fewer vesicular profiles in its cytoplasm (Figure 23). The contour of its inner border which fronts on a basement membrane is less smooth and exhibits greater numbers of surface projections and infoldings (Figures 22 and 23). Occasionally this basement membrane extends into the infoldings formed by surface projections, but is most often identified with fetal endothelium. In fact, wherever fetal endothelium is identified, a supporting basement membrane separates it from the overlying trophoblast (Figures 22, 23 and 25). For the most part, the endothelium remains relatively thick as in the preceding stage (Figures 23 and 25). However, a few cells do appear reduced in width (Figure 22). Such cells exhibit a paucity of cytoplasmic organelles and minimal pinocytotic activity (Figures 22 and 23).

Cytochemistry

Cytochemical observations of the 14th day placental labyrinth reveal that the hydrolysis products of the three nucleotide phosphates used as substrates occur at similar fine structural sites, but at slightly different intensities (Figures 22-25). When ATP is used as

substrate, discrete granules of lead phosphate are primarily found on the maternal surface membrane of trophoblast II (Figure 25). To a much lesser extent, final product is also noted on the fetal and maternal surface membranes of trophoblast I (Figure 25). Here there appears to be no direct relationship between the sites of localization and surface modifications such as evaginations and invaginations. However, in trophoblast II more activity is found where its plasma membrane forms numerous evaginations and tubuler infoldings (Figure 25). Within the cytoplasm of T II moderate sized vesicles are seen which contain deposits of final reaction product (Figure 25). Although many of these vesicles may be continuous with the outer surface of T II, those occurring near the inner border have probably separated from surface infoldings as caveolae. In no other instance is final reaction product deposited within the cytoplasm of this layer. The inner surface of T II as well as T III and the fetal endothelium are free of enzymatic activity (Figure 25).

When ADP is used as substrate, less activity occurs than with ATP, but the distribution of final product is seen at the same fine structural sites (Figures 22 and 23). On the other hand, when AMP is used as substrate, final reaction product is limited to the outer surface membrane of trophoblast I (Figure 24). In areas where trophoblast I cells from opposite sides of a maternal blood space are closely apposed, final reaction product is particularly abundant on the outer surface membranes and their numerous microvilli (Figure 24). In addition, smaller precipitates of lead phosphate are seen where accumulations of amorphous material of moderate electron density occur in the intercellular spaces between T I and T II (Figure 24). Here activity is local-

ized throughout the amorphous material and not with bordering plasma membranes. Whether this localization represents non-specific staining by lead ions (metalophilia) or true enzymatic activity is uncertain. However, no such staining is found in control preparations. Such staining of amorphous material is more frequently seen at 22 days of gestation and will be considered then in greater detail.

As on the 12th day, the plasma membranes of maternal blood cells display a dense coat of final reaction product resulting from the hydrolysis of all three nucleotide phosphate substrates (Figures 22, 23 and 25). On the other hand, fetal blood elements exhibit no activity.

Placental Labyrinth of the 18th Day

Ultrastructure

By the 18th day of gestation all remaining cords of undifferentiated epitheliod trophoblast have been vascularized. Thus the placental labyrinth has reached its greatest development. For the most part, the layers of trophoblast appear as at 14 days (Figures 28, 29, 30, 32 and 34). Trophoblast I is highly attenuated with its greatest depth across the region occupied by nuclei (Figures 26 and 27). Here the perinuclear cytoplasm is rich in golgi elements, RNP granules and vesicular profiles of RER which are filled with a granular material of medium electron density (Figures 26 and 27). Occasionally the contents of such RER profiles appear to be released into the maternal blood space as "micro-apocrine secretions" (Figure 27).

A slight increase in the numbers of microvillus-like projections are seen on the outer surface of T I (Figures 28 and 29). In the thicker regions of this layer, trophoblast cells from the opposite sides of the maternal blood space are frequently closely apposed. When they

meet, typical desmosomal attachments are seen (Figure 26). However, in the thinner regions of T I, adjacent cells are attached by tight junctions (zonula occludens) (Figures 30 and 32). Occasionally the intercellular space between T I and T II is confluent with the maternal blood space through openings which occur between adjacent T I cells. These openings also allow terminal bulbous enlargements of T II to extend into the maternal blood space (Figure 33). Although the extent of interdigitation between the processes of T I and T II has not appreciably increased by the 18th day, the outer limiting membrane of T II has become highly irregular with extensive evaginations and infoldings (Figures 28-32). It is commonly possible to trace these infoldings two-thirds or more of the way through the cell. It appears that many of these tubular infoldings become pinched off to form caveolae and vacuoles, but it is difficult to differentiate these from cross sections of tubules (Figures 32, 34 and 35). The thicker regions of T II are rich in cytoplasmic contents as they are in the preceding stage (Figure 34). Distinct desmosomes, although infrequent, are found between T I and T II (Figure 35).

By the 18th day of gestation, the common junction between T II and T III forms a more distinct series of undulations with secondary irregularities superimposed (Figure 32). The cellular attachments between these two layers, as mentioned earlier, consist of small tight and intermediate junctions. The former junction is characterized by the absence of an intercellular space and the investment of its intracellular aspect by a condensation of slightly dense parallel

fibrils (Figures 30 and 32). The latter junction is characertized by the presence of an extremely narrow intercellular space and conspicuous bands of dense fibrillar material in the adjacent cytoplasm (Figure 35). By the 18th day the inner limiting membrane of trophoblast III has also become more irregular with greater numbers of cytoplasmic processes and infoldings (Figures 29-32). Folds from this inner surface frequently extend near to infoldings on the outer undulating surface which gives T III a beaded appearance (Figure 32). The Trophoblast III appears thinner than T II, but also has numerous vesicular profiles and other cytoplasmic organelles. In addition to these structures, T III has numerous lipid inclusions which are infrequently seen in the other cell layers (Figures 28, 29 and 36).

One of the salient features which is first observed on this day is the appearance of extraembryonic connective tissue elements between the basement membrane fronting T III and the fetal endothelium (Figure 36). These elements consist mainly of stellate mesenchymal cells which are rich in cytoplasmic organelles and exhibit extensive outpocketings (blebbing) of their outer nuclear envelope (Figure 36). Such connective tissue elements are better described in later stages.

Probably the most striking changes seen over the preceding stage occur in the lining of the fetal allantoic vessels. Here the endothelial cells which rest on a continuous basement membrane become more attenuated with some areas reduced to a thin flange (Figures 28, 31 and 36). In these thinner regions pores or fenestrations are frequently seen (Figures 36 and 37). The interendothelial junctions are characterized

by liplike cytoplasmic flaps which extend into the capillary lumen (Figures 28, 33, 34 and 38). These flaps are attached by small tight junctions (Figures 34 and 38). When compared with the other three layers of trophoblast, the endothelial cells contain the largest amount of rough endoplasmic reticulum, but the least number of pinocytotic profiles (Figures 29, 30 and 39). However, evidence for pinocytotic activity is much greater than in the preceding two stages. Evidence for this activity occurs predominantly on the outer plasma membrane (Figures 34 and 38).

Cytochemistry

On the 18th day of gestation activity to adenosine nucleotide phosphates appears to be distributed identically with that seen in the previous stage, with the exception of activity to AMP which is now localized at the same sites as that of ATP and ADP (Figures 26-37 and 39). With ATP as substrate, activity is still predominantly deposited in relation to the plasma membrane lining the outer surface of T II and its tubular infoldings (Figures 30, 32 and 34). In many areas where the inner and outer surface membranes of T I and II are more closely apposed, dense clusters of lead phosphate fill the intercellular spaces (Figure 30). However, when the two membranes are divergent, activity appears associated with membranes as dense precipitates (Figures 30, 32 and 34). The activity on the limiting membranes of trophoblast I, as in the previous stage, is less than that seen on T II (Figures 32 and 34). Again, no final reaction product is found on the inner surface of T II or on the surface membranes of T III and fetal endothelium (Figures 30, 33 and 34).

When ADP is used as substrate, considerably more activity is seen than at the preceding stage. Its fine structural localization, however, appears the same. This localization is also consistent with that just described for the activity to ATP (Figures 26, 28, 29, 31 and 33).

The most striking cytochemical change observed on the 18th day is the distribution and intensity of the activity to AMP in various areas of the labyrinthine trophoblast. While activity to AMP is limited to the outer plasma membrane of T I on the 14th day, it now appears, in addition, on the surface membranes bordering the intercellular spaces between T I and II and in the tubular infoldings of T II (Figures 35, 36, 37 and 39). In some areas of the labyrinth, final reaction product occurs predominantly on the surface membranes of trophoblast I and is especially abundant on the outer plasma membrane bordering the maternal blood space (Figure 36). In other areas of trophoblast I, however, very little final reaction product is found in relation to its membranes (Figures 37 and 39). Ultrastructurally no apparent differences exist between these two areas.

Infrequently small amounts of activity to ADP and AMP are seen in the intercellular space between trophoblast II and III (Figures 29, 35 and 39), but never on the inner surface membranes of T III or on the limiting membranes of the fetal endothelium.

On the 18th day, as on all days of gestation, the plasma membranes of maternal blood cells display adenosine nucleotide phosphatase activity, whereas fetal blood cells are always negative (Figure 32).

Placental Labyrinth of the 22nd Day

Ultrastructure

At 22 days of gestation (term), trophoblast I is characterized by

being extremely attenuated except in regions where nuclei are located (Figures 40 and 41). As in the preceding stage, its cytoplasm is rich in free RNP granules, golgi microvesicular profiles and rough endoplasmic reticulum (Figures 40 and 41). Trophoblast II, which appears as the thickest layer of the labyrinthine barrier, exhibits little change. The extensive evaginations and infoldings described in the previous stage now occupy most of its width, thus reducing the thickness of the placenta barrier (Figures 42-45). These evaginations appear as long slender processes which frequently interdigitate with other similar processes, but less frequently with evaginations of T I (Figure 46). The tubular infoldings or pockets resulting from these evaginations are greatly dilated and are actively involved in pinocytosis as is evidenced by numerous vesicular caveolae which occur at their margins (Figure 40). Frequently a homogenous or fibrin-like material of moderate electron density is found lying within the interstices between T I and II (Figures 40 and 41). Although the presence of this material is unaccompanied by obvious evidence of cell deterioration, it is interpreted as the earliest stage of trophoblastic degeneration.

The thicker cytoplasmic regions of T II and T III exhibit numerous caveolae, vesicular profiles and organelles as in the preceding two stages (Figures 40 and 41). Large lipid droplets, however, are still limited to T III (Figure 42). Except in its perinuclear region, the effective width of T III is markedly reduced (Figures 47 and 48). This appears to be brought about both by an attenuation of its cytoplasm and by basal infoldings which now more closely approach its outer limiting surface (Figures 40 and 41). In all three trophoblast layers, mitochondria are seen in which the matrix and inner membranes are of such a similar density that the cristae are only discerned with difficulty

(Figures 40, 41, 47 and 48). Therefore, the mitochondria are easily confused with other opaque bodies.

By the 22nd day of gestation the extraembryonic connective tissue elements, first described on the 18th day, are commonly found intervening between the basement membrane fronting T III and the fetal endothelium. These elements occur in spaces of varying widths and consist primarily of mesenchymal cells and collagen and reticular fibrils (Figures 43-48). In areas between adjacent allantoic capillaries, these spaces are particularly wide and contain greater numbers of connective tissue cells and fibrils (Figures 43-46). However, in regions directly between T III and the fetal endothelium, usually not more than a single connective tissue cell with associated fibrils is found (Figures 47 and 48). As mentioned on the 18th day, the mesenchymal cells are of a flattened stellate nature and contain numerous strands of rough endoplasmic reticulum, free RNP granules, microvesicular profiles and other cytoplasmic organelles. Evidence of active pinocytosis is also seen. The nuclei of these cells frequently exhibit large outfoldings of their outer envelope which contain a flocculant material of medium electron density (Figures 43, 44 and 46). The endothelium on the 22nd day, as on the previous, is greatly attenuated and exhibits a few irregular microvilli which extend from its inner surface into the capillary lumen (Figures 42-45). In addition to liplike cytoplasmic flaps and pore areas, numerous pinocytotic vesicles are seen.

Cytochemistry

At 22 days of gestation, the three nucleotide phosphate substrates (ATP, ADP and AMP) appear to be equally well hydrolyzed with their final reaction product being deposited at the same fine structural sites as on

the 18th day (Figures 40-43). Generally on this day, a more intense and equal distribution of activity to all substrates is seen related to the limiting membranes of trophoblast I and II. However, in the thicker regions of trophoblast I, only occasional deposits of final product are seen (Figures 40 and 41). In the intercellular space between trophoblast I and II and in the infoldings of T I where frequent accumulations of fibrin-like material are found, precipitates of final reaction product of varying diameters appear distributed throughout the fibrin-like material and less related to the bordering plasma membranes (Figures 40 and 41).

Placental Labyrinth of the 25th Day

Ultrastructure

1. Normal trophoblast

Between the 12th and 22nd days of gestation, the rat placental labyrinth only occasionally exhibits alterations which might be interpreted as degenerative changes. However, when pregnancy in the rat is extended three days beyond the time of normal parturition, certain areas of the trophoblast show a complete spectrum of internal degenerative changes. On the other hand, adjacent regions show fewer degenerative processes and occasionally exhibit only slight changes over that of 22 days. Therefore, as a matter of convenience of description, an account of these areas showing the least amount of change will be given first, followed by a description of regions showing greater degenerative changes.

In the more normal appearing areas of the labyrinth, trophoblast I has regular thick and thin regions as in previous stages (Figures 49 and 50). The cytoplasm extending across the thin regions is quite

attenuated and often exhibits pores (Figure 50), short irregular projections and caveolae which are frequently seen to coalesce to form larger vesicles and vacuoles (Figures 51 and 52). The caveolae occur predominantly on the outer surface of trophoblast I where they are most often located near the bases of cytoplasmic projections (Figures 50-52). In the thicker regions of T I, cytoplasmic projections and caveolae are less frequent. However, numerous mitochondria, granular endoplasmic reticulum, free ribosomes and golgi elements with associated microvesicular profiles are abundant as described in preceding stages (Figure 49). The cisternae of the granular endoplasmic reticulum in these thicker areas frequently appear distended and contain a granular to fibrillar material of moderate electron density (Figure 53).

On the 25th day, the accumulation of moderately dense fibrinous-like material first described on the 22nd day of gestation not only occurs in the intercellular spaces between T I and T II, but on their cytoplasmic borders and infoldings (Figures 51 and 52).

Trophoblasts II and III appear much thinner at this stage, which in many areas effectively reduces the overall thickness of the placental barrier to not more than two or three microns (Figure 50). However, in other areas, due to an increased number of connective tissue cells found intervening between T III and the fetal endothelium, the placental barrier appears much thicker than at 22 days (Figure 51). Scattered throughout the cytoplasm of T II and T III are numerous vesicles and tubular profiles, many of which contain a granular material of medium electron density (Figures 49 and 54). The larger profiles have electron transparent centers, but are

coated with a granular material which resembles that found within the intercellular spaces and, therefore, probably represent caveolae or tubular infoldings of plasma membranes. In addition to these vesicles and tubular profiles, larger oval structures resembling degenerating mitochondria are seen (Figures 52 and 54). The irregular and deeply penetrating folds of the inner plasma membrane of T III noted earlier, now form the perimeter of large distended spaces and extend close to the basement membrane of the fetal endothelium as pedicle-like processes (Figure 49). The distended spaces within these folds contain finger-like projections from adjacent surfaces of T III and various amounts of a granular to fibrillar material which resembles the material surrounding fetal mesenchymal elements.

At this stage, relative to the preceding, greater numbers of connective tissue cells are found directly between T III and the fetal endothelium (Figure 51). These cells are surrounded by collagen, reticular and elastic fibrils which are embedded in a matrix of granular material of moderate electron density. Some of the mesenchymal cells are quite large and exhibit a well differentiated cytoplasm which includes numerous mitochondria, tubular shaped, rough endoplasmic reticulum, rosettes of ribosomes, golgi microvesicular profiles and pinocytotic vesicles. The fetal endothelium exhibits a tremendous increase in pinocytotic activity which occurs predominantly on its outer surface (Figures 49-51). Pores, irregular projections and lip-like cytoplasmic flaps at inter-endothelial junctions are evident (Figure 50).

2. Degenerating trophoblast

In areas of the labyrinth where advanced degrees of degeneration are most apparent, usually not more than one of the three trophoblast layers exhibit extensive cytoplasmic deterioration (Figures 55-58). The cytoplasm of the remaining layers, however, does appear abnormally granular or fibrillar in texture and contains organelles in various stages of degeneration. Very frequently, the areas of more advanced degeneration correspond to the thicker regions of the particular layer involved (Figures 55-58). Although no direct correlation can be made between the extent of degeneration and the amount of fibrin deposited, there appears to be more cytoplasmic deterioration in areas where intercellular spaces and tubular infoldings of plasma membranes are occluded with fibrin (Figures 55 and 56). With this brief introduction, a more detailed description of the individual layers of the labyrinth follows.

In the thicker regions of trophoblast I, where degenerative changes are most apparent (Figure 55), the cytoplasm loses its homogenous texture and becomes abnormally clumped and vacuolated. Most individual organelles are indistinguishable except for skeins of rough endoplasmic reticulum, which appear irregular and with their membranes occasionally whorled in the form of myelin figures. The overall appearance of such cells is one characterizing foamy degeneration. In the thinner areas of trophoblast I, where less extensive degenerative changes are seen, the cytoplasm has a granular to fibrillar appearance and contains degenerating mitochondria (Figure 59). In addition to fragmented cristae, these mitochondria have either a centrally rarified matrix, or a matrix which is of such density that at first glance they appear as dense bodies (Figures 57 and 59).

In many cases there are fewer RNP granules associated with membranes of the endoplasmic reticulum (Figure 57). Although rough bundles and free strands of fine filaments are not apparent at this stage, they are particularly evident in areas of degeneration (Figure 56). Where fibrin is particularly abundant in the tubular infoldings of the outer plasma membranes of trophoblast II, the immediately surrounding cytoplasm appears scanty and highly disorganized (Figure 56). The mitochondria appear ballooned and contain a moderately dense granular matrix. Other small and intermediate sized oval profiles containing a dense granular material are seen, but do not differ morphologically from cross sections of tubular infoldings which contain fibrin. The fibrous material observed in this infolding of T II frequently exhibits a periodicity characteristic of fibrin (Figure 56). As in trophoblast I, the cytoplasm in the thinner regions of trophoblast II has a granular to fibrillar texture (Figures 57, 60 and 61) and contains distorted mitochondria. On the other hand, vaceolae are still apparent, which is interpreted as evidence of pinocytotic activity.

In many areas trophoblast III appears highly disorganized and vacuolated (Figures 57 and 58). What little cytoplasm does exist has a fibrillar texture and is primarily located near the inner and outer surface membranes (Figure 57). Mitochondria are characteristically fragmented as are other organelles. The mesenchymal cells intervening between trophoblast III and the fetal endothelium also exhibit degenerative changes (Figure 59). The mitochondria appear swollen and fragmented with vacuolated matrices (Figure 59). In these cells the cisternae of the rough endoplasmic reticulum which contain granular material of moderate electron density are slightly

dilated and often appear continuous with the fibrillar cytoplasm at the periphery of the cell. Occasionally the outer limiting membrane of these cells is continuous with short fibrils which extend into the extracellular space (Figure 59). The connective tissue space surrounding the mesenchymal cells is filled with either numerous parallel arrays of collagen and reticular fibrils or a dense fibrous mat (Figure 61). The basement membranes underlying trophoblast III and supporting the fetal endothelium appear within normal limits of width and are indistinguishable from those of 22 days (Figure 59 and 61). The fetal endothelium appears intact, but its cytoplasm also has a definite granular to fibrillar texture and exhibits degenerating mitochondria and a few pinocytotic vesicles (Figures 57, 58, 60 and 61).

Cytochemistry

Although enzymatic activities to the three nucleotide phosphate substrates can be determined at the same fine structural sites as seen in the previous stage, day 22, (Figure 59, 61 and 62), the final reaction product obtained on the 25th day of gestation exhibits less association with surface membranes and is more often deposited in intercellular accumulations of fibrin. Also, in regions of trophoblast I which show extensive degeneration, the hydrolysis product of all three substrates used is diffusely scattered throughout the cytoplasm (Figure 55), whereas similar areas of trophoblast II show little to no activity (Figure 56). When ATP is used as a substrate, intense activity occurs in the intercellular space between T I and T II where it is distributed within clumps of fibrin either as dense clusters or as fine granular deposits of lead phosphate (Figure 59). The outer surface membrane of

T I displays less activity than the surface membranes bordering the accumulations of fibrin which in either case is less than that seen on day 22. Frequently fine granular deposits of lead phosphate are seen within the cytoplasm of T I (Figure 59). Here no specific localization to organelles or degenerating profiles occurs. Similar fine granular deposits are also frequently observed in the basement membrane underlying trophoblast III.

With ADP as substrate, the final reaction product most often displays a pattern of localization similar to that with ATP (Figures 57, 60 and 61). However, random areas of trophoblast I occasionally exhibit more activity on their outer plasma membrane (Figure 58).

The least amount of enzyme activity on the 25th day occurs when AMP is used as substrate (Figure 62). Here, dense accumulations of final reaction product are seen related to fibrin, but only patchy deposits occur on the plasma membranes of T I and II (Figure 62). In control sections no metalophilia is seen in either fibrin deposits or in areas of focal degeneration (Figures 49, 50, 51, 52 and 54).

Visceral Yolk Sac of the 12th Day

Ultrastructure

The 12 day rat visceral yolk sac appears, when examined with the electron microscope, as a three layered structure. The surface epithelium is composed of a single layer of columnar cells, frequently of a pyramidal shape, which lie upon a narrow visceral basement membrane (Figures 4, 63 and 64). Immediately below this membrane is a connective tissue space in which endothelium-lined vitelline capillaries and mesenchymal cells are surrounded by a network of collagen and reticular fibrils (Figures 65-68). The inner surface of the visceral yolk sac

is formed by another continuous basement membrane (serosal) which is covered by a single layer of squamous mesothelial cells lining the exocelom (Figures 69 and 70). The apical or free border of the columnar epithelial cells is evaginated to form numerous tall and slender microvilli which are frequently branched and may end in terminal bulbous enlargements (Figures 71-73). The plasma membrane surrounding the microvilli as well as the cell surface has an extraneous coat with a furry or spike-like appearance (Figure 73). Between the bases of many microvilli, the plasma membrane is invaginated to form crypts or tubules which may branch and extend for various distances into the apical cytoplasm (Figures 71 and 74). Tubules parallel or diagonal to the cell surface suggest that these invaginations may also form a network of laterally intercommunicating canaliculi. The cytoplasm directly beneath the microvilli sometimes has a fibrillar texture similar to that referred to as the terminal web in the intestinal epithelium (Figures 72 and 73). This meshwork of fine filaments is also continuous with the microvillous projections and probably functions as a cytoskeleton.

The apical cytoplasm of the endodermal cells is filled with numerous small membrane bound vesicles which show considerable heterogeneity in size (0.1 - 0.5 u), content and electron density (Figures 71 and 77). Many of these vesicles represent either cross sections of the tubular invaginations or portions of variable size which have become pinched from their contact with the surface membrane to form pinocytotic vesicles. In the former case, the limiting membrane of the vesicles has a dark inner rim of spike-like material typical of that which coats the cell surface. The center of the vesicle is usually electron transparent (Figures 71, 73 and 74).

In the latter case, the matrix of the pinocytotic vesicles contains varying amounts of fine granular material which makes them difficult to distinguish from other small electron dense vesicles (Figures 71-77). Because of the nature of large "absorption vacuoles" to be described in the supranuclear cytoplasm, it is likely that many of these pinocytotic vesicles are involved in the transport of small absorbed fat particles to the larger vacuoles. Some of the other smooth surfaced vesicles (microbodies) may be interpreted as either golgi microvesicular profiles, which are found in abundance in the perinuclear region (Figure 63), or lysosome-like bodies. Occasionally aggregates of tubular or vesicular profiles merge to form larger vesicles surrounded by an often irregular and somewhat indistinct membrane (Figures 75 and 76). Their matrix appears as a finely granular material with varying amounts of electron density. Other small vesicles in the apical cytoplasm also coalesce; however, the membrane which comes to surround them is not completely closed so that the material in the vacuoles seems to merge with the surrounding cytoplasm (Figures 76 and 78). Here the impression is gained that ribosome rich cytoplasm is being engulfed.

The supranuclear cytoplasm also contains numerous spherical bodies which show great heterogeneity in content and range from 0.5 to 5 u in diameter (Figures 71-79). These bodies appear to be formed by several means, but are probably best distinguished from one another by their morphology. The first population to be described is represented by spherical bodies which contain either a finely granular material of considerable electron density or a uniformly floccular material with less electron density (Figures 71, 74, 76 and 77). Areas of dense particulate materials or degenerative profiles, however, are frequently found in both.

In either case the vacuoles are bound by a single but distinct membrane. The second population of vacuoles characteristically contains clusters of small lipid droplets which are in a complex association with both granular clumps of electron dense material and the irregular limiting membranes (Figures 71, 72 and 75-79). These "absorption vacuoles" vary in size and appear to gain in mass through the coalescence of similar vacuoles and small vesicular profiles from the apical cytoplasm. In addition to lipid clusters and coarse granular material, the larger vacuoles contain whorls of membranes in the form of myelin figures, circular profiles reminiscent of those described in the apical cytoplasm (pinocytotic vesicles) and open areas which are electron transparent (Figure 78). The exact relationships between the vesicles in the apical cytoplasm and the different vacuoles in the supranuclear cytoplasm are uncertain, but suggestive of progressive stages in either the breakdown of absorbed materials or the disposal of degenerating cytoplasmic organelles.

In addition to vacuoles and vesicles, the supranuclear cytoplasm has an abundance of ribosomes which occur singly or in rosettes and give the cytoplasm a granular appearance (Figures 76-79). The mitochondria are usually oval to elongated with their long axis frequently oriented parallel to the long axis of the cells. Some of the mitochondria are swollen and vesiculated, conditions which are usually interpreted as signs of progressive degeneration. Additional indications of degeneration are the fragmenting of cristae, focal rarifaction of the mitochondral matrix and subsequent whorling of inner membranes which produce a myelin figure appearance (Figures 72, 75 and 78). Sheets of rough surfaced endoplasmic reticulum are found scattered throughout the supra-

nuclear cytoplasm and appear to be oriented in the long axis of the cell, as are the mitochondria (Figure 63). They are moderately dilated and contain a granular material of medium electron density.

The nuclei of the visceral yolk sac endoderm are eccentrically located toward the base of the cells (Figures 63, 64, 65 and 68). Because of the irregular shape of the nuclei, many sections show both perpendicular and tangential cuts through its limiting envelope. The perpendicular sections show small dilitations between the inner and outer nuclear membranes, which are frequently interrupted by points of fusion (Figures 75, 77, 78 and 79). These points of fusion appear as nuclear pores in sections that are tangential to the nuclear envelope (Figures 71, 72 and 78). Occasionally small lipid inclusions are seen in the nucleoplasm (Figures 65, 77 and 80).

The perinuclear and basal cytoplasm contain numerous polysomes, ribosomes, granular endoplasmic reticulum, golgi-like microvesicular profiles and mitochondria (Figures 63, 64, 65 and 81). Large lipid droplets, which frequently indent the surface of the nucleus, are predominantly seen in the basal cytoplasm (Figures 64, 65, 69, 80 and 81). There, large lipid deposits appear to gain in size through the coalescence of smaller droplets (Figure 65). The outer surface of the lipid material appears to be in close association with periodically spaced rosettes of polyribosomes (Figure 81), the significance of which is not known.

The lateral surfaces of the visceral endodermal cells, which are closely apposed to those of similar adjoining cells, show several types of attachment. Near the apical surface, adjoining cells are attached by terminal bars, which seal off the yolk sac lumen from the intercellular spaces (Figures 72 and 75). The intracellular aspect of the plasma

membrane at these zones of adhesion are invested with a fibrillar material which is continuous with the terminal web. The mid-lateral cell surfaces have small finger-like projections which form simple to complex interdigitations (Figures 63, 64, 77 and 78). Such interdigitations are highly developed at the base of adjoining cells (Figures 64, 65 and 68). Desmosomes are infrequently found.

The basal cell surface has many complex infoldings and is actively involved in pinocytosis. This activity is indicated by the presence of small invaginations and microvesicular profiles within the basal cytoplasm (Figure 81).

The basement membrane of the visceral yolk sac epithelium is a thin homogeneous reticular structure which follows the contour of the basal cell surface and maintains a close and direct apposition to it. This membrane separates the visceral cells from the underlying connective tissue space (Figures 69 and 81). The connective tissue of this space is of the areolar type and the formed elements observed in it are mesenchymal cells, and collagen and reticular fibrils. The mesenchymal cells, which are elongated with finely branched cell processes, are most abundant in villous areas where they are in close association with the vitelline capillaries (Figures 67 and 70). The cytoplasm of these cells is rich in rough surfaced endoplasmic reticulum and rosettes of free ribosomes (Figures 67 and 70). Lipid droplets and mitochondria are also common components. The greatly dilated cisternae of the rough endoplasmic reticulum are probable sites of the synthesis of the precursors to the collagen fibrils which run in various directions through the connective tissue space.

The endothelium of the vitelline capillaries is usually quite thin, except in areas where nuclei and other cytoplasmic organelles

are found (Figure 66). In the thinner parts of the cytoplasm, fenestrations occur which are individually bridged by a thin diaphragm (Figure 67). Other areas of the cytoplasm become so attenuated that only parallel plasma membranes are distinguishable (Figure 67).

The mesothelium of the exocoelomic cavity is separated from the connective tissue space by a thin, homogeneous and often discontinuous serosal basement membrane (Figures 67, 69 and 70). This serous membrane is composed of a single layer of flattened mesothelial cells with centrally placed round to oval nuclei which frequently show lipid inclusions (Figures 66 and 70). Its cytoplasm, like that of the mesenchymal elements of the connective tissue space, is rich in organelles. The rough endoplasmic reticulum consists of intercommunicating stacks of paired membranes which are oriented parallel to the long axis of the cells (Figures 66, 69 and 70). Free rosettes of ribosomes, mitochondria, lysosome-like bodies and lipid droplets are dispersed between the layers of endoplasmic reticulum whose cisternae are dilatated with a granular material of medium electron density (Figures 66, 69 and 70). The surface membranes of the mesothelial cells are relatively smooth except for occasional pinocytotic invaginations and pseudopod-like evaginations. These evaginations occur predominantly near intercellular junctions and extend into the exocoelomic cavity (Figures 67, 69 and 70). The mesothelial cells are held together by either tight junctions, desmosomes or interdigitating finger-like projections (Figures 67, 69 and 70).

Cytochemistry

The lead phosphate resulting from the enzymatic hydrolysis of the substrate ATP is clearly demonstrated in the 12 day visceral yolk sac as intensely electron dense granular deposits. No enzyme activity is

seen with either adenosine mono- or diphosphates (Figures 67, 69, 71, 74 and 81). The most reactive site that survives fixation in glutaraldehyde is at the luminal surface of the visceral endodermal cells. Here, a dense deposition of final product, several hundred angstroms thick, occurs in a beaded fashion along the surface membranes of the microvilli (Figures 63, 64, 72, 75 and 76). The invaginated crypts or tubules whose plasma membranes are continuous with that of the luminal surface, are either completely filled or coated with a granular layer of final reaction product (Figures 72 and 75). Many of the membrane bound vesicles in the apical cytoplasm (pinocytotic vesicles) show activity related to the inner surface of their limiting membrane and/or to their contents. The final reaction product of these vesicles found deeper in the apical cytoplasm appears spotty. Occasionally such vesicles are seen to be in close relation with the large lipid containing "absorption vacuoles" (Figure 72). The cytoplasmic contents of the nuclear regions show no activity (Figures 68 and 75-79).

The lateral surfaces of the visceral endodermal cells also exhibit deposits of the final product (Figures 63, 72, 75-78). The specialized zones of adhesion such as the terminal bar, however, contain no enzymatic activity (Figure 77). On the other hand, relatively large, round or oval accumulations of final product fill the intercellular spaces between the specialized interdigitating folds of adjacent cell surfaces (Figures 63 and 68). Such activity also occurs in the complex infoldings of the basal cell surface (Figure 65). In all cases, final reaction product is localized in the visceral basement membrane (Figures 63, 65, 66 and 68). Because this activity consists of finer granular deposits of lead phosphate than that which is usually seen associated with cell surfaces,

it is not clear whether this type of localization represents true enzyme activity within the basement membrane itself or a diffusion of reaction product formed on basal surface membranes of the endodermal cells with which it is in close contact.

Final reaction product is sparsely distributed in the connective tissue space (Figure 65). Some of this finely diffuse activity appears to have been absorbed non-specifically to the surface membranes of a few mesenchymal elements (Figure 66). A more discrete reaction, however, is prominent where these cells are in contact with other cells (Figure 66). The fenestrated endothelium of the vitelline capillaries is enzymatically unreactive as is its basement membrane except for certain areas where they are in close apposition to the visceral basement membrane (Figures 65 and 66). Here again, this localization probably represents diffusion of final reaction product. No activity is seen in the serosal basement membrane (Figure 70). In control studies where visceral yolk sacs are incubated in equimolar concentrations of B glycerophosphate or substrate free media, no reaction is seen. Visceral yolk sacs prefixed for 10 minutes in 2% osmium textroxide and subsequently incubated in a substrate complete medium also show no reaction product.

Visceral Yolk Sac of the 14th Day

Ultrastructure

On the 14th day of gestation, the visceral yolk sac appears much as it does on the 12th (Figure 82). In the apical cytoplasm only subtle changes are apparent. Included among these are a more evident terminal web, located beneath the microvilli, and a slight increase in the numbers of surface invaginations (Figures 83 and 85). Many of these invaginations

are seen in longitudinal section which more readily demonstrates their network of intercommunicating canaliculi. Below this, membrane bound pinocytotic vesicles and lysosome-like bodies of varying size and electron density are seen (Figure 84). Some of the smaller vesicles have an extremely dense content which is surrounded by a less electron dense zone. Such vesicles are typical of those seen transporting small absorbed fat particles through the cytoplasm of intestinal epithelial cells (Figure 84).

The supranuclear cytoplasm contains numerous spherical bodies or vesicles which are similar to those described as the first population in the supranuclear cytoplasm of the 12 day endodermal cells (Figures 86 and 87). The second population of "absorption vacuoles" which contained clusters of lipid droplets are no longer present. Medium sized vacuoles containing clumped granular material, myelin figures and electron optically empty areas are present, however (Figure 85). At this stage, relative to that of 12 days, the perinuclear cytoplasm appears to contain more rough endoplasmic reticulum and mitochondria (Figures 82 and 86). Also, fewer golgi microvesicular profiles and nuclear lipid inclusions are seen. On the other hand, nuclei are still frequently indented by lipid droplets which predominantly occupy the infra-nuclear cytoplasm (Figure 88). The lateral cell surfaces remain closely apposed except for an occasional dilatation.

By this day, the connective tissue space has increased in width through an increase in both collagen fibrils and mesenchymal cells. The endothelial lining of the vitelline capillaries shows evidence of pinocytotic activity (Figures 89 and 90). This activity is predominantly seen on the luminal side of the endothelial cells. It is dif-

ficult to say, however, in which direction these vesicles are moving. Finally, the serosal basement membrane is indistinct (Figure 90).

Cytochemistry

At 14 days of gestation, the visceral yolk sac possesses enzymes capable of hydrolyzing both adenosine di- and triphosphates. However, under identical conditions, the visceral cells demonstrate much greater hydrolytic capacity with ATP than with ADP (Figures 84 and 91). No activity is demonstrated with AMP or B glycerophosphate (Figure 92).

When ATP is used as substrate, the final reaction product occurs at the same fine structural localizations as it did on the 12th day (Figures 82-88). The deposits on the apical surface membrane, however, appear as a dense continuous layer of lead phosphate rather than as dense beads (Figures 83 and 84). Similarly, a more continuous deposition of final product fills the intercellular spaces where adjoining cells are closely apposed or interdigitated (Figures 85-87). It should be noted that many of the pinocytotic vesicles and invaginations of the apical cytoplasm show enzymatic reactions which make them difficult to distinguish from vesicles containing electron dense materials other than final reaction product (Figure 84). As on the 12th day, the supra-, peri-, and infranuclear cytoplasm contain no reactive sites for these substrates. The activity located on the basal surface membrane and its infoldings appears as large oval precipitates (Figure 88). However, those deposits in the visceral basement membrane are much smaller and diffusely localized (Figure 88). Some lead deposits are found in that portion of the connective tissue space underlying the visceral basement membrane (Figure 88). Finally, no reaction occurs either in the serosal basement membrane or where cells of the mesothelium are in contact with

each other (Figure 89).

When ADP is used as substrate, a reaction of moderate intensity occurs which is limited in distribution to microvilli, tubular invaginations and pinocytotic vesicles of the apical cytoplasm (Figure 91). Here, the final product occurs in a beaded fashion, interrupted by unreactive sites, along the outer surface of the plasma membrane; somewhat less or no staining occurs in the intercellular spaces.

Visceral Yolk Sac of the 18th Day

Ultrastructure

By the 18th day of gestation, the epithelial cells of the visceral yolk sac no longer appear columnar, but are tall cuboidal cells with dome shaped apical surfaces (Figure 93). The microvillous projections of this surface also undergo a decrease in height and appear more blunt and often pleomorphic (Figure 94). In the apical cytoplasm directly below the clear zone of the terminal web, numerous small vesicular profiles of varying electron density and tubular invaginations of the surface membrane are seen as in the previous stages (Figures 93, 94 and 95).

The supranuclear as well as the perinuclear cytoplasm also exhibit little change in the number and distribution of mitochondria, rough endoplasmic reticulum and golgi microvesicular profiles. Greater numbers of dense vesicles of variable size are found (Figure 96). These vesicles appear progressively larger from the apical to the perinuclear region. Other vesicles in the supranuclear cytoplasm, which frequently have an ill-defined and discontinuous limiting membrane, resemble those of the first population described in the 12 and 14 day visceral endoderm cells (Figures 93, 94, 95 and 97).

Although lipid inclusions are occasionally found within the basally situated nuclei, the surrounding basal cytoplasm appears to be free of lipid droplets (Figures 93, 95 and 98).

The lateral intercellular spaces between adjoining endodermal cells, which on the 14th day consist of only occasional dilatations between the closely apposed surface membranes, on the 18th day more frequently appear as large dilatations which are interrupted by finger-like projections (Figures 93 and 98). These cytoplasmic projections extend from apposing cell surfaces into the intercellular spaces where they tend to overlap one another forming irregular or cup shaped spaces. Such spaces are less well developed toward the apical surface of the cells (Figure 95). Here, the adjoining plasma membranes are attached by junctional complexes which seal off the yolk sac cavity from the intercellular space of the visceral epithelium. Additional desmosomes are often seen between overlapping cytoplasmic extensions along the mid-lateral cell surface. Occasionally accumulations of granular material and vesicular profiles of moderate electron density are seen in the intercellular spaces (Figure 93). It cannot be determined, however, if these profiles are free of cellular attachments or are cross sections of adjacent cytoplasmic projections.

In many neighboring endodermal cells, the lateral cell surfaces are still as closely apposed as those observed on the 14th day (Figures 97 and 99). The basal cell surface and the underlying visceral basement membrane exhibit no change over the preceding stage, but an increase in the amount of intercellular fibrils is apparent in the connective tissue space.

The cytoplasm of the mesothelial cells on the 18th day appear to

be dominated by rosettes of ribosomes and granular endoplasmic reticulum whose dilated cisternae contain granular material of moderate electron density (Figure 100). Other cytoplasmic organelles and lipid droplets are dispersed between the layers of endoplasmic reticulum. The basal surface membranes of the mesothelial cells are frequently associated with a fine feltwork of moderately dense material which in turn is closely interwoven with fibrils of the connective tissue space. In areas where this fibrous material is particularly abundant, cell boundaries as well as the serosal basement membrane are ill-defined and sometimes barely discernable (Figure 100). The amniotic surface membranes of the mesothelium exhibit little change over that of 14 days except for a slight increase in the number of cytoplasmic evaginations which project into the exocoelomic cavity.

Cytochemistry

Although enzymatic activity in the 18 day visceral yolk sac hydrolyzes both adenosine di- and triphosphates as on the 14th day of gestation, the fine structural localization and intensity of the reactions differ. At this stage, the final reaction product resulting from enzymatic hydrolysis of ATP is found on the apical and lateral plasma membranes of the endodermal cells as in the previous stage, but not on the basal surface membranes (Figures 93, 95 and 98). In some of the endodermal cells, the lead phosphate deposits on the apical surface and its microvillous projections are less intense than others (Figures 93 and 95). However, in both cases the apical cytoplasm exhibits the same moderate amount of activity related to the inner membranes and/or contents of tubular surface invaginations and pinocytotic vesicles.

Occasionally a few of the larger and moderately electron dense

vesicles also display deposits of lead phosphate (Figure 93).

ATPase activity on the lateral surface membranes, which at this stage are either closely apposed or separated by large intercellular spaces, is less intense than on the apical surface (Figure 98). Frequently the lateral surfaces of adjoining endodermal cells exhibit no enzymatic activity for this substrate (Figures 93 and 95). There appears, however, to be no correlation between the degree of association of adjacent lateral surfaces and the presence or absence of enzymatic activity.

The basal surface of the endodermal cells, as mentioned earlier, is unreactive (Figures 93 and 98). Although fine deposits of lead phosphate do occur in the visceral basement membrane, no activity is found associated with the connective tissue elements or the endothelium of the vitelline capillaries (Figures 93 and 98).

The serosal basement membrane and the outer and lateral plasma membranes of the mesothelium are unreactive as in the previous stage. At this stage, however, clusters of lead phosphate granules are found along the inner plasma membranes (Figure 100). These deposits appear to be equally distributed on smooth surface and those surfaces with numerous cytoplasmic projections.

When ADP is used as substrate, fewer deposits of lead phosphate are found on the apical surface and its tubular invaginations than on the 14th day (Figures 97 and 99). At this stage, slight activity is still apparent in the intercellular spaces where adjoining lateral plasma membranes are closely apposed (Figures 97 and 99).

Visceral Yolk Sac of the 22nd Day

Ultrastructure

At 22 days of gestation, the endodermal cells of the visceral yolk sac epithelium appear much lower than on the 18th day (Figures 101 and 102). The microvilli on the apical surface of these cells appear uniformly short and less branched. The apical system of tubular invaginations, which are surrounded by numerous small dense vesicles, are particularly evident at this stage and are identified by a characteristic dense outer rim surrounding a less dense central core (Figures 103, 104 and 105). Frequently cross sections of microvilli are seen within these central cores which indicate that many tubular invaginations encircle the bases of microvilli (Figure 103). In other instances, longitudinal sections of the tubular system, which are oriented at right angles to the cell surface, are seen to either terminate in bulbous enlargements and/or to be continuous with other vesicular invaginations (Figure 105). As mentioned earlier, this pattern is highly suggestive of a canalicular system in the apical cytoplasm which is continuous with the outer cell surface.

The expanse of cytoplasm between the basally situated nuclei and the apical surface in most cells is pervaded with great numbers of vesicles and vacuoles ranging from .1 u to 4 or 5 u in diameter (Figures 106, 107 and 108). The smaller of these structures, which contain granular material of varying electron density, appear as those described in earlier stages (golgi microvesicular profiles or vesicles pinched off from surface invaginations) (Figures 103, 104, 107 and 109). However, the larger vesicles and vacuoles, in addition to having ill-defined and often discontinuous limiting membranes, exhibit a varying

content of dense vesicular profiles, myelin-like figures and electron translucent areas. These vacuoles have a definite residual body appearance (Figures 108, 110 and 111). It is in the electron translucent areas where the limiting membrane is particularly disrupted. A progressive series of stages showing the breakdown of large vacuoles can be traced to the stage where the entire vacuolar content is freely exposed to the cytoplasm (Figures 107-111). Similar appearing areas, which are also free of limiting membranes, are found in the basal cytoplasm (Figures 112-114). Since this region is relatively free of large vacuoles, these areas may represent accumulations of glycogen rather than disintegrated vacuoles. In some of the endoderm calls, even the small vesicular profiles exhibit electron translucent areas, but usually not dense profiles and myelin-like figures (Figures 101 and 105). Some of the intermediate sized vacuoles, which have a fairly homogenous matrix of moderately electron dense material, have an irregular limiting membrane characteristic of a structure which is gaining in mass through the coalescence of numerous small vesicles (Figures 105, 107 and 109).

In those cells which exhibit a greater number of large and intermediate sized vesicles and vacuoles, the cytoplasmic organelles, although scattered between the vacuoles, predominantly occur in the basal, lateral and perinuclear regions (Figures 105, 106, 108, 114 and 115). On the other hand, in cells where fewer vacuoles occur, the organelles are abundant in all regions of the cytoplasm (Figures 101, 102 and 116). This pattern of distribution closely parallels that seen on the 18th day except that at this stage greater numbers of golgi microvesicular profiles are found in the peri- and supranuclear cytoplasm. In the

more apical region, the golgi profiles are still indistinguishable from small tubules and vesicles of the canalicular system (Figures 102, 108, 114 and 116).

The mitochondria on the 22nd day of gestation are either spherical or elongated and have long internal membranes which for the most part are intact and clearly discernable (Figures 102, 116 and 117). The granular endoplasmic reticulum appears as either paired membranes enclosing narrow elongated cisternae or as vesicular profiles (Figures 102, 112 and 116). In both instances, the cisternae contain granular material of moderate electron density.

No obvious signs of degeneration or aging are apparent in the cytoplasmic organelles in the 22 day placental labyrinth other than the general observation that mitochondria appear somewhat smaller than those seen in earlier stages of the visceral endoderm.

By the 22nd day of gestation, the large intercellular dilatations, which were first described on the 18th day, are more highly developed and extend from tight junctions at the apical surface down to the visceral basement membrane of all adjoining endodermal cells (Figures 106, 107, 114 and 115). In addition, greater amounts of a flocculant material are found within these intercellular spaces (Figures 113, 117 and 118).

The basal surface of the endodermal cells, like that of the lateral surface, has extensive infoldings and cytoplasmic evaginations which extend to the visceral basement membrane as pedicle-like foot processes (Figures 102, 115 and 118). Frequently wedges of cytoplasm, which also have surface evaginations and infoldings, intervene between the base of an adjoining cell and its underlying visceral basement membrane. Here

the two apposing cell surfaces loosely interdigitate (Figures 115 and 117).

Along the base of the endodermal cells, the visceral basement membrane approximates the contours of the plasma membrane and frequently extends into the basal infoldings (Figure 117). Whereas this membrane in previous stages appeared relatively thin, it is now thickened with frequent spaces which give it a lace-like appearance (Figures 112 and 117). Toward the underlying connective tissue space, the reticular fibrils of the basement membrane often merge with a feltwork of connective tissue fibrils which surround the mesenchymal cells (Figures 117 and 118). All of the fibrils appear to be infiltrated and coated by an amorphous matrix.

The mesenchymal cells within the connective tissue space are stellate and exhibit cytoplasmic organelles of which free ribosomes, granular endoplasmic reticulum and microvesicular profiles are most abundant (Figure 115). Wherever vitelline capillaries occur, these mesenchymal cells are found in close association with the vessels' supporting basement membrane (Figures 102, 112, 117 and 118). The endothelial cells lining the vitelline capillaries are highly attenuated and exhibit cytoplasmic fenestrations as well as cytoplasmic flaps which occur at interendothelial junctions (Figures 117 and 118).

The mesothelium and its serosal basement membrane exhibit little change over that of 18 days except for a slight increase in the number of microvilli on the inner surface of the mesothelium (Figure 101).

Cytochemistry

On the 22nd day of gestation, enzyme activity in the visceral yolk sac hydrolyzes not only adenosine di- and triphosphates, but also adenosine monophosphate. Of these substrates, the most intense reaction

is obtained with ATP, the final product of which is almost entirely limited to the luminal surface of the visceral epithelium (Figures 106, 107 and 111). Here the lead phosphate deposits appear more uniform than on the 18th day and occur as either a continuous coat or as closely spaced beads.

When ADP is used as substrate, a more intense reaction occurs than on the 18th day. The final product of this activity is confined to the same fine structural localizations as with ATP, but with much less intensity (Figures 103, 109 and 116). Additional deposits of lead phosphate are dispersed throughout accumulations of granular material which are occasionally found within the yolk sac cavity and/or uterine lumen. In areas where this material is particularly close to the visceral epithelium, activity on the microvillous projections appears scanty (Figures 104 and 107). However, no change occurs in the amount of activity present within pinocytotic vesicles and tubular invaginations (Figure 104).

The most striking enzymatic feature on the 22nd day is the appearance of activity toward AMP. Although this activity is dispersed in a somewhat spotty fashion, it has the same fine structural localizations in the endodermal cells as activity with the other two adenosine phosphate substrates (Figures 101, 102 and 105).

The cytoplasmic contents of the endodermal cells show no activity with the three substrates except for some reaction product confined to apically situated pinocytotic vesicles and tubular surface invaginations (Figures 103, 104, 105 and 107). Here the activity is related to the inner surface of their limiting membrane and/or to their contents as in earlier stages. The content of these vesicles and invaginations, which

is particularly well demonstrated in sections incubated with ADP, is identical with the granular material in the yolk sac cavity (Figure 104). This appearance is highly suggestive of movement of materials into the visceral endoderm.

The lateral surfaces of the endodermal cells, which at this stage all loosely interdigitate, show no deposits of final product proximal to the apical tight junction (Figures 102, 106, 107 and 114). Also, no enzyme activity occurs at the basal surface of these cells, or where intervening basal surfaces interdigitate (Figures 112, 115 and 118). On the other hand, the underlying visceral basement membrane, as in the earlier stages, contain some reaction product or metalophilia when incubated with adenosine di- and triphosphates (Figures 113, 115 and 117). At this stage, the lead phosphate deposits occur primarily on the reticular-like fibrils which often appear to be continuous with the fibrous elements of the connective tissue space. Other elements of this space, such as mesenchymal cells and vitelline vessels, display no activity (Figures 112, 115, 117 and 118).

Cytochemical observations of enzyme activity in the mesothelium and its supporting basement membrane are limited to reactions in which AMP is used as substrate. In such instances, final reaction product occurs only in the mesothelium where it is sparsely deposited between tightly apposed lateral cell surfaces and on microvillous projections of the inner cell surface (Figure 101).

Visceral Yolk Sac of the 25th Day

Ultrastructure

By the 25th day of gestation, the visceral yolk sac epithelium has undergone further reduction in width and now appears to consist of

squamous to low cuboidal endodermal cells which often overlap one another at their lateral margins (Figures 119 and 126). The microvilli on the apical surface of these cells are similar to those of the preceding stage except for occasional terminal bulbous enlargements which appear to coalesce while still attached to the microvilli (Figures 122 and 123). The uterine lumen and/or yolk sac cavity in regions of these enlargements is filled with a granular material of moderate electron density which is not unlike the content of the bulbous enlargements.

The cytoplasmic content of adjacent endodermal cells differs considerably at this stage. Generally fewer numbers of surface invaginations, vesicles and vacuoles are found (Figures 128-131). In some cells, however, large vesicles of varying electron density and content are so numerous that the cytoplasm and its organelles are crowded to the cell periphery (Figures 120 and 126). On the other hand, most cells exhibit a more even distribution of cytoplasmic organelles among which smaller vesicular profiles are scattered. Of course, intermediate stages are frequently seen.

The larger vesicular profiles in the endodermal cells appear to be in various stages of disintegration and contain dense myelin figures and electron translucent areas as described in the 22nd day visceral epithelium (Figures 122 and 127). A greater number of the smaller vesicular profiles are electron translucent at this stage (Figures 123 and 126). Of these, many are opened at one end in the shape of a horse shoe (Figure 123).

The cytoplasmic organelles of the 25th day endodermal cells exhibit little change over the preceding stage. The mitochondria are discernable, but their inner membranes are often disrupted. Granular endoplasmic

reticulum and ribosomes are present and impart an overall granular appearance to the cytoplasmic background. Golgi profiles appear to be abundant, but again are indistinguishable from other microvesicular profiles which are now found in all regions of the cell. Some pinocytotic activity is evident at the basal and apical cell surfaces. When such vesicles loose their continuity with the cell surface, they become indistinguishable from other small profiles.

At this stage, small and intermediate sized lipid droplets reappear within the cytoplasm of the endodermal cells, but show no particular pattern of distribution such as that seen in early stages (Figures 119, 121, 122 and 131).

On the 25th day of gestation, fewer adjoining endodermal cells exhibit large intercellular dilatations with interrupting cytoplasmic projections as on the 22nd day. In some instances, this pattern is changed to a complex system of folds formed by lateral interdigitations of adjoining cell processes (Figures 125 and 132). In other instances, the plasma membranes are closely apposed with only a narrow intercellular space and exhibit few irregularities in their course to the basal cell surface (Figures 123 and 131). In the latter, the intercellular space is frequently reduced as at the location of tight junctions (Figure 123). The intracellular aspect of such areas also exhibit the characteristic band of fine filaments (tonofibrils).

The basal surface of the endodermal cells appear relatively smooth and have few infoldings and pedicle-like foot processes (Figures 119, 123, 126, 127 and 131). The thickened visceral basement membrane in most areas is tightly compressed against the basal surface by mesenchymal elements of the connective tissue space and no longer displays a lace-like

appearance (Figures 119, 122 and 123). As compared with the previous stage, collagen and reticular fibrils are more dense and completely fill the relatively unoccupied areas of the connective tissue space (Figures 119, 124, 126, 131 and 132).

The dense serosal basement membrane on which the mesothelium rests is well defined and frequently merges with fibrils of the connective tissue space, as does the visceral basement membrane (Figures 119, 124, 126, 132 and 133).

The mesothelium of the 25th day visceral yolk sac consists of spindle shaped serous cells of varying widths as seen in earlier stages (Figures 121, 123 and 124). In addition to ribosomes and granular endoplasmic reticulum, the cytoplasm at this stage is also richly provided with branching bundles of fine filaments (Figures 133 and 134). Other common components of the cell include bulbous mitochondria with disrupted cristae and focally rarified matricies, vacuoles with a varying content of granular material and myelin figures, pinocytotic vesicles and small lipid droplets (Figures 119, 123, 124 and 133). Microvilli are quite numerous on the amniotic surface of the mesothelium at this stage. They are most abundant in the more widely separated regions (Figures 124, 125, 126, 133 and 134).

An additional observation on the 25th day of gestation is that the ratio of mesenchyme to visceral epithelium is greatly increased and best appreciated in areas where the combined thickness of the connective tissue elements and mesothelium is greater than that of the endodermal cells (Figures 122, 124 and 132). This change is brought about by the gradual decrease in height of the endodermal cells and the increase in mesenchymal elements.

Cytochemistry

On the 25th day of gestation, enzyme activity in the visceral yolk sac continues to hydrolyze mono-, di- and triphosphates at the same fine structural sites and, with the exception of ADP, at the same intensities as described on the 22nd day (Figures 119-134).

At this stage, the apical surface membranes of the endodermal cells display approximately equal activity to adenosine di- and triphosphates substrates (Figures 119, 120, 124, 125 and 131), except in areas where accumulations of granular material overlie the visceral epithelium. Here activity to ADP is not only sparse, as in similar areas of the previous stage, but is frequently absent (Figures 121-123). On the other hand, slight to moderate activity to ATP is always present in such areas (Figures 126, 127 and 134). The deposits of lead phosphate, which are related to the granular material within the yolk sac cavity, are also smaller and less numerous with ADP than with ATP (Figures 120 and 121).

Although enzyme activity with all three substrates occurs in relation to the plasma membrane of surface invaginations, very few tubular and vesicular profiles situated below the terminal web display deposits of lead phosphate at this stage.

With the exception of widely dispersed deposits of lead phosphate, which are occasionally seen in relation to connective tissue elements (Figure 121), all remaining enzymatic activity in the visceral yolk sac is confined to the mesothelium. Their activity with ATP yields a moderate deposition of final reaction product on the lateral and inner surface membranes of the serous cells (Figures 125, 126 and 134). With AMP as substrate, sparse activity occurs which is limited to the inner cell surface (Figure 133). No deposition of final product occurs when ADP is used as substrate (Figures 119 and 123).

The distribution of adenosine mono-, di- and triphosphatase activities in the rat placental labyrinth and visceral yolk sac on the 12th, 14th, 18th, 22nd and 25th days of gestation are summarized in Tables I and II. Also presented is an evaluation of the relative intensities of the individual enzymatic activities as determined by visual examination. A discussion of the distribution of these enzymatic activities along the surface membranes of fetal and maternal blood cells at various stages of gestation has been reported elsewhere.[3]

[3] Connell, R. S. and Bacon, R. L. Nucleoside phosphatases of fetal and maternal blood cells; an electron microscopic study. Science, 1965, 150, 503.

Table I

NUCLEOSIDE PHOSPHATASE ACTIVITY IN GLUTARALDEHYDE-FIXED RAT VISCERAL YOLK SAC USING SEVERAL PHOSPHATE SUBSTRATES

	ATP					ADP					AMP				
days	12	14	18	22	25	12	14	18	22	25	12	14	18	22	25
AS	+++	+++	+++	+++	+++	−	++	+	++	+++	−	−	−	+	+
LS	+++	+++	++	−	−	−	+	+	−	−	−	−	−	−	−
BS	+++	+++	−	−	−	−	−	−	−	−	−	−	−	−	−
CT	+	+	−	−	−	−	−	−	−	−	−	−	−	−	−
Mes	+	−	++		++	−	−			−	−	−		+	+

AS = Apical Surface of Endodermal Cells

LS = Lateral Surface " "

BS = Basal Surface " "

CT = Connective Tissue Elements

Mes = Mesothelium

+++ = Intense

++ = Moderate

+ = Slight

− = None

Table II

NUCLEOSIDE PHOSPHATASE ACTIVITY IN GLUTARALDEHYDE-FIXED RAT PLACENTAL LABRINTH USING SEVERAL PHOSPHATE SUBSTRATES

		ATP					ADP					AMP				
days		12	14	18	22	25	12	14	18	22	25	12	14	18	22	25
MBC		+++	+++	+++	+++	+++	++	++	++	++	++	++	++	++	++	++
T_I	m		+	++	+++	+		+	++	+++	++		+++	+++	+++	+
	f		+	++	++	+		+	++	++	+		+	++	++	+
T_{II}	m		+++	+++	+++	++		++	+++	+++	++		+	+++	+++	+
	f		−	−	−	−		−	−	−	−		−	−	−	−
T_{III}	m		−					−	−	−	−		−	−	−	−
	f		−	−	−	−		−	−	−	−		−	−	−	−
En	m		−	−		−		−	−	−	−		−	−	−	−
	f		−	−	−	−		−	−	−	−		−	−	−	−
FBC		−	−	−	−	−		−	−	−	−		−	−	−	−

MBC = Maternal Blood Cells

T_I = Trophoblast I

T_{II} = Trophoblast II

T_{III} = Trophoblast III

En = Capillary Endothelium

FBC = Fetal Blood Cells

m = maternal, f = fetal

+++ = Intense

++ = Moderate

\+ = Slight

− = None

DISCUSSION

Labyrinthine Placenta

When observed with the light microscope at increasing gestational ages, the labyrinthine barrier of the rat chorio-allantoic placenta is seen to consist of exceedingly thin laminae of cytoplasm separating maternal and fetal blood streams. Therefore, the difficulty of establishing the nature of the epithelial cytoplasm forming the confining walls of the maternal blood channels is at once apparent.

Duval (4), who was among the first investigators to undertake a comprehensive study of the development and growth of the rodent placenta, described the trophoblast of the rat labyrinth as disappearing a few days before parturition, leaving only fetal endothelium between the maternal and fetal blood streams. Jenkinson (164), a contemporary of Duval, disagreed with this interpretation and produced evidence in the form of placental casts which showed that the trophoblast persisted throughout gestation. This study, however, was reported in an obscure Dutch journal and was consequently lost to the literature during the period that the chorio-allantoic placentas of eutherian mammals were being classified. Subsequently, Duval (4) extended his morphological observations of a disappearing trophoblast to include the lagamorph placenta. This observation was later confirmed by Chipman (5). As a result of these studies, Duval's description of an extreme reduction in the number of layers comprising the rodent placental barrier became widely accepted.

In 1926, H. W. Mossman (2), in studying the rabbit placenta and placental transmission, corroborated the early observations of Duval and Chipman and introduced the term hemoendothelialis to describe the separating membrane in the late rabbit placenta. Unfortunately, due to

the lack of evidence contrary to Duval's description (excluding the work of Jenkinson), the chorio-allantoic placentas of rats and most rodents were classified as being hemoendothelial by subsequent investigators. Although Hard (41), Wislocki et al. (37), Bridgman (167) and Amoroso (54) pointed out that evidence for so classifying the rodent placenta was inconclusive, methods to prove otherwise were limited by the resolving power of the light microscope and by the existing histological methods.

With the great resolving powers of the electron microscope, Dempsey and Wislocki (96) and Wislocki and Dempsey (97) were able to show in the rat and rabbit placentas that trophoblast intervenes between maternal blood and fetal endothelium throughout pregnancy. Subsequent ultrastructural examinations have confirmed the presence of trophoblast in the term rat placental labyrinth. There has been no unanimous agreement, however, among these few reports as to the number of layers or to the cytological nature of the trophoblastic layers.

Dempsey and Wislocki (96) initially reported that on the 15th, 17th and 21st days of gestation, the rat placental labyrinth consisted of endothelial lined fetal capillaries, a delicate and fine fibrillar supporting basement membrane which often appeared double, and several attenuated sheets of overlapping trophoblast, of which the middle and inner layers consisted of separate discrete cells and the outer layer bordering the maternal blood space of syncytially fused cells.

In a later and more definitive study, Wislocki and Dempsey (97) re-examined the rat placenta on the 15th, 17th and 21st days of gestation and interpreted the labyrinth as consisting of two or three thin, overlapping sheets of individual cytotrophoblasts. Schiebler and Knoop (98), on the other hand, reported that the inner layer of trophoblast

appears syncytial on the 20th and 21st days of gestation and that only a single basement membrane occurs between the syncytial trophoblastic layer and the fetal endothelium. Owers and Mossman (100), utilizing perfusion fixation and a newer embedding medium, confirmed the syncytial nature of the inner layer of trophoblast, but found the labyrinthine barrier to consist of only two layers of trophoblast. More recently, Jollie (101) has studied the fine structure of the rat placental labyrinth from the day of its establishment through term. At all stages the labyrinth was reported as possessing an outer and middle layer of cytotrophoblast (trophoblasts I and II), an inner syncytial layer (element III) and a trabecular capillary with an underlying basement membrane. In a comparative study of the hemochorial placenta, Enders (45) has given a similar description for the term rat placental labyrinth, but has suggested that the middle layer of trophoblast (T II) is also syncytial.

The discrepancies between these descriptions may be accounted for by the limitations of available facilities in the past years. Furthermore, the components of the placental labyrinth may be subject to considerable variation as has been proposed by Owers and Howerter (121). Since the area covered by electron micrographs at even low powers of magnification is only a fraction of the entire placental labyrinth, it would seem unlikely that any group of investigators, utilizing a technique as time consuming as electron microscopy, would quickly come upon all the different structural appearances that have been reported.

The present investigation of the rat placental labyrinth at increasing gestational ages confirms the observations of the more recent of these studies in which three attenuated layers of trophoblast are described. The present study also confirms the presence of distinct

basement membranes underlying trophoblast III and the fetal endothelium. In addition, the occurrence of allantoic mesenchymal cells in the potential connective tissue space which intervene between the two basement membranes is demonstrated for the first time in this study.

In order to resolve the discrepancies as to the cellular or syncytial nature of the three trophoblast layers, electron micrographs of extensive areas of the placental labyrinth were taken on the 14th, 18th and 22nd days of gestation and appropriate montages made. Distinct cell bounderies between trophoblast I cells were easily demonstrated at all stages. On the other hand, owing to the presence of deeply penetrating and complex folds of their surface membranes, it cannot be stated with certainty that trophoblasts II and III are syncytial. Cell membranes, however, were never observed extending between the inner and outer surfaces of these layers even after tracing their cytoplasm around several consecutive allantoic capillaries. On occasions, nuclei could be found which were clearly not separated by cell membranes. It is, therefore, concluded that trophoblasts II and III are syncytial throughout gestation and that trophoblast I and the fetal endothelium are cellular. Even if occasional lateral cell membranes were to persist in trophoblasts II and III, tight junctions, which have been reported as acting as a barrier to transport (168), would most likely prevent lateral diffusion into the intercellular space between adjacent cells of the same layer.

The origin(s) of the three layers overlying the fetal endothelium of the labyrinth is not yet known. Dr. Mossman, however, in a personal communication with Enders (45), has suggested that in the rodent placenta the three layers may contain three sources of trophoblast, the giant cells, the trager epithelium and the true chorionic epithelium. Jollie

(101), having considered the possibility that allantoic mesenchyme may accompany the allantoic vessels as they penetrate the parenchymal trophoblast[4], has inferred that the innermost layer might be allantoic mesenchyme rather than trophoblast. Because of this uncertainty, he has designated this layer as "element III". Although the present work includes observations on the 12 day placental labyrinth, intermediate stages in the formation of the vascular trophoblastic lamellae which would help resolve this question were not found.

The occurrence of alternating tight and intermediate junctions (168) between the plasma membranes of trophoblast II and III, however, would suggest that these two layers are of similar origin. A search of the literature reveals no instances where elements of such diverse origins as allantoic mesenchyme and chorionic trophoblast are joined by cell junctions. Furthermore, by the 18th day of gestation, occasional mesenchymal cells can be found in the placental labyrinth and are readily identified by their well developed granular endoplasmic reticulum. These cells, which are coated by an external lamina, are separated from "element III" and the fetal endothelium by distinct basement membranes (basal laminae). As gestation advances there is an increase in the numbers of these cells and a slight increase in the thickness of the two basement membranes. Therefore, if "element III" were of allantoic mesenchyme, one would expect to find, at least in the later stages of gestation, a basal lamina separating this layer from trophoblast II. Since only cell junctions are observed along the common border of these two syncytial layers, it is suggested that "element III"

[4]Dr. D. L. Gunberg (1966) has made preliminary observations which would suggest that at least some of the fetal vessels in the placental labyrinth have their origin from blood islands found within the ectoplacental cone.

is trophoblastic in origin and, therefore, might well be designated as trophoblast III. This interpretation is in agreement with that of Mossman (169).

If one agrees that the parenchymal cords of undifferentiated cellular trophoblast give rise to the definitive vascular labyrinth, the means by which trophoblast II and III become syncytial remains to be answered. The results presented in this study do not resolve this question. It is unlikely, however, that these layers become syncytial through a series of nuclear divisions without cell division since autoradiographic observations indicate that H^3 labelled thymidine incorporation does not occur in the vascular labyrinth from the time of its formation until the day before term (170). It is more likely that trophoblasts II and III become syncytial through progressive coalescence and break down of their plasma membranes. Such a method for the formation of the syncytium from cytotrophoblast has been alluded to and described in the human placenta (65, 75, 76, 77, 78, 79, 80 and 81).

Since mitotic figures are observed exclusively in the parenchymal cords of epitheliod trophoblast, it would appear that this tissue functions as a reservoir for subsequent labyrinthine growth.

On the 12th day of gestation, fetal vessels from the allantois have just made contact with the base of the ectoplacental cone. Therefore, most of the labyrinthine placenta appears as numerous branching cords of avascular trophoblast separated from each other by maternal blood sinuses. Many of these parenchymal trophoblast cells exhibit an ultrastructural organization similar to that which has been interpreted as being typical for undifferentiated cells in general (171); there is very little granular endoplasmic reticulum and a great abundance of free ribosomes. Jollie (101) has also described the plasma membranes

of the parenchymal cells as being parallel, closely apposed, relatively smooth and free of desmosomes. This ultrastructural organization is comparable to that described for the inner cell mass of the rat blastocyst at six days of gestation (172). Although areas with similar morphological features are observed in the present study, the parenchymal trophoblast cells are also seen to assume three other distinct morphological appearances. The fine structural appearance of these cells is strikingly similar to that of the three trophoblastic elements which comprise the junctional zone of the rat placenta (173). The first type of parenchymal trophoblast cells are loosely arranged and have pleomorphic microvillous projections which either extend into the maternal blood sinus or into the interstices which are in open continuity with the maternal circulation. The cells are attached by desmosomes and possess a paucity of endoplasmic reticulum, but have numerous vacuoles with varying contents, liposomes, free ribosomes, bundles of fibrils and swollen mitochondria. This description is similar to that which characterizes the trophoblastic giant cells on the 12th day of gestation (173).

Unlike the giant trophoblast-like cells, the plasmalemma of the second type of parenchymal trophoblast cells is not modified into microvillous projections even when directly exposed to the maternal blood space. The cells are attached to each other by desmosomes and contain granular endoplasmic reticulum disposed in tubular arrays which roughly parallel each other. This description describes very well the trophospongial (spongiotrophoblast) cells which constitute the innermost layer of the junctional zone (173). The third morphological type of parenchymal trophoblast appears much lighter than the other cell types due to the presence of relatively large areas of the cytoplasm which are relatively void of cytoplasmic organelles. Although the tissue

sections were not counterstained with lead hydroxide which has been accepted as a method for demonstrating glycogen at the electron microscopic level (174), these areas of less dense cytoplasm could represent the accumulation and/or storage of glycogen for subsequent fetal utilization. This type of cell is characteristic of glycogen cells which are typically found in the junctional zone (173). Since evidence from autoradiographic studies (170) suggest that the three trophoblastic elements of the junctional zone are derived from undifferentiated trophoblastic parenchyma of the ectoplacental cone, it is tempting to infer that the three morphological types of trophoblast are intermediate stages in the formation of giant trophoblast cells, trophospongium and glycogen cells, respectively. Furthermore, since a great abundance of free ribonucleoprotein granules and a poorly developed endoplasmic reticulum are characteristic of rapidly proliferating cells synthesizing protein for growth (175), it is suggested that the parenchymal trophoblast cells which possess these features (and were the only cells in the present study to undergo cell division) differentiate into labyrinthine trophoblast and trophoblastic elements of the junctional zone.

In the earlier part of this century, placental exchange was largely based on the number of layers interposed between the fetal and maternal circulations. A comparison of physiological studies involving sodium transfer across Grosser's four placental types would seem to bear out the validity of this correlation. In these studies, it was observed that the rate of sodium passage is more rapid and complete in the three layered hemochorial placenta (176, 177, 178 and 179) than in the six layered epitheliochorial placenta (180). However, the physiologic

advantage alluded to in the hemochorial placenta would appear to be offset in the rat by the functional disadvantage of the laminated arrangement of the trophoblastic cells as revealed by electron microscopy. Thus, with respect to cell surfaces and layers, the rat placental labyrinth would appear to be as complex as syndesmochorial and epitheliochorial placentas. Undoubtedly, the number of layers and their thickness play roles in the rate of passage of highly diffusable substances such as oxygen and carbon dioxide. It is now clear from results obtained by a number of investigators that many substances are actively transported across the placental barrier or at least undergo the process of facilitated diffusion (146, 181, 182, 183, 184, 185). It would, therefore, appear that the total thickness of the placental barrier is of minor importance in the overall task of transfer.

Although the labyrinthine barrier consists of four cytoplasmic layers throughout gestation, the surface membranes of each display specialized structures which in other tissues are commonly interpreted as devices which not only facilitate transport but also amplify the area of membrane across which absorption takes place. Included in these specialized structures are endothelial and trophoblastic fenestrations, microvillus-like cytoplasmic evaginations which are capable of impounding sizable droplets of fluid, at least two distinct forms of micropinocytosis and deep infoldings of the surface membranes, some of which form long channels that bud off small vacuoles or caveolae at their end.

Labyrinthine fenestrations which are first identified in trophoblast I on the 14th day of gestation and in the fetal endothelium on the 18th day are extremely interesting in that they assume two different structural appearances. Both types of fenestrae are pores roughly 400

to 700 Å in diameter. The first type is bridged by a thin membrane or central diaphragm and appear comparable to endothelial fenestrations which are presumed to facilitate transendothelial transport to various tissues, e.g., kidney (186, 187), thyroid (188, 189, 190), adrenal cortex (191, 192), anterior pituitary (193), ciliary process and choroid plexus (194, 195) and exocrine pancreas (196). The second type of fenestration appears to be open as is evidenced by the continuity of the plasma membrane around the margins of the pore and the absence of a central diaphragm. An amorphous material, however, is present. Similar fenestrations without diaphragms, but with hazy material within their openings, have been described in the glomerulus (197) and in capillaries of the thyroid gland (198). Wissig (198) has interpreted the hazy material as a segment of the rim of the pore that is included in the section. This explanation would most likely explain the presence of the amorphous material seen within the pores in trophoblast, and the fetal endothelium, especially since the thickness of the tissue is at least as thick if not thicker than the diameter of fenestrations. Elfvin (199), who has studied capillary fenestrations in the adrenal medulla of the rat, disagrees with both assumptions that the hazy material represents the front and back wall of the halved fenestrations and that fenestrae are true openings. Nevertheless, two morphologically different fenestrae can be identified in the present study. Tillack (200) has also observed open pores in trophoblast I but was unable to demonstrate them in the fetal endothelium.

As yet, fine structural studies have not revealed the structural significance of open fenestrations, but it can be assumed that in the placental labyrinth they further facilitate the passage of large

molecules. The fact that ferritin is seen within trophoblast II and the basement membrane underlying the fetal endothelium after only two minutes of circulation in the pregnant rat would support this assumption (200). Diffusion through intercellular spaces between trophoblast I and endothelial cells would seem to be denied by the tight junctions. Furthermore, evidence of transport vesicles with ferritin inclusions are not observed so quickly in these cells (200, 201). As a result of pore formation, then, the functional thickness of the labyrinth is reduced and by the 18th day post coitum trophoblasts II and III remain as the only cytoplasmic barriers to placental transport.

It is interesting to note that despite the presence of fenestrations, trophoblast I and the fetal endothelium also demonstrate other specialized structures for absorption and transport. In addition to vastly increasing the surface area, the thin, irregularly arranged pleomorphic folds and/or microvillous projections described on the free surface of trophoblast I from the twelfth day through to term may produce localized regions of relative stasis of the maternal plasma. Furthermore, these structures are frequently branched and occasionally have distally expanded tips. Such features would also tend to cause interference with the flow of maternal plasma (45) and thus facilitate absorption. It is in the regions of these structures where caveolae are principally situated. Caveolae are the second form of micropinocytosis alluded to earlier and will be considered in greater detail further along in the discussion.

Frequently throughout gestation adjacent pleomorphic folds and/or evaginations of trophoblast I are seen to coalesce at their distal tips and thus entrap droplets of maternal plasma, which are then taken into

the cytoplasm in membrane bound vacuoles. These surface projections are also seen to bend back upon themselves so that their distal tips approach the cell surface. The tips then fuse with the cell membrane in such a way as to form vacuoles like those described above. Similar folds are also seen projecting into the lumina of the fetal capillaries from the margins of the endothelial cells. These thin folds appear as early as the 14th day and may occur on one or on both of the adjoining cells. Kisch (202) has demonstrated that similar flaps in capillaries in the left ventricle of the guinea pig heart are not microvillous projections as they appear in transverse sections, but are folds extending for various distances along the cell boundaries. Although the marginal folds of the labyrinthine capillaries are seen to bend back so that their edges approach the cell surface, stages where they actually fuse with the cell membrane were not observed. The formation of marginal vacuoles by such folds have been described in the counter current system of capillaries of the choroid rete of the fish eye (203, 204), in the blood vessels in the normal fetal central nervous system of the rabbit (205), in the brains of animals in the course of experimental edema (206), and in the capillaries of the traumatized sciatic nerve of the rat (205). Fawcett (207) has suggested that the frequency of marginal folds and vacuoles in mammalian blood vessels is not great enough to be regarded as a quantitatively important mode of transport under normal conditions. He does suggest, however, that these intraluminal projections might have a significant hemodynamic effect. They may increase resistance to blood flow near the vessel wall and thus favor a more rapid streamline flow in the center of the vessel; or they may increase resistance and retard flow by creating peripheral turbulence. The

latter function would seem to be more applicable to the folds in the fetal vessels of the placental labyrinth as a retarded blood flow would facilitate the exchange of materials including respiratory gases.

The endothelial cells lining the fetal capillaries of the placental labyrinth also display evidence of micropinocytosis which becomes more abundant with increasing gestational age. These small smooth-surfaced invaginations of the cell membrane are seen along both the luminal and basal surfaces of the endothelial cells, but are more numerous along the latter. Vesicles of similar size are also found free in the cytoplasm. These uniformly alveolate or flask-shaped vesicles appear as those described in the capillary endothelium (208, 209) and later observed in smooth and striated muscle and many other cell types. Because these microvesicles occur on both surfaces of endothelial cells in general, Palade (208) has suggested that they serve as vehicles for fluid transport, forming on the luminal surface, moving across the cell and discharging their contents at the basal surface of the capillary. Moore and Ruska (210) have offered the term cytopempsis to describe this activity, but suggest that it may occur in both directions across the cell. Cytopempsis, as interpreted by these authors, differs from pinocytosis in that the former is concerned with fluid being moved completely across the cell, while the latter activity is concerned with fluid incorporated within the cell.

Recent transport studies have shown that electron opaque particles introduced into the pericapillary connective tissue of the cornea are taken up by pinocytotic vesicles at the basal surface of the endothelium (211, 212) equally as well as particles introduced into the blood vessel are taken up by the luminal surface of the endothelium (213, 214, 215,

216). In fact, Staubesand (217) has demonstrated the simultaneous transport of different marker particles by vesicles in opposite directions across both mesothelial cells and capillary endothelium following the injection of one kind of marker particle into the serous cavity and another into the blood stream.

Presently, then, several generalizations can be made concerning micropinocytotic activity in the placental labyrinth. First, they appear to form equally as well on one side of a cell as the other. Second, they form quite rapidly as intermediate stages in their formation are rarely observed. Third, they apparently are slow to separate from the plasmalemma since they accumulate in large numbers along the inner surface of the membrane while relatively few vesicles are found free in the cytoplasm. On this basis, it is tempting to infer that the preponderance of alveolate shaped vesicles on the basal surface membrane of the fetal endothelium indicates that the preferred direction of transport by micropinocytosis is towards the luminal surface of the fetal capillary rather than towards the basal surface as first implied by Palade (208). Furthermore, it would appear that the transport of ferritin by such vesicles is unidirectional. Tillack (200) has demonstrated in the near term rat placenta that ferritin is transported across the fetal endothelium by vesicles only when introduced into the fetal circulatory system. When injected into the maternal circulation, ferritin particles are found free in the cytoplasm of the fetal endothelium.

In addition to micropinocytosis vesicles typical of endothelium, the luminal surface of the fetal endothelium occasionally displays a second type of micropinocytotic vesicle which is characterized by having

a noticeably thick and fuzzy appearing limiting membrane. Such vesicles, which are called caveolae, also occur in trophoblast I, but are most numerous in trophoblast II. It is the current speculation that vesicles with extraneous coats provide for the selective uptake of certain classes of substances such as proteins, whereas uptake in the smooth surfaced vesicles is thought to be undiscriminating (207, 218, 219, 220, 221, 222). Since caveolae and external surface coatings (glycocalyx), which are described as possessing properties suitable for selective binding of particular classes of ions or molecules to the cell surface prior to the formation of pinocytotic vesicles (223, 224), are common features of the visceral endodermal cells. A more detailed account of their functional significance will be deferred until the discussion of the visceral yolk sac placenta.

Trophoblast II, which is a relatively thick layer as compared to the other layers of trophoblast and the fetal endothelium, also becomes functionally thinner as gestation advances. This reduction is effected by the appearance of surface infoldings or channels which frequently extend two-thirds or more the distance across the cytoplasm to the common border between trophoblast II and III. As gestation proceeds, these infoldings become more extensive and complex. The cytoplasm between the channels and the fetal surface of trophoblast II displays numerous vacuoles of various sizes which often occur as strings spanning the width of the cell. This appearance suggests that materials which have gained access to the intercellular space between trophoblast I and II may flow into the infoldings and become absorbed in the vacuoles which form by the abscission of the distal ends of the channels. It cannot be stated with certainty, however, that all of the vacuoles are

free in the cytoplasm rather than being cross sections of the channels and/or their invaginations. Some of the smaller vacuoles may also represent golgi microvesicular profiles which commonly occur in the thicker regions of this layer. In addition to the smooth surfaced vacuoles, the cytoplasm of trophoblast II contains thick-walled caveolae which appear in greater numbers towards the end of gestation. These structures arise from the outer or maternal surface membrane as well as from the surface membranes lining the infoldings or channels. Since the caveolae do not accumulate in large numbers along the inner surface of the membrane as do smooth surfaced pinocytotic vesicles, they must detach as rapidly as they form and move into the cytoplasm. The appearance of both smooth surfaced vacuoles and small caveolae in trophoblast II suggests that some materials are selectively transported across this syncytial layer. It may be that the vacuoles participate in bulk transfer of fluids and materials, whereas the caveolae may participate in selective absorption. The infoldings of trophoblast II greatly increase the surface area for absorption and certainly reduce the distance across which materials are transported.

Trophoblast III also displays smooth surfaced cytoplasmic vacuoles and surface infoldings along its basal or inner plasmalemma. These infoldings, although not as complex as those on the outer surface of trophoblast II, become more extensive with advancing gestational age and at term frequently give the appearance of pedicel-like foot processes which are directed toward the endothelial basement membrane. Similar basal membrane structures have been observed at the bases of cells of the proximal convoluted tubules whose function is that of reabsorption of a number of metabolites and of substantial amounts of water for the

maintenance of homostasis (187, 225) in the submaxillary gland, choroid plexus and ciliary body, all of which are particularly noted for water transport (226). The basal infoldings in these tissues, however, differ from those along the basal or inner surface of trophoblast III in that mitochondria are situated among their infoldings. Ruska and associates (227) have suggested that the mitochondria among the infoldings of renal tubular cells participate as an energy generator for pushing water into blood vessels against a pressure gradient. Kurosumi (228) has interpreted the absence of mitochondria among the basal infoldings of secretory cells as indicating that water flow is the reverse of that in renal tubular cells and that water easily flows from blood capillaries into gland cells with a negligible amount of energy consumption. Since tracer studies indicate that there is an extremely rapid rate of turnover of water between the fetus and amniotic fluid and the fetus and the maternal system (177, 178, 229, 230, 231, 232), it may be suggested that the basal infoldings of trophoblast III provide for a great increase in the cytoplasmic surface area for the active transport of fluids. Furthermore, since these infoldings become more extensive towards term, one would expect the rate of fluid transfer to be greater during late gestation. A similar interpretation has been suggested for the complex infoldings along the basal surface of the human syncytial and cytotrophoblasts (74, 95).

The mechanism(s) by which materials are transported across the common border between trophoblast II and III is an extremely challenging question. Since the adjoining surface membranes of the two layers are closely apposed throughout their entire extent and are attached to one another by closely spaced tight and intermediate junctions which may

act as barriers to transport (168, 233), it would seem that transport to either side of the labyrinthine barrier would be denied. Although smooth surfaced vacuoles and caveolae are found free within the cytoplasm of both layers, at no stage of gestation were these adjoining surface membranes observed in the process of forming pinocytotic vesicles. In fact, other than a few simple surface interdigitations, the two surface membranes do not exhibit any of the specializations which have been implicated in facilitating transport. Tillack (200) has demonstrated that the transport of ferritin across the common border of trophoblasts II and III is more rapid from fetal to maternal circulation. When injected into the maternal blood stream, only a few molecules of ferritin were present in trophoblast III after two hours. These molecules were found free within the cytoplasm. On the other hand, ferritin injected into the umbilical vein appeared in vacuoles within trophoblast II after five minutes. Tillack was unable, however, to give an explanation for the mechanism by which these molecules were transported.

A number of investigators (48, 74) have suggested that waste products of fetal metabolism such as creatine, creatinine and urea are so readily diffusable that their excretion would probably not be associated with the formation of granules and vacuoles. Nevertheless, the surface infoldings as well as the vesicles and vacuoles within the cytoplasm of the three layers of trophoblast may possibly be involved in the movement of granular and fluid wastes from the fetal to maternal blood.

Because of the simultaneous presence of fenestrae, smooth surfaced pinocytotic vesicles and vacuoles and caveolae throughout gestation, it is tempting to infer that they indicate separate placental exchange

routes for separate transportable materials, i.e., transport of small molecules such as water and respiratory gases via the fenestrations and pinocytotic vesicles and transport of serum proteins by caveolae. The entrapment of materials within these vesicles, however, does not insure either their confinement in the cell or their unaltered passage across the cell. Furthermore, transport across the placental barrier undoubtedly depends on the physical, physicochemical and biochemical properties of both the materials and the cell membranes, as well as regulatory mechanisms on both sides of the placenta (234).

From the 12th day through the 18th day of gestation, the surface membranes of the trophoblast cells bordering the maternal blood sinus exhibit specialized structures which may be interpreted as mechanisms for the release of secretory materials. The first of these structures which are predominantly found along the free surfaces of the 12 day parenchymal trophoblast cells are represented by clavate microvilli. These structures are irregularly oriented and have globular expanded tips which contain granular material of moderate electron density. Such microvilli along the free surface of 12 day trophoblast I cells also contain globular vesicles. Since free floating vesicles and granular materials similar to the expanded tips and their contents are found in the maternal blood space, it is assumed that the tips of the microvilli become pinched off their narrow bases. Similar microvilli with extremely expanded tips which presumably become detached have been described in the choroid plexus (195, 235), in the carpal organ of the pig (236) and in the intrahepatic bile ducts (228). Maxwell and Pease (195), in studying the fine structure of the ependymal cells of the choroid plexus, have designated the border composed of polyp-like

microvilli as the "polypoid border". Van Breeman and Clemente (237) have suggested that the pinching off of the expanded tips of polypoid microvilli may represent apocrine secretions at the submicroscopic level.

The second type of secretory projection appears to be formed as a result of a local solation of the outer plasma membrane. Although present in the parenchymal trophoblast cells, this type of projection is more commonly found along the free surfaces of trophoblast I cells. Here, they usually occur in regions which are pervaded with granular endoplasmic reticulum, free ribosomes and golgi microvesicular profiles. Such regions are characteristic of those of many protein secretory cells. The interior of these projections are of little contrast, but do contain various amounts of a finely granular material and small globular vesicles. The granular material may represent portions of the cytoplasm as well as the finely flocculated product of the granular endoplasmic reticulum, which occasionally appears to be in the process of discharging its cisternal content into the lumen of the secretory projections. Whether all of the globular vesicles are derived from the cytoplasm or represent portions of the front and back wall of the halved projections which are infolded due to strong hydrostatic pressures in the maternal blood space is not known. The low density of the interior of the projection, however, does imply that they contain a high water content (228). Similar secretory extensions have been reported as occurring on the apical surface of gland cells in a variety of tissues. They have been observed in the thyroid gland (238, 239), eccrine and apocrine sweat glands (240, 241, 242), gastric parietal cells (243, 244), epithelia of bile ducts (228) and epithelia of excretory ducts of the submaxillary gland (245). In these tissues it

is believed that the apocrine projections become decapitated or ruptured and through the opening the secretion together with a small amount of cytoplasm is discharged. Further investigation is needed before a definite statement can be made concerning the functional significance of the "microapocrine secretions".

On the basis of known synthetic activities of the placenta, however, one could speculate that these microapocrine projections represent the mechanism for the release of proteolytic (121) enzymes and/or chorionic gonadotrophic hormones. Proteolytic enzymes may in part be responsible for the atrophy (246, 247) and subsequent autolysis (248) of the primary decidua. This cytolytic activity correlates well with the time when both clavate microvilli and absorption vacuoles are most numerous in the trophoblast cells. If these secretions are of a proteolytic nature and thus facilitate the invasion of the uterine wall, the vacuoles in the giant-like cells may then represent phagocytosed decidual debris. In any case, the similarity between the granular material in these vacuoles and that in the maternal blood space would certainly suggest a direct relationship between the two. As yet, the exact site of chorionic gonadotrophic hormone production, which is responsible for stimulating the ovaries and hence supporting normal pregnancy, has not been unequivocally established in the rodent placenta (249). Since this function has been tentatively assigned to the giant cells and the adjacent spongiotrophoblast (249, 250, 251), it is tempting to infer that the secretory projections found along their free surfaces contain chorionic gonadotrophic hormone which is to be released into the maternal blood space.

Fat droplets encountered in the labyrinth from the 12th day of

gestation through term are found exclusively in trophoblast III. Many of these inclusions which range in size from 1 to 2 microns appear distorted and have irregular outlines which are probably due to fixation, dehydration and embedding (175, 252). The fact that the lipid takes up relatively little osmium tetroxide may suggest that they are highly saturated (175). Bridgman (167) has pointed out that these lipid droplets diminish shortly before term. In the present study, however, lipid reduction appears to occur only when gestation is prolonged three days beyond the normal time of parturition. At this time, all evidence of lipid inclusions is absent. The functional significance of this lipid is at present a matter of conjecture. Histochemical studies and ultrastructure evidence presented here and elsewhere, however, would suggest that they are not the morphological counterparts found in the villous syncytiotrophoblast of the human placenta which represent the hormones estrogen and progesterone.

Early histochemical studies demonstrated that lipid droplets in the placental labyrinth are birefringent and give an intense carbonyl reaction (37, 253, 254). Since these properties, at the time, were considered to be characteristic of those of other steroid hormone-producing cells, the labyrinthine trophoblast was suspected as being the site of steroid hormonal synthesis (48). This supposition was subsequently weakened by studies which showed that these properties are not limited to lipids in hormone-producing cells (255). Furthermore, on morphological grounds, Schiebler and Knoop (99) hypothesized that the giant trophoblast cells are responsible for steroid-hormone secretion. The validity of this hypothesis would seem to be supported by the histochemical and biochemical studies of Deane et al. (249).

These investigators assayed the placentas of mice and rats for 3 ol hydroxysteroid dehydrogenase activity which is known to play a key role in the biosynthesis of active steroid hormones. This enzymatic activity which has also been reported in the syncytiotrophoblast of the human placenta (256) was histochemically limited to the giant trophoblast cells. Even when incubations were continued overnight, no detectable activity was found in the labyrinthine portion of the placentas.

Terzakis (75) has described granules which may represent the hormones estrogen and progesterone in the human syncytiotrophoblast as being moderately electron dense with distinct limiting membranes and arising within golgi membranes. Although the lipid droplets within trophoblast III are of a similar size and electron density as these granules, they are not confined by a detectable limiting membrane nor are they particularly associated with golgi elements. Except for a softer electron density and a limited distribution, these lipid inclusions are typical of those in the human placenta which have been interpreted as being nutritive (75, 95). On this basis, it is suggested that the lipid inclusions in trophoblast III are either nutritive in nature (in which case their proximity to the fetal circulation would decrease the distance of active transport and thus increase the efficiency of energy utilization) or serve as a local store of energy and a potential source of short carbon chains that can be utilized by the trophoblast in the synthesis of its lipid containing components, such as membranes.

Visceral Yolk Sac Placenta

The ultrastructure of the visceral yolk sac placenta, which has been described sequentially from the 12th to 22nd days, clearly indicates that this membrane has a dynamically complex cytological structure which undergoes a series of morphological changes during this interval. Until recently, there had not been a closely seriated fine structural study of the rat visceral yolk sac including important stages before and after the rupture of Reichert's membrane. Within the last year, however, Lambson (257) and Schultz et al. (258) have published observations on the fine structure of this membrane at increasing gestational ages. The former study is concerned with the mechanisms utilized in the visceral epithelium for the transport of ferritin molecules at different stages of gestation, whereas, the latter study is concerned with the cytochemical demonstration of lysosomal areas in the visceral epithelium at various stages of development. For the most part, the present findings are in agreement with these as well as other descriptions of the yolk sac ultrastructure (guinea pig, 155; rat, 48, 97, 139, 156, 157; human, 90; rabbit, 108). Therefore, only those structural features of the rat visceral yolk sac which previously have been either unemphasized or perhaps unnoticed will be considered in the present discussion.

Throughout gestation the apical surface of the visceral endodermal cells are crowned by long and slender microvilli which are frequently branched and closely spaced. The surface membrane between the bases of many microvilli is invaginated to form crypts or tubules which may branch and extend for various distances into the apical cytoplasm. Between the 14th and 18th days of gestation these invaginations become

more extensive and form a complex interconnected series of canaliculi which are frequently seen to be directly continuous with large vacuoles in the apical cytoplasm. It would thus appear that the apical surface of the visceral epithelium is modified for bulk absorption. It is also interesting to note that the apical canalicular system becomes more extensive during the period when Reichert's membrane and with it the parietal yolk sac and chorion leave rupture and recoil to the margin of the chorio-allantoic placenta. Such an elaborate absorptive surface suggests greater absorptive activity after direct exposure of the visceral endoderm to the uterine contents.

The plasma membrane limiting the microvilli as well as the invaginations and canaliculi is further modified for absorptive activities at all stages of gestation by the presence of a fuzzy appearing extraneous coating 200 to 300 Å thick. Excrescences of this kind, which were first noted on microvilli of gall bladder epithelium by Yamada (259), have since been observed on the free and invaginated surfaces of a variety of different cell types (260, 261, 262). These extraneous coatings, which are variously named, but here will be called a glycocalyx (223), have been generally accepted as consisting of a polysaccharide rich material capable of acting as a filter, retarding the passage of particles, molecules or ions above a certain size and also as binding certain substances preferentially by virture of the chemical nature of groupings available. Thus, such a glycocalyx is thought to exert an influence on the composition of the environment close to the external surface of the plasma membrane of the cell.

Choi (224, 263) and Brandt and Pappas (264) have shown that the extracellular coating on the luminal surface of the toad bladder epi-

thelium and the plasma membrane of the amoeba is capable of selectively binding colloidal particles or proteins which are subsequently taken into the toad bladder epithelium and amoeba by pinocytosis or phagocytosis. Roth and Porter (220, 222) have similarly reported that the extracellular polysaccharide rich coating of surface invaginations of mosquito oocytes is responsible for the selective absorption of proteins. In the visceral yolk sac, however, Lambson (257) has observed the absorption of ferritin molecules and other unrelated compounds, i.e., thorotrast and saccharated iron oxide, which were obviously not attached to the extraneous coating (glycocalyx) of the apical invaginations and canaliculi. On the basis of these observations, he concludes that specific attachment to the surface coating may not be necessary for the entrance of protein into the visceral endodermal cells.

On the basis of the present cytochemical observations that adenosine mono-, di- and triphosphatase activities are distributed along the apical surface of the visceral endodermal cells, it is tempting to infer that the glycocalyx coating this border contains hydrolytic enzymes which play an active role in extracellular digestion. Fawcett (207) has suggested that the ultimate stages of intraluminal digestion may be carried out with great efficiency in the glycocalyx and that the resulting small molecules would then be free to enter the cell by traversing the limiting membrane of the microvilli. A sequence of such activities has been recently described for the absorption of fat in the rat intestinal epithelium (265). The results of this investigation favored the interpretation that a hydrolysis of triglycerides occurs at the cell surface and that the resulting monoglycerides and free fatty acids diffuse through the microvillar membrane.

From the 12th day of gestation to term, the apical cytoplasm of the visceral endodermal cells contain numerous vesicles and vacuoles of varying diameters, content and density. Many of these structures appear to represent progressive stages in absorptive activities, whereas, others are probably autophagic vacuoles and golgi elements. The absorption vacuoles and vesicles are readily identified by their luminal coating of fuzzy material (glycocalyx) and form by either an abscission of the dilated distal ends of apical canaliculi or by caveolae. Once free within the apical cytoplasm these structures either coalesce to form larger vacuoles or fuse directly with larger preformed absorption vacuoles (multivesicular bodies). A similar process of vesicle interaction has been noted in intestinal epithelium (266) and in proximal convoluted kidney tubules (267, 268, 269, 270).

Small and smooth surfaced vesicles which are indistinguishable from golgi elements which are characteristically found in abundance in the perinuclear cytoplasm, are also numerous in the apical cytoplasm. These vesicles are frequently observed in the process of fusing with the absorption and multivesicular vacuoles as well as with intermediate sized vacuoles which appear to be engulfing the surrounding ribosomal rich cytoplasm (autophagic vacuoles). Since acid phosphatase has been localized in these multivesicular and dense bodies (258), it is reasonable to suggest that the golgi-like vesicles, which in the rat prostatic, seminal vesicle (271) and intestinal epithelium (272) have been described as "pure" or "virgin" lysosomes, discharge hydrolytic enzymes into the absorption and autophagic vacuoles. These enzymes could then take part in either the breakdown of the ingested materials or synthesis of new products. In vitro studies of the visceral yolk sac have shown

that it is able to produce lytic enzymes (273) as well as to synthesize several compounds (139, 274). The vacuoles containing dense granular material and myelin figures so characteristically found in the latter stages of gestation, might then represent residual bodies which store materials not utilized by the visceral endodermal cells. Similar transformation of lysosomal vesicles to dense or residual bodies has been described as occurring during the intracellular digestive process in mammalian tissue culture cells (275). Furthermore, it has been shown that lysosomes perform the function of storage of metabolically inert materials (276).

This scheme of absorptive activity would appear to be consistent with experimental studies of the sequential absorption of colloidal gold, saccharated iron, lipids, colloidal carbon, egg albumin, bovine gamma globulin, salivary gland virus (133, 134), thorotrast (135, 257) and ferritin (257) from the uterine lumen. In these studies the various materials were described as entering the visceral endodermal cells in fuzzy-lined apical invaginations which, once free within the cytoplasm, coalesced to form large multivesicular bodies. Except for ferritin, there was no evidence reported that any of these materials were subsequently transported from the epithelial cells to the subjacent connective tissues, vitelline vessels or mesothelium. As for ferritin, it appeared in apical vacuoles at all stages of gestation, but was transported to the vitelline vessels and mesothelium on only the 20th and 21st days of gestation (257). It would thus appear that the visceral endodermal cells undergo some change near the end of pregnancy which allows the transport of certain materials. The fact that the placental labyrinth acts as a barrier to the transport of ferritin in a fetal

direction (200, 201) strengthens existing evidence (145, 148, 149) that the yolk sac is an important means of protein transport to the developing rat. It is well known that antibodies as well as other homologous and heterologous proteins are transported to the fetus during the last part of gestation (141, 142, 143, 144, 145, 146, 147, 148, 149, 150, 151, 152, 153). One might say, then, that the visceral epithelium of the yolk sac is unselective so far as absorption is concerned, but highly selective in the materials which it transports to the fetus. Since it has been shown that the visceral endoderm concentrates azodyes (277), some of which are known teratogens (278), the ability to absorb, segregate and store a wide variety of materials may well be interpreted as a defense mechanism to protect the developing fetus from potentially injurious substances within the uterine and/or yolk sac cavity.

Although the evidence is highly circumstantial, several suggestions may be proposed for the subsequent activities of the apical vacuoles. It could be suggested that the vacuoles which exhibit irregular and indistinct limiting membranes are in the process of breaking up and releasing their digested content into the surrounding cytoplasm. The raw materials thus exposed could be utilized for intracellular use or resynthesized by the granular endoplasmic reticulum and sequestered into the cisternae of the highly developed perinuclear complex of smooth endoplasmic reticulum for subsequent extracellular use. Recent ultrastructural studies of fat absorption in the rat intestinal epithelium suggest that triglycerides are synthesized by the endoplasmic reticulum from fatty acids and monoglycerides which are free within the cytoplasm (265). The vacuoles in the visceral endodermal cells which appear to be incorporating small golgi-like vesicles may actually be in the process

of budding off small vesicles which also contain materials (altered by digestive and/or synthetic activities) for extracellular use. Some of the small vesicles in the perinuclear cytoplasm may also represent cytopemptic vesicles which contain unaltered materials such as antibodies and other proteins destined for fetal utilization.

Throughout the greater part of gestation the lateral surfaces of the endodermal cells are closely apposed and attached at their apices by tight junctions which prevent the diffusion of materials from the yolk sac cavity or uterine lumen into the lateral intercellular spaces. By the 18th day, however, many of the lateral surface membranes proximal to the apical tight junctions become infolded which results in the formation of large intercellular dilatations. On the 22nd day, these intercellular dilatations are observed between all of the endodermal cells. Such structural changes would certainly provide a greater surface area for the exchange of materials. During these stages of gestation many smooth surface golgi-like vesicles are seen in close association with the basal and lateral cell surfaces. Since these golgi elements contain granular material which is optically similar to both that found in the intercellular spaces and apical vacuoles, it is suggested that some of the golgi vesicles in the perinuclear and basal cytoplasm are transport vesicles for the various materials which are to be elaborated extracellularly. Such a route has been described in the intestinal epithelium for the discharge of fat (266, 279, 280). This interpretation is also consistent with that given for the appearance of ferritin containing vesicles deep within the visceral endodermal cytoplasm (257).

In a discussion of the yolk sac ultrastructure, Schultz (258) has

proposed two alternate interpretations for the inter-relationships of the fuzzy-lined pinocytotic vesicles with larger vacuoles in the apical cytoplasm. In addition to serving the process of endocytosis, Schultz suggests that the vacuoles, fuzzy-lined vesicles and apical canalicular system may serve as a route for either the elimination of membrane remnants and residual materials or the elimination of secretory products from the yolk sac epithelial cells. In the latter case, the secretory product is presumed to form in the endoplasmic reticulum and accumulate in the apical vacuoles. Although Schultz's observations as well as those of other investigators do not provide structural evidence of secretory activities, it has been demonstrated, in tissue culture studies, that the visceral yolk sac is secretory in nature (131). Secretory activity as outlined by Schultz has not been observed in the present study. On the 12th through the 25th days of gestation, however, the apical surface of the visceral epithelium exhibits prominent granular filled clavate microvilli which, due to the presence of similar free floating vesicles in the yolk sac cavity and uterine lumen, are interpreted, as in other tissues, as being secretory in nature (195, 228, 235, 236, 237). As gestation advances the microvilli are observed to fall in height and become pleomorphic. Such structural changes have also been interpreted as indicating greater secretory activity (228).

The vacuoles in the apical cytoplasm which variously contain myelin figures, clumps of granular material, small vesicular profiles and clusters of membrane bound lipid droplets are of particular interest. Lambson (257) has observed the occurrence of similar lipid containing vacuoles in the visceral endodermal cells from the 16th to 21st days of gestation. In the present study, however, these vacuoles appear ex-

clusively on the 12th day of gestation and except for the presence of lipid clusters are similar to the acid phosphatase containing multivesicular bodies described by Schultz as completely disappearing by the 14th day of gestation. It is quite likely that these vacuoles represent the storate depots for anisotropic lipid which has been described as being maximally absorbed and stored in the supranuclear cytoplasm of the visceral epithelium on the 13th day of gestation (48, 131). Sorokin and Padykula (131) have shown that cholesterol-rich lipid which is absorbed in vitro appears within the supranuclear cytoplasm in smooth surfaced vesicles which similarly concentrate in large vacuoles. Whether fat enters the yolk sac endoderm by particulate absorption (pinocytosis) of unhydrolyzed triglycerides (266, 281) or by the diffusion of monoglycerides and free fatty acids which are resynthesized by the smooth endoplasmic reticulum (265, 282, 283, 284) is not known. Although the present study does not resolve this question, the presence of osmiophilic vesicles beneath the apical surface membrane and the occurrence of a well developed complex of smooth endoplasmic reticulum in the supranuclear cytoplasm suggests that both mechanisms of entry may occur. Lipid droplets which are clearly not membrane bound also occur in the perinuclear and basal cytoplasm. Although this lipid appears to be ultrastructurally identical to that in the apical cytoplasm, its actual relationship to the membrane enclosed droplets is not known.

Throughout gestation lipid inclusions are found within the nuclei of the endodermal and mesothelial cells. Luse and associates (132, 133, 134) have described similar nuclear inclusions in the rabbit and mouse yolk sac and in the intestinal epithelia of newborn rats. These investi-

gators suggest that different materials (colloidal iron and carbon and salivary gland virus) may enter the nuclei of these cells through either nuclear pores or by pinocytosis.

After passing through the visceral epithelium, macromolecules, as have been shown experimentally, enter the fetus by way of the vitelline vessels and the mesothelium (145, 149, 257). Ultrastructurally, both of these structures exhibit features which have been described as facilitating diffusion and transport (207). The endothelial lining of the vitelline vessels becomes increasingly attenuated with advancing gestational age and exhibits frequent fenestrations and pinocytotic vesicles. In addition to pinocytotic activity there is a striking increase in the surface area of the mesothelium towards term by the formation of numerous surface evaginations.

Cytochemistry

Ultrastructural studies of the rat placental barrier have not only revealed the persistence of trophoblast throughout gestation, but have shown that it also consists of three discrete cytoplasmic layers. Its continued presence favors the supposition advanced through histochemical studies that phosphatase enzyme activities are principally located in the trophoblast rather than in the fetal endothelium (37, 41). Since the thickness of the labyrinthine barrier is at the lower limits of resolution with the light microscope, recent histochemical studies have not been able to ascertain with which layers of trophoblast these enzyme activities are associated (38).

Utilizing current methods for electron cytochemistry, it has now been possible to describe the fine structural localization of ATP-, ADP- and AMPase activities in the labyrinthine and visceral yolk sac placentas. The localization of enzyme-active sites in cells at the electron microscope level, however, depends on the degree of tissue preservation and the amount of enzyme activity that survives the rigors of tissue preparation and histochemical incubation. Therefore, before discussing the possibilities as to the significance of the present cytochemical findings, a brief account should be made with regard to the methods utilized in this study as well as to the specificity of the adenosine nucleoside phosphatase reactions.

Glutaraldehyde as employed in the present study has been described as a powerful inhibitor of a number of enzyme activities. Farquhar and Palade (285), in a recent cytochemical study of amphibian epidermis, found that 60 to 70 percent of ATPase activity is lost during glutaraldehyde fixation. It has also been shown that many plasma

membrane nucleoside phosphatase activities, demonstrated in the presence of magnesium (160) or manganese ions (286, 287), as well as nucleoside diphosphatase activities in the endoplasmic reticulum (287, 288) and golgi saccules (286), are far more inhibited by a 60 to 90 minute fixation in cold 5 to 6 percent glutaraldehyde (159) than by overnight fixation in cold 4 percent formaldehyde (289). In an additional comparative study of the inhibitory effects of glutaraldehyde and formaldehyde fixation on ATPase activity, Goldfischer and associates (290) found that activity on the surface membranes of capillary endothelial cells of the rat kidney survives overnight fixation in 4 percent formaldehyde-calcium, but fails to do so with 60 to 90 minutes of 5 percent glutaraldehyde-cacodylate fixation. On the basis of these findings, Goldfischer and associates (290) recommend that formaldehyde fixation be used for phosphatase cytochemistry in order to avoid this source of error. In the present study, however, the distribution of ATP-, ADP- and AMPase activities was found to be essentially the same whether the tissues were fixed in formaldehyde-calcium or glutaraldehyde. Furthermore, the intensities of the three reactions appeared to be much greater in the latter fixative. It would appear that adenosine nucleoside phosphatase activities in the placental labyrinth and visceral yolk sac are inhibited more by overnight formaldehyde fixation than by glutaraldehyde fixation. Similar observations have been described for nucleoside triphosphatase activity on the plasma membranes of cells in the proximal convoluted tubules of the rat kidney (291). In addition to preserving greater levels of enzymatic activities, the use of glutaraldehyde was found, as in other tissues (159, 292, 293), to provide a far superior maintenance of ultra-

structure when compared with formaldehyde.

The appearance of myelin figures and irregular pale areas where part of the cytoplasm seems to be washed out are readily recognized structural artifacts produced during glutaraldehyde fixation and incubation (285, 290). Sabatini and associates (292) have cautioned that the quality of glutaraldehyde fixation decreases, despite buffering to pH 7.4, when its pH falls below 3.5 as a result of impurities or oxidation. Farquhar and Palade (285) have also warned that contaminants in glutaraldehyde such as glutaric and tartaric acid may inhibit nucleoside phosphatase activities. Although it would have been desirable to have used redistilled glutaraldehyde, only that with a pH above 3.5 (Union Carbide) was utilized in the present study.

Pb^{2+}, which is used as the phosphate trapping agent in the Wachstein Meisel method (160), has also been described as markedly inhibiting nucleoside phosphatase activities (285, 294, 295, 296, 297). In an attempt to avoid such inhibition, the placental tissues were incubated according to the method of Padykula and Herman (298). This method differs from that of Wachstein and Meisel (160) in that calcium instead of lead is used as the phosphate capture agent. The localization of the enzyme activities obtained with this method, however, was not as sharp as that demonstrated with the Wachstein Meisel medium.

Since the extent to which glutaraldehyde and Pb^{2+} inhibit ATP-, ADP- and AMPase activities has not been established in the present study, one must bear in mind that the absence of final reaction product along the surface membranes of trophoblast III, connective tissue cells and labyrinthine and vitelline vessels may actually indicate the presence of low levels of enzyme activity which have been inhibited.

Recently a number of investigators have discussed the advantages and disadvantages of using blocks of tissue in electron histochemistry (159, 286, 290, 292, 299, 300, 301). Holt and Hicks (299) and Goldfischer and associates (290) have shown that when tissue sections exceed 50 u in thickness, the exposure of the cells to the fixative is not uniform, a fixation gradient occurs from the periphery to the center of the block and the exact time of exposure of the cells to the fixative cannot be accurately estimated. As a result of these difficulties, a false localization of enzyme activity in the well fixed periphery of the block may arise from the diffusion of soluble enzymes or reaction product from the inadequately fixed core (290). False localization in tissue blocks may also occur as a result of the potentially different rates of penetration of histochemical substrates and capture reagents (292, 301). Goldfischer and associates (290) have shown that false reactions may be consistently avoided when frozen sections not thicker than 60 u are used. The use of frozen sections, however, has been repeatedly shown to cause structural artifacts (285, 292, 301).

In the present study, comparisons were made of the distribution and intensities of final reaction product between 50 u frozen sections and small unfrozen blocks of the placental labyrinth and visceral yolk sac. The results of this comparison indicated that no differences in the enzymatic activities occurred between the two procedures. Since unfrozen tissues consistently provided better preservation of fine structure, it was preferred to work mainly with tissue blocks while using frozen sections as controls. In future studies, however, it would be desirable to use 50 u sections cut on the recently developed Smith

Farquhar tissue chopper which avoids specimen freezing (302, 303).

It is extremely difficult to ascertain cytochemically the specificity of phosphatase reactions in prefixed tissues. Although specific substrates have been used in the present study, it has been reported that nonspecific alkaline phosphatase, apyrase, Ca^{++} and Mg^{++} activated ATPase and SH-dependent-independent- and sensitive enzymes are capable of splitting phosphates from ATP (304, 305, 306, 307, 308, 309, 310, 311, 312, 313). Similarly, ADP and AMP substrates may be hydrolyzed by apyrase, adenosine 5' nucleotidase (AMPase) and adenylate kinase (314). Biochemically, many of these enzymes have been characterized as to their specific activators and inhibitors. Nucleosidetriphosphatases extracted from plasma membranes are described as being activated by Mg^{++} and further stimulated by the simultaneous addition of Na^{+} and K^{+} (295, 315, 316, 317, 318, 319, 320, 321). Only the Na^{+} and K^{+} dependent activity is specifically inhibited by ouabain and is, therefore, referred to as the ATPase enzyme participating in active cation transport (316, 322).

On the basis of these biochemical studies, attempts have been made to characterize nucleoside phosphatase activities, demonstrated at the ultrastructural level, in terms of activation by Na^{+}, K^{+} and Mg^{++} and inhibition by ouabain, p-chloromercuribenzoic acid and n-ethyl maleimide (285, 323, 324). The results of these experiments, however, have been negative in that the enzymatic activities were neither totally inhibited or markedly activated by these agents. These findings may well indicate that aldehyde fixation, in addition to partially inhibiting enzyme activities, may also alter the sensitivities of nucleoside dephosphorylating enzymes to activators and inhibitors (297, 323). On the other hand,

since the ratio between $Mg^{++} + Na^{+} + K^{+}$ activated enzyme and Mg^{++} activated enzyme varies with the tissue (295, 321, 325, 326) and preparation procedure (319, 321, 327), one would expect the chances of determining activation and inhibition through a qualitative cytochemical procedure to be rather limited. Farquhar and Palade (285) have suggested that slight differences in the intensities of the final reaction product may be due to variations in the thickness of the tissue specimens rather than to specific activators and inhibitors.

Although specific activators (other than Mg^{++}) and inhibitors have not been used in this investigation, several assumptions may be made as to the specificity of the three enzyme reactions reported here. First, it may be assumed that the hydrolysis of the three nucleoside phosphate substrates is not due to a nonspecific alkaline phosphatase. Recently, Ahmed and King (328) have reported that 0.001 M arsenate strongly inhibits placental alkaline phosphatase and that this inhibition could not be reversed by magnesium. Since the tissue specimens in this study were washed in 0.1 M dimethylarsenic acid (Na cacodylate) for periods of at least 24 hours prior to incubation, it may be assumed that alkaline phosphatase activity is inhibited. This assumption would appear to be verified by the fact that when equimolar concentrations of sodium glycerophosphate or phenylphosphate were substituted as substrate, there was no evidence of dephosphorylating activity even after extended periods of incubation. Furthermore, when the tissues were incubated according to the Gomori method (329) for the demonstration of alkaline phosphatase, no reaction occurred at the light microscope level when the tissues had been prewashed in sodium cacodylate. Similarly, when control tissues were incubated in a substrate free medium, no reaction occurred. This would indicate that the final reaction product

observed in the experimental tissues is not due to a nonspecific binding of lead with protein.

Since the possibility exists that the commercially available adenosine nucleoside phosphate substrates contain inorganic phosphate contaminants and that a nonspecific hydrolysis of the substrates could occur before or during the cytochemical incubation (301), tissues were incubated in a medium containing precipitated lead phosphate. The distribution of the lead phosphate deposits in these cloudy controls, when compared with enzymically deposited lead phosphate, was sparsely and diffusely localized with no particular association with cell membranes.

The striking similarity in the distribution of ATP, ADP and AMP hydrolysis products raises the question as to whether a single nucleoside phosphatase might not be responsible for all of the activity. In the yolk sac, this possibility is rendered less likely by the fact that there is a sequential appearance of activity with the three substrates. On the 12th day of gestation, ATP is hydrolyzed, but not ADP or AMP. On the 14th and 18th days, both ATP and ADP substrates are hydrolyzed and on the 22nd and 25th days even AMP to a limited degree. Furthermore, the distribution and intensities of the final reaction product vary with the three substrates. These findings suggest that at least three different nucleoside phosphatase activities (ATPase, ADPase and AMPase) are present at different stages of gestation in the visceral yolk sac placenta. Similar interpretations have been given for the specificity of golgi localized testicular phosphatases (301) and nucleoside phosphatases in cerebral capillaries (330). Although it cannot be stated with certainty that the three activities in the placental labyrinth are not properties of the same enzyme (apyrase), it has been demonstrated

by biochemical analysis that the human placenta contains ATP-, ADP- and AMPase activities (331).

Many tissues known to be actively engaged in fluid transport show a histochemical localization of nucleoside phosphatase activities restricted to, or predominantly associated with, cell membranes in electron microscope preparations. These tissues include the mammalian kidney tubules (290, 332, 333), gall bladder (334), colon (335), urinary bladder (336), ciliary epithelium (337), corneal endothelium and epithelium (338, 339) and frog epidermis (285). Since biochemical studies indicate that cation-activated adenosine nucleoside phosphatases are associated with plasma membranes (320), it is suggested here, as in the aforementioned investigations, that ATP-, ADP- and AMPase activities, distributed on the surface membranes of the placental labyrinth and visceral yolk sac, function in the regulation of electrolyte and water transport across the placental barrier and in some way monitor the passage of these substances as well as macromolecules.

Since pinocytotic vesicles including caveolae have been shown to be active in the transport of substance across the placental barrier (200, 201, 257), it is conceivable that the nucleoside phosphatase enzymes, as suggested by Marchesi and Barrnett (324, 340), might function in the formation or activation of cell membranes which form the vesicles. If this is the case, then it may be significant that the maternal surface of trophoblast II and the apical surface of the visceral epithelium, which are the surfaces most actively engaged in pinocytotic activities, demonstrate the most intense enzymatic activity throughout gestation. Many of the pinocytotic vesicles at these sites also demonstrate final reaction product associated with their luminal surface. Marchesi and

Barrnett (324) have suggested that ATPase activity within pinocytotic vesicles could function to maintain the electrolyte differences between the contents of the vesicle and that of the cytoplasm. In this case, the enzyme might function as a cation pump similar to that described biochemically in other tissues (316, 322). Similarly, the association of ATP-, ADP- and AMPase activities with the lateral surface membranes of the visceral endodermal cells might serve to maintain electrolyte gradients across the membranes (341). No explanation is apparent for the abrupt loss of these enzyme activities along the basal and lateral surface membranes of the yolk sac epithelium on the 18th day of gestation. This loss, however, can be correlated with the dilation of the intercellular spaces which occurs at that time.

The absence of ATP-, ADP- and AMPase enzyme activities in the endothelial cells of the labyrinthine and vitelline vessels is consistent with similar observations showing that nucleoside phosphatase activities are not present in the endothelial cells of the rat glomerular and peritubular capillaries of the kidney, and vessels in the small intestine, thyroid, retina and cerebral cortex (324, 341, 342). Marchesi and associates (324, 341) have suggested that the lack of enzymatic activity in endothelial cells may have some bearing on the peculiar permeability properties of these vessels.

The observation of final reaction product in the visceral basement membrane and connective tissue space surrounding the vitelline vessels on the 12th and 14th days of gestation is also consistent with findings in the retina (324, 341) and brain (330, 342). Although the possibility exists that this localization is artifactual, Marchesi and associates (324, 341) hypothesize that an enzymatically active basement membrane

may actually facilitate transport of some materials rather than serving as a barrier.

Torack and Barrnett (330) suggest that the barrier function of cerebral capillaries resides in the lack of nucleoside phosphatase activity in the endothelial membranes. Although it would appear that the labyrinthine and vitelline vessels also lack adenosine nucleoside phosphatase activities, transport studies (200, 201, 257) indicate that the endothelium of these vessels and their accompanying basement membranes do not act as a barrier to the passage of ferritin. Since the fetal capillaries of the rat placenta are fenestrated, a good deal of transport may occur through these openings. If so, one might expect the endothelial cells to possess little or no transport adenosine nucleoside phosphatase activity. Such has been the interpretation for the absence of nucleoside phosphatase activity in kidney, intestinal and thyroid vessels (324).

The lag in appearance of ADP- and AMPase activities in the visceral yolk sac may suggest that they assume functional roles in the later stages of gestation. Similarly, the variations observed in the intensities of the reactions in both the placental labyrinth and visceral yolk sac at different stages of gestation may suggest that the three substrates (ATP, ADP and AMP) play active roles at different stages of gestation.

On the 22nd and 25th days of gestation large accumulations of extraneous materials are frequently seen in association with the visceral epithelium. In these areas enzyme activity on the apical surface of the endodermal cells is absent. On the other hand, adjacent areas which are free of the extraneous material exhibit intense re-

actions. Since it has been shown that surface coatings are capable of bringing about an inactivation of critical enzymes in the erythrocyte stroma (343), it is suggested that the absence of enzyme activity is a result of their inactivation by the extraneous material.

Ageing

Aside from progressive morphological changes, the question arises as to whether, beginning some time late in gestation, the placenta undergoes regressive or degenerative changes which have an unfavorable effect on placental exchange. In reviews of the literature, Wislocki (344) and Villee (345) have emphasized the fact that there is relatively little substantial data upon which to answer this question.

Biochemical methods of determining the amount and direction of placental change have shown that in a clinically normal human pregnancy the placenta exhibits a decline in oxygen consumption, a decrease in glycogen content, a loss in the ability to produce glucose and glycogen, and a marked decrease in lactate production as gestation approaches term (346, 347, 348, 349, 350). These changes have been interpreted as indicating that the placenta undergoes unfavorable senescence during late gestation.

Metabolic ageing has also been demonstrated through histochemical studies. Placental ribonucleoprotein, seen as cytoplasmic basophilia in light microscope preparations and as free and attached ribosomes in electron microscope preparations, has been shown to undergo a steady decline with increasing gestational age, whereas acid and alkaline phosphatase activities, which are minimal in amount during the first trimester, increase steadily towards term (31, 36, 48, 71, 351, 352). In late gestation, however, alkaline glycerophosphatase as well as adenosine triphosphatase, esterase and succinic dehydrogenase activities also decline (38, 48, 344). The storage of lipid and glycogen substances are also seen to diminish perceptibly toward the end of gestation (48, 137, 139). The fact that these changes do not occur in a regular

sequence has been interpreted by Huggett (353) as indicating that different functions are exercised by the placenta at different ages. The validity of this hypothesis would appear to be substantiated by the histochemical and biochemical studies of McKay et al. (29, 30), Padykula (38) and Padykula and Richardson (139). These authors reported that when the glycogen content and certain enzymatic activities decline in the human and rat placentas they appear in the fetal liver with good temporal correlation. Such observations would also support the hypothesis first advanced by Claude Bernard (354) that the placenta functions in part as a fetal liver in the synthesis and storage of glycogen and in the secretion of glucose for fetal utilization. As for the decline in cytoplasmic basophilia, Wislocki and associates (355) have suggested that the ribonucleoprotein (basophilia) represents a provision for the synthesis of proteins necessary for fetal growth until this function is assumed by the fetal liver. Therefore, rather than equating decreasing metabolic activities with placental ageing, Padykula (99) and Wislocki and Padykula (48) have suggested that terminal changes should be interpreted as a redistribution of the functional activities of the placental-fetal complex.

Unfavorable terminal morphological changes that occur in the human placenta to which more attention has been devoted, have been variously described. According to Hertig (356), Hellman (357), Shanklin (358) and Fox (359), the earliest and most frequently noted manifestations of placental ageing are the deposition of fibrin, calcium and fibrinoid in the intervillous spaces and the gathering of syncytial nuclei in small areas on one side of the chorionic villus as "buds" or "knots". Villee (346) has observed an increase in the solid fraction of the term placenta

which McKay and associates (32) attribute to the thickening of basement membranes of fetal capillaries and trophoblast cells. More severe degenerative changes such as ischemic necrosis due to dense accumulations of intervillous fibrin and hemorrhagic infarctions have been described as occurring in a variable number of chorionic villi (32, 360, 361). To what extent these morphological changes effect the overall efficiency of placental exchange, however, is still a matter of conjecture.

Obvious morphological age changes such as those observed in the term human placenta have not been described as occurring in either the term chorio-allantoic or yolk sac placentas of the rat (131). This difference is thought to be due to the relatively brief gestation period of the rat (22 days) as compared with that for humans (9 months) (344). Therefore, age changes in the rat placental labyrinth and visceral yolk sac have very little time in which to express themselves. There have been no studies designed, however, to determine whether the definitive placentas of mammals with long gestation show more terminal age changes than those with short gestation. Even though obvious morphological age changes have not been reported as occurring in the rodent placenta, Flexner et al. (6) have shown that there is a sharp decline in the rate of transport of radioactive sodium across the chorio-allantoic placenta of the rat just as there is in the human placenta during the last ten percent of intrauterine life (7). On the other hand, in vivo transport studies of antibodies across the visceral yolk sac would indicate that there is a steady increase in the rate of transfer from the 17th day of gestation to term (145, 146, 153). Sorokin and Padykula (131) suggest that this increase rate of transport may be directly related to the growth or expansion of the visceral yolk sac

during this period. An increase in transfer rate towards term, however, does not necessarily indicate increased efficiency. For example, Padykula and Wilson (156) found that the absorption of vitamin B_{12} intrinsic factor complex by the rat visceral yolk sac from 13 days of gestation to term increases only 5-fold whereas the weight of the membranes increases 50-fold. Such evidence would suggest a decreased absorptive capacity by the visceral yolk sac at term.

When ultrastructurally compared with the extraembryonic membranes in early pregnancy, the near term placental labyrinth and visceral yolk sac of the rat are found to undergo a kaleidoscopic series of morphological changes. For the most part, these changes probably reflect a series of steps in the differentiation and function of these membranes. Therefore, one must exercise caution in distinguishing between progressive and regressive age changes.

In the present study, the most noticeable terminal changes in the placental labyrinth which may be correlated with those changes attributable to ageing in the mature human placenta (48, 71, 78, 79) are a decrease in the overall thickness of the three layers of trophoblast, an increase in the incidence of mesenchymal cells and fibrils in the connective tissue space between trophoblast III and the fetal endothelium and an increase in the thickness of the basal laminae supporting these two layers. In the visceral yolk sac there is also a gradual increase in the numbers of mesenchymal cells and fibrils in the connective tissue space between the endodermal cells and the mesothelium and also a marked thickening of both the visceral and serosal basement membranes (basal laminae). A proliferation of mesenchymal cells near the end of gestation correlates well with the burst of tritium labelling observed in

both the placental labyrinth and visceral yolk sac on the 22nd day of pregnancy (170). An overgrowth of connective tissue elements has been considered a manifestation of morphological ageing or regression (131) and may well result in a decreased rate of active transport across the placental labyrinth and visceral yolk sac. The possibility that thickened basement membranes would retard the passage of various materials is strengthened by the observations of Farquhar and associates (197) who described the glomerular basement membrane as being a main barrier to filtration.

The only obvious evidence of unfavorable fine structural change in the rat placenta which may be related to early stages of degeneration is the occasional occurrence of deposits of fibrin-like material in the intercellular space between normal appearing trophoblast I and II layers and in the surface infoldings and/or channels of the latter. Whether the deposition of fibrin is initiated by some degenerative change undetectable by such a technique as electron microscopy is a matter of speculation and will be considered in greater detail further along in the discussion. It is reasonable to assume, however, that the deposition of fibrin in such areas would not only hinder active transport across the placental barrier, but would also decrease the rate of exchange of O_2 and CO_2 as well as the diffusion of wastes from the fetal to maternal circulations.

Both the deposition of intervillous fibrin (leading to thromboses) (362) and the diffuse thickening of fetal capillary and trophoblastic basement membranes (32) have been interpreted as causing a terminal decline in the rate of sodium transfer across the human placental barrier. Transposing the same principle to the rat placenta, it is tempting

to infer that these unfavorable morphological changes may also account, in part, for the terminal decline in sodium transport across the rodent placental barrier (6, 7).

Unlike regressive changes or ageing in the human placenta, there is no obvious decrease in the size and number of microvilli along the surface membranes bordering the maternal blood space nor is there a decrease in the number of trophoblastic elements comprising the placental barrier. In the visceral yolk sac, however, the epithelial brush border does fall in height and the microvilli appear pleomorphic and less branched. Since it has been demonstrated that the yolk sac is secretory in nature (131), these changes may reflect a functional state of the endodermal cells rather than terminal regressive changes as interpreted by other investigators (48). It is well known that an active discharge of secretions from secretory epithelia is accompanied by a disappearance or a decline in number and in length of microvilli (228).

Jollie (101) has interpreted cytoplasmic vacuolation, dilatation of cisternae of endoplasmic reticulum and mitochondrial ballooning in trophoblasts I and III on the 21st day of gestation as being evidence of degenerative changes. Since these cytomorphic changes are in accord with degenerative changes observed in trophoblastic giant and trophospongial cells (junctional zone elements), which have been shown to have a fixed life-span equivalent to the gestation period of the species, both in utero (363, 364) and in extrauterine grafts (365), Jollie (101) has suggested that the components of the placental labyrinth may also possess a similar fixity in life-span which would account for the selective changes observed in trophoblasts I and III. Although similar fine structural changes in the labyrinth were observed in the present study, it is felt that their interpretation warrants further consideration.

For example, the increase in cytoplasmic vacuolation of the layers of trophoblast at term may well reflect an increase in transport activities across the placental barrier as discussed earlier. Ballooned mitochondria with fragmented cristae and focally rarefied matrices occur in early as well as late stages of gestation and, therefore, may represent an osmotic problem introduced during specimen preparation rather than a manifestation of ageing. Mitochondria in the visceral yolk sac, however, do undergo structural alterations with increasing gestational age which may possibly be correlated with decreasing metabolic activity and, therefore, ageing. On the 12th day of gestation, the mitochondrial population appears homogeneous and exhibits a typical internal structure of transverse cristae. By the 22nd day, the population is decidedly heterogeneous. In addition to having transverse cristae, some of the mitochondria have longitudinally oriented cristae and others possess cristae which are transversely oriented at one end and longitudinally at the other. Karnovsky (366) has shown that there is a definite correlation between the fine structural arrangement of the inner mitochondrial membranes in the proximal tubular cells of the nephron of Rana pipiens and the degree of cytochrome oxidase activity which is considered to be an exclusively mitochondrial enzyme. In the summer, the mitochondria of the proximal tubules were found to have a high degree of cytochrome oxidase activity and transversely oriented cristae. In the winter, the cytochrome oxidase activity was found to be low or absent and the mitochondrial population heterogeneous with respect to the orientation of their inner membranes. Since mitochondria in the visceral yolk sac appear to undergo similar fine structural changes with increasing gestational age, it is tempting to infer that cytochrome

oxidase activity decreases in the term visceral yolk sac and that such morphological changes are regressive in nature.

Although the individual layers of trophoblast comprising the placental labyrinth may possibly have a fixed life-span, experimental evidence would suggest that terminal morphological changes in the yolk sac are imposed on the membrane and do not result from its inherent senility. Sorokin and Padykula (131) have reported that when near term visceral yolk sacs are cultured, the epithelial brush border increases in height, glycogen storage begins anew, enzymic levels remain elevated at an age corresponding to term in vivo and the explants preserve good morphology for considerable periods of time beyond the normal length of gestation. Furthermore, when parturition has been delayed either naturally or experimentally with the aid of hormones, placental membranes of rats (367), rabbits (368), cattle (369) and man (370) have survived for some time beyond the date of parturition normal for the species.

With regard to prolonged pregnancy, reports concerning concomitant metabolic, morphological and physiological changes in placental membranes are available, but the findings for the most part are conflicting and often confusing (371, 372, 373, 374, 375, 376, 377). As a result of the difficulty in the diagnosis of prolonged pregnancy, most morphological changes in the human placenta have been described as differing only in degree from the normal terminal regressive changes alluded to earlier in the discussion. Consequently, many investigators have concluded that postmature placentas show no increased degenerative changes over mature placentas (371, 378, 379).

In the domestic cow, prolonged gestation is a definite clinical

entity and occurs when the fetus is homozygous for a recessive autosomal gene, and is borne by a cow heterozygous for the gene. In such a genetically conditioned prolonged gestation, pregnancy which normally is 270 to 285 days has been reported to extend to 365 days in the Holstein-Friesian and up to 510 days in the Guernsey, the fetus being alive in utero during the post-term period. Morphological evidence indicates that the bovine placenta removed from such cows with prolonged pregnancies show retrogressive changes which are foreshadowed in the placentomes taken from normal cows at term (369). In rabbits and rats, pregnancy has been experimentally prolonged by treatment of the mother with either progesterone, estrone, gonadotrophins, mechanical interference or hypophysectomy (see Boe (367) for a review of the literature).

After administration of gonadotrophic extracts derived from the urine of pregnant women, rabbit fetuses remained alive and continued to grow for 4 to 6 days beyond the normal time of parturition, but eventually died when they became too large to be delivered (368). Tuchmann-Duplessis (380) has prolonged pregnancy in the rat for 3 or 4 days and reports that both the placental and fetal weights increase during this period. Since the placentas appeared quite normal at the end of the protracted periods, Tuchmann-Duplessis suggested that the placenta is able to function in fetal maternal exchange for a longer period of time than it normally does without showing ageing phenomena. Observations in the present study, however, do not support this suggestion, as fine structural changes, which are interpreted as ageing or regression, are found in the rat placenta when pregnancy is prolonged beyond the normal time of parturition. Furthermore, the maximum time of which pregnancy could be successfully prolonged with the fetuses being alive in utero

was found to be 3 days (a total gestation period of 25 days). When gestation exceeded this length of time, the incidence of dead fetuses increased tremendously and at 26 days of gestation all fetuses were dead.

Of all the studies of prolonged gestation, a review of the literature indicates that only that of Boe (367) has been concerned to any extent with histological changes in the rat extraembryonic membranes. In this study, he reports that gestation in rats which normally deliver at 22½ days could be successfully extended to 24½ days. The most marked histological changes observed in the chorio-allantoic placenta at this stage were a variable amount of necrosis and hyalinization of the junctional zone elements. Other than a rather pronounced hyperemia of the maternal blood channels with occasional deposits of a homogeneous pink substance (presumably fibrin), the labyrinthine portion of the placentas with living fetuses were described as exhibiting very little change as compared with the histological picture at 22½ days (term). When gestation was prolonged to 25 and 26 days, however, the trabeculae of the labyrinth appeared shrunken, homogeneous and entirely pinkish (hyalinized). All of the fetuses were also reported as being dead in utero on these days. On the 25th day of prolonged gestation in the present study, the junctional zone was found to exhibit similar degenerative changes as those described by Boe (ischemic necrosis due to dense accumulations of fibrin and hemorrhagic infarctions). In addition to changes in the junctional zone, however, degenerative changes were also found to occur in the trabeculae of the placental labyrinth. Since many of the trabeculae of the term placental labyrinth have a total thickness (2-3 u) which is at the lower limits of practical resolution of the light microscope, it is understandable why Boe, who utilized the light microscope for his study,

did not detect degenerative changes in the placental labyrinth.

The fact that pregnancy extended beyond 24½ days was not compatible with fetal survival in his study, whereas gestation extended to 25 days in this study was, may possibly be accounted for by either the less stringent method of timing pregnancy in the former study, the differences in the dates of gestation when hormonal substances were administered to the mothers or a strain variation in length of normal gestation. In the present study, estrogen and progesterone were given to the mothers daily from the 20th day to the 24th day of pregnancy, whereas Boe gave daily doses of gonadotrophic extracts on either the 16th through 21st days of gestation or on the 19th through the 21st days. In view of recent evidence which suggests that the persistence of trophoblastic elements is maintained by progesterone (364), which is in turn related to the action of chorionic gonadotrophins, it is tempting to suggest that, in Boe's study, the circulating levels of progesterone gradually declined to a level at 24½ days where gestation was maintained, but not the integrity of the placental barrier, which, once lost, resulted in the death of the fetuses. It is noteworthy that the incidence of dead fetuses was much lower when gonadotrophic extracts were given over the six day period (16 to 21 days).

The most consistent morphological changes observed in the placental labyrinth when gestation is prolonged to 25 days are the increased incidence of connective tissue cells and fibrils intervening between trophoblast III and the fetal endothelium and the occurrence of a moderately electron dense amorphous material surrounding each of the trophoblast layers as well as the connective tissue cells and fibrils and the fetal endothelium. According to McKay et al. (32), an increased

production of intercellular glycoproteins, mucopolysaccharides, and collagen is associated with ischemia. An increase in mucopolysaccharide production has also been associated with anoxia (381). This extracellular appearing lamina or glycocalyx is also somewhat similar to the amorphous electron dense fibrinoid substance so frequently noted in the rat (99, 382), guinea-pig (105), carnivore (47) and man (Nitabuch's layer) (383) as separating the maternal and fetal components of the placenta. Bradbury et al. (384) have suggested that the fibrinoid material in the mouse placenta acts as a barrier to prevent the egress of fetal antigens into the mother. It is, therefore, tempting to transpose the same principle to the extracellular coating observed in prolonged gestation and suggest that it behaves as an immunological no-man's land, walling the fetus from chemical interaction with the mother.

On the 25th day of gestation, there is also an increased deposition of fibrin-like material in the intercellular spaces between trophoblasts I and II and in the infoldings or channels along the outer surface of the latter layer. When this material occludes the surface infoldings of trophoblast II, it exhibits a periodicity similar to that which is characteristic for fibrin (Figures 55 and 56). In these sites the trophoblastic cytoplasm appears rarefied with few obvious ribonucleoprotein granules, the plasma membranes are indistinct and the mitochondria are ballooned and appear granular with no apparent inner membranes. In other areas where accumulations of fibrin-like material occlude the intercellular spaces the three layers of trophoblast appear abnormally granular or fibrillar and exhibit areas of focal necrosis. In such areas the cytoplasm is either highly vacuolated (foamy degenera-

tion) or totally disorganized and rarefied. In addition, the limiting membranes are indistinct. Even the more normal appearing trophoblast exhibits some degree of degenerative changes (e.g., cytoplasmic vacuolation, dilatation of cisternae of endoplasmic reticulum, mitochondrial disruption and focal disintegration of plasma membranes). As for the fetal vessels, the endothelial lining appears intact, but the cytoplasm also has a definite granular to fibrillar texture and exhibits degenerating organelles.

Whether the deposition of fibrin is initiated by degenerative changes in the placental labyrinth or by thrombi in the maternal blood channels is not known. Although fibrin deposits are generally regarded as a feature of normal placental ageing (385, 386, 387), the present observations would suggest that its deposition leads to ischemic necrosis and, therefore, is an early sign of placental degeneration. A similar deposition of fibrin with related ischemic necrosis has been described at the fine structural level in erythroblastic placentas (388).

As far as can be determined by a literature search, there have been no <u>in vivo</u> studies of the visceral yolk sac in prolonged gestation.

Unlike the labyrinthine placenta, the visceral yolk sac does not exhibit obvious areas of cellular deterioration when gestation has been extended three days beyond the normal time of parturition. The visceral epithelium, however, does become attenuated so that it appears to consist of overlapping squamous to low cuboidal endodermal cells. As compared with term, the lateral surface membranes of adjoining cells exhibit loose interdigitations and for the most part are closely apposed. In addition to being attached by desmosomes, the lateral surface membranes

are also joined through intermediate junctions (zonula adherens). This appearance, when added to the fact that the basal surface of the endodermal cells appear relatively smooth and have few infoldings and pedicel-like foot processes as compared with term, suggests that there may be a reduction in the amount of fluid transport across the visceral yolk sac at this stage. Such an appearance, however, may also be a structural attempt for the conservation of fluids.

Although the cytoplasm of the endodermal cells appears abnormally granular or fibrillar and contains ballooned mitochondria, both of which are features described as being regressive changes in the term guinea pig yolk sac placenta (155), it is difficult to evaluate the significance of the numerous vesicles and vacuoles which contain myelin-like figures and granular materials of varying densities. The mesothelium, like the visceral epithelium, for the most part, exhibits no remarkable structural abnormalities at the electron microscope level such as those observed in the placental labyrinth. Nevertheless, the mesothelial cell cytoplasm frequently appears abnormally granular and contains an increased number of branching bundles of fine fibrils and ballooned mitochondria.

Since the visceral and serosal basal laminae are decidedly thickened and the connective tissue space packed with fibrils, it would appear that the mesenchymal cells not only continue to flourish in prolonged gestation, but are stimulated to produce heavy deposits of extracellular fibrils and ground substance. Such an overgrowth of the visceral yolk sac by connective tissue elements in an <u>in vitro</u> study has been described as leading to the loss of the membrane's histological integrity, the formation of foci of necrosis and eventually the death

of the cultures (131). Whether the overgrowth of the connective tissue elements foreshadows the regressive changes observed in the visceral epithelium and mesothelium is not known. It is reasonable to assume, however, that the deposition of extracellular material by the mesenchymal cells increasingly separates the endodermal and mesothelial cells from functional interactions. Such interactions may possibly be necessary for the maintenance of specific morphological and biochemical characteristics of the visceral yolk sac (131).

Ageing Cytochemistry

On the 25th day of gestation, the three nucleoside phosphatase activities are found to be distributed at the same fine structural sites as described on the 22nd day (term), but at different intensities (see Table II). In the placental labyrinth there is a marked decrease in the amount of final reaction product deposited along the fetal and maternal surface membranes of trophoblast I and the maternal surface of trophoblast II. Where deposits of fibrin occur in the intercellular spaces, the final product is less associated with the bordering surface membranes and is predominantly deposited in the accumulations of fibrin. In areas where trophoblast I exhibits extensive necrosis, the hydrolysis products of all three substrates are diffusely scattered throughout the cytoplasm. On the other hand, areas of ischemic necrosis in trophoblast II are free of such activity.

In the visceral yolk sac ATPase and AMPase activities, which are distributed along the free surfaces of the visceral epithelium and mesothelium, exhibit little change over that described on the 22nd day of gestation. ADPase activity along the apical surface of the endodermal cells, however, appears to increase in intensity.

The complete absence of lead staining in control sections would suggest that the distribution of lead phosphate in fibrin deposits, accumulations of granular material and areas of focal degeneration are not due to nonspecific metallophilia.

On the basis of these observations, it would appear that the visceral yolk sac is as enzymatically active on the 25th day of gestation as on the 22nd day (term). As for the placental labyrinth, the decline in ATP-, ADP- and AMPase nucleoside activities might well be regarded as

a regressive change, especially if one assumes that these enzymes are involved in the regulation of transport activities.

Since electron microscopy presents great obstacles to adequate histological sampling, it is extremely difficult, if not impossible, to determine the extent to which regressive and degenerative changes effect normal placental functions. There is certainly a need for further morphological as well as biochemical and physiological studies of placental membranes in postmaturity.

SUMMARY

The ultrastructure and fine structural localization of adenosine mono-, di- and triphosphatase enzyme activities in the rat labyrinthine and visceral yolk sac placentas are described on the 12th, 14th, 18th and 22nd days of gestation with supplementary observations on specimens experimentally prolonged three days beyond the time of normal parturition.

At all stages, the vascular placental labyrinth is composed of three trophoblastic layers supported by a basal lamina and a fetal capillary consisting of a basal lamina bearing a lining of endothelial cells. In order from the maternal blood sinus to the fetal capillary lumen, these layers are: (a) trophoblast I, a cellular layer; (b) trophoblast II, a syncytial layer; (c) trophoblast III, also a syncytial layer; and (d) fetal endothelium. Throughout gestation these layers exhibit features which have been described as facilitating transport.

In addition to vascular trophoblastic lamellae, the 12 day placental labyrinth possesses numerous cords of avascular trophoblast which are described as probable intermediate stages in the differentiation of junctional zone elements (giant trophoblast cells, spongiotrophoblast and glycogen cells) and vascular labyrinthine trophoblast.

The final reaction product resulting from the hydrolysis of adenosine mono-, di- and triphosphatase substrates was deposited, in all stages, at the same fine structural localization. Of these substrates, less activity was displayed with ADP. Fine granular deposits of lead phosphate were confined to the surface membranes of trophoblast I and the maternal surface of trophoblast II. In the post mature labyrinth the intensities of all three enzyme activities were markedly reduced in areas of cellular degeneration.

At all stages of gestation the visceral yolk sac is composed of a single layer of endodermal cells resting on a highly vascularized layer of splanchnic mesoderm. The mesenchymal elements comprising this layer form a loose meshwork of connective tissue cells and fibrils which surround and support the vitelline vessels. A serosal basal lamina separates the visceral yolk sac from the mesothelium that lines the exocoelomic cavity. The complex cytological structure of the endodermal cells clearly indicates that the visceral yolk sac is engaged in functional activities throughout gestation.

With increasing age the visceral endodermal cells and mesothelial cells showed decided variations in activity of the enzymes studied. On the 12th day of gestation, ATP is hydrolyzed but not ADP or AMP. On the 14th and 18th days, both ATP and ADP substrates are hydrolyzed and on the 22nd day even AMP to a limited degree. In the postterm visceral yolk sac very little change is observed in the distribution and intensities of the three enzyme reactions.

Progressive changes in the fine structure and distribution of adenosine mono-, di- and triphosphatase enzyme activities in these placental tissues are compared and discussed at increasing gestational ages.

REFERENCES

1. Grosser, O. Vergleichende Anatomie und Entwicklungsgeschichte der Placenta mit besonderer Berucksichtigung des Menschen, W. Braunmuller. Vienna and Leipzig, 1909.

2. Mossman, H. W. The rabbit placenta and the problem of placental transmission. Am. J. Anat., 1926, 37, 433-497.

3. Mossman, H. W. Comparative morphogenesis of the fetal membranes and accessory uterine structures. Contr. Embryol. Carneg. Instit., 1937, 26, 129-246.

4. Duval, M. Le placenta des rongeurs: le placenta du lupin. J. Anat., Paris, 1889, 25, 399-573.

5. Chipman, W. Observations on the placenta of the rabbit with special reference to the presence of glycogen, fat and iron. Lab. Reports of Royal College of Physicians, Edinburgh, 1903, 8, 227.

6. Flexner, L. B. and Gellhorn, A. Comparative physiology of placental transfer. Am. J. Obstet. and Gynec., 1942, 43, 965.

7. Flexner, L. B., Cowie, D. B., Hellman, C. M., Wilde, W. S. and Vosburgh, G. T. Permeability of human placenta to sodium in normal and abnormal pregnancies and supply of sodium to human fetus as determined with radioactive serum. Am. J. Obstet. and Gynec., 1948, 55, 469.

8. Widdas, W. F. Inability of diffusion to account for placental glucose transfer in the sheep and consideration of the kinetics of a possible carrier transfer. J. Physiol., 1952, 118, 23.

9. Verzar, F. and McDougall, E. J. Absorption from the intestine. London: Longmans, Green, 1936.

10. Bloor, W. R. Biochemistry of the fatty acids and their compounds, the lipids. New York: Reinhold Publishing Corp., 1943.

11. Bourne, G. The distribution of alkaline phosphatase in various tissues. Quan. J. Exp. Physiol., 1943, 32, 1-17.

12. Davson, H. and Danielli, J. F. The permeability of natural membranes. New York: Macmillan, 1943.

13. Sumner, J. B. and Somers, G. F. Chemistry and methods of enzymes. New York: Academic Press, 1943.

14. Green, A. A. and Colowick, S. P. Chemistry and metabolism of the compounds of phosphorous. Ann. Rev. of Biochem., 1944, 155-186.

15. Mann, T. and Lutwuk-Mann, C. Non-oxidative enzymes. Ann. Rev. of Biochem., 1944, 25-58.

16. Wilmer, H. A. Correlation between functional activity of the renal tubule and its phosphatase content. Arch. Path., 1944, 37, 227-237.

17. Hafez, E. S. E. Uterine and placental enzymes. A review. Acta Endocrinol., 1964, 46, 217-229.

18. Hagerman, D. D. Enzymatic capabilities of the placenta. Fed. Proceed., 1964, 23, 785-790.

19. Page, E. W. and Glendening, M. B. Enzymes of the human placenta. In L. B. Flexner (Ed.) Gestation, Transactions of the first conference. New York: Josiah Macy Jr. Foundation, 1954, 225-229.

20. Wislocki, G. B. and Dempsey, E. W. Histochemical reactions of the placenta of the pig. Am. J. Anat., 1946, 78, 181-226.

21. Dempsey, E. W. and Deane, H. W. The cytological localization, substrate specificity and pH optimum of phosphatases in the duodenum of the mouse. J. Cell. and Comp. Physiol., 1946, 27, 159-179.

22. Dempsey, E. W. and Wislocki, G. B. Further observations on the distribution of phosphatases in mammalian placentas. Am. J. Anat., 1947, 80, 1-33.

23. Wimsatt, W. A. Observations on the morphogenesis, cytochemistry and significance of the binucleate giant cells of the placenta of ruminants. Am. J. Anat., 1951, 89, 233-281.

24. Weeth, H. J. and Herman, H. A. A histological and histochemical study of bovine oviducts, uterus and placenta. Res. Bull. Univ. Missouri Agric. Exp. Station, 1952, 501.

25. Foley, R. C., Reece, R. P. and Leathem, J. H. Histochemical observations of the bovine uterus, placenta and corpus luteum during early pregnancy. J. Anim. Science, 1954, 13, 131.

26. Bjorkman, N. Morphological and histochemical studies on the bovine placenta. Acta Anat., 1954, 22, 1-91.

27. Wislocki, G. B. and Wimsatt, W. A. Chemical cytology of the placenta to two North American shrews (Blarina brevicauda and Sorex fumeus). Am. J. Anat., 1947, 81, 269-307.

28. Wislocki, G. B. and Dempsey, E. W. Histochemical reactions in the placenta of the cat. Am. J. Anat., 1946, 78, 1-45.

29. McKay, D. G., Adams, E. C., Hertig, A. T. and Danziger, S. Histochemical horizons in human embryos. I. Five millimeter embryo - Streeter Horizon XIII. Anat. Rec., 1955, 122, 125-151.

30. McKay, D. G., Adams, E. C., Hertig, A. T. and Danziger, S. Histochemical horizons in human embryos. II. 6 and 7 millimeter embryos - Streeter Horizon XIV. Anat. Rec., 1956, 126, 433-463.

31. Dempsey, E. W. and Wislocki, G. B. Histochemical reactions associated with basophilia and acidophilia in the placenta and pituitary gland. Am. J. Anat., 1945, 76, 277-301.

32. McKay, D. G., Hertig, A. T., Adams, E. C., and M. V. Richardson. Histochemical observations on the human placenta. Am. J. Obst. and Gynec., 1958, 12, 1-36.

33. Sharov, I. I. Phosphatases in human placenta. Byulletin Eksperimental noi Biologii Meditsiny, 1963, 56, 64. Fed. Proc. Tran. Suppl., 1964, 23, 750.

34. Wielenga, G. and Willighagen, R. G. The histochemistry of the syncytiotrophoblast and the stroma in the normal full-term placenta. Am. J. Obst. and Gynec., 1962, 84, 1059-1064.

35. Wachstein, M., Meager, J. G., and Ortiz, J. Enzymatic histochemistry of the term human placenta. Am. J. Obst. and Gynec., 1963, 87, 13-26.

36. Wislocki, G. B. and Dempsey, E. W. The chemical histology of the human placenta and decidua with reference to mucopolysaccharides, glycogens, lipids and acid phosphatase. Am. J. Anat., 1948, 83, 1-41.

37. Wislocki, G. B., Deane, H. W. and Dempsey, E. W. The histochemistry of the rodent's placenta. Am. J. Anat., 1946, 78, 281-321.

38. Padykula, H. A. A histochemical and quantitative study of enzymes of the rat's placenta. J. Anat., 1958, 92, 118-129.

39. Bulmer, D. Esterase and acid phosphatase activities in the rat placenta. J. Anat., 1965, 99, 513.

40. Hard, W. L. The distribution of alkaline phosphatase in the fetal membranes and placenta of the guinea pig. Anat. Rec., 1944, 89, 532-533.

41. Hard, W. L. A histochemical and quantitative study of phosphatases in the placenta and fetal membranes of the guinea pig. Am. J. Anat., 1947, 78, 47-77.

42. Pritchard, J. J. The distribution of alkaline phosphatase in the pregnant uterus of the rat. J. Anat., 1947, 81, 352-364.

43. Wislocki, G. B. The anatomy of the placental barrier. In L. B. Flexner (Ed.) Gestation, Transactions of the first conference. New York: Josiah Macy Jr. Foundation, 1954, p. 165.

44. Wimsatt, W. A. Some aspects of the comparative anatomy of the mammalian placenta. Am. J. Obst. and Gynec., 1962, 84, 1568-1594.

45. Enders, A. C. A comparative study of the fine structure of the trophoblast in several hemochorial placentas. Am. J. Anat., 1965, 116, 29-68.

46. Dempsey, E. W., Wislocki, G. B., and Amoroso, E. C. Electron microscopy of the pig's placenta with special reference to the cell membranes of the endometrium and chorion. Am. J. Anat., 1955, 96, 65-101.

47. Amoroso, E. C. Histology of the placenta. Brit. Med. Bull., 1961, 17, 81-95.

48. Wislocki, G. B., and Padykula, H. A. Histochemistry and electron microscopy of the placenta. In W. Young (Ed.) Sex and internal secretions. Baltimore: Williams and Wilkins, 1961, pp. 883-957.

49. Bjorkman, N. On the ultrastructure of the pig's placenta. Int. J. Fertil., 1963, 8, 868. (Abstract)

50. Bjorkman, N. The fine morphology of the area of foetal-maternal apposition in the equine placenta. Ztschr. Zellforsch., 1965, 65, 285-289.

51. Assheton, R. The morphology of the ungulate placenta particularly the development of that organ in sheep and notes upon the placenta of elephant and hyrax. Phil. Tran. B., 1960, 198, 143-220.

52. Wimsatt, W. A. New histological observations on the placenta of the sheep. Am. J. Anat., 1950, 87, 391-458.

53. Wimsatt, W. A. Observations on the morphogenesis, cytochemistry and significance of the binucleate giant cells of the placenta of ruminants. Am. J. Anat., 1951, 89, 233-281.

54. Amoroso, E. C. Placentation. In A. S. Parkes (Ed.) Marshall's physiology of reproduction. New York: Longmans, Green and Co., 1952, pp. 127-311.

55. Bjorkman, N. and Bloom, G. On the fine structure of the foetal-maternal junction in the bovine placentome. Ztschr. Zellforsch., 1957, 45, 649-659.

56. Bjorkman, N. and Sollen, P. Morphology of the bovine placenta at normal delivery. Acta. Vet. Scand., 1960, 1, 347-362.

57. Amoroso, E. C. Histology of the placentas. Brit. Med. Bull., 1961, 17, 81-95.

58. Hamilton, W. J., Harrison, R. J., and Young, B. A. Aspect of placentation in certain cervidae. J. Anat. Lond., 1960, 94, 1-33.

59. Ludwig, K. S. On the fine structure of the maternal-fetal connection in the placentoma of the sheep (ovis aries L.). Experientia, 1962, 18, 212-213.

60. Bjorkman, N. Ultrastructure features of the ovine placentome. Proc. 5th Int. Conf. E. M., 1962, 00-9.

61. Bjorkman, N. Fine structure of the ovine placentome. J. Anat., 1965, 99, 283-297.

62. Lawn, A. M., Chiquoine, A. D. and Amoroso, E. C. The ultrastructure of the placenta of the sheep and the goat. J. Anat., 1963, 97, 306.

63. Dempsey, E. W. and Wislocki, G. B. Electron microscopic observations on the placenta of the cat. J. Biophys. and Biochem. Cytol., 1956, 2, 743-754.

64. Lawn, A. M. and Chiquoine, A. D. The ultrastructure of placental labyrinth of the ferret, (Mustela putorius furo). J. Anat., 1965, 99, 47-69.

65. Boyd, J. D. and Hamilton, W. J. Electron microscopic observations on the cytotrophoblast contribution to the syncytium in the human placenta. J. Anat., 1966, 100, 535-548.

66. Wislocki, G. B. and Streeter, G. L. On the placentation of the macaque (Macaca mulata) from the time of implantation until the formation of the definitive placenta. Contr. Embryol., 1938, 27, 1-66.

67. Hertig, A. T. and Rock, J. Two human ova of the pre-villous stage, having a developmental age of about seven and nine days respectively. Contr. Embryol., 1945, 31, 65-84.

68. Bargmann, W. and Knoop, A. Electronenmikroskopische untersuchungen an plazentarzotten des menschen. Ztschr. Zellforsch., 1959, 50, 472-493.

69. Dempsey, E. W. and Wislocki, G. B. Electron microscopy of human placental villi. Anat. Rec., 1953, 117, 609. (Abstract)

70. Boyd, J. D. and Hughes, A. F. Observations on human chorionic villi using the electron microscope. J. Anat., 1954, 88, 356-362.

71. Wislocki, G. B. and Dempsey, E. W. Electron microscopy of the human placenta. Anat. Rec., 1955, 123, 133-168.

72. Sawasaki, C., Mori, T., Inone, T., and Shimmi, K. Observations on the human placental membrane under the electron microscope. Endocrinol. Japan., 1957, 4, 1-11.

73. Terzakis, J. and Rhodin, J. A. G. Ultrastructure of human term placenta. Anat. Rec., 1961, 139, 279. (Abstract)

74. Rhodin, J. A. G. and Terzakis, J. The ultrastructure of the human full term placenta. J. Ultrastruct. Res., 1962, 6, 88-106.

75. Terzakis, J. A. The ultrastructure of normal human first trimester placenta. J. Ultrastruct. Res., 1963, 9, 268-284.

76. Carter, J. E. The ultrastructure of the human trophoblast. Transcript of 2nd Rochester Trophoblast Conf., 1963, 7-27.

77. Carter, J. E. Morphologic evidence of syncytial formation from the cytotrophoblastic cells. Am. J. Obstet. and Gynec., 1964, 23, 647-656.

78. Lister, U. M. Ultrastructure of the human mature placenta. I. The maternal surface. J. Obstet. and Gynec. Brit. Cwlth., 1963, 70, 373-386.

79. Lister, U. M. Ultrastructure of the human mature placenta. II. The fetal surface. J. Obstet. and Gynec. Brit. Cwlth., 1963, 70, 766-776.

80. Lister, U. M. Ultrastructure of the early human placenta. J. Obstet. and Gynec. Brit. Cwlth., 1964, 71, 21-32.

81. Enders, A. C. Formation of syncytium from cytotrophoblast in the human placenta. Am. J. Obstet. and Gynec., 1965, 25, 378-386.

82. Pierce, G. B. Jr., Midgley, A. R. Jr. and Beals, T. F. An ultrastructural study of differentiation and maturation of trophoblast of the monkey. Lab. Invest., 1964, 13, 451-464.

83. Midgley, A. R. Electron microscopic studies of human choriocarcinoma and monkey trophoblast. Transcript of 2nd Rochester Trophoblast Conf., 1963, 42-57.

84. Wynn, R. M. Fine structure of the transplanted human choriocarcinoma and its endocrine function. Transcript of 2nd Rochester Trophoblast Conf., 1963, 58-90.

85. Pierce, G. B. Jr. and Midgley, A. R. Jr. The origin and function of human syncytiotrophoblastic giant cells. Am. J. Path., 1963, 43, 153-173.

86. Wynn, R. M. and Davies, J. Ultrastructure of hydatidform mole. Correlative electron microscopic and functional aspects. Am. J. Obstet. and Gynec., 1964, 90, 293-307.

87. Midgley, A. R. Jr., Pierce, G. B. Jr., Deneau, G. A. and Gosling, J. R. G. Morphogenesis of syncytrophoblast in vivo; an autoradiographic demonstration. Science, 1963, 141, 349.

88. Richart, R. Studies of placental morphogenesis. I. Radioautographic studies of human placenta utilizing tritiated thymidine. Proc. Soc. Exp. Biol. Med., 1961, 106, 829-831.

89. Bourne, G. L. and Lacy, D. Ultrastructure of human amnion and its possible relation to the circulation of amniotic fluid. Nature, 1960, 186, 925-954.

90. Bourne, G. The human amnion and chorion. Chicago: Year Book Publishers, Inc., 1962, p. 81.

91. Falck Larsen, J. Electron microscopy of the human placenta. Transcript of 2nd Rochester Trophoblast Conf., 1963, 280-300.

92. Terzakis, J. Morphological considerations in the metabolism of the human placenta. Transcript of 2nd Rochester Trophoblast Conf., 1963, 28-41.

93. Yoshida, Y. Glycogen formation in the cytotrophoblast of human placenta in early pregnancy as revealed by electron microscopy. Exper. Cell. Res., 1964, 34, 293.

94. Yoshida, Y. Ultrastructure and secretory function of the syncytial trophoblast of human placenta in early pregnancy. Exper. Cell. Res., 1964, 34, 305.

95. Strauss, L., Goldenberg, N., Hirotu, K. and Okudaira, Y. Structure of the human placenta; with observations on the ultrastructure of the terminal chorionic villous. Birth Defects Symposium on the Placenta, 1965, 1, 13-26.

96. Dempsey, E. W. and Wislocki, G. B. Electron microscopy of the rat's placenta. Anat. Rec., 1953, 117, 581-582. (Abstract)

97. Wislocki, G. B. and Dempsey, E. W. Electron microscopy of the placenta of the rat. Anat. Rec., 1955, 123, 33-64.

98. Schiebler, T. H. and Knoop, A. Electron microscopic studies on the structure of the rat placenta. Verhandl. Anat. Ges., 1960, 82-88.

99. Schiebler, T. H. and Knoop, A. Histochemical and electron microscopic studies on the rat placenta. Ztschr. Zellforsch., 1959, 50, 494-552.

100. Owers, N. and Mossman, H. W. New observations by electron microscopy on the structure of the placental barrier of the white rat, Mus norvegicus. Anat. Rec., 1963, 145, 269. (Abstract)

101. Jollie, W. A. Fine structural changes in placental labyrinth of the rat with increasing gestational age. J. Ultrastruct. Res., 1964, 10, 27.

102. Kirby, D. R. S. and Bradbury, S. The hemo-chorial mouse placenta. Anat. Rec., 1965, 152, 279-282.

103. Falck Larsen, J. Electron microscopy of the chorioallantoic placenta of the rabbit. I. The placental labyrinth and multinucleated giant cells of the intermediate zone. J. Ultrastruct. Res., 1962, 7, 535-549.

104. Wynn, R. M. and Davies, J. Comparative electron microscopy of the hemochorial placenta. Am. J. Obstet. and Gynec., 1965, 91, 533-549.

105. Davies, J., Dempsey, E. W. and Amoroso, E. C. The subplacenta of the guinea pig: An electron microscopic study. J. Anat., 1961, 95, 311-324.

106. Enders, A. C. Light and electron microscopic observations on the villi of the hemochorial placenta of the armadillo. Anat. Rec., 1958, 130, 297.

107. Enders, A. C. Electron microscopic observations on the villous haemochorial placenta of the nine-banded armadillo (Dasypus novemcinctus). Anat. Rec., 1960, 94, 205-215.

108. Falck Larsen, J. Histology and fine structure of the avascular and vascular yolk sac placentae and obplacental giant cells in the rabbit. Am. J. Anat., 1963, 112, 269.

109. Hamilton, W. J., Boyd, J. D. and Mossman, H. W. Human embryology. Baltimore: The Williams and Wilkins Co., 1952.

110. Jollie, W. P. and Jollie, L. G. The fine structure of the yolk sac of the spiny dogfish. Anat. Rec., 1966, 154, 363. (Abstract)

111. Jollie, W. P. and Jollie, L. G. The fine structure of the ovarian follicle of the ovoviviparous poeciliid fish, Lebistes reticulatus. I. Maturation of follicular epithelium. J. Morphol., 1964, 114, 479.

112. Jollie, W. P. and Jollie, L. G. The fine structure of the ovarian follicle of the ovoviviparous poeciliid fish, Lebistes reticulatus. II. Formation of follicular pseudoplacenta. J. Morphol., 1964, 114, 503.

113. Turner, C. L. Viviparity superimposed upon ovo-viviparity in the Goodeidae, a family of cyprinodont teleost fishes of the Mexican plateau. J. Morphol., 1933, 55, 207-251.

114. Turner, C. L. Follicular pseudoplacenta and gut modifications in anableped fishes. J. Morphol., 1940, 67, 91-101.

115. Weeks, H. C. A review of placentation among reptiles with particular regard to function and evolution of the placenta. Proc. Zool. Soc., London, 1935, 2, 625.

116. Hillemann, H. H. The vertebrate organism. O.S.C. Cooperative Assoc., Corvallis, 1960, 55-56.

117. Hill, J. P. The early development of Didelphys aurita. Quant. J. Micr. Sci., 1918, 63, 91.

118. Wimsatt, W. A. Cytochemical observations on the fetal membranes and placenta of the bat, Myotis lucifugus. Am. J. Anat., 1949, 84, 63-141.

119. Bridgman, J. A morphological study of the development of the placenta of the rat. I. An outline of the development of the placenta of the white rat. J. Morphol., 1948, 83, 61-86.

120. Asai, F. Zur Entwicklung und Histophysiologie des Dottersacks der Nagen mit Entypie des keim-felds und zur Frage der sogenannten Riesenzellen. Anat. Hefte (Arbeiten), 1914. Cited by J. Bridgman in: A morphological study of the development of the placenta of the white rat. J. Morphol., 1948, 83, 61-86.

121. Owers, N. and Howerter, B. New histochemical and electron microscopical observations on the placenta of the rat. Anat. Rec., 1966, 154, 398. (Abstract)

122. Litwer, G. Uber die Sekretion and Resorption in dem Dotterentoderm-zellen bei graviden weissen Mausen. Ztschr. Zellforsch., 1928, 8, 135-152.

123. Branca, A. Recherches sur la vesicule ombilicale. III. La vesicule ombilicale des rongeurs. Arch. de Biol., 1923, 33, 605-670.

124. Gerard, P. Recherches morphologiques et experimentales sur la vesicule ombilicale des rongeurs a feuillets inversees. Arch. de Biol., 1926, 35, 269-293.

125. Goldman, E. E. Die aussere und innere sekretion des gesunden und kranken organismus in Lichte der "Vitalen Farbung". Beitr. Z. Klin. Chirug., 1909, 64, 192-265.

126. Wislocki, G. B. Experimental studies on fetal absorption. Contrib. Embryol. Carnegie Inst. Wash., 1920, 11, 47-59.

127. Wislocki, G. B. Further experimental studies on fetal absorption. Contrib. Embryol. Carnegie Inst. Wash., 1921, 13, 89-101.

128. Everett, J. W. Morphological and physiological studies of the placenta in the albino rat. J. Exp. Zool., 1935, 70, 243-286.

129. Al-Abbass, A. H. and Schultz, R. L. Phagocytic activity of the rat placenta. J. Anat., 1966, 100, 2, 349-359.

130. Stephens, R. J. Histology and histochemistry of the placenta and fetal membranes in the bat, Jadarida brasiliensis cynocephala (with notes on maintaining pregnant bats in captivity). Am. J. Anat., 1962, 111, 259-286.

131. Sorokin, S. P. and Padykula, H. A. Differentiation of the rat's yolk sac in organ culture. Am. J. Anat., 1964, 114, 457-478.

132. Luse, S. A. The morphologic manifestations of uptake of materials by the yolk sac of the pregnant rabbit. In C. A. Villee (Ed.) Gestation, transactions of the fourth conference. New York: Josiah Macy Jr. Foundation, 1957, 115-141.

133. Luse, S., Davies, J. and Smith, M. Electron microscopy of experimental inclusions in cytoplasm and nuclei of yolk sac cells. Fed. Proc., 1959, 18, 491. (Abstract)

134. Luse, S., Davies, J. and Clark, S. L. Electron microscopy of nuclear inclusions. Am. J. Path., 1959, 35, 686. (Abstract)

135. Carpenter, S. J. and Ferm, V. H. Electron microscopic observations on the uptake and storage of thorotrast by rodent yolk sac epithelial cells. Anat. Rec., 1966, 154, 327. (Abstract)

136. Goldman, E. E. Die aussere und innere sekretion des gesunden und kranken organismus im Lichte der "Vitalen Farbung". Teil II. Bruns. Beitrage Z. Klin. Chirug., 1912, 78, 1-108.

137. Wislocki, G. B. and Padykula, H. A. Reichert's membrane and the yolk sac of the rat investigated by histochemical means. Am. J. Anat., 1953, 92, 117-151.

138. Bulmer, D. and Dickson, A. D. Observations on the carbohydrate materials in the rat placenta. J. Anat., 1960, 94, 46-58.

139. Padykula, H. A. and Richardson, D. A correlated histochemical and biochemical study of glycogen storage in the rat placenta. Am. J. Anat., 1964, 114, 457-478.

140. Dempsey, E. W. and Wislocki, G. B. Observations on some histochemical reactions in the human placenta, with special reference to the significance of the lipids, glycogen and iron. Endocrinology, 1944, 35, 409-429.

141. Brambell, F. W. R., Hemings, W. A. and Rowlands, W. T. The passage of antibodies from the maternal circulation into the embryo in rabbits. Proc. Roy. Soc., London, 1948, 135, 390-403.

142. Brambell, F. W. R., Hemings, W. A., Henderson, M., Parry, H. J. and Rowlands, W. T. The route of antibodies passing from the maternal to foetal circulation in rabbits. Proc. Roy. Soc., London, 1949, 136, 131-144.

143. Brambell, F. W. R., Hemings, W. A., Henderson, M. and Rowlands, W. T. The selective admission of antibodies to the foetus by the yolk sac splanchnopleure in rabbits. Proc. Roy. Soc., London, 1950, 137, 239-252.

144. Brambell, F. W. R., Hemings, G. P., Hemings, W. A., Henderson, M., and Rowlands, W. T. The route by which antibodies enter the circulation after injection of immune serum into the exocoel of foetal rabbits. Proc. Roy. Soc., London, 1951, 138, 188-204.

145. Brambell, F. W. R. and Halliday, R. The route by which passive immunity is transmitted from mother to foetus in the rat. Proc. Roy. Soc., London, 1956, 145, 170-178.

146. Brambell, F. W. R. The development of fetal immunity. Macy Foundation Conferences on Gestation, 1957, 4, 143-201.

147. Smith, A. E., and Schechtman, A. M. Significance of the rabbit yolk sac. A study of the passage of heteologous proteins from mother to embryo. Develop. Biol., 1962, 4, 339-360.

148. Anderson, J. W. The placental barrier to gamma globulins in the rat. Am. J. Anat., 1959, 104, 403.

149. Mayersbach, H. Zur Fraye des Proleinnberganges voh den Mutter zum Foelen. I. Befunde an Ratten am Ende der Schwangerschaft. Ztschr. Zellforsch., 1958, 48, 479-504.

150. Davies, J. Transmission of proteins across the rabbit placenta using the fluorescent antibody method. Transactions of the fifth conference on Gestation, Josiah Macy Jr. Foundation, New York, 1959.

151. Leissring, J. C. and Anderson, J. W. The transfer of serum proteins from mother to young in the guinea pig. I. Prenatal rates and routes. Am. J. Anat., 1961, 109, 149-156.

152. Leissring, J. W. and Leissring, J. C. The transfer of serum proteins from mother to young in the guinea pig. II. Histochemistry of tissues involved in prenatal transfer. III. Postnatal studies. Am. J. Anat., 1961, 109, 157-174.

153. Brambell, F. W. R. and Hemings, W. A. The transmission of antibodies from mother to fetus. In C. A. Villee (Ed.) The placenta and fetal membranes. Baltimore: Williams and Wilkins Co., 1960, 71-84.

154. Davies, J. Survey of research in gestation and the developmental sciences. Baltimore: Williams and Wilkins Co., 1960.

155. Dempsey, E. W. Electron microscopy of the visceral yolk sac epithelium of the guinea pig. Am. J. Anat., 1953, 93, 331-364.

156. Padykula, H. A. and Wilson, T. H. Differentiation of absorptive capacity in the visceral yolk sac of the rat. Anat. Rec., 1960, 136, 254. (Abstract)

157. Lambson, R. O. and Jollie, W. P. Ultrastructural variations in phago-/pino-cytosis activity throughout gestation in normal rat visceral yolk sac. J. Appl. Phys., 1963, 34, 2529. (Abstract)

158. Lyons, W. R. Pregnancy maintained in hypophysectomized oophorectomized rats injected with estrone and progesterone. Proc. Soc. Exp. Biol. Med., 1943, 54, 65-68.

159. Sabatini, D. D., Bensch, K. and Barrnett, R. J. Cytochemistry and electron microscopy. The preservation of cellular ultrastructure and enzymatic activity by aldehyde fixation. J. Cell. Biol., 1963, 17, 19-58.

160. Wachstein, M. and Meisel, E. Histochemistry of hepatic phosphatases at a physiological pH. Am. J. Clin. Path., 1957, 27, 13-23.

161. Luft, J. H. Improvements in epoxy resin embedding methods. J. Biophys. Biochem. Cytol., 1961, 9, 409-414.

162. Richardson, K. C., Jarrett, L. and Finke, E. Embedding in epoxy resins for ultrathin sectioning in electron microscopy. Stain Techn., 1960, 35, 313-323.

163. Reynolds, E. S. The use of lead citrate at high pH as an electron-opaque stain in electron microscopy. J. Cell. Biol., 1963, 17, 208-213.

164. Jenkinson, J. W. Observations on the histology and physiology of the placenta of the mouse. Tijdschr. ned. dierk. Ver., 1902, 2, 124.

165. Huber, G. C. The development of the albino rat, Mus norvegicus albinus. J. Morphol., 1915, 26, 247-358.

166. Keibel, F. Ueber die grenze zwischen mutterlichen und fetalem gewebe. Anat. Anz., 1915, 48, 255.

167. Bridgman, J. A morphological study of the development of the placenta of the rat. II. An histological and cytological study of the development of the chorio-allantoic placenta of the white rat. J. Morphol., 1948, 83, 195-223.

168. Farquhar, M. G. and Palade, G. E. Junctional complexes in various epithelia. J. Cell. Biol., 1963, 17, 375-412.

169. Mossman, H. W. Personal communication. 1966.

170. Jollie, W. P. Radioautographic observations on variations in desocyribonucleic acid synthesis in rat placenta with increasing gestational age. Am. J. Anat., 1964, 114, 161-172.

171. Slauterbach, D. B. and Fawcett, D. W. The development of the cnidoblasts of hydrin, an electron microscope study of cell differentiation. J. Biophys. Biochem. Cytol., 1959, 5, 441-452.

172. Schlafke, S. and Enders, A. C. Observations on the fine structure of the rat blastocyst. J. Anat., 1963, 97, part 3, 353-360.

173. Jollie, W. P. Fine structural changes in the junctional zone of the rat placenta with increasing gestational age. J. Ultrastruct. Res., 1965, 12, 420-438.

174. Revel, J. P. Electron microscopy of glycogen. J. Histochem. Cytochem., 1964, 12, 104-114.

175. Fawcett, D. W. An atlas of fine structure. The cell. Philadelphia: W. B. Saunders, 1966.

176. Flexner, L. B. and Pohl, H. A. The transfer of radioactive sodium across the placenta of the white rat. J. Cell. Comp. Physiol., 1941, 18, 49-59.

177. Flexner, L. B. and Pohl, H. A. Transfer of water across the placenta of the guinea pig. Am. J. Physiol., 1941, 132, 594-611.

178. Gellhorn, A. and Flexner, L. B. Transfer of water across the placenta of the guinea pig. Am. J. Physiol., 1942, 136, 750-756.

179. Flexner, L. B. and Pohl, H. A. The transfer of radioactive sodium across the placenta of the rabbit. Am. J. Physiol., 1941, 134, 344-349.

180. Gellhorn, A., Flexner, L. B. and Pohl, H. A. The transfer of radioactive sodium across the placenta of the sow. J. Cell. Comp. Physiol., 1941, 18, 393-400.

181. Page, E. W., Glendening, M. B., Margolis, A., and Harper, H. A. Transfer of D- and L-histidine across the human placenta. Am. J. Obst. and Gynec., 1957, 73, 589.

182. Bothwell, T. H., Pribilla, W. F., Mebust, W., and Finch, C. A. Iron metabolism in the pregnant rabbit - iron transport across the placenta. Am. J. Physiol., 1958, 193, 615.

183. Dancis, J., Lind, J., Oratz, M., Smolens, J., and Vara, P. Placental transfer of proteins in human gestation. Am. J. Obst. and Gynec., 1961, 82, 167.

184. Steinberg, J. Placental transfers: modern methods of study. Am. J. Obst. and Gynec., 1962, 84, 1731.

185. Hagerman, D. D. and Villee, C. A. Transport functions of the placenta. Physiol. Revs., 1960, 40, 313-330.

186. Longley, J. B., Banfield, W. G. and Brindley, D. C. Structure of the rete mirable in the kidney of the rat as seen with the electron microscope. J. Biophys. Biochem. Cytol., 1960, 7, 103-106.

187. Rhodin, J. A. G. The diaphragm of capillary endothelial fenestrations. J. Ultrastruct. Res., 1962, 6, 171.

188. Dempsey, E. W. and Peterson, R. R. Electron microscopic observations on the thyroid glands of normal hypophysectomized, cold exposed and thiouracil-heated rats. Endocrinology, 1955, 56, 46-58.

189. Ekholm, R. The ultrastructure of the blood capillaries in the mouse thyroid gland. Ztschr. Zellforsch., 1957, 46, 139-146.

190. Ekholm, R. and Sjostrand, F. S. The ultrastructural organization of the mouse thyroid gland. J. Ultrastruct. Res., 1957, 1, 178.

191. Ross, M. H. Annulate lamellae in the adrenal cortex of the fetal rat. J. Ultrastruct. Res., 1962, 7, 373-382.

192. Zelander, T. Ultrastructure of the mouse adrenal cortex. J. Ultrastruct. Res., 1959, 2, 1-111.

193. Farquhar, M. G. Fine structure and function in capillaries of the anterior pituitary gland. Angiology, 1961, 12, 270-292.

194. Pappas, G. D. and Tennyson, V. M. An electron microscopic study of the passage of colloidal particles from the blood vessels of the ciliary processes and choroid plexus of the rabbit. J. Cell. Biol., 1962, 15, 227-239.

195. Maxwell, D. S. and Pease, D. C. The electron microscopy of the choroid plexus. J. Biophys. Biochem. Cytol., 1956, 2, 467-474.

196. Ekholm, R. and Edlund, Y. Ultrastructure of the human exocrine pancreas. J. Ultrastruct. Res., 1959, 2, 453-481.

197. Farquhar, M. G., Wissig, S. L. and Palade, G. E. Glomerular permeability. I. Ferritin transfer across the normal glomerular capillary wall. J. Exp. Med., 1961, 47, 113-347.

198. Wissig, S. L. The anatomy of secretion in the follicular cells of the thyroid gland. I. The fine structure of the gland in the normal rat. J. Biophys. Biochem. Cytol., 1960, 7, 419.

199. Elfvin, L. G. The ultrastructure of the capillary fenestrae in the adrenal medulla of the rat. J. Ultrastruct. Res., 1965, 12, 687-704.

200. Tillack, T. W. The transport of ferritin across the placenta of the rat. Lab. Invest., 1966, 15, 896-909.

201. Jollie, W. P. and Jollie, L. G. Visualization of transport of electron opaque colloids in placental membranes of the rat. Sixth International Congress for Electron Microscopy, Kyoto. In: R. Uyeda (Ed.) Electron microscopy, 1966, 2, 423-424.

202. Kisch, B. Electron microscopy of the cardiovascular system: an electron microscopic study with applications to physiology. Springfield, Ill.: Charles C. Thomas, 1960.

203. Fawcett, D. W. and Wittenberg, J. Structural specializations of endothelial cell junctions. Anat. Rec., 1962, 142, 231.

204. Fawcett, D. W. Comparative observations on the fine structure of blood capillaries. In J. L. Orbison and D. Smith (Ed.) The peripheral blood vessels. Blatimore: Williams and Wilkins, 1963, pp. 17-44.

205. Donahue, S. A relationship between fine structure and function of blood vessels in the central nervous system of rabbit fetuses. Am. J. Anat., 1964, 115, 17-26.

206. Luse, S. A. and Harris, B. Electron microscopy of the brain in experimental edema. Neurosurg., 1960, 17, 439-446.

207. Fawcett, D. W. Surface specializations of absorbing cells. J. Histochem. Cytochem., 1965, 13, 75-91.

208. Palade, G. E. The fine structure of blood capillaries. J. Appl. Phys., 1953, 24, 1424.

209. Holter, H. Pinocytosis. Int. Rev. Cytol., 1960, 8, 481-504.

210. Moore, D. H. and Ruska, H. The fine structure of capillaries and small arteries. J. Biophys. Biochem. Cytol., 1957, 3, 457-462.

211. Kaye, G. I. and Pappas, G. D. Studies on the cornea. I. The fine structure of the rabbit cornea and the uptake and transport of colloidal particles by the cornea. J. Cell. Biol., 1962, 12, 457.

212. Kaye, G. I. Studies on the cornea. III. The fine structure of the frog cornea and the uptake and transport of colloidal particles by the cornea in vivo. J. Cell. Biol., 1962, 15, 241-258.

213. Wissig, S. An electron microscope study of the permeability of capillaries in muscle. Anat. Rec., 1958, 130, 467.

214. Florey, H. Exchange of substances between the blood and tissues. Nature, 1961, 192, 908.

215. Palade, G. E. Transport in quanta across the endothelium of blood capillaries. Anat. Rec., 1960, 136, 254.

216. Palade, G. E. Blood capillaries of the heart and other organs. Circulation, 1961, 24, 368-384.

217. Staubesand, J. Zur Histophysiologie des hertzbeutels. II. Electronmikroskopische untersuchungen uber die passage von metallsoben durch mesotheliale membranen. Ztschr. Zellforsch., 1963, 58, 915-952.

218. Anderson, E. Oocyte differentiation and vitellogenesis in the roach, Periplaneta Americana. J. Cell. Biol., 1964, 20, 131-155.

219. Andres, K. H. Mikropinozytose in zentral nerven system. Ztschr. Zellforsch., 1964, 64, 63-73.

220. Roth, T. F., and Porter, K. R. Specialized sites on the cell surface for protein uptake. Fifth Internat. Congr. Electron Microsc. In S. S. Breese, Jr. (Ed.) New York: Academic Press, 1962, 2, pp. LL-4.

221. Palay, S. L. Alveolate vesicles in Purkinje cells of rat cerebellum. J. Cell. Biol., 1963, 19, 89A-90A.

222. Roth, T. F., and Porter, K. R. Yolk protein uptake in the oocyte of the mosquito, Aedes aegypti L. J. Cell. Biol., 1964, 20, 313-332.

223. Bennett, H. S. Morphological aspects of extracellular polysaccharides. J. Histochem. Cytochem., 1963, 11, 2-13.

224. Choi, J. K. The fine structure of the urinary bladder of the toad, Bufo marinus. J. Cell. Biol., 1963, 16, 53-72.

225. Sjostrand, F. S. and Rhodin, J. A. G. The ultrastructure of the proximal convoluted tubules of the mouse kidney as revealed by high resolution electron microscopy. J. Exp. Cell. Res., 1953, 4, 426.

226. Pease, D. C. Infolded basal plasma membranes found in epithelia noted for their water transport. J. Biophys. Biochem. Cytol., 1956, 2, 203.

227. Ruska, H., Moore, D. H. and Weinstock, J. The base of the proximal convoluted tubule cells of rat kidney. J. Biophys. Biochem. Cytol., 1957, 3, 249-254.

228. Kurosumi, K. Electron microscopic analysis of secretion. In G. H. Bourne and J. F. Danielli (Ed.) International review of cytology. New York: Academic Press, 1961, pp. 1-124.

229. Plentl, A. A. Rate of exchange of sodium and potassium between the amniotic fluid and maternal system. Proc. Soc. Exper. Biol. and Med., 1954, 86, 432.

230. Hutchinson, D. R., Hunter, C. B., Nesten, E. D., and Plentl, A. A. Exchange of water and electrolytes in the mechanism of amniotic fluid formation and relationship to hydramnios. Surg. Gynec. Obst., 1955, 100, 391.

231. Vosburgh, G. J., Flexner, L. B., Cowie, D. B., Hellman, L. M., Proctor, N. K., and Wilde, W. S. The rate of renewal in women of the water and socium of the amniotic fluid as determined by tracer techniques. Am. J. Obstet. and Gynec., 1948, 56, 1156.

232. Plentl, A. A. The origin of amniotic fluid. In Transactions of the fourth conference on gestation. New York: Josiah Macy Jr. Foundation, 1957.

233. Muir, A. R. and Peters, A. Quintuple layered membrane junctions at terminal bars between endothelial cells. J. Cell. Biol., 1962, 12, 443-448.

234. Page, E. Transfer of materials across the human placenta. Am. J. Obstet. and Gynec., 1957, 74, 705.

235. Millen, J. W. and Rogers, G. E. An electron microscopic study of the choroid plexus in the rabbit. J. Biophys. Biochem. Cytol., 1956, 2, 407-416.

236. Kurosumi, K. Protoplasma, 1958, 49, 116. Cited by Kurosumi, K. Electron microscopic analysis of secretion. In G. H. Bourne and J. F. Danielli (Ed.) International review of cytology. New York: Academic Press, 1961, pp. 1-124.

237. Van Breemen, V. L., and Clemente, C. D. Silver deposition in the central nervous system and the hematoencephalic barrier studied with the electron microscope. J. Biophys. Biochem. Cytol., 1955, 1, 161-166.

238. Braunsteiner, H., Fellinger, K., and Pakesch, F. Electron microscopic observations on the thyroid. Endocrinology, 1953, 123-133.

239. Ichikawa, A., and Irie, M. Acta. Anat., Nippon, Tokyo, 1957, 32, 93. Cited by Kurosumi, K. Electron microscopic analysis of secretion. In G. H. Bourne and J. F. Danielli (Ed.) International review of cytology. New York: Academic Press, 1961, pp. 1-124.

240. Kitamura, T. Arch. Histol. Japan, 1958, 14, 575. Cited by Kurosumi, K. Electron microscopic analysis of secretion. In G. H. Bourne and J. F. Danielli (Ed.) International review of cytology. New York: Academic Press, 1961, pp. 1-124.

241. Iijima, T. Acta. Anat., Nippon, Tokyo, 1959, 34, 649. Cited by Kurosumi, K. Electron microscopic analysis of secretion. In G. H. Bourne and J. F. Danielli (Ed.) International review of cytology. New York: Academic Press, 1961, pp. 1-124.

242. Kurosumi, K., Kitamura, T., and Iijima, T. Arch. Histol. Japan, 1959, 16, 523. Cited by Kurosumi, K. Electron microscopic analysis of secretion. In G. H. Bourne and J. F. Danielli (Ed.) International review of cytology. New York: Academic Press, 1961, pp. 1-124.

243. Kurosimi, K., Shibasaki, S., Uchida, G., and Tanaka, Y. Arch. Histol. Japan, 1958, 15, 587. Cited by Kurosumi, K. Electron microscopic analysis of secretion. In G. H. Bourne and J. F. Danielli (Ed.) International review of cytology. New York: Academic Press, 1961, pp. 1-124.

244. Shibasaki, S. Acta. Ant., Nippon, Tokyo, 1959, 34, 19. (Abstract) Cited by Kurosumi, K. Electron microscopic analysis of secretion. In G. H. Bourne and J. F. Danielli (Ed.) International review of cytology. New York: Academic Press, 1961, pp. 1-124.

245. Nakanishi, T. J. Chiba. Med. Soc., 1959, 35, 474. Cited by Kurosumi, K. Electron microscopic analysis of secretion. In G. H. Bourne and J. F. Danielli (Ed.) International review of cytology. New York: Academic Press, 1961, pp. 1-124.

246. Krehbiel, R. H. Cytological studies of the decidual reaction in the rat during early pregnancy and in the production of deciduomata. Physiol. Zool., 1937, 10, 212-234.

247. Velardo, J. T., Dawson, A. B., Olsen, A. G., and Hisaw, F. L. Sequence of histological changes in the uterus and vagina of the rat during prolongation of pseudopregnancy associated with the presence of deciduomata. Am. J. Anat., 1953, 93, 273-305.

248. Jollie, W. P., and Bencosme, S. A. Electron microscopic observations on primary decidua formation in the rat. Am. J. Anat., 1965, 116, 217-236.

249. Deane, H. W., Rubin, B. L., Driks, E. C., Lobel, B. L., and Leipsmer, G. Trophoblastic giant cells in placentas of rats and mice and their probable role in steroid-hormone production. Endocrinology, 1962, 70, 407-419.

250. Jones, C. I. The disappearance of the X-zone of the mouse adrenal cortex during first pregnancy. Proc. Roy. Soc. of London (Biol.), 1952, 139, 398-410.

251. Dickson, A. D., and Bulmer, D. Observations on the placental giant cells of the rat. J. Anat., 1960, 94, 418-424.

252. Davies, J. Survey of research in gestation and the developmental sciences. Baltimore: The Williams and Wilkins Company, 1960.

253. Ashbel, R., and Seligman, A. M. A new reagent for the histochemical demonstration of active carbonyl groups. A new method for staining ketonic steroids. Endocrinology, 1949, 44, 565-583.

254. Wislocki, G. B. The Ashbel-Seligman reaction for carbonyl groups in the placentas of man and animals. Anat. Rec., 1952, 112, 438.

255. Deane, H. W. In S. L. Palay (Ed.) Frontiers in cytology. New Haven: Yale University Press, 1958, p. 227.

256. Wattenberg, L. W. Microscopic histochemical demonstration of steroid 3 ol dehydrogenase in tissue sections. J. Histochem. Cytochem., 1958, 6, 225-232.

257. Lambson, R. O. An electron microscopic visualization of transport across rat visceral yolk sac. Am. J. Anat., 1966, 118, 21-52.

258. Schultz, P. W., Reger, J. F. and Schultz, R. L. Effects of Triton WR-1339 on the rat yolk sac placenta. Am. J. Anat., 1966, 119, 199-234.

259. Yamada, E. The fine structure of the gall bladder epithelium of the mouse. J. Biophys. Biochem. Cytol., 1955, 1, 445-458.

260. Ito, S., and Winchester, R. The fine structure of the gastric mucosa in the bat. J. Cell. Biol., 1963, 16, 541-577.

261. Ito, S. The surface coating of enteric microvilli. Anat. Rec., 1964, 148, 294.

262. Peachey, L., and Rasmussen, H. Structure of the toad's urinary bladder as related to its physiology. J. Cell. Biol., 1961, 10, 529-553.

263. Choi, J. K. Electron microscopy of absorption of tracer materials by toad (Bufo marinus) bladder epithelium. Anat. Rec., 1962, 142, 22.

264. Brandt, P. W., and Pappas, G. D. An electron microscopic study of pinocytosis in ameba. I. The surface attachment phase. J. Biophys. Biochem. Cytol., 1960, 8, 675-687.

265. Cardell, R. R., Badenhausen, S. and Porter, K. R. The morphology of fat absorption in the rat intestinal epithelial cell. Sixth International Congress for Electron Microscopy, Kyoto. In: R. Uyeda (Ed.) Electron microscopy, 1966, 2, 587-588.

266. Palay, S. L. and Karlin, L. J. An electron microscopic study of the intestinal villus. II. The pathway of fat absorption. J. Biophys. Biochem. Cytol., 1959, 5, 373-384.

267. Straus, W. Segregation of an intravenously injected protein by droplets of the cells of rat kidneys. J. Biophys. Biochem. Cytol., 1957, 3, 1037-1040.

268. Miller, F. Hemoglobin absorption by the cells of the proximal convoluted tubule in mouse kidney. J. Biophys. Biochem. Cytol., 1960, 8, 689-718.

269. Trump, B. F. An electron microscopic study of the uptake, transport and storage of colloidal materials by the cells of the vertebrate nephron. J. Ultrastruct. Res., 1961, 5, 291-310.

270. Miller, F., and Palade, G. Lytic activities of renal protein absorption droplets. An electron microscopical and cytochemical study. J. Cell. Biol., 1964, 23, 519-553.

271. Brandes, D. Observations on the apparent mode of formation of "pure" lysosomes. J. Ultrastruct. Res., 1965, 12, 63-80.

272. Moe, H., Rostgaard, J., and Behnke, O. On the morphology and origin of virgin lysosomes in the intestinal epithelium of the rat. J. Ultrastruct. Res., 1965, 12, 396-403.

273. New, D. A. T., and Stein, K. F. Cultivation of postimplantation mouse and rat embryos on plasma clots. J. Embryol. Exp. Morph., 1964, 12, 101-111.

274. Popp, R. A. Comparative metabolism of blastocyts, extraembryonic membranes, and uterine endometrium of the mouse. J. Exp. Zool., 1958, 138, 1-23.

275. Gordon, G. B., Miller, L. R., and Bensch, K. B. Studies on the intracellular digestive process in the mammalian tissue culture cells. J. Cell. Biol., 1965, 25, 41-55.

276. Wattiaux, R., Wibo, M. and Baudhuin, P. Influence of the injection of Triton WR-1339 on the properties of rat-liver lysosomes. In: A. V. S. de Reuck and M. P. Cameron (Eds.) Ciba Foundation Symposium on Lysosomes. Boston: Little Brown and Company, 1963, pp. 176-196.

277. Ferm, V. H., Free, H. J., and Shires, D. L. Concentration of azoproteins in yolk sac placenta of the rat. Proc. Soc. Exp. Biol. Med., 1959, 100, 456-459.

278. Gillman, J., Gilbert, C., Gillman, T., and Spence, I. A preliminary report of hydrocephalus, spina bifida, and other congenital anomalies in the rat produced by trypan blue. S. Afr. J. Med. Sci., 1948, 13, 47-90.

279. Weiss, J. M. The role of the golgi complex in fat absorption as studied with the electron microscope with observations on the cytology of duodenal absorptive cells. J. Exp. Med., 1955, 102, 775-788.

280. Ashworth, C. T., Slembridge, V. A., and Sanders, E. Lipid absorption, transport and hepatic assimilation studied with electron microscopy. Am. J. Physiol., 1960, 198, 1326-1328.

281. Palay, S. L., and Revel, J. P. Morphology of fat absorption. In: H. C. Menz (Ed.) Lipid transport. Springfield, Ill.: Charles L. Thomas Co., 1964.

282. Hofmann, A. F., and Borgstrom, B. Physico-chemical state of lipids in intestinal content during their digestion and absorption. Fed. Proc., 1962, 21, 43-50.

283. Senior, J. R. Intestinal absorption of fats. J. Lipid Res., 1964, 5, 495-521.

284. Rostgaard, J., and Barrnett, R. J. Fine structural observations of the absorption of lipid particles in the small intestine of the rat. Anat. Rec., 1965, 152, 325-349.

285. Farquhar, M. G., and Palade, G. E. Adenosine triphosphatase localization in amphibian epidermis. J. Cell. Biol., 1966, 30, 359-379.

286. Novikoff, A., and Goldfischer, S. Nucleosidediphosphatase activity in the golgi apparatus and its usefulness for cytological studies. Proc. Natl. Acad. Sci., 1961, 47, 802-810.

287. Novikoff, A. B., Essner, E., Goldfischer, S., and Heus, M. Nucleosidephosphatase activities of cytomembranes. Symp. Intl. Soc. Cell. Biol., 1962, 1, 149-192.

288. Novikoff, A. B., and Heus, M. A microsomal nucleoside diphosphatase. J. Biol. Chem., 1963, 238, 710-716.

289. Baker, J. R. The histochemical recognition of lipine. Quant. J. Micr. Sci., 1946, 37, 441-470.

290. Goldfischer, S., Essner, E., and Novikoff, A. B. The localization of phosphatase activities at the level of ultrastructure. J. Histochem. Cytochem., 1964, 12, 72-95.

291. Spater, H. W., Novikoff, A. B., and Masek, B. Adenosine triphosphatase activity in the cell membranes of kidney tubule cells. J. Biophys. Biochem. Cytol., 1958, 4, 765-770.

292. Sabatini, D. D., Miller, F. and Barrnett, R. J. Aldehyde fixation for morphological and enzyme histochemical studies with the electron microscope. J. Histochem. Cytochem., 1964, 12, 57-71.

293. Torack, R. M. Adenosine triphosphatase activity in rat brain following differential fixation with formaldehyde, glutaraldehyde and hydroxyadipaldehyde. J. Histochem. Cytochem., 1965, 13, 191-205.

294. Novikoff, A. B., Hausman, D. H., and Podber, E. The localization of adenosine triphosphatase in liver: in situ staining and cell fractionation studies. J. Histochem. Cytochem., 1958, 6, 61

295. Bonting, S. L., Caravaggio, L. L. and Hawkins, N. M. Studies on sodium-potassium activated adenosine triphosphatase. IV. Correlation with cation transport sensitive to cardiac glycosides. Arch. Biochem. Biophys., 1962, 98, 413-419.

296. Scarpelli, D. G., and Craig, E. L. The fine localization of nucleoside triphosphatase activity in the retina of the frog. J. Cell. Biol., 1963, 17, 279-288.

297. Essner, E., Novikoff, A. B., and Quitana, N. Nucleoside triphosphatase activities in rat cardiac muscle. J. Cell. Biol., 1965, 25, 201-215.

298. Padykula, H. A. Factors affecting the activity of adenosine triphosphatase and other phosphatases as measured by histochemical techniques. J. Histochem. Cytochem., 1955, 3, 161-169.

299. Holt, S. J. and Hicks, R. M. The localization of acid phosphatase in rat liver cells as revealed by combined cytochemical staining and electron microscopy. J. Biophys. Biochem. Cytol., 1961, 11, 47-66.

300. Holt, S. J. and Hicks, R. M. Specific staining methods for enzyme localization at the subcellular level. Brit. Med. J., 1962, 18, 214-219.

301. Tice, L. W. and Barrnett, R. J. The fine structural localization of some testicular phosphatases. Anat. Rec., 1963, 147, 43-64.

302. Smith, R. E. and Farquhar, M. G. Preparation of thick sections for cytochemistry and electron microscopy by a non-freezing technique. Nature, 1963, 200, 691.

303. Smith, R. E. and Farquhar, M. G. Preparation of nonfrozen sections sections for electron microscope cytochemistry. Scient. Instr., News, 1965, 10, 13.

304. Pillai, R. K. Dephosphorylation in muscle extracts. Biochem. J., 1938, 32, 1087-1099.

305. Schmidt, G., and Thannhauser, S. J. Intestinal phosphatase. J. Biol. Chem., 1943, 149, 369-385.

306. Kalckar, H. M. Adenylpyrophosphatase and myokinase. J. Biol. Chem., 1944, 153, 355-367.

307. Moog, F., and Steinback, H. B. Adenylpyrophosphatase in chick embryos. J. Cell. Comp. Physiol., 1945, 25, 133-144.

308. Steinback, H. B., and Moog, F. Localization of adenylpyrophosphatase in cytoplasmic granules. J. Cell. Comp. Physiol., 1945, 26, 75-83.

309. Novikoff, A. B., Podber, E. and Ryan, J. Intracellular distribution of phosphatase activity in rat liver. Fed. Proc., 1950, 9, 210.

310. Maengwyn-Davies, G. D., Friedenwald, J. S. and White, R. T. Histochemical studies of alkaline phosphatase in the tissues of the rat using frozen sections. II. Substrate specificity of enzymes hydrolyzing adenosine triphosphate, muscle and yeast adenylic acids and creatine-phosphate at high pH; the histochemical demonstration of myosin ATPase. J. Cell. Comp. Physiol., 1952, 39, 395-447.

311. Novikoff, A. B., Hecht, L., Podber, E. and Ryan, J. Phosphatases of rat liver. I. The dephosphorylation of adenosine triphosphate. J. Biol. Chem., 1952, 194, 153-170.

312. Padykula, H. A. and Herman, E. The specificity of the histochemical method for adenosine triphosphatase. J. Histochem. Cytochem., 1955, 3, 170-195.

313. Freiman, D. G. and Kaplan, N. Studies on the histochemical differentiation of enzymes hydrolyzing adenosine triphosphatase. J. Histochem. Cytochem., 1960, 8, 159-170.

314. Hori, S. H. and Chang, J. P. Histochemical study of adenosine triphosphatase in cytoplasm. J. Histochem. Cytochem., 1963, 11, 71-79.

315. Skou, J. C. The influence of some cations on an adenosine triphosphatase from peripheral nerves. Biochim. Biophysica. Acta., 1957, 23, 394.

316. Post, R. L., Merritt, C. R., Kinsolving, C. R. and Albright, C. D. Membrane adenosine triphosphatase as a participant in the active transport of sodium and potassium in the human erythrocyte. J. Biol. Chem., 1960, 235, 1796-1802.

317. Skou, J. C. Further investigations on a $mg^{++} + Na^{+}$-activated adenosine triphosphatase possibly related to the active linked transport of $Na^{+} + K^{+}$ across the nerve membrane. Biochim. Biophysica. Acta., 1960, 42, 6.

318. Bonting, S. L., Simon, K. A. and Hawkins, N. M. Studies on sodium potassium-activated adenosine triphosphatase. I. Quantitative distribution in several tissues of the cat. Arch. Biochem. Biophys., 1961, 95, 416-423.

319. Dunham, E. T. and Glynn, I. M. Adenosinetriphosphatase activity and the active movements of alkali metal ions. J. Physiol., 1961, 156-274.

320. Hoffman, J. F. Cation transport and structure of the red cell plasma membrane. Circulation, 1962, 26, 1201-1213.

321. Skou, J. C. Preparation from mammalian brain and kidney of the enzyme system involved in active transport of Na^{+} and K^{+}. Biochim. Biophys. Acta., 1962, 58, 314.

322. Kinsolving, C. R., Rost, R. L. and Bearer, D. L. Sodium plus potassium transport adenosine triphosphatase activity in kidney. J. Cell. Comp. Physiol., 1963, 62, 85.

323. Novikoff, A. B., Drucker, J., Shin, W. Y. and Goldfischer, S. Further studies of the apparent adenosinetriphosphatase activity of cell membranes in formol-calcium fixed tissues. J. Histochem. Cytochem., 1961, 9, 434.

324. Marchesi, V. T. and Barrnett, R. J. The localization of nucleosidephosphatase activity in different types of small blood vessels. J. Ultrastruct. Res., 1964, 10, 103-115.

325. Bonting, S. L. and Caravaggio, L. L. Studies on sodium-potassium-activated adenosine-triphosphatase. V. Correlation of enzyme activity with cation flux in six tissues. Arch. Biochem. Biophysics., 1963, 101, 37-46.

326. Skou, J. C. Enzymatic basis for active transport of Na and K across cell membrane. Physiol. Rev., 1965, 45, 596.

327. Landon, E. J. and Norris, J. L. Sodium and potassium-dependent adenosine triphosphatase activity in a rat kidney endoplasmic reticulum function. Biochim. Biophysica. Acta., 1963, 71, 266.

328. Ahmed, Z. and King, E. J. Kinetics of placental alkaline phosphatase. Biochim. Biophys. Acta., 1960, 45, 581-592.

329. Pearse, A. G. E. Histochemistry, theoretical and applied. (2nd Ed.) Boston: Little Brown and Co., 1960.

330. Torack, R. M. and Barrnett, R. J. The fine structural localization of nucleoside phosphatase activity in blood-brain barrier. J. Neuropath. Exptl. Neuro., 1964, 23, 46-59.

331. Cerletti, P., Fronticelli, C., and Zichella, L. Adenosine nucleotidases of human placenta. Clin. Chim. Acta., 1960, 5, 439-443.

332. Novikoff, A. B., Essner, E., Goldfischer, S. and Heus, M. Nucleoside phosphatase activities of cytomembranes. In: R. J. C. Harris (Ed.) The interpretation of ultrastructure. New York: Academic Press, 1962, 149-192.

333. Wachstein, M. and Besen, M. Electron microscopic study in several mammalian species of the reaction product enzymatically liberated from adenosinetriphosphate in the kidney. Lab. Invest., 1964, 13, 476-489.

334. Kaye, G. I., Lane, N., Wheeler, H. O. and Whitlock, R. T. Fluid transport in the rabbit gall bladder: a combined physiological and electron microscopic study. Anat. Rec., 1965, 151, 369. (Abstract)

335. Otero-Vilardebo, L. R., Lane, N., and Godman, G. C. Localization of phosphatase activities in colonic goblet and absorptive cells. J. Cell. Biol., 1964, 21, 486-490.

336. Bartoszewicz, W. and Barrnett, R. J. Fine structural localization of nucleoside phosphatase activity in the urinary bladder of the toad. J. Ultrastruct. Res., 1964, 10, 599-609.

337. Kaye, G. I. and Pappas, G. D. Studies on the ciliary epithelium and zonule. III. The fine structure of the rabbit ciliary epithelium in relation to the localization of ATPase. J. Micr., 1965, 4, 497-563.

338. Kaye, G. I. and Tice, L. W. Electron microscopic localization of adenosinetriphosphatase activity in relation to transport in the corneal endothelium. Bull. N.Y. Acad. Med., 1964, 40, 76.

339. Kaye, G. I. and Tice, L. W. Studies on the cornea. V. Electron microscopic localization of adenosinetriphosphatase activity in the rabbit cornea in relation to transport. Inv. Ophthal., 1965, 5, 22.

340. Marchesi, V. T., and Barrnett, R. J. The demonstration of enzymatic activity in pinocytotic vesicles of blood capillaries with the electron microscope. J. Cell. Biol., 1963, 17, 347-556.

341. Marchesi, V. T., Sears, M. L. and Barrnett, R. J. Electron microscopic studies of nucleoside phosphatase activity in blood vessels and glia of the retina. Inv. Ophthal., 1964, 3, 1-21.

342. Torack, R. M., Besen, M. and Becker, N. H. Localization of adenosinetriphosphate in capillaries of the brain as revealed by electron microscopy. Neurology, 1961, 11, 71-76.

343. Storti, E., Vaccari, F. and Baldini, E. Changes in red cells metabolism in presence of incomplete antibodies. Experientia, 1956, 12, 108. Cited by Altman, K. I. Some enzymologic aspects of the human erythrocyte. Am. J. Med., 1959, 27, 936-951.

344. Wislocki, G. B. Morphological aspects of ageing in the placenta. In G. E. W. Wolstenholme and E. C. P. Millar (Eds.) Ciba Foundation Colloquia on Ageing. Vol. 2, Ageing in Transient Tissues, London, J. and A. Churchill, Ltd., 1956, pp. 105-117.

345. Villee, C. A. Metabolism of the placenta. Am. J. Obstet. and Gynec., 1962, 84, 1684-1694.

346. Villee, C. A. Biochemical evidence of ageing in the placenta. In G. E. W. Wolstenholme and E. C. P. Millar (Eds.) Ciba Foundation Colloquia on Ageing. Vol. 2, Ageing in Transient Tissues, London, J. and A. Churchill, Ltd., 1956, 129-147.

347. Loeser, H. Atmung und Garung der uberlebenden Placenta des Menschen sowie deren Beeinflussung durch Hormone nebst dem Milchsaurestoffwechsel der ubenden Placenta im trachtigen Tiere. Arch. Gynaek., 1932, 148, 118-148.

348. Wang, H. W., and Hellman, L. M. John Hopk. Hosp. Bull., 1941, 73, 31. Cited by Villee, C. A. Biochemical evidence of ageing in the placenta. In G. E. W. Wolstenholme and E. C. P. Millar (Eds.) Ciba Foundation Colloquia on Ageing. Vol. 2, Ageing in Transient Tissues, London, J. and A. Churchill, Ltd., 1956, 129-147.

349. Page, E. W. Obstet. Surv. Baltim., 1948, 3, 615. Cited by Villee, C. A. Biochemical evidence of ageing in the placenta. In G. E. W. Wolstenholme and E. C. P. Millar (Eds.) Ciba Foundation Colloquia on Ageing. Vol. 2, Ageing in Transient Tissues, London, J. and A. Churchill, Ltd., 1956, 129-147.

350. Hellman, L. M., Harris, B. A. and Andrews, M. C. Johns Hopk. Hosp. Bull., 1950, 87, 203. Cited by Villee, C. A. Biochemical evidence of ageing in the placenta. In G. E. W. Wolstenholme and E. C. P. Millar (Eds.) Ciba Foundation Colloquia on Ageing. Vol. 2, Ageing in Transient Tissues, London, J. and A. Churchill, Ltd., 1956, 129-147.

351. Singer, M. and Wislocki, G. B. The affinity of syncytium, fibrin and fibrinoid of the human placenta for acid and basic dyes under controlled conditions of staining. Anat. Rec., 1948, 102, 175-193.

352. Wislocki, G. B. and Bennett, H. S. The histology and cytology of the human and monkey placenta, with special reference to the trophoblast. Am. J. Anat., 1943, 73, 335-449.

353. Huggett, A. St. G. Chronological changes in placental function. In G. E. W. Wolstenholme and E. C. P. Millar (Eds.) Ciba Foundation Colloquia on Ageing. Vol. 2, Ageing in Transient Tissues, London, J. and A. Churchill, Ltd., 1956, pp. 118-128.

354. Bernard, C. Recherches sur l'origine de la glycogenie dans la vie embryonnaire; nonvelle fonction du placenta. Comptes Rendus des Seances et Memoires de la Societe de Biologie. Tome premier de la troisieme serie, 1859.

355. Wislocki, G. B., Dempsey, E. W. and Fawcett, D. W. Some functional activities of the placental trophoblast. Obstet. Gynec. Survey, 1948, 5, 604-614.

356. Hertig, A. H. Involution of tissues in fetal life: a review. J. Gerontol., 1946, 1, 96-117.

357. Hellman, L. M. Novaks gynecologic and obstetric pathology. (3rd Ed.) Philadelphia and London: W. B. Saunders Co., 1952, pp. 534-562.

358. Shanklin, D. R. The human placenta. Obstet. and Gynec., 1958, 11, 129-138.

359. Fox, H. The significance of villous syncytial knots in the human placenta. J. Obstet. Gynaec. Brit. Cwlth., 1965, 72, 347-355.

360. Tenney, B. Syncytial degeneration in normal and pathologic placentas. Am. J. Obstet. and Gynec., 1937, 37, 1024-1028.

361. Thomsen, K. Zur Morphologie und Genese der sog. Placentarinfarkte Arch. Gynak., 1962, 185, 221-247.

362. Flexner, L. B. The functional role of the placenta. Gestation, Transactions of the first conference. New York: Josiah Macy Jr. Foundation, 1955, 11-52.

363. Jollie, W. P. The incidence of experimentally produced abdominal implantations in the rat. Anat. Rec., 1961, 141, 159-168.

364. Jollie, W. P. Action of progesterone in determining persistence of placental elements during parturitional delay in the rat. Endocrinology, 1962, 71, 573-579.

365. Jollie, W. P. The persistence of trophoblast on extrauterine tissues in the rat. Am. J. Anat., 1960, 106, 109-119.

366. Karnovsky, M. J. The fine structure of mitochondria in the frog nephron correlated with cytochrome oxidase activity. Exp. Molec. Path., 1963, 2, 347-366.

367. Boe, F. Studies on prolonged pregnancy in rats. Acta Path. et Microbiol. Scandinav., 1938, Suppl. 36, 1-146.

368. Snyder, F. F. The prolongation of pregnancy and complications of parturition in the rabbit following induction of ovulation near term. Johns Hopk. Hosp. Bull., 1934, 54, 1-23.

369. Holm, L. W., Salvatore, C., and Zeele-Minning, P. The histology of the postterm bovine placenta. Am. J. Obstet. and Gynec., 1964, 88, 479-489.

370. Clifford, S. H. Postmaturity. In S. Z. Levine (Ed.) Advances in pediatrics. Chicago: Year Book Publ., 1957, 9, 13-63.

371. Nesbitt, R. E. L. Prolongation of pregnancy: a review. Obstet. Gynec. Survey, 1955, 10, 311-361.

372. Clifford, S. H. Postmaturity with placental dysfunction. Clinical syndrome and pathologic findings. J. Pediatrics, 1954, 44, 1-13.

373. Cushner, I. M. Postmaturity. Sinai Hosp. J., 1964, 12, 39-47.

374. Gruenwald, P. The fetus in prolonged pregnancy. Am. J. Obstet. and Gynec., 1964, 89, 503-509.

375. Mead, P. B., and Stewart, C. M. Prolonged pregnancy. Am. J. Obstet. and Gynec., 1964, 89, 495-502.

376. Prytowsky, H. Postmaturity. Northwest Med., 1965, 64, 103-106.

377. Wentworth, P. Macroscopic placental calcification and its clinical significance. J. Obstet. Gynaec. Brit. Cwlth., 1965, 72, 215-223.

378. Reynolds, F. N. Problems of postmaturity. Proc. Roy. Soc. Med., 1938, 31, 781.

379. Masters, M., and Clayton, S. G. Calcification of human placenta (question of relationship to prolonged pregnancy). J. Obstet. Gynaec. Brit. Cwlth., 1940, 47, 437.

380. Tuchmann-Duplessis, H. Discussion in G. E. W. Wolstenholme and E. C. P. Millar (Eds.) Ciba Foundation Colloquia on Ageing. Vol. 2, Ageing in Transient Tissues, London, J. and A. Churchill, Ltd., 1956, p. 127.

381. Angevine, D. M. Structure and function of normal connective tissue. In Transactions, first conference on connective tissue. New York: Josiah Macy Jr. Foundation, 1950.

382. Bulmer, D., Dickson, A. D. The fibrinoid capsule of the rat placenta and the disappearance of the decidua. J. Anat., 1961, 95, 300-310.

383. Bardawil, W. A. and Toy, B. L. The natural history of chorio-carcinoma: problems of immunity and spontaneous regression. Ann. N.Y. Acad. Sci., 1959, 80, 197.

384. Bradbury, W. D., Billington, W. D., and Kirby, D. R. S. Histo-chemical and electron microscopical study of the fibrinoid of the mouse placenta. J. Roy. Micro. Soc., 1965, 84, 199-211.

385. Hertig, A. T. Pathological aspects. In C. A. Villee (Ed.) The placenta and fetal membranes. Baltimore: Williams and Wilkins, 1960.

386. Kline, B. S. Microscopic observations of the placental barrier in transplacental erythrocytoxic anemia (erythroblastosis fetalis) and in normal pregnancy. Am. J. Obstet. and Gynec., 1948, 56, 226-237.

387. Paine, C. G. Observations on placental histology in normal and abnormal pregnancy. J. Obstet. and Gynaec. Brit. Cwlth., 1957, 64, 668.

388. Zacks, S. I., and Blazar, A. S. Chorionic villi in normal pregnancy, pre-eclamptic toxemia, erythroblastosis and diabetes mellitus. A light and electron microscope study. Obstet. and Gynec., 1963, 22, 149-167.

ULTRASTRUCTURAL AND CYTOCHEMICAL STUDIES OF THE EXTRAEMBRYONIC MEMBRANES OF THE RAT

by

Reid Sandford Connell Jr., M.S.

Volume 2

A THESIS
Presented to the Department of Anatomy
and the Graduate Division of the University of Oregon Medical School
in partial fulfillment of
the requirements for the degree of
Doctor of Philosophy

June 1967

FIGURE 1

A schematic representation of the labyrinthine barrier of the rat hemotrichorial placenta. This barrier typically consists of four discrete cytoplasmic elements which intervene between maternal and fetal blood streams. From the maternal blood sinus (MBS) inward to the lumen of the allantoic capillary (FBC), in order these are: (a) trophoblast I (T 1), an attenuated cellular layer which extends pleomorphic evaginations into the sinus; (b) trophoblast II (T 11), a relatively thick syncytial layer which is loosely associated with trophoblast I and closely apposed in a series of undulations with trophoblast III (T 111); (c) trophoblast III, a relatively thin syncytial layer which has numerous short cytoplasmic projections and infoldings on its inner surface; (d) fetal endothelium (En), an attenuated cellular layer with an underlying basement membrane (BM).

BM - basement membrane

EN - endothelium

FBC - fetal blood capillary

MBS - maternal blood space

T 1 - trophoblast I

T 11 - trophoblast II

T 111 - trophoblast III

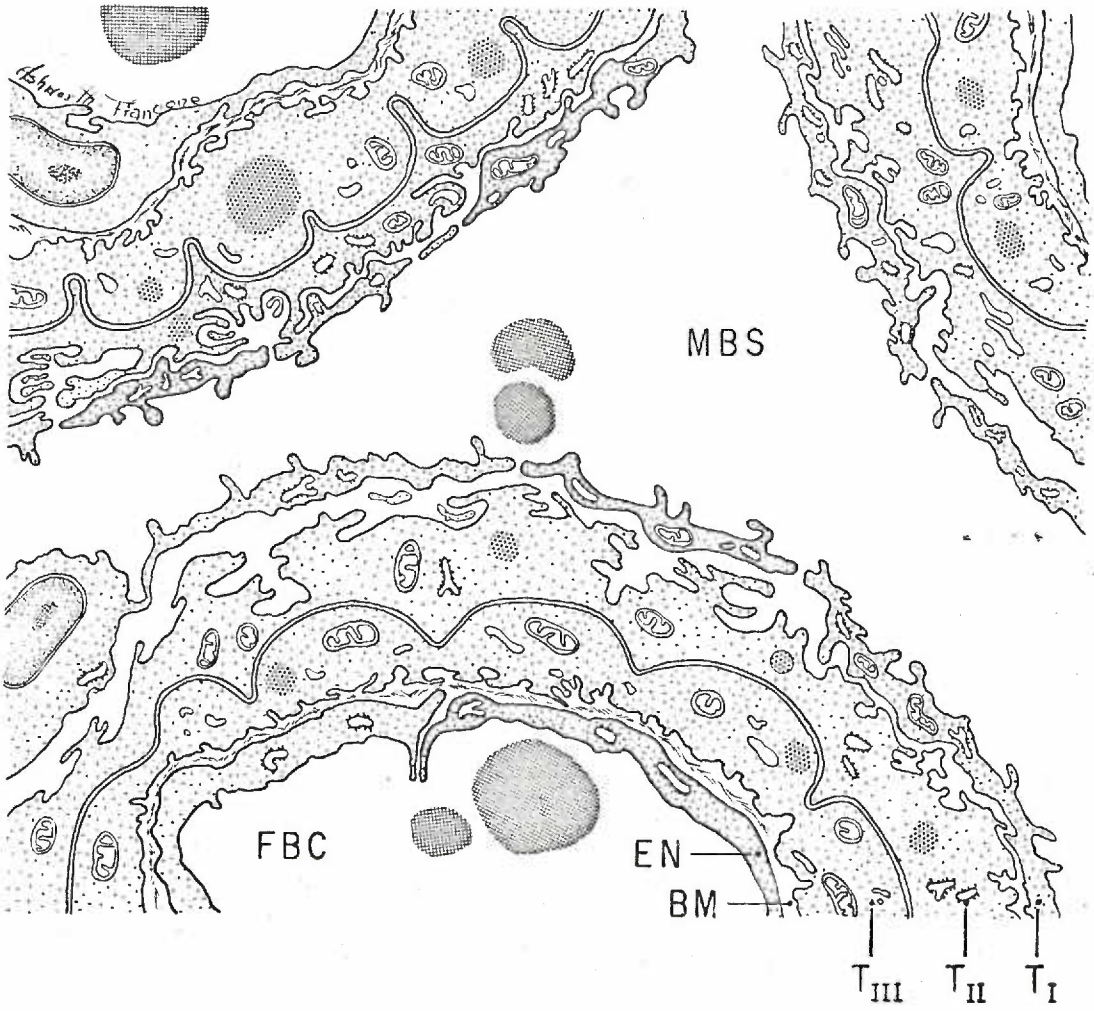
MBS
FBC
EN
BM
T_{III}
T_{II}
T_I

FIGURE 2

A schematic representation of the maternal and fetal placental components of the 12-14 day old gestation sac as seen by cutting at right angles to the long axis of the uterine horn.

AM - amnion

AV - allantoic vessel

CSM - circular smooth muscle

DB - decidua basalis

DC - decidua capsularis

ES - endodermal sinus

Ex - exocoelom

GTC - giant trophoblast cell layer

LSM - longitudinal smooth muscle

Mes - mesometrium

MG - metrial gland

PL - placental labyrinth

PYS - parietal yolk sac

RM - Reichert's membrane

ST - spongiotrophoblast

UC - umbilical cord

UL - uterine lumen

VYS - visceral yolk sac

YSC - yolk sac cavity

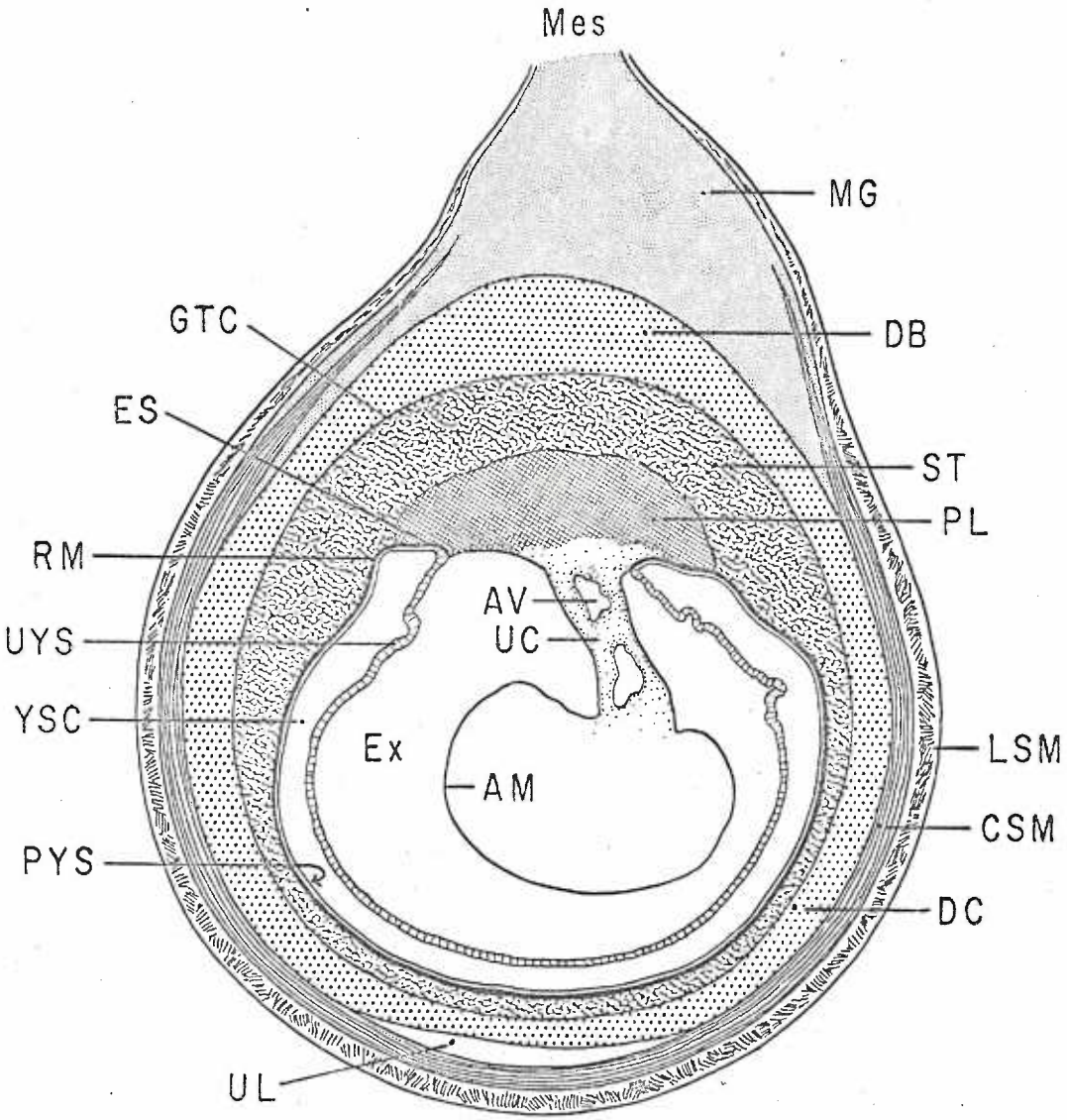
Mes
MG
GTC
DB
ES
ST
PL
RM
AV
UC
UYS
YSC
Ex
LSM
AM
CSM
PYS
DC
UL

FIGURE 3

A schematic representation of the maternal and fetal placental components of the 18-22 day old gestation sac as seen by cutting at right angles to the long axis of the uterine horn.

AM - amnion

AV - allantoic vessel

CSM - circular smooth muscle

DB - decidua basalis

DP - decidua parietalis

ES - endodermal sinus

Ex - exocoelom

GTC - giant trophoblast cell layer

LSM - longitudinal smooth muscle

Mes - mesometrium

MG - metrial gland

PL - placental labyrinth

PYS - parietal yolk sac

RM - Reichert's membrane

ST - spongiotrophoblast

SVYS - smooth visceral yolk sac

UC - umbilical cord

UL - uterine lumen

VVYS - villous visceral yolk sac

YSC - yolk sac cavity

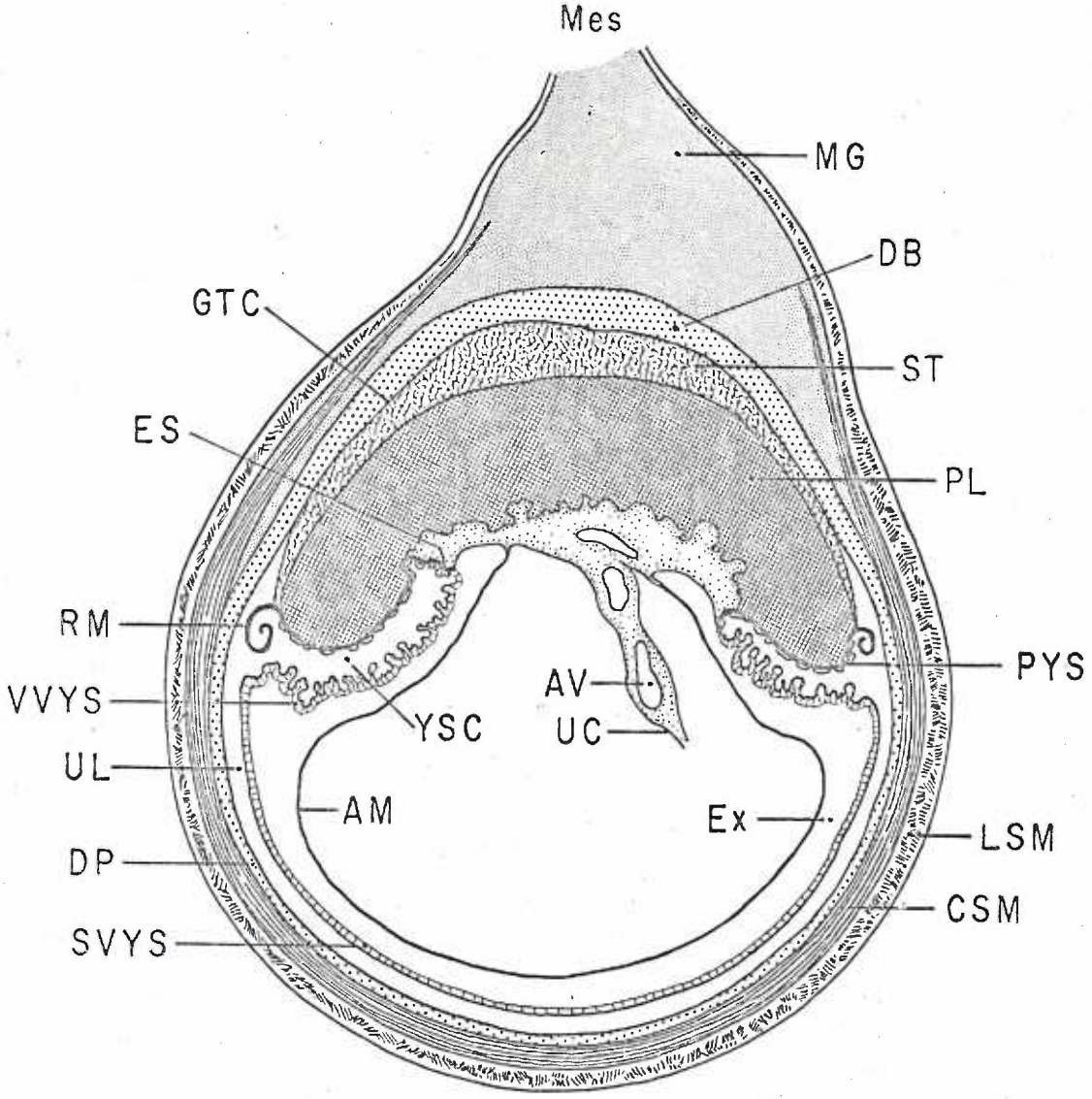
Mes
MG
DB
GTC
ST
ES
PL
RM
PYS
VVYS
AV
YSC
UC
UL
AM
Ex
LSM
DP
CSM
SVYS

FIGURE 4

A schematic drawing of the rat visceral yolk sac fine structure during the second trimester. The visceral epithelium consists of simple columnar cells linked together by terminal bars and supported by a narrow visceral basement membrane (VBM). The apical cytoplasm which is crowned by an irregular border of microvilli (MV) displays an assortment of surface invaginations, absorption vacuoles (Abs V), vesicles and dense bodies (DB). Well developed mitochondria (Mi) and granular endoplasmic reticulum (RER) are distributed throughout the cytoplasm, but large lipid inclusions (Lip) at this stage, occur typically below the nuclei (Nuc). The connective tissue space (CTS) beneath the visceral endoderm (VE) contains a loose meshwork of connective tissue cells (CTC), fibrils and vitelline capillaries (VC). An attenuated layer of mesothelial cells (Mes) which are supported by the serosal basement membrane (SBM), separate the visceral yolk sac from the underlying exocoelomic cavity.

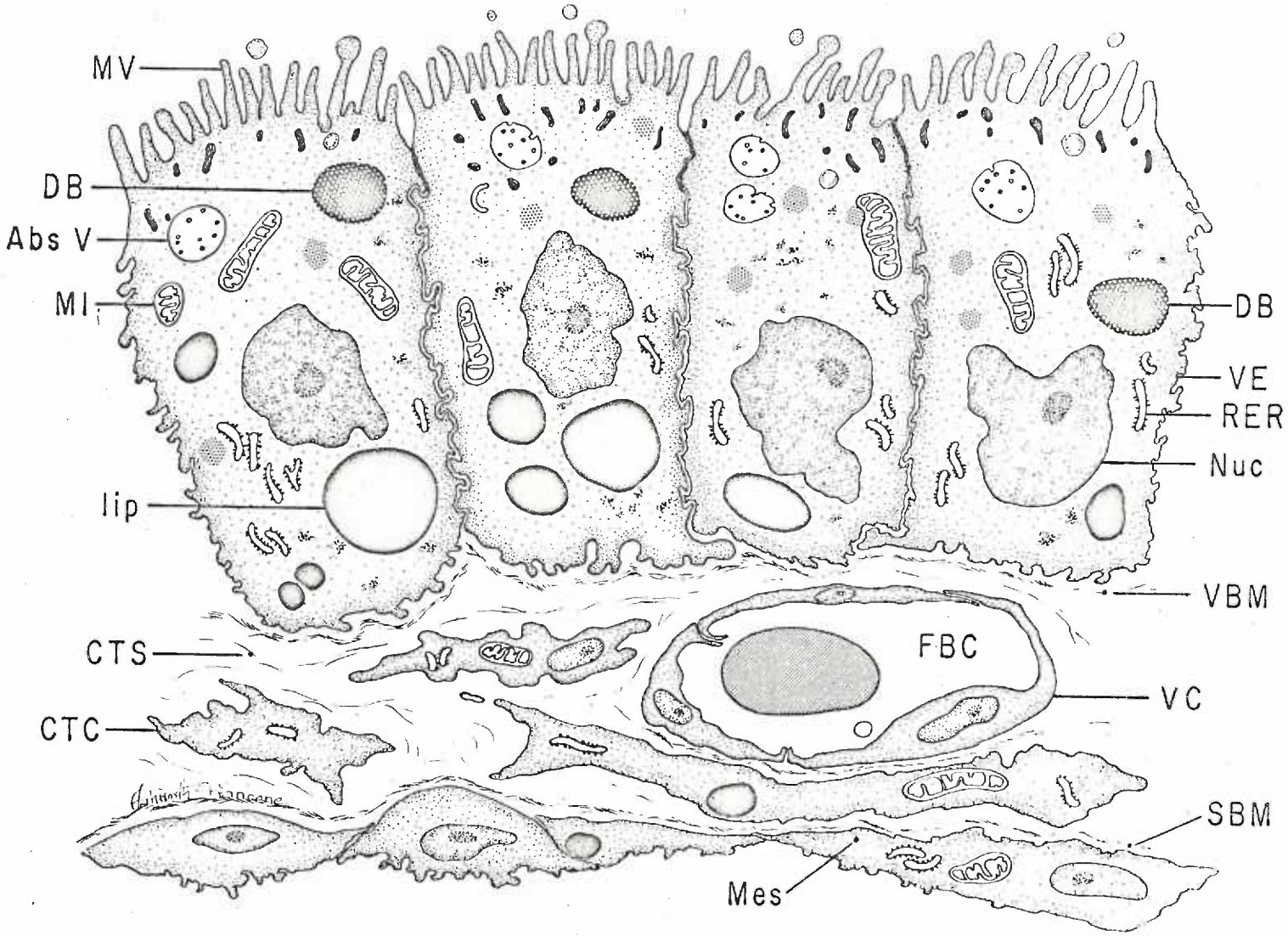
MV
DB
Abs V
MI
lip
CTS
CTC
FBC
VC
VBM
DB
VE
RER
Nuc
SBM
Mes

Abs V - absorption vacuole

CTC - connective tissue cell

CTS - connective tissue space

DB - dense body

FBC - fetal blood cell

Lip - lipid

Mes - mesothelium

Mi - mitochondria

MV - microvilli

Nuc - nucleus

RER - rough endoplasmic reticulum

SBM - serosal basement membrane

VBM - visceral basement membrane

VC - vitelline capillary

VE - visceral endoderm

ABBREVIATIONS FOR FIGURES 5 - 62

BM	-	basement membrane
Co	-	collagen fibrils
CTC	-	connective tissue cell
CTS	-	connective tissue space
Des	-	desmosome
EL	-	external lamina
En	-	endothelium
ER	-	endoplasmic reticulum
F	-	fenestrations
FBC	-	fetal blood capillary
Fi	-	fibrils
FRBC	-	fetal red blood cell
G	-	golgi elements
IS	-	intercellular space
Jct	-	cell junction
Li	-	lipid
Ly	-	lysosome
MB	-	multivesicular body
MBS	-	maternal blood space
MF	-	marginal fold
Mi	-	mitochondria
ML	-	maternal leukocyte
MP	-	maternal platelet

MRBC	-	maternal red blood cell
My	-	myelin figure
N	-	nucleus
PC	-	perinuclear cisterna
PV	-	pinocytotic vesicle (caveolae)
Ri	-	ribosome (polysome)
T 1	-	trophoblast I
T 11	-	trophoblast II
T 111	-	trophoblast III
TJ	-	tight junction
V	-	vacuole
v	-	vesicle
ZA	-	zonula adheren (intermediate junction)

FIGURE 5

Cross sectional view of a portion of a cord of 12 day avascular parenchymal trophoblast incubated with ATP as substrate. Magnification 12,900 X. A maternal blood space (MBS) is seen in the upper left corner of the figure. The layers of trophoblastic cells appear loosely associated and display cytoplasmic evaginations which project into wide intercellular spaces (IS). These spaces are interrupted at irregular intervals by cell junctions (Jct). Globular deposits of final reaction product (lead phosphate) occur in the intercellular spaces and along the surface membranes of trophoblast cells.

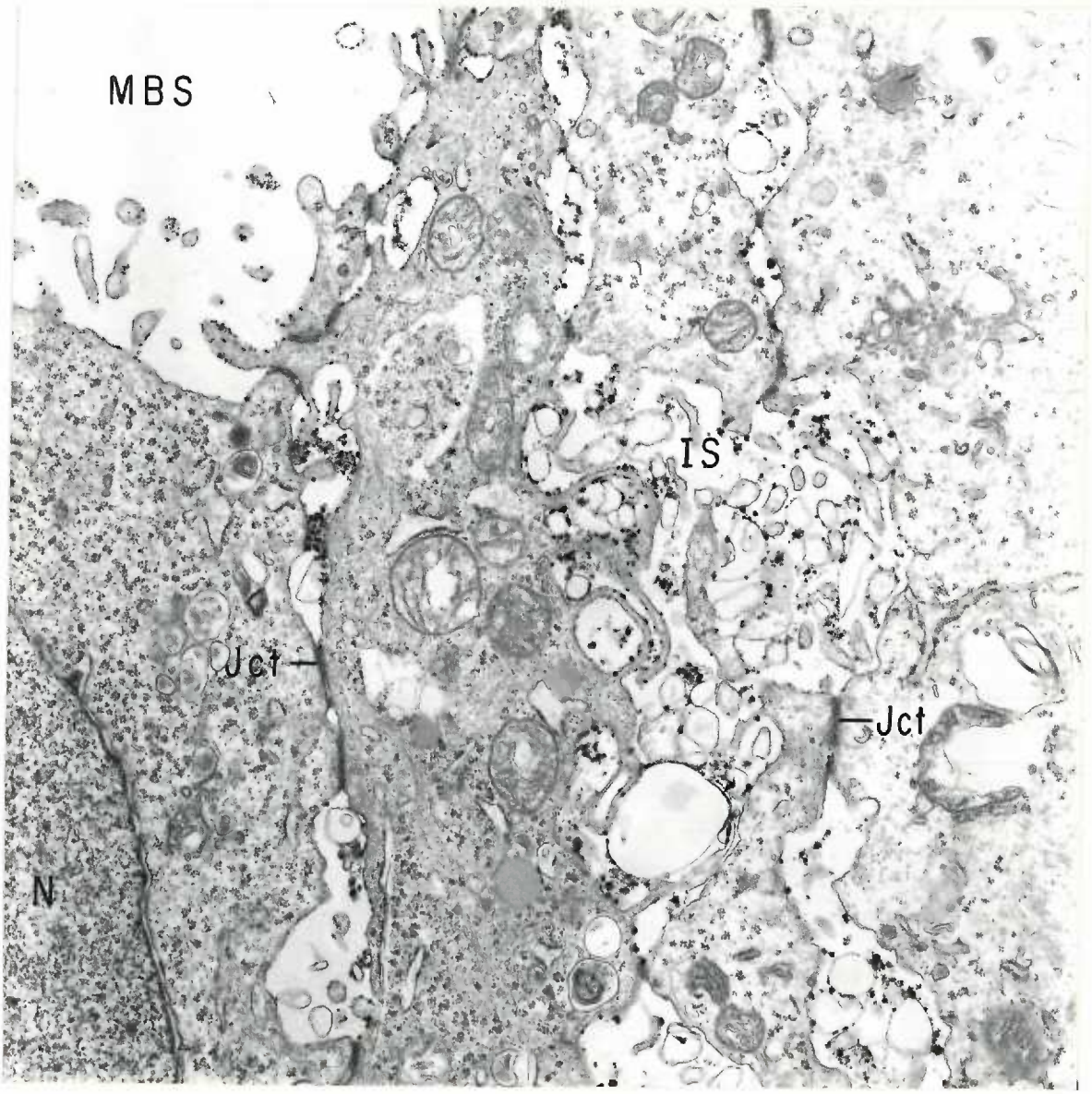

5

FIGURE 6

Twelve day avascular parenchymal trophoblast incubated with AMP as substrate. Magnification 12,900 X. The outer layer of trophoblast bordering the maternal blood space (MBS) is greatly attenuated and displays relatively few cytoplasmic organelles as compared with the inner layer of trophoblast which is characterized by the presence of numerous polyribosomes and lipid inclusions (Li). Deposits of final reaction product are distributed along the outer surface membrane of the inner layer of trophoblast cells.

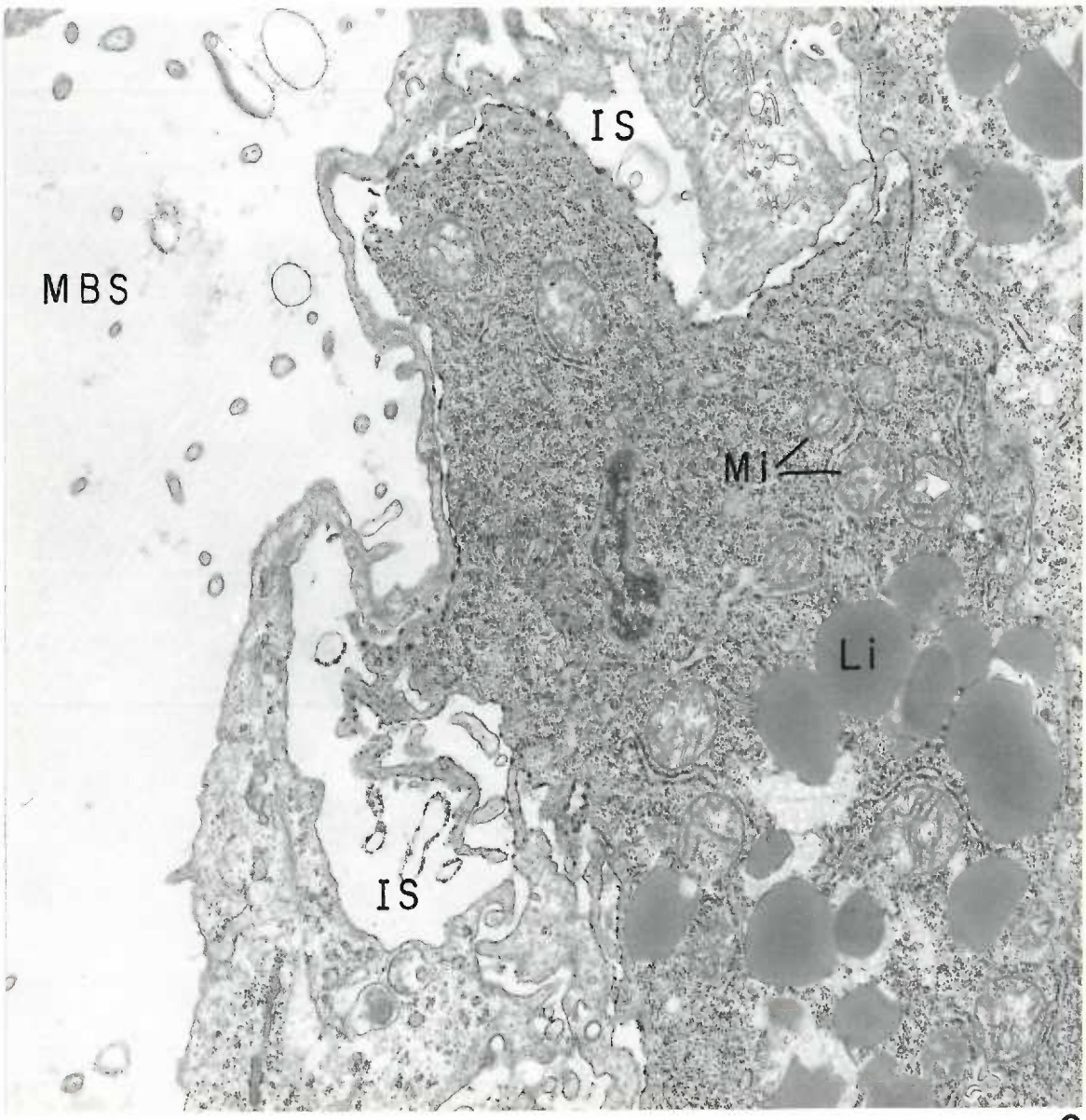

6

FIGURE 7

Portions of several 12 day trophoblast cells. Magnification 12,900 X. The attenuated outer trophoblast cell appears to be in the process of releasing a disrupted mitochondrion and a small vacuolar structure into the maternal blood space (MBS). The long lumen of the granular endoplasmic reticulum (ER) in the inner trophoblast cells displays two possible sites of continuity with the intercellular space (arrows). Note the continuity between the perinuclear cisternae (PC) and the dilated lumen of the granular endoplasmic reticulum (ER).

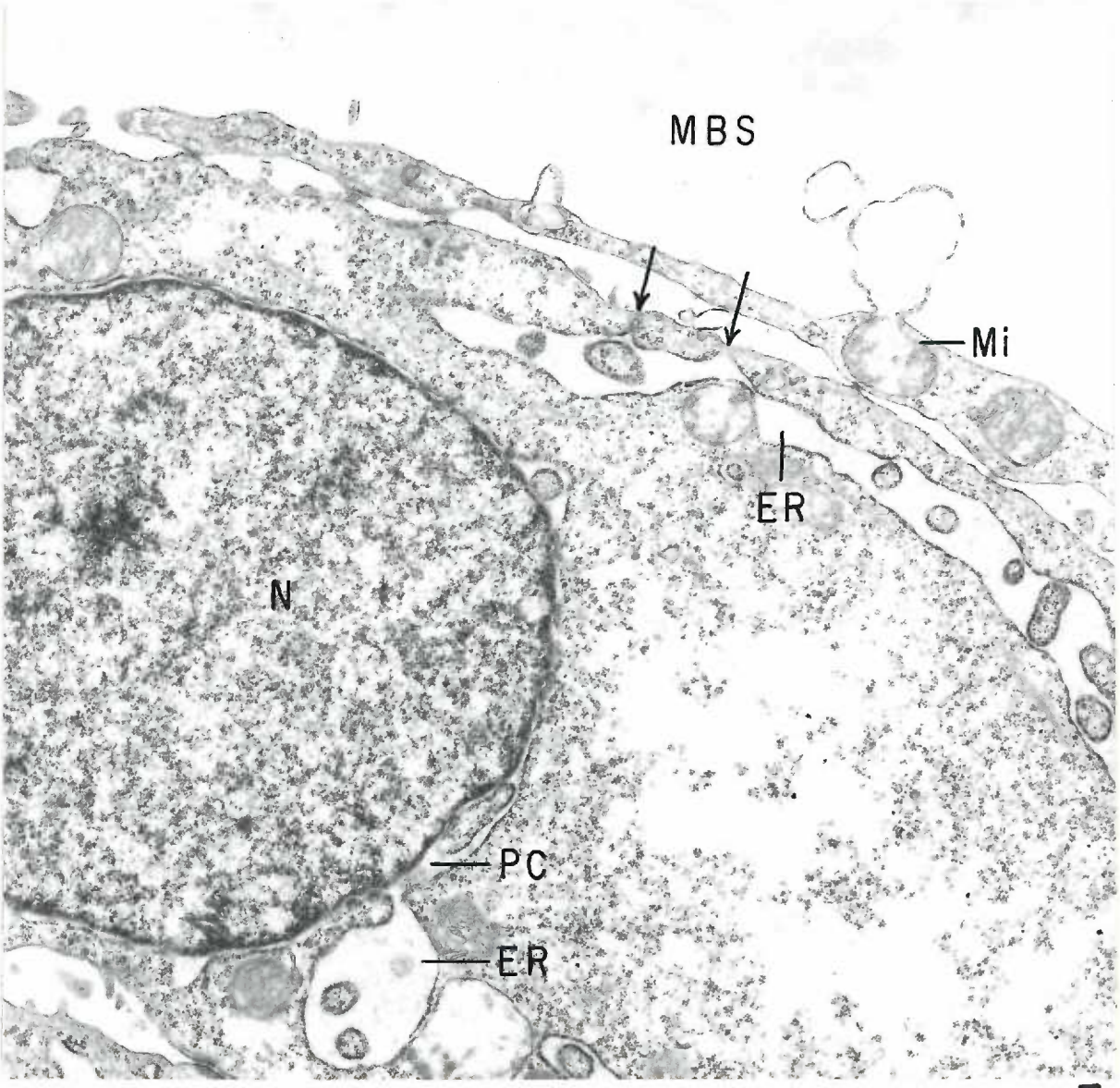

7

FIGURE 8

Twelve day avascular trophoblast incubated with ADP as substrate. Magnification 12,900 X. Sparse deposits of final reaction product are irregularly distributed along the surface membranes bordering intercellular spaces (IS). The inner and outer trophoblast cells are attached by irregularly spaced desmosomes (Des). A large golgi zone (G) is seen in the perinuclear cytoplasm.

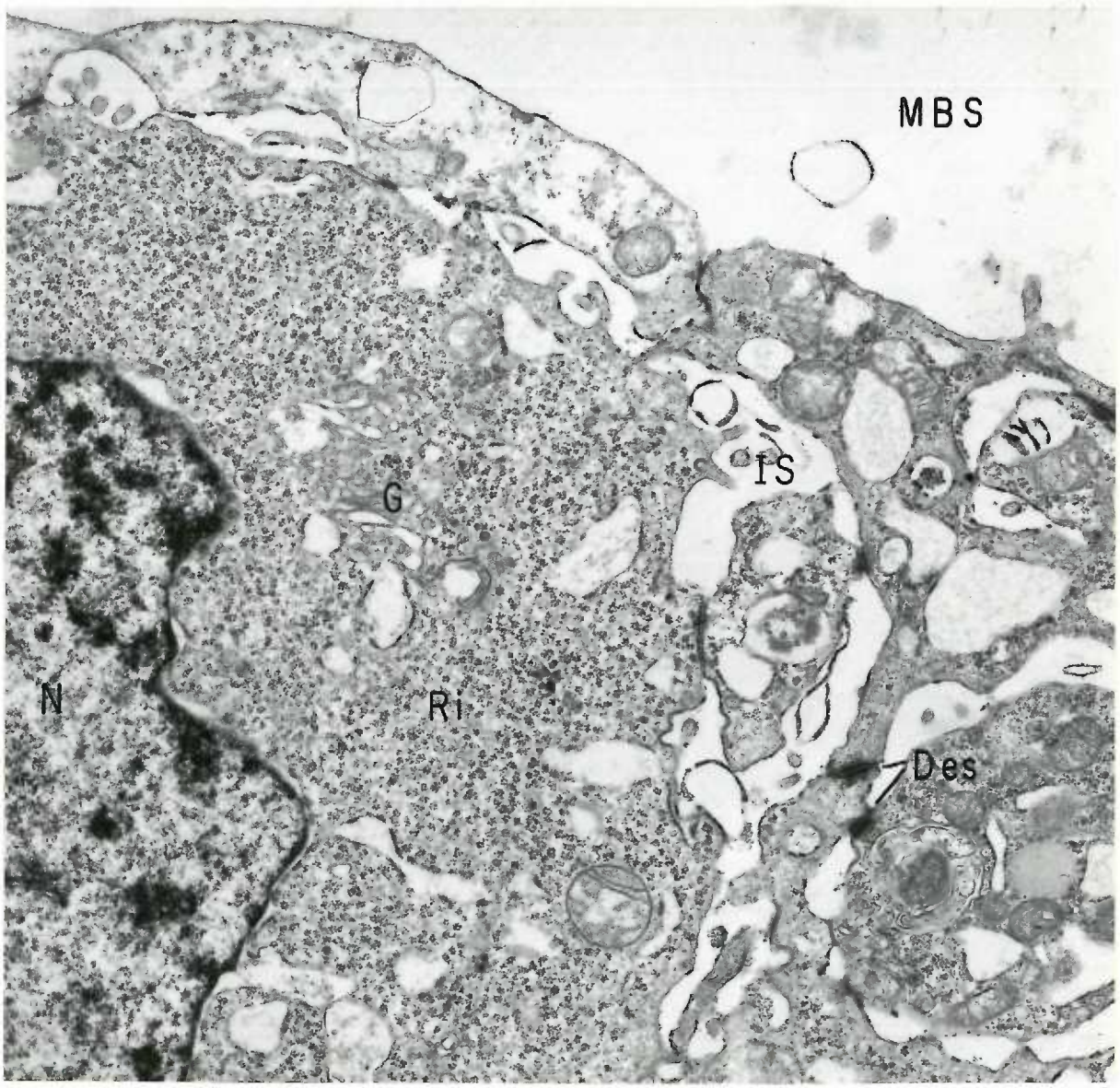

8

FIGURE 9

Twelve day avascular trophoblast incubated with ATP as substrate. Magnification 12,900 X. In this particular section where large accumulations of granular or flocculant material fill the maternal blood space (MBS), final reaction product is absent from the surface membranes of the trophoblast cells. The cytoplasm of the outer trophoblast cell contains ribosomes (Ri) and skeins of intercommunicating granular endoplasmic reticulum (ER) which are oriented with the long axis of the cell.

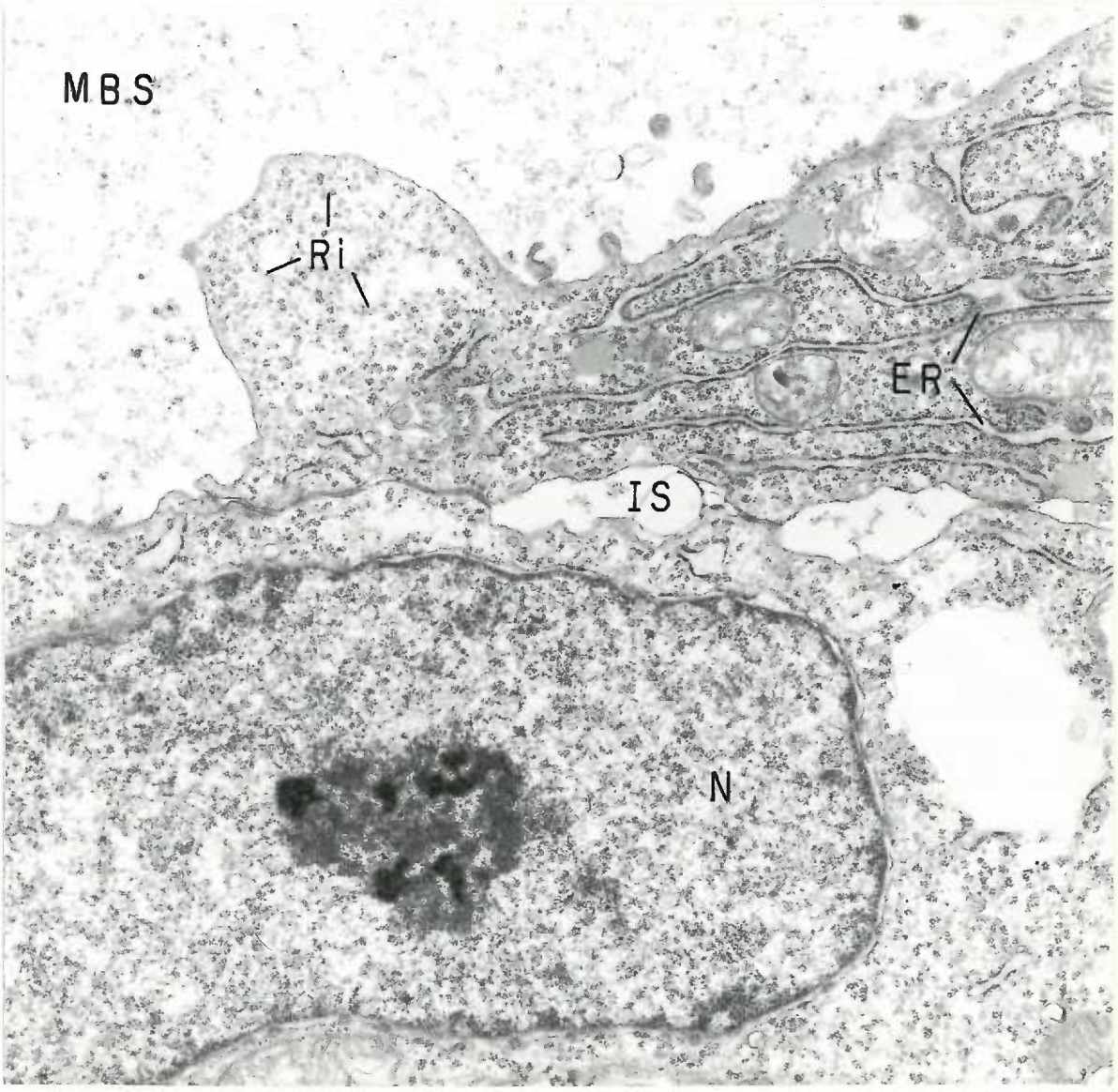

9

FIGURE 10

Tangential section through the 12 day avascular trophoblast incubated with ATP as substrate. Magnification 12,900 X. Final reaction product occurs as individual granules and clusters of granules which are irregularly deposited along the surface membranes and their evaginations. Deposits of lead phosphate are also associated with the flocculent material and vesicular profiles seen within the maternal blood spaces (MBS). Note particularly that the surface membrane of a maternal platelet (MP) in the right side of the figure is coated by dense globular deposits of final reaction product.

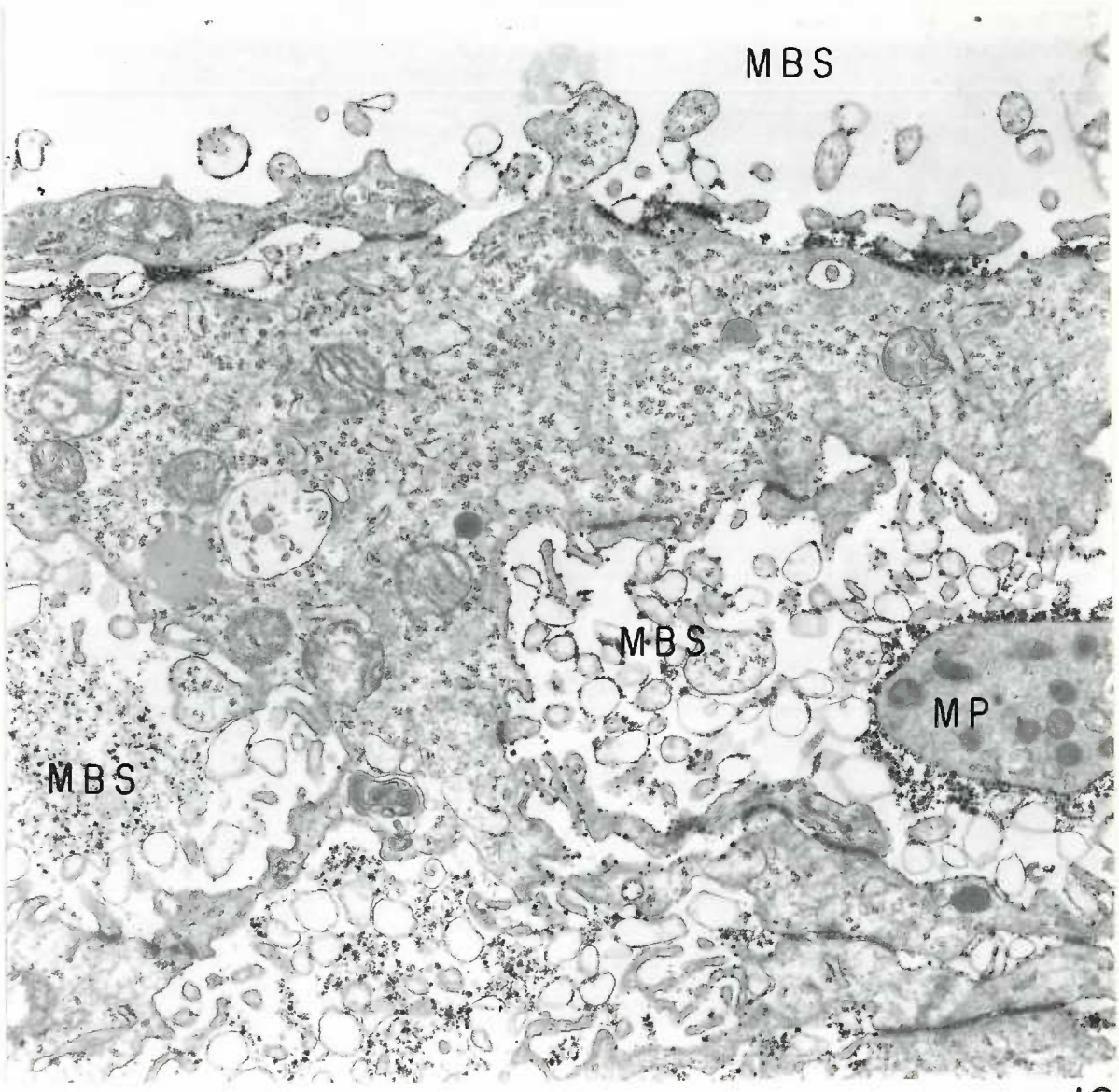

10

FIGURE 11

Twelve day avascular trophoblast incubated with AMP as substrate. Magnification 12,900 X. Note the long and slender evaginations of the free surface of the outer trophoblast cell. Some of the projections have terminal bulbous enlargements (arrows) which contain granular material similar to that seen in the maternal blood space (MBS). In addition to polyribosomes (Ri) the cytoplasm contains numerous fine fibrils (Fi). The mitochondria (Mi) appear ballooned and exhibit disruption of their matrices. Fine deposits of lead phosphate are distributed throughout the granular material in the maternal blood space and in the intercellular space (IS) in the lower left corner of the figure. Very little final reaction product occurs on the surface membranes of the trophoblast cells.

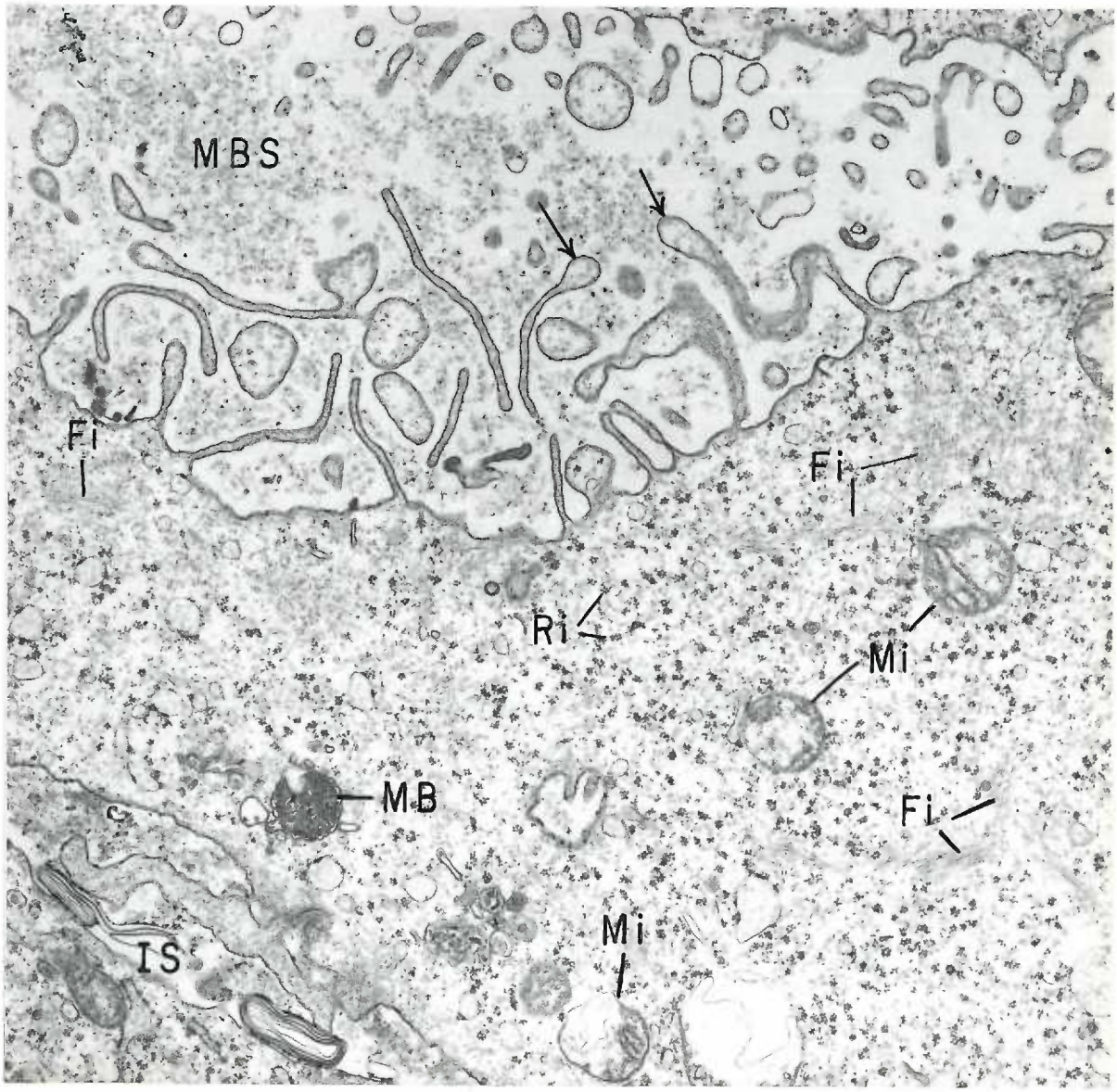

II

FIGURE 12

Twelve day avascular trophoblast incubated with AMP as substrate. Magnification 12,900 X. Final reaction product is distributed as described in Figure 11. The individual fibrils (Fi) or groups of fibrils found within the trophoblastic cell cytoplasm closely resemble the tonofibrils of epithelial cells. The fibrils are generally oriented parallel to the long axis of the trophoblast cells and some of them terminate in desmosomes (Des). Note the disrupted appearance of the mitochondria (Mi).

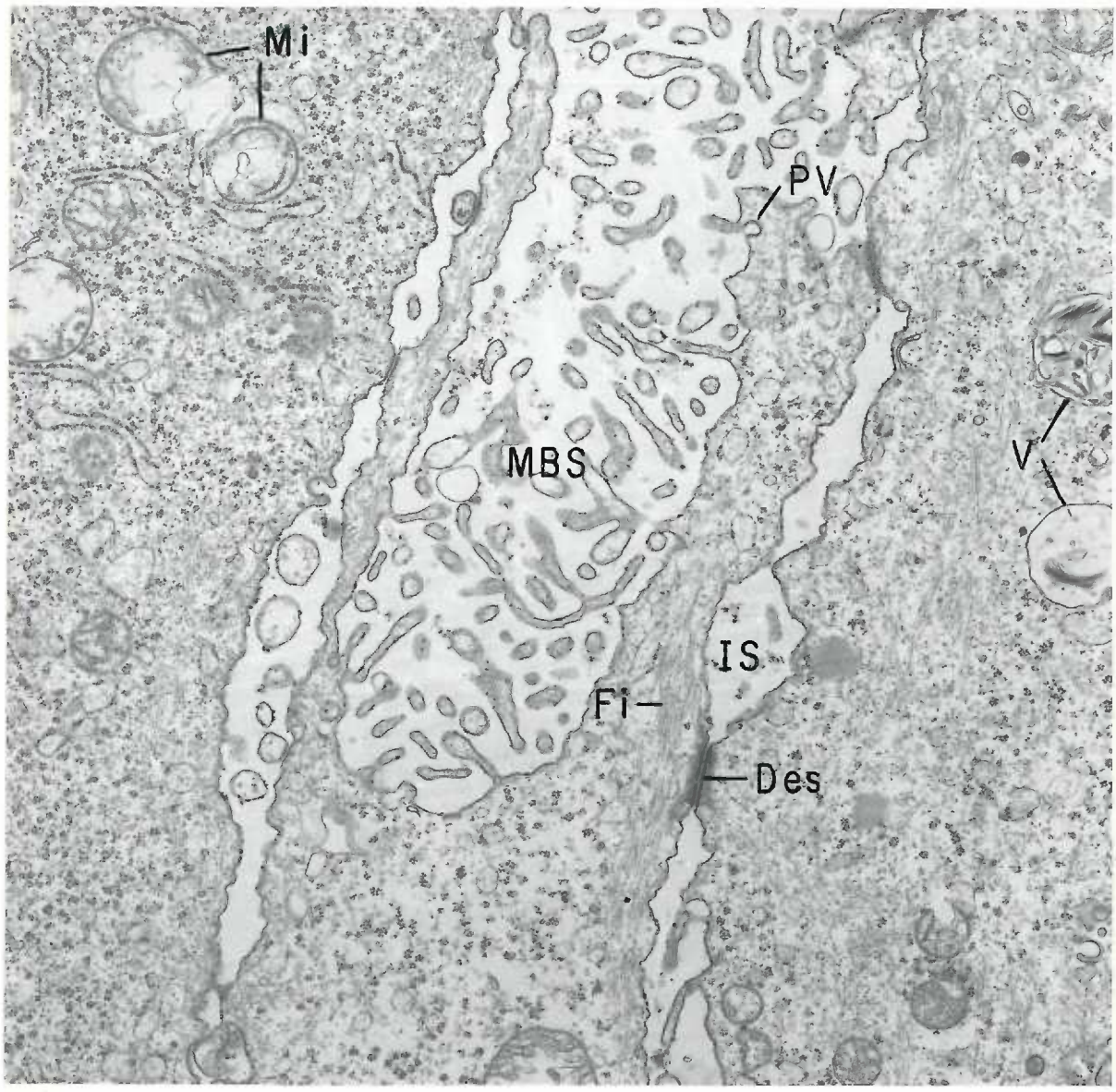

12

FIGURE 13

Twelve day avascular trophoblast incubated with ATP as substrate. Magnification 7,800 X. Final reaction product is distributed as described in Figure 10. The trophoblast cell at the bottom of the figure exhibits large spherical vacuoles (V) which have poorly defined limiting membranes and contain a granular or flocculent material of moderate electron density.

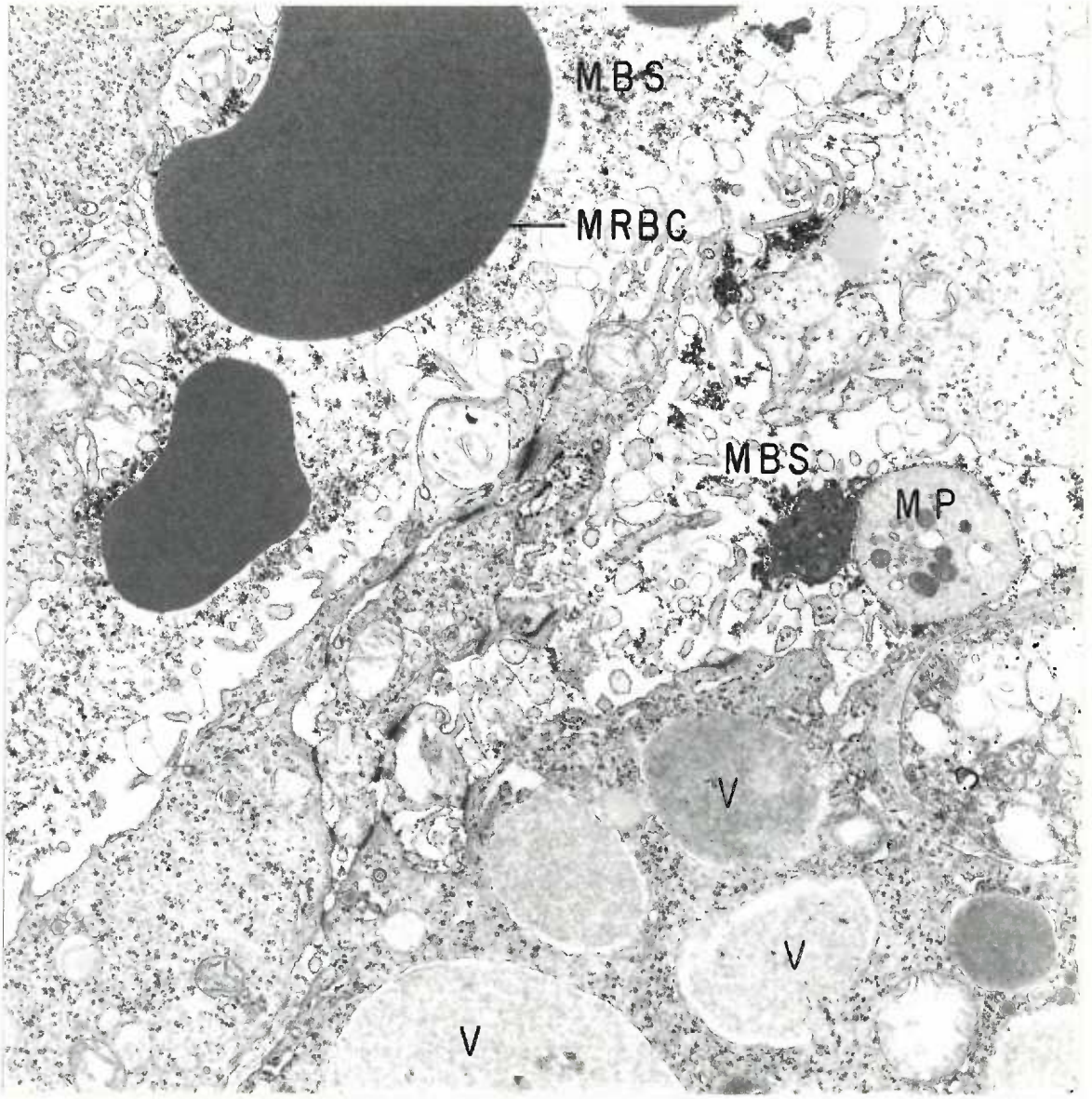

13

FIGURE 14

Twelve day avascular trophoblast incubated with ATP as substrate. Magnification 12,900 X. A leukocyte (ML) within the maternal blood space (MBS) displays globular deposits of final reaction product along the outer aspect of its limiting plasma membrane. Fewer and finer precipitates of final product are deposited along the surface membranes of bordering trophoblast cells and tubular and vesicular profiles.

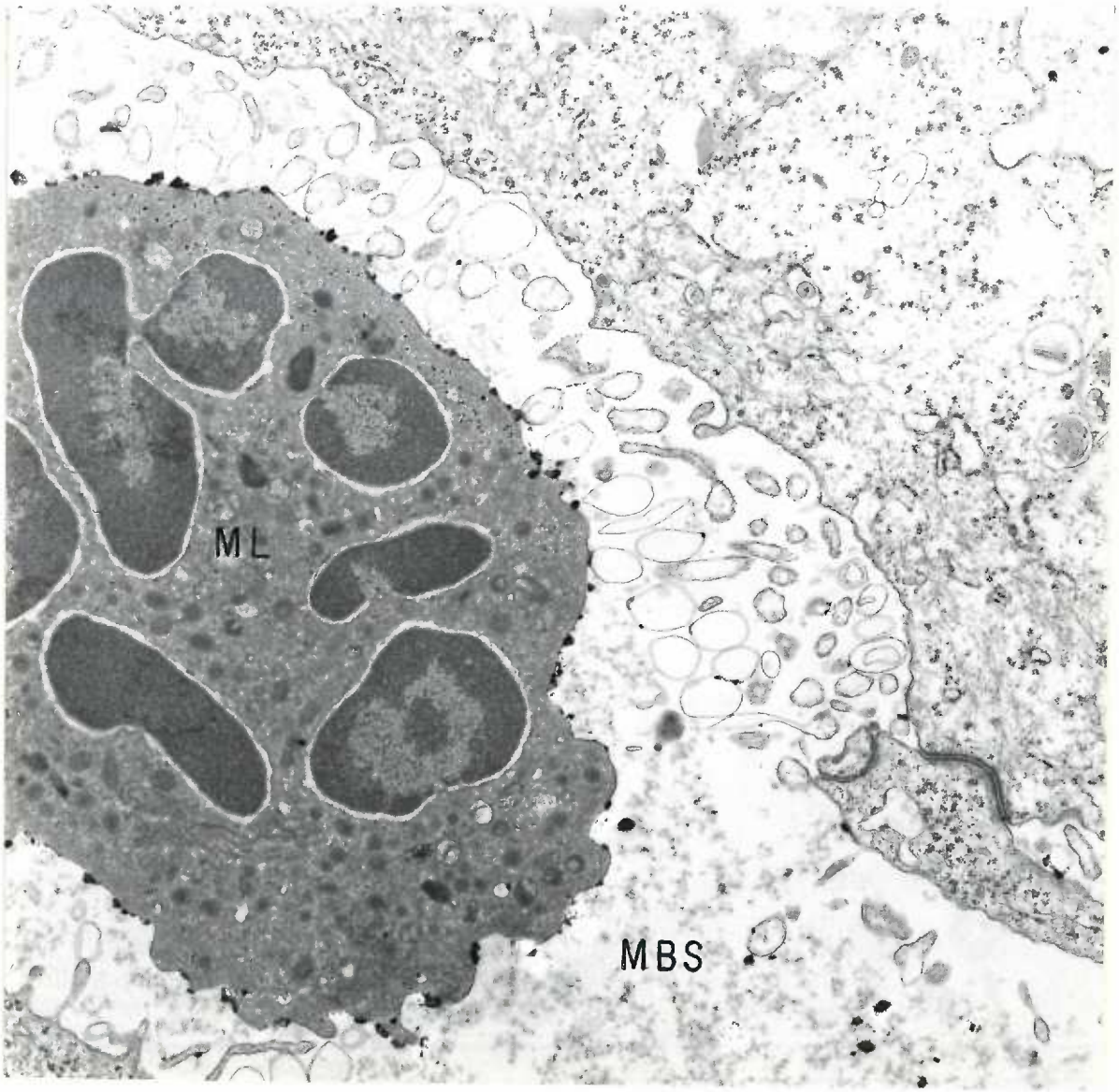

14

FIGURE 15

Portions of two 12 day trophoblast cells incubated with ATP as substrate. Magnification 12,900 X. In the presence of large accumulations of granular material in the maternal blood space (MBS), final reaction product is absent along the bordering surface membranes. Note the long bundles of fibrils (Fi) which converge upon the desmosomes (Des). In addition to polyribosomes and distended profiles of granular endoplasmic reticulum (ER), the cytoplasm of the two trophoblast cells displays golgi elements (G) and a number of disrupted mitochondria (Mi).

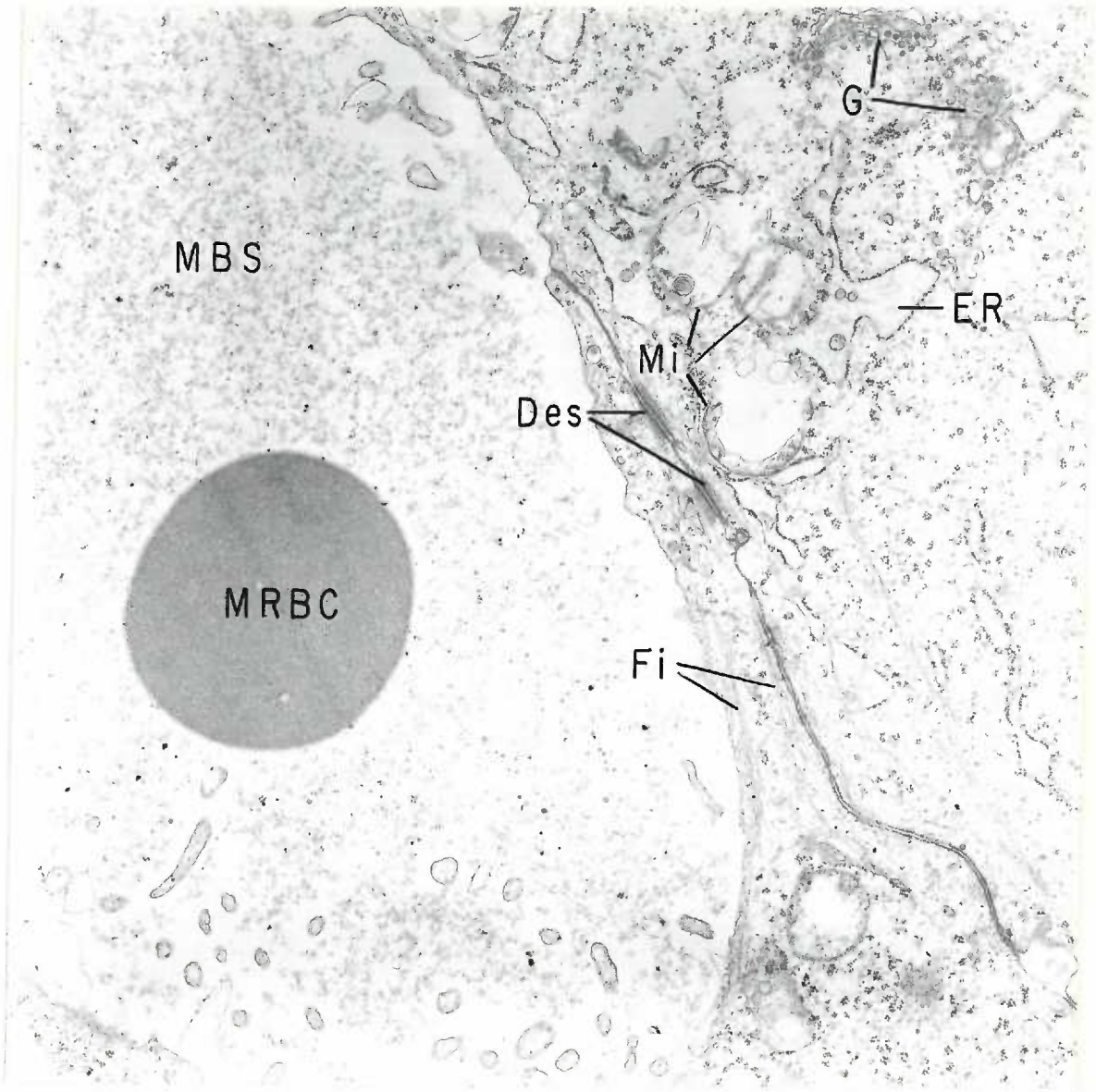

15

FIGURE 16

Twelve day avascular trophoblast incubated with ADP as substrate. Magnification 12,900 X. Although ADPase activity is very sparse at this stage, occasional deposits of final reaction product are found in the intercellular spaces (IS) and along the surface membranes bordering these spaces. The outer trophoblast cell bordering the maternal blood space (MBS) displays a vacuole (V) which contains a myelin-like concentric system of membranes. Mitochondria (Mi) in the inner trophoblast cell exhibit fragmented cristae and focal rarefacation of their matrices.

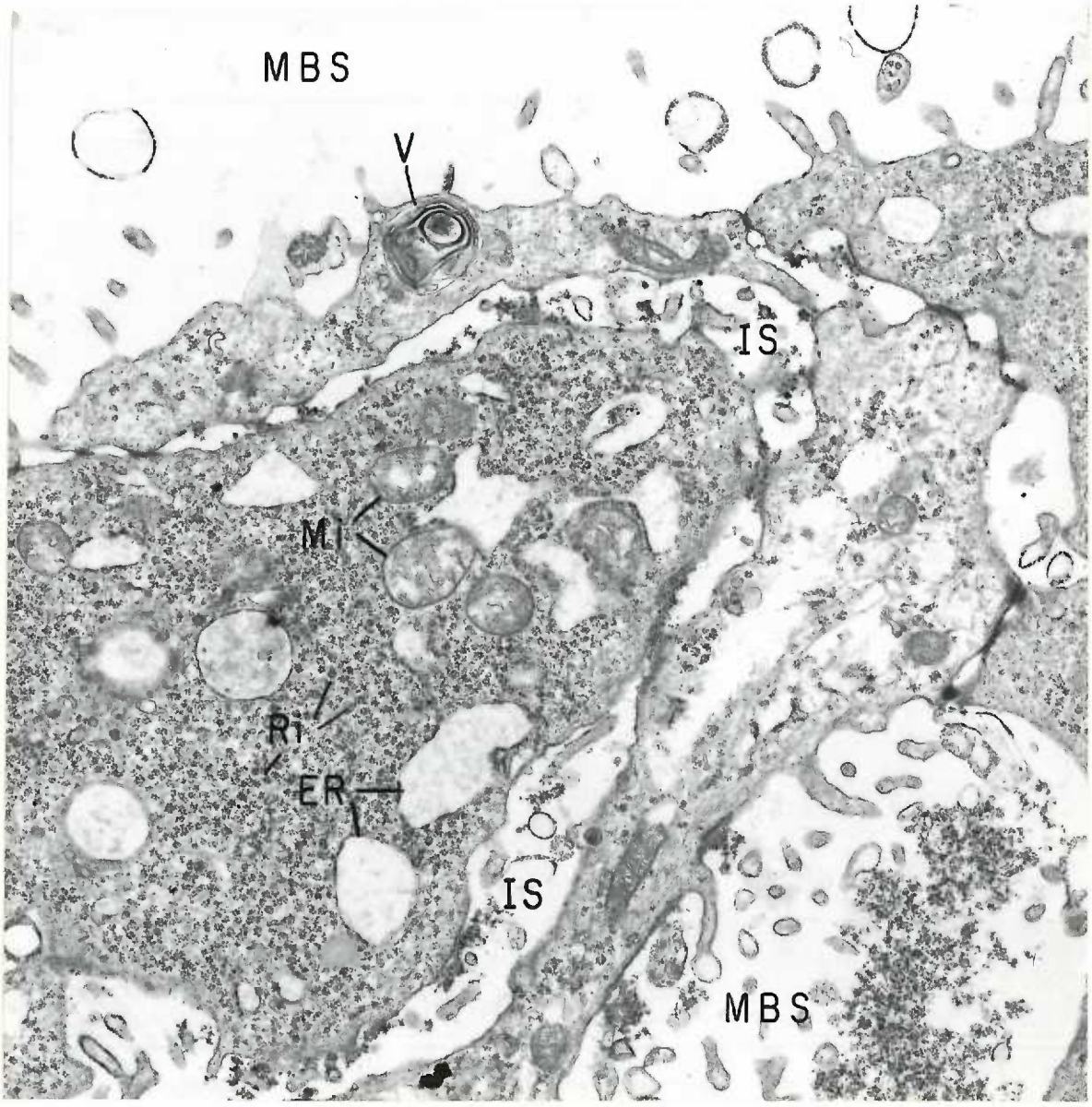

16

FIGURE 17

Twelve day avascular trophoblast incubated with ADP as substrate. Magnification 12,900 X. ADPase activity is localized as described in Figures 8 and 16. The cytoplasm of the inner trophoblast cells is strikingly pervaded with polyribosomes (Ri).

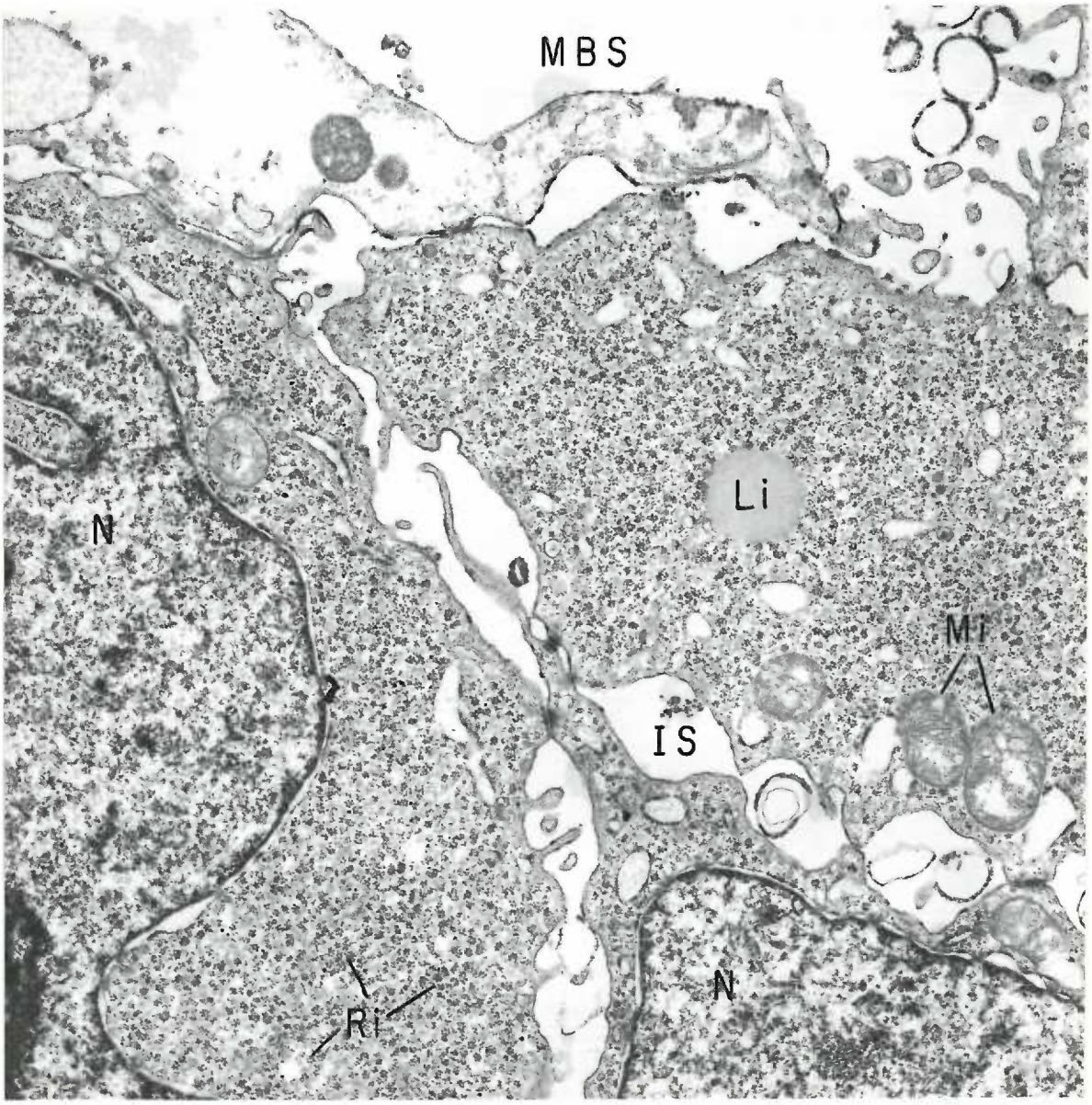

17

FIGURE 18

Twelve day avascular trophoblast incubated with ATP as substrate. Magnification 7,800 X. This figure shows an inner trophoblast cell in metaphase of mitotic division. Sparse deposits of final reaction product are found along the surface membranes of the trophoblast cells and are scattered throughout the granular material within the intercellular space (IS).

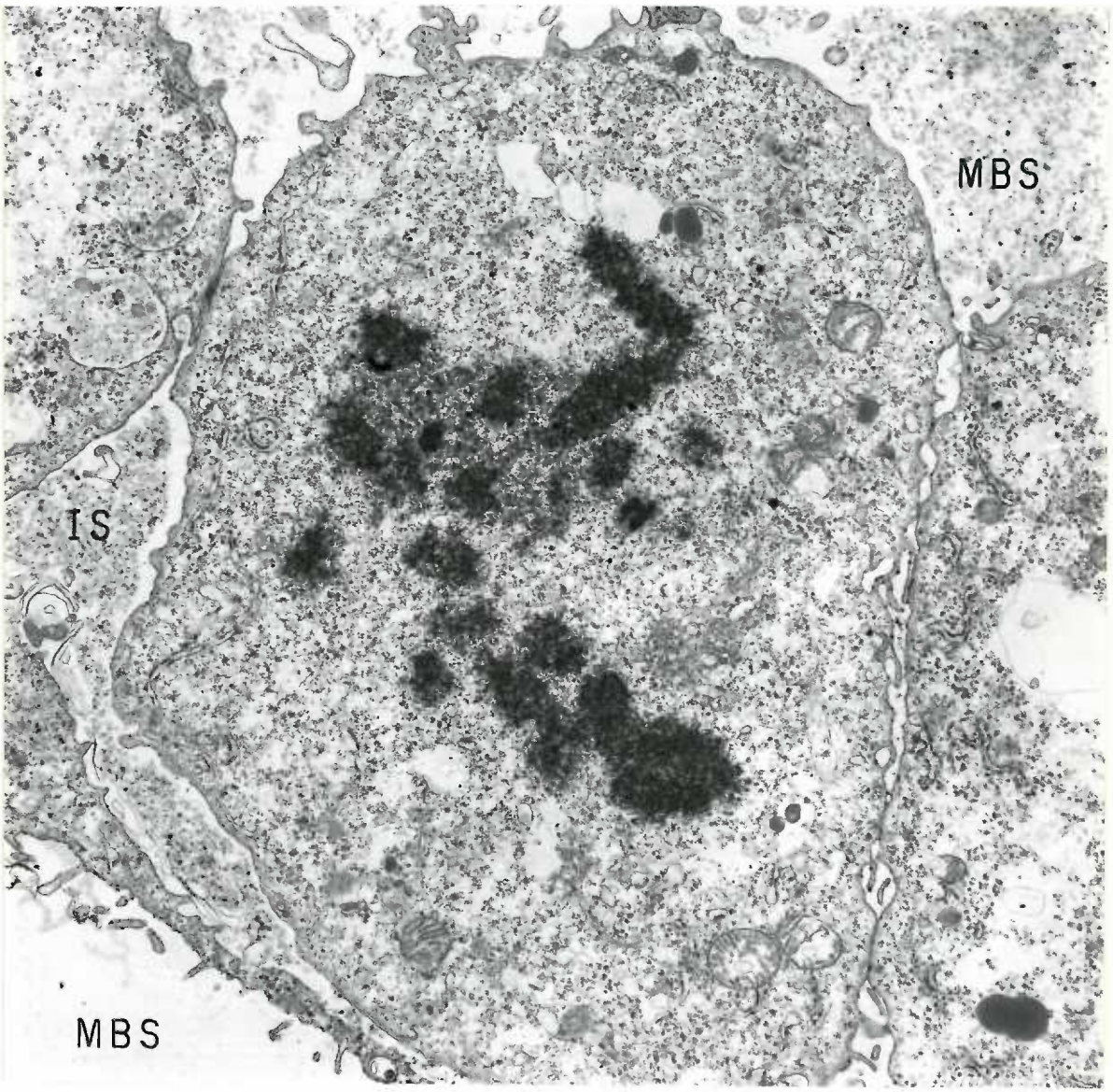

18

FIGURE 19

Twelve day avascular trophoblast incubated with ATP as substrate. Magnification 12,900 X. ATPase activity is localized as described in Figure 10. Note that the large vacuole (V) in the middle of the trophoblast contains a homogenous material similar in texture to hemoglobin and, therefore, may possibly represent a phagocytized fragment of a maternal erythrocyte.

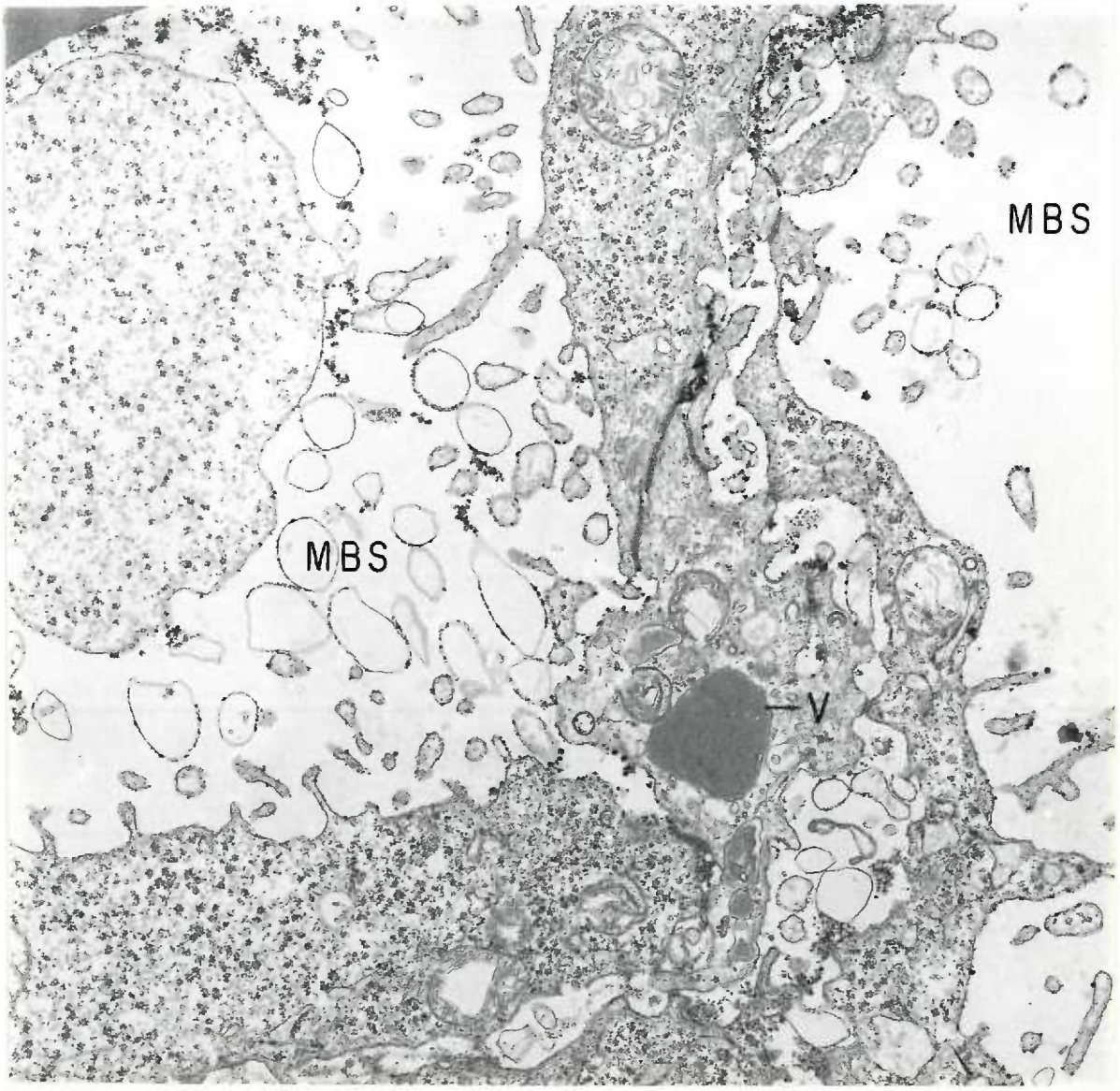

19

FIGURE 20

Cross section of a 12 day trophoblast cell bordering a maternal blood space (MBS). Magnification 12,900 X. The cytoplasm is richly provided with polyribosomes, expanded profiles of granular endoplasmic reticulum (ER), disrupted mitochondria (Mi), golgi elements (G), multivesicular bodies (MB), and myelin figures (My). ATPase activity is absent along the free surface membrane, but occasional punctate deposits of lead phosphate are seen on the surface membranes bordering the intercellular space (IS) at the lower left corner of the figure.

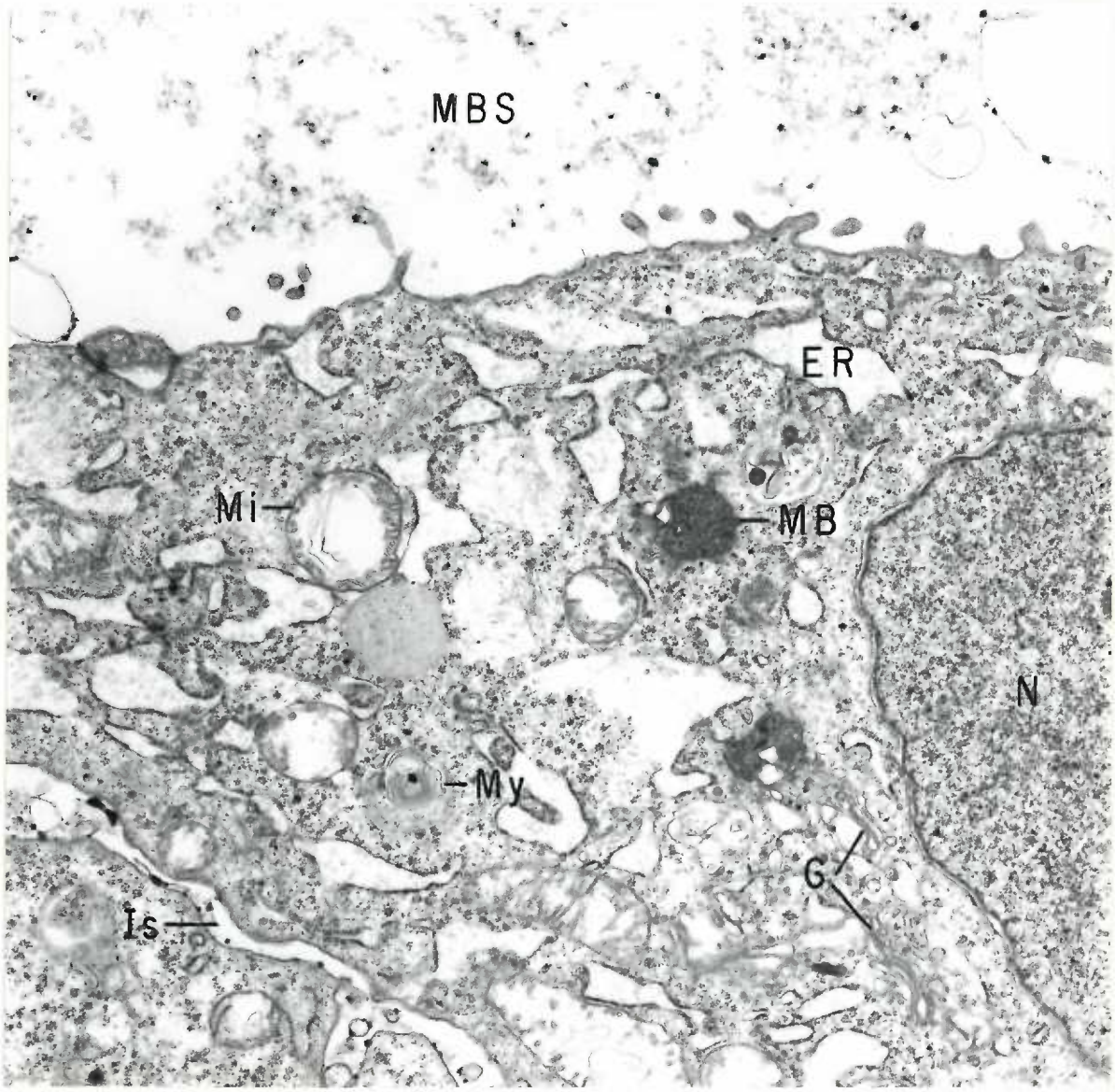

20

FIGURE 21

Twelve day vascular placental labyrinth. Magnification 12,900 X. Three layers of trophoblast (T 1, T 11 and T 111) are seen intervening between a maternal blood space (MBS) and the basement membrane (BM) of a fetal capillary (FBC). Large pleomorphic evaginations with globular expanded tips extend from the free surfaces of trophoblast I and the fetal endothelium. Trophoblast III characteristically exhibits lipid (Li) inclusions.

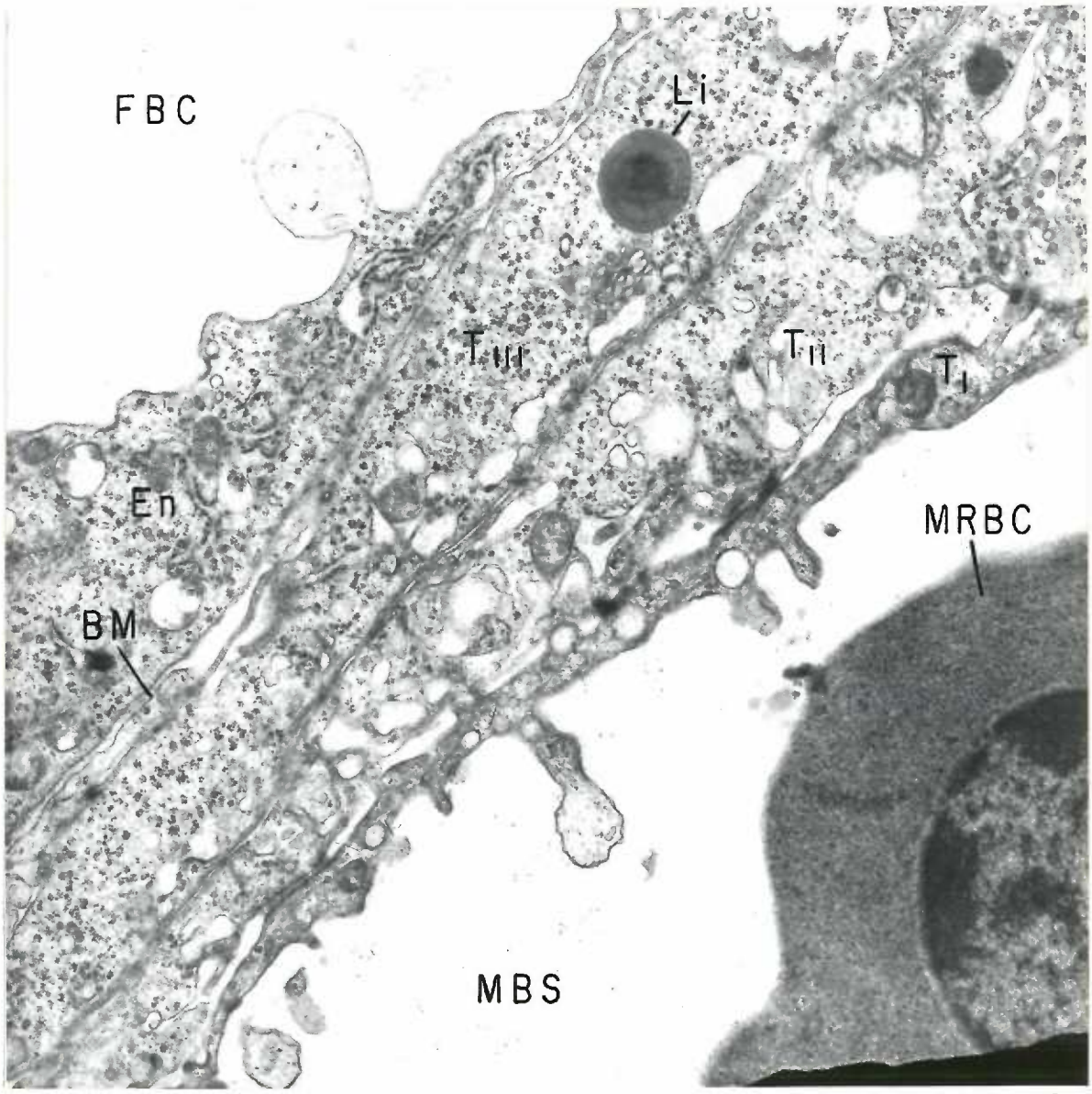

21

FIGURE 22

Fourteen day placental labyrinth incubated with ADP as substrate. Magnification 18,600 X. Final reaction product coats the surface membranes of maternal erythrocytes (MREC) located within a maternal blood space (MBS). Precipitates also appear on the surface membranes of trophoblast I (T 1), on the maternal surface of trophoblast II (T 11) and in the space between trophoblast I and II. Trophoblast III (T 111) as well as the endothelium (En) lining the fetal capillary (FBC) lack activity. Note that adjacent cell membranes of trophoblast II and III are closely apposed. Points of contact between these two layers appear as small intermediate junctions (zonula adherens) (arrows). Trophoblast III, which fronts on the basement membrane (BM) supporting the fetal endothelium, exhibits numerous surface projections and infoldings.

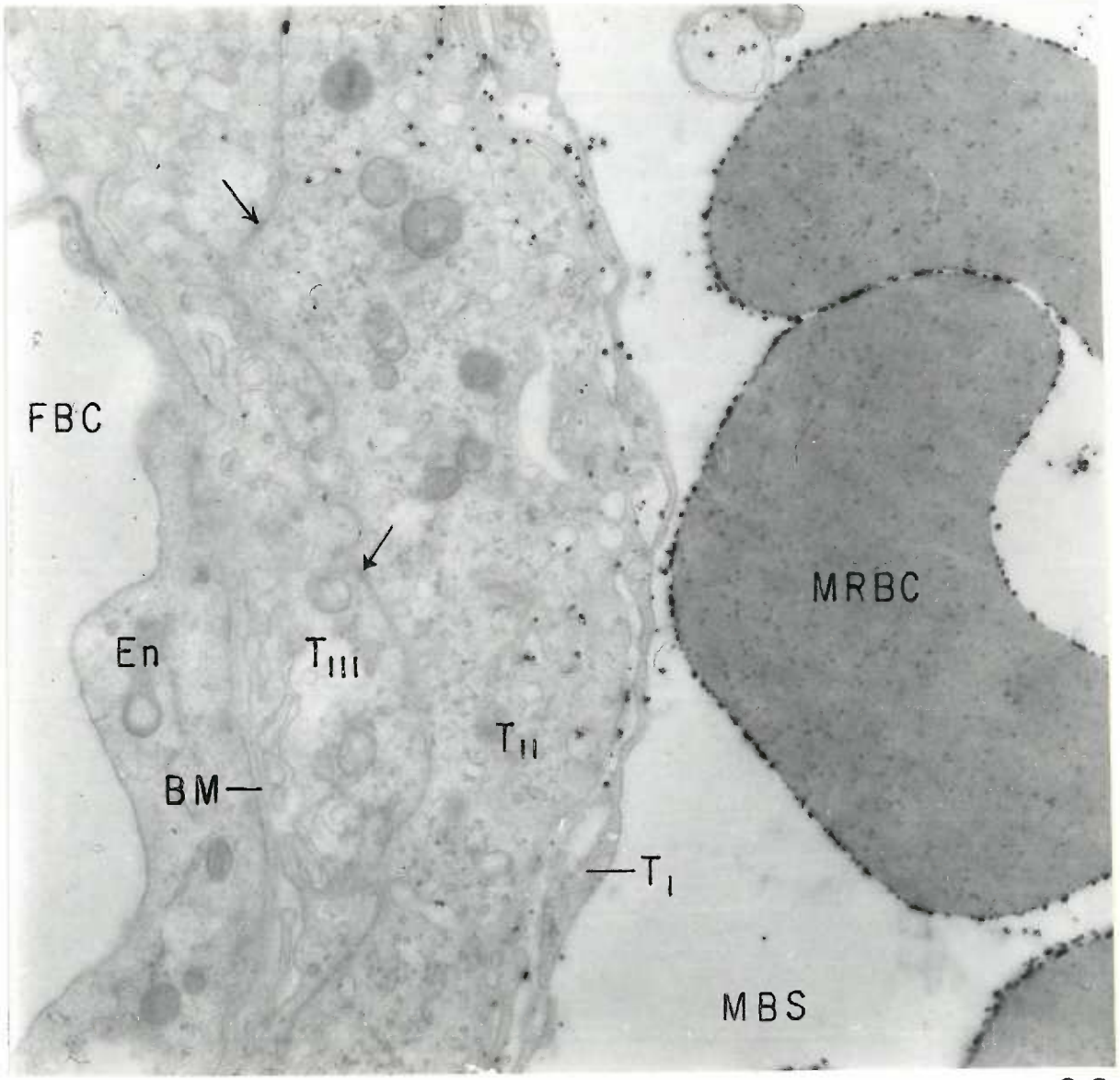

22

FIGURE 23

Fourteen day placental labyrinth incubated with ADP as substrate. Magnification 18,600 X. The distribution of final reaction product in this electron micrograph is the same as that shown in Figure 22. Trophoblast I (T 1) appears extremely attenuated and exhibits distinct fenestrations (short arrows) which are closed by a thin diaphragm of amorphous material. Trophoblast II (T 11) contains numerous ribosomes and vesicles. Some moderate sized vesicles within the cytoplasm of this layer contain final reaction product (long arrows). These vesicles appear to be infoldings of the surface plasma membrane which have either separated from the cell surface or are continuous with the intercellular space between trophoblast I and II. Note the paucity of cytoplasmic organelles in the capillary endothelium (En).

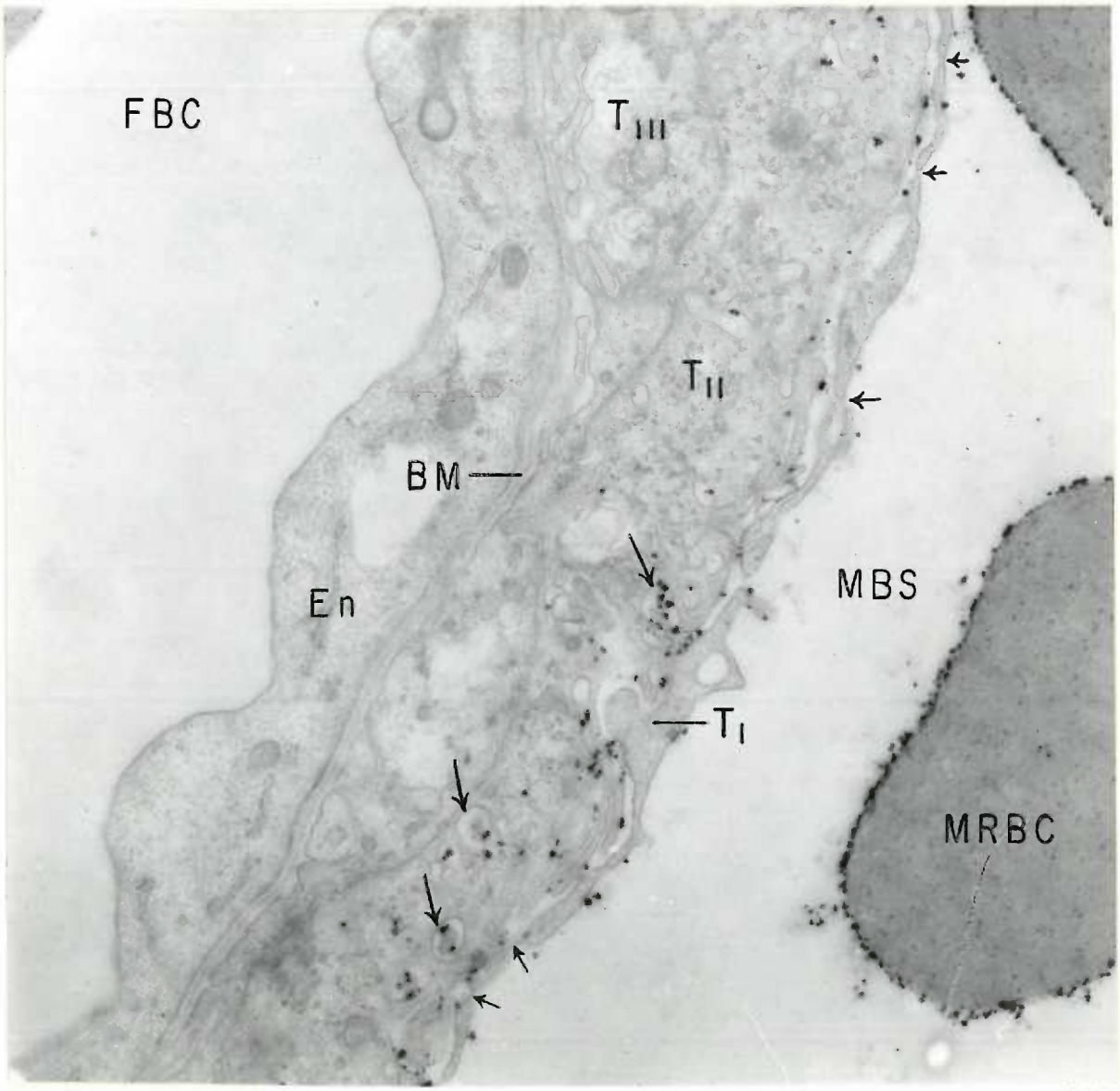

23

FIGURE 24

Fourteen day placental labyrinth incubated with AMP as substrate. Magnification 18,600 X. In this photomicrograph the closely apposed surfaces of two trophoblast I cells (T 1) extend numerous cytoplasmic projections which mutually interdigitate and thus break up the maternal blood space (MBS) into small irregular channels. Final reaction product is particularly abundant on the outer surface membranes of these cytoplasmic projections. Smaller precipitates of lead phosphate are seen throughout the amorphous material occurring in the intercellular space (IS) between trophoblast I and II (T 11).

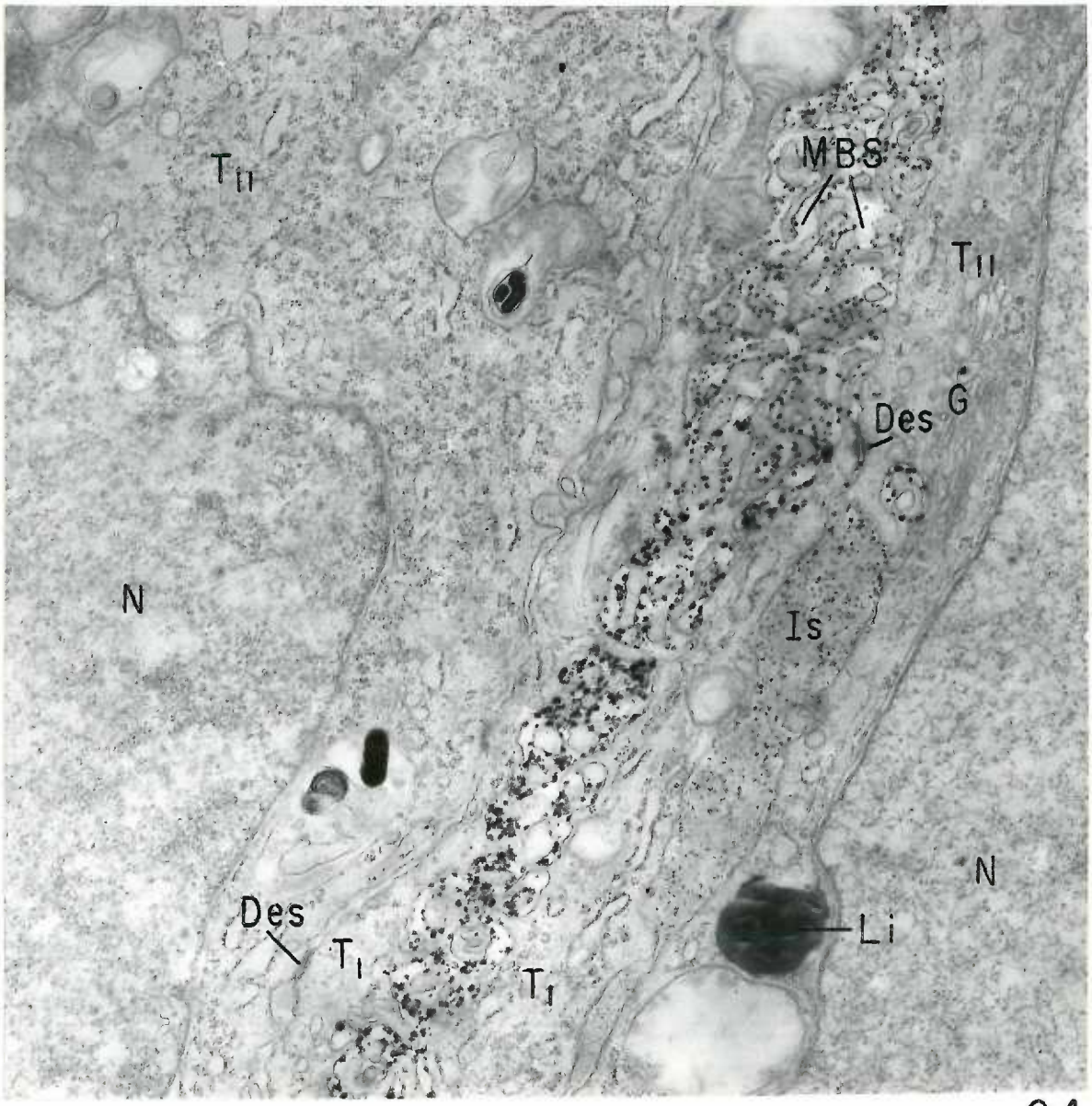

24

FIGURE 25

Fourteen day placental labyrinth incubated with ATP as substrate. Magnification 18,600 X. Deposits of reaction product are most abundant on the maternal surface of trophoblast II (T 11). Less activity occurs on the inner and outer surface membranes of trophoblast I (T 1). Note the mutually interdigitating cytoplasmic evaginations of trophoblasts I and II (arrows).

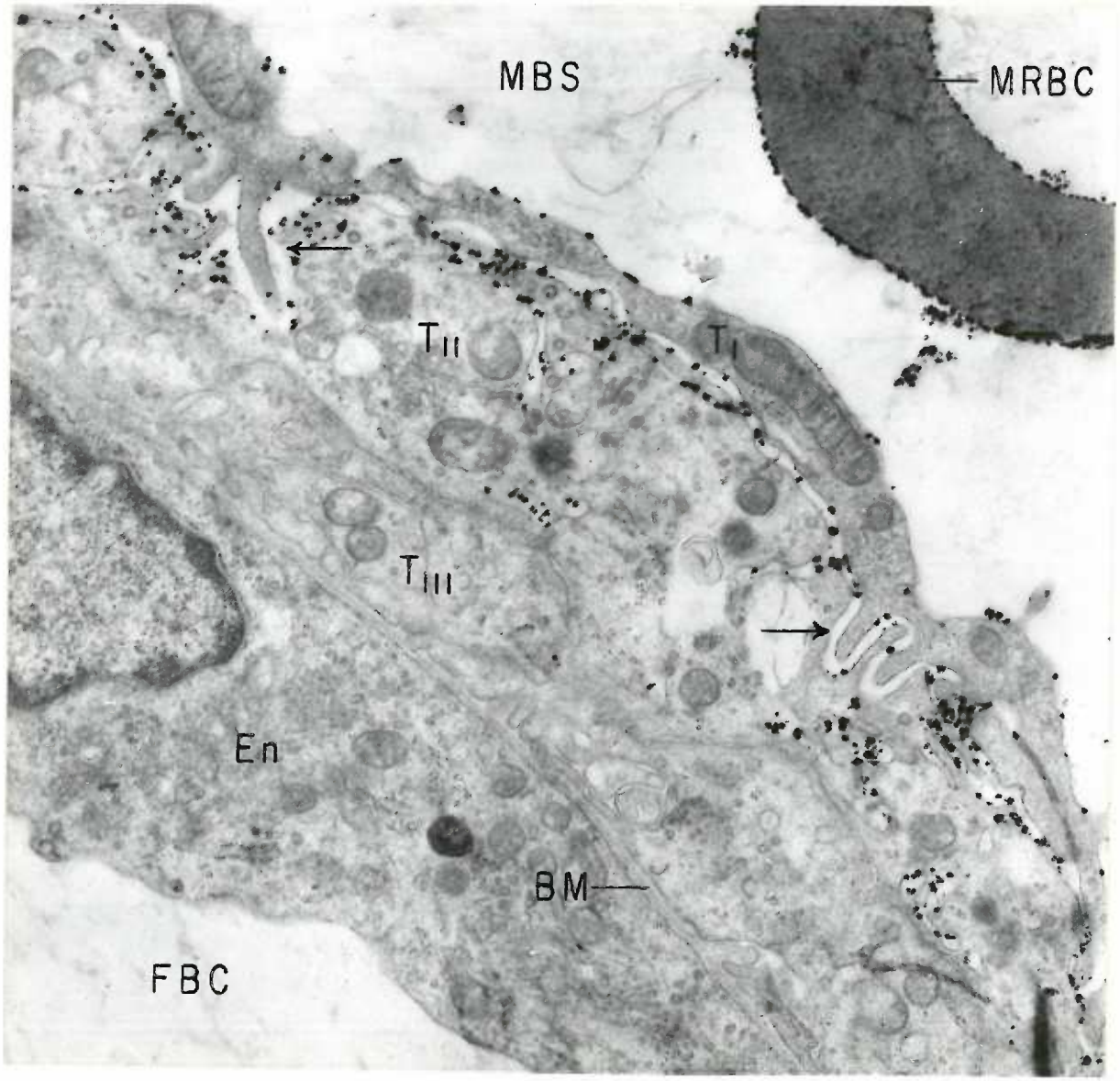

25

FIGURE 26

Eighteen day placental labyrinth incubated with ADP as substrate. Magnification 11,780 X. Deposits of final reaction product are distributed along the surface membranes of trophoblast I (T 1) and on the maternal surface of trophoblast II (T 11) and its tubular infoldings. The thickest diameter of the fetal endothelium (En) and trophoblast I corresponds to the position of their nuclei. Note that these cells attenuate abruptly on either side of their nuclei to form thin cytoplasmic layers.

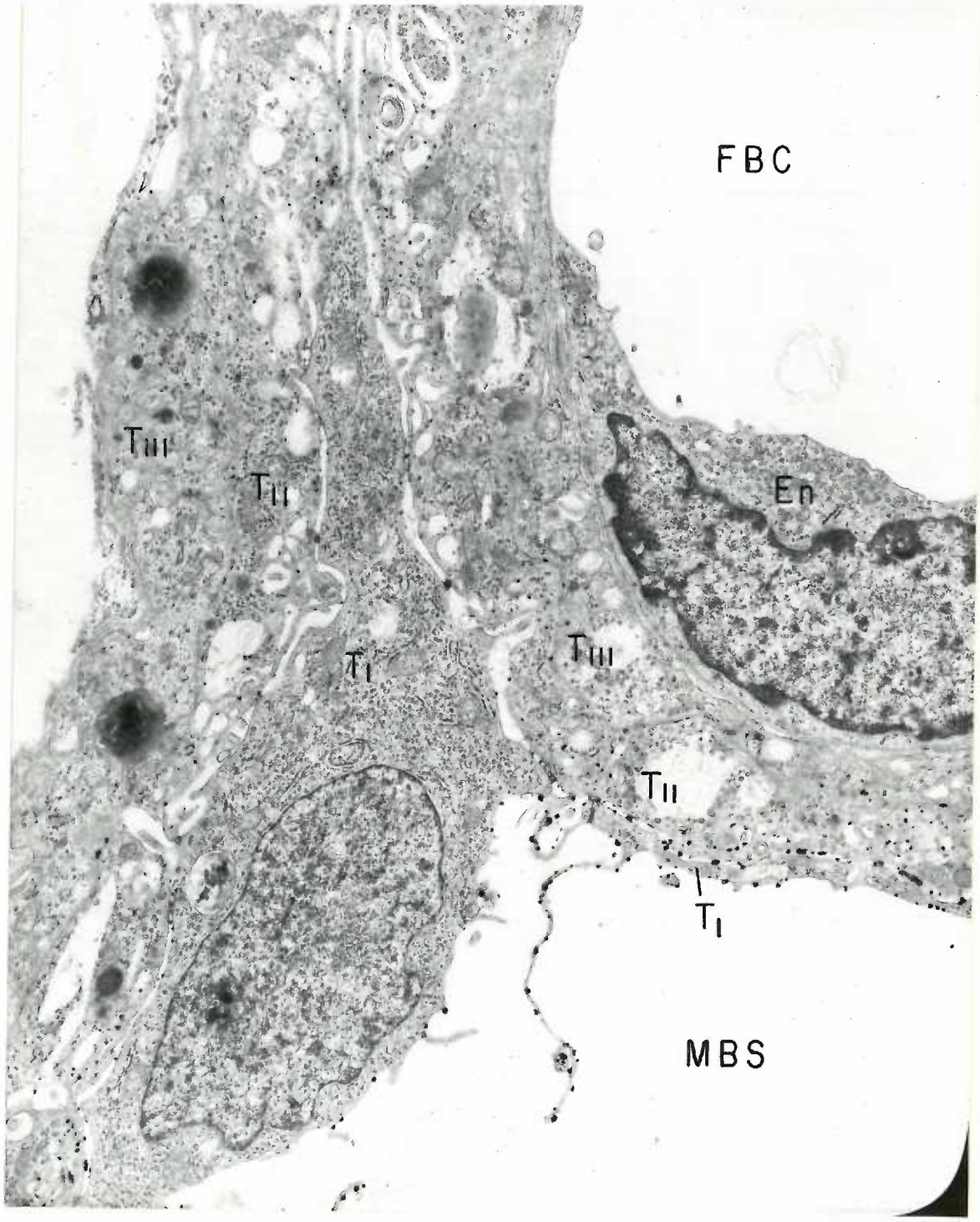
FBC
TIII
TII
En
TI
TIII
TII
TI
MBS

FIGURE 27

Eighteen day trophoblast I cell incubated with ATP as substrate. Magnification 18,600 X. Discrete deposits of final reaction product are distributed along the outer surface membrane and its microvillous projections. The perinuclear cytoplasm is rich in golgi elements (G), ribosomes (Ri) and vesicular profiles of granular endoplasmic reticulum (ER) which contain a granular material of medium electron density. One of the profiles appears to be in the process of releasing its contents into the maternal blood space (MBS).

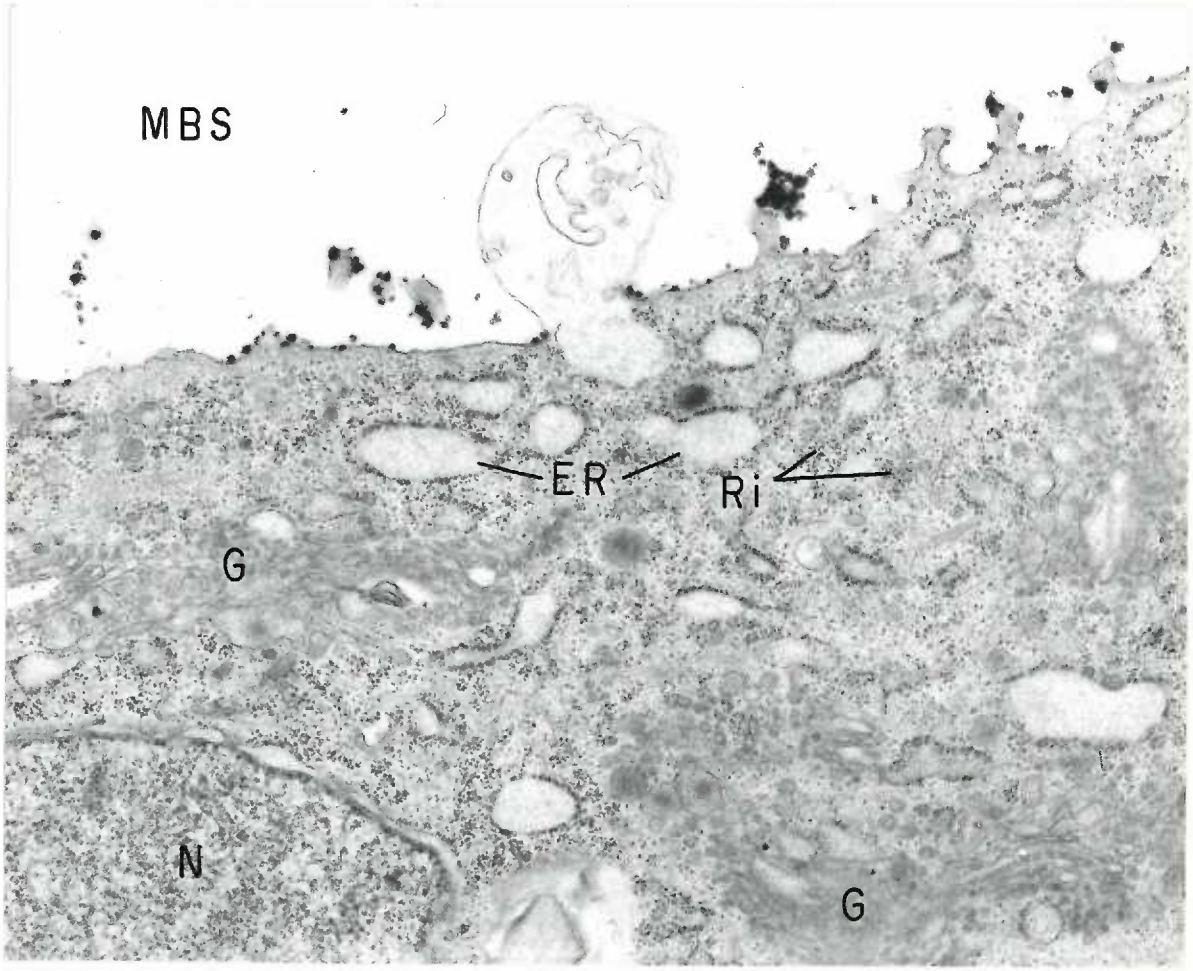

27

FIGURE 28

Eighteen day placental barrier incubated with ADP as substrate. Magnification 4,940 X. This electron micrograph demonstrates a complete cross section through an allantoic vessel. A process of a fibroblast (CTC) is seen in the connective tissue space (CTS) in the upper left corner of the figure. Note that basement membranes separate this cell from the overlying trophoblast and the underlying endothelium (En). Final reaction product appears as described in Figure 26.

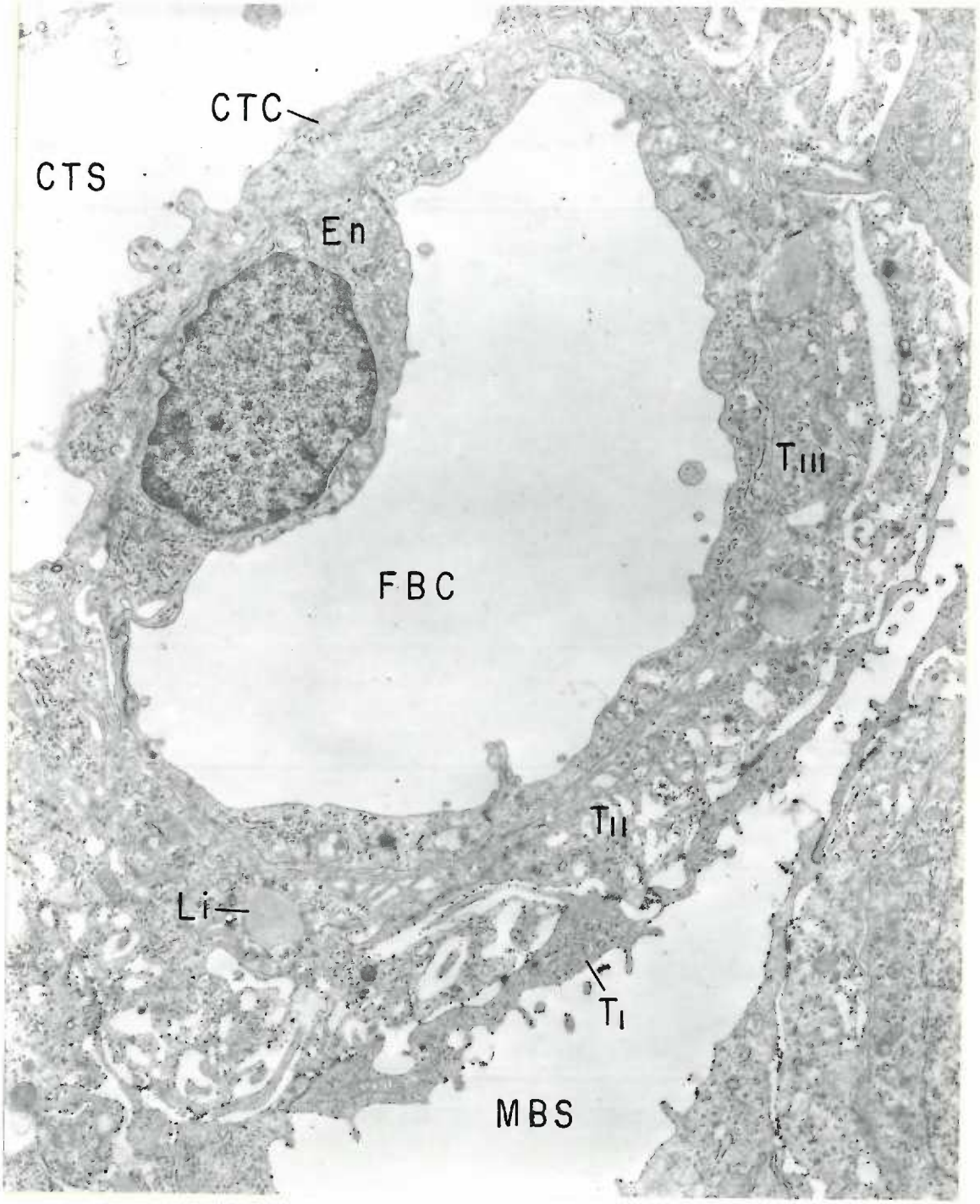

28

FIGURE 29

Enlarged portion of Figure 28. Magnification 11,780 X. The three layers of trophoblast can be seen clearly. Note the extensive infoldings and cytoplasmic projections of the maternal surface of trophoblast II (T II). Many of these infoldings, two of which are indicated (arrows), closely approximate the fetal surface of this layer. Large lipid inclusions (Li) occur in trophoblast III (T III). ADPase activity, as in Figure 26, is distributed along the surface membranes of trophoblast I (T I) and on the maternal surface membrane of trophoblast II.

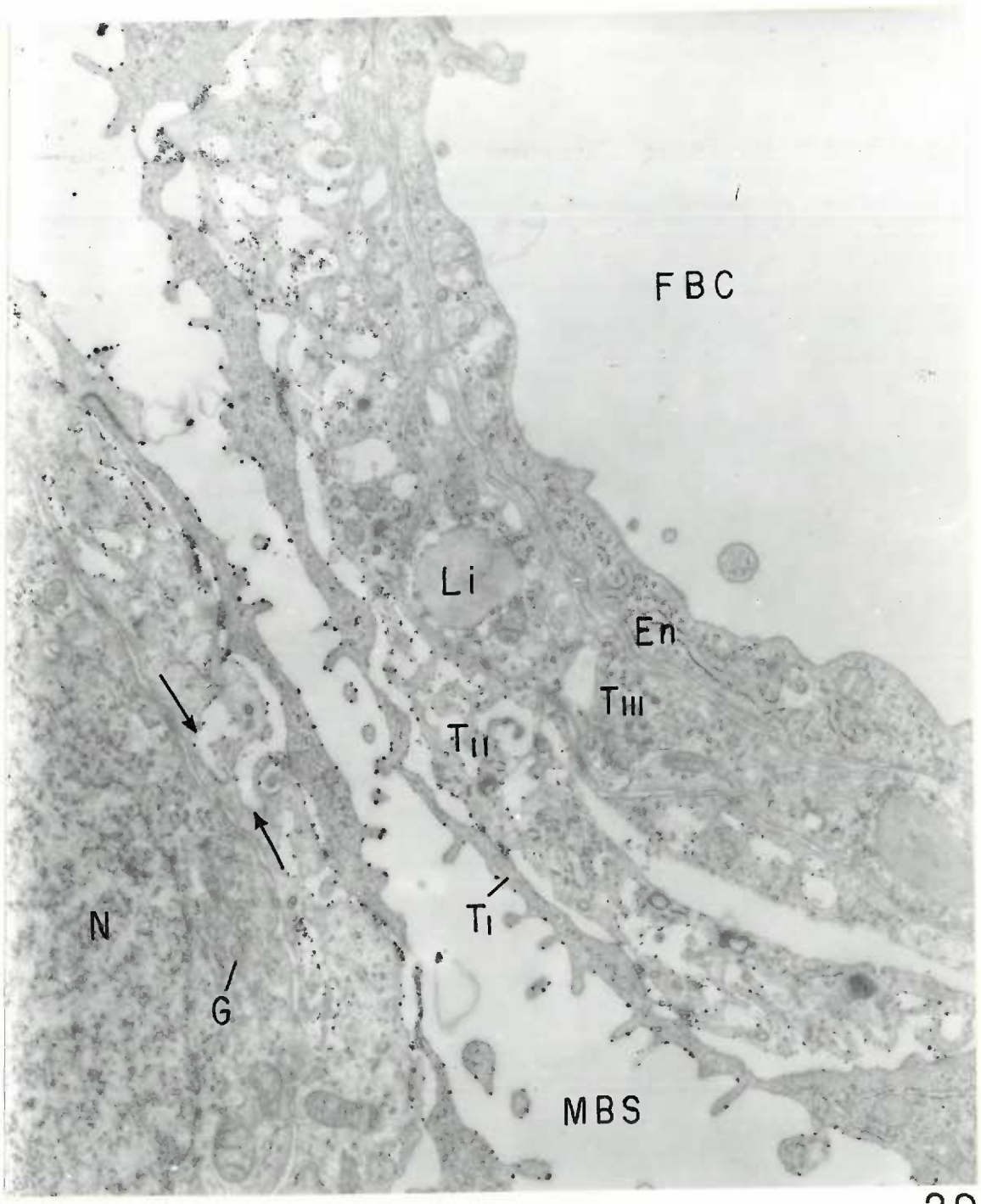
FBC
Li
En
TIII
TII
TI
N
G
MBS

FIGURE 30

Eighteen day placental labyrinth incubated with ATP as substrate. Magnification 18,600 X. Final reaction is deposited along the highly infolded surface membrane of trophoblast II (T II) and to a lesser extent along the surface membranes of trophoblast I (T I). A tight junction (TJ) is seen between two overlapping trophoblast I cells. The absence of an intercellular space along much of the common border between trophoblasts II and III is interpreted as evidence of their fusion to form tight junctions (zonula occludens) (arrows). On close examination a condensation of fine fibrils is seen associated with these junctions.

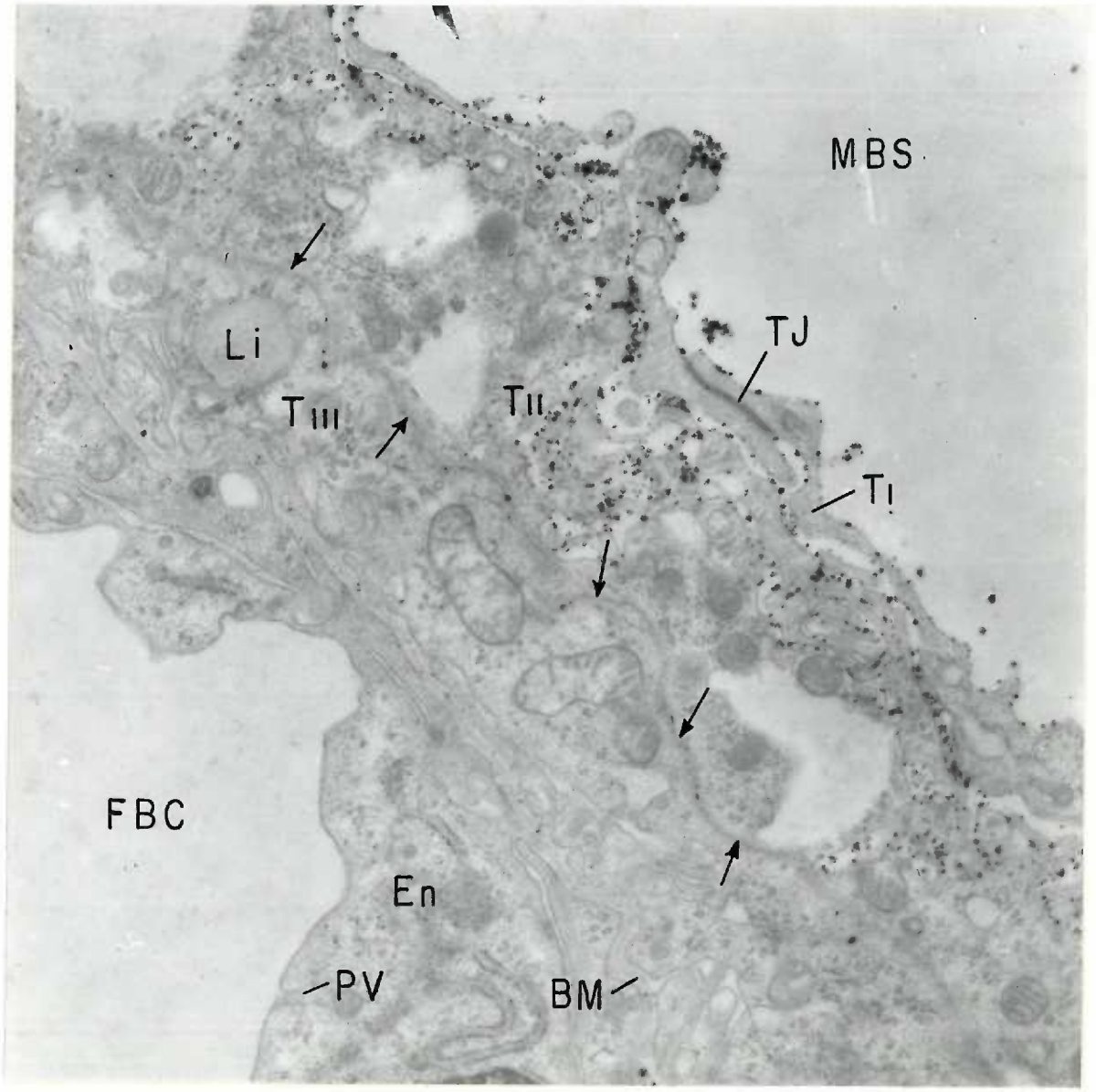

30

FIGURE 31

Eighteen day placental labyrinth reacted for ADPase activity. Magnification 7,800 X. Final reaction product occurs as described in Figure 26. The outer limiting membrane of trophoblast II (T 11) is highly irregular and has infoldings which closely approximate its inner plasma membrane. The thick portion of trophoblast III (T 111) seen in the lower corner of the figure contains numerous polysomes and golgi elements (G).

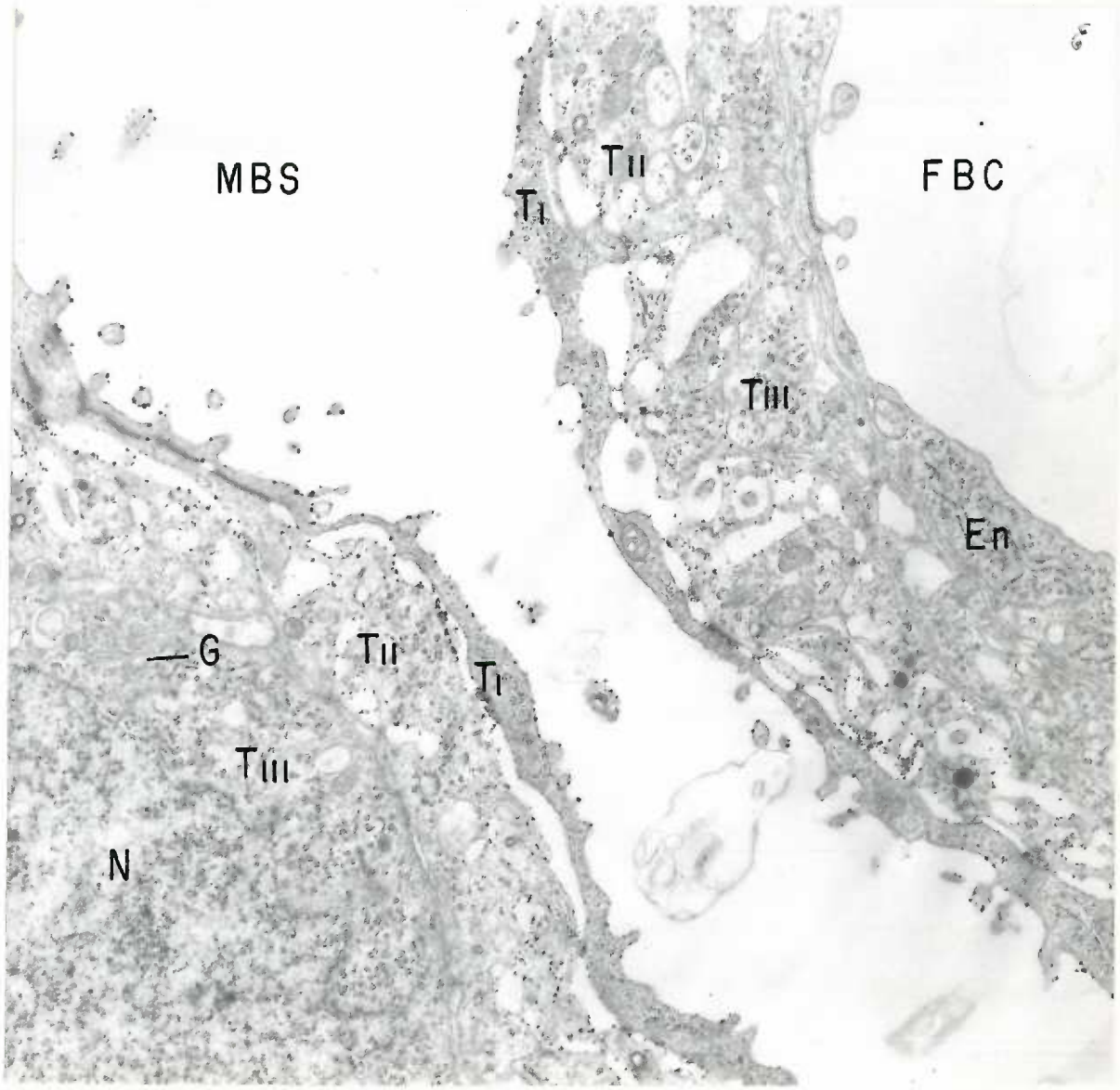

31

FIGURE 32

Eighteen day placental labyrinth reacted for ATPase activity. Magnification 18,600 X. Moderate deposits of final reaction product are distributed along the surface membranes of trophoblast I (T 1) and along the outer surface of trophoblast II (T 11) and its tubular infoldings as in Figure 30. Note that ATPase activity also coats the external surface membrane of the maternal erythrocyte (MRBC) and not that of the fetal red blood cell (FRBC). The common junction between trophoblast II and III (arrows) forms a series of undulations which impart a somewhat beaded appearance to trophoblast III (T 111).

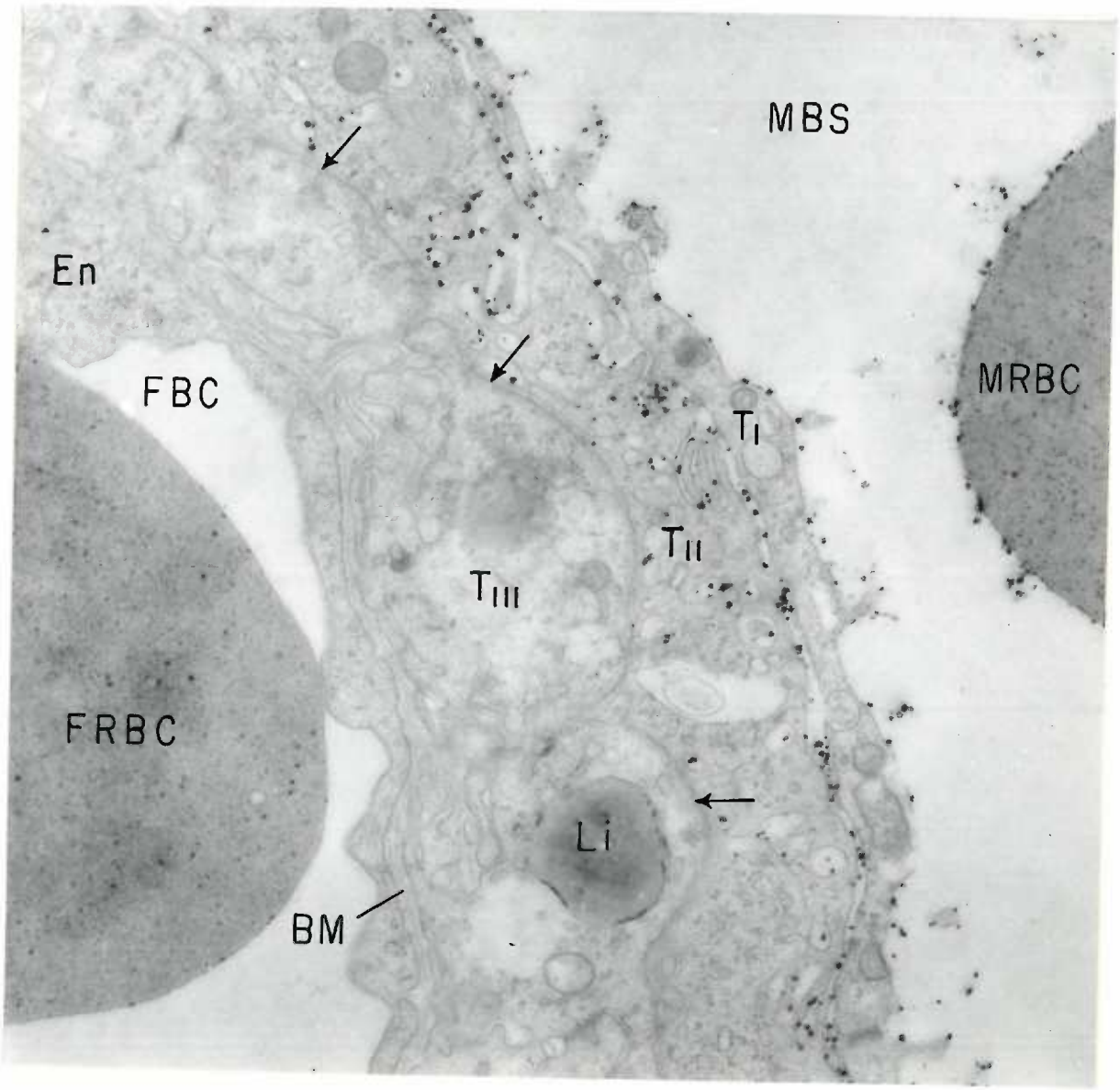

32

FIGURE 33

Eighteen day placental labyrinth incubated with ADP as substrate. Magnification 12,900 X. Final reaction product is distributed as described in Figure 26. The intercellular space (IS) between trophoblasts I (T 1) and II (T 11) is confluent with the maternal blood space (MBS) through an opening between two trophoblast I cells. A large bulbous projection of trophoblast II extends through this opening.

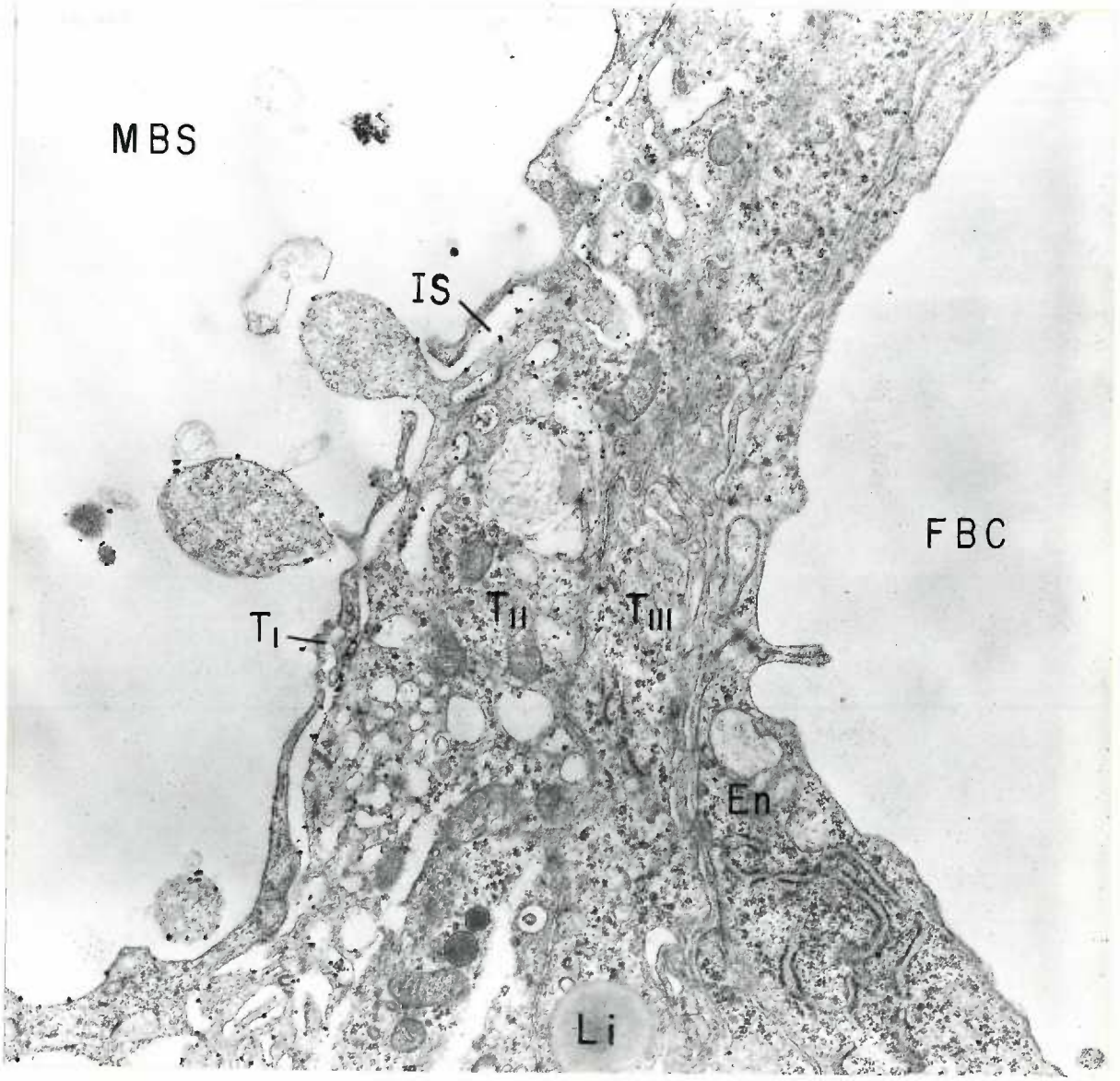

33

FIGURE 34

Eighteen day placental labyrinth incubated with ATP as substrate. Magnification 18,600 X. Final reaction product is distributed as described in Figure 32. Trophoblast I (T 1) is highly attenuated and exhibits fenestrations (long arrows). Trophoblasts II (T 11) and III (T 111) are richly provided with cytoplasmic organelles as in preceding stages. The fetal endothelium (En) shows massive pinocytotic activity (PV) along its basal surface and liplike cytoplasmic flaps (short arrows) at its interendothelial junction.

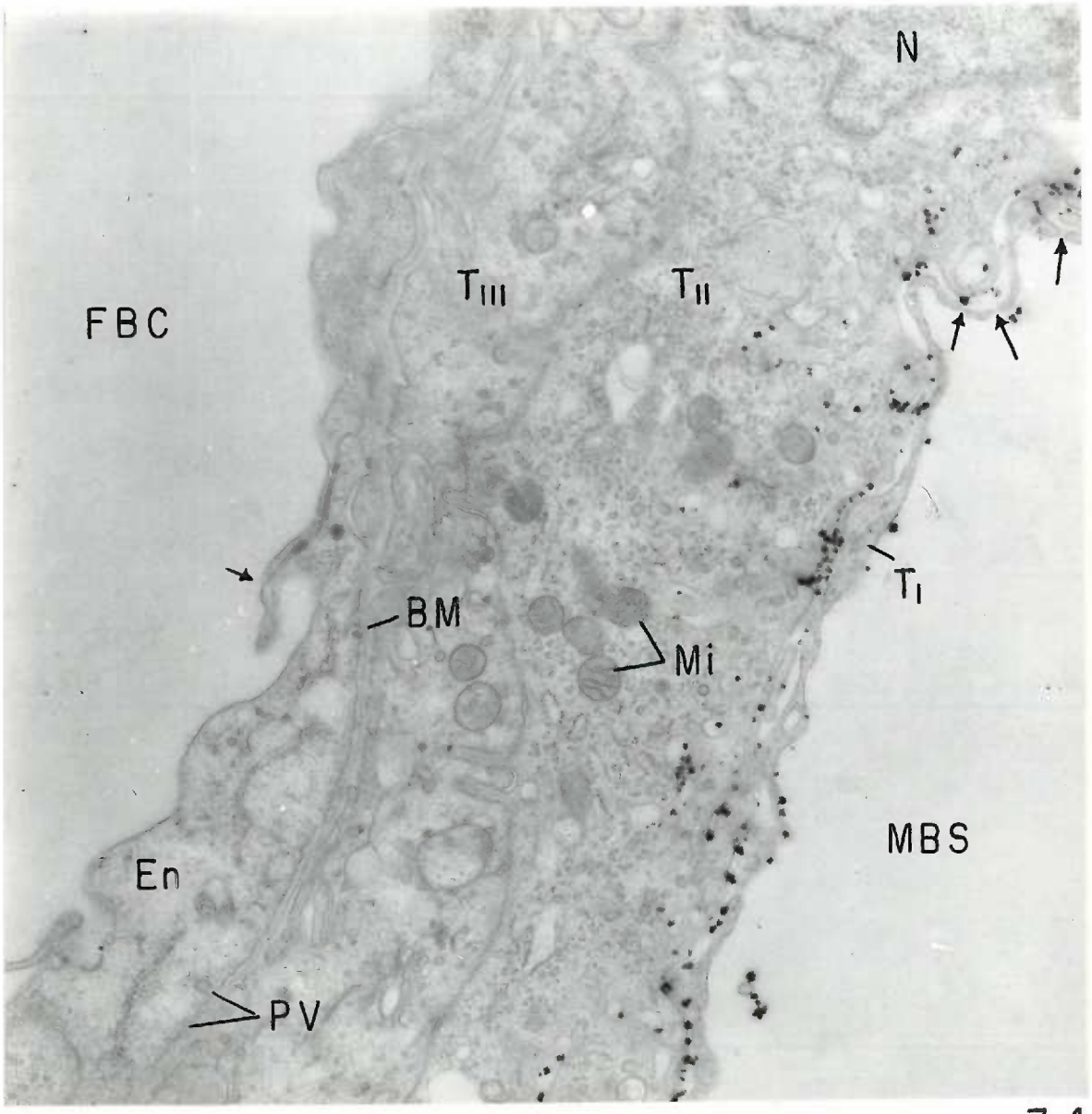

34

FIGURE 35

Eighteen day placental labyrinth incubated with AMP as substrate. Magnification 12,900 X. Globular deposits of final reaction product occur along the surface membranes of trophoblasts I (T 1) and II (T 11). This figure exhibits the intercellular attachment devices which are characteristic of the junctions between the constituents of the labyrinthine barrier. Desmosomes (macula adherens) (Des) occur at irregular intervals between trophoblasts I and II. Intermediate junctions (zonula adherens) (ZA) alternate with tight junctions (zonula occludens) (TJ) throughout the entire border between trophoblasts II and III (T 111). These tight junctions can be seen to better advantage in Figure 30. Tight junctions also occur between the overlapping endothelial (En) cells of the allantoic capillaries (FBC).

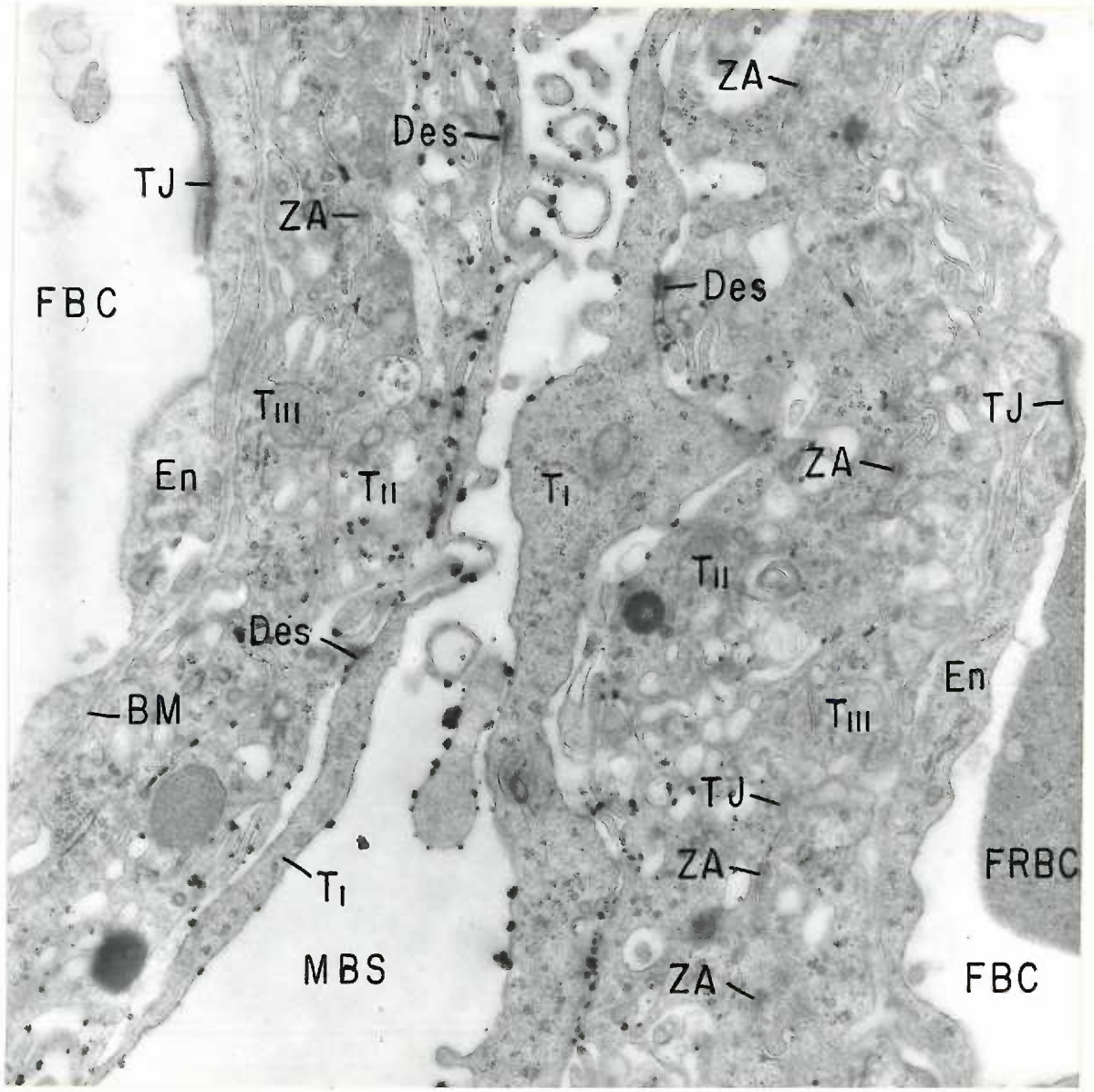
ZA
Des
TJ
ZA
FBC
Des
TIII
TJ
En
TII
TI
ZA
TII
Des
BM
En
TIII
TJ
ZA
FRBC
TI
MBS
ZA
FBC

35

FIGURE 36

Eighteen day placental labyrinth reacted for AMPase activity. Magnification 4,940 X. Final reaction product is intensely distributed along the outer surface membrane of trophoblast I (T 1). Less activity occurs along the common border between trophoblasts I and II (T 11) except where the two surface membranes are closely apposed. The lipid droplets (Li) which characteristically occur in trophoblast III (T 111) have irregular and distorted outlines due to fixation and dehydration. Note the continuity between the perinuclear cisternae (PC) and the lumen of the granular endoplasmic reticulum (ER) in the two mesenchymal cells (CTC) directly below the allantoic capillary (FBC).

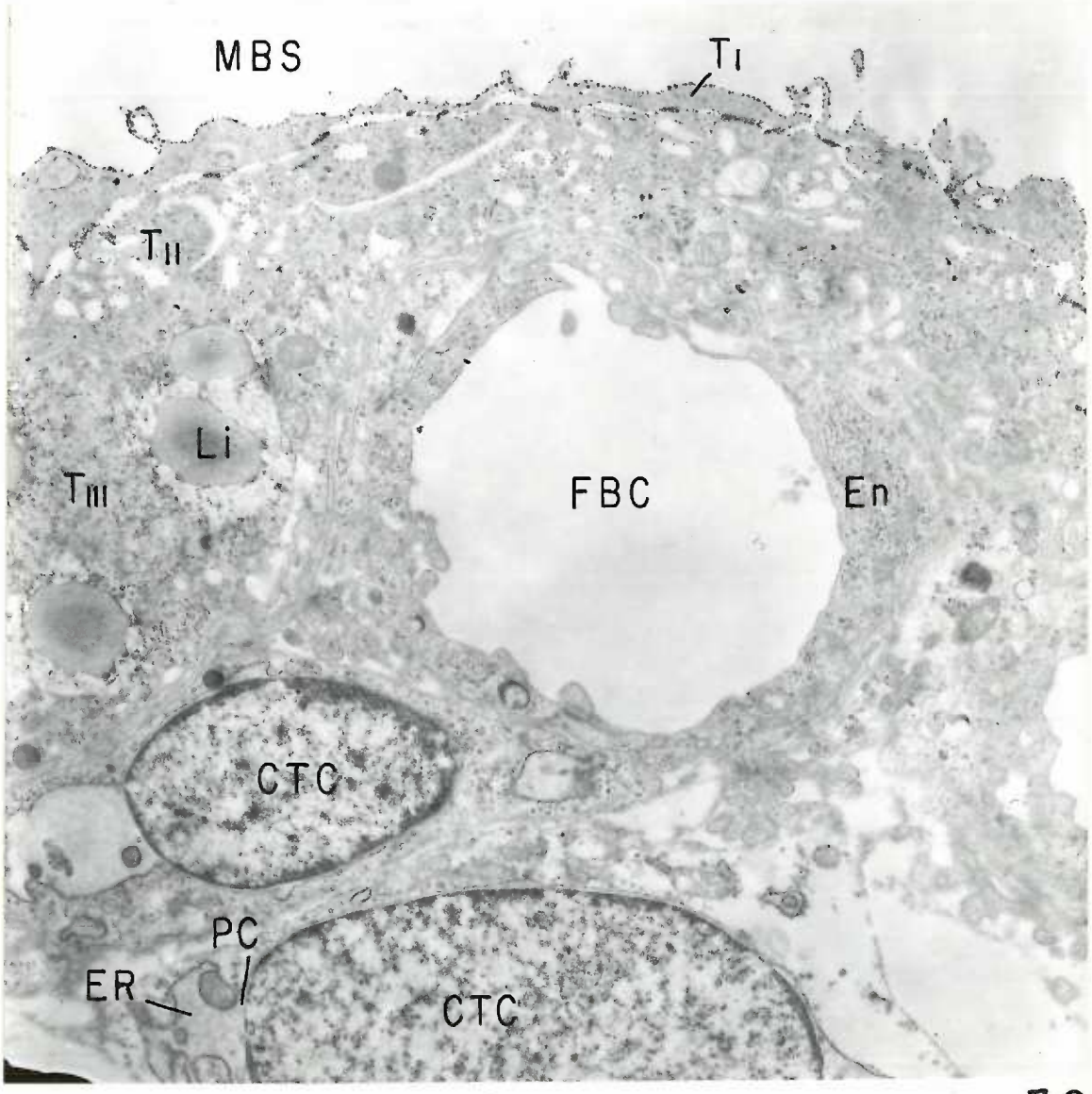

36

FIGURE 37

Eighteen day placental labyrinth incubated with AMP as substrate. Magnification 12,900 X. AMPase activity is distributed as described in Figure 35. As in previous stages, the thicker portion of trophoblast I (T 1) is richly provided with polysomes (Ri), granular endoplasmic reticulum (ER) and golgi elements (G).

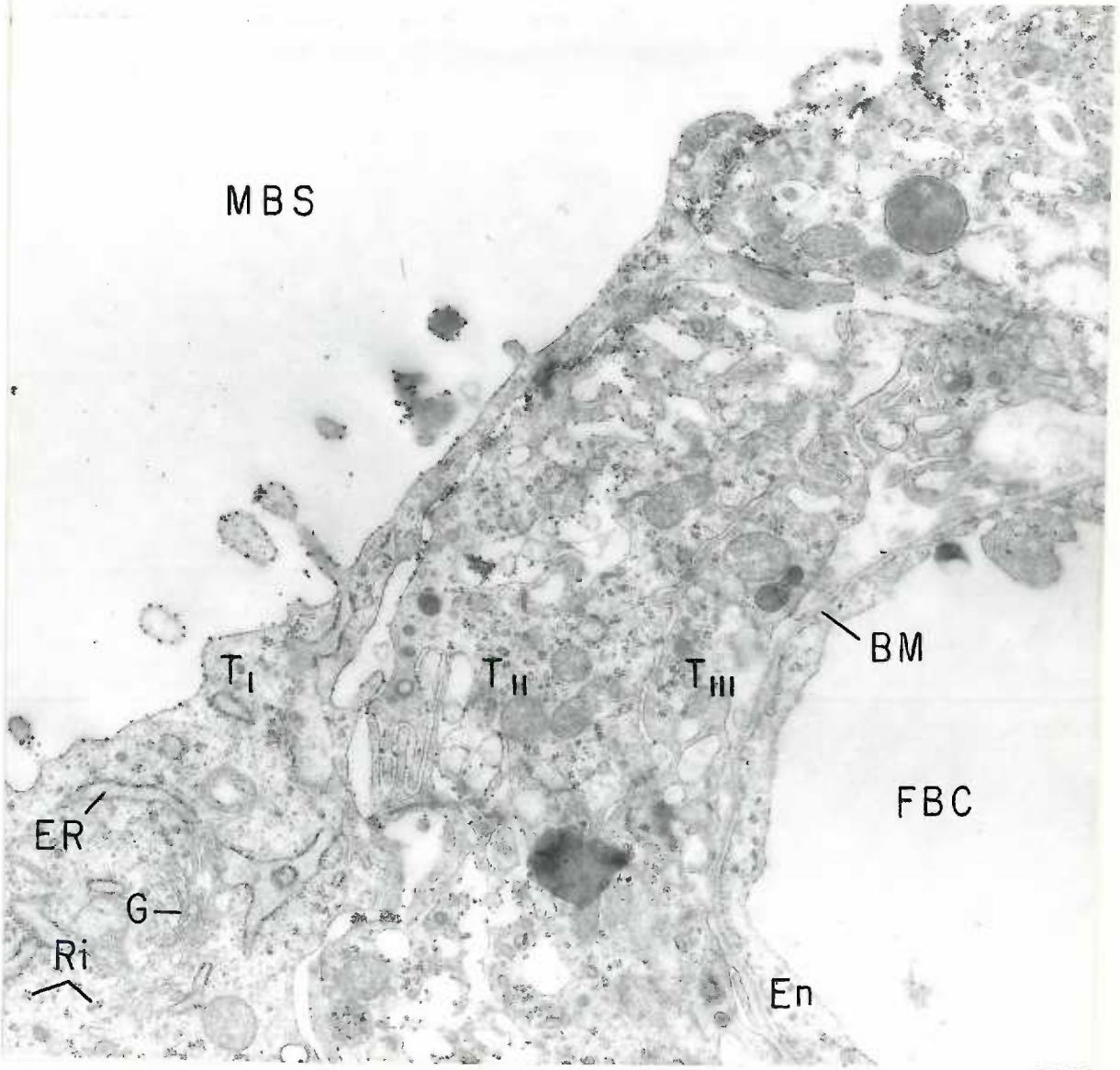

37

FIGURE 38

Eighteen day allantoic capillary. Magnification 18,600 X. Note that the interendothelial junctions are characterized by liplike cytoplasmic folds (arrows) which extend into the capillary lumen (FBC). These marginal folds are attached at their bases by tight junctions (TJ). Evidence of active pinocytosis (PV) is most apparent on the basal surface of the endothelium (En). On close examination two basal laminae (BM) are discernable between trophoblast III (T III) and the capillary endothelium.

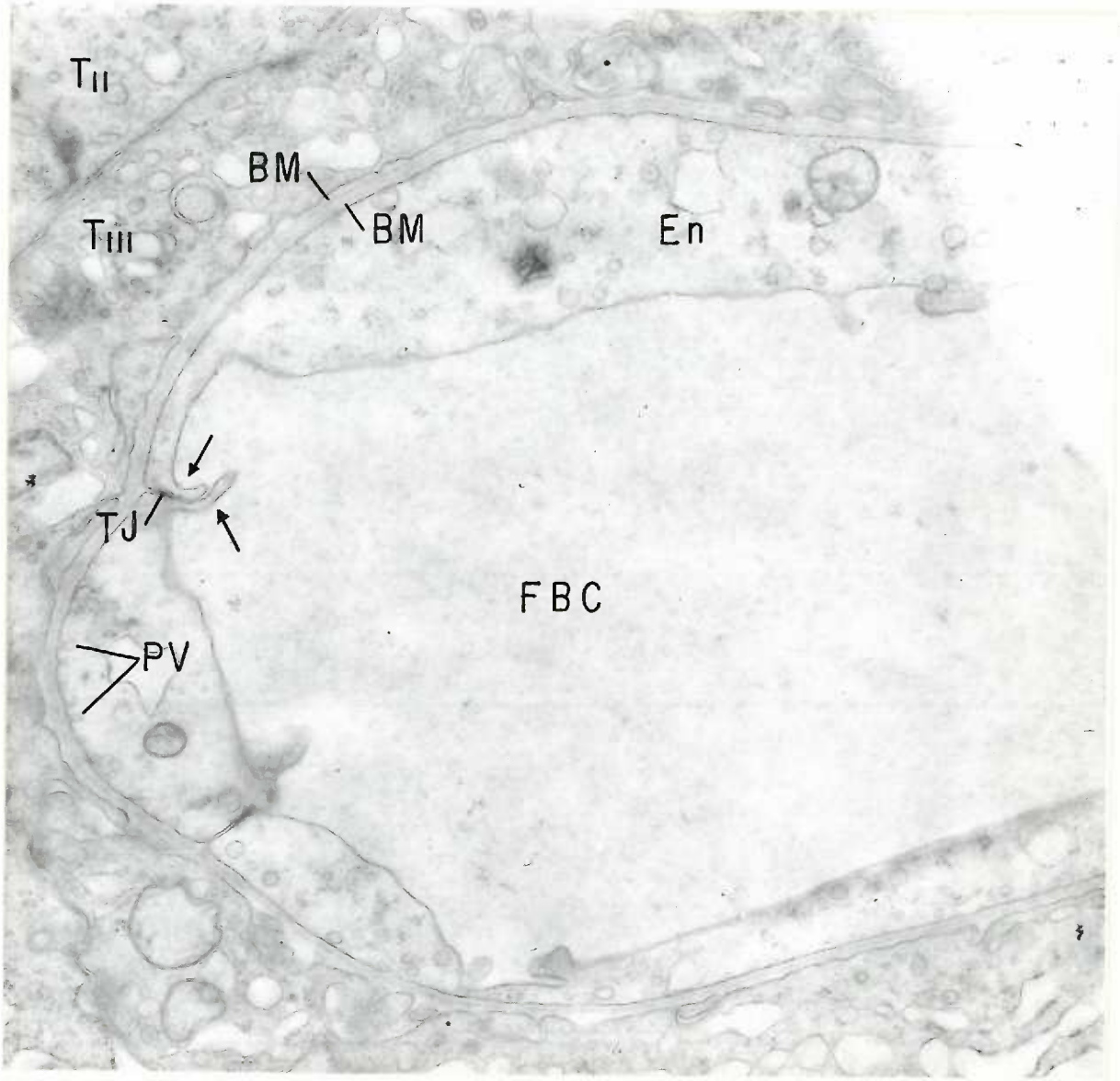

38

FIGURE 39

Eighteen day placental labyrinth incubated with AMP as substrate. Magnification 12,900 X. Final reaction product occurs as described in Figure 35. Note that many of the mitochondrial membranes (Mi) are not sharply defined and that their internal structure is disrupted. The focal rarification of the cytoplasm in trophoblast II (T 11) probably represents artifact produced during fixation or incubation.

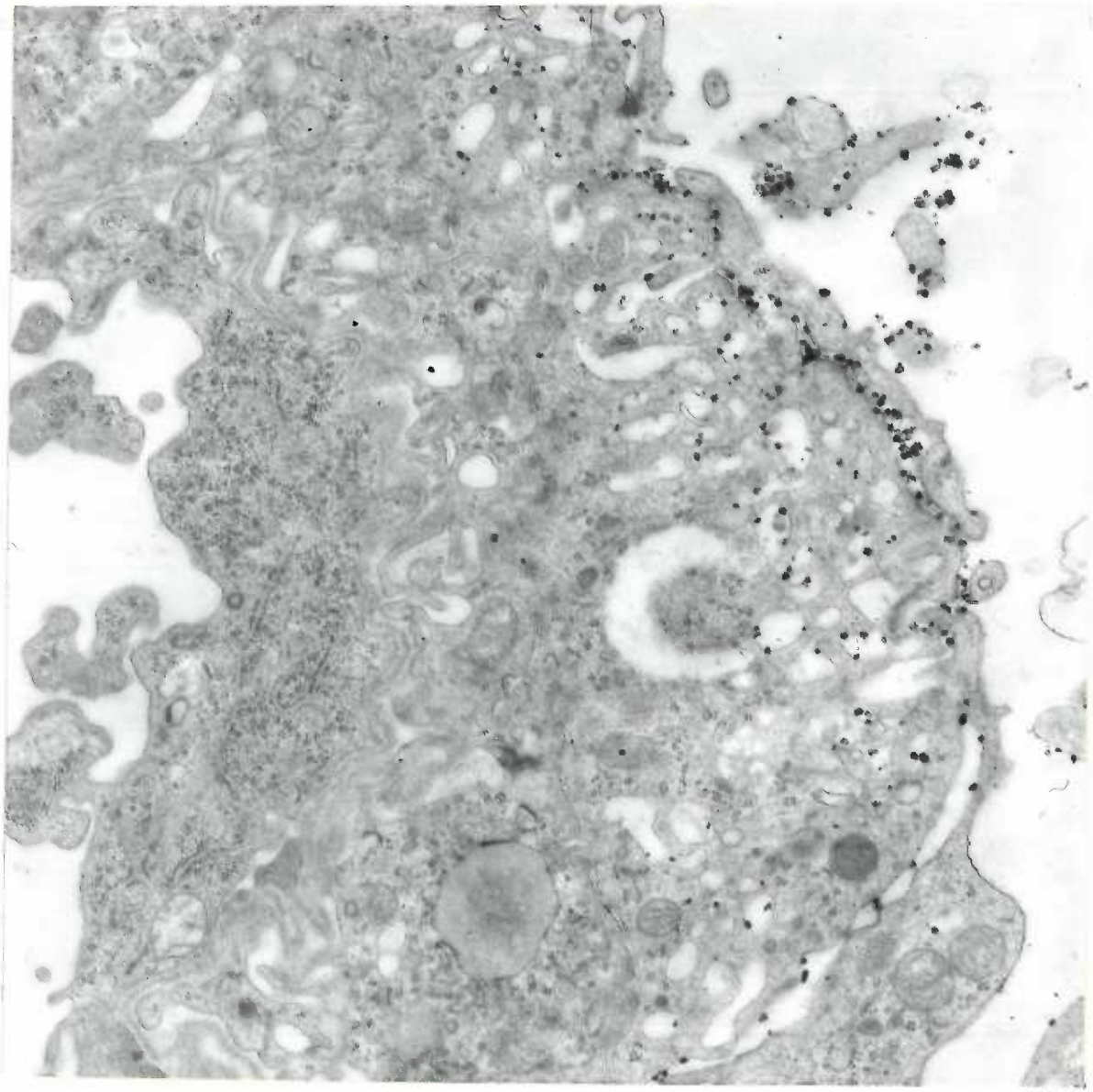

39

FIGURE 40

Twenty-two day placental labyrinth incubated with ATP as substrate. Magnification 12,900 X. Final reaction product is predominantly deposited in association with the fibrin-like material (short arrows) seen within the intercellular spaces between trophoblast I (T 1) and II (T 11) and in the channels or surface infoldings of trophoblast II. Note that activity along the free surface of trophoblast I is exceedingly sparse. The thicker region of trophoblast I is richly provided with granular endoplasmic reticulum (ER), polysomes and golgi-like microvesicular profiles (G). The maternal surface of trophoblast II is highly infolded and exhibits caveolae (PV) and many thick walled microvesicles. Note that two distinct basal laminae (long arrows) separate the allantoic endothelium (En) from trophoblast III (T 111).

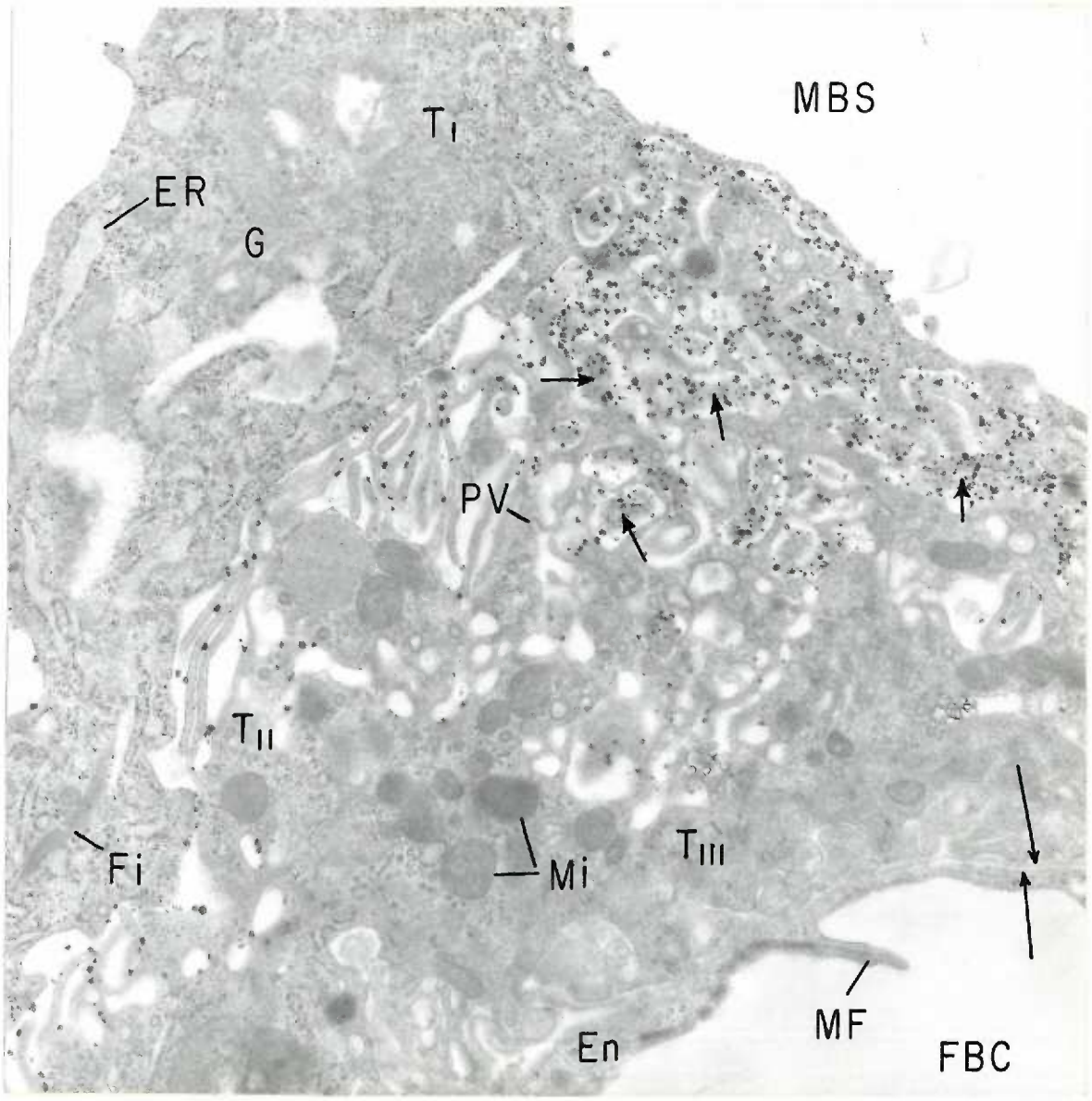

40

FIGURE 41

Twenty-two day placental labyrinth incubated with ADP as substrate. Magnification 12,900 X. ADPase activity exhibits a similar distribution to that of ATPase activity in Figure 40. Two distinct basal laminae (arrows) can be seen intervening between trophoblast III (T III) and the capillary endothelium (En). Each basal lamina conforms closely to the irregular contours of its respective plasma membranes.

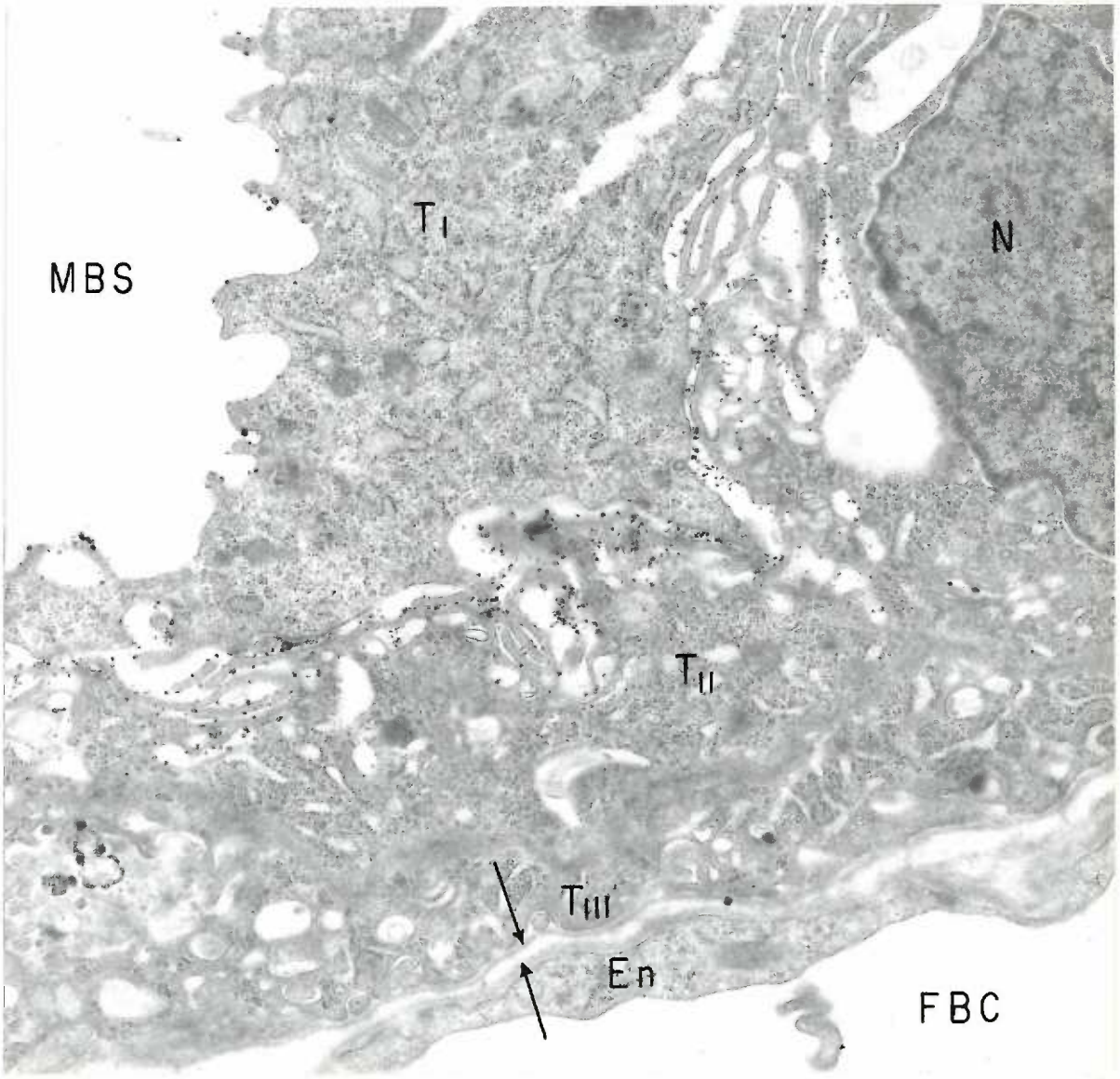

41

FIGURE 42

Twenty-two day placental labyrinth demonstrating a cross section of an allantoic capillary (FBC). Magnification 4,100 X. In marked contrast to Figure 40, ATPase activity is intensely distributed along the surface membranes of trophoblast I (T 1) and along the highly infolded surface membrane of trophoblast II (T 11). Globular and punctate deposits of lead phosphate also occur in the intercellular space between these two layers. The common border between trophoblast II and III (arrows), as well as the basement membrane (BM) and underlying capillary endothelium (En), are free of activity. Note that lipid (Li) inclusions are limited to trophoblast III (T 111).

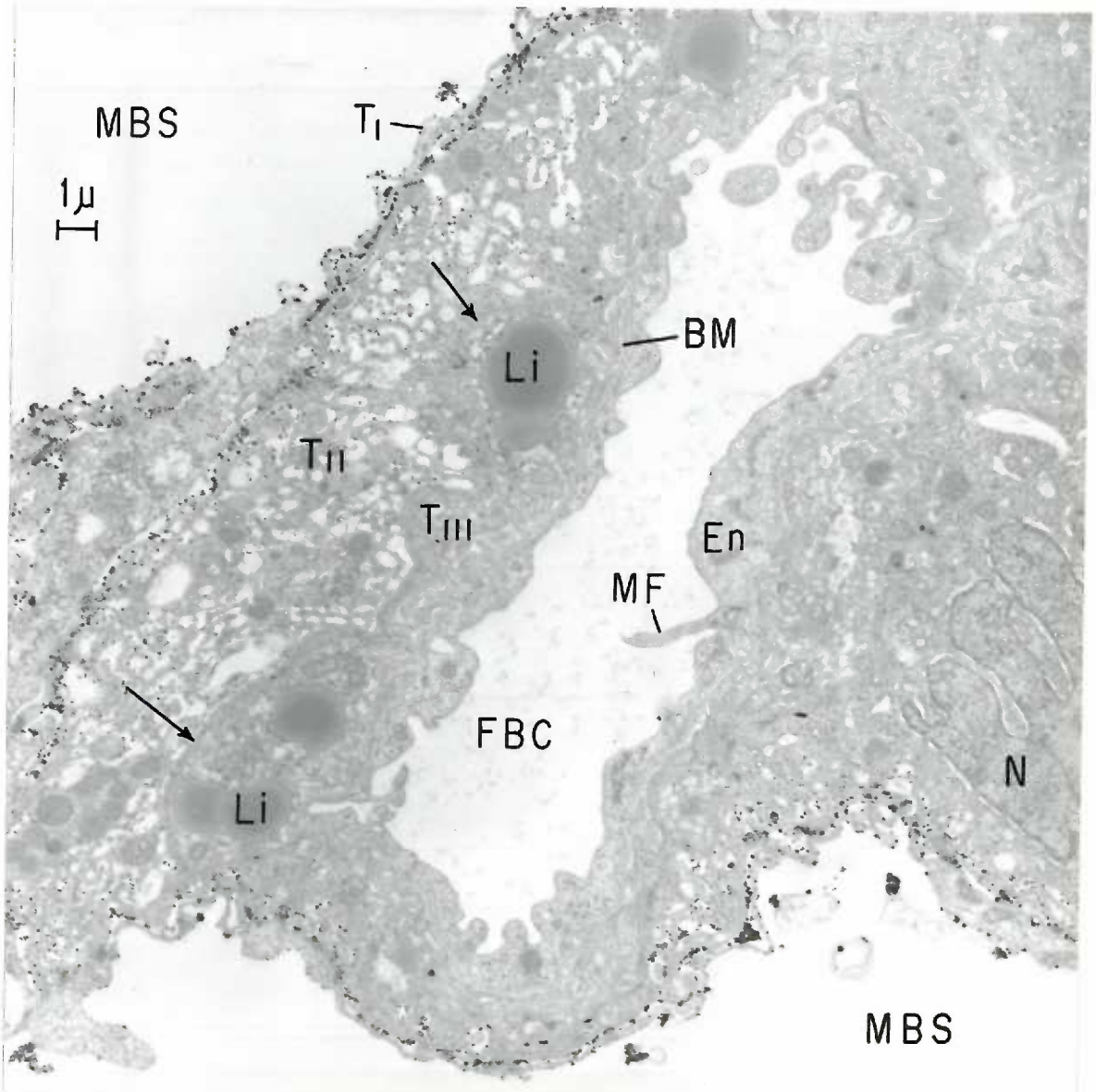

42

FIGURE 43

A longitudinal portion of the 22 day placental labyrinth incubated with ADP as substrate. Magnification 4,110 X. Dense deposits of final reaction product are distributed along the surface membranes of trophoblast I (T 1) and along the surface infoldings of trophoblast II (T 11). A portion of an allantoic capillary (FBC) is seen in the upper right corner of the figure. Note the presence of allantoic mesenchymal cells (CTC) and fibrils (Co) in the connective tissue space (CTS) between the two portions of trophoblast III (T 111) and the allantoic capillary. The mesenchymal cell in the center of the figure shows a large dilatation in its perinuclear cisterna (PC).

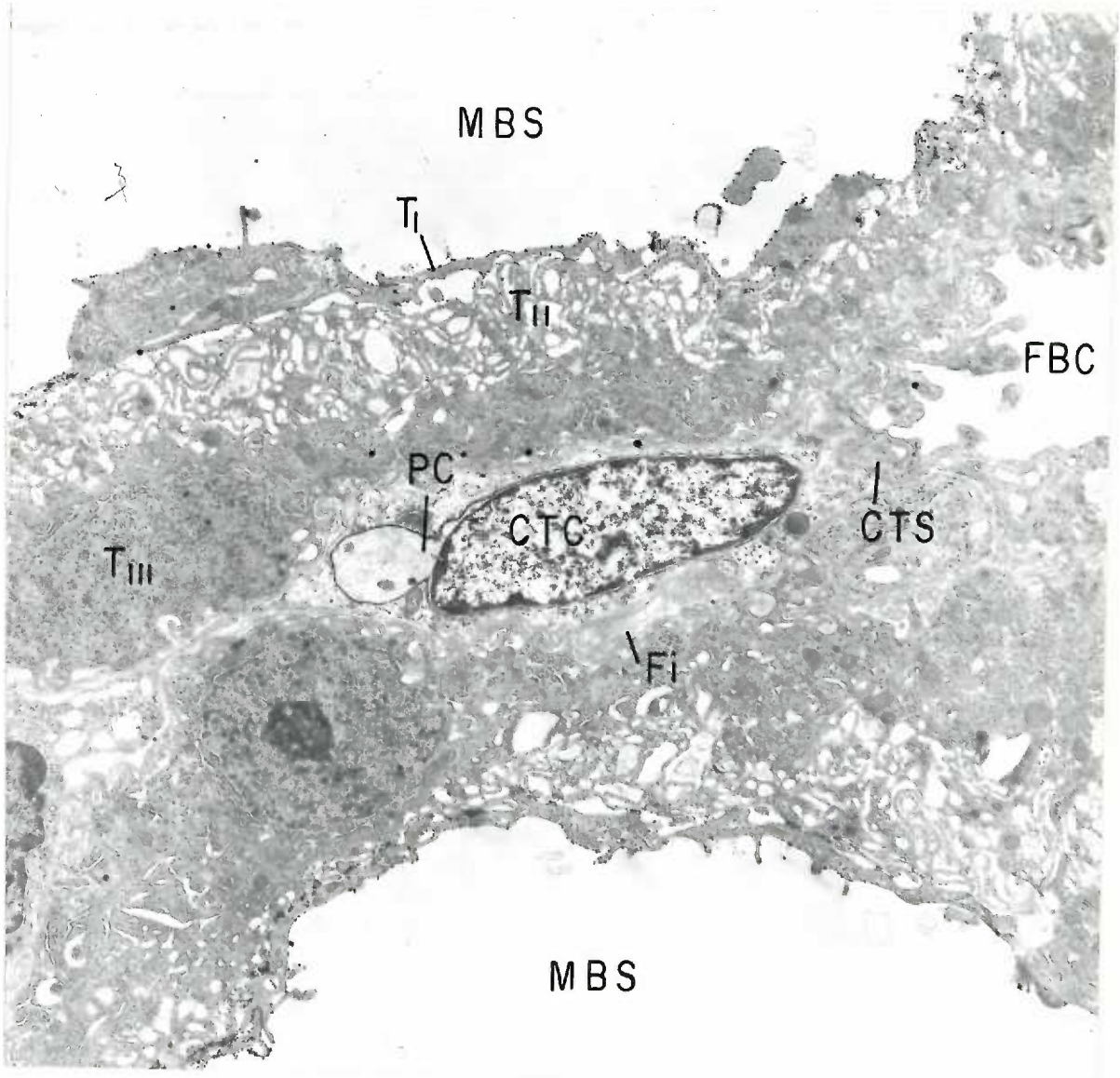

43

FIGURE 44

Twenty-two day placental labyrinth demonstrating the fine structural localization of AMPase activity. Magnification 3,420 X. Beaded deposits of final reaction product are distributed along the surface membranes of trophoblast I (T 1) and along the surface infoldings of trophoblast II (T 11). A large connective tissue space (CTS) containing portions of several mesenchymal cells (CTC) is seen between two allantoic capillaries (FBC).

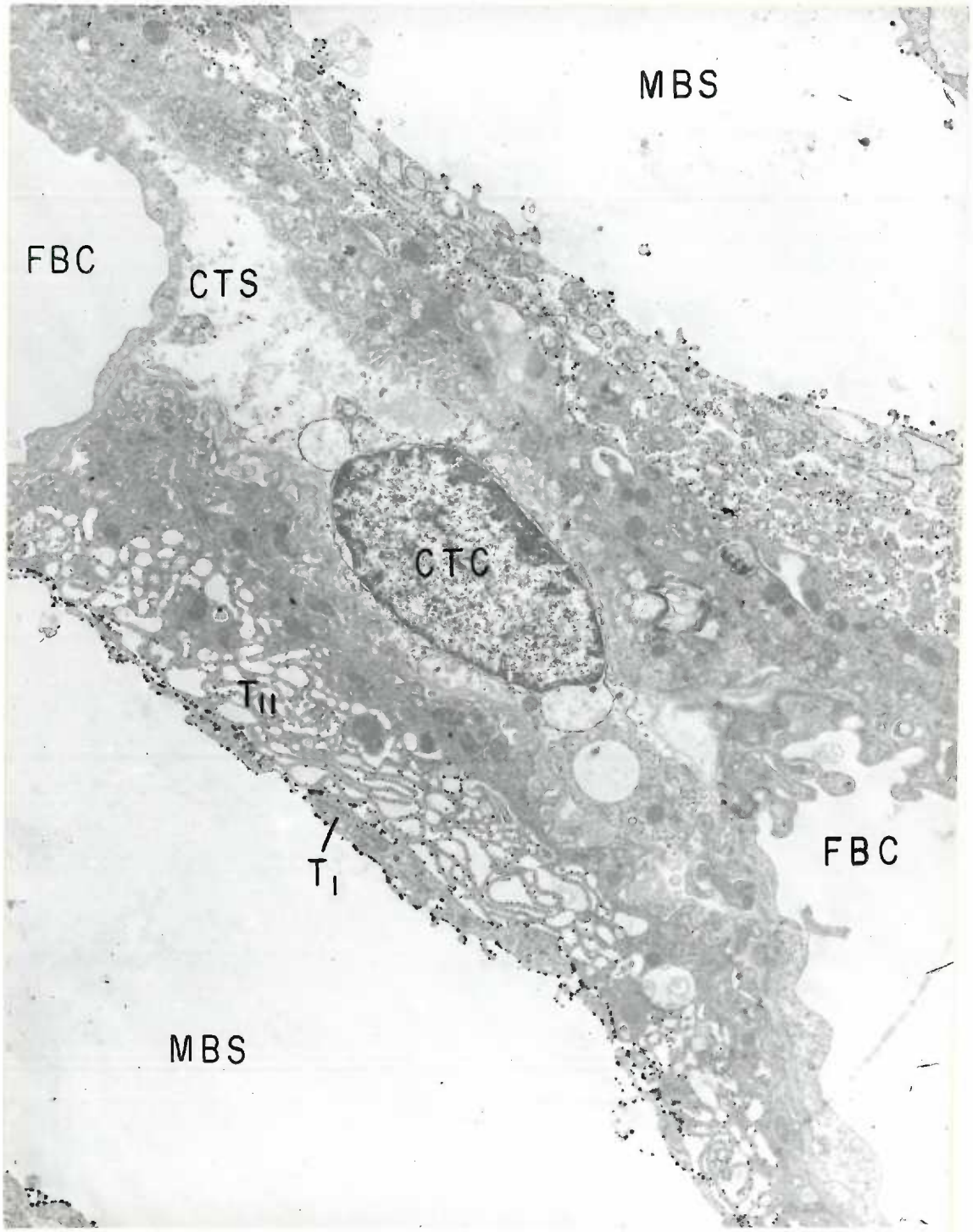

44

FIGURE 45

Longitudinal portion of a 22 day placental labyrinth treated for AMPase activity. Magnification 4,110 X. Final reaction product is distributed as described in Figure 44. A collapsed allantoic capillary (FBC) is seen at the bottom of the figure. The connective tissue space (CTS) directly above this capillary contains portions of several mesenchymal cells (CTC), one of which is richly provided with granular endoplasmic reticulum.

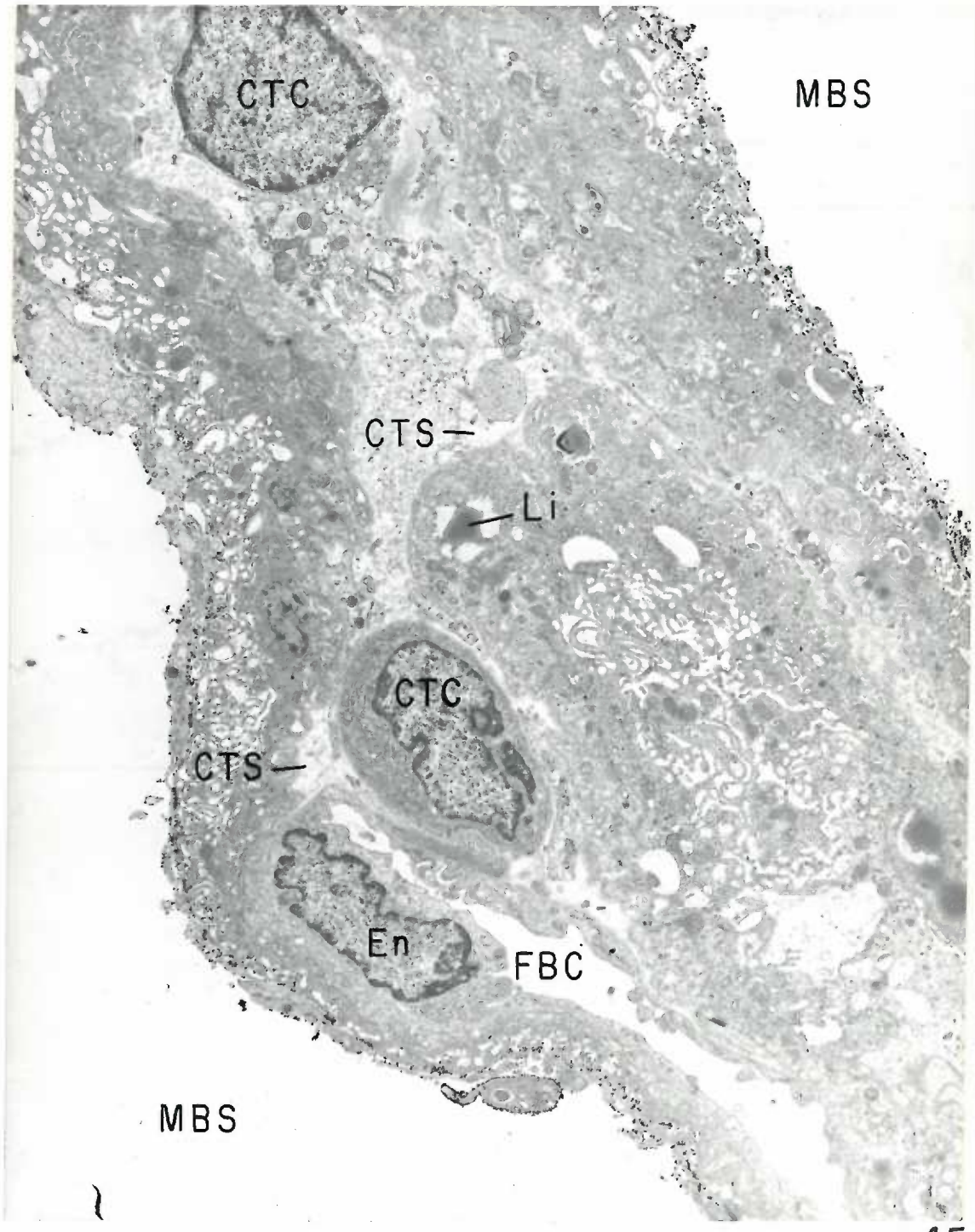

45

FIGURE 46

Enlarged portion of Figure 44. Magnification 12,175 X. Note that the numerous infoldings or channels of the middle layer of trophoblast (T 11) extend almost to the junction between trophoblast II and III (arrows). The mesenchymal cell (CTC) in the center of the connective tissue space (CTS) exhibits two rather large dilatations in its perinuclear cisterna (PC).

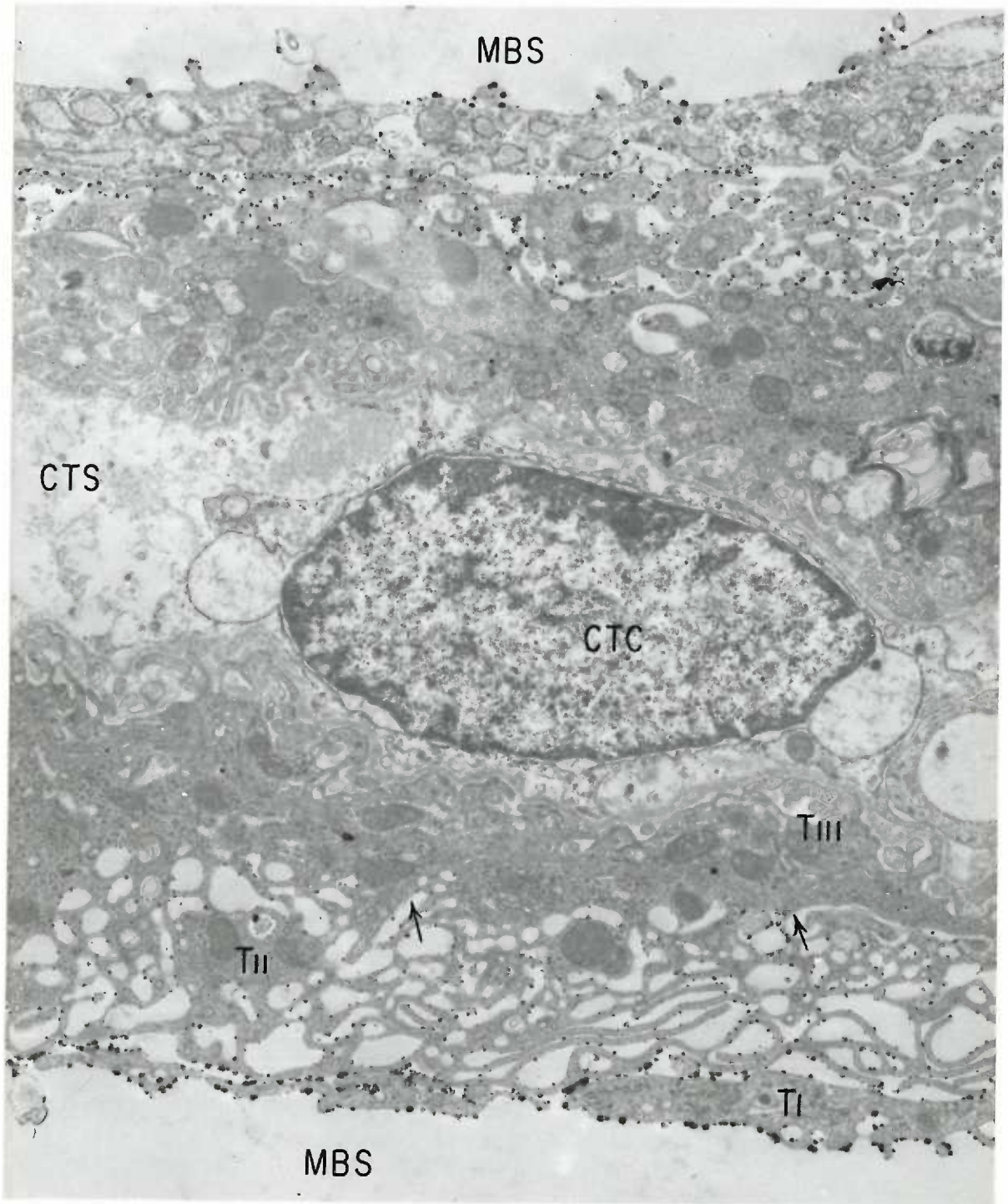

46

FIGURE 47

Twenty-two day placental labyrinth incubated with ADP as substrate. Magnification 12,900 X. ADPase activity is distributed as described in Figure 43. Compare the thickness of the nuclear portion of trophoblast III (T III) with the combined thickness of the remaining cytoplasmic layers. Note the areas of trophoblast I (T 1) which are extremely attenuated and the fenestration which occurs in the upper right corner of the figure (arrow). The basement membrane (BM) underlying trophoblast III appears more extensive than in the preceding stage.

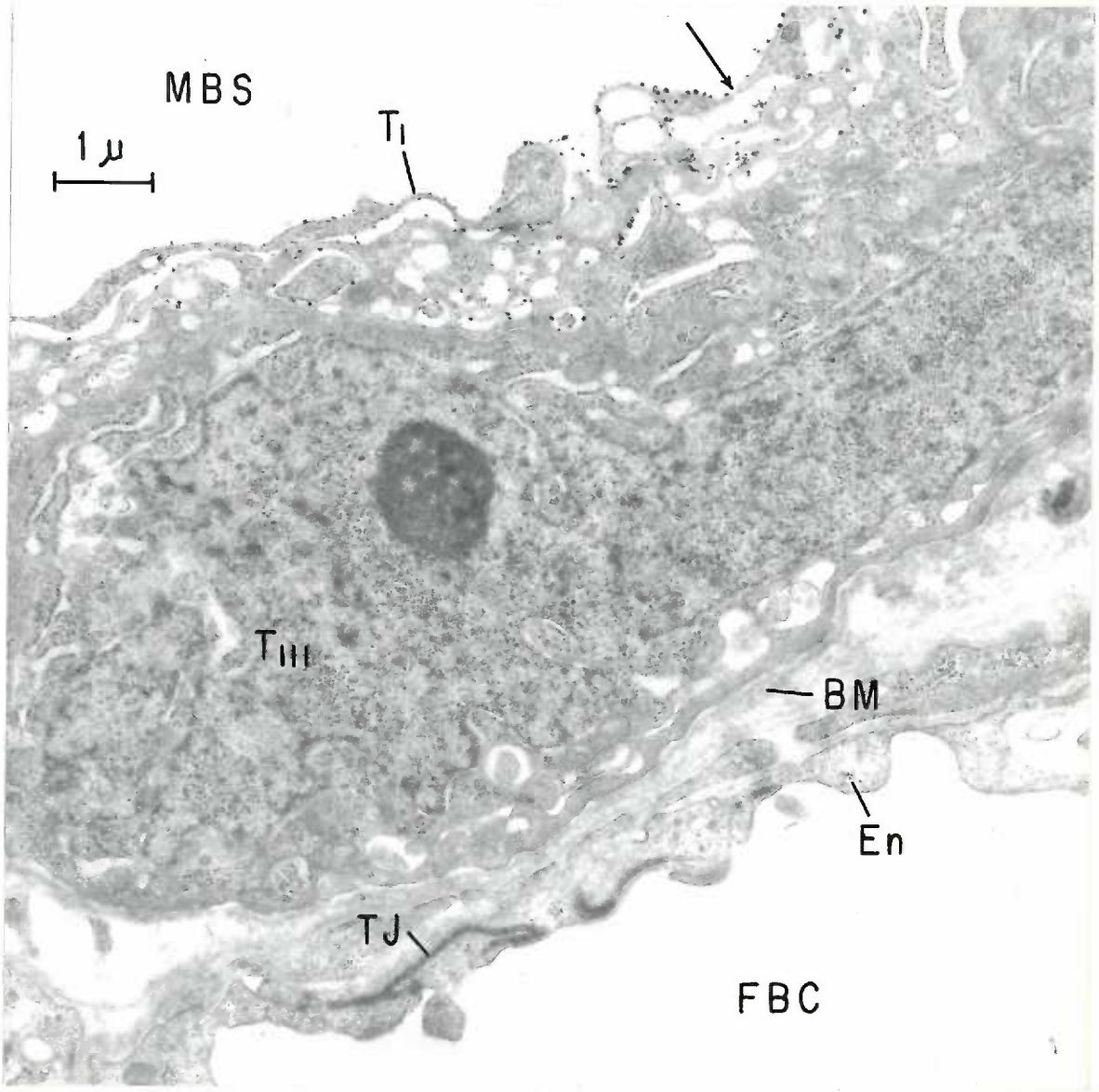

47

FIGURE 48

Twenty-two day placental labyrinth incubated with AMP as substrate. Magnification 7,800 X. AMPase activity is distributed as described in Figure 44. A rather large connective tissue space (CTS) intervenes between trophoblast III (T III) and the allantoic capillary (FBC). This space contains an elongated mesenchymal cell (CTC) which is richly provided with cytoplasmic organelles and shows evidence of active pinocytosis. Small pinocytotic vesicles also occur along the basal surface of the attenuated capillary endothelium (En).

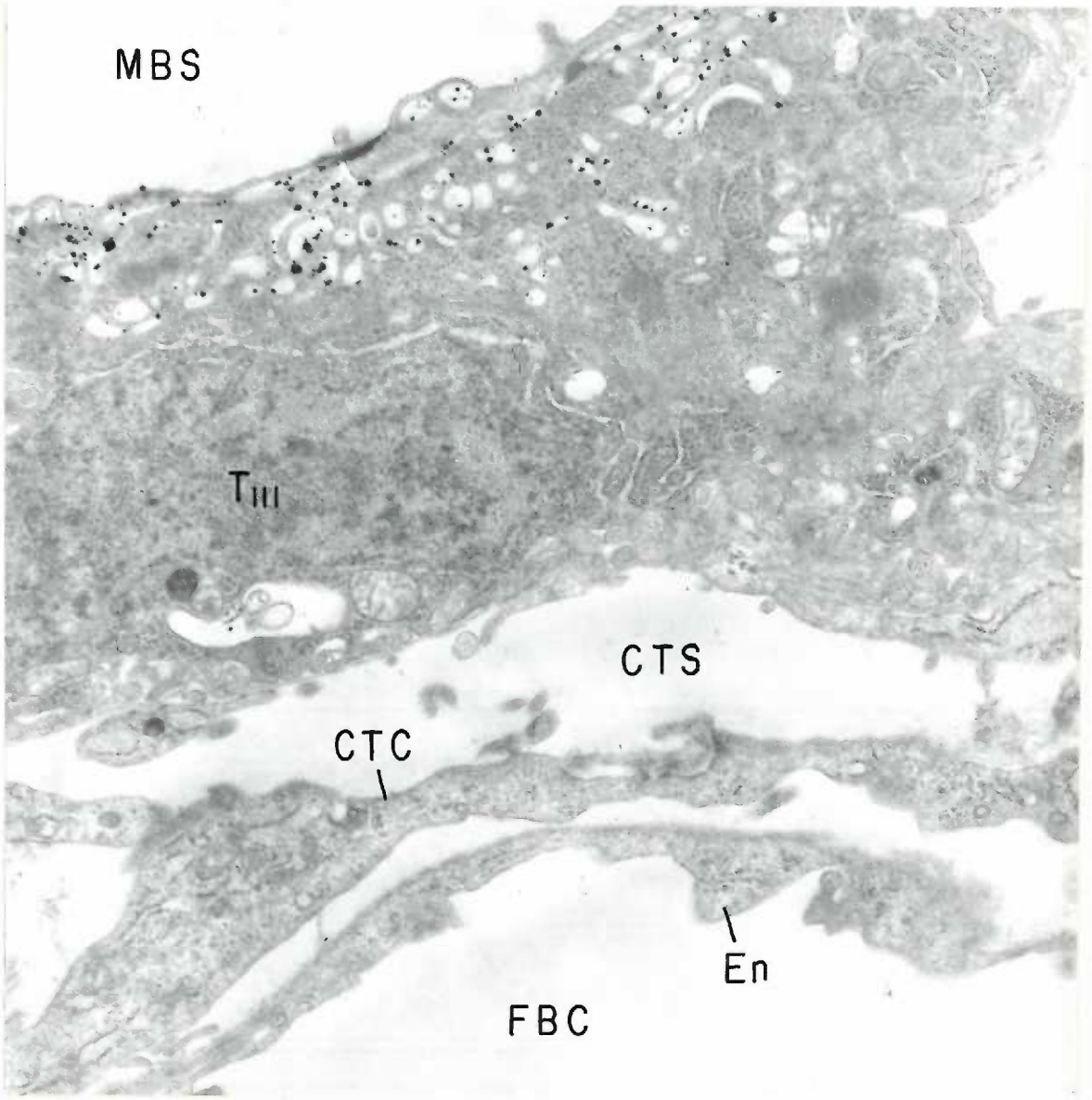

48

Figures 49-62 are of the labyrinthine portion of the chorio-allantoic placenta of rats whose pregnancies were artifically prolonged to 25 days (three days beyond the normal time of parturition).

FIGURE 49

Twenty-five day placental labyrinth incubated in a substrate free medium as a control preparation for an ATPase reaction. Magnification 12,900 X. Evidence of lead phosphate deposition is completely absent. As in preceding stages, the thicker regions of trophoblast I (T 1) are richly provided with ribosomal studded endoplasmic reticulum (ER), polysomes, golgi elements (G) and microvesicular profiles. Lysosome-like bodies are also seen in this layer (Ly). A homogenous appearing material of moderate electron density fills the intercellular spaces (IS) between trophoblast I and II (T 11). Note the massive number of thick walled vesicles in the cytoplasm adjacent to the surface infoldings of trophoblast II. Trophoblast III (T 111) appears markedly reduced in thickness over the previous stages. The extensively infolded plasma membrane of this layer gives the appearance of pedicel-like foot processes which are directed inward toward the endothelial basement membrane (BM).

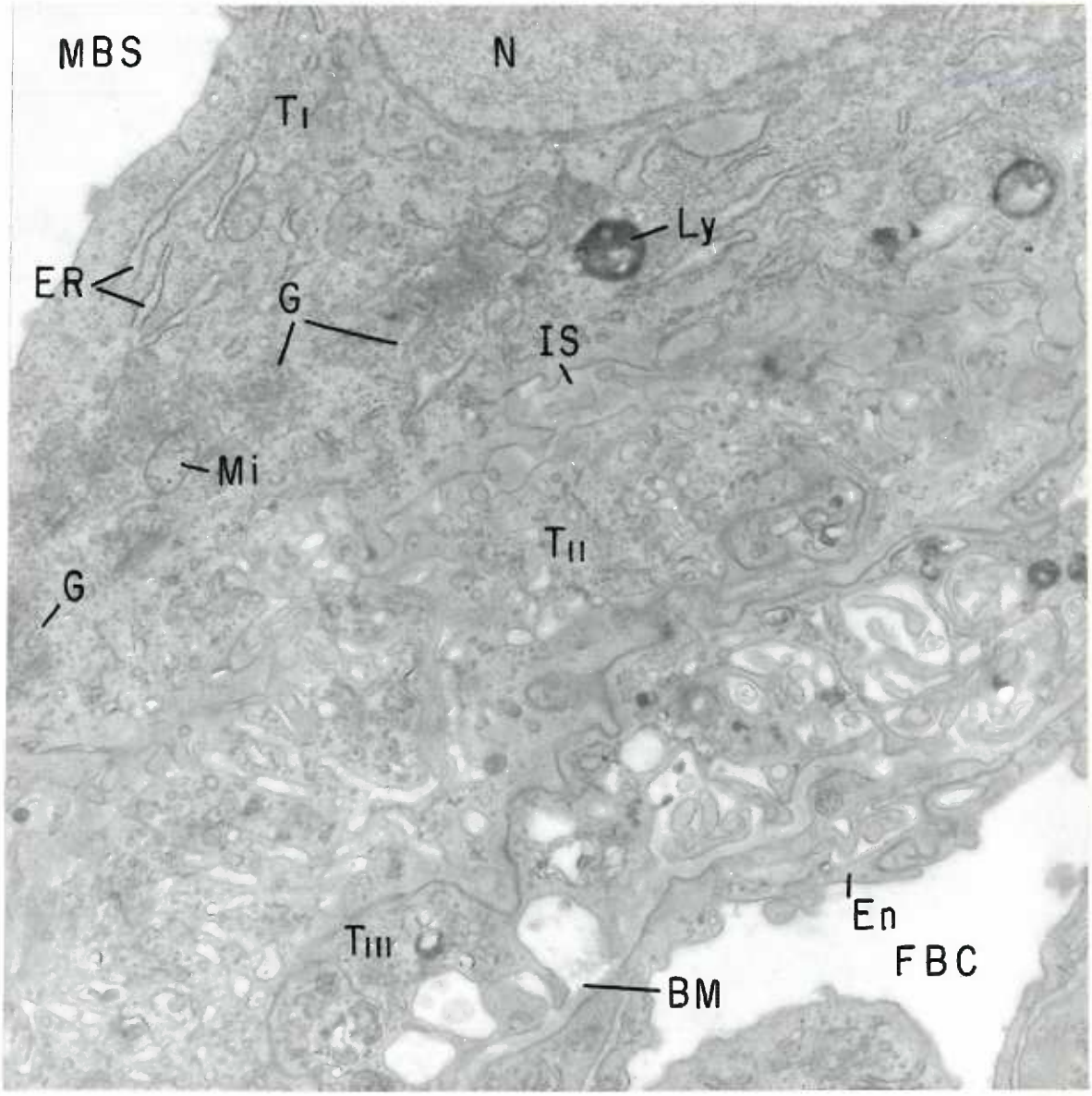

49

FIGURE 50

ATPase control preparation of the 25 day placental labyrinth incubated in a substrate free medium. Magnification 12,900 X. Final reaction product is completely absent from this preparation. The trophoblast I (T 1) cells bordering the maternal blood space contain small vesicular structures and show distinct fenestrations in their more attenuated regions (short arrows). In contrast to its thicker regions such as those in Figure 49, trophoblasts II (T 11) and III (T 111) display fewer organelles and a distinctly more fibrous and granular cytoplasm. Note the evidence of massive pinocytotic activity (PV) in the endothelium (En) lining the allantoic capillary (FBC) in the upper portion of the figure. Two closely apposed marginal folds (MF) project from the surfaces of the attenuated margins of two endothelial cells at the bottom of the figure. Several fenestrations (long arrows) in the endothelium occur adjacent to these folds. The extensive infolding and extreme attenuation of the four cytoplasmic layers effectively reduces the overall thickness of the placental barrier to not more than two microns.

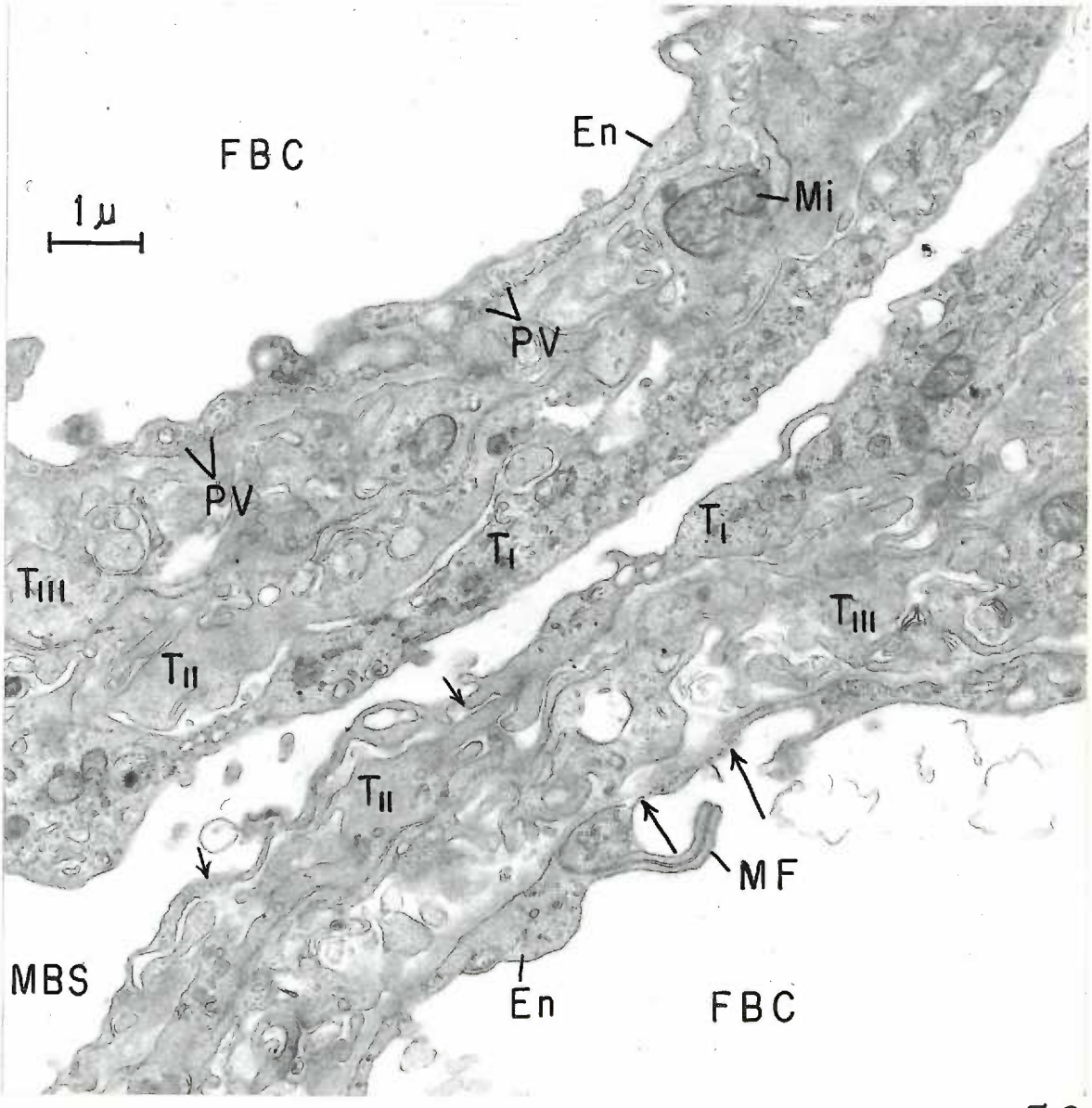

50

FIGURE 51

Control preparation of a 25 day placental labyrinth incubated in an ATP free medium. Magnification 12,900 X. Evidence for ATPase activity is absent. Trophoblast I (T 1) is greatly attenuated and exhibits caveolae (PV) near the bases of several cytoplasmic projections. Note the increase in numbers of mesenchymal cells (CTC) intervening between trophoblast III (T 111) and the allantoic capillary (FBC). These cells are invested by a layer of material which has the same fine structure as the basal laminae underlying trophoblast III and the fetal endothelium. The mesenchymal cell in the upper right corner of the figure is richly provided with cytoplasmic organelles. The endothelium (En) of allantoic capillary exhibits evidence of pinocytotic activity (PV) on both surfaces.

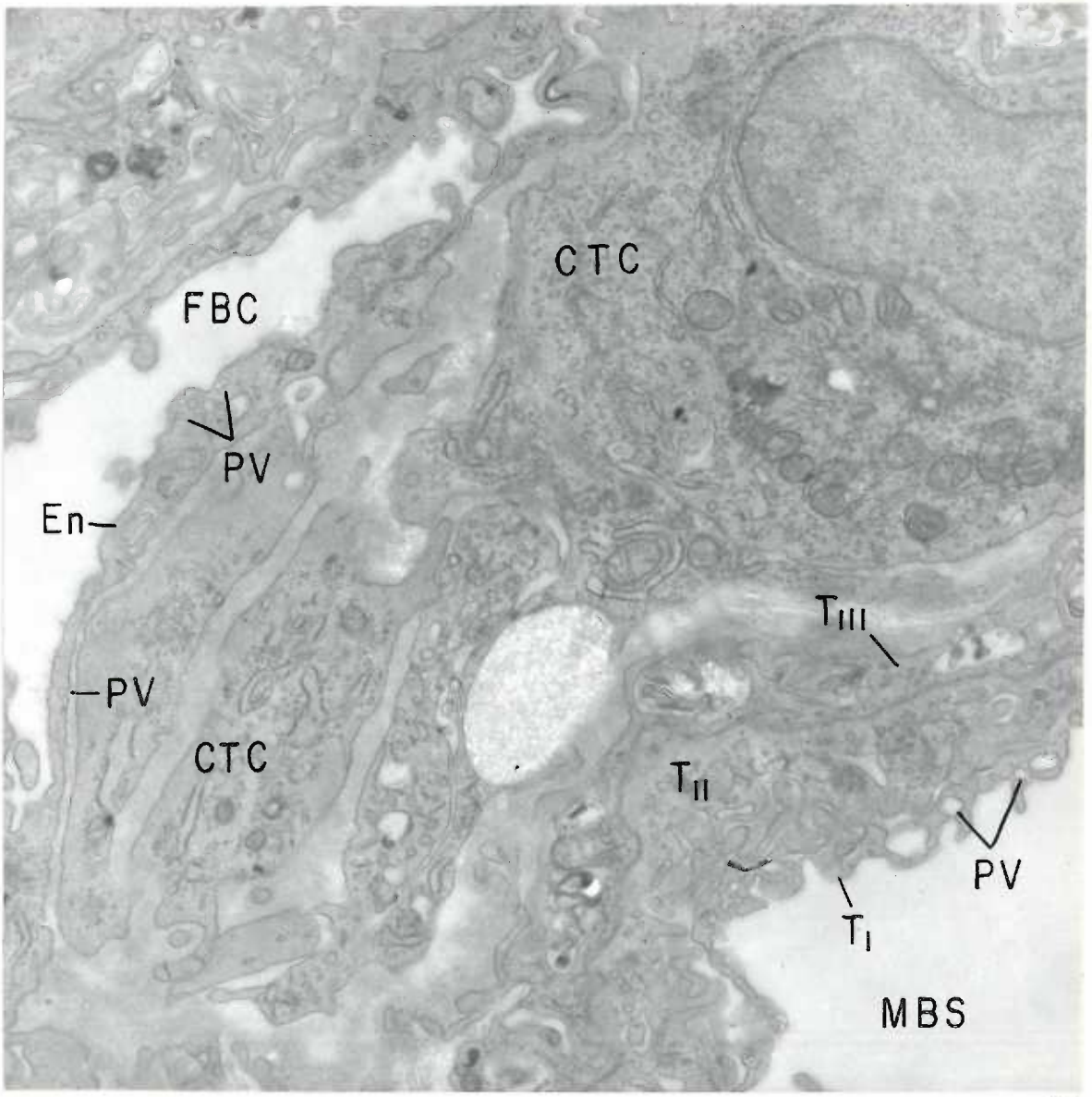

51

FIGURE 52

AMPase control preparation of a 25 day placental labyrinth. Magnification 12,900 X. Evidence of final reaction product is completely absent. Note that many of the mitochondria (Mi) in trophoblast II (T II) and III (T III) appear ballooned and have fragmented cristae and focally rarified matrices.

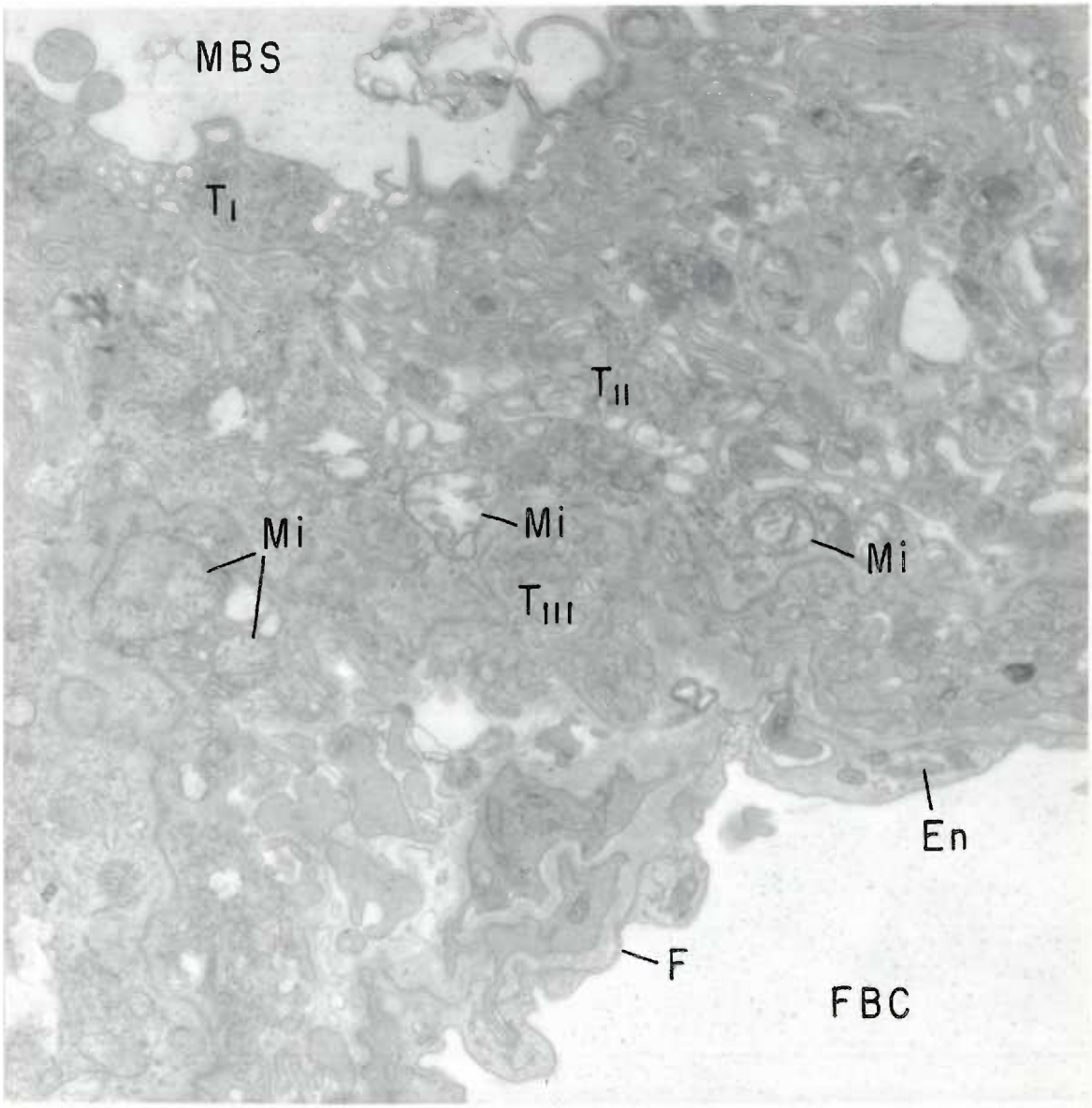

52

FIGURE 53

Portion of a trophoblast I cell from a 25 day placental labyrinth incubated with ATP as substrate. Magnification 12,900 X. Punctate deposits of final reaction product occur along the outer surface of the cell membrane and its microvillous projections. The cytoplasm is richly provided with polysomes (Ri), golgi elements (G) and granular endoplasmic reticulum (ER) whose cisternae are greatly distended by accumulations of cell product. Randomly oriented groups of filaments (Fi) associated in fine bundles are also seen in the cytoplasm.

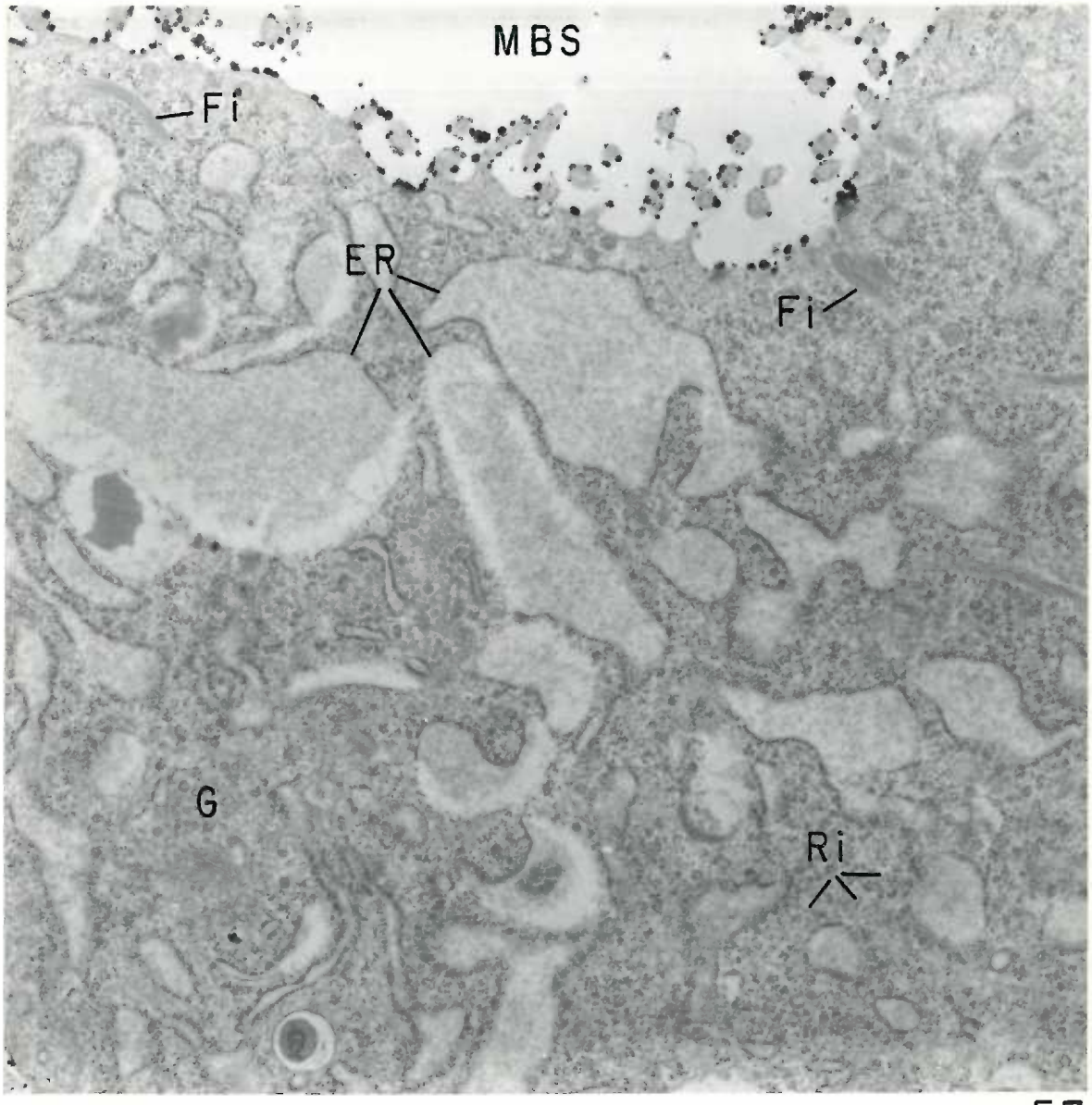

53

FIGURE 54

ATPase control preparation of a 25 day placental labyrinth. Magnification 12,900 X. As in Figures 49, 50 and 51, no evidence of final reaction product occurs when ATP is deleted from the incubation medium.

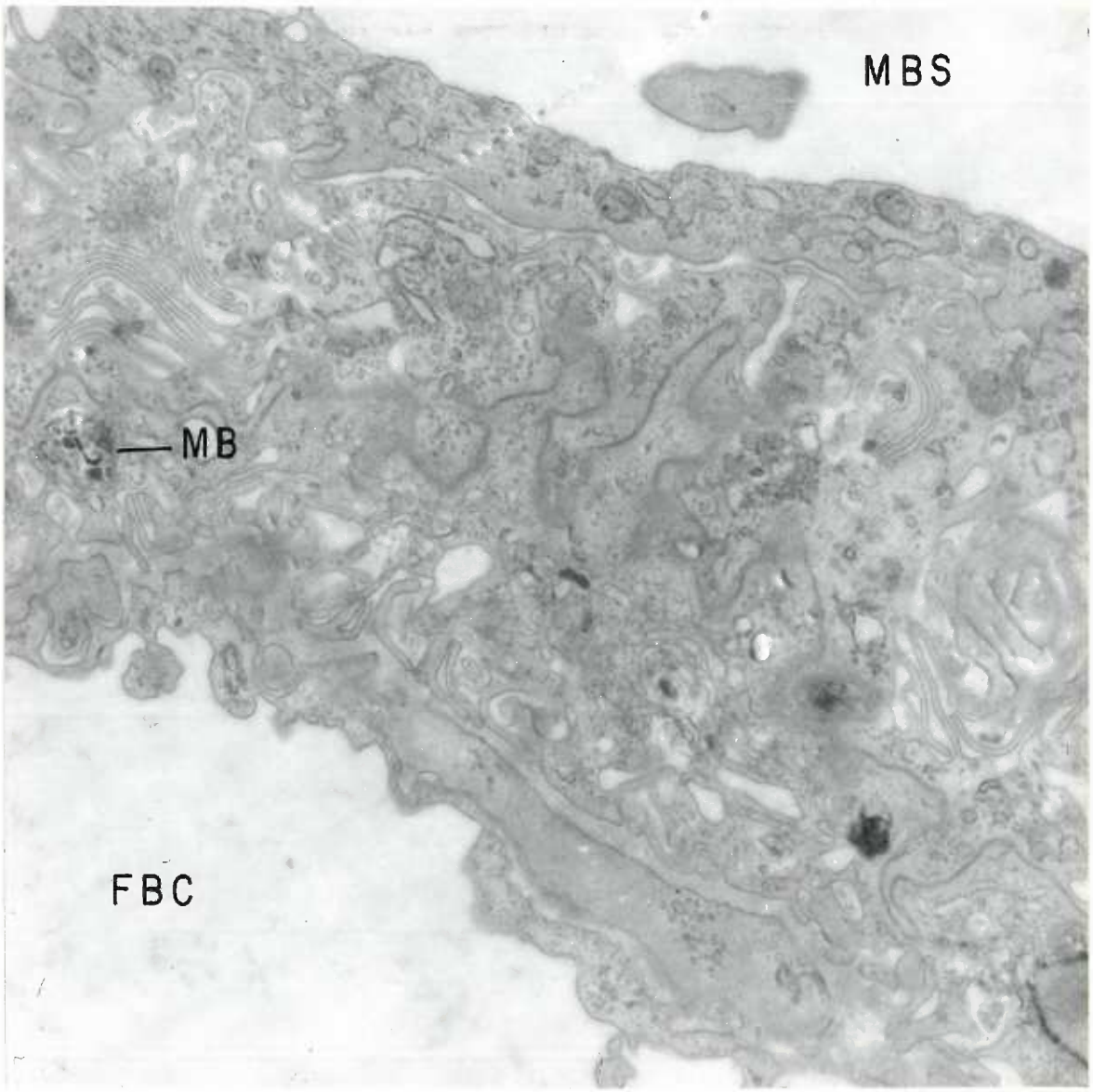

54

FIGURE 55

Twenty-five day placental labyrinth incubated with AMP as substrate. Magnification 5,400 X. Trophoblast I (T 1) appears to be in an advanced stage of degeneration with a highly clumped and vacuolated cytoplasm. Lead phosphate deposits are non-specifically scattered throughout the cytoplasm of this layer. Many of the infoldings of trophoblast II (T 11) as well as the intercellular spaces (IS) between trophoblast I and II are occluded with fibrin-like material (short arrows). Several areas of focal degeneration (long arrows) are also seen in trophoblast II. In these areas the cytoplasm is sparse and myelin (My) figures are apparent. Trophoblast III (T 111), the two intervening basal laminae and the capillary endothelium (En) are intact.

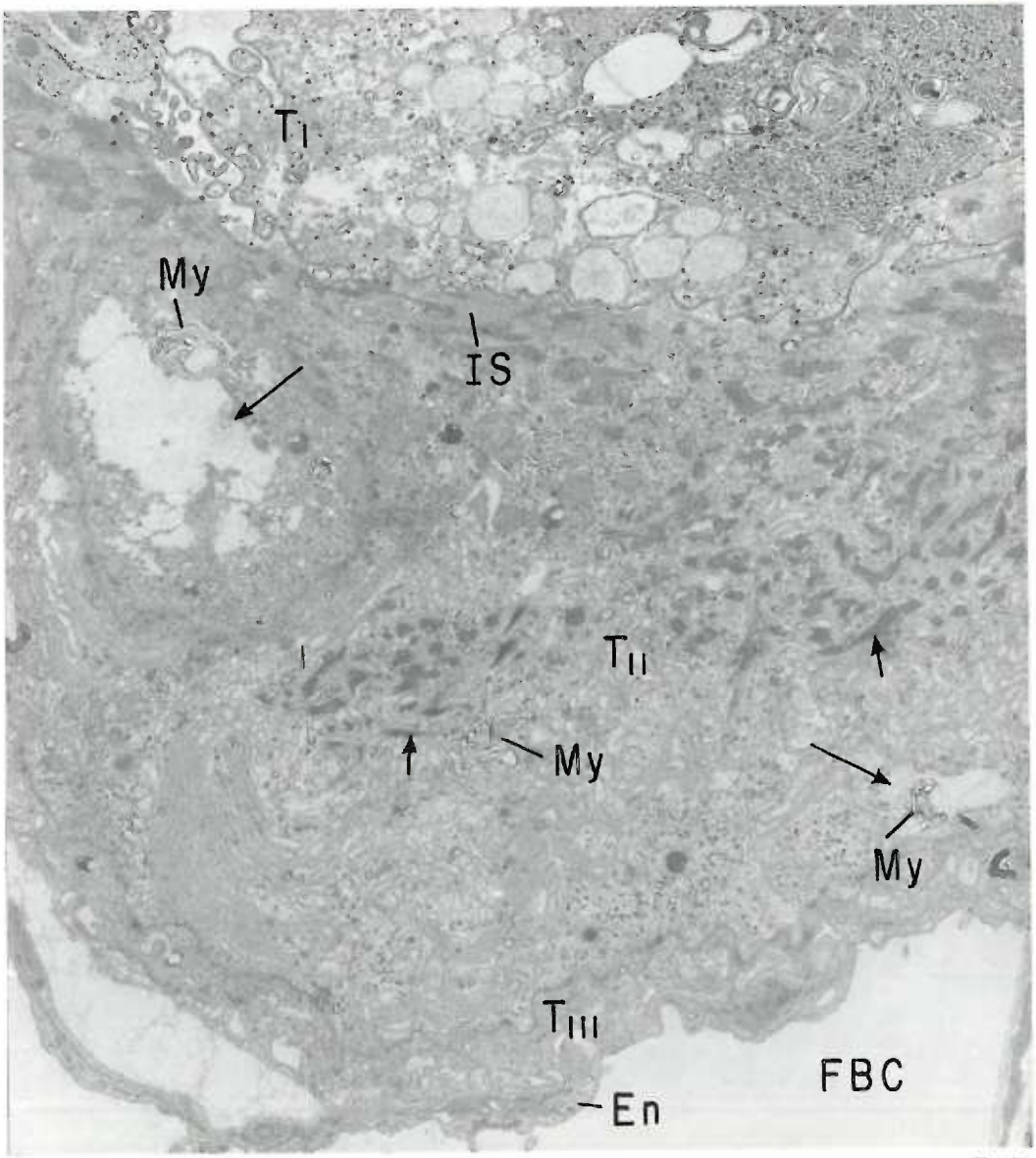

55

FIGURE 56

Twenty-five day placental labyrinth incubated with AMP as substrate. Magnification 18,600 X. Globular deposits of final reaction product are distributed throughout the fibrin-like material which fills the intercellular space (IS) between trophoblast I (T 1) and II (T 11). Activity localized to surface membranes is extremely sparse. The cytoplasm of trophoblast I appears granular and contains longitudinally oriented bundles of fine fibrils (Fi). The cytoplasm of trophoblast II is sparse and the surface infoldings and/or vacuoles are filled with a dense fibrous material which exhibits a periodicity characteristic of fibrin (arrows). Mitochondria (Mi) are ballooned and have disrupted cristae.

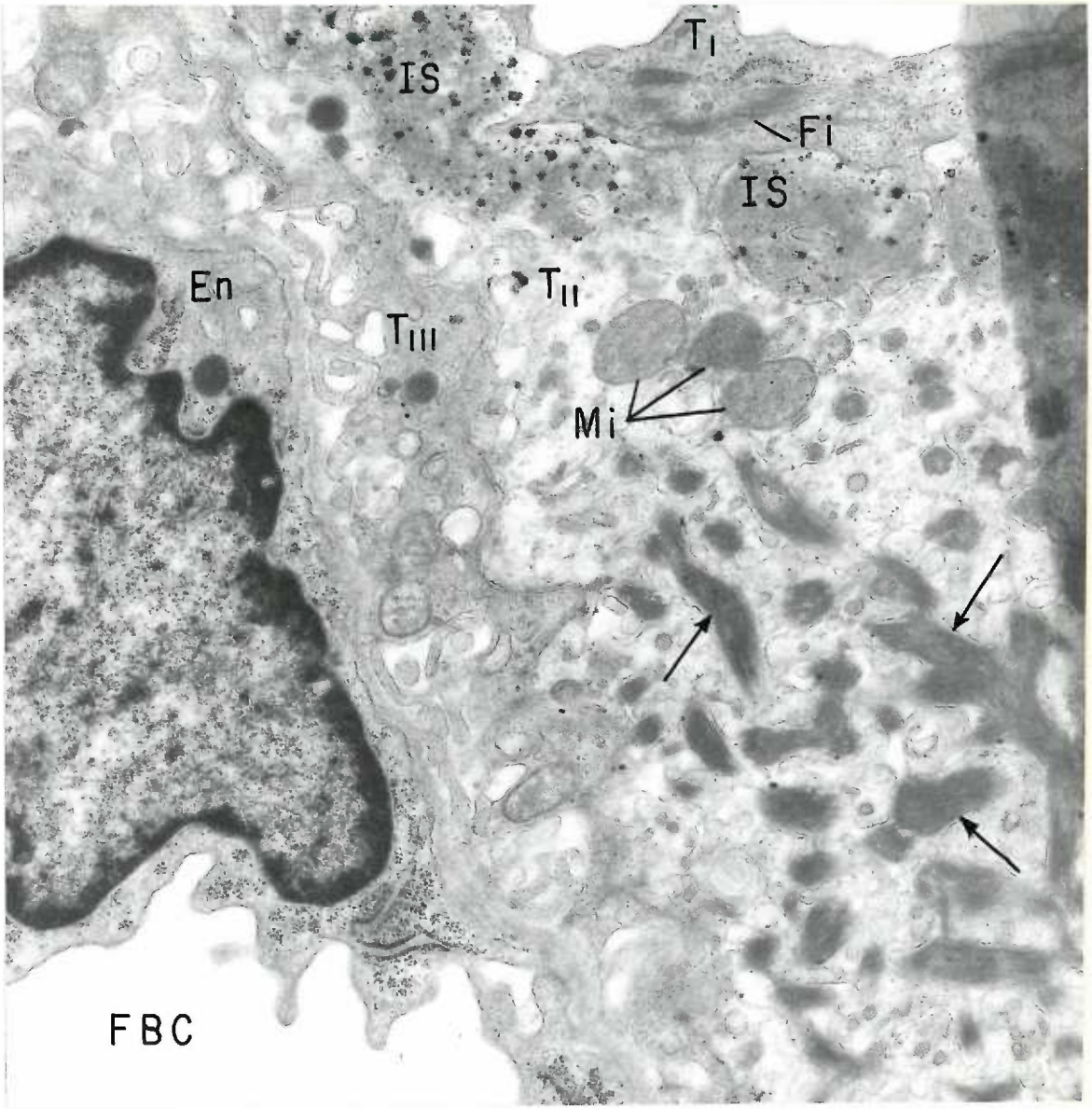

56

FIGURE 57

Twenty-five day placental labyrinth reacted for ADPase activity. Magnification 18,600 X. Globular deposits of final reaction product are distributed throughout the fibrin-like material in the intercellular space between trophoblast I (T 1) and II (T 11) and to a lesser extent along the surface membranes bordering this space. Only sparse activity occurs on the free surface of trophoblast I. The cytoplasm of trophoblast III (T 111) is centrally rarified and exhibits a granular to fibrillar texture as does the cytoplasm of the other layers. The surface membranes of the barrier are not sharply defined and occasionally appear to fade away (arrow) suggesting focal plasma membrane disruption. Cytoplasmic organelles also are not sharply defined.

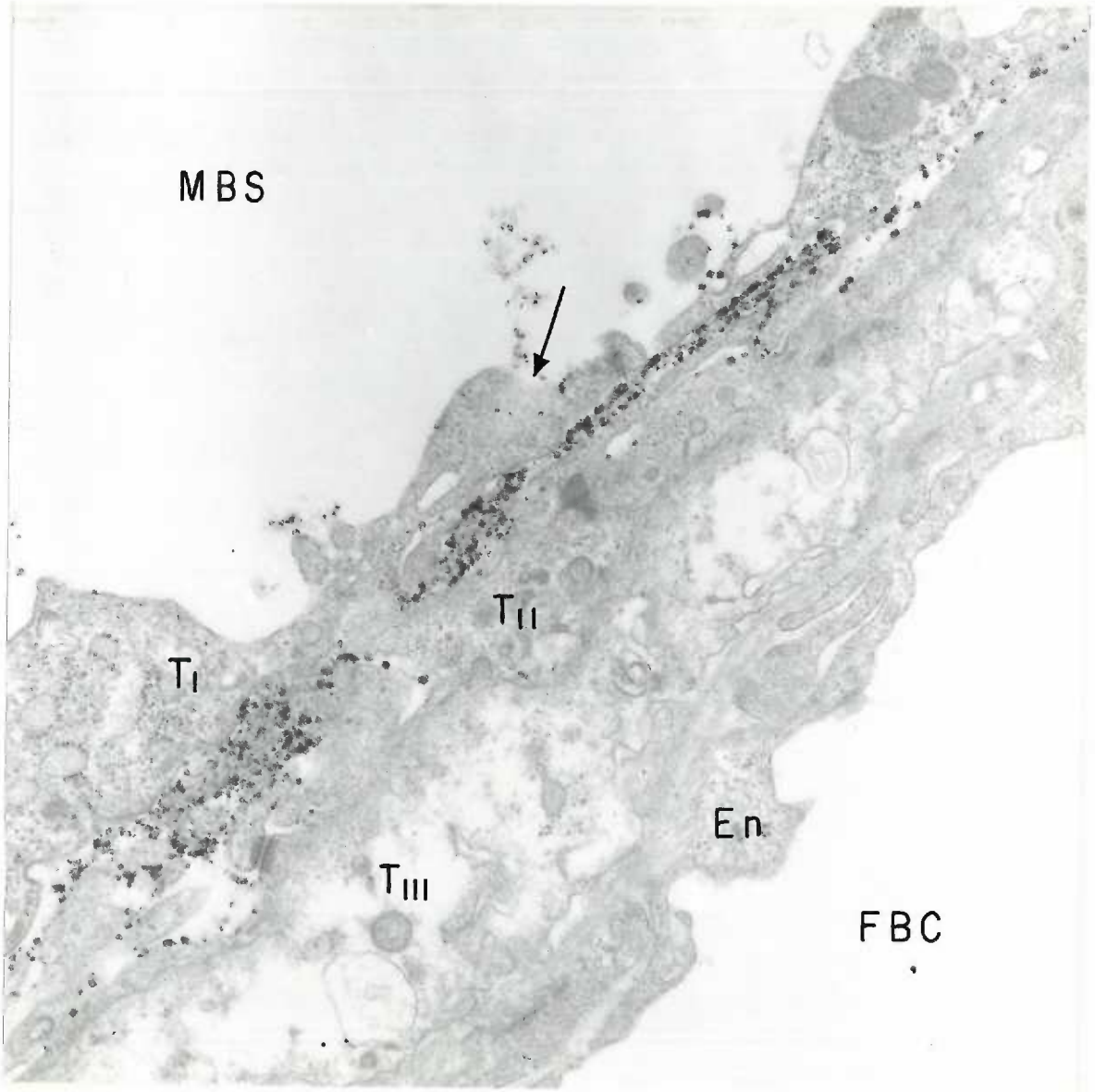

57

FIGURE 58

Twenty-five day placental labyrinth incubated with ADP as substrate. Magnification 7,800 X. Final reaction product is distributed as described in Figure 57, except that more deposits of lead phosphate occur along the free surface of trophoblast I (T 1). The cytoplasmic detail of the four layers is ill-defined and the mitochondria (Mi) are ballooned and have disrupted and rarified matrices. Fenestrations (arrows) are seen in the more attenuated areas of the capillary endothelium (En).

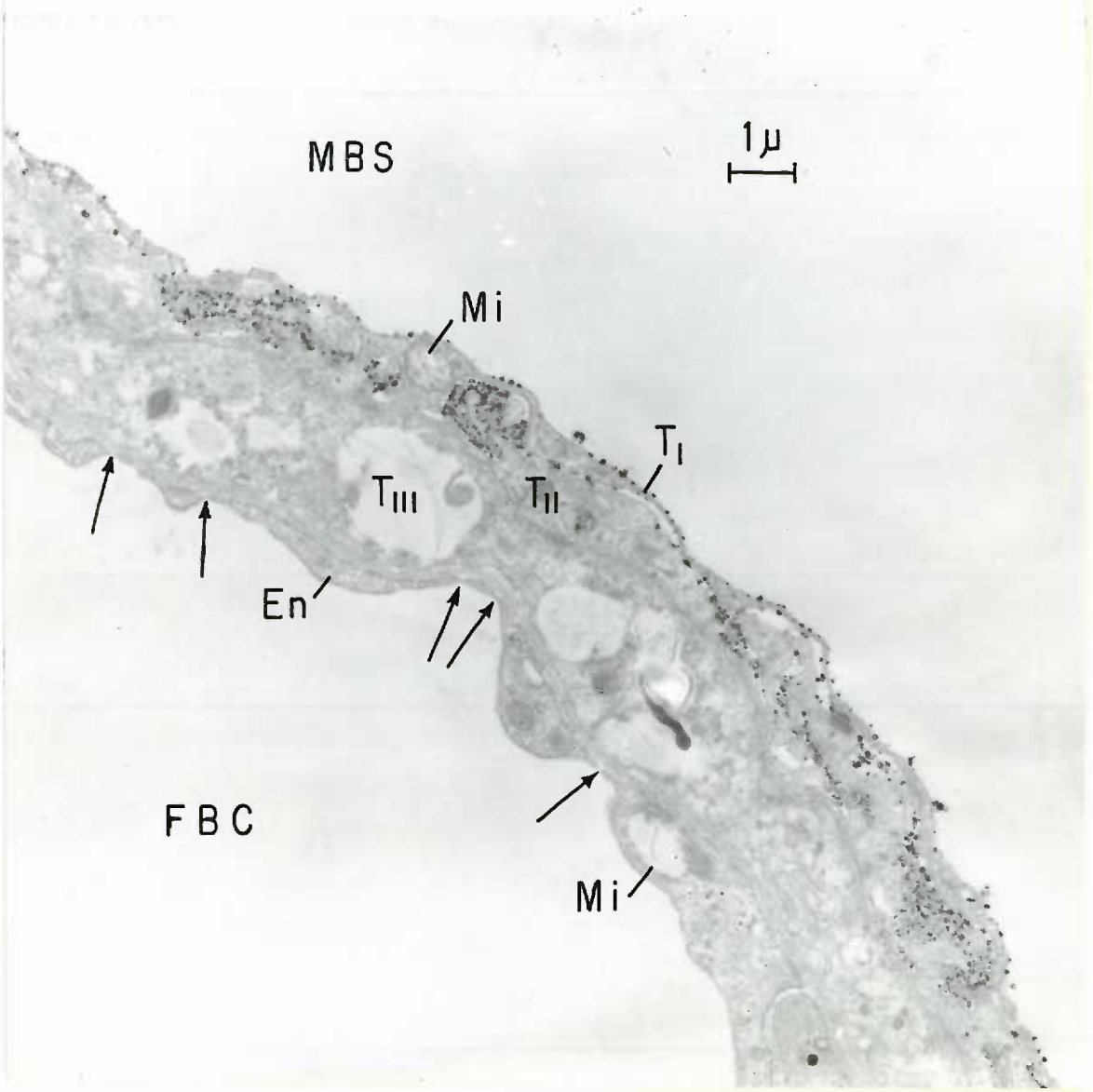

58

FIGURE 59

Twenty-five day placental labyrinth reacted for ATPase activity. Magnification 7,800 X. Final reaction product is distributed throughout clumps of fibrin-like material which occur in the intercellular space between trophoblast I (T I) and II (T II) and in the surface infoldings and/or vacuoles of trophoblast II. Activity is also distributed along the surface membranes of these layers. Both trophoblast I and II exhibit focal areas where lead phosphate occurs nonspecifically deposited throughout the cytoplasm. The limiting membrane of the mesenchymal cell (CTC) bordering the capillary endothelium (En) is indistinct and appears to be continuous with short fibrils which extend from the peripheral cytoplasm into the extracellular space and basal lamina of the allantoic capillary (FBC). Mitochondria (Mi) in the mesenchymal cell as well as in trophoblast I are swollen and fragmented with vacuolated matrices.

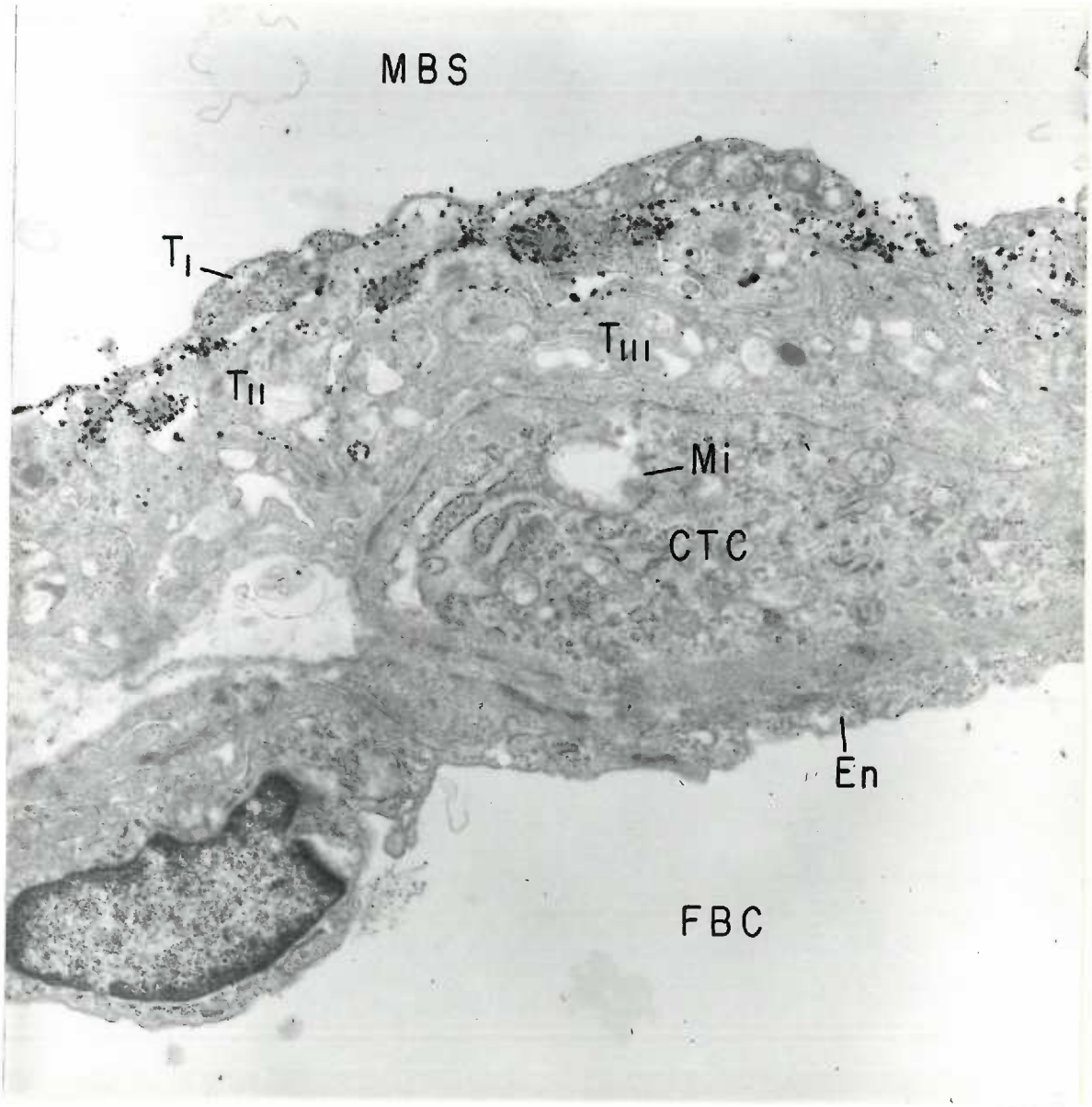

59

FIGURE 60

Twenty-five day placental labyrinth reacted for ADPase activity. Magnification 18,600 X. Final reaction product is distributed as described in Figures 57 and 58. The cytoplasm of the mesenchymal cell (CTC) intervening between trophoblast (T III) and the capillary basement membrane has a granular to fibrillar appearance as do the other cytoplasmic layers and contains disrupted organelles.

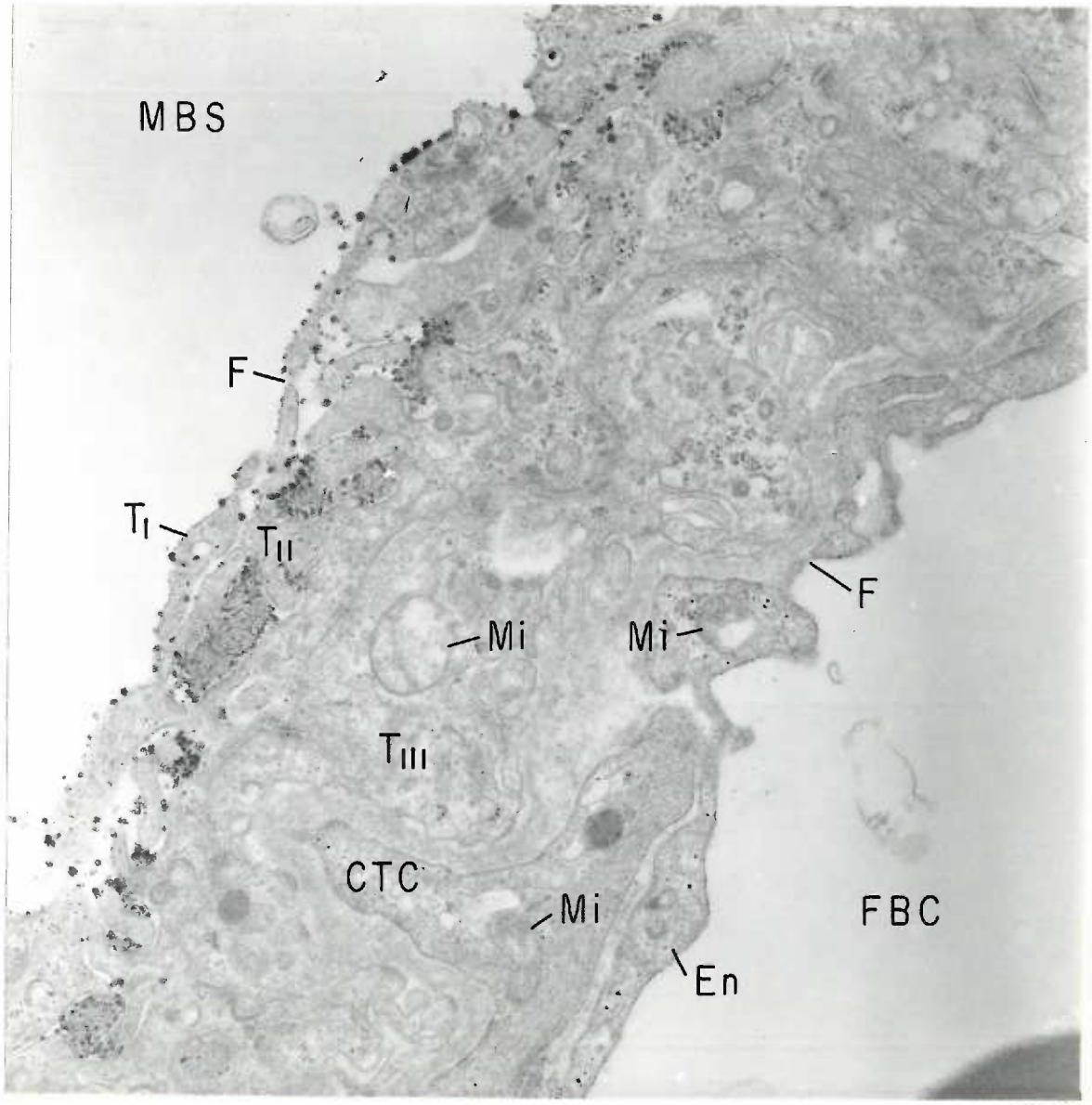

60

FIGURE 61

Twenty-five day placental labyrinth incubated with ADP as substrate. Magnification 7,800 X. Activity with this substrate is distributed as described in Figures 57 and 58. Note that the external lamina (EL) which envelopes the mesenchymal cells (CTC) intervening between trophoblast III (T III) and the capillary endothelium (En) is thickened and reticulated.

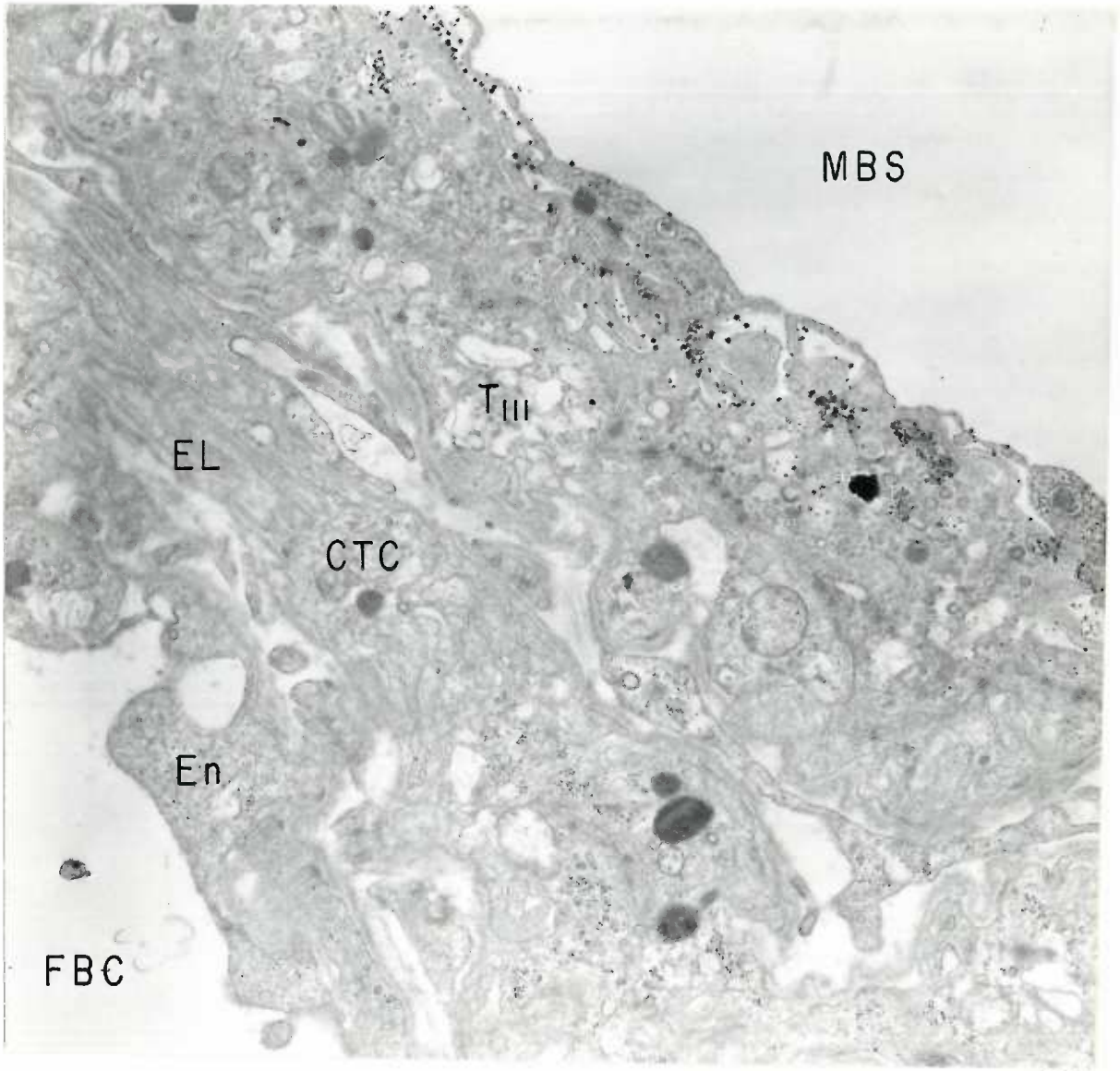

61

FIGURE 62

Twenty-five day placental labyrinth incubated with AMP as substrate. Magnification 12,900 X. Final reaction product is deposited as described in Figure 56. Trophoblast I (T 1) and the capillary endothelium (En) are richly provided with microvesicular profiles and other cytoplasmic organelles. Trophoblasts II and III are greatly attenuated and remain closely apposed. The matrices of the mitochondria (Mi) in all layers are either dense or disrupted.

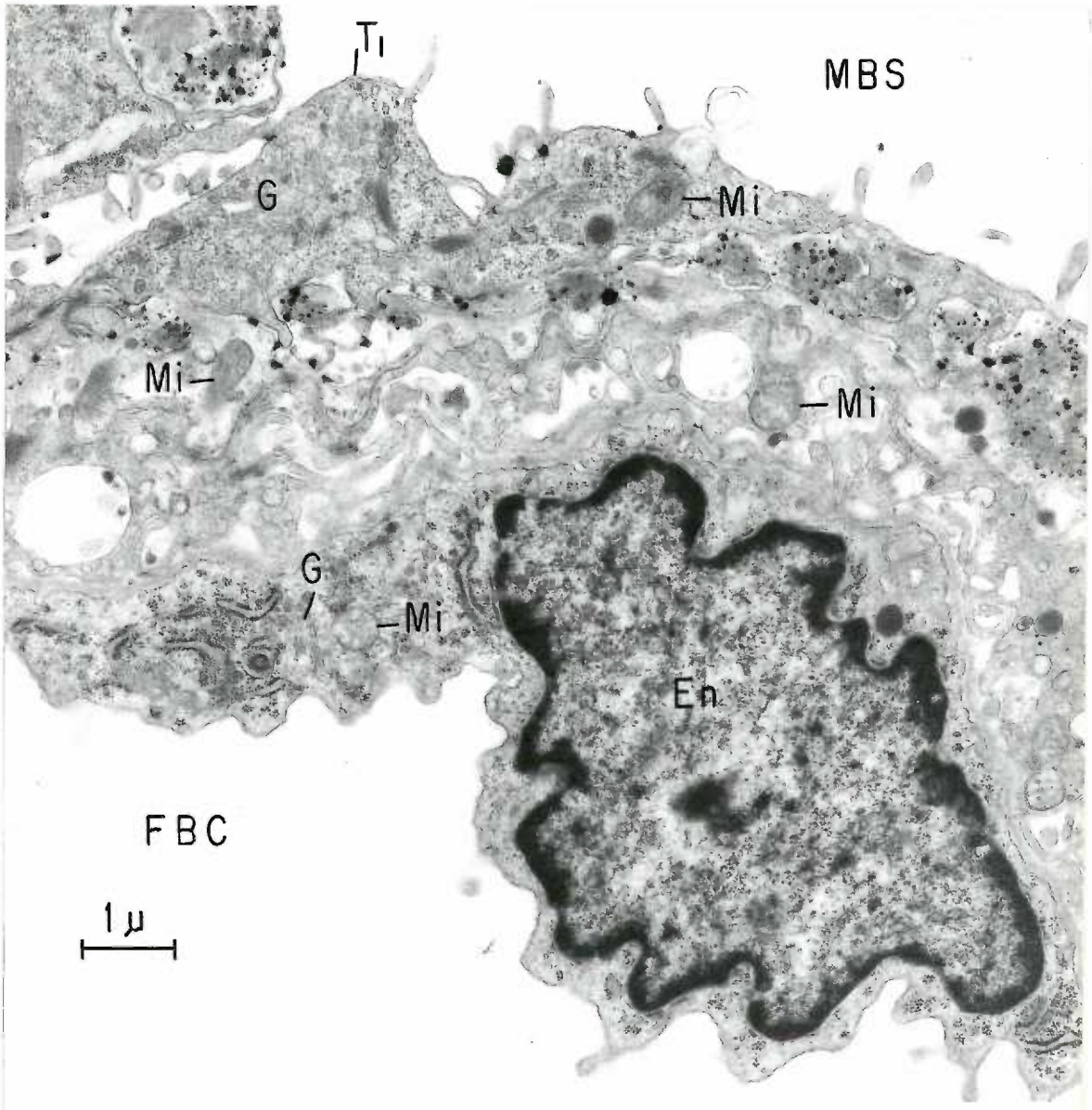

62

ABBREVIATIONS FOR FIGURES 63 - 134

Abs V	-	absorption vacuole
AC	-	apical canal
Co	-	collagen fibrils
CP	-	circular profiles
CTC	-	connective tissue cell
CTS	-	connective tissue space
Des	-	desmosome
En	-	endothelium
ER	-	endoplasmic reticulum
Ex	-	exocoelom
FRBC	-	fetal red blood cell
Fi	-	fibrils
G	-	golgi elements
IS	-	intercellular space
Li	-	lipid
Ly	-	lysosome
Mes	-	mesothelium
Mi	-	mitochondria
Mv	-	microvilli
My	-	myelin figure
N	-	nucleus
PV	-	pinocytotic vesicle
Ri	-	ribosomes

SBM - serosal basement membrane

TB - terminal bar

TJ - tight junction

To - tonofibrils

TW - terminal web

UL - uterine lumen

V - vacuole

v - vesicle

VBM - visceral basement membrane

VC - vitelline capillary

VE - visceral entoderm

YSC - yolk sac cavity

FIGURE 63

Twelve day visceral endoderm incubated with ATP as substrate. Magnification 7,800 X. The apical cytoplasm is crowned by a brush border of microvilli (Mv) which are coated with granular deposits of final reaction product. Many small vesicles (v) and large absorption vacuoles (Abs V) appear below the apical cell surface. An abundance of mitochondria (Mi) and endoplasmic reticulum (ER) are distributed throughout the cytoplasm and the golgi-like microvesicular profiles (G) are most concentrated in the supranuclear regions. Dense deposits of lead phosphate also fill the intercellular spaces between adjoining endodermal cells.

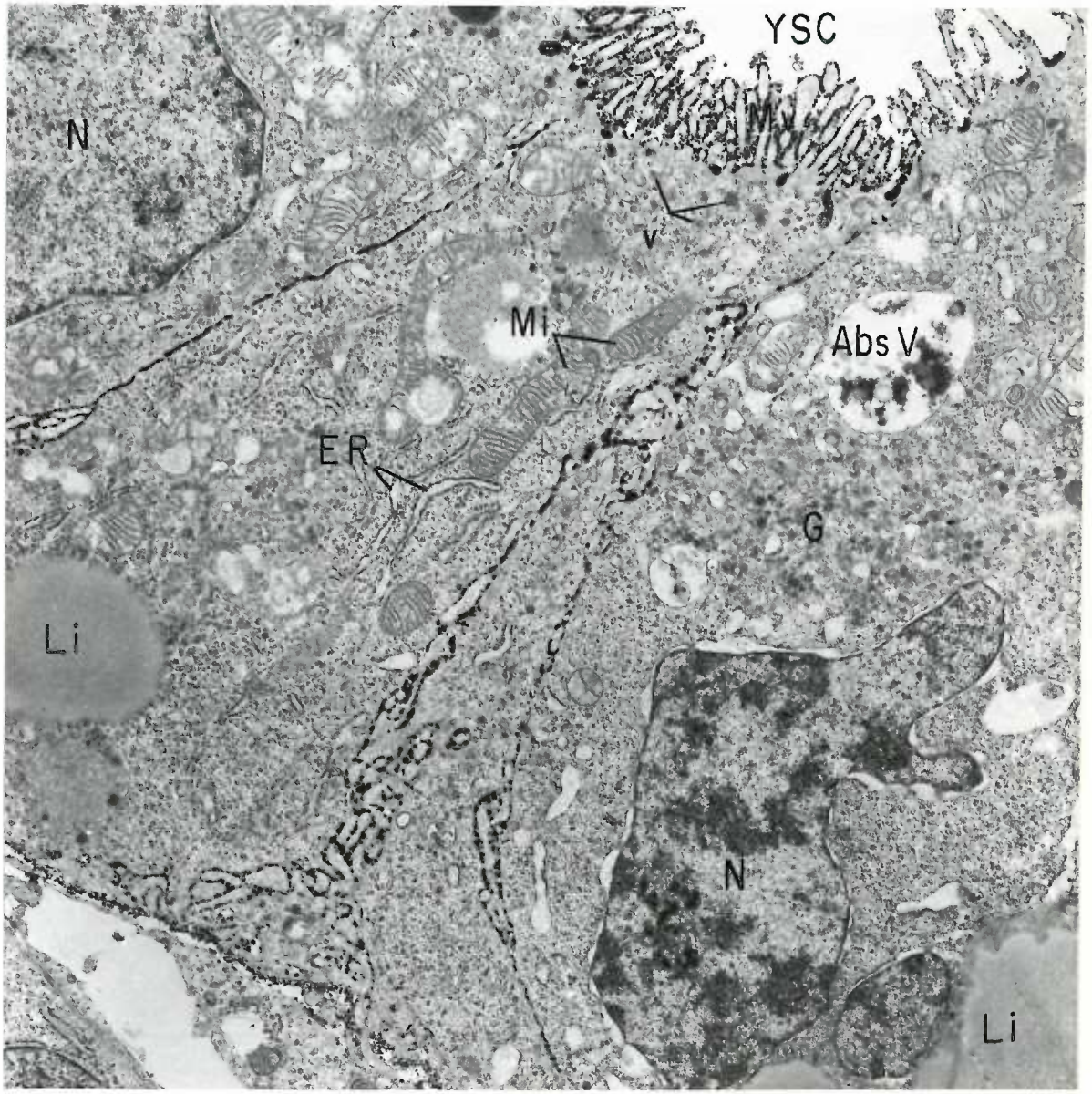

63

FIGURE 64

Low power electron micrograph of several 12 day visceral endodermal cells incubated with ATP as substrate. Magnification 8,170 X. The apical cytoplasm of these cells contain numerous vacuoles (V) of various sizes. The perinuclear and basal cytoplasm is rich in endoplasmic reticulum and polyribosomes (Ri). A cluster of large homogeneous lipid droplets (Li) are seen in close relation with the basal surface of the endodermal cell on the right. Smaller lipid clusters are also seen above the nuclei (N). Note that lateral surface membranes between the adjoining cells become more complex toward the visceral basement membrane.

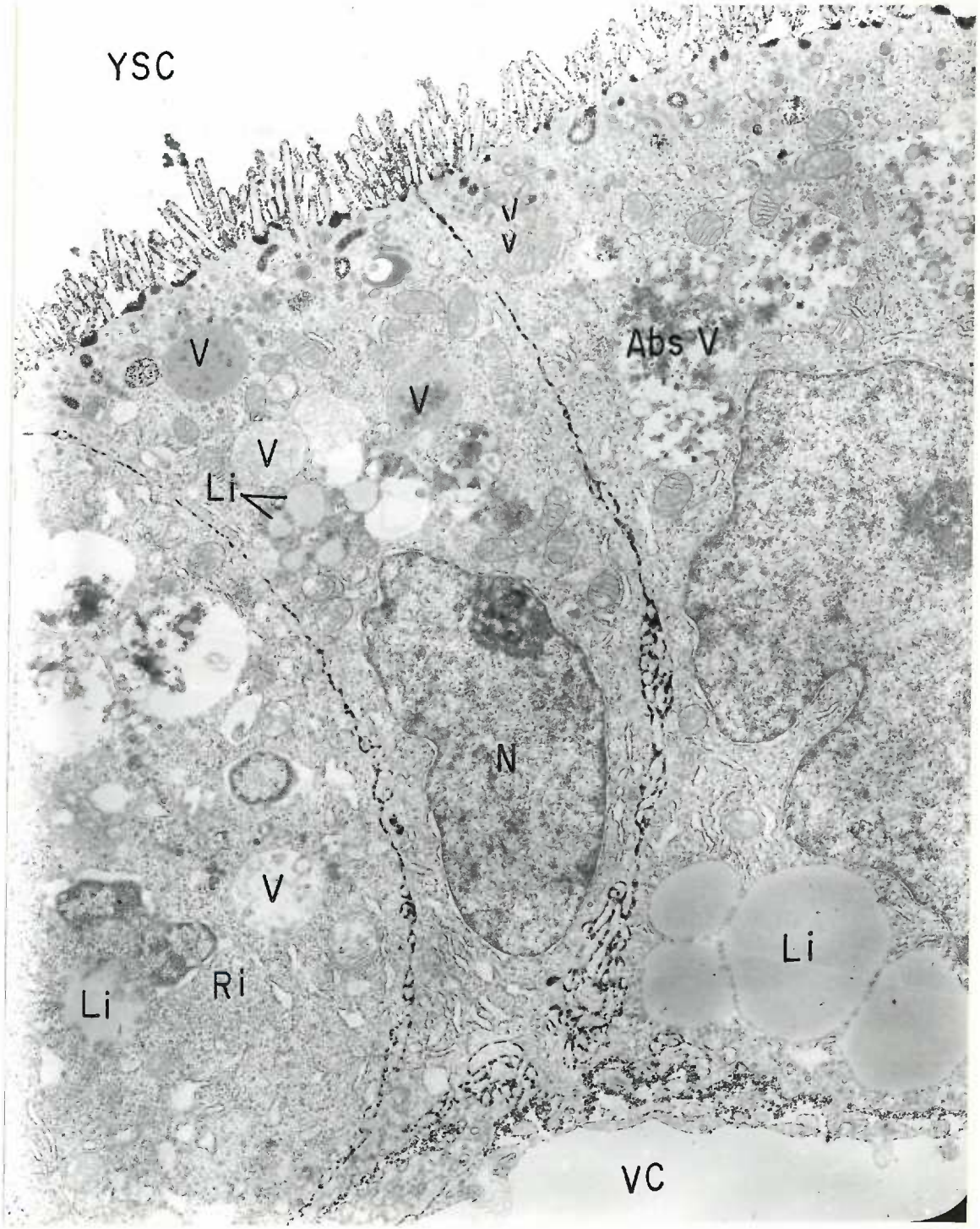

64

FIGURE 65

Basal portion of a 12 day visceral yolk sac incubated with ATP as substrate. Magnification 7,800 X. Accumulations of final product fill the intercellular spaces between the highly interdigitated folds of adjoining endodermal cell surfaces. Fine granular deposits of lead phosphate also occur in the visceral basement membrane (VBM) and to a lesser extent throughout the underlying connective tissue space (CTS) and serosal basement membrane (SBM). At points where the vitelline capillary (VC) is in close contact with the visceral basement membrane, diffuse granules occur on the outer plasma membrane of the endothelium (En). This localization probably represents diffusion of the final reaction product as other areas of the capillary endothelium are devoid of such deposits. No activity is seen in the mesothelium (Mes) lining the exocoelom (Ex). Note the presence of a small lipid (Li) inclusion in the nucleus of the endodermal cell in the upper right hand corner of the figure.

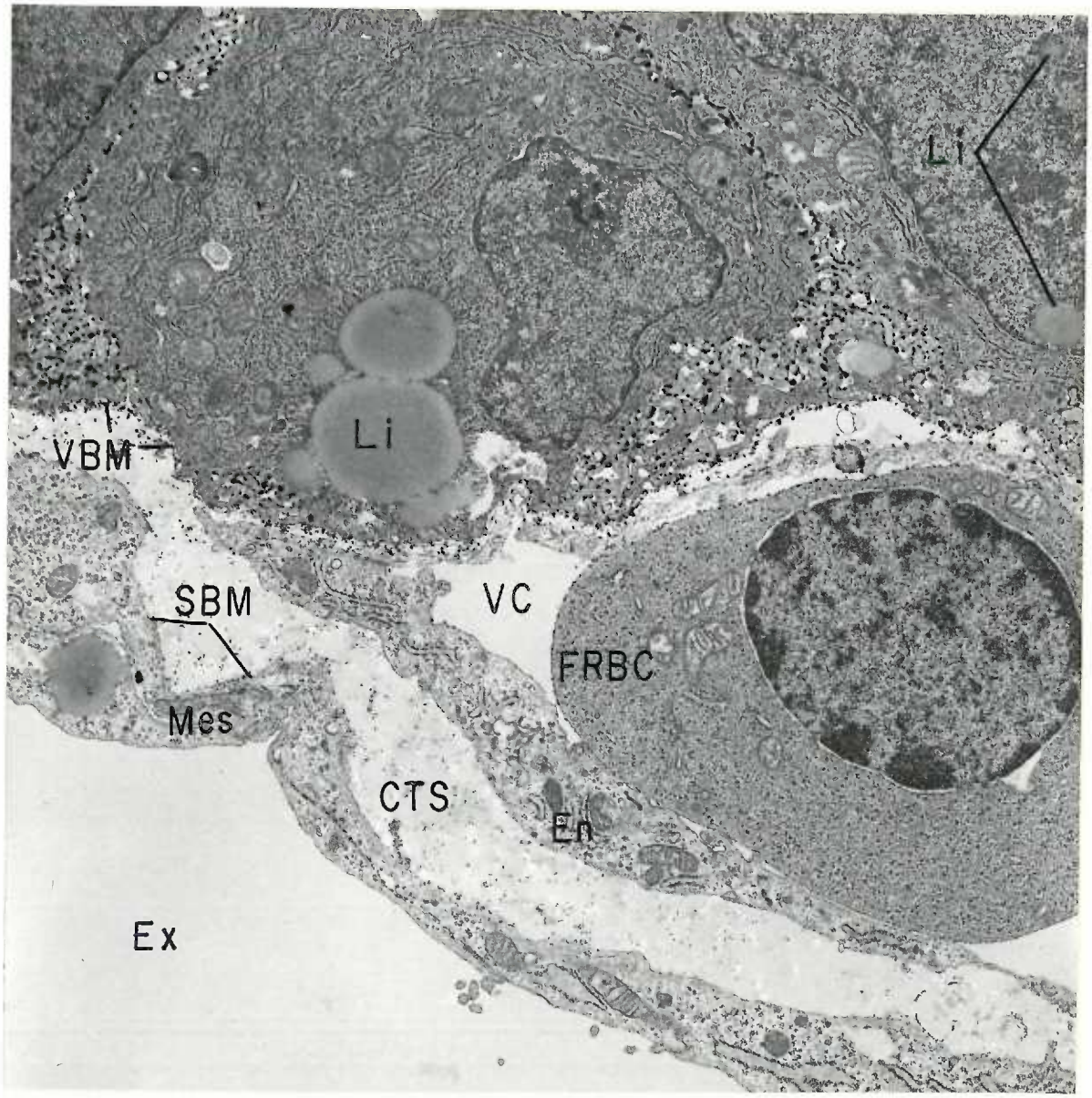

65

FIGURE 66

Basal portion of a 12 day visceral yolk sac incubated with ATP as substrate. Magnification 7,800 X. Part of a mesenchymal cell (CTC) and a vitelline capillary (VC) containing a fetal nucleated red blood cell (FRBC) are seen intervening between the visceral basement membrane and the mesothelium lining and exocoelomic cavity (Ex). The cytoplasm of the mesothelium (Mes) is particularly rich in polyribosomes and possesses a well developed granular endoplasmic reticulum (ER) which is oriented parallel to the long axis of the cell. Note the presence of a lipid inclusion (Li) within the mesothelial cell nucleus.

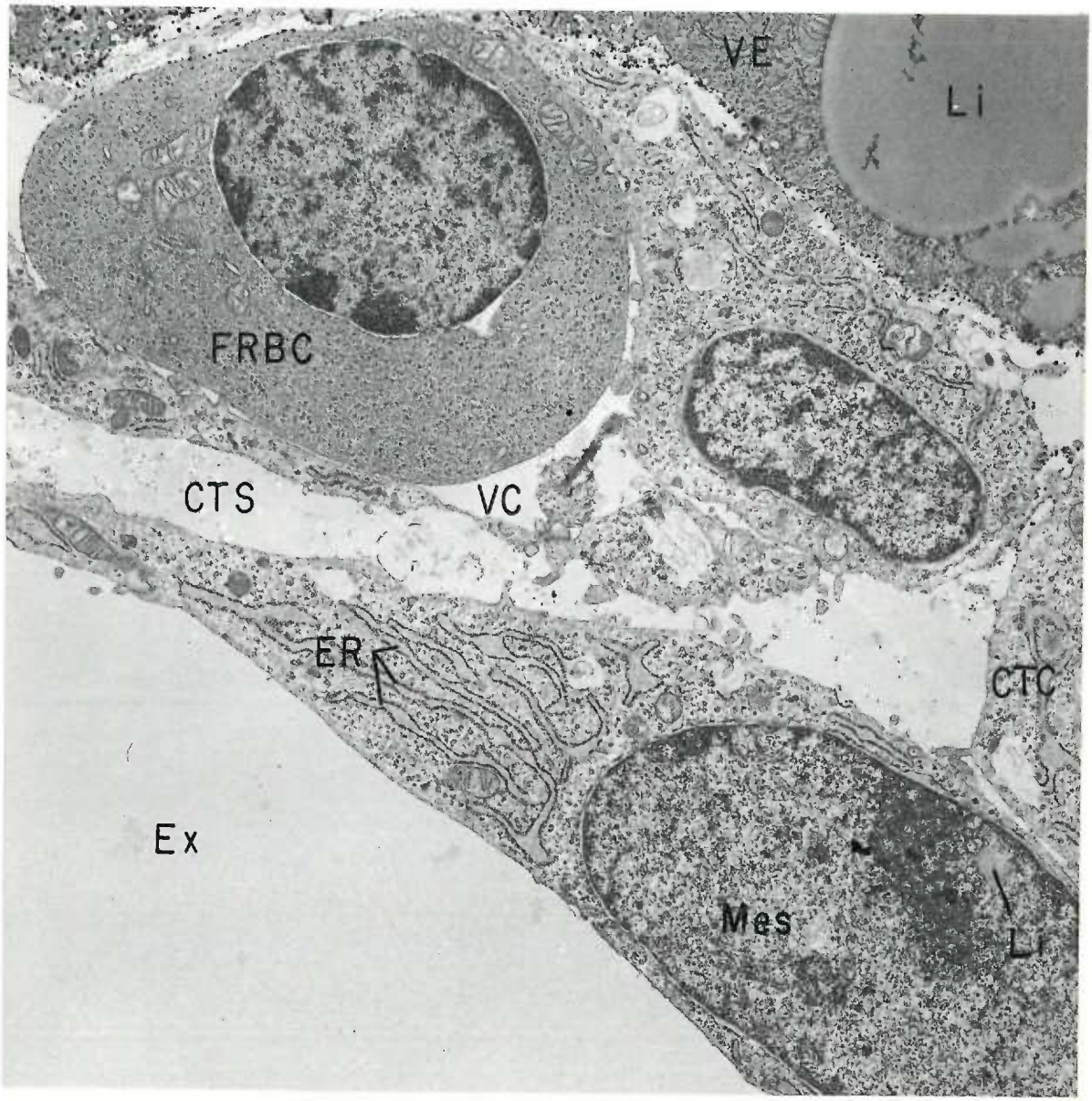

66

FIGURE 67

A portion of a 12 day visceral yolk sac incubated with ADP as substrate. Magnification 8,170 X. The connective tissue space (CTS) between the vitelline capillary (VC) and mesothelium (Mes) is occupied by a portion of a mesenchymal cell (CTC) and a loose network of collagen fibrils (Co). The capillary endothelium (En) is characterized by fenestrations (long arrows) and areas of extreme attenuation (short arrows). Note that at this stage the basal lamina of the serosal basement membrane (SBM) is poorly developed. Both the mesenchymal cell and mesothelium display a well developed cytoplasm.

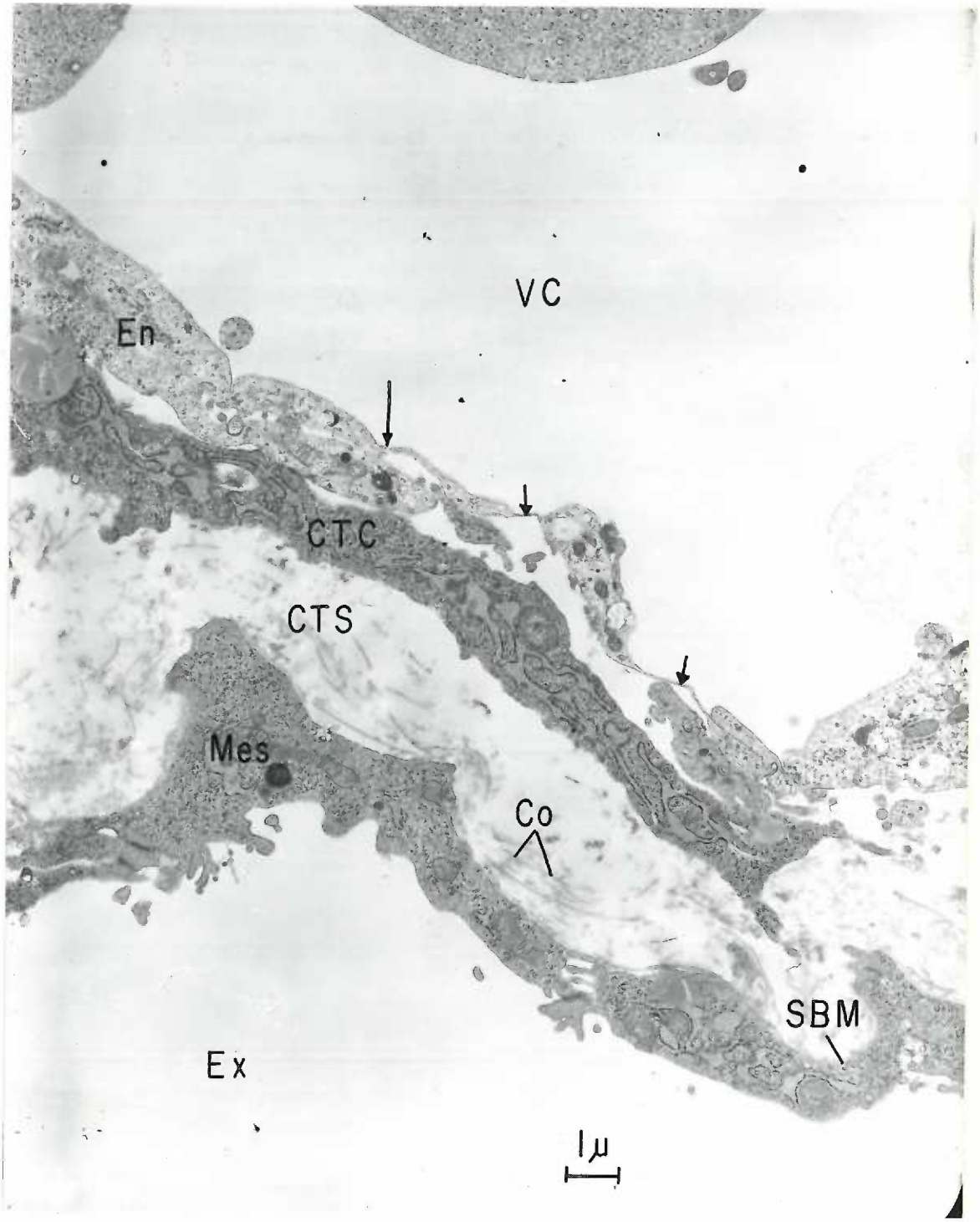
VC
En
CTC
CTS
Mes
Co
SBM
Ex
1μ

FIGURE 68

Cross section through the basal portion of several endodermal cells of a 12 day visceral yolk sac incubated with ATP as substrate. Magnification 7,800 X. Lipid (Li) is found in large droplets below the basally located polymorphic nucleus. The granular deposits of final reaction product which occur along the lateral surface membranes of the endodermal cells appear progressively smaller towards the visceral basement membrane. The endothelium (En) of a vitelline capillary (VC) lying directly below the visceral basement membrane is rich in cytoplasmic organelles.

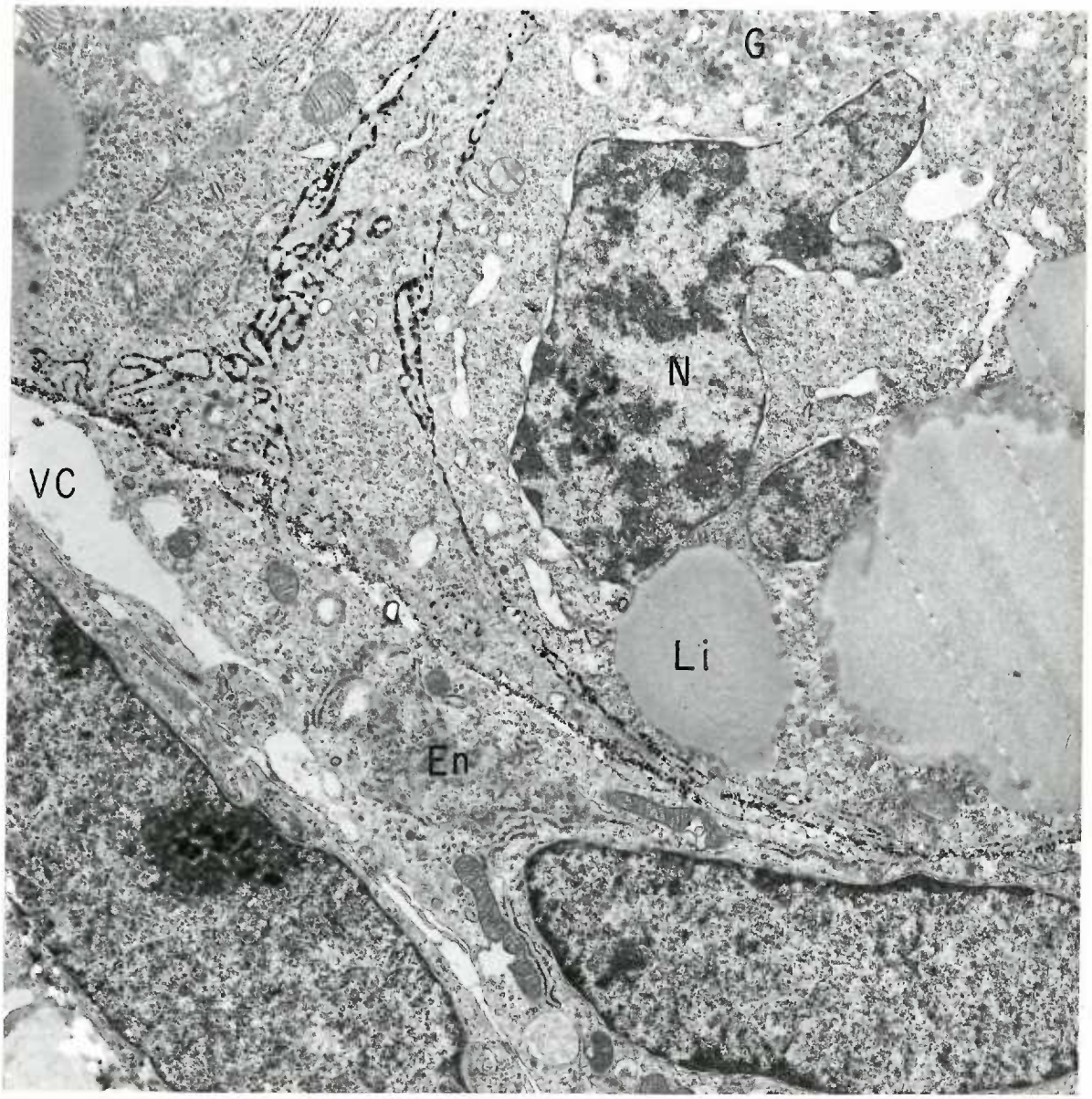

68

FIGURE 69

Basal portion of a 12 day visceral yolk sac incubated with ADP as substrate. Magnification 12,900 X. In this micrograph the dense zone of the basal lamina of the visceral basement membrane (VBM) is well developed and can be traced along the contour of the base of the endodermal cells. The basal lamina of the serosal basement membrane (SBM) is less well developed at this stage. The cisternae of the granular endoplasmic reticulum (ER) are greatly distended with a granular material of medium electron density. The free surface membrane of the mesothelium (Mes) is relatively free of surface evaginations except near junctions between adjoining cells. Evidence of enzymatic activity using ADP as substrate is completely absent.

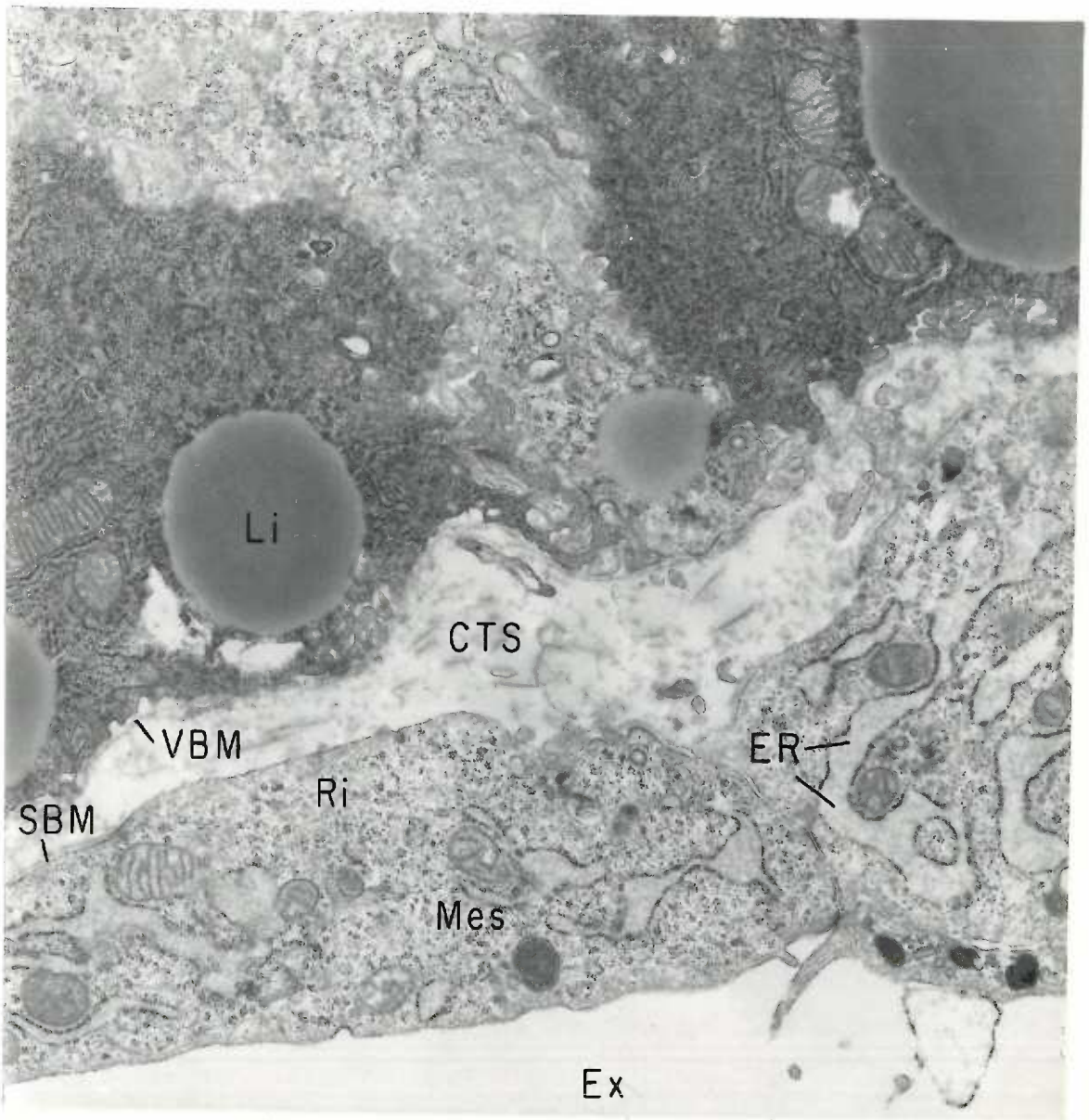

69

FIGURE 70

Basal portion of a 12 day visceral yolk sac incubated with ATP as substrate. Magnification 7,800 X. A process of a fetal mesenchymal cell (CTC) separates the attenuated capillary endothelium (arrows) from the mesothelium (Mes) lining the exocoelom (Ex). Fine granular deposits of final reaction product occur in the intercellular space between the two adjoining mesothelial cells. Note, particularly, the highly developed system of intercommunicating granular endoplasmic reticulum (ER) in both the mesenchymal and mesothelial cells.

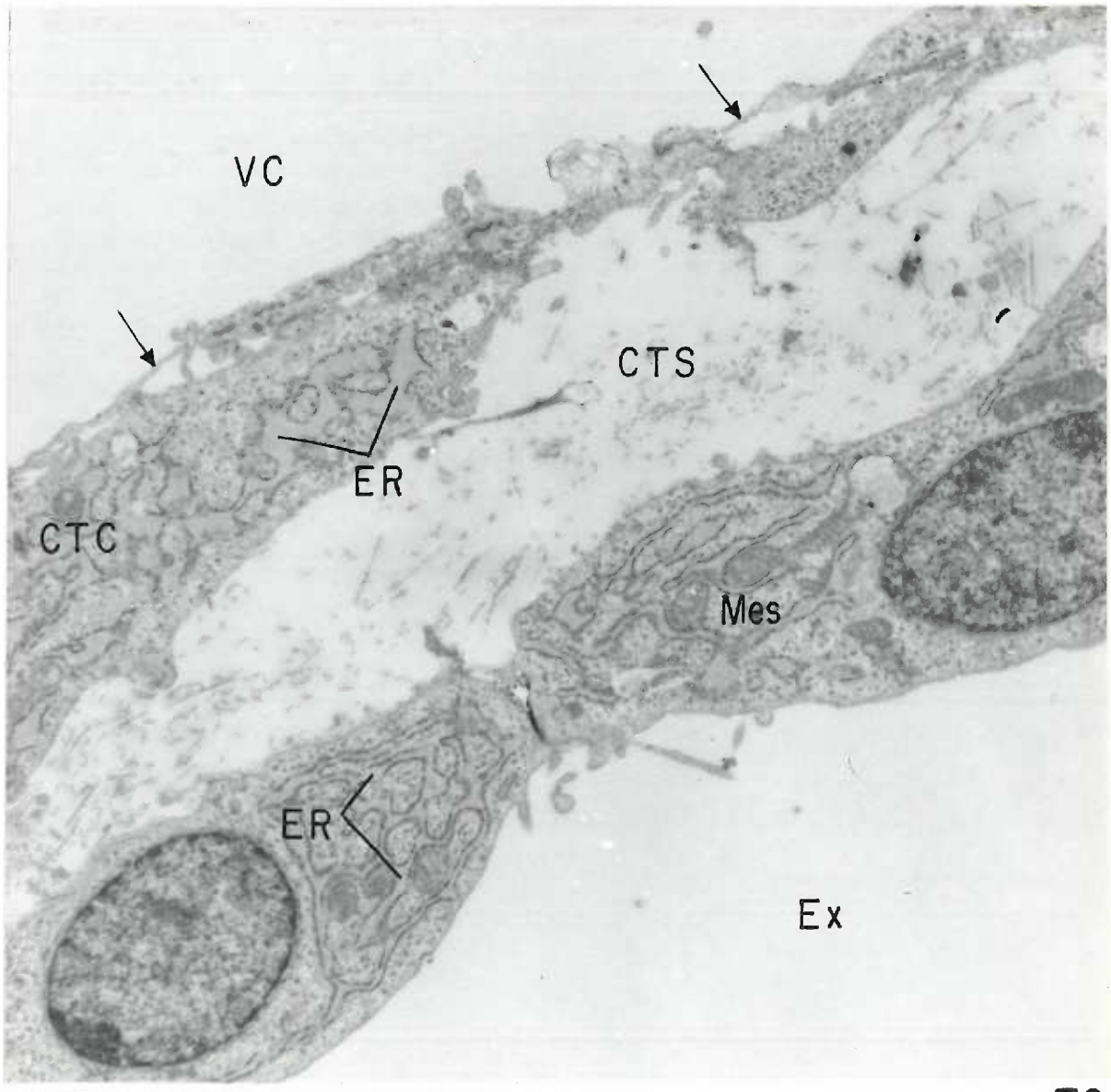

70

FIGURE 71

Apical portion of a 12 day visceral endodermal cell incubated with ADP as substrate. Magnification 12,900 X. Evidence of enzymatic activity with this substrate is absent. The free surface of this cell is formed by numerous irregular and branching microvilli. The surface plasma membrane is invaginated to form crypts or canaliculi (AC) which extend for various distances into the apical cytoplasm. These canaliculi are lined by a glycocalyx. The apical region also contains numerous small membrane bound vesicles (v) which show considerable heterogeneity in size (0.1-0.8 u) content and electron density. The moderately sized vesicles (asterisks) with an inner rim of fuzzy material and electron translucent centers represent cross sections or separated portions of the canalicular system, whereas the smaller vesicles may represent pinocytotic vesicles, golgi vesicles and/or lysosome-like bodies. In addition to the microvesicular profiles, the supranuclear cytoplasm contains large spherical vacuoles (V) of considerable heterogeneity. Some contain either a finely granular material or a floccular material (V 2). One of the latter appears to be merging with a large absorption vacuole which characteristically contains clusters of small lipid droplets.

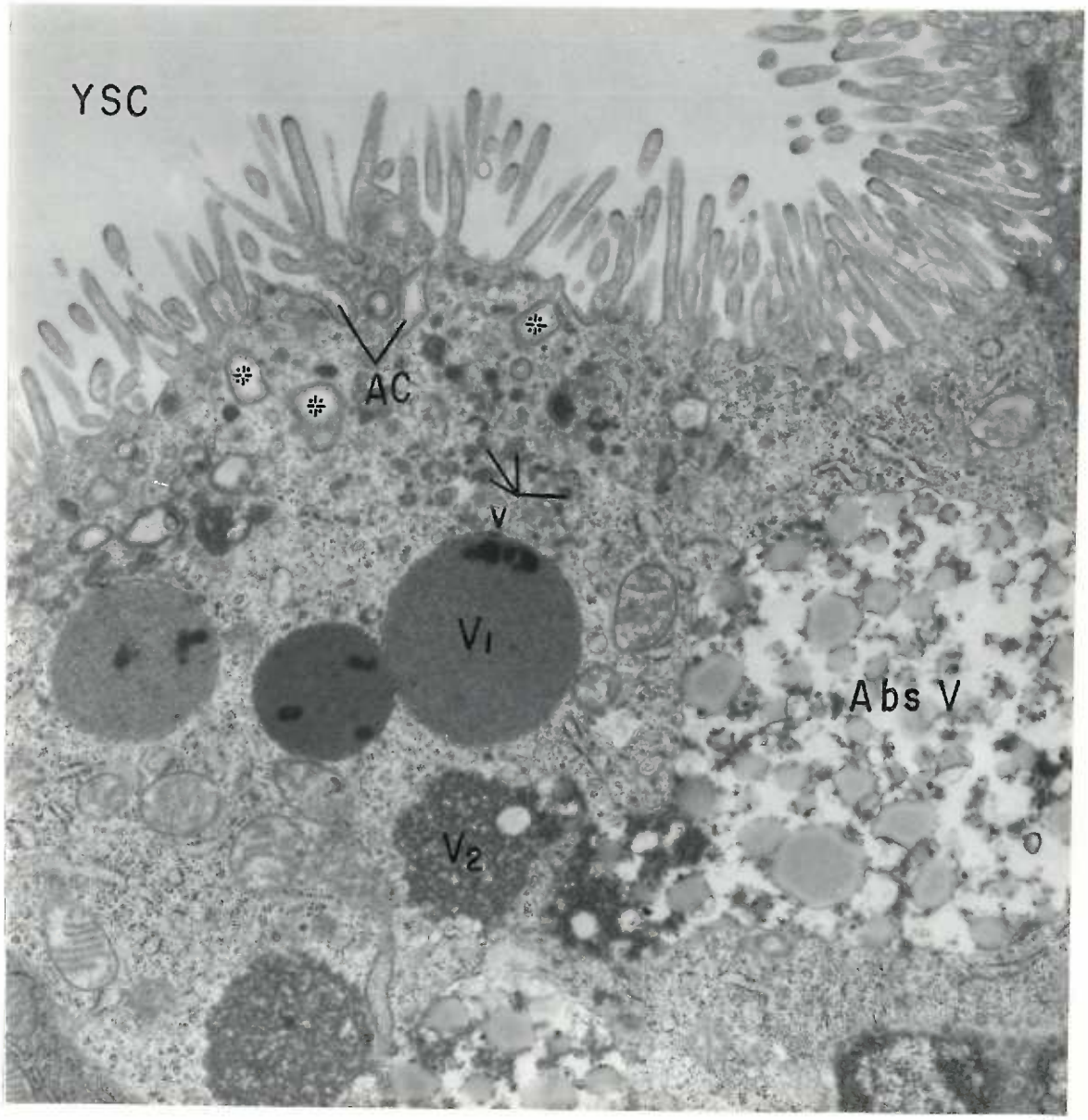

71

FIGURE 72

ATPase preparation showing the apical portion of two 12 day visceral endodermal cells. Magnification 12,900 X. Final reaction product is deposited as dense beads along the outer surface membrane of the microvilli and in the intercellular space along the lateral surface membranes. Note that globular deposits of lead phosphate are heaviest between the bases of microvilli where the plasma membrane is invaginated to form crypts or canaliculi (AC). No reaction product is seen in the intercellular space where the lateral cell membranes form a tight junction. Many of the vesicles in the apical cytoplasm show final product related to the inner surface of their limiting membrane and/or to their contents (long arrows). Such a vesicle (short arrows) appears to be merging with a large absorption vacuole (Abs V).

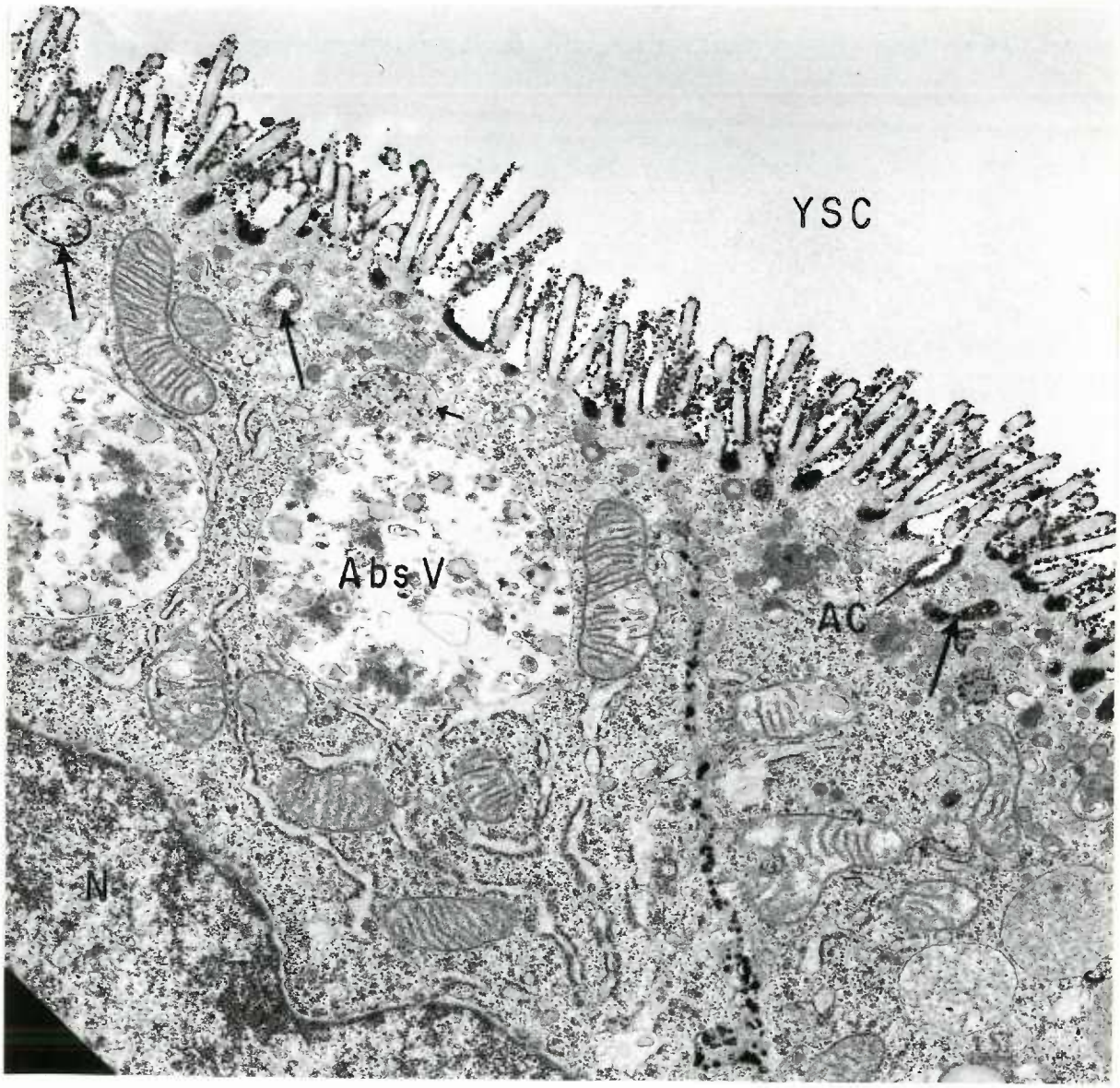

72

FIGURE 73

Apical portion of several 12 day visceral endodermal cells fixed in cacodylate buffered osmium tetroxide. Magnification 18,600 X. The microvilli projecting from the free surface of the endodermal cells are irregularly oriented and frequently have globular expanded tips which appear to be released into the yolk sac cavity (asterisk). Straight filaments run longitudinally in the interior of the microvilli and extend downward into the apical cytoplasm where they join fine filaments comprising the terminal web (TW). The plasmalemma of the microvilli exhibits a fuzzy extraneous surface coating (glycocalyx) which is also seen lining the inner surface of canalicular surface invaginations (long arrows) and smaller pinocytotic vesicles (short arrows).

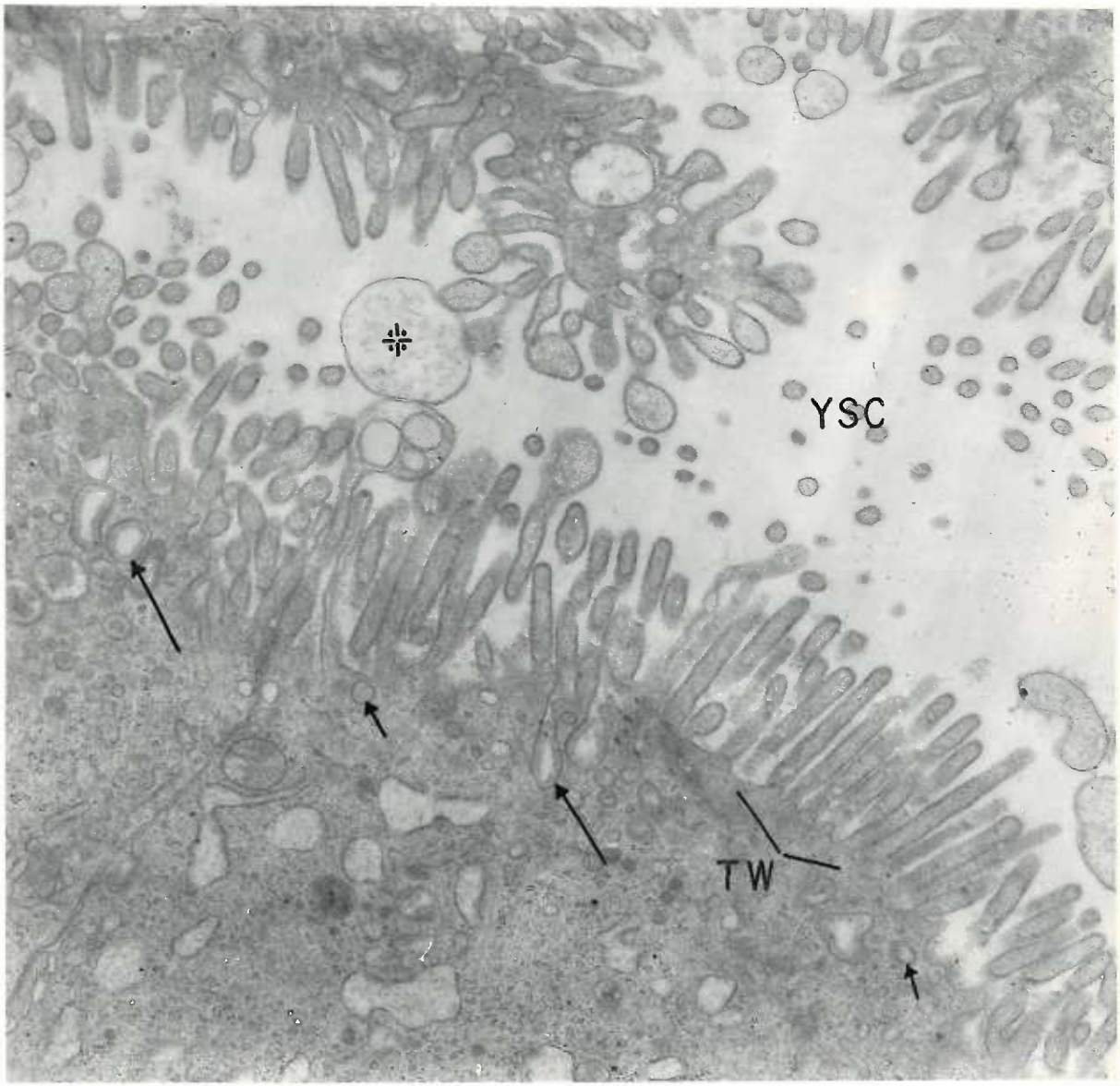

73

FIGURE 74

Apical portion of several 12 day visceral endodermal cells incubated with ADP. Magnification 12,900 X. As in Figure 71, evidence of enzymatic activity with this substrate is absent. The endodermal cells are held together at their apices by tight junctions (TJ) and along their lateral margins by small desmosomes (Des). Dense microvesicular profiles (v), vacuoles (V) with varying content and apical canals (AC) with a characteristic dense fibrous material on their luminal surface are evident. Note that several vacuoles (arrows) at the bottom of the figure contain small lipid droplets and clumps of granular material enclosed by a loose fitting and irregular membrane.

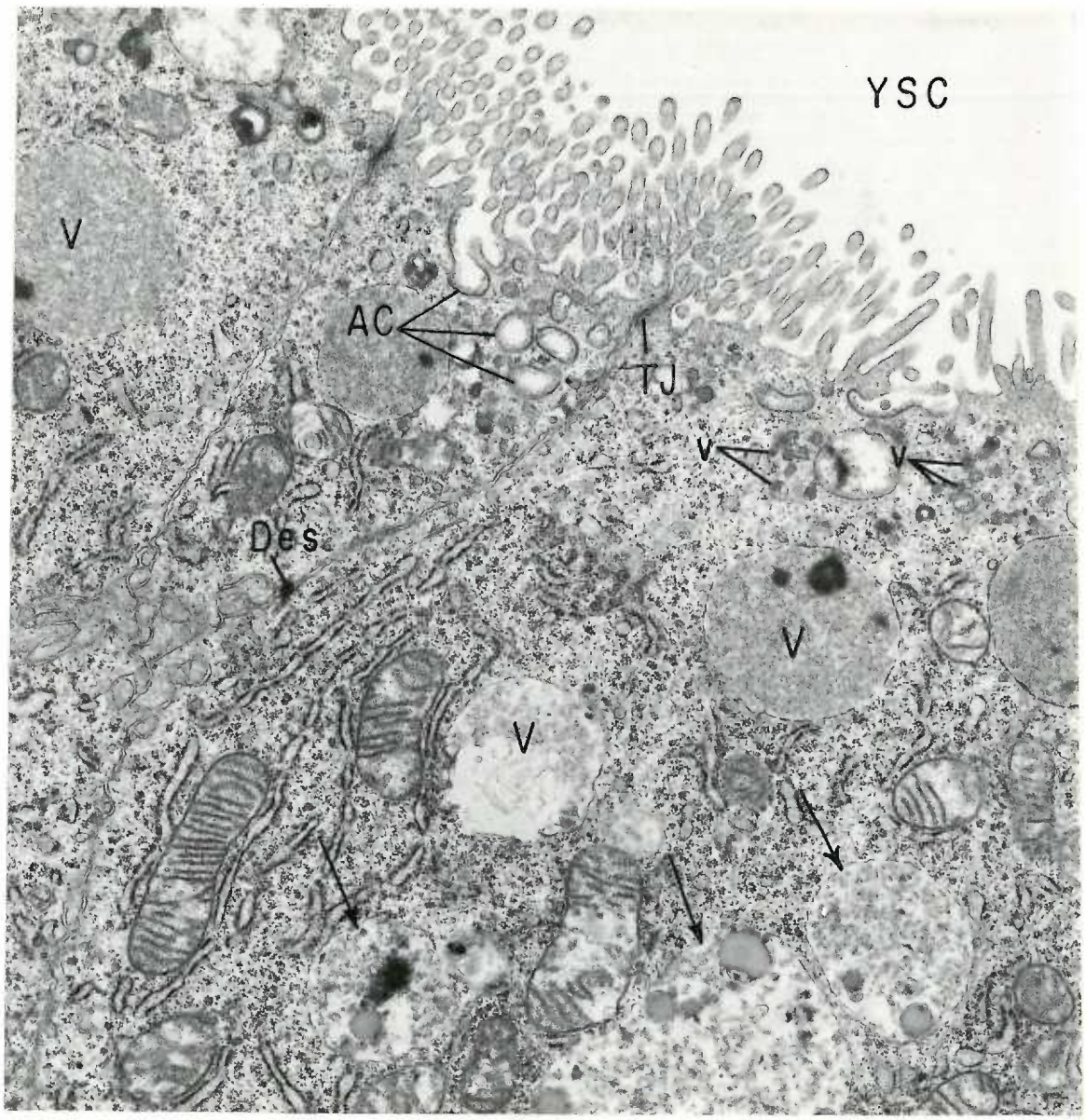

74

FIGURE 75

Apical portion of the 12 day visceral yolk sac incubated with ATP as substrate. Magnification 12,900 X. Final reaction product is distributed as described in Figure 72. Note the large degenerating mitochondrion (Mi) in the left endodermal cell.

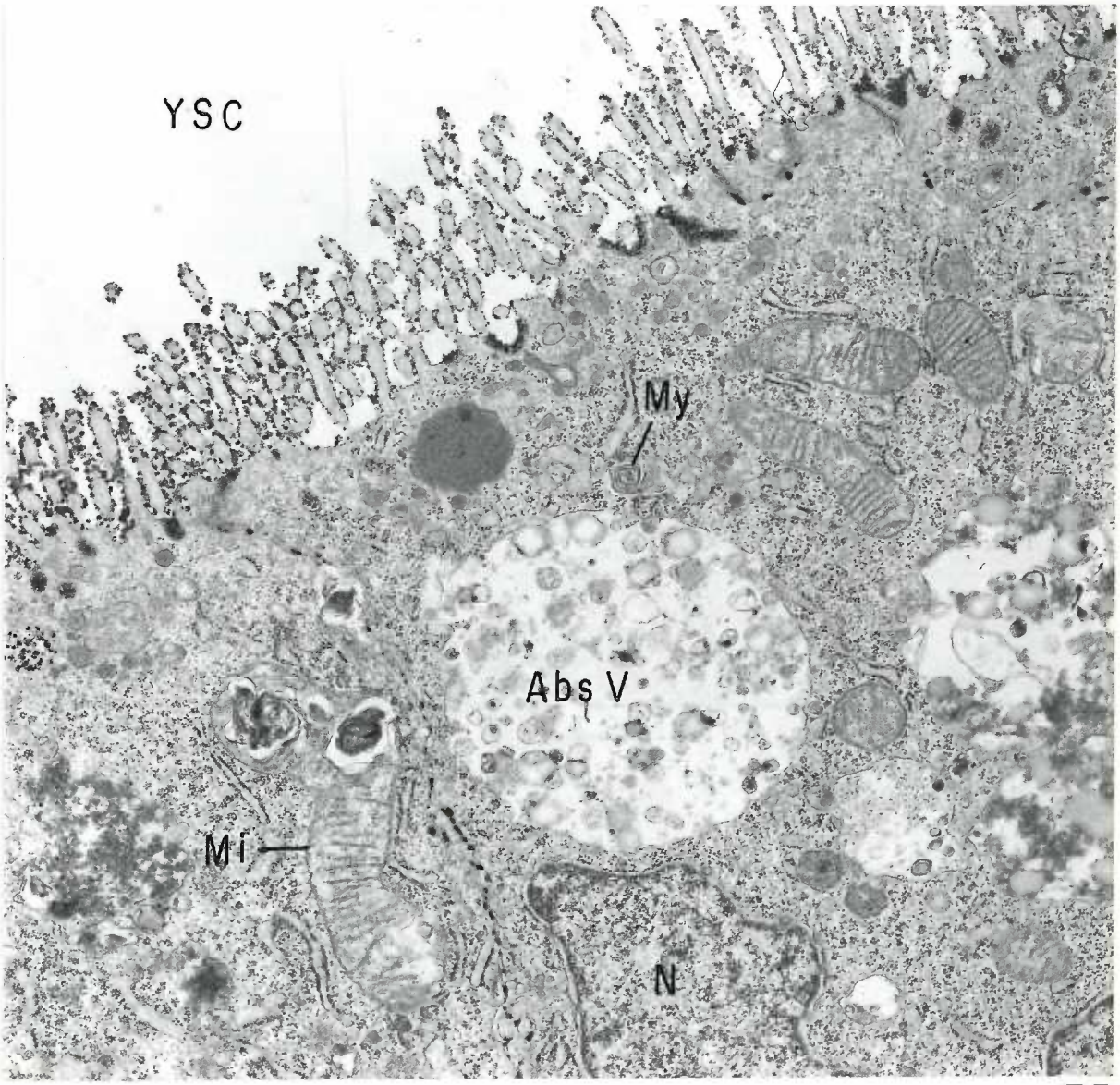

75

FIGURE 76

Detail of the cytoplasm of several 12 day visceral endodermal cells incubated with ATP as substrate. Magnification 12,900 X. Final reaction product is distributed as described in Figure 72. Two microvesicular profiles in the apical cytoplasm of the left endodermal cell appear to be coalescing with a moderately sized vacuole (arrow). The supranuclear cytoplasm contains large vacuoles (V) which are suggestive of successive stages in either the breakdown or synthesis of some material and/or in the formation of large absorption vacuoles (Abs V).

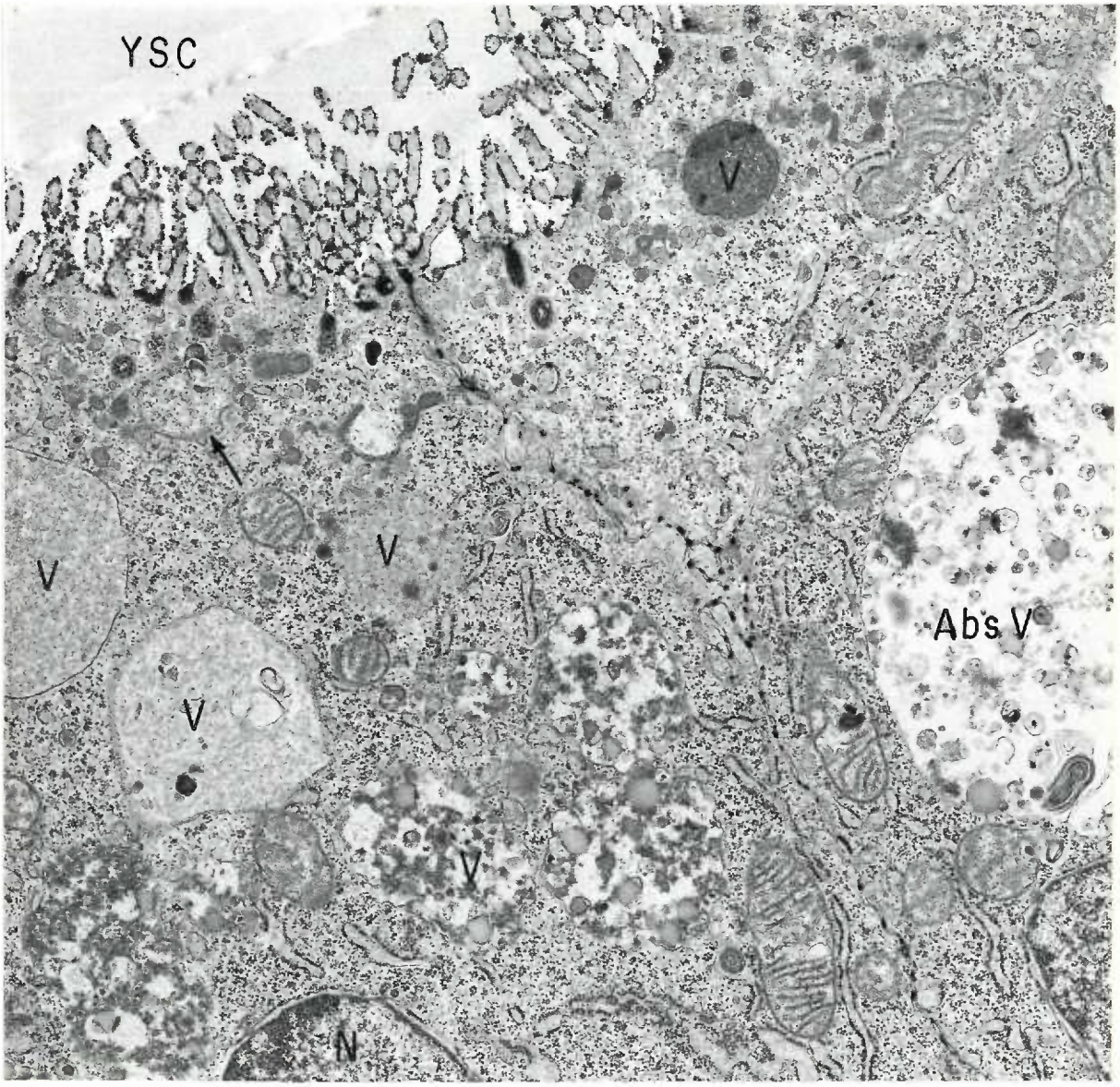

76

FIGURE 77

Section through the apex of two 12 day visceral endodermal cells reacted for ATPase. Magnification 12,900 X. As in Figure 72, final reaction product occurs as beaded deposits at the luminal surface of the visceral epithelium and fills the intercellular space between the two apposing lateral plasma membranes in an interrupted fashion. In addition to vesicles (v), vacuoles (V) and mitochondria, the cytoplasm is richly provided with rosettes of polyribosomes (Ri).

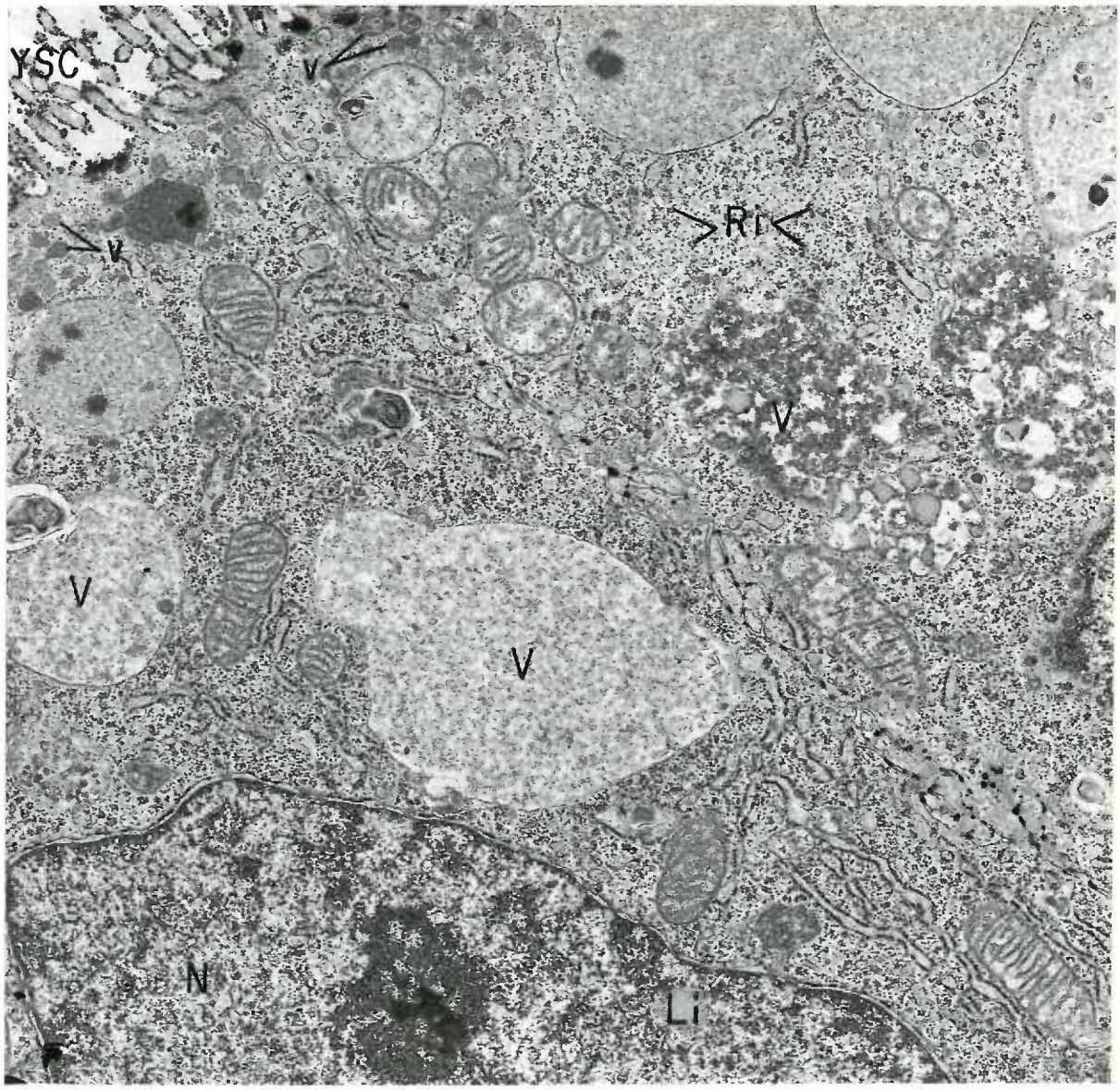

77

FIGURE 78

Supranuclear portion of two 12 day endodermal cells incubated with ATP as substrate. Magnification 12,900 X. In addition to lipid clusters (Li) and coarse granular material, the large absorption vacuole (Abs V) in the right hand endodermal cell contains a myelin figure (My), circular profiles (CP) and open areas which are electron transparent. The perinuclear cisterna of the nucleus on the right is traversed at irregular intervals by nuclear pores which in tangential sections, such as that shown in the left hand nucleus, appear as circular openings (arrows).

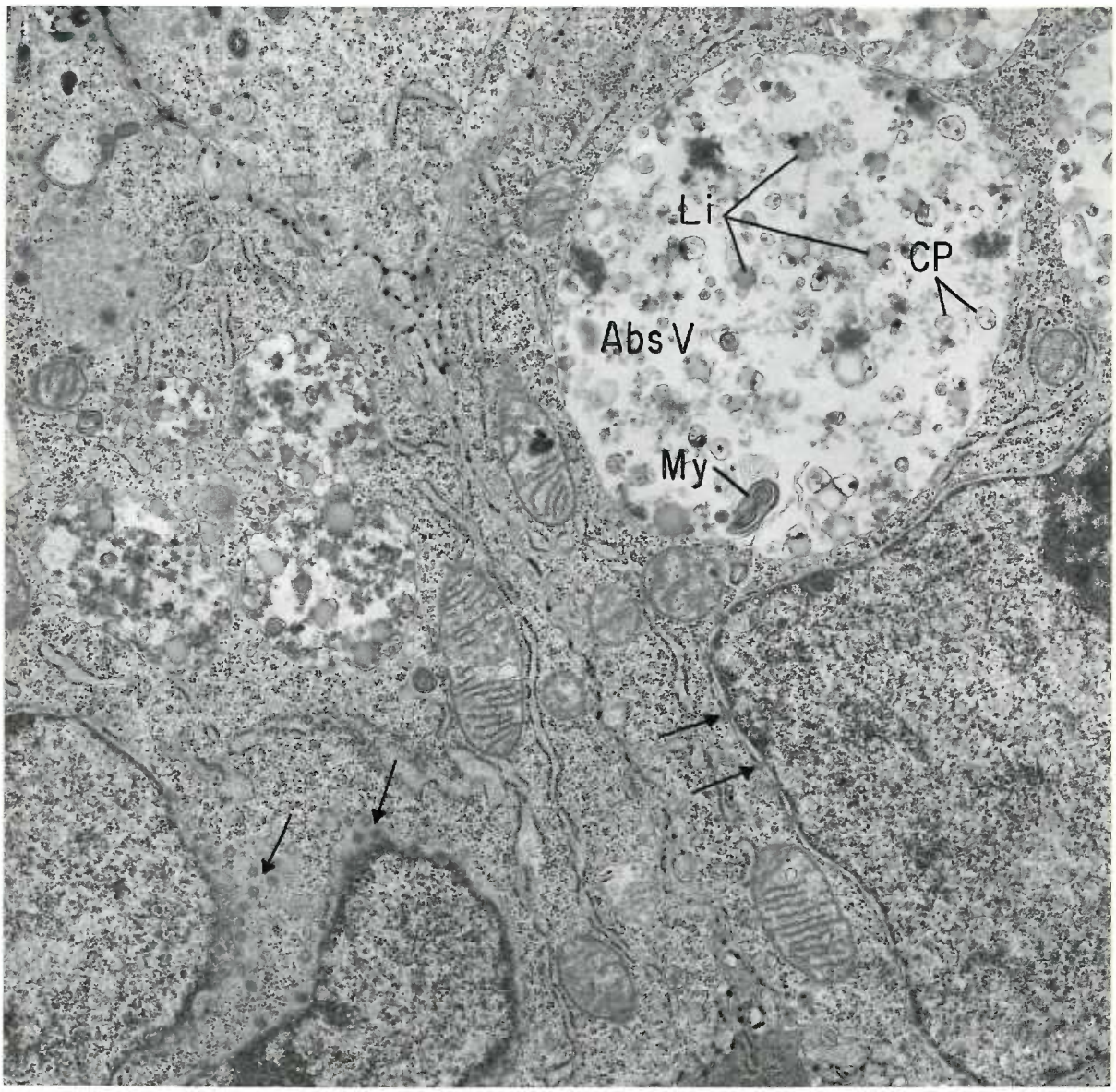

78

FIGURE 79

Supranuclear portion of two 12 day visceral endodermal cells reacted for ATPase. Magnification 12,900 X. Final reaction product is deposited as described in Figure 77. Golgi-like microvesicular profiles (G) are evident in the perinuclear cytoplasm.

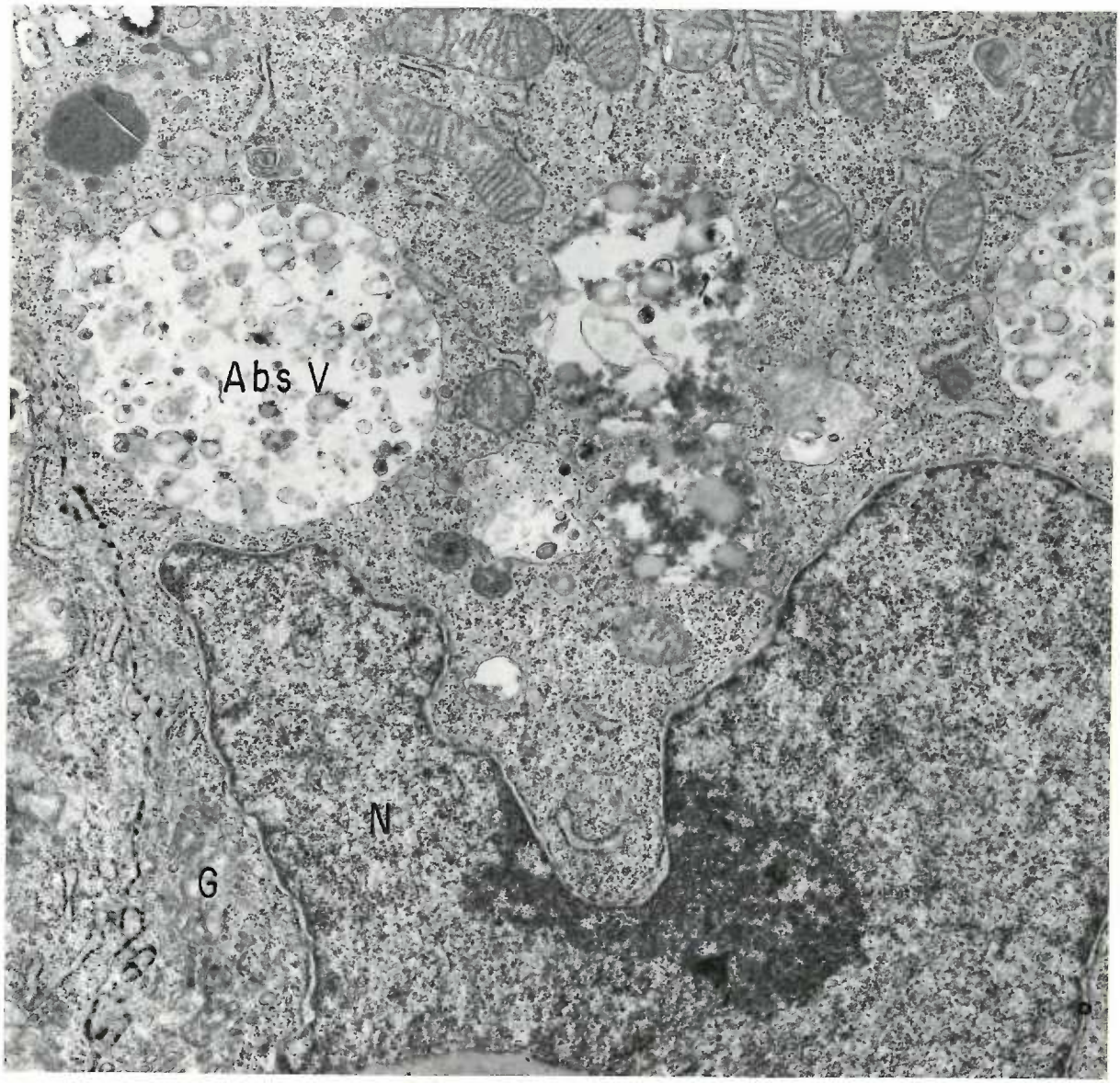

79

FIGURE 80

Basal surface of a 12 day visceral yolk sac incubated with ATP as substrate. Magnification 8,170 X. Final reaction product is present throughout the intercellular spaces as discrete deposits and in the visceral basement membrane and connective tissue space (CTS) as fine precipitates. A rather large homogeneous lipid droplet (Li) is seen in close association with the concave basal surface of a nucleus (N) which itself displays a small lipid inclusion.

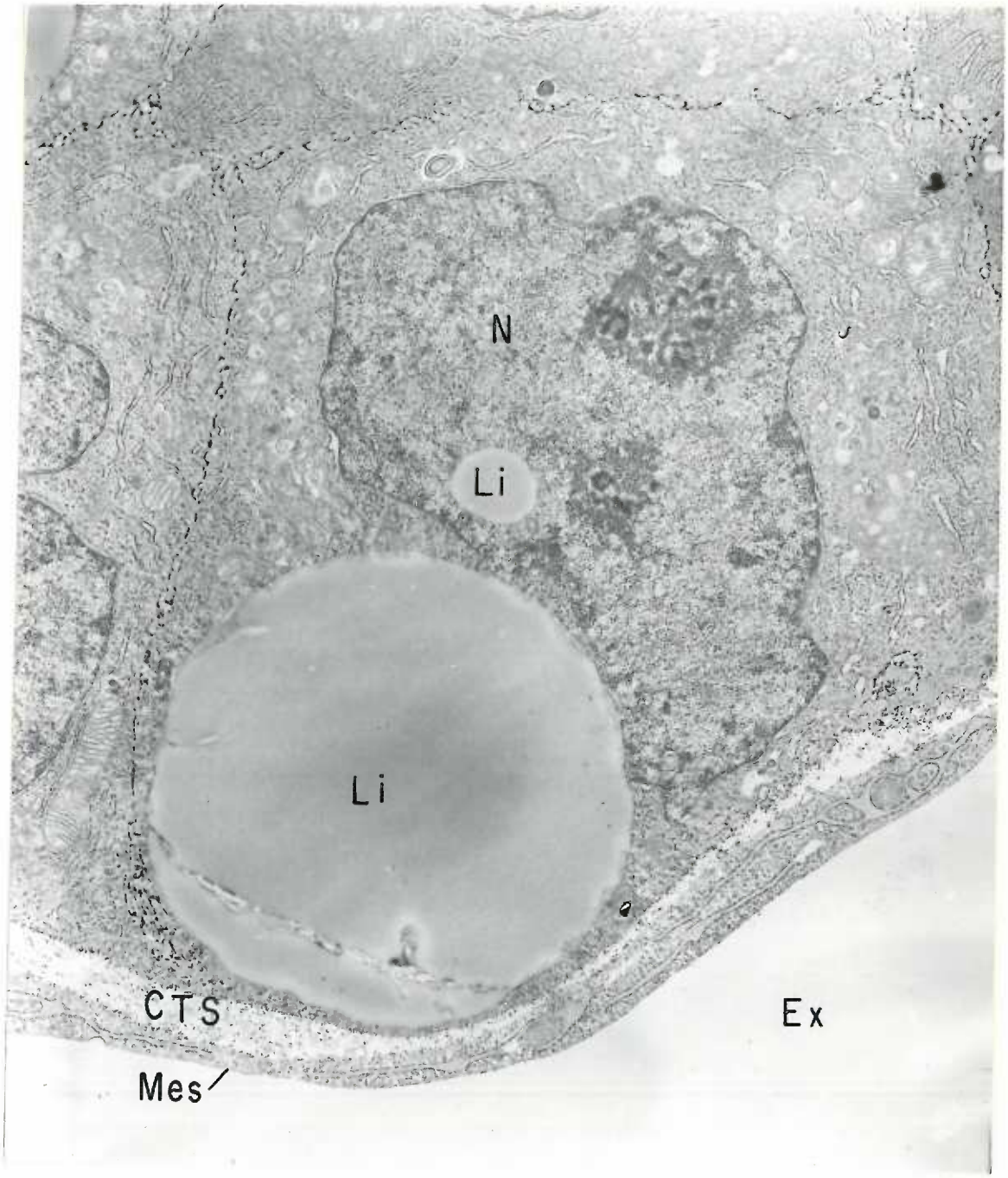

80

FIGURE 81

Basal portion of the 12 day visceral endoderm incubated with ATP. Magnification 12,900 X. Enzyme activity with this substrate appears to be entirely absent at this stage. Active pinocytosis (PV) is seen on the basal surface of the endoderm. Note the intense reduction of osmium at several points along the interface between the lipid droplets (Li) and the surrounding cytoplasm. Also note the close association of polyribosomes with the surface of the lipid droplets.

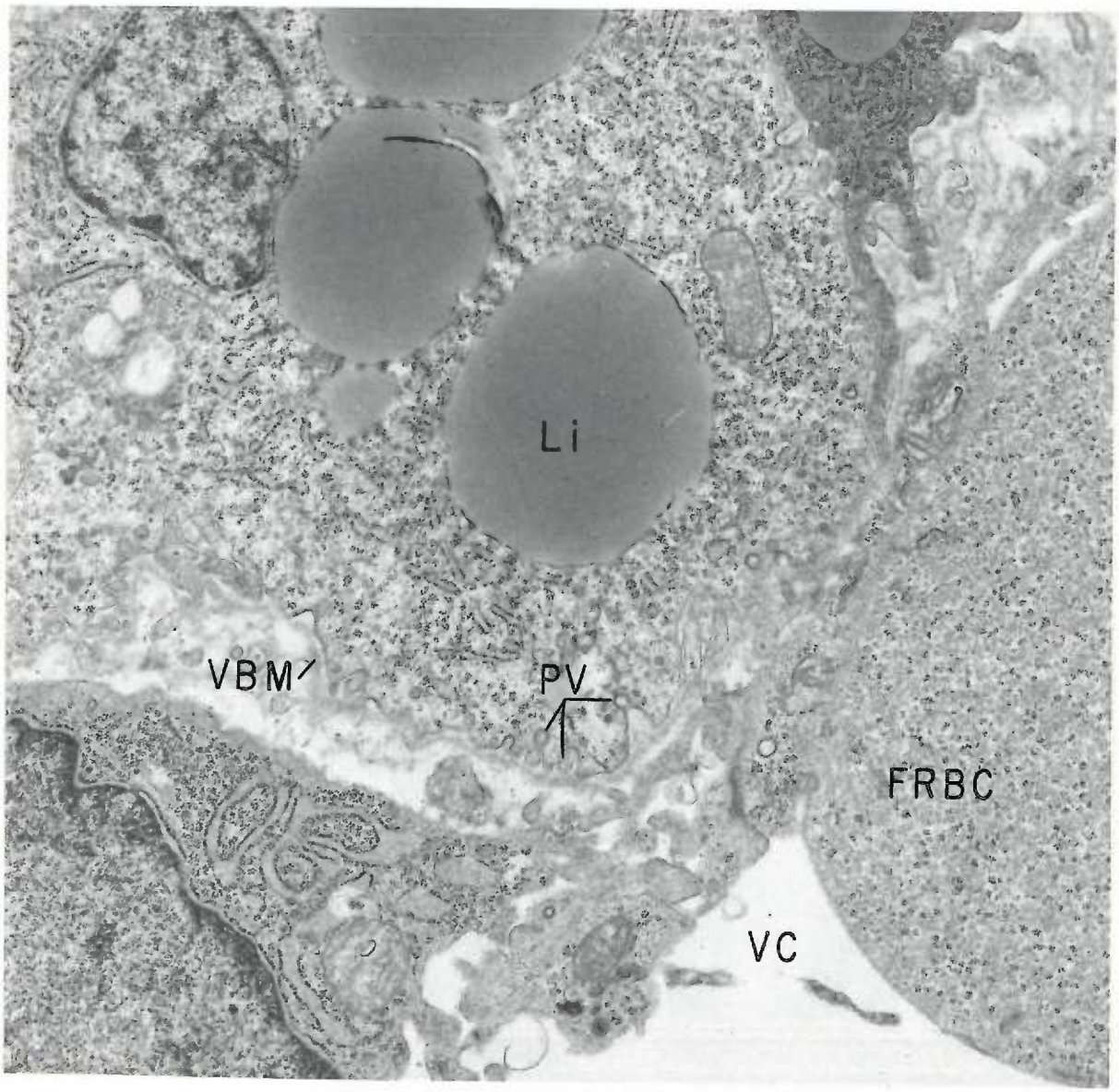

81

FIGURE 82

General view of the 14 day visceral yolk sac incubated with ATP as substrate. Magnification 2,603 X. This tangential section through the visceral endoderm illustrates the disposition of cytoplasmic organelles and inclusions. Final reaction product is deposited as dense precipitates which exactly outline the lateral margins as well as the apical brush border of the visceral endodermal cells. Finer deposits of final product outline the visceral basement membrane which separates the endodermal cells from the underlying connective tissue cells (CTC) and collagen fibrils (Co). A portion of a vitelline capillary (VC) is seen in the lower left hand corner of the connective tissue space (CTS).

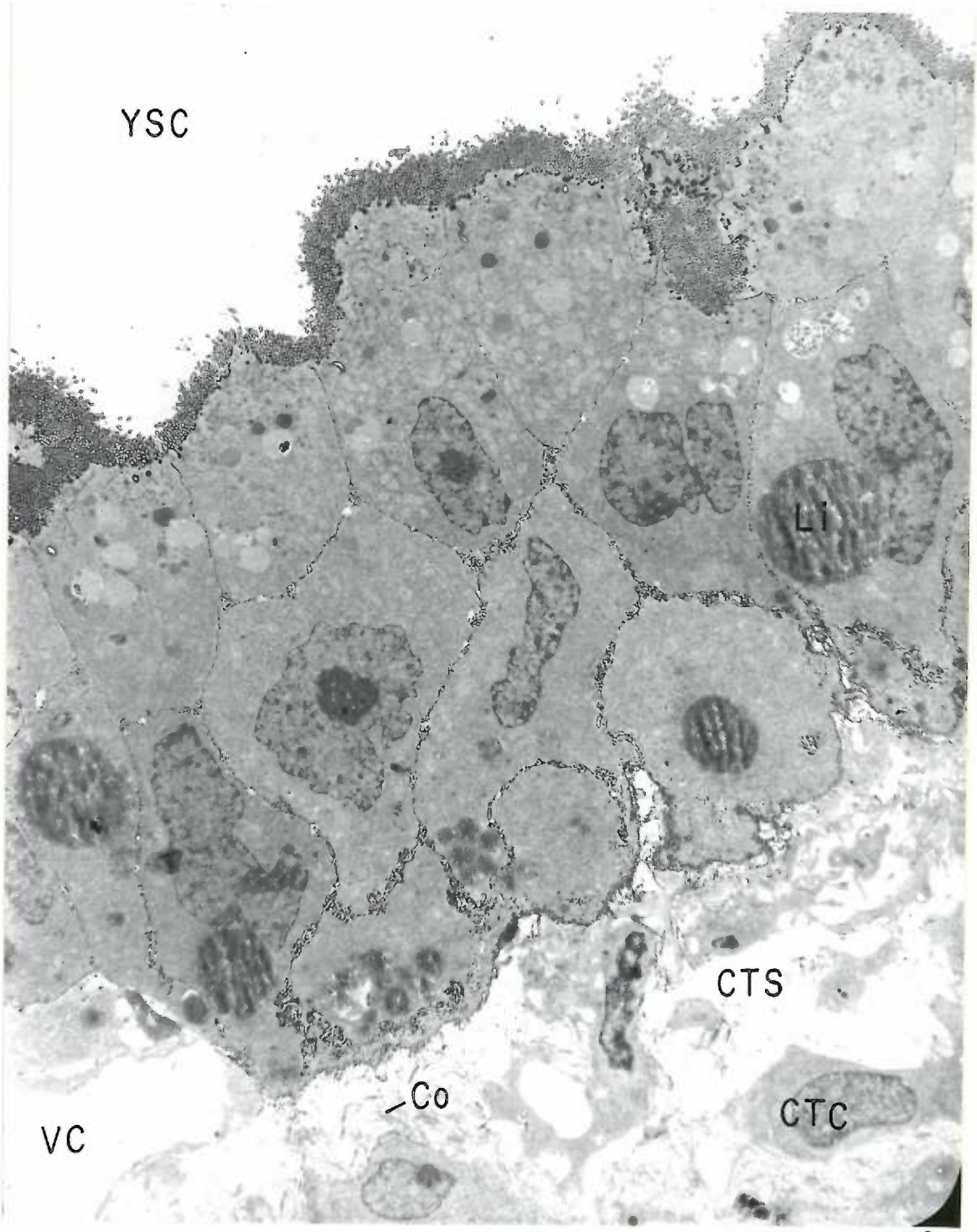

82

FIGURE 83

Apical portion of several 14 day visceral endodermal cells incubated with ATP as substrate. Magnification 18,600 X. Final reaction product is deposited primarily as a confluent dense precipitate at the surface of microvilli (Mv). Between adjoining endodermal cells proximal to the apical junctional complex (TB), deposits are punctate and interrupted. Final product is also seen in the apical cytoplasm where it occurs in relation to the inner surface or contents of canaliculi (short arrows). Numerous vesicles (v) and vacuoles (V) containing dense granular material are apparent. One of the larger vacuoles (long arrow) situated below the brush border has final product distributed through its granular contents.

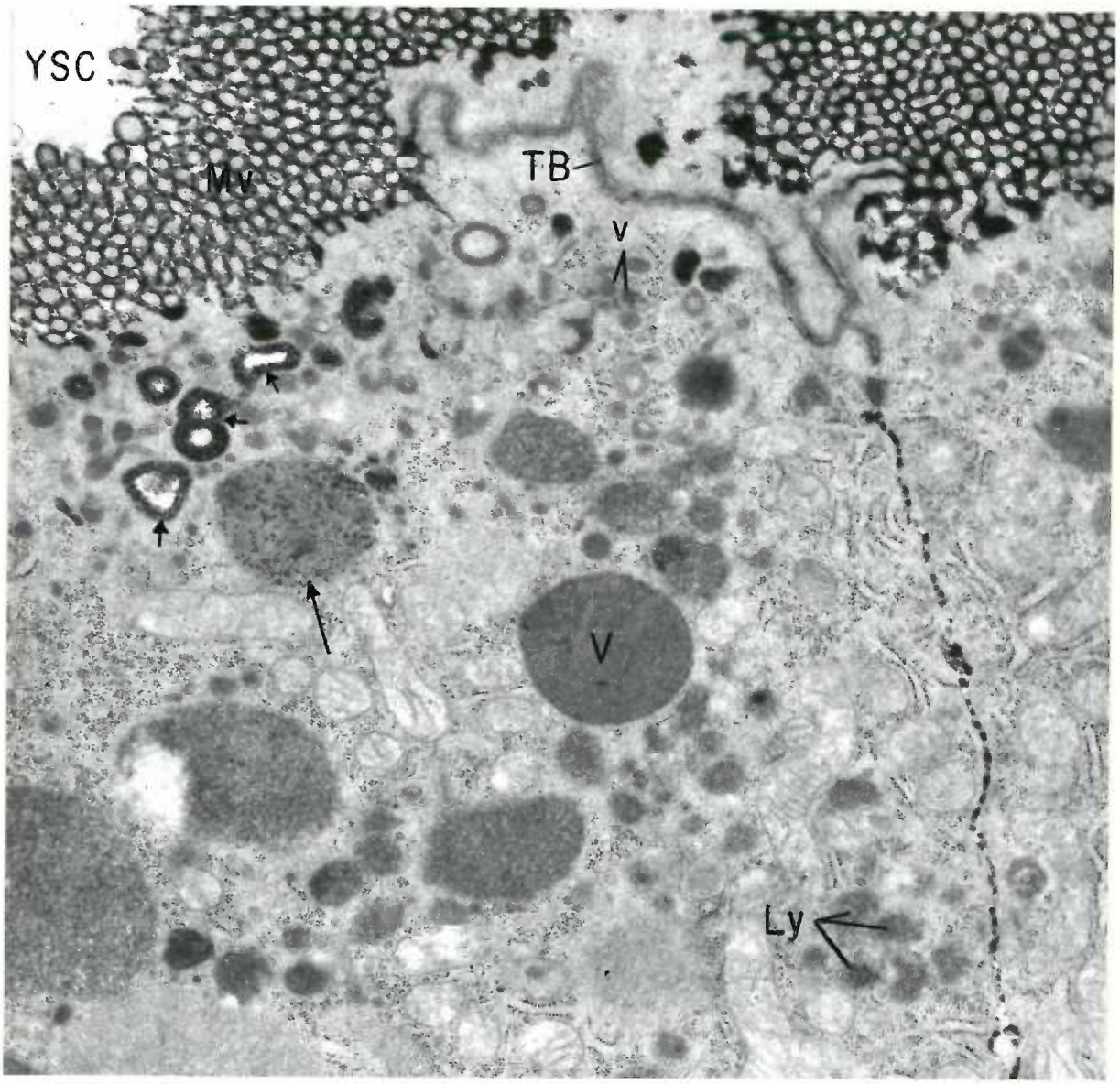

83

FIGURE 84

Oblique section through the apical portion of 14 day visceral endodermal cells incubated with ATP as substrate. Magnification 18,600 X. Globular deposits of final reaction product appear most dense on the apical surface membrane and in the invaginations between adjacent microvilli. Note the excessive breadth of the terminal web (TW) which appears continuous with the terminal bar (TB) formations seen in the upper left and lower right margins of the figure. In the terminal web and the subjacent cytoplasm are numerous small membrane bound vesicles (v) and tubules (AC) which contain electron dense material indistinguishable from final reaction product. These structures are interpreted as either pinocytotic vesicles or portions of the apical canalicular system.

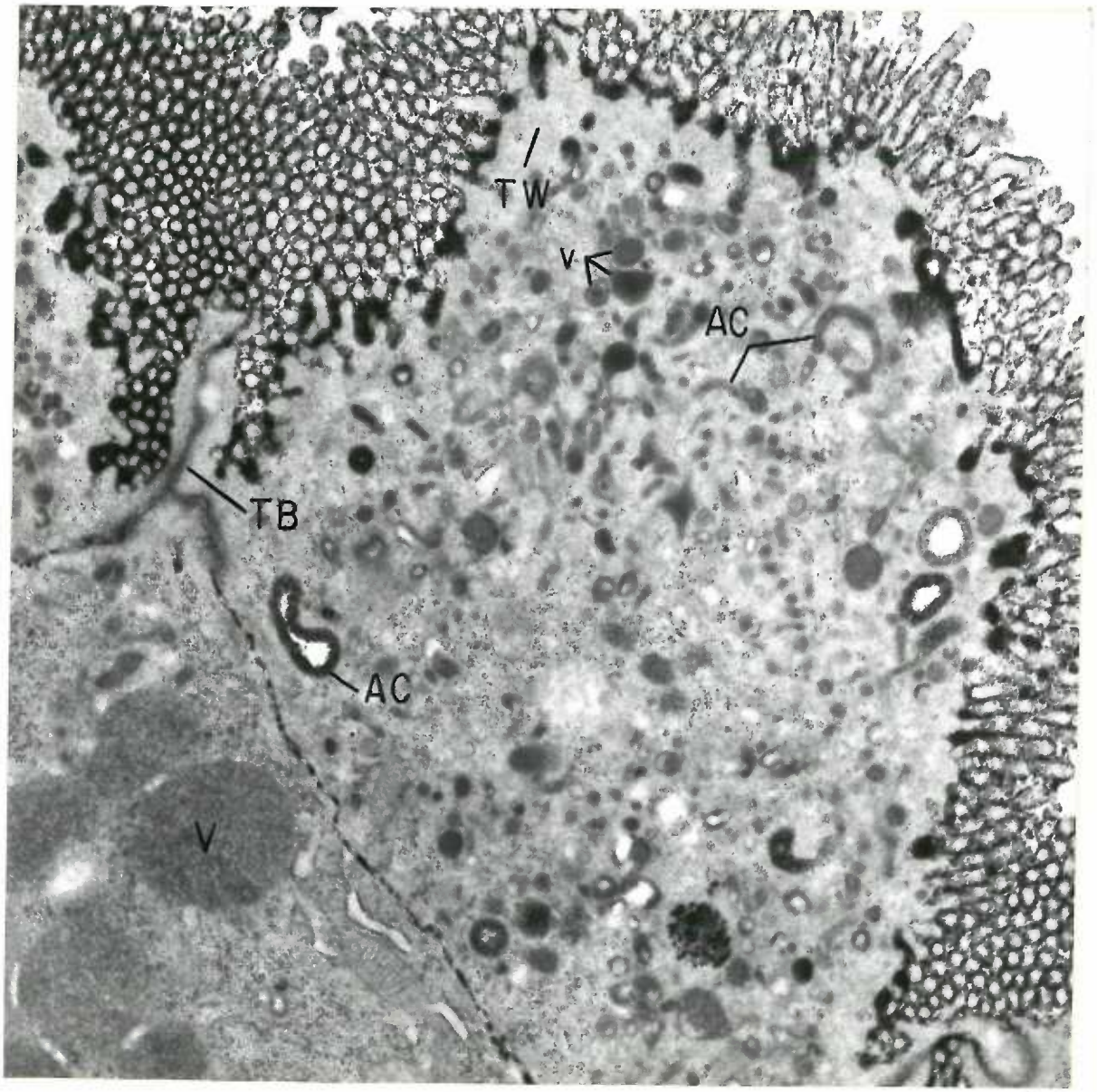

84

FIGURE 85

Oblique section through a group of 14 day visceral endodermal cells incubated with ATP as substrate. Magnification 11,780 X. Note that not all of the apical canaliculi (AC) in the upper right corner of the figure show final reaction product. This may indicate that such canals are no longer continuous with the cell surface.

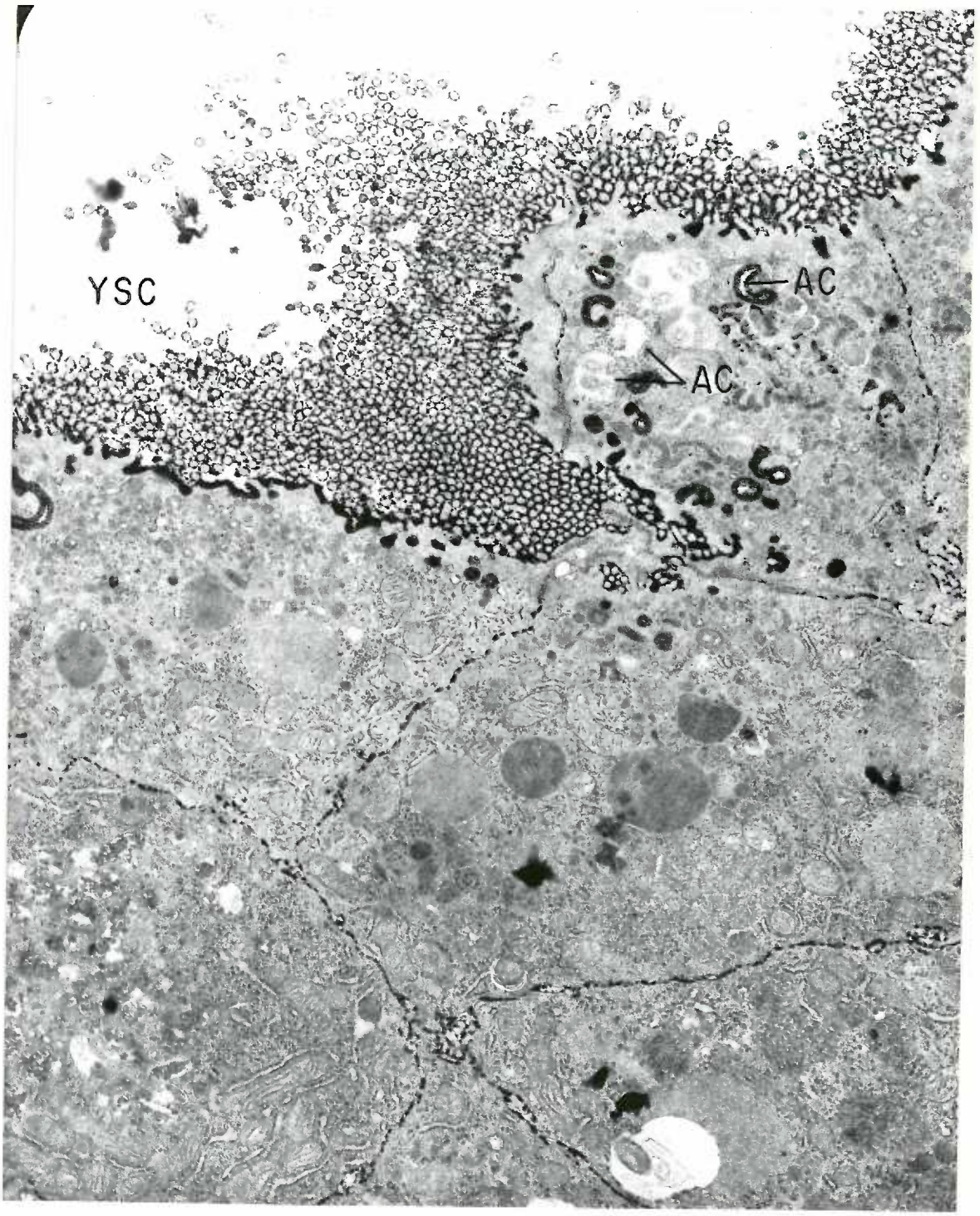

85

FIGURE 86

Tangential section through the 14 day visceral yolk sac endoderm displaying the regional contents of the cytoplasm as well as the distribution of final reaction product resulting from the enzymatic hydrolysis of ATP. Magnification 11,780 X. The perinuclear region is characterized by cisternal profiles of granular reticulum between which are dispersed numerous mitochondria (Mi) and polysomes (Ri). In addition to these organelles, the supranuclear cytoplasm contains vesicles (v) and vacuoles (V) of varying granular content. The denser vesicles are lysosomal-like bodies. The apical cytoplasm as seen in the endodermal cell on the middle-right side of the figure is predominated by microvesicular and tubular profiles of the canalicular system (AC). The distribution of final reaction product is the same as described in Figures 82, 83 and 85.

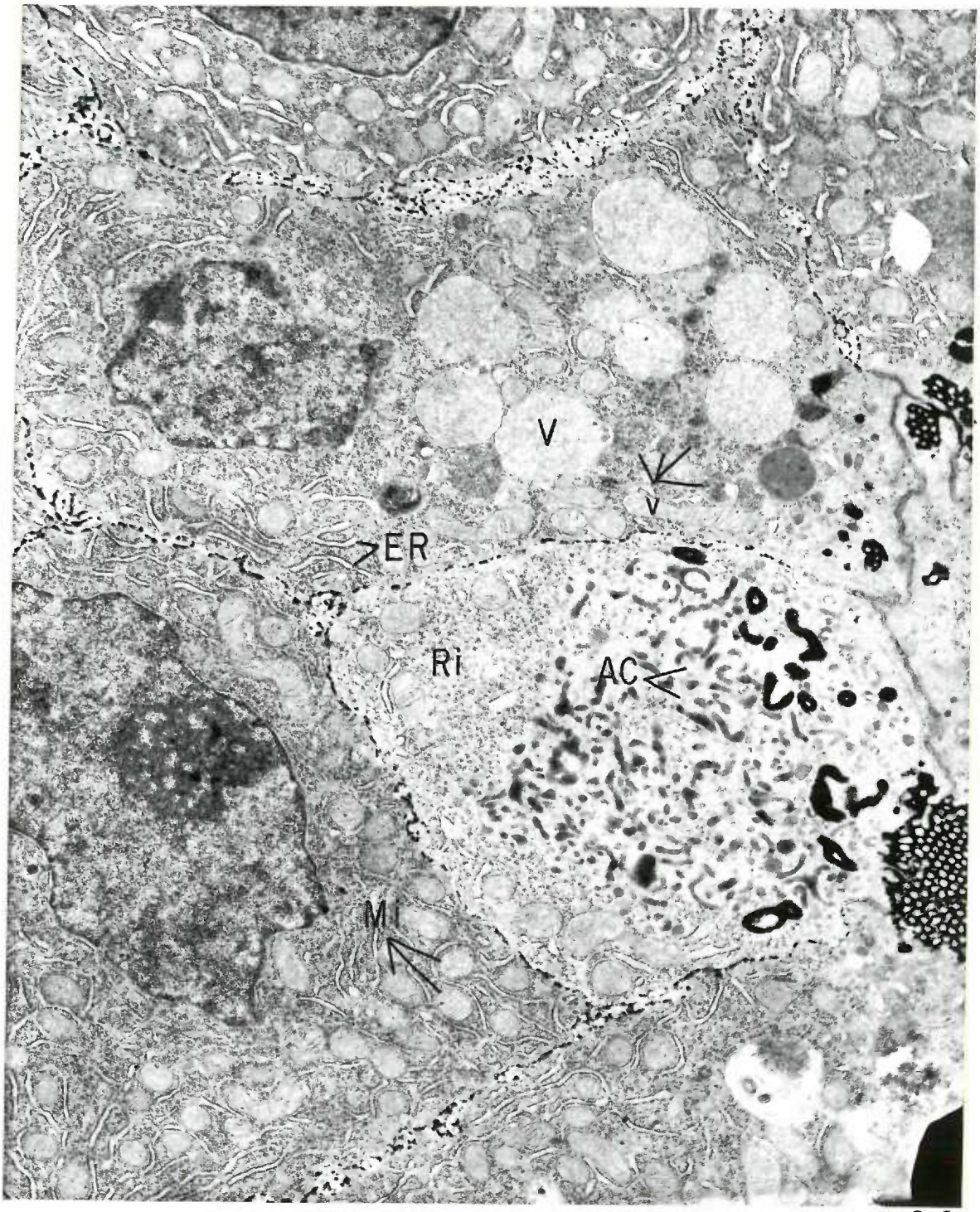
V
v
ER
Ri
AC
Mi

FIGURE 87

A cross section through the supranuclear cytoplasm of three 14 day visceral endodermal cells incubated with ATP as substrate. Magnification 18,600 X. In addition to a heterogeneous population of vacuoles (V) and vesicles (v), the supranuclear cytoplasm also displays an abundance of polysomes, granular reticulum and oval and elongated mitochondria. The electron transparent vacuoles (asterisk), which occasionally contain membranous profiles observed in this photomicrograph, are interpreted as artifacts produced during fixation or incubation.

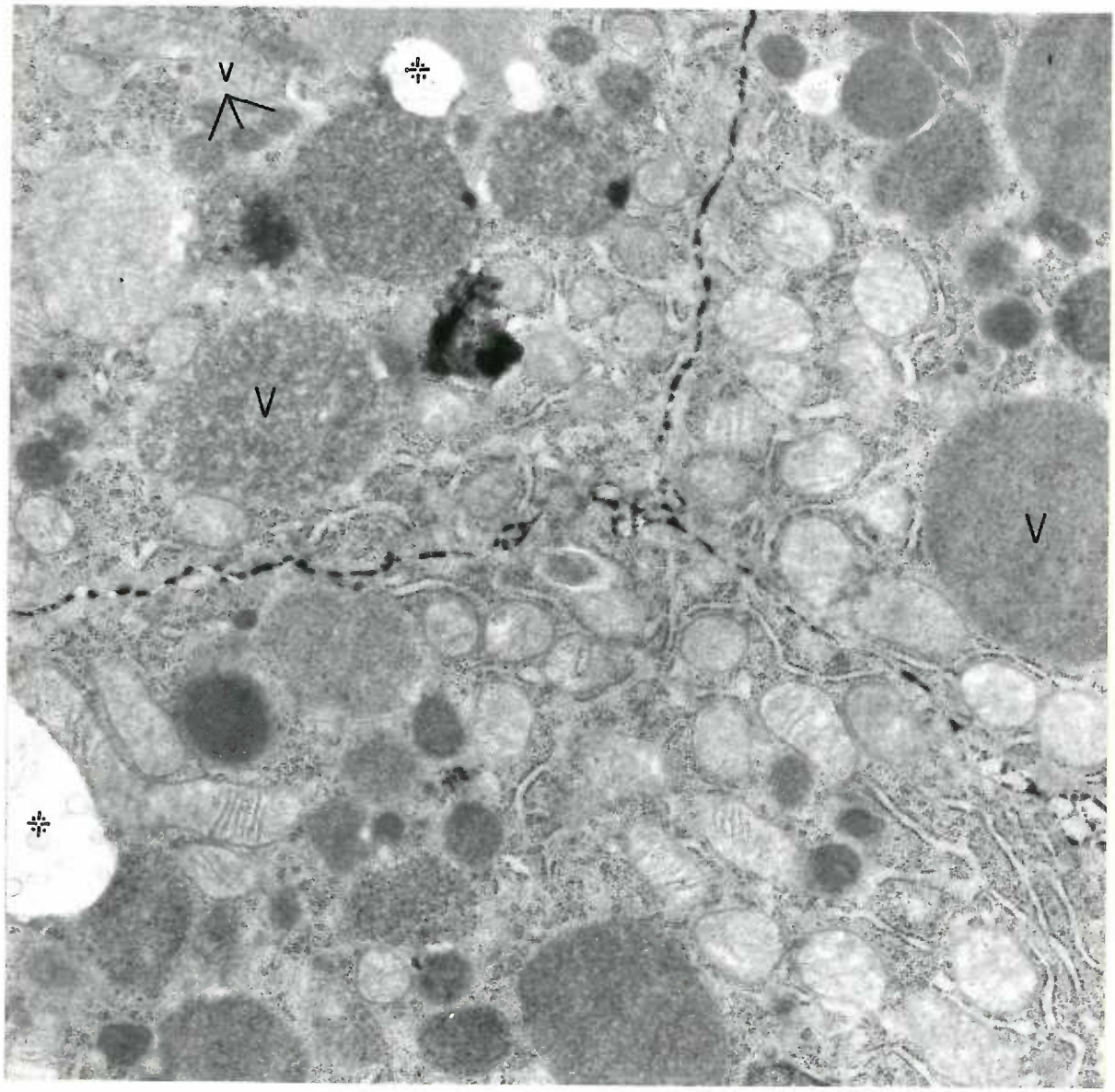

87

FIGURE 88

Basal portion of a group of 14 day visceral endodermal cells incubated with ATP as substrate. Magnification 8,170 X. Note that the final reaction product deposited on and between the visceral basement membrane is of a much finer texture than that occurring in the intercellular spaces. Fine precipitates are also seen related to adjacent surface membranes of mesenchymal cell processes (CTC) and collagen fibrils (Co). The endothelium of an underlying vitelline capillary (VC) and a fetal nucleated blood cell (FRBC) exhibit no activity. Large lipid droplets (Li) are typically seen in the basal cytoplasm; they occur as well in underlying mesenchymal cells.

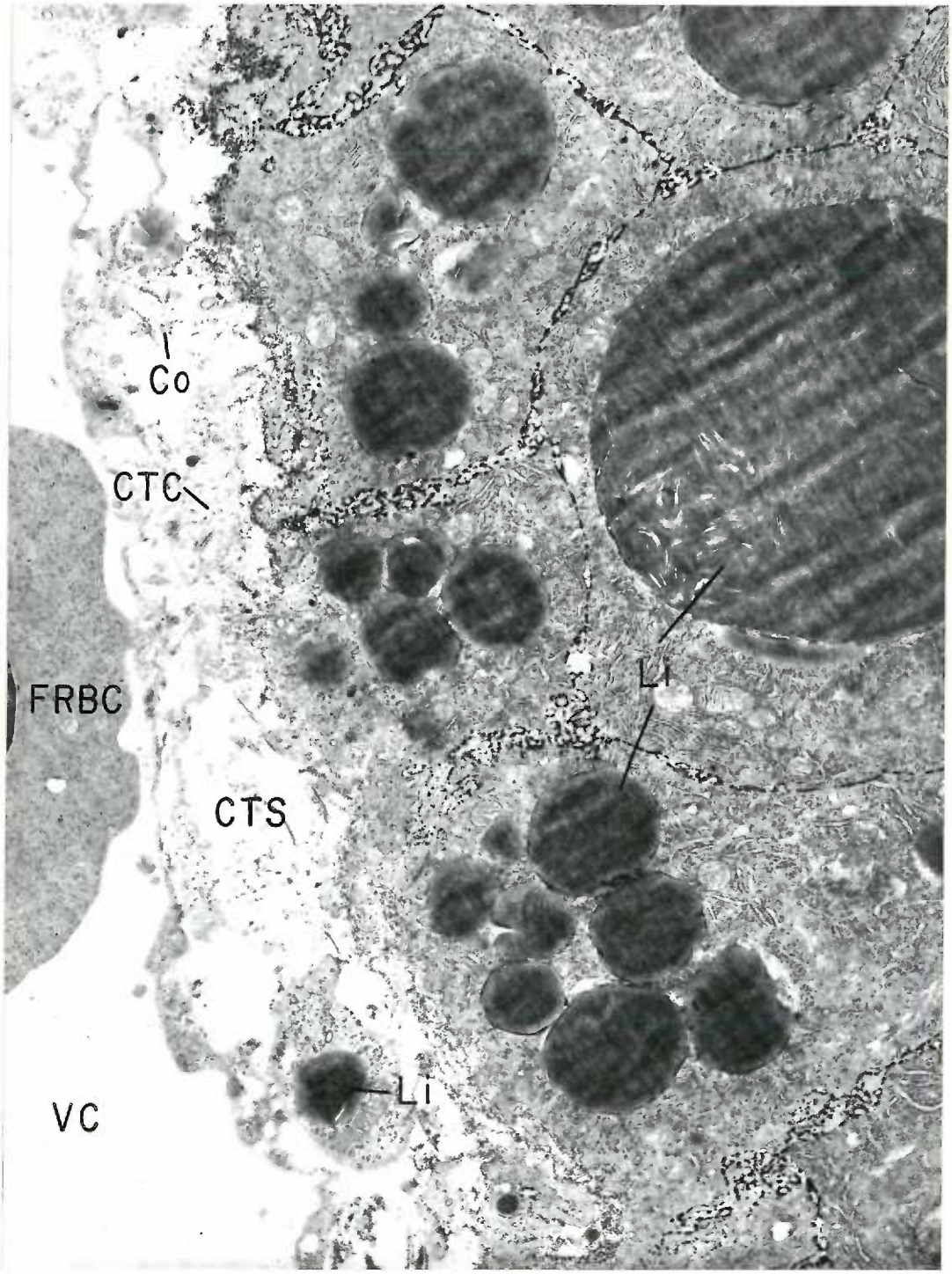
Co
CTC
FRBC
CTS
VC
Li
Li

FIGURE 89

Basal portion of the 14 day visceral yolk sac incubated with ATP as substrate. Magnification 8,170 X. A process of a fetal mesenchymal cell (CTC) separates the endothelium (En) of a vitelline capillary (VC) from the mesothelium (Mes) and its poorly developed serosal basement membrane. No evidence of final reaction product is apparent.

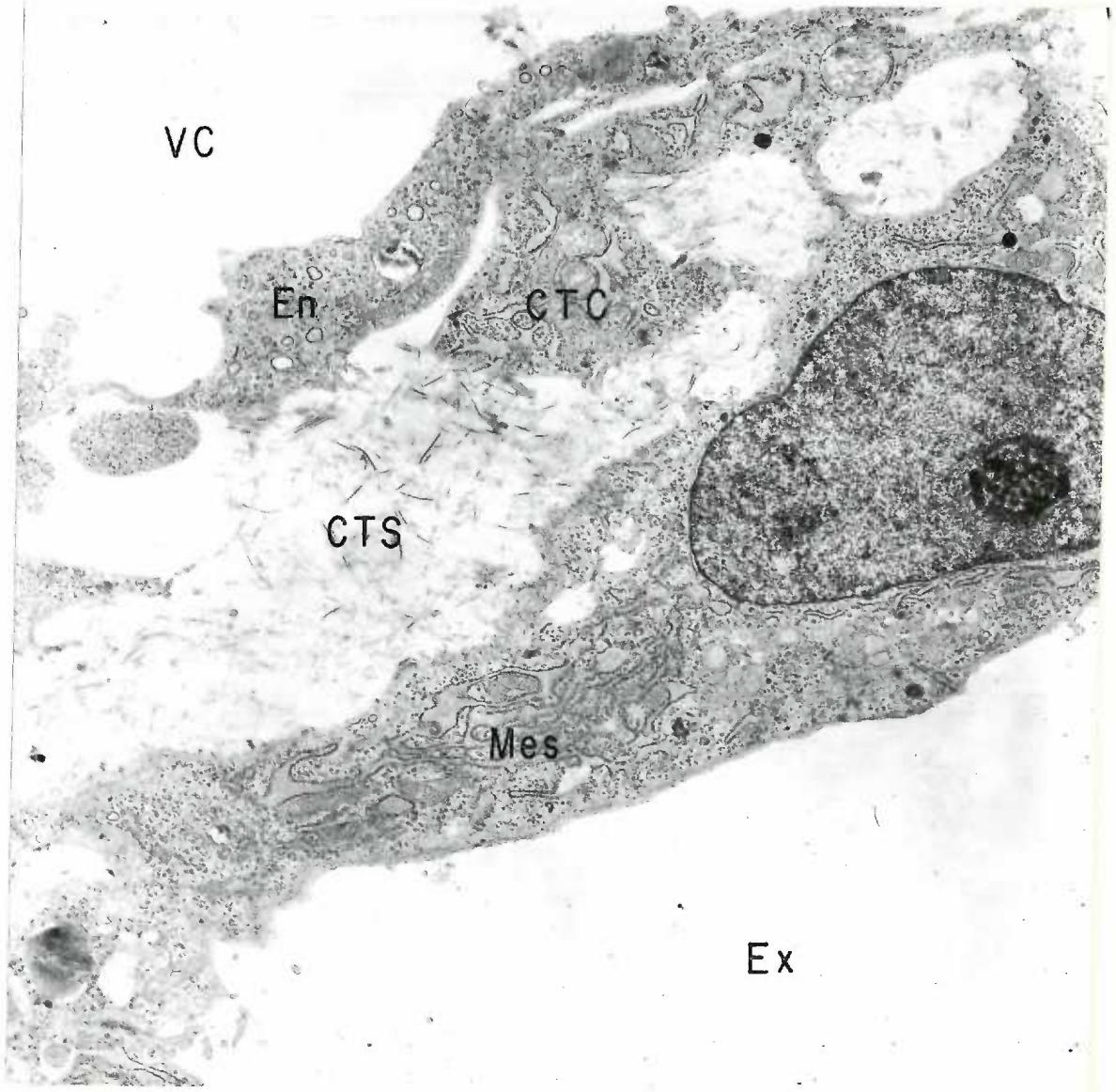
VC
En
CTC
CTS
Mes
Ex

FIGURE 90

Basal portion of a 14 day visceral yolk sac. Magnification 18,600 X. This preparation, which was incubated with AMP, exhibits no activity to this substrate. Pinocytotic vesicles (PV) or caveolae with particularly dense walls are seen along the luminal surface of an endothelial cell (En) lining a vitelline capillary. Loose strands of collagen fibrils intervene between and occasionally appear continuous with the basement membrane of the vitelline capillary and the poorly developed serosal basement membrane. The mesothelial cells (Mes) lining the exocoelom appear rich in polysomes and granular endoplasmic reticulum.

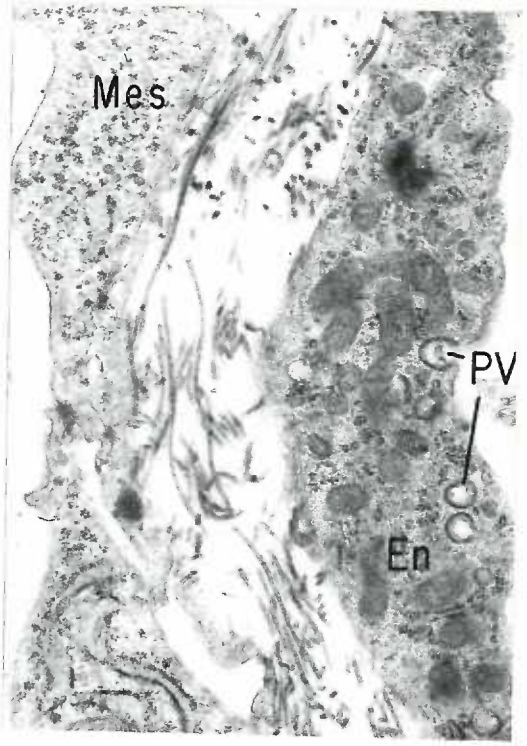

90

FIGURE 91

Striated border and apical cytoplasm of the 14 day visceral yolk sac endoderm incubated with ADP as substrate. Magnification 18,600 X. A moderate deposition of final reaction product is seen along the surface membranes of microvilli and in the canalicular invaginations between the bases of microvilli. Directly below the striated border a complex system of apical canaliculi (AC) is evident. Some of the profiles indicate clearly that the canals are probably joined together to form a continuous membrane-limited labyrinth in the apical cytoplasm.

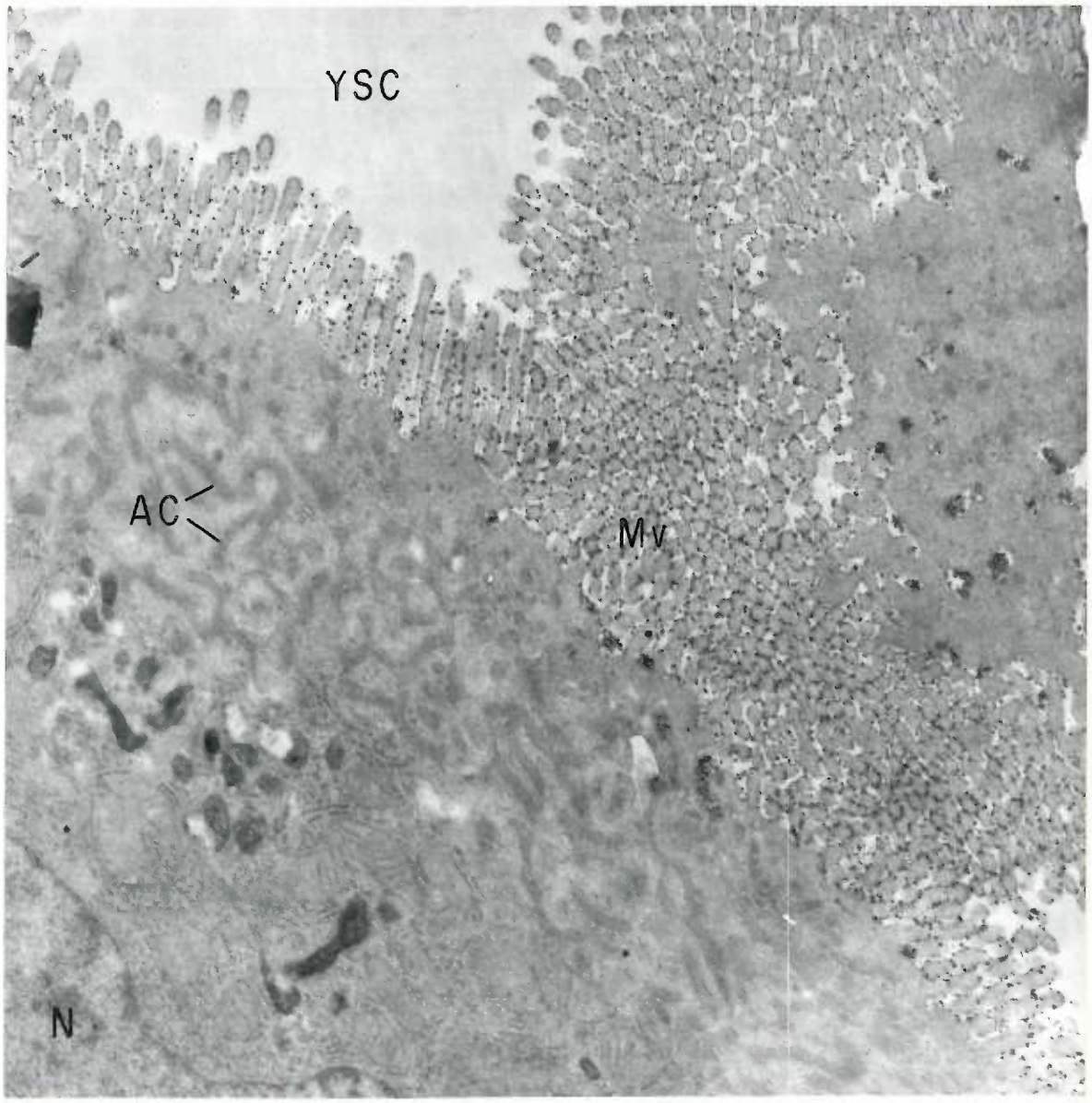
YSC
AC
Mv
N

FIGURE 92

Apical portion of two 14 day visceral endodermal cells incubated with AMP as substrate. Magnification 18,600 X. Evidence of enzyme activity with this substrate is not apparent at this stage.

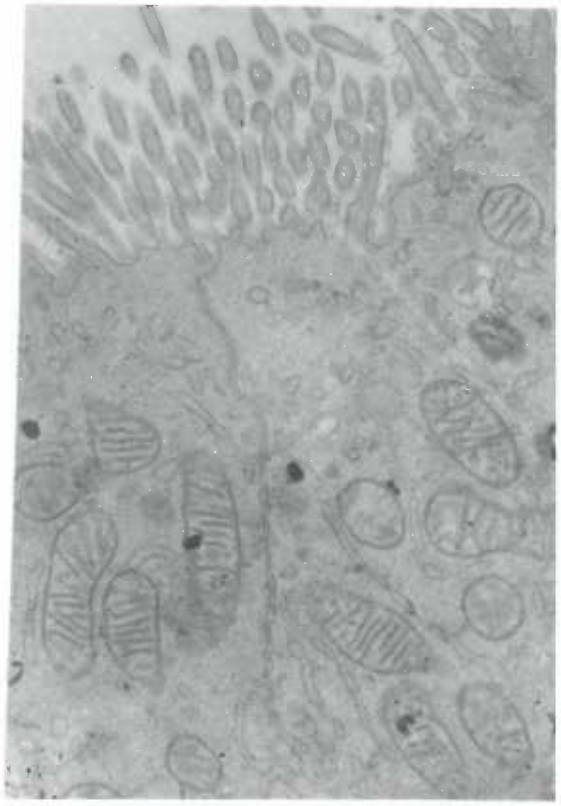

92

FIGURE 93

Cross section of an 18 day visceral yolk sac incubated with ATP. Magnification 7,800 X. Final reaction product is moderately deposited along the outer membranes of microvilli and in relation to the luminal surface and/or contents of vesicles which are considered portions of apical canalicular invaginations (short arrows). A large vacuole seen directly below the brush border on the right contains lead phosphate precipitates dispersed throughout its granular contents (long arrow). Note that activity, in this particular section, is not present on lateral surface membranes, which, proximal to the apical terminal bars (TB), are provided with folds projecting into distended intercellular spaces (IS). The basal surface of the endodermal cells and the visceral basement membrane (VBM) as well as the underlying capillary endothelium (En) are also unreactive.

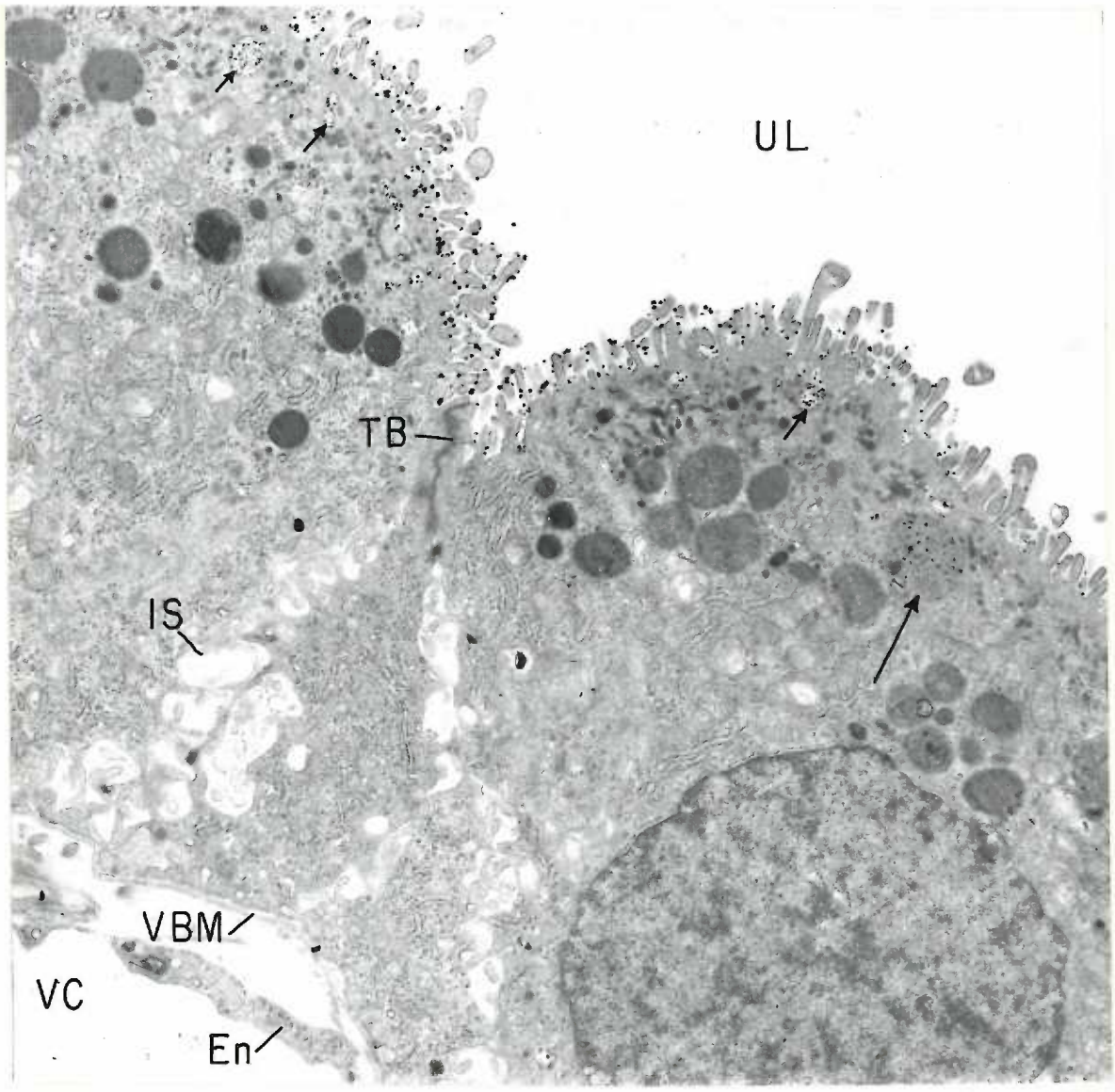

93

FIGURE 94

Detail of the apical portion of two 18 day visceral endodermal cells. Magnification 18,600 X. As compared with that of 14 days (Figure 91), the microvillous projections have undergone a decrease in height and appear blunt and often pleomorphic. The apical cytoplasm directly below the terminal web (TW) contains numerous large, dense and granular vacuoles (V) and small vesicular profiles (v). The cell on the left demonstrates a direct communication between an apical canal and a moderately-sized vesicle (arrow).

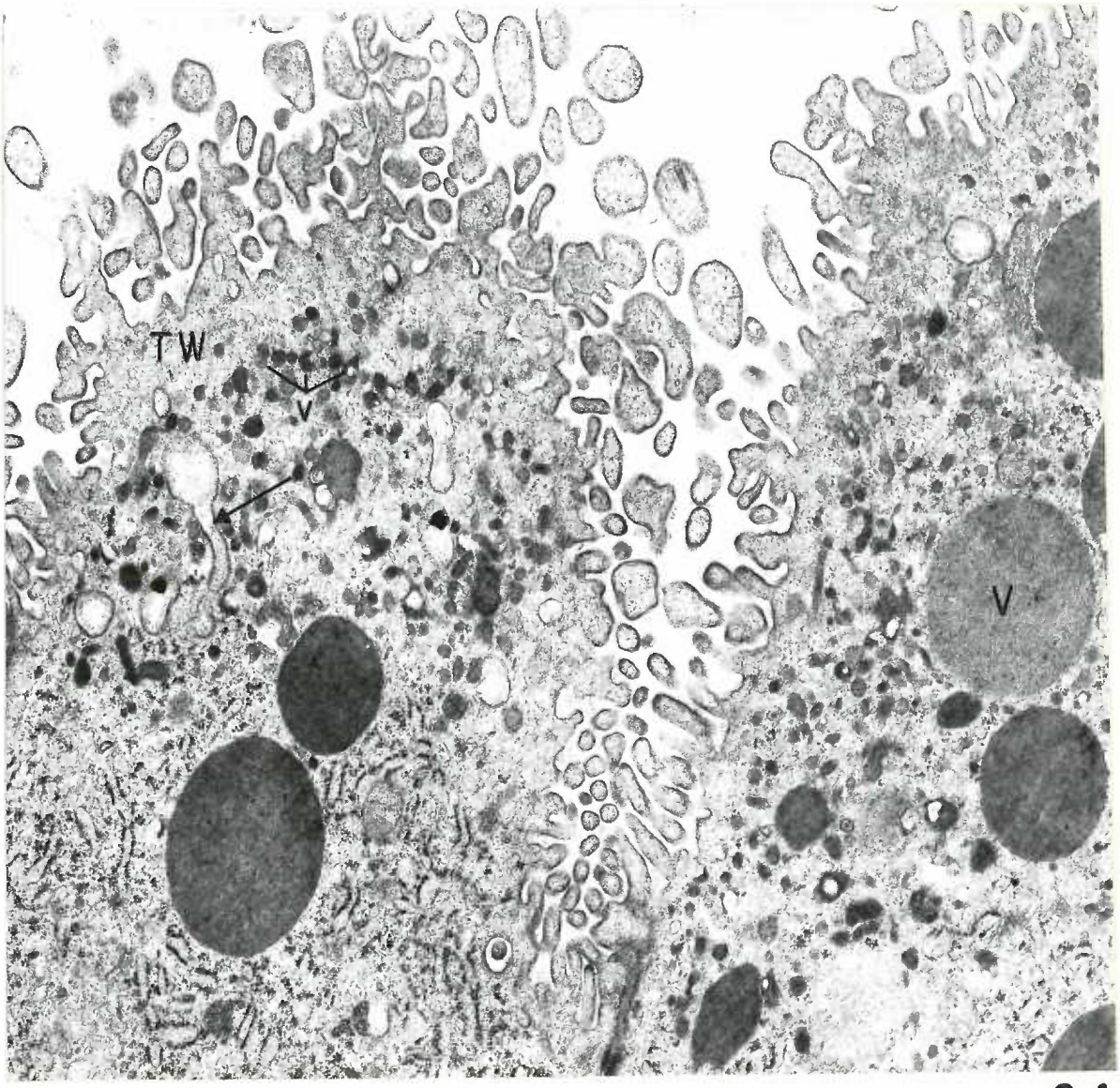

94

FIGURE 95

Apical portion of several 18 day visceral endodermal cells incubated with ATP. Magnification 12,900 X. Note that final reaction product is deposited primarily as a confluent dense precipitate at the outer surface of microvilli on the left, whereas, deposits on those to the right of the figure are punctate and interrupted. Note also that at 18 days the intercellular space depicted is not distended along its entire length. A cluster of lipid droplets are seen within the nucleus at the bottom of the figure.

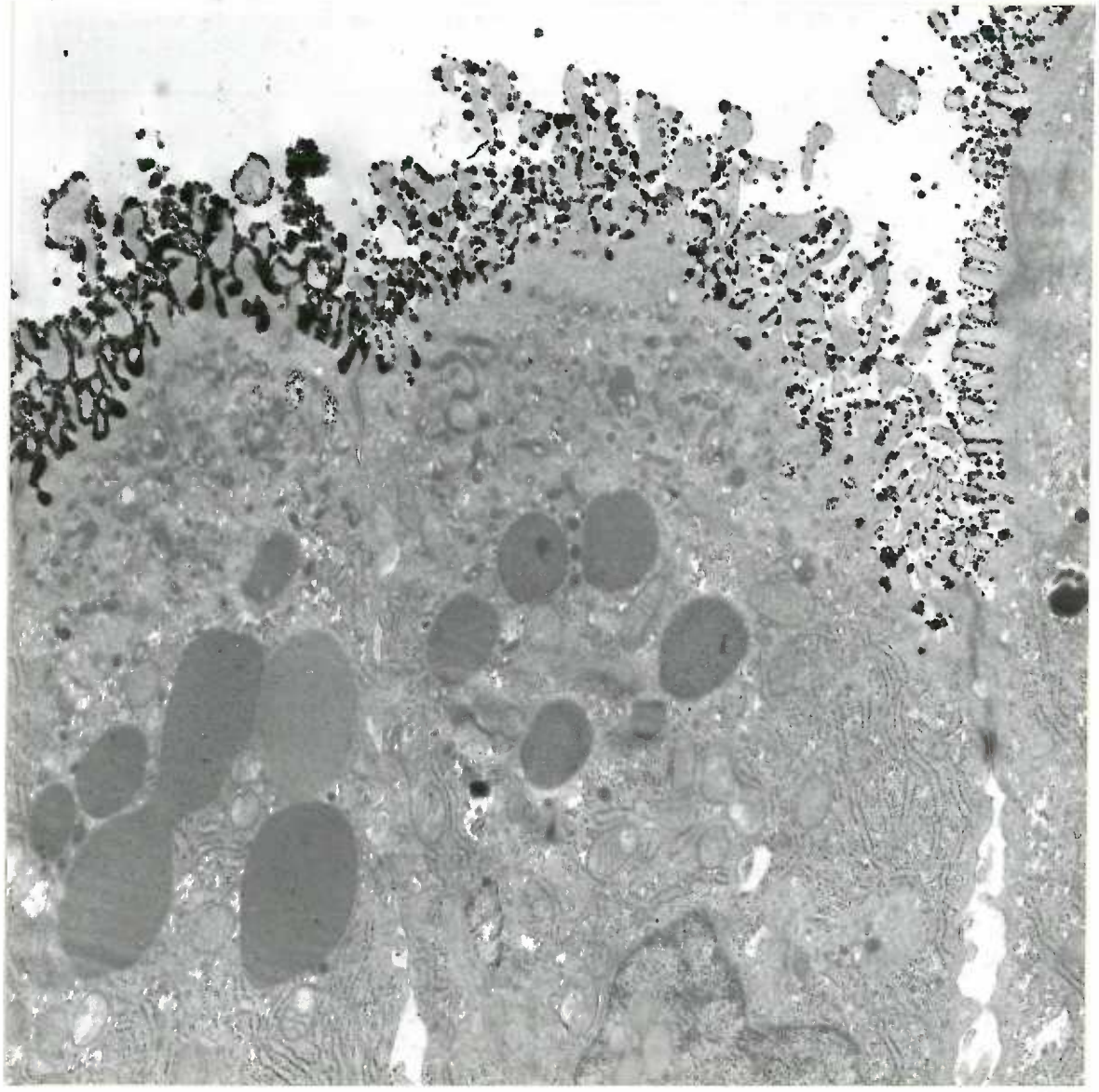

95

FIGURE 96

Low magnification electron micrograph of the 18 day visceral yolk sac epithelium. Magnification 3,420 X. This figure demonstrates the large number of electron dense vesicles and vacuoles which generally appear progressively larger from the apical to the supranuclear cytoplasm and are typical of the 18 day visceral yolk sac epithelium.

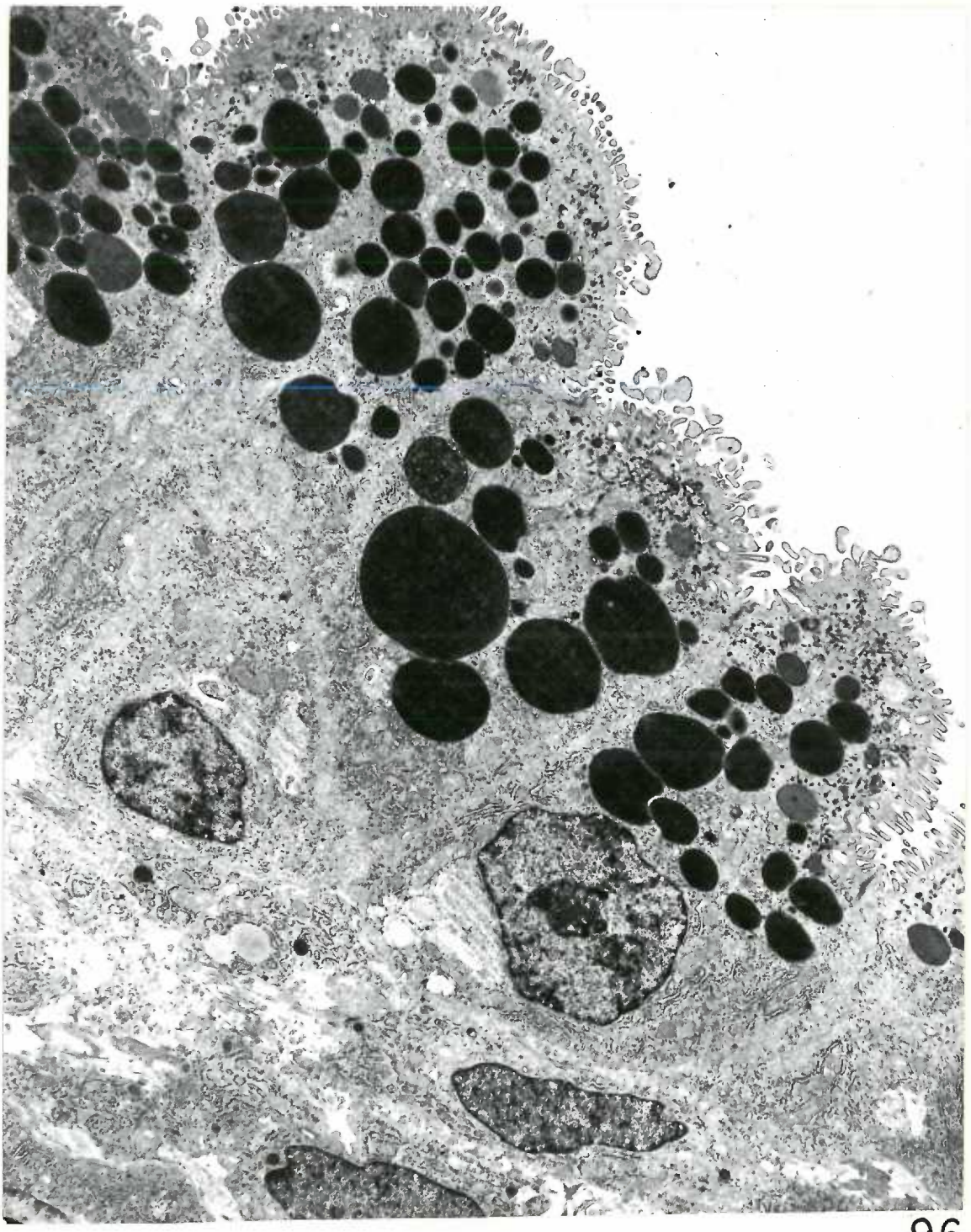

96

FIGURE 97

Microvillous border and apical cytoplasm of three endodermal cells incubated with ADP. Magnification 18,600 X. Granules of final reaction product are sparsely deposited on the apical surface membrane and on the inner surface of a number of tubular and vesicular profiles (arrows) seen within the apical cytoplasm. Sparse deposits of reaction product also occur in the intercellular space where the lateral surface membranes are closely apposed.

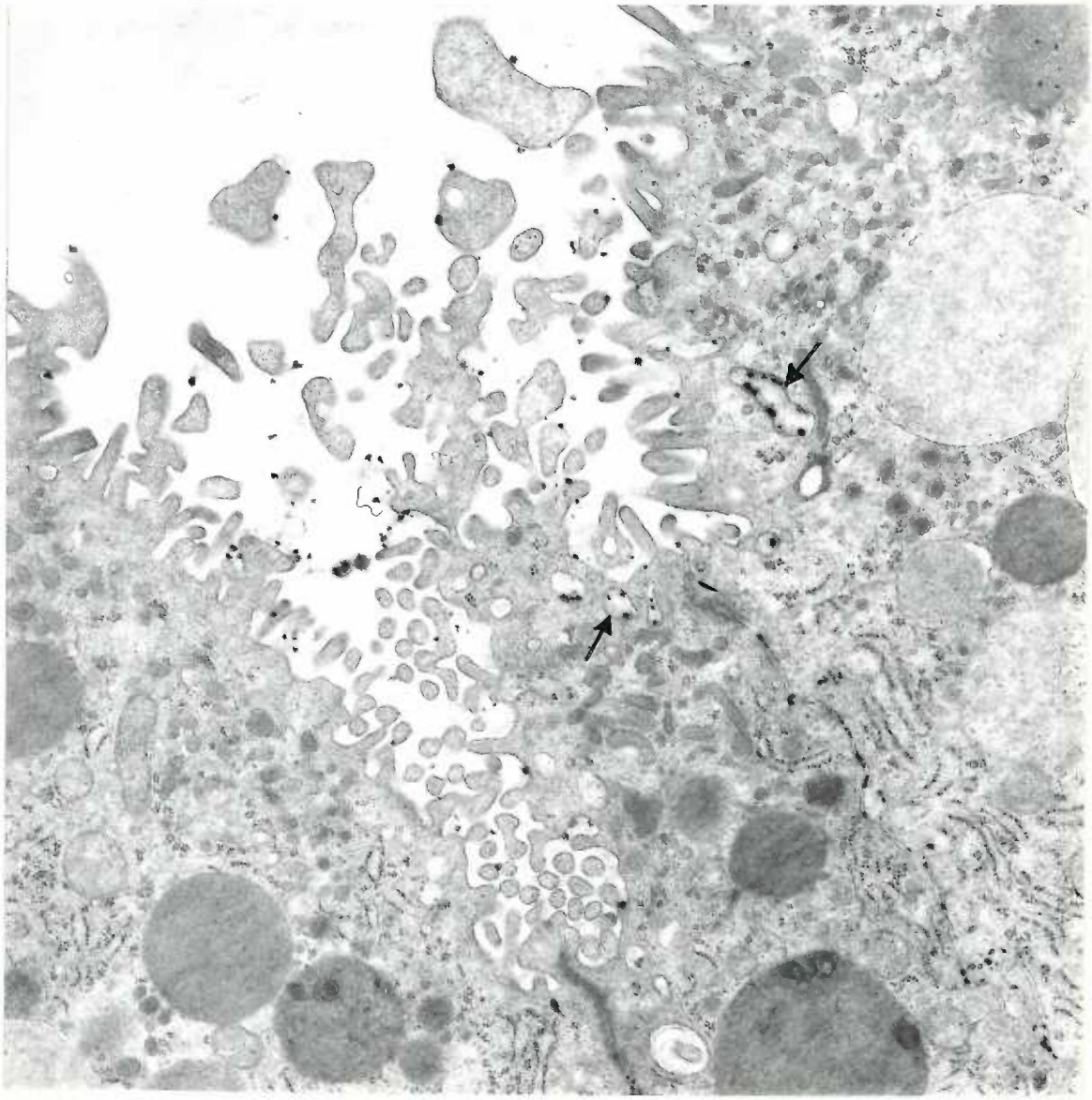

97

FIGURE 98

Basal portion of an 18 day visceral yolk sac incubated with ATP. Magnification 12,900 X. Punctate deposits of final reaction product occur on the lateral surface membranes of two endodermal cells bordering a distended intercellular space (IS). Note that the basal surface of the endodermal cell is unreactive, whereas the visceral basement membrane (VBM) has fine precipitates present throughout its matrix.

FIGURE 99

Apical portion of two visceral endodermal cells incubated with ADP. Magnification 18,600 X. Final reaction product is deposited as described in Figure 97. Note the well developed mitochondria and granular endoplasmic reticulum which extend well into the apical cytoplasm. The tangential cut through the nucleus (N) at the left margin of the figure reveals a fibrous lamina (long arrow) and a number of nuclear pores (short arrows).

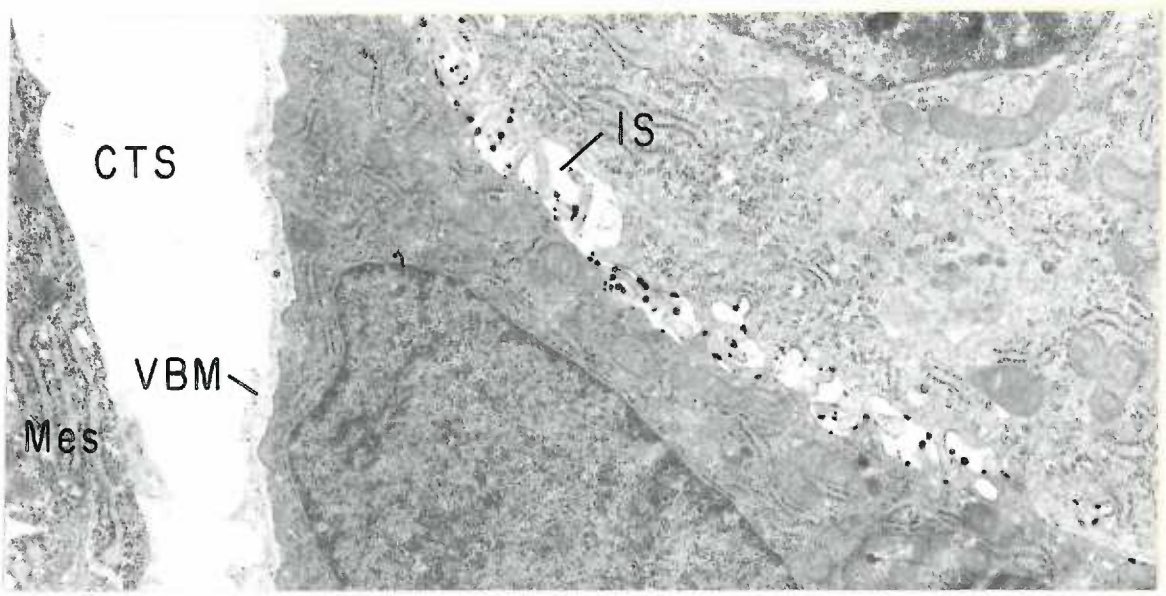

98

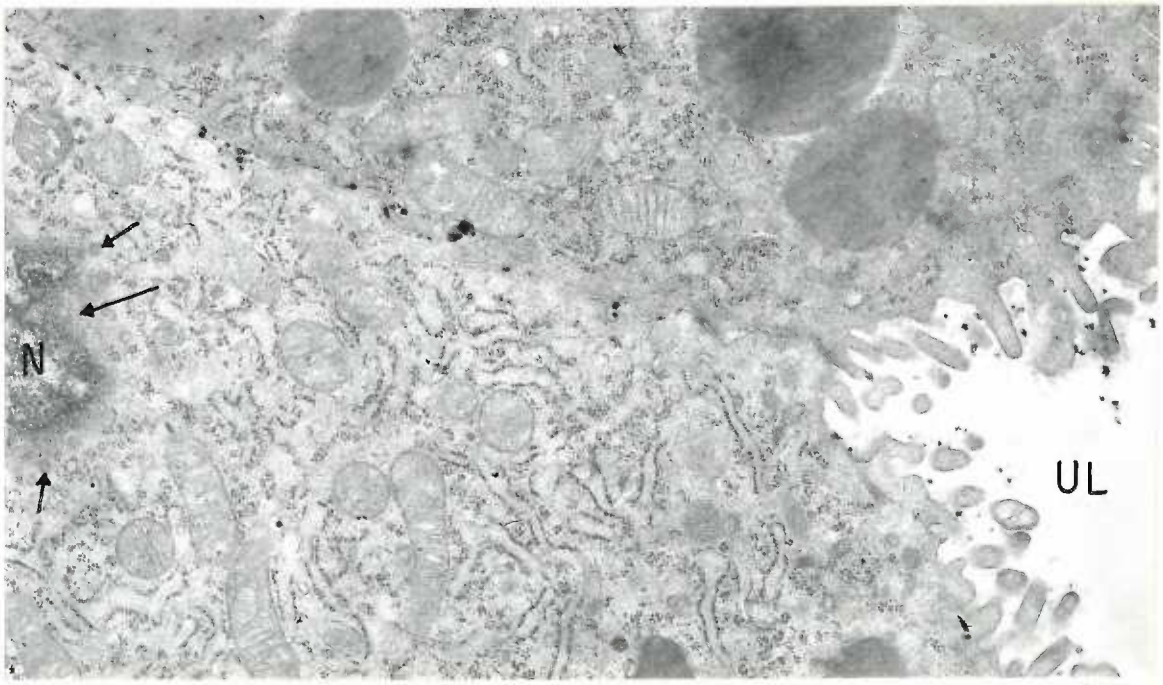

99

FIGURE 100

Portions of two mesothelial cells of the 18 day visceral yolk sac incubated with ATP. Magnification 18,600 X. Deposits of final reaction product are present along outer surface membranes facing the exocoelom (Ex). The mesothelial cytoplasm displays an abundance of polyribosomes, granular endoplasmic reticulum and several lipid inclusions (Li). Note the increase in fibrous elements adjacent to the serosal basement membrane (SBM). Also note that lead phosphate precipitates do not occur in the serosal basement membrane.

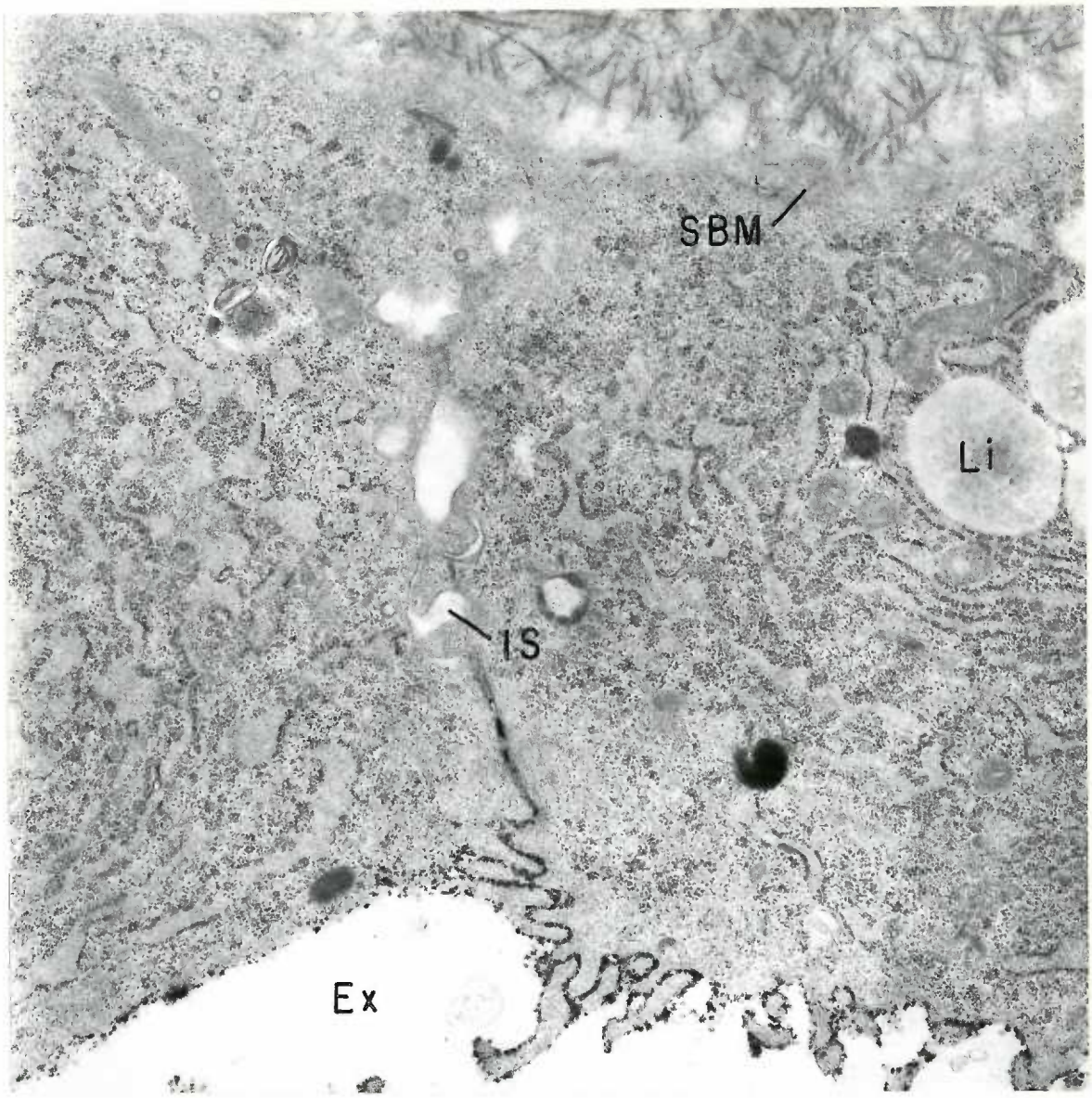

100

FIGURE 101

Electron micrograph of a section through the entire thickness of the visceral yolk sac placenta on the 22nd day of gestation. Magnification 7,800 X. Note that the visceral epithelium is much lower than on the 14th or 18 days and that large intercellular spaces (IS) are prominent. The visceral and serosal basement membranes (VBM, SBM) are well developed and separate the visceral endodermal cells (VE) from the mesothelial cells (Mes) which line the exocoelom (Ex). The connective tissue space (CTS) appears to contain more collagen fibrils (Co) than previous stages. Final reaction product resulting from the enzymatic hydrolysis of AMP is sparsely deposited on the outer surface of the microvillous projections which extend from both the luminal surface of the visceral epithelium and the free surface of the mesothelium. No activity is found along either the lateral or basal surface membranes of endodermal cells.

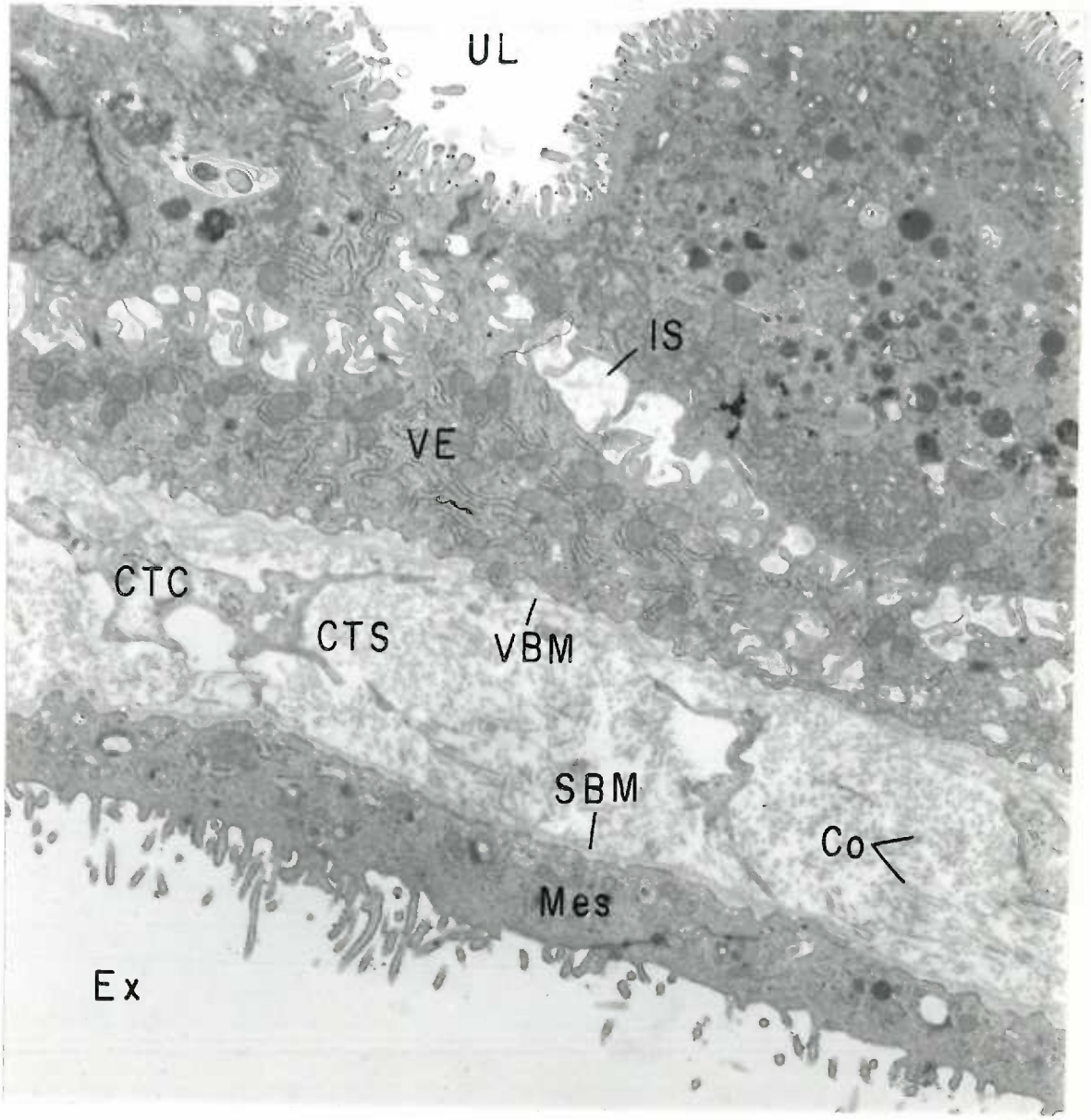

101

FIGURE 102

General view of the 22 day visceral endoderm incubated with AMP. Magnification 12,900 X. As in Figure 101, activity is localized along the outer surface of microvilli. Note the elaborate and loosely interdigitating folds of the lateral surface of adjoining endodermal cells. Similar interdigitations are seen along the basal surface of the endodermal cells. Mitochondria, granular endoplasmic reticulum and microvesicular profiles appear uniformly distributed throughout the cell, whereas the golgi zone (G) is primarily located in the basal cytoplasm. Vacuoles (V) and vesicles (v) of varying content and electron density are seen in the cytoplasm above the golgi zone. The limiting membrane of the vesicles and vacuoles are irregular as though they were increasing in size through the coalescence of smaller golgi-like vesicles.

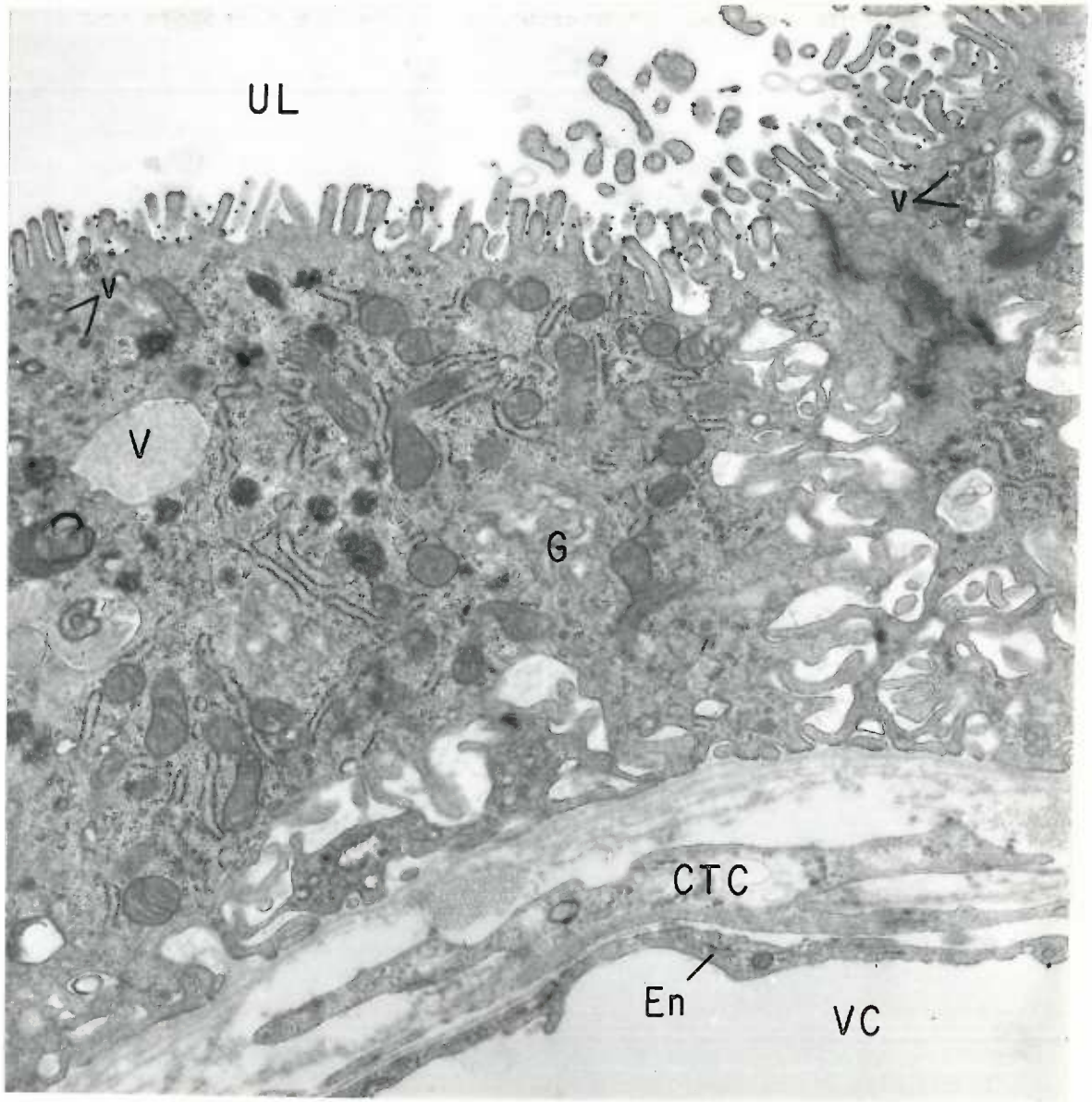

102

FIGURE 103

Oblique section through the apical portion of two 22 day visceral endodermal cells incubated with ADP. Magnification 12,900 X. Final reaction product is moderately deposited along the outer surface of the microvilli. Activity within the apical cytoplasm occurs in relation to the inner surface of circular or tubular vesicles which represent invaginations of the apical surface membrane (AC). Occasional cross sections of bases of microvilli are seen within these profiles which would indicate that the plasma membranes of the microvilli are continuous with the walls of the canaliculi (arrows). The apical cytoplasm contains numerous microvesicular profiles. The two endodermal cells are attached at their apex by a terminal bar (TB). Note the fine fibrils which radiate from this junction along the lateral cell margin.

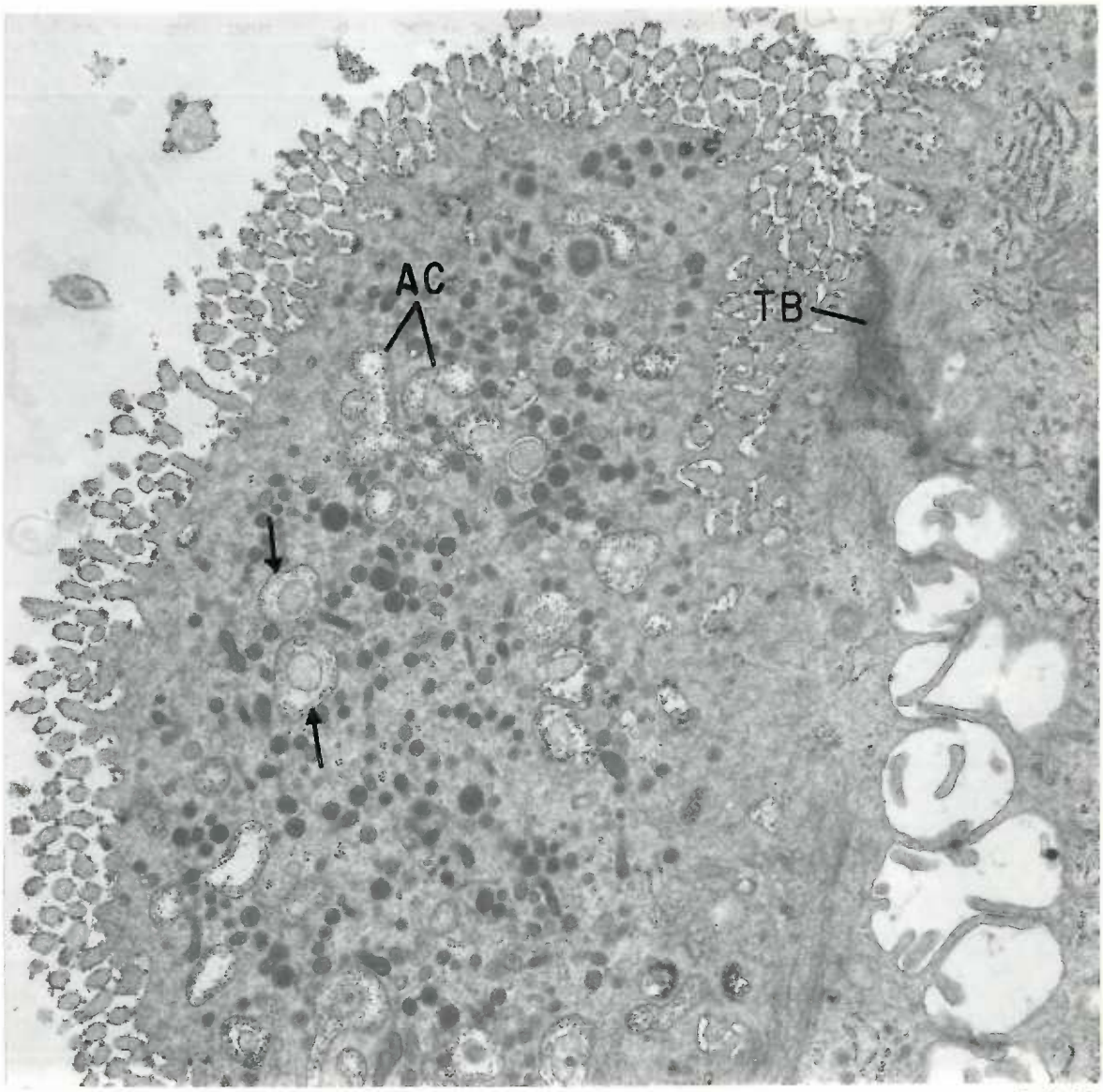

103

FIGURE 104

Detail of the free surface of two 22 day visceral endoderm cells incubated with ADP as substrate. Magnification 12,900 X. Compare the distribution of final reaction product with that seen in Figure 103. Wherever large accumulations of extracellular material occur in close relationship to the microvilli of the visceral epithelium, only sparse deposits of activity occur along the surface plasma membrane, whereas large deposits of lead phosphate are seen throughout the extraneous material. A few of the canalicular invaginations (AC) between the bases of the microvilli contain granular material mixed with reaction product which is similar to that seen in the uterine lumen (UL). This is suggestive of an inward movement of extraneous materials.

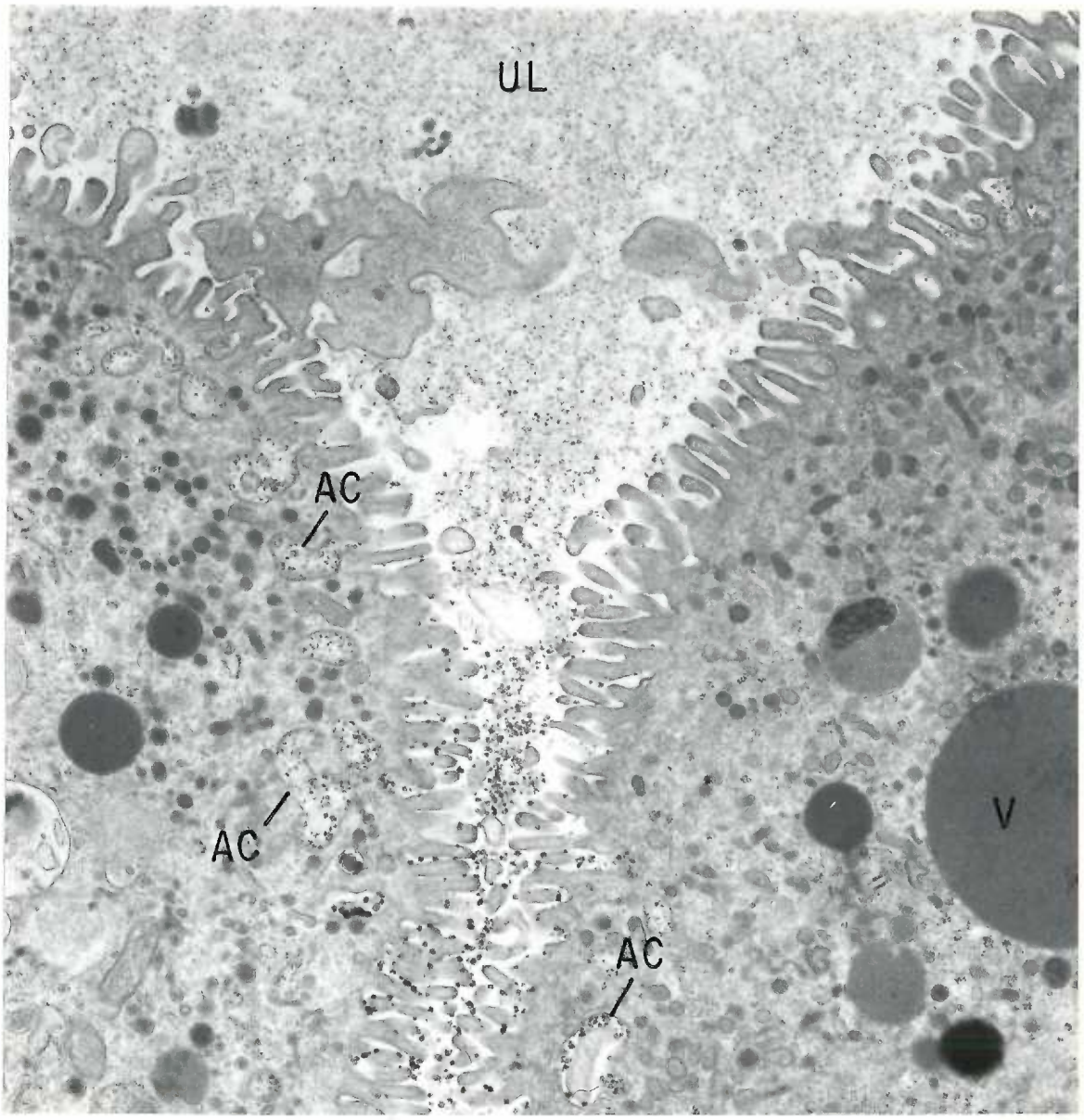

104

FIGURE 105

Apical section of two 22 day visceral endodermal cells incubated with AMP. Magnification 12,900 X. As in Figures 101 and 102, only slight activity occurs along the apical surface membrane. Directly below the microvillous border a direct connection can be seen between a tubular canal and a cross section of a surface invagination (long arrow). In addition to profiles of the apical canal system (AC) the apical and supranuclear cytoplasm contain numerous vesicles and vacuoles of various sizes which are irregular in outline and contain granular material of varying electron densities. Whether these structures are or will be transformed into lysosomes is not clear. A golgi zone (G) is apparent at the bottom of the figure. Note that some of the mitochondria show either longitudinally oriented cristae or cristae oriented transversely at one end and longitudinally at the other (short arrows).

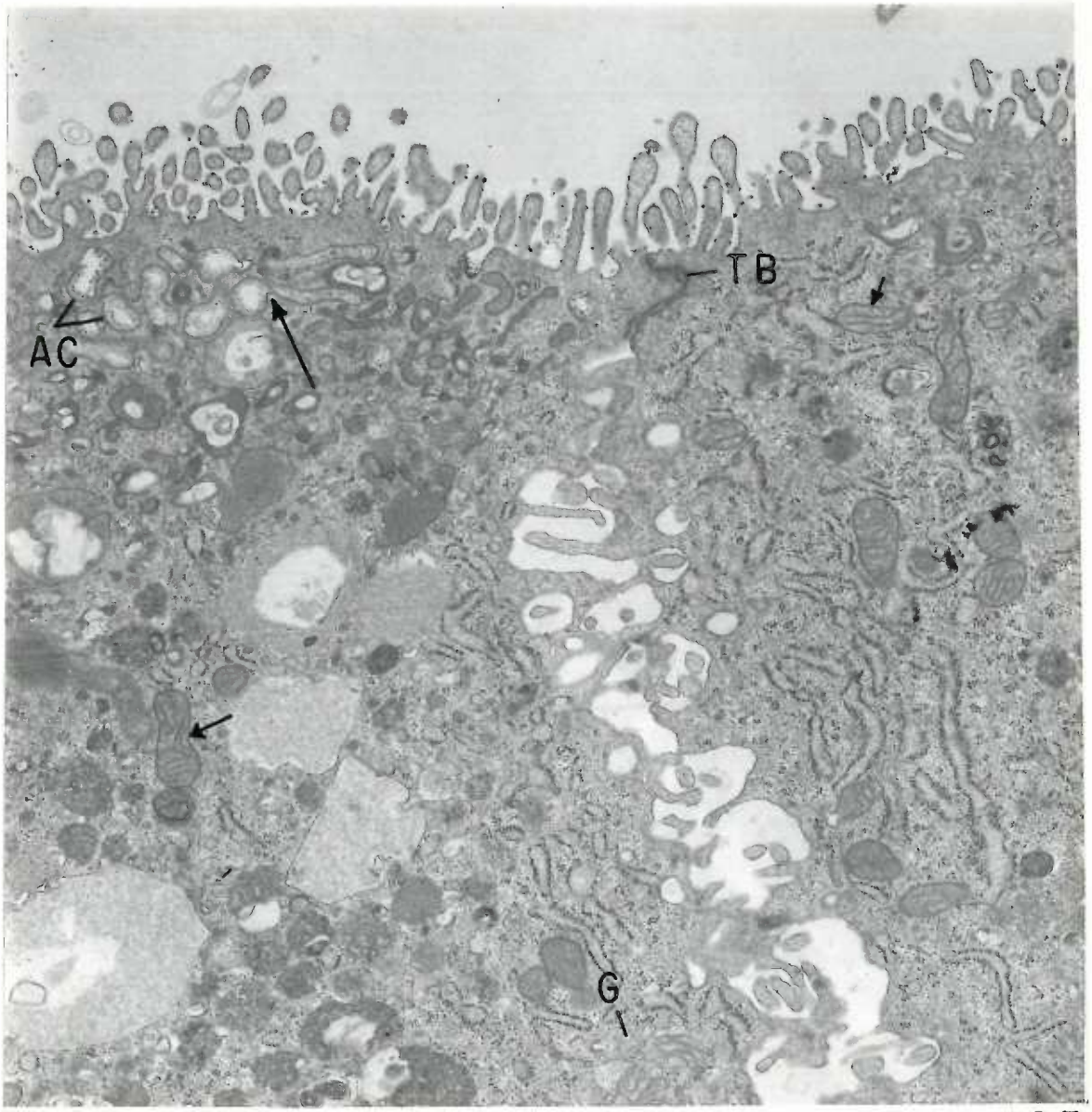

105

FIGURE 106

General view of the 22 day visceral epithelium incubated with ATP. Magnification 8,170 X. Adjoining endodermal cells are firmly attached at their apices by tight junctions. Proximal to the terminal bars (TB), finger-like cytoplasmic projections from apposing lateral cell surfaces loosely interdigitate to form intercellular pockets (IS) which contain a flocculent material of moderate electron density. Desmosomes occur at irregular intervals between interdigitating lateral and basal projections (arrows). Final reaction product resulting from the enzymatic hydrolysis of ATP is limited to the apical surface membrane where it occurs as a confluent dense precipitate.

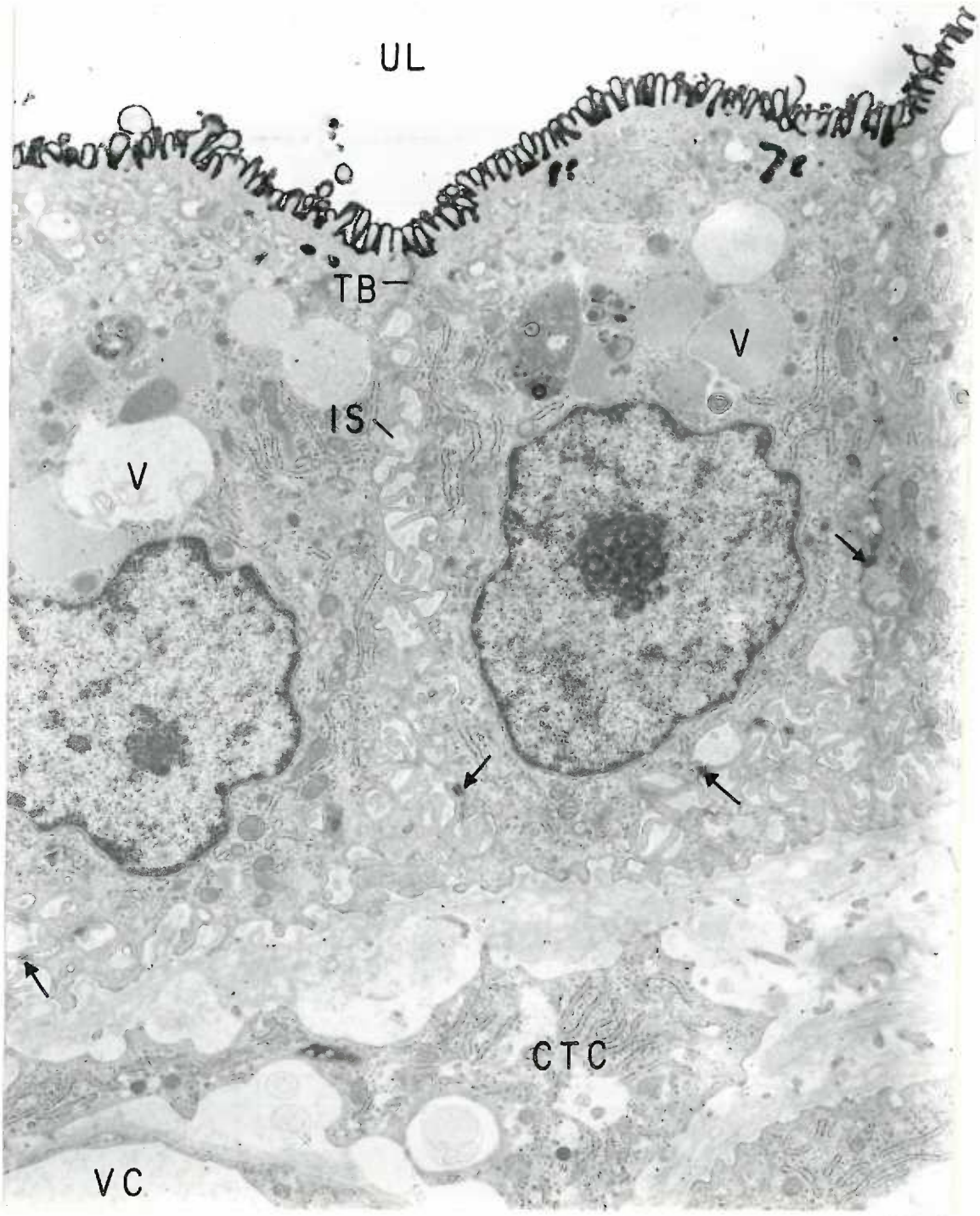

106

FIGURE 107

Apical portion of two 22 day visceral endodermal cells incubated with ADP. Magnification 12,900 X. Activity with this substrate is deposited along the outer surface of microvilli and along the inner surface and/or contents of surface invaginations. At the apical end of the intercellular space the lateral plasma membranes of the endodermal cells are firmly attached by a terminal bar (TB). The cytoplasm displays a great number of vesicles (v) and vacuoles (V) ranging from 0.1 to 4.5 u in diameter. The larger vacuoles in the cell to the left have a homogeneous dense content and are surrounded by a more distinct membrane than the vacuoles in the cell to the right. The cytoplasm of right endodermal cell is also lighter and contains fewer mitochondria and profiles of granular endoplasmic reticulum than the cell on the left. As in Figure 105, note the longitudinal orientation of the cristae mitochondriales (arrow).

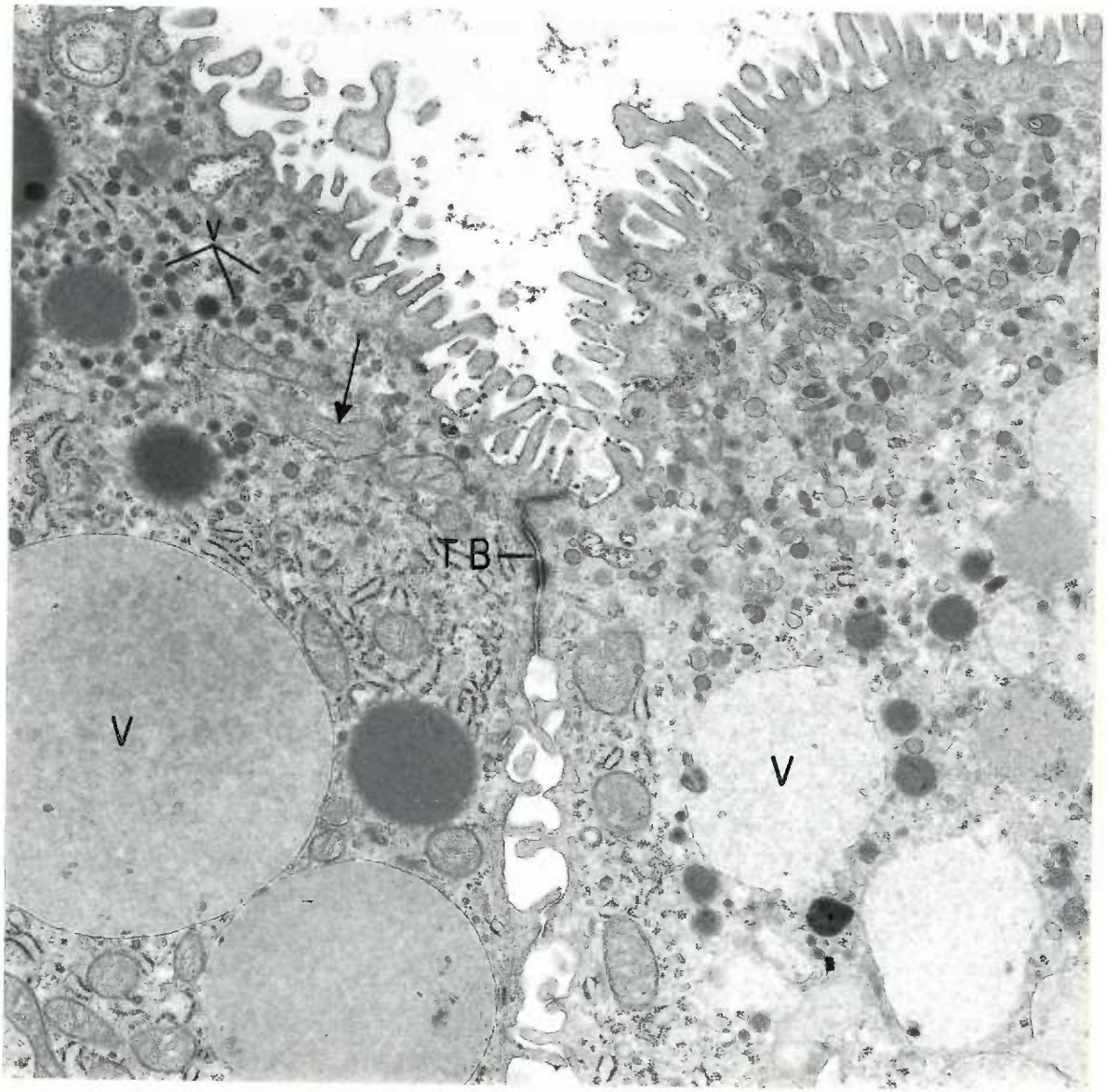

107

FIGURE 108

Detail of the apical surface and supranuclear cytoplasm of two 22 day visceral endoderm cells incubated with ATP. Magnification 12,900 X. The final reaction product occurs as dense beaded deposits at the surface of the microvilli and in the depressions and canaliculi between the bases of the microvilli. No ATPase activity is seen along the lateral surface membranes or in the intercellular space. A well developed golgi zone (G) consisting of both lamellar systems of cisternae and small vesicles is seen in the supranuclear cytoplasm in the lower left corner of the figure. Microvesicular profiles of a similar size and density are also seen in the apical cytoplasm. It is difficult, however, to say which are golgi vesicles, lysosomes or pinocytotic vesicles. Note that some of the vacuoles display electron translucent areas. A mitochondrion with longitudinally oriented cristae is indicated by an arrow.

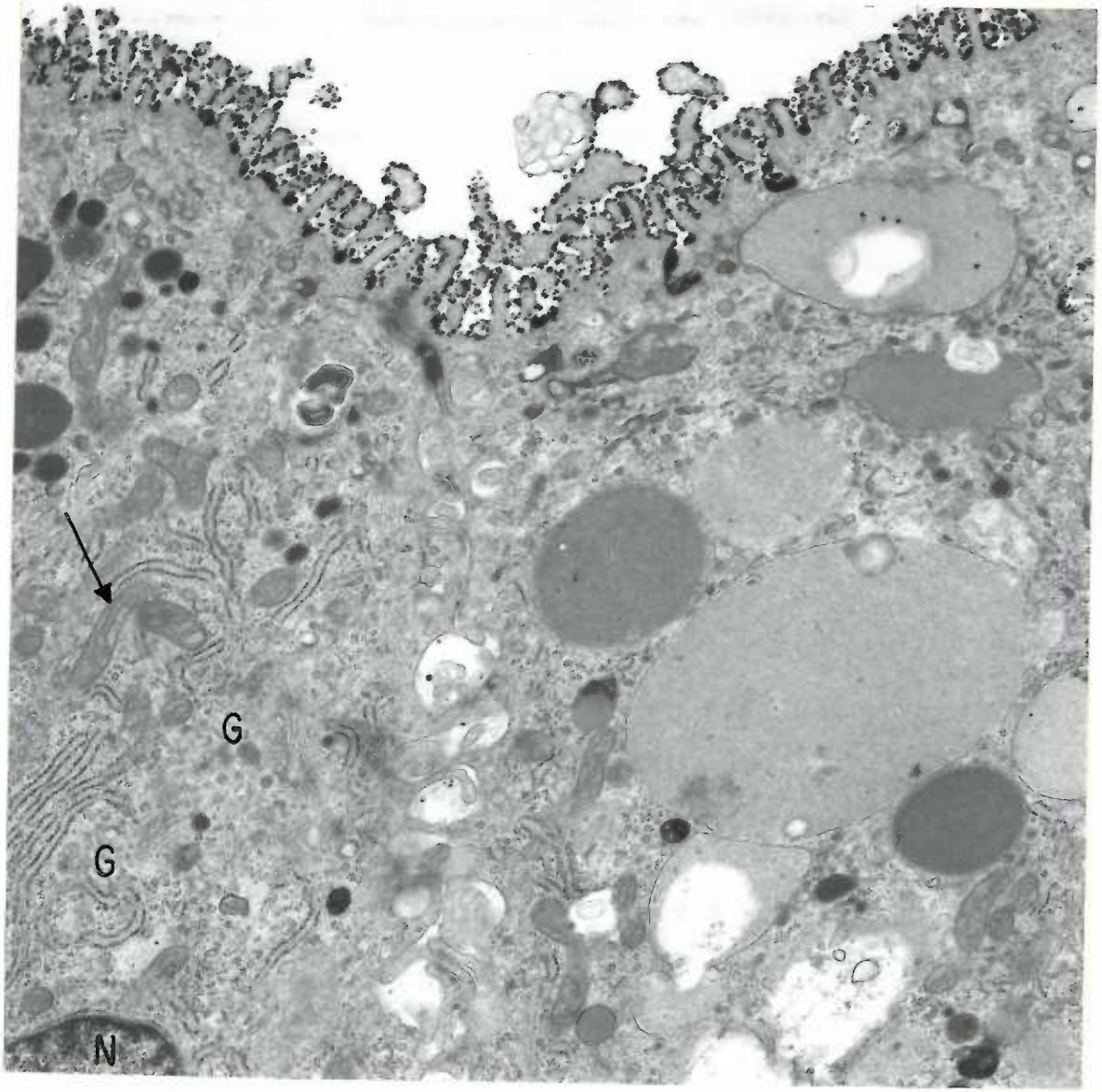

108

FIGURE 109

Apical portion of a 22 day visceral endodermal cell incubated with ADP as substrate. Magnification 12,900 X. In this preparation, the large number of microvesicular profiles which occur within the apical cytoplasm cannot be identified as being golgi elements, pinocytotic vesicles or profiles of apical canals. Final reaction product occurs on the outer surface membranes of microvilli as described in Figure 103.

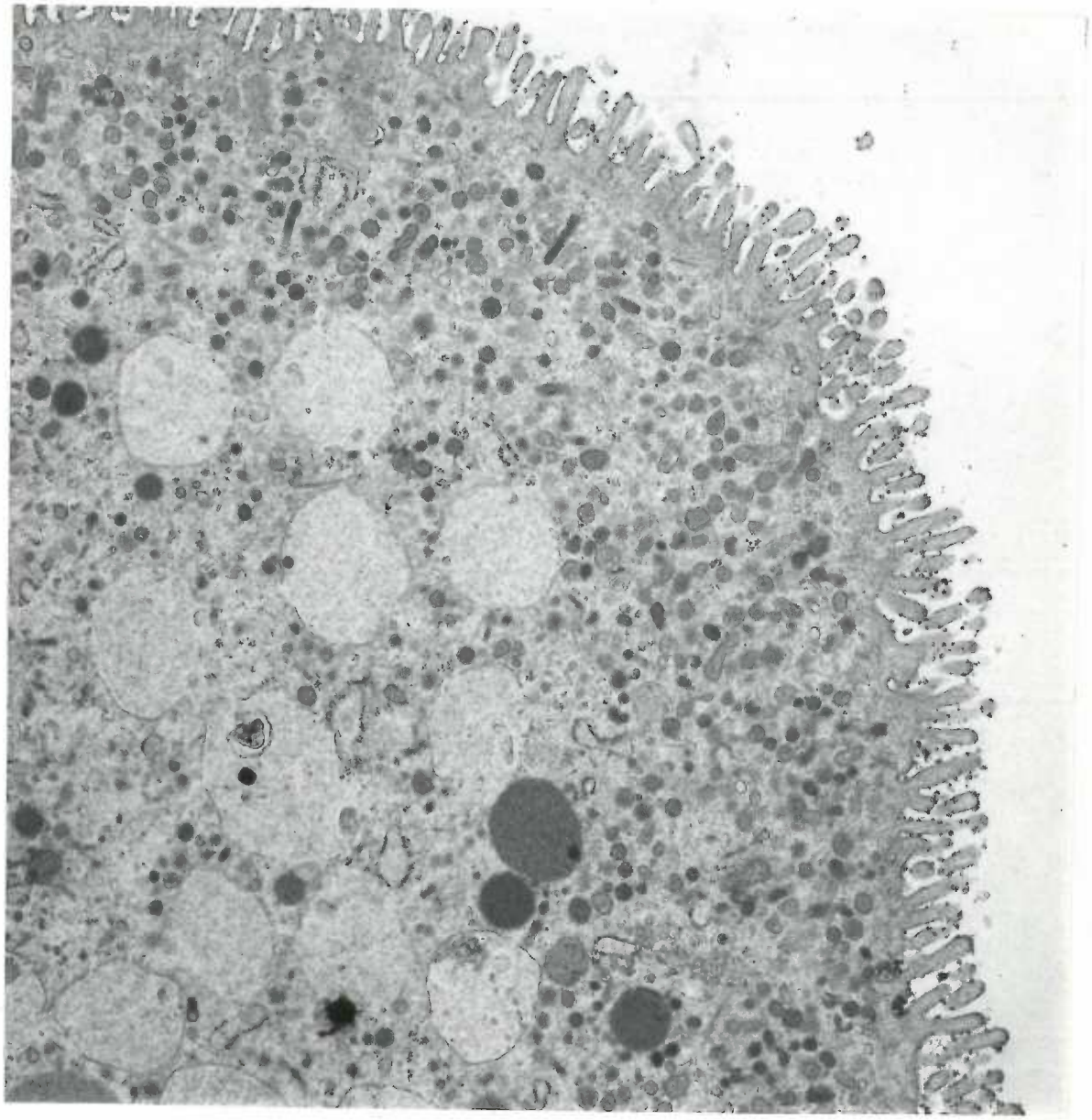

FIGURE 110

Cross section through the apical portion of two apposing 22 day visceral endodermal cells incubated with ATP. Magnification 12,900 X. This electron micrograph demonstrates the varied appearance of the vesicles and vacuoles in the apical cytoplasm. In addition to having ill-defined and often discontinuous limiting membranes, many of the vesicles and vacuoles contain one or more dense figures and/or myelin-like concentric systems of membranes intermingled with a fine granular material of either low or moderate electron density. Note the close association of disrupted vacuoles with the large area of less dense cytoplasm (asterisk) seen in the center of the figure. The varied appearance of the vesicles and vacuoles may represent successive stages in the breakdown or synthesis of some material. A well developed junctional complex is seen near the free surface of the epithelium in the lower right corner of the figure. Dense deposits of lead phosphate resulting from the enzymatic hydrolysis of ATP are seen on the outer surface membranes of microvilli.

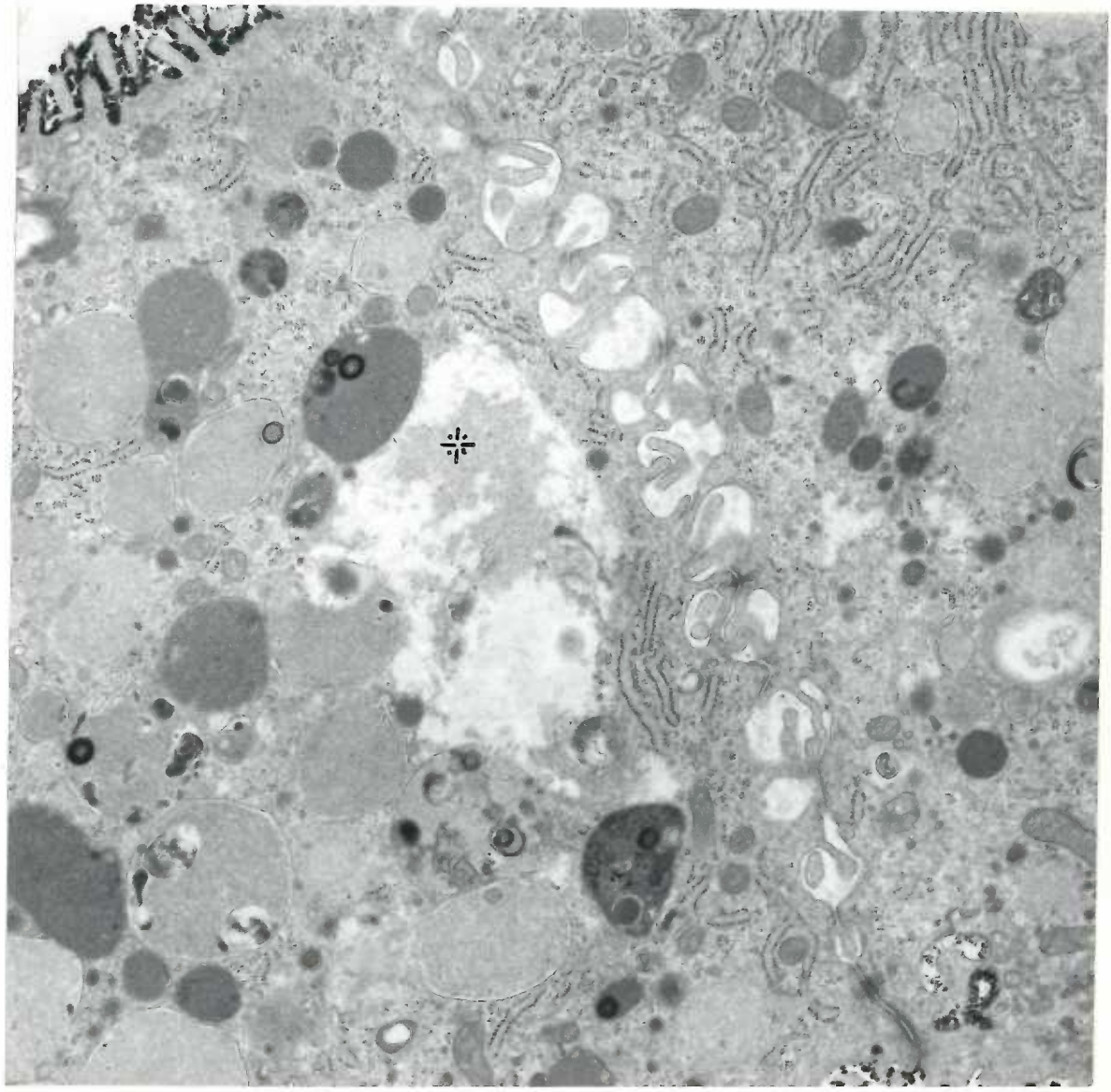

110

FIGURE 111

Apical portion of two adjacent 22 day visceral endodermal cells incubated with ATP. Magnification 12,900 X. Dense deposits of final reaction product are visible at the cell surface as seen in Figures 106, 108 and 110. Note the close association of golgi microvesicular profiles with the disrupted vacuole in the lower left corner of the figure (arrow). Parallel arrays of granular endoplasmic reticulum are prominent in the supranuclear cytoplasm.

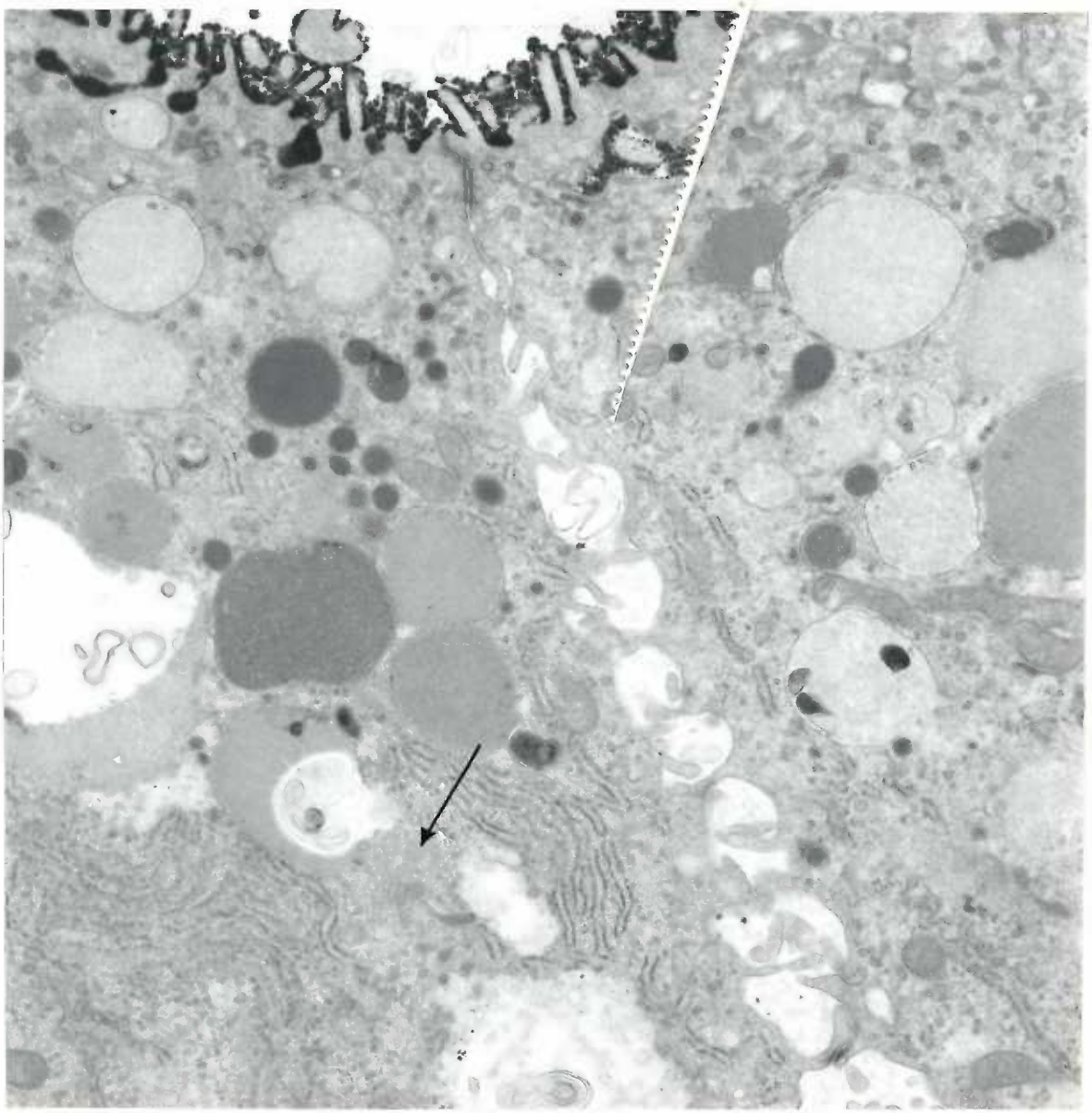

III

FIGURE 112

Basal portion of two 22 day visceral endodermal cells incubated with AMP. Magnification 12,900 X. Final reaction product does not occur on either the basal or lateral cell surfaces. The visceral basement membrane (VBM) as well as the underlying mesenchymal cells (CTC) and vitelline capillary (VC) are also unreactive with this substrate. Cytoplasmic projections from apposing lateral cell surfaces form a labyrinthine appearing complex of loosely interdigitating folds. Similar projections and infoldings are seen along the basal cell surfaces. Microvesicular profiles (v) are abundant near the basal border. A large spherical area of less dense cytoplasm is seen on the right side of the micrograph (asterisk).

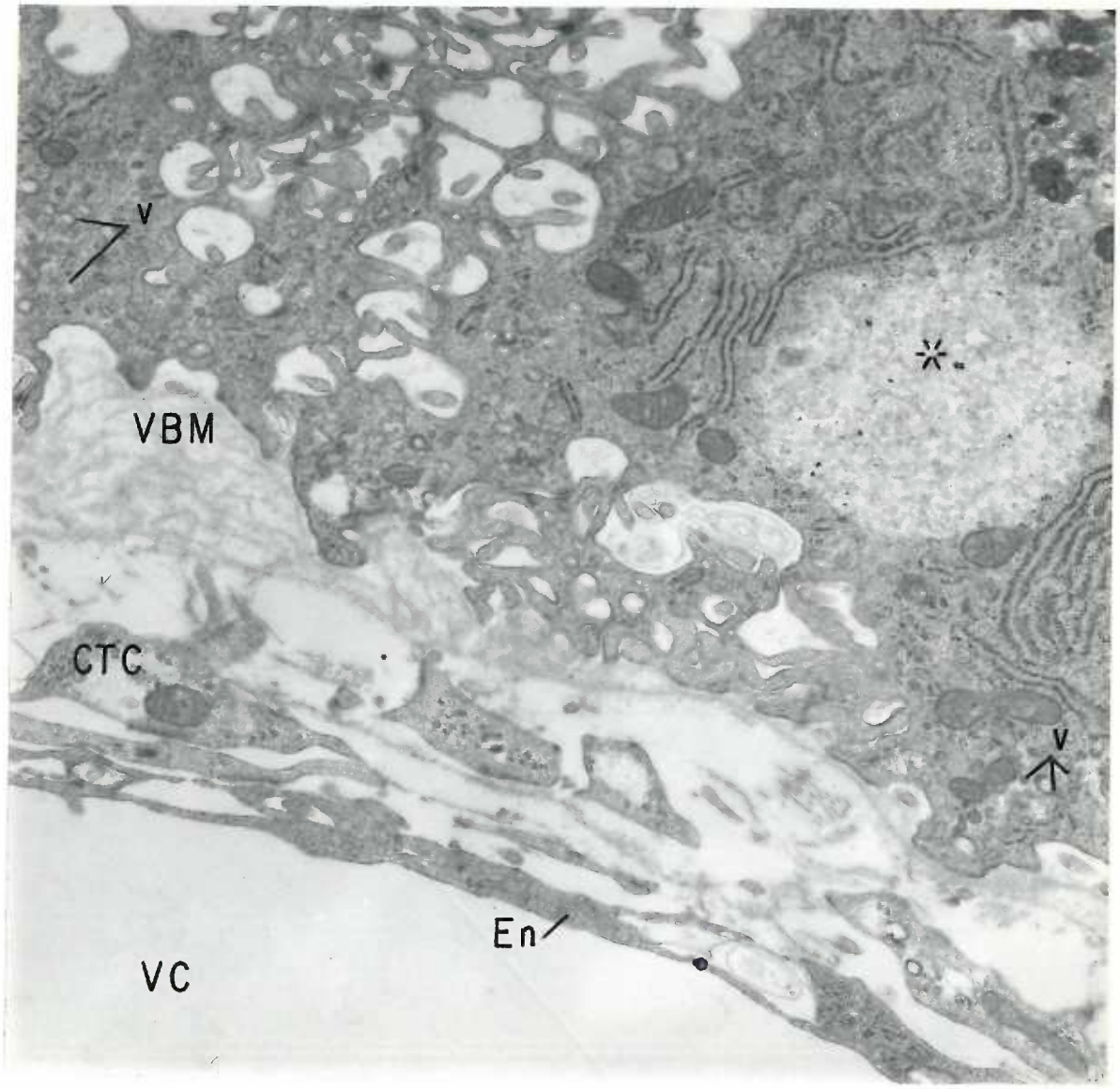

112

FIGURE 113

Cross section through the base of a villus of a 22 day visceral yolk sac showing the basal portions of four endodermal cells resting on a well developed visceral basement membrane. Magnification 12,900 X. A fine flocculent material of low electron density is seen in the intercellular spaces. Several areas of less dense cytoplasm, some of which contain myelin-like concentric systems of membranes, occur in the upper left cell. Note the close association of golgi microvesicular profiles with such areas (arrows). These areas could represent digested vacuoles or artifacts produced during fixation and/or incubation. Lead phosphate deposits resulting from an incubation with ATP appear in both the visceral basement membrane and the fibrous elements of the connective tissue space.

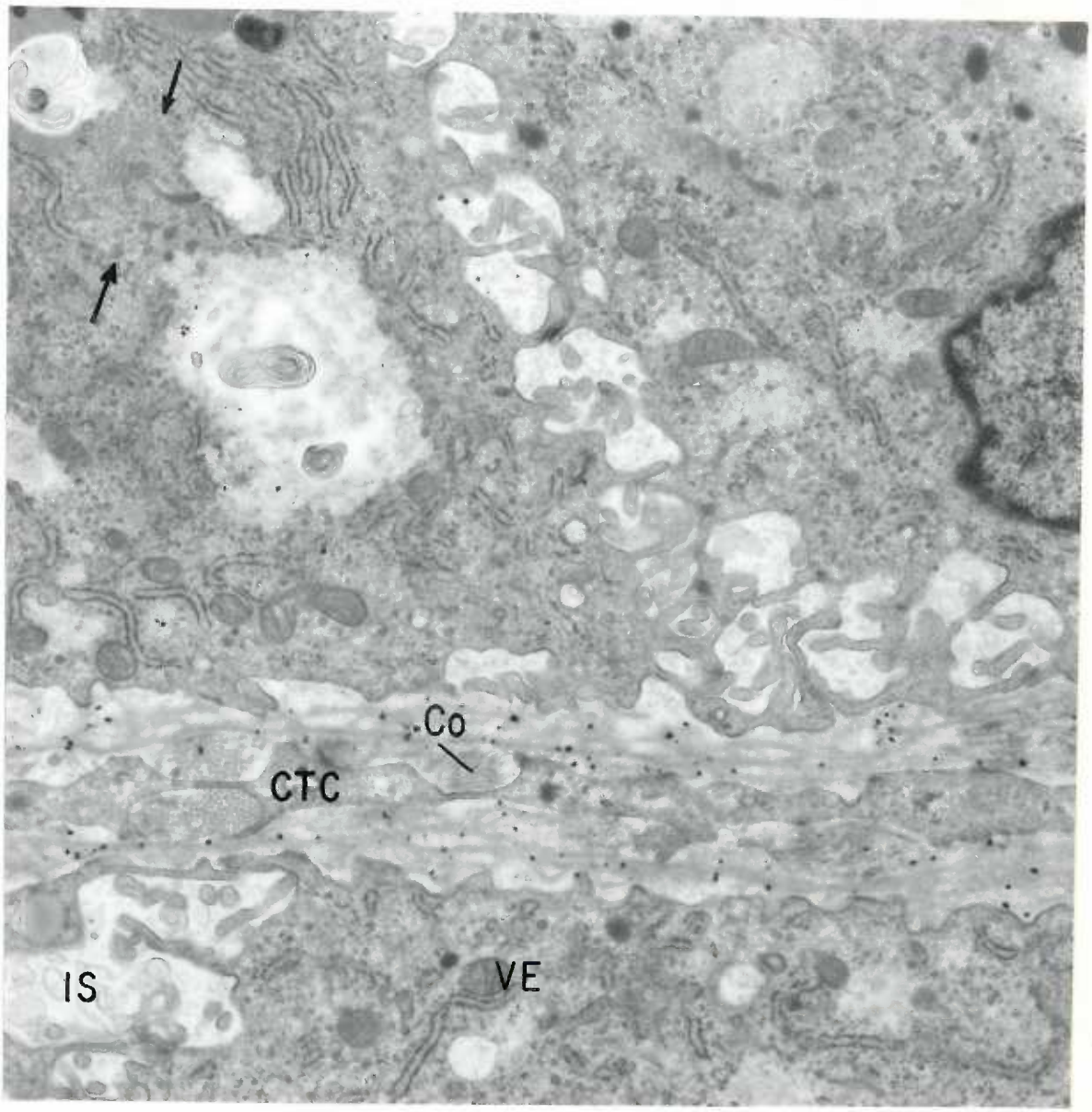

113

FIGURE 114

Oblique section through the supranuclear cytoplasm of several 22 day visceral endodermal cells incubated with ADP as substrate. Magnification 12,900 X. No evidence of activity is seen along the lateral surface membranes, in the distended intercellular spaces or in the supranuclear cytoplasm. Mitochondria, golgi-like microvesicular profiles and strands of granular endoplasmic reticulum are primarily disposed along the lateral margins of the endodermal cells, whereas vacuoles and larger vesicles occur in the center of the cells. The central cytoplasm of the lower right cell, which is seen at a deeper level than the other two cells, exhibits a prominent golgi zone (G). Note the close association of less dense cytoplasm with the disrupted vacuoles (asterisk).

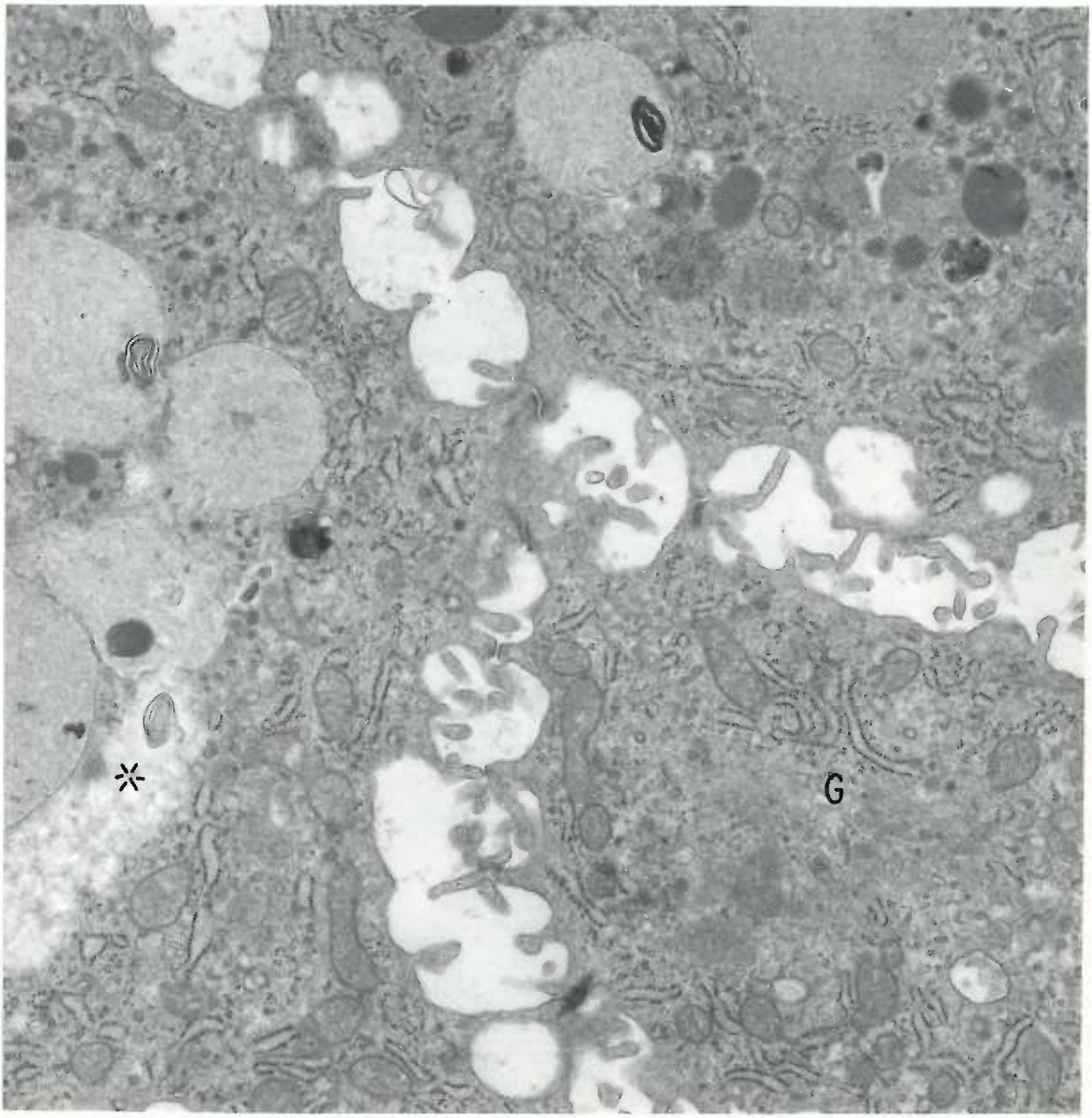

114

FIGURE 115

Detail of the basal portion of a 22 day visceral yolk sac incubated with ADP. Magnification 12,900 X. Activity in this region is limited to trace deposits of lead phosphate found along the visceral basement membrane (VBM). The basal cytoplasm of the two endodermal cells as well as the cytoplasm of the large mesenchymal cell (CTC) seen within the connective tissue space (CTS) contain an abundance of polysomes, granular endoplasmic reticulum and microvesicular profiles. The basal surfaces of the endodermal cells have infoldings and cytoplasmic processes that rest on the visceral basement membrane. A small portion of an adjacent endodermal cell (VE) containing a lipid droplet intervenes between the endodermal cell on the right and its underlying visceral basement membrane. A portion of a vitelline capillary is seen in the lower left corner of the figure.

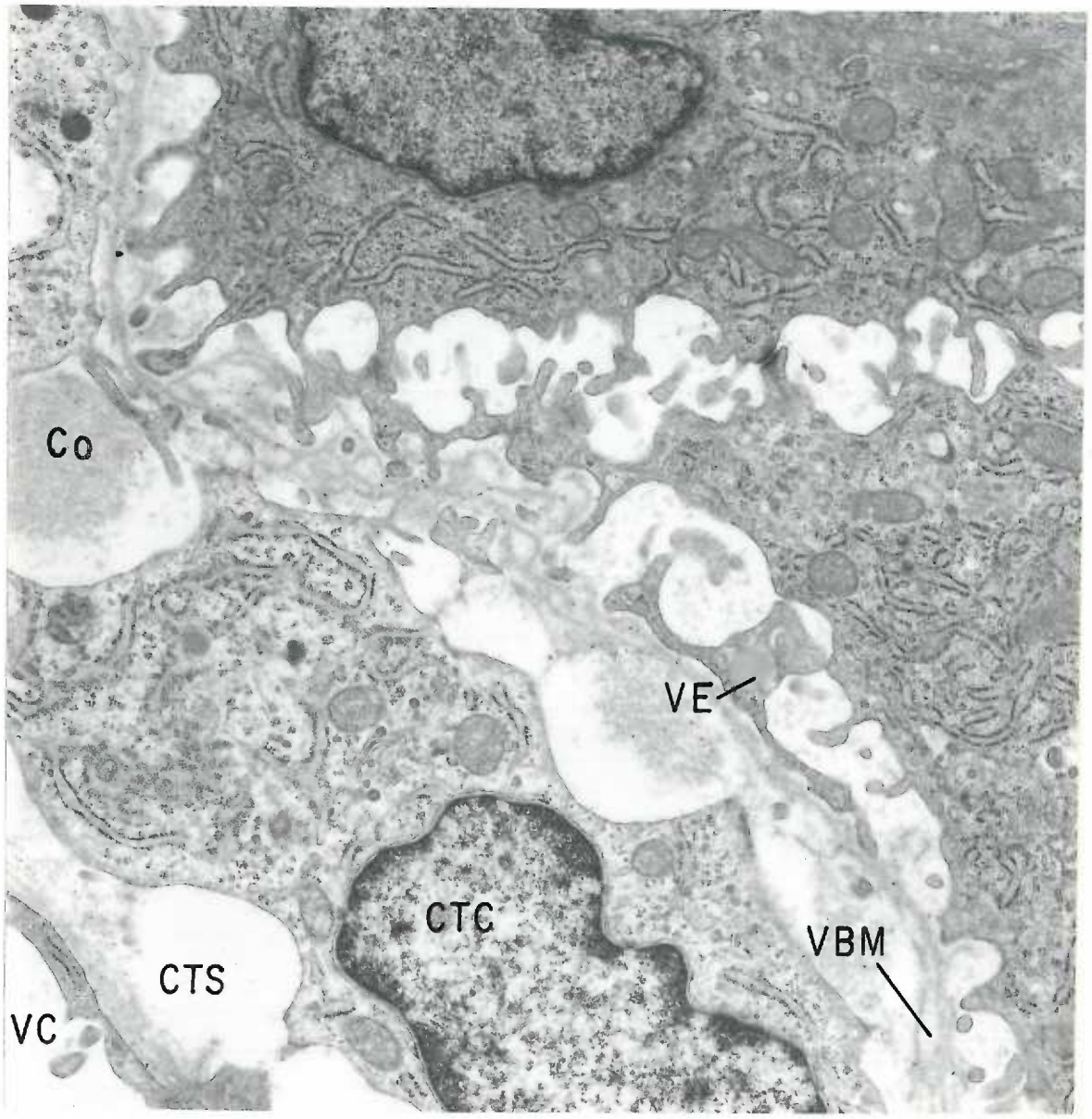

115

FIGURE 116

Apical portion of several 22 day visceral endodermal cells incubated with ADP. Magnification 12,900 X. Punctate deposits of final reaction product occur along the outer aspect of the free surface of the plasma membrane and its microvillous projections. In addition to large numbers of smooth surfaced vesicles and vacuoles described in other figures, the apical and supranuclear cytoplasm contain ribosomes, mitochondria and ribosome-studded profiles of endoplasmic reticulum containing a finely granular material of moderate electron density.

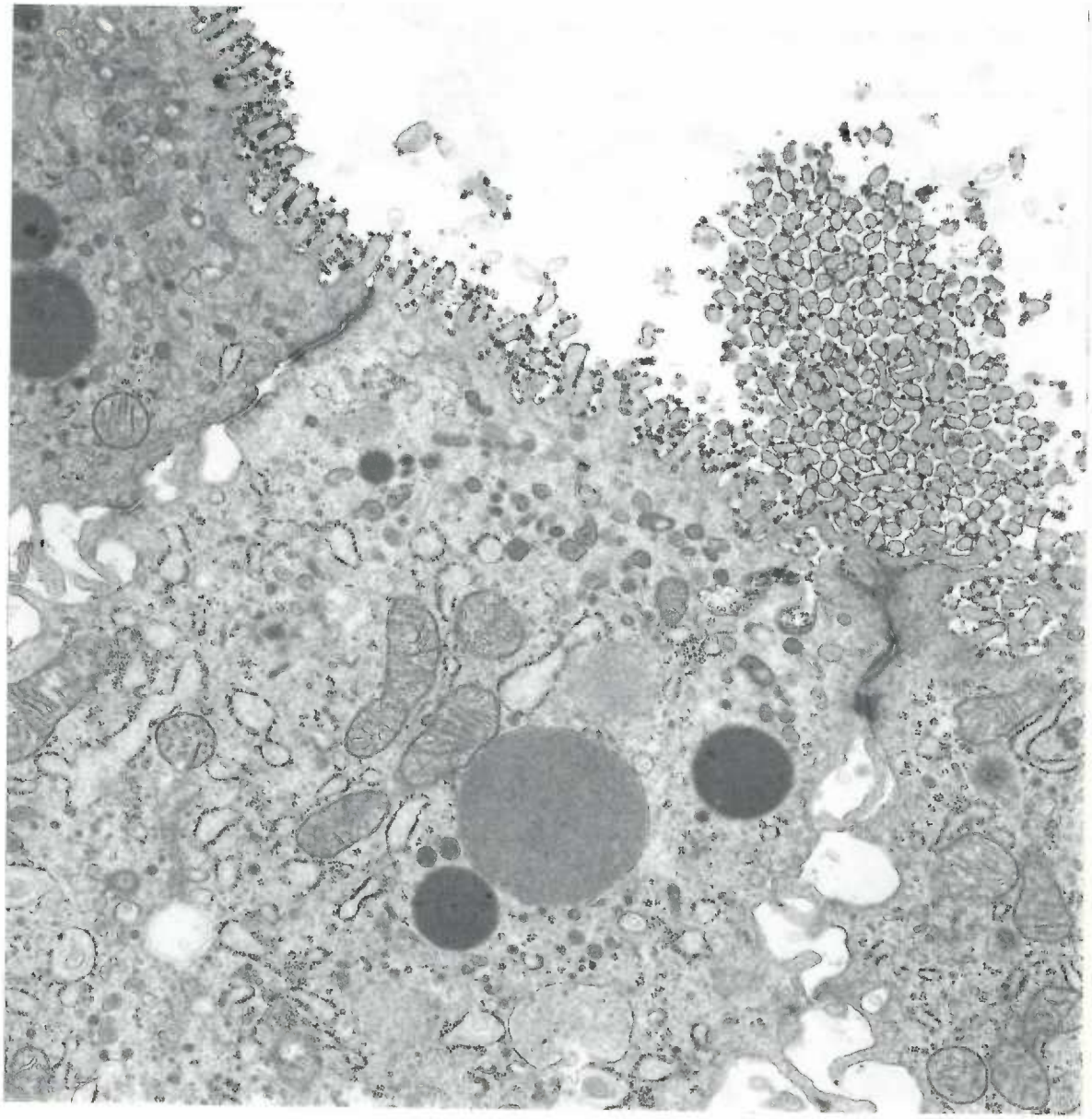

116

FIGURE 117

Cross section through the basal portion of a 22 day visceral yolk sac incubated with ATP. Magnification 12,900 X. Deposits of lead phosphate appear as described in Figure 113. The basal lamina of the thick visceral basement membrane (VBM), which has a lacy appearance, follows the contour of the base of the visceral epithelium and extends into the interstices between the basal projections.

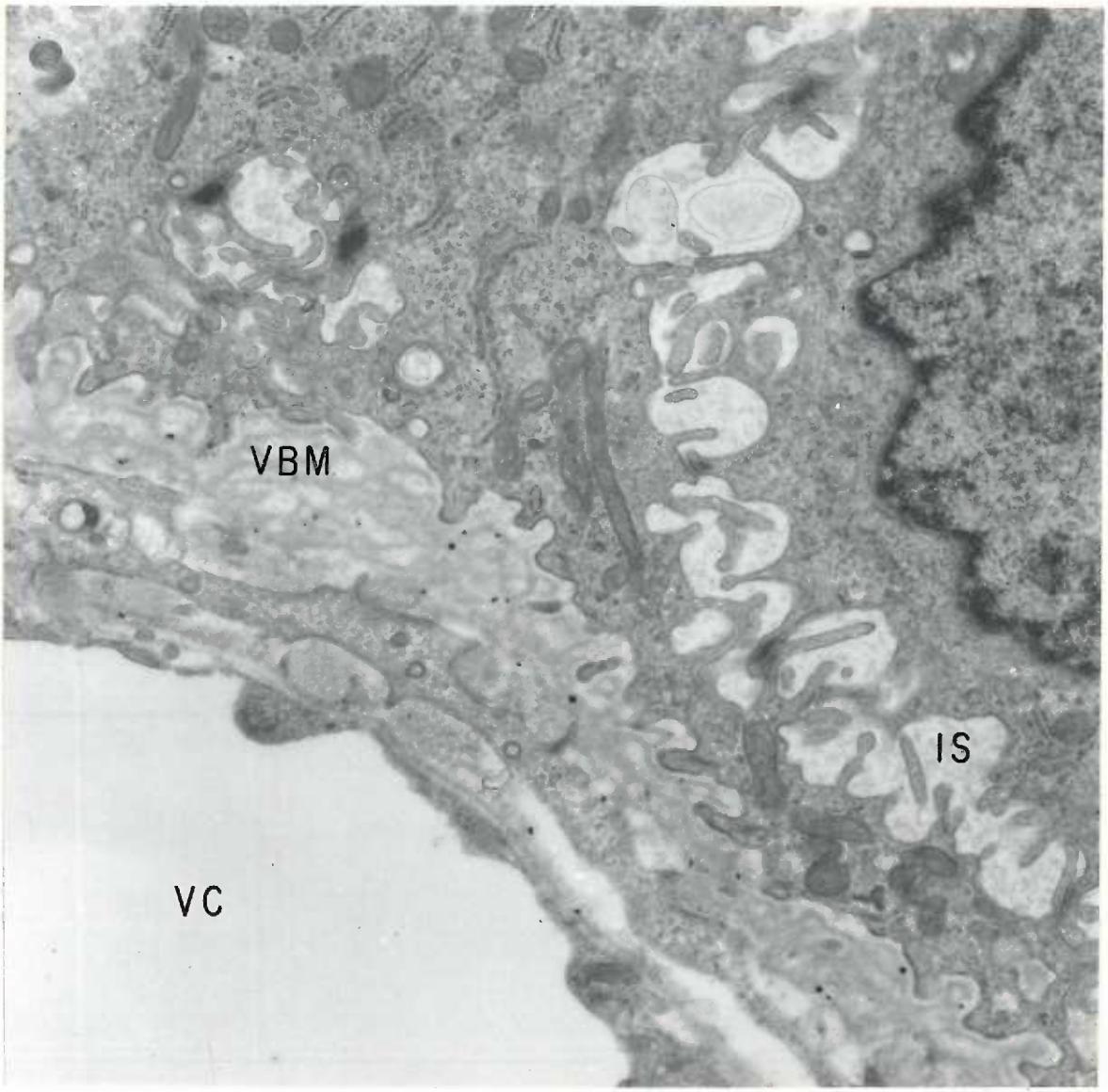

117

FIGURE 118

Basal portion of a 22 day visceral yolk sac incubated with ATP. Magnification 12,900 X. As compared with Figure 113, only an occasional deposit of lead phosphate appears in the visceral basement membrane. A fine flocculent material is seen within the intercellular space between the two endodermal cells (long arrows). Similar appearing material also occurs in the lumen of a vitelline capillary (VC). Note that the endothelium becomes extremely attenuated and exhibits cytoplasmic pores or fenestrations (short arrows).

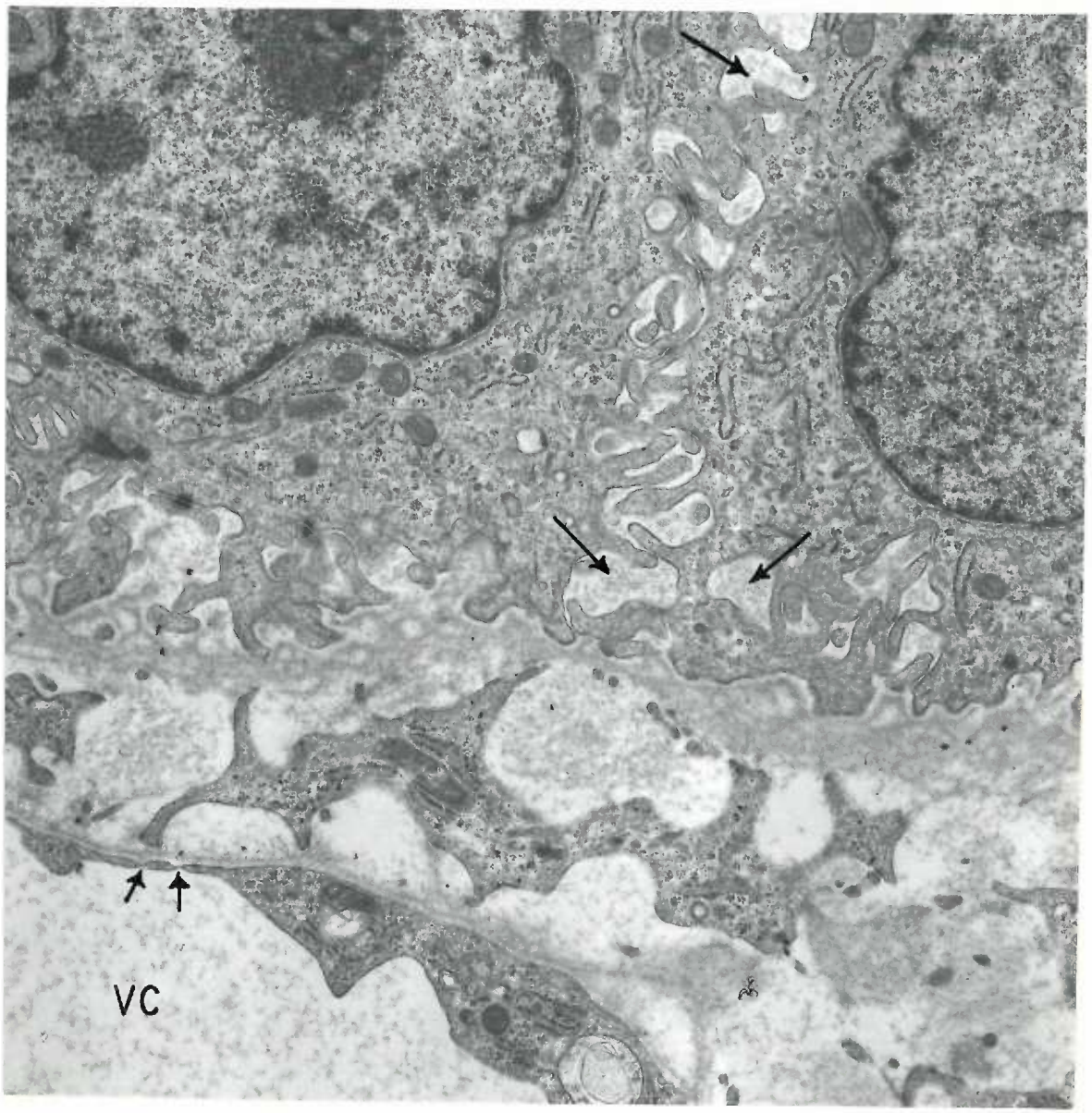
VC

Figures 119-134 are of visceral yolk sac placentae from rats whose pregnancies were artificially prolonged to 25 days (three days beyond the normal time of parturition).

FIGURE 119

General view of the 25 day visceral yolk sac incubated with ADP as substrate. Magnification 4,940 X. The visceral epithelium (VE) consists of squamous cells whose overlapping lateral surfaces tightly interdigitate (arrows). The basal surface of the endodermal cells appears relatively smooth and rests on a well developed visceral basement membrane (VBM). The underlying connective tissue space (CTS) is densely packed with collagen fibrils (Co) and mesenchymal cells (CTC). The serosal basement membrane (SBM) which separates the mesothelium from the connective tissue space is also well developed. Note that lipid droplets (Li) appear in the visceral endoderm and the mesothelium (Mes). Final reaction product is limited to the luminal surface of the visceral epithelium and its microvillous projections.

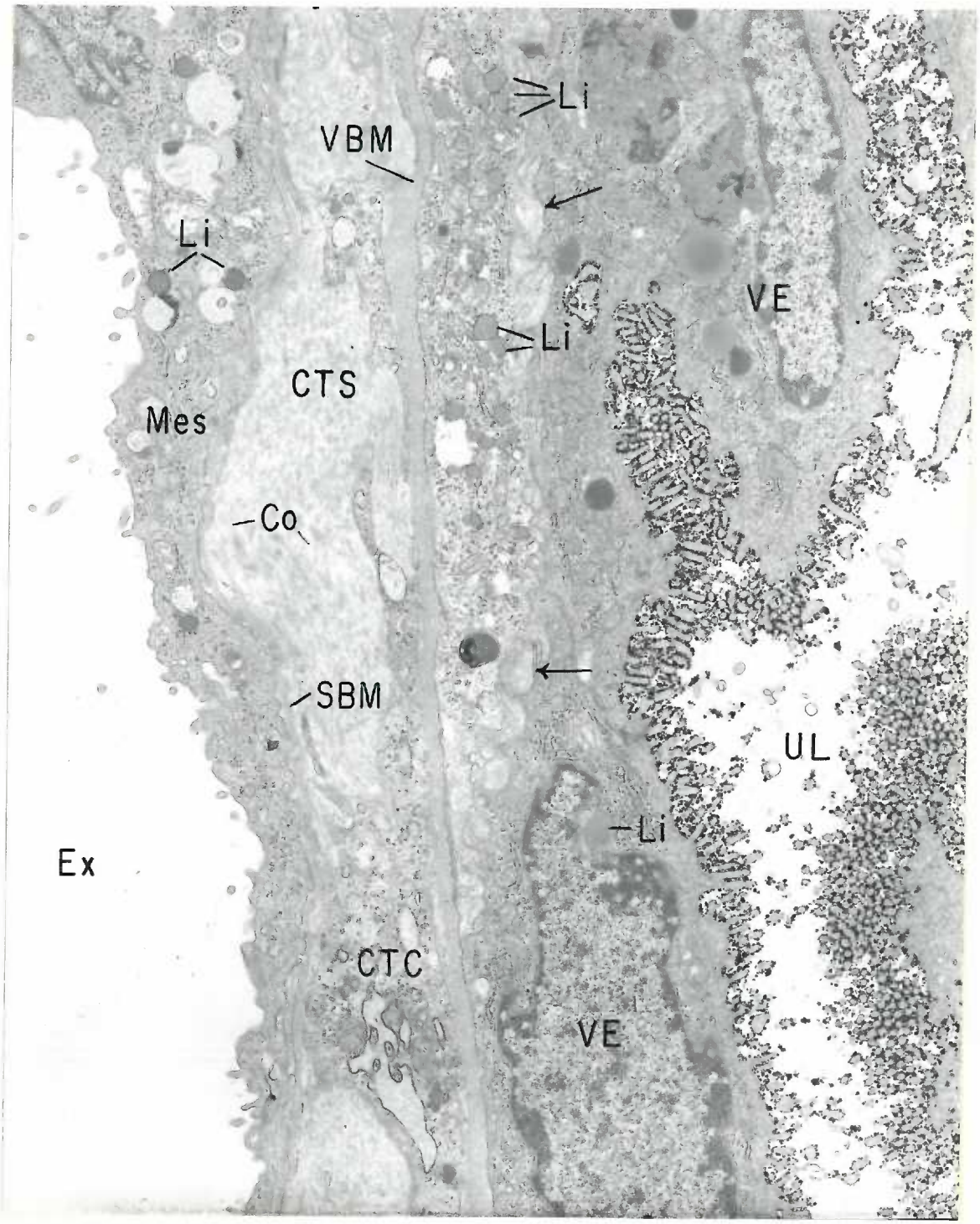
Li
VBM
Li
Li
VE
CTS
Mes
Co
SBM
UL
Li
Ex
CTC
VE

FIGURE 120

Cross section through a villous of the 25 day visceral yolk sac incubated with ATP as substrate. Magnification 4,940 X. A number of finely branched mesenchymal cell processes (CTC) intervene between the visceral basement membranes (VBM) of diametrically apposed endodermal cells (VE). Note the large number of closely spaced vesicles and vacuoles (V) which dominate the endodermal cytoplasm on the right side of the figure. The uterine cavity (UL) in the upper left corner contains a granular material throughout which dense precipitates of lead phosphate are distributed. The bordering microvilli display only sparse deposits of final product whereas, those microvilli extending into a clear uterine space (UL) in the lower right corner, display a dense coat of final product.

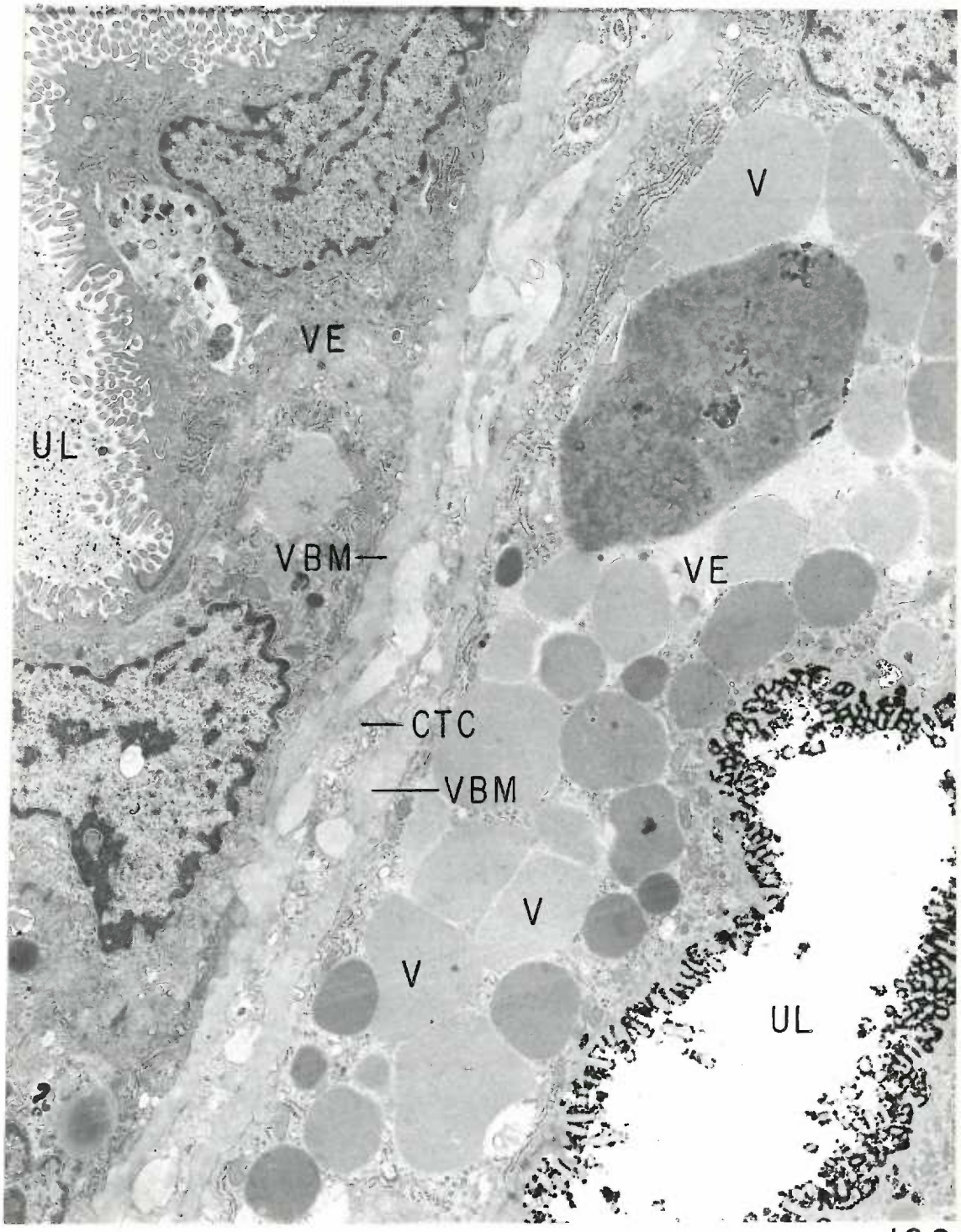

120

FIGURE 121

Twenty-five day visceral yolk sac incubated with ADP as substrate. Magnification 4,110 X. Fine deposits of lead phosphate are scattered throughout the accumulation of granular material which overlies the visceral epithelium (VE). In this area final reaction product is absent from the luminal surface membrane and its microvillous projections. Irregular deposits of lead phosphate, however, are seen in the connective tissue space (CTS).

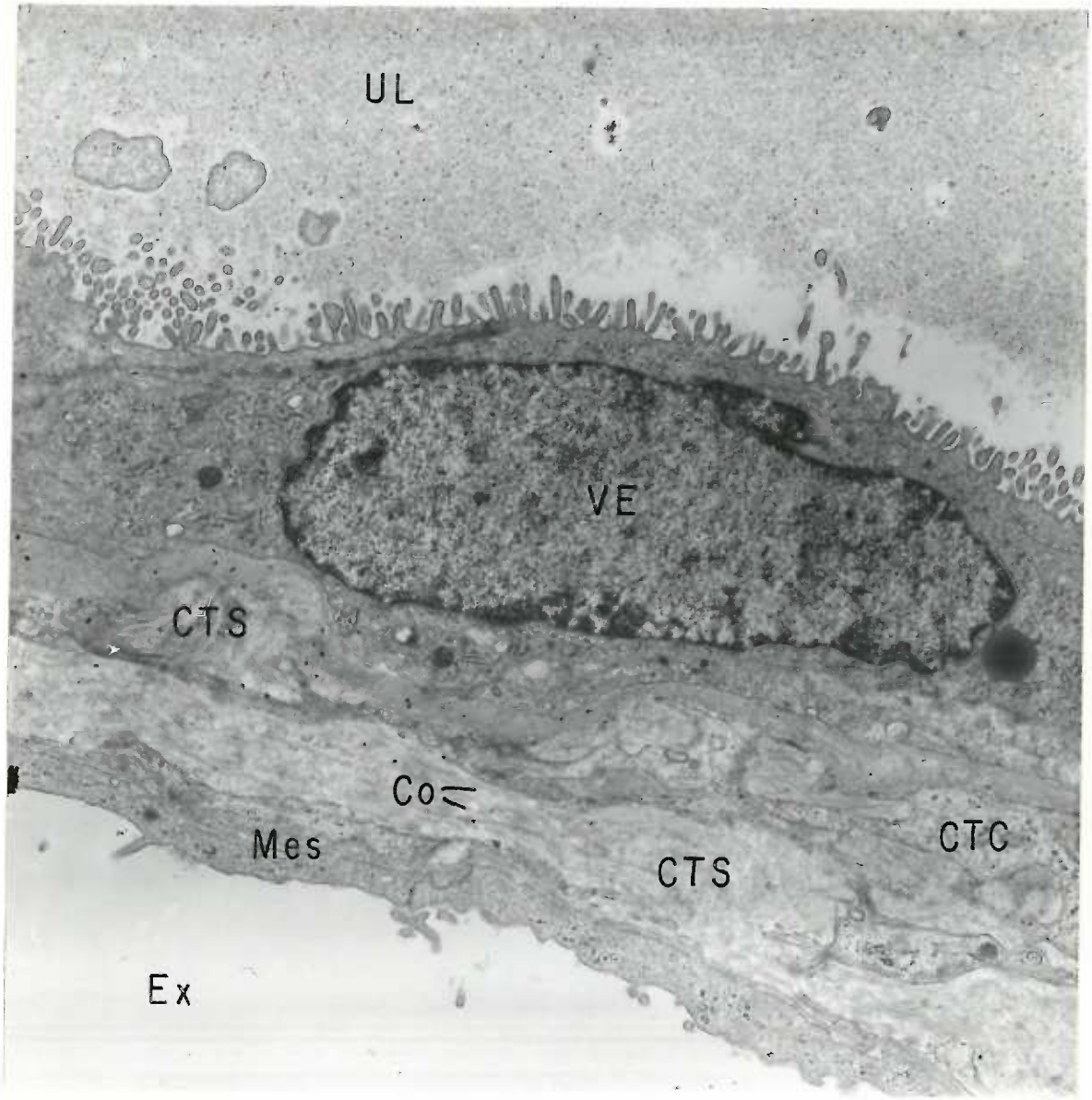
UL
VE
CTS
Co
Mes
CTS
CTC
Ex

FIGURE 122

Twenty-five day visceral yolk sac incubated with ADP as substrate. Magnification 4,110 X. A few microvilli on the free surface of the middle endodermal cell have globular expanded tips (arrows) which contain granular material similar in electron density to the material seen within the uterine lumen (UL). Large vacuoles (V) with dense inner profiles are evident. A mesenchymal cell (CTC) intervenes between the visceral (VBM) and serosal basement membranes (SBM). The cytoplasm of this cell contains ribosomes, fine fibrils and granular endoplasmic reticulum (ER) whose dilated cisternae contain a fine granular material. As in Figure 121, final reaction product is absent from the free surface of the visceral epithelium.

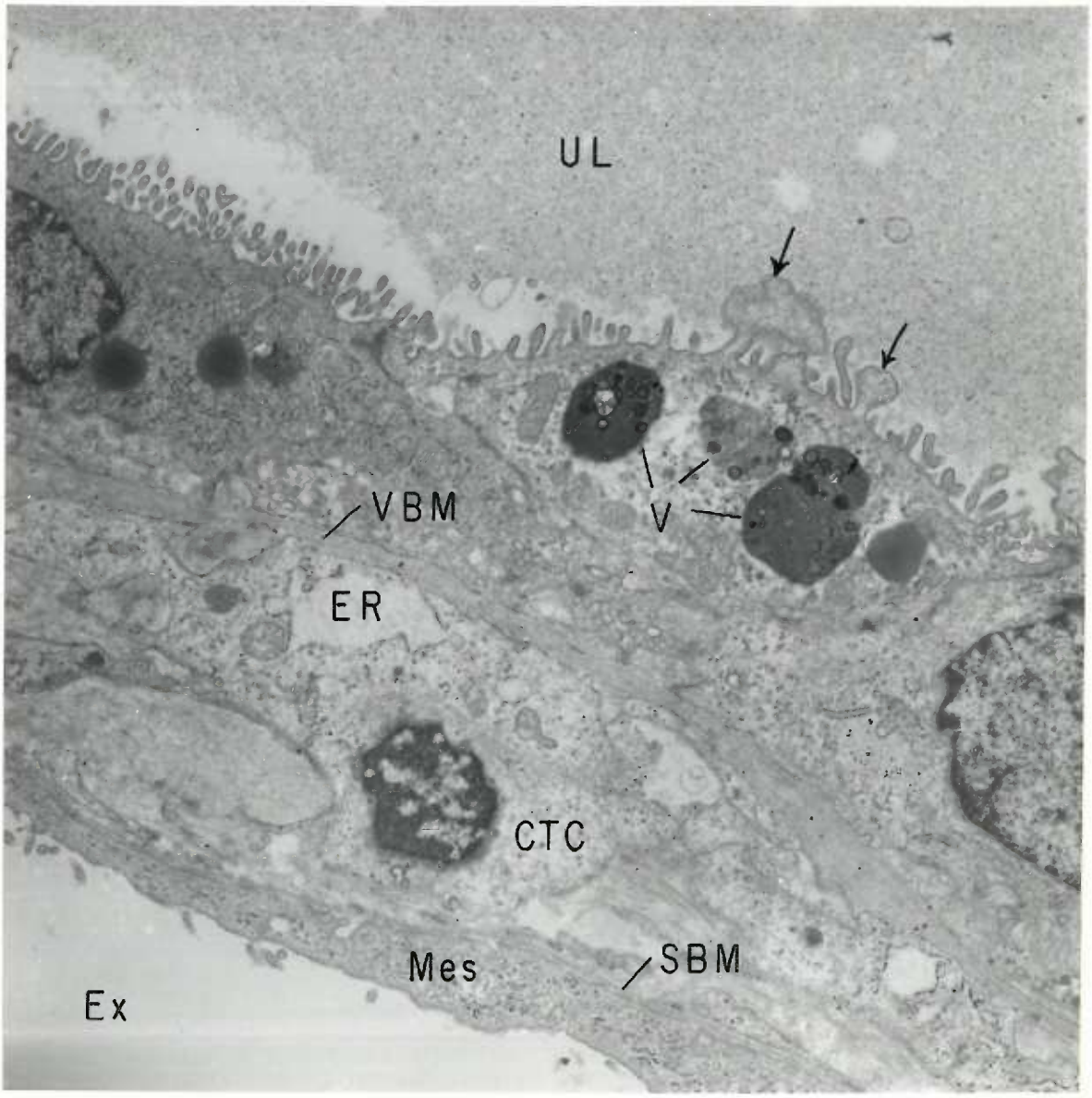

122

FIGURE 123

Twenty-five day visceral yolk sac incubated with ADP as substrate. Magnification 8,170 X. The globular expanded tips of a number of microvilli have coalesced to form large bulbous enlargements filled with a flocculent or granular material of moderate electron density (arrows). Note that the endodermal cytoplasm is richly provided with microvesicular profiles (v). Only an occasional deposit of lead phosphate is found at the surface of microvilli and throughout the connective tissue space.

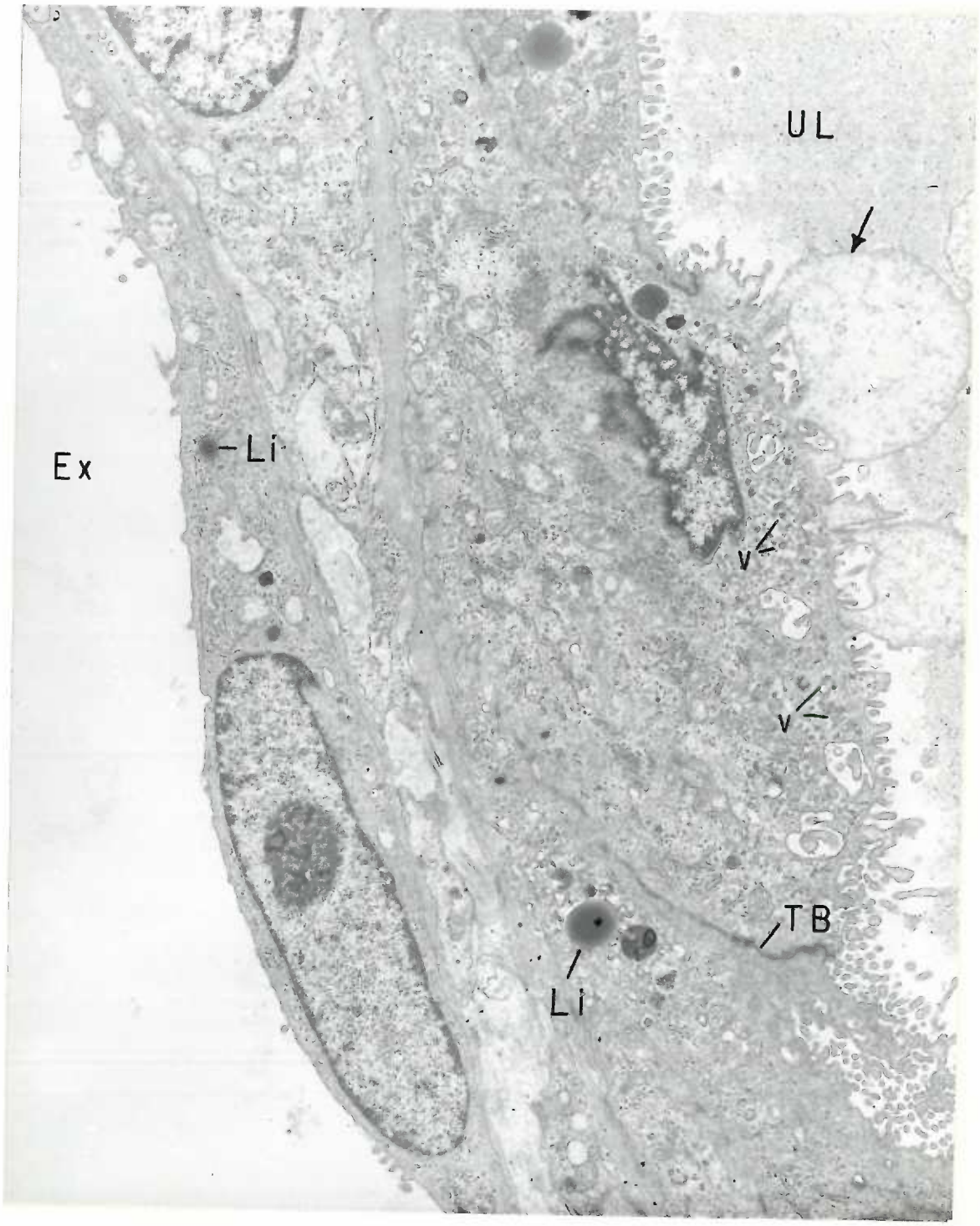

123

FIGURE 124

Twenty-five day visceral yolk sac incubated with ATP as substrate. Magnification 12,900 X. Final reaction product along the luminal surface of the visceral endoderm (VE) occurs as relatively large and closely spaced beads of lead phosphate. Activity along the lateral (long arrows) and luminal surfaces of the mesothelium (Mes), on the other hand, appears as small irregularly distributed deposits. Note that some of the mitochondria show longitudinally oriented cristae (short arrows).

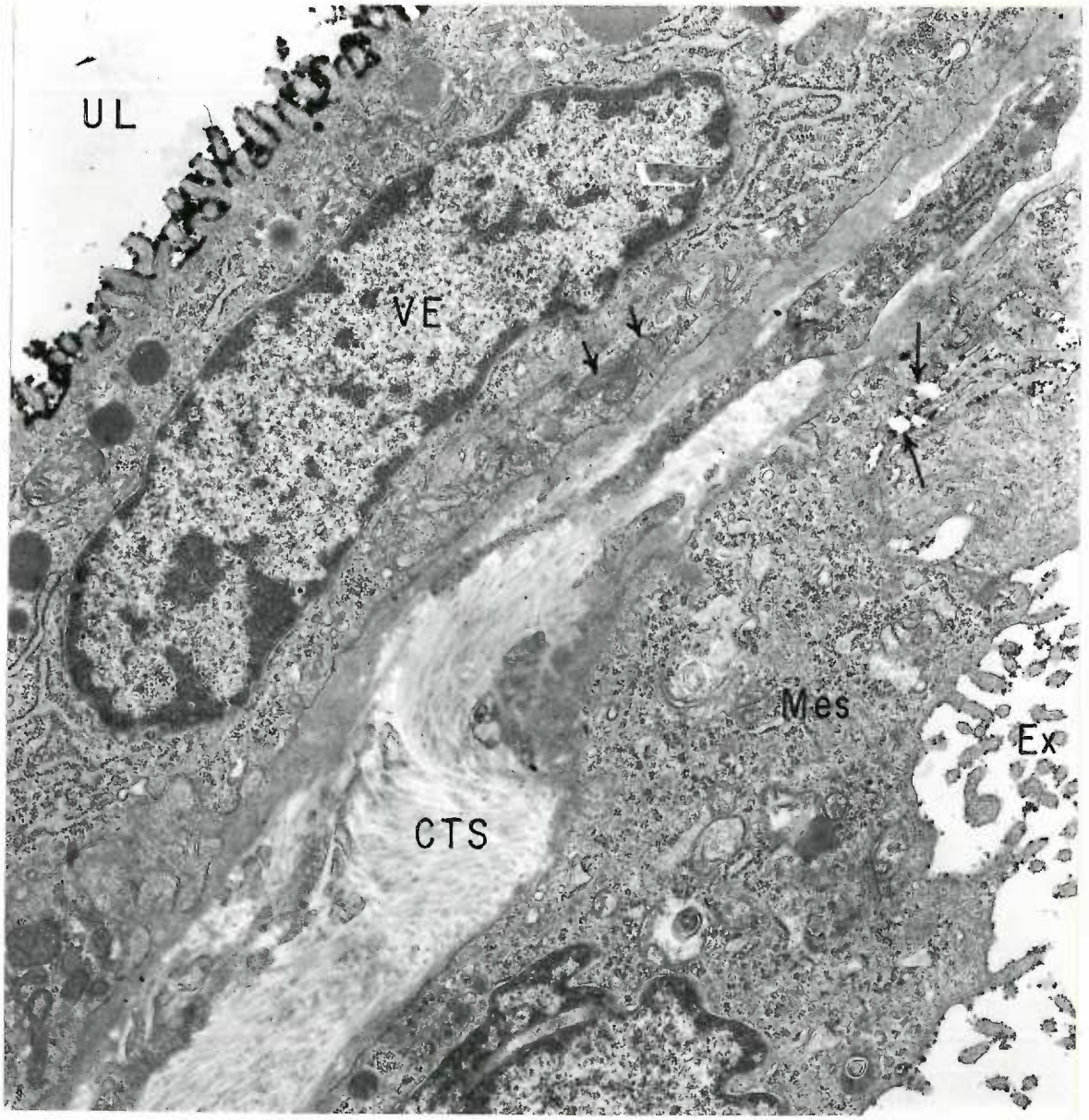

124

FIGURE 125

Twenty-five day visceral yolk sac incubated with ATP as substrate. Magnification 12,900 X. Complex plications of the lateral plasma membranes greatly reduce the width of the endodermal intercellular space (long arrows). Final reaction product along the free surfaces of the mesothelium and visceral epithelium appears as described in Figure 124. Note that ATPase activity is present on the extracellular side of the lateral plasma membranes and in the intercellular spaces of the mesothelium (short arrows), but not on those of the visceral endoderm.

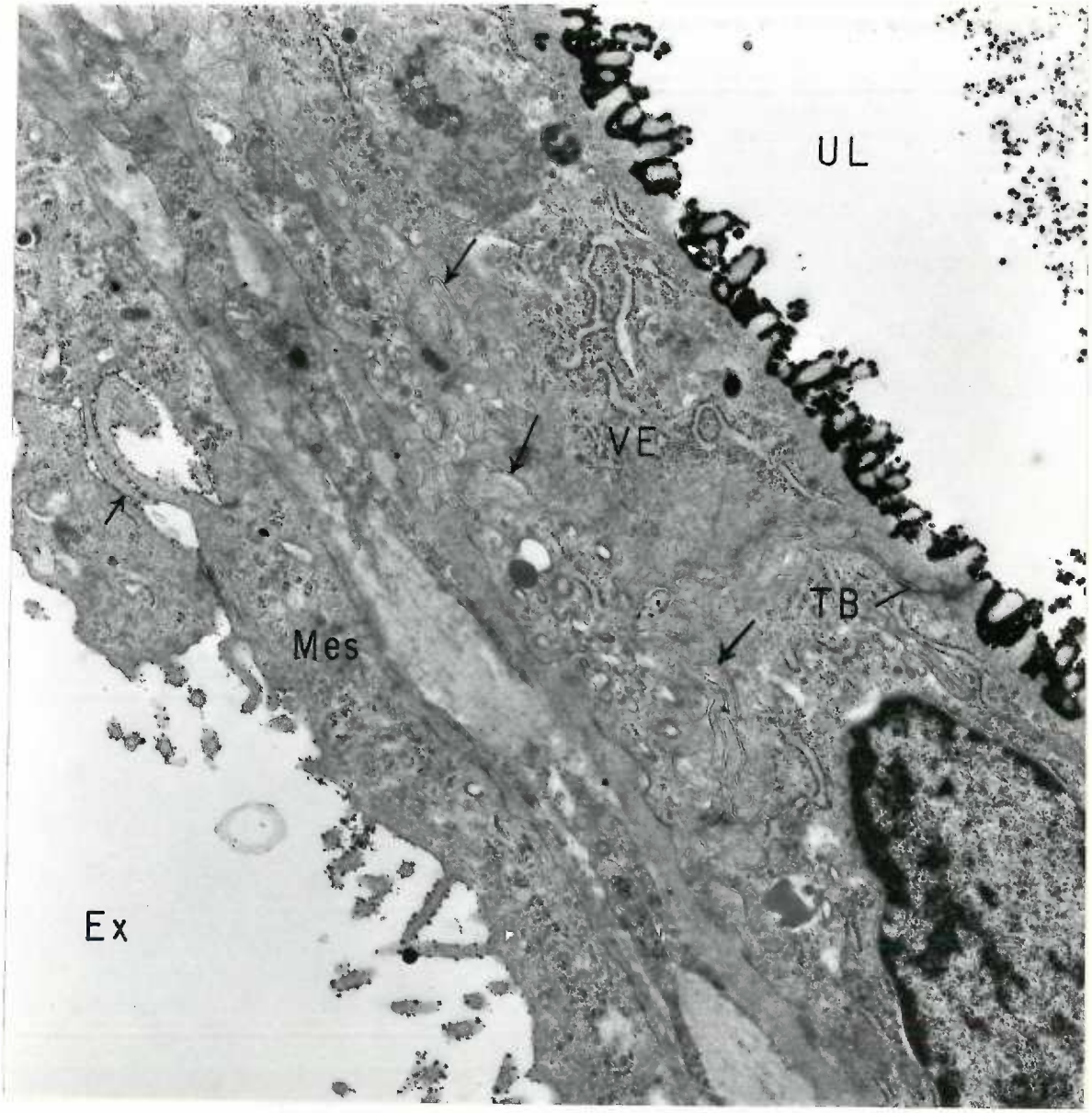

125

FIGURE 126

Twenty-five day visceral yolk sac incubated with ATP as substrate. Magnification 12,900 X. Final reaction product is distributed as described in Figures 124 and 125. Note, however, that only moderate deposits of activity occur where the free surface of the visceral epithelium is bordered by large accumulations of granular material. A number of rather large vacuoles (V) together with small vesicular profiles (v) are scattered throughout the endodermal cytoplasm. Mitochondria with longitudinally oriented crisate are evident (arrows).

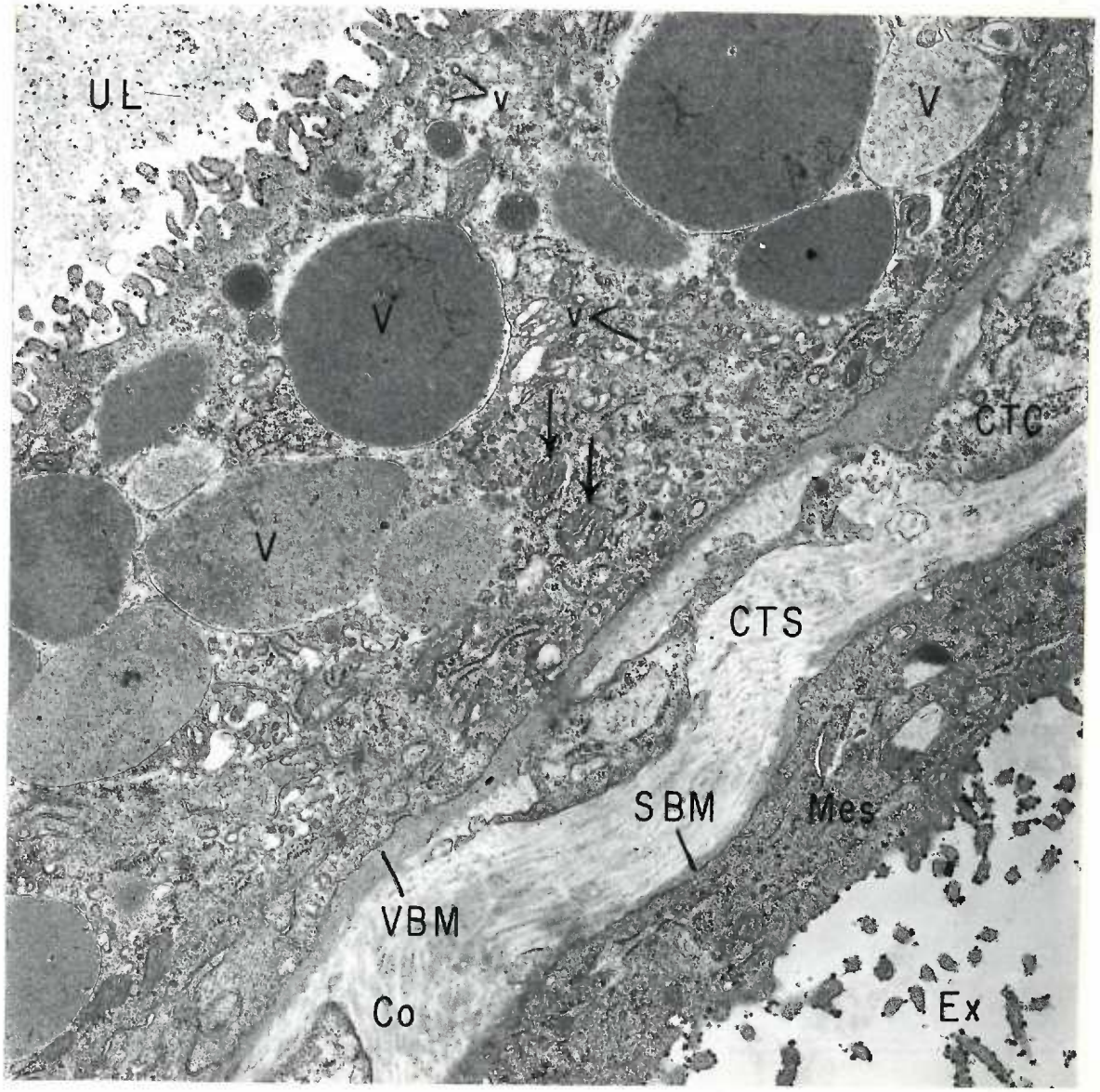

126

FIGURE 127

Twenty-five day visceral yolk sac incubated with ATP as substrate. Magnification 12,900 X. ATPase activity is distributed as described in Figure 126. The larger vacuoles (V) within the endodermal cytoplasm appear irregular in shape with discontinuous limiting membranes and contain agglomerations of myelin-like concentric systems of membranes intermingled with granules and vesicular profiles of varying densities. The overall appearance of such structures is that of residual bodies or disintegrating vacuoles.

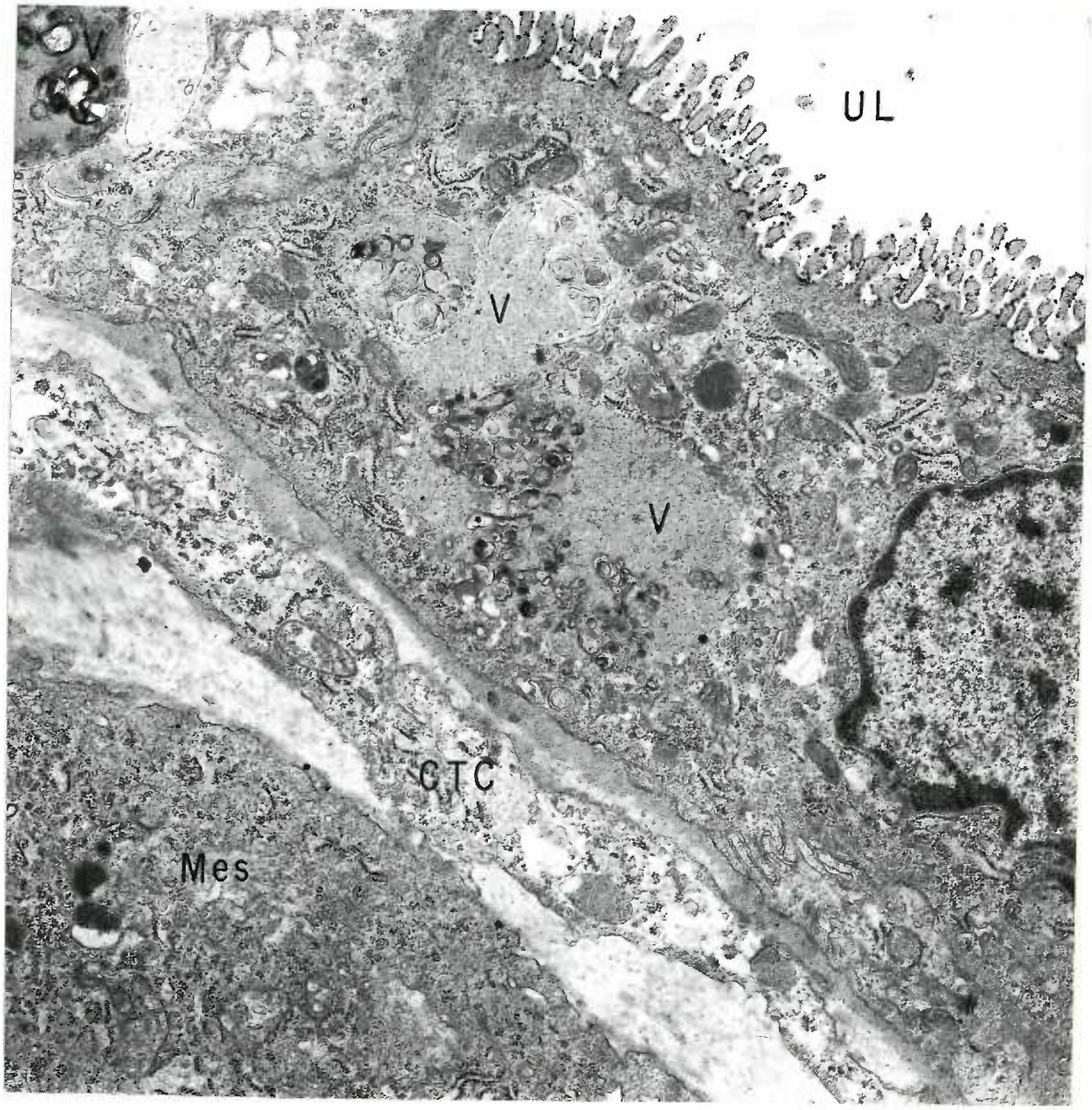

127

FIGURE 128

Twenty-five day visceral yolk sac incubated with AMP as substrate. Magnification 12,900 X. Final reaction product occurs as sparse deposits at the luminal surface of the visceral epithelium. Cytoplasmic projections from the lateral surfaces of adjoining endodermal cells loosely interdigitate to form large intercellular spaces (IS) which contain flocculent material of low electron density. A number of mesenchymal cell processes (CTC) intervene between the visceral epithelium and an underlying vitelline capillary (VC).

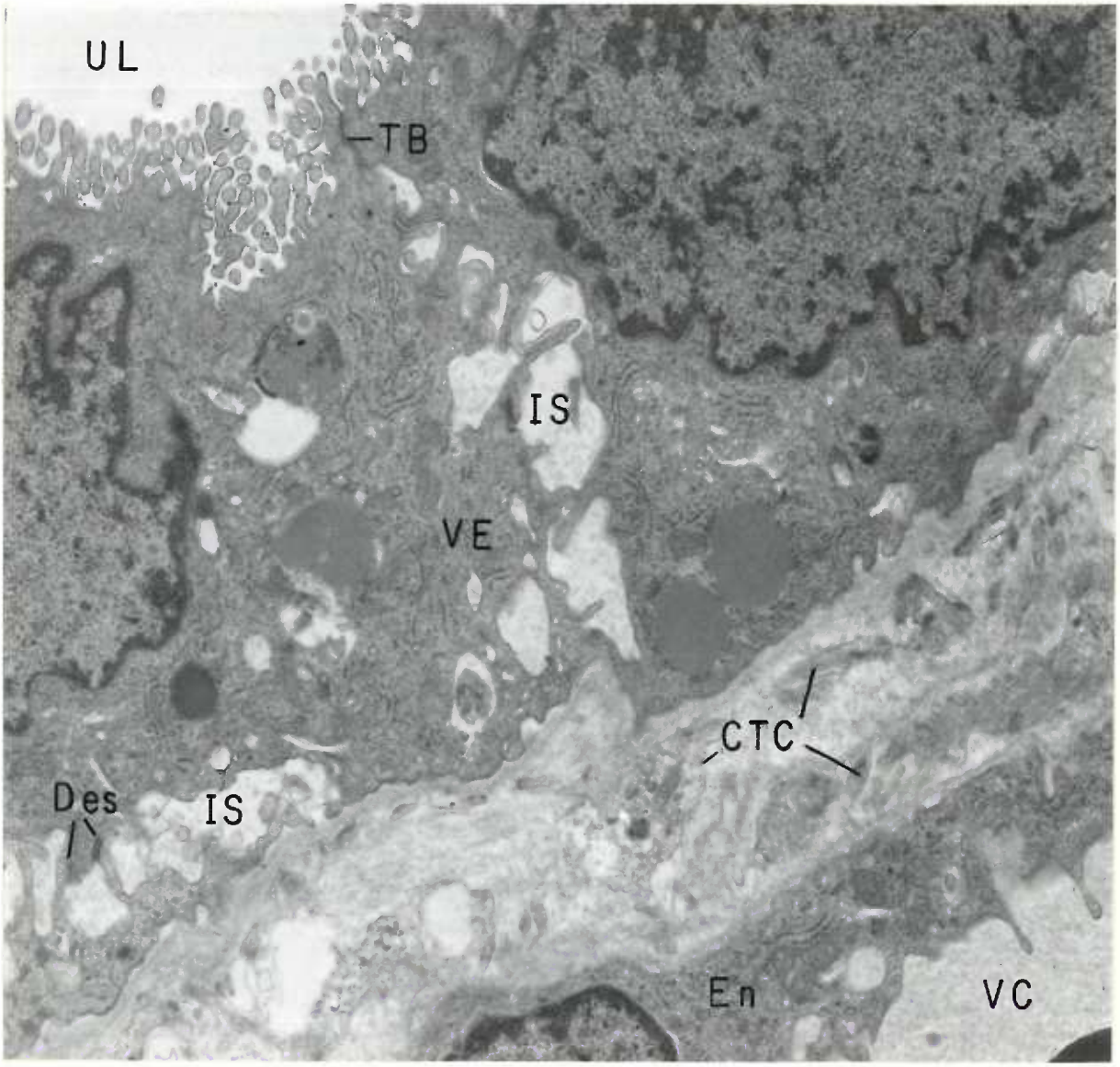

128

FIGURE 129

Twenty-five day visceral yolk sac incubated with AMP as substrate. Magnification 18,600 X. Sparse deposits of final product are distributed along the luminal surface of microvilli. A typical junctional complex is seen at the apical end of the intercellular space. Note the tonofibrils (To) converging upon the desmosome from the adjacent cytoplasm. Numerous fibrils (Fi) are also seen in the basal cytoplasm.

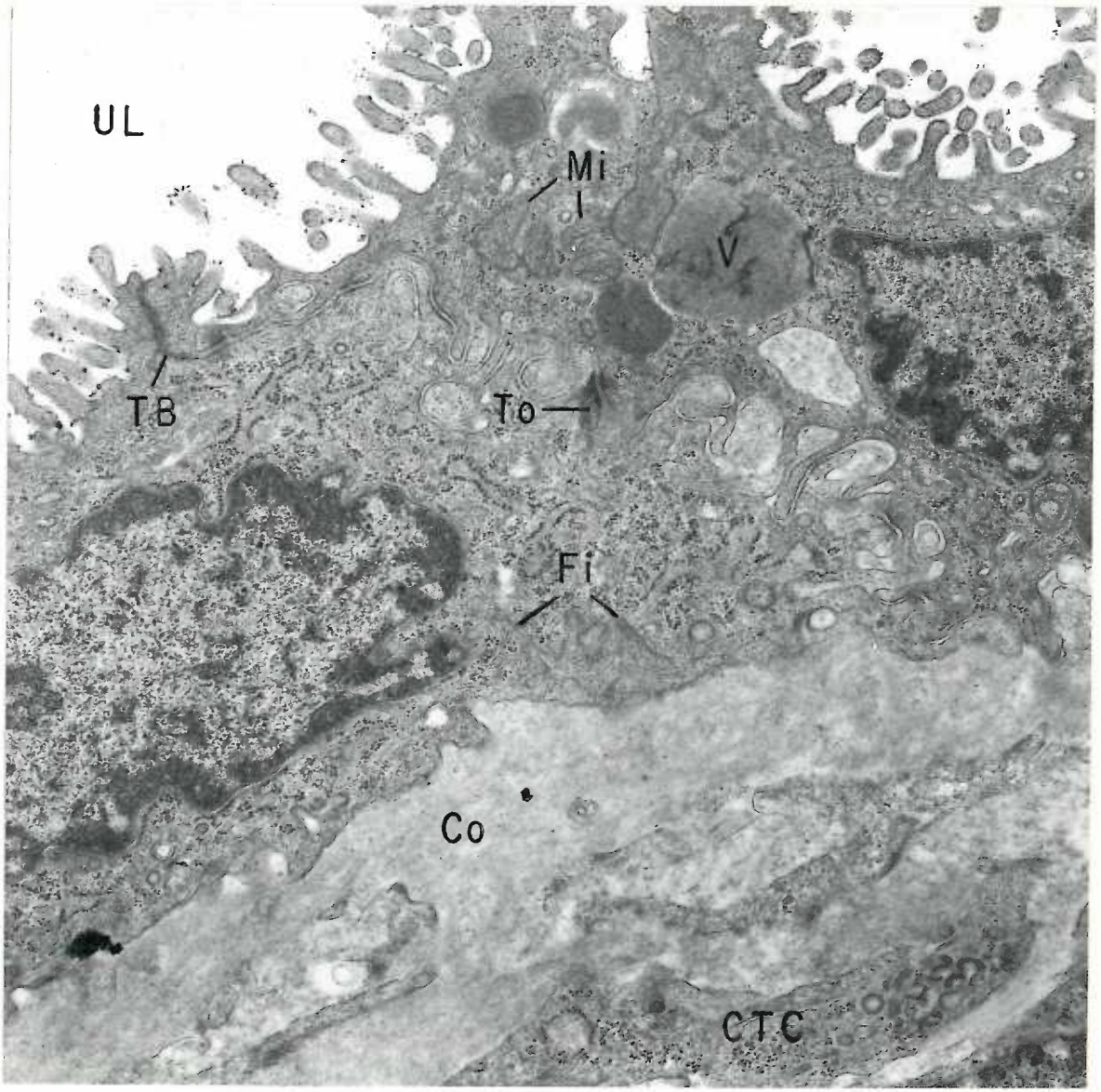

129

FIGURE 130

Twenty-five day visceral yolk sac incubated with AMP as substrate. Magnification 12,900 X. Final reaction product occurs as described in Figure 128. The cytoplasm of both the endodermal cells (VE) and the endothelial cells (En) lining the underlying vitelline capillary (VC) is richly provided with free ribosomes (Ri) and granular endoplasmic reticulum. Pinocytotic activity (PV) is evident along the basal surface of the endoderm and along the luminal surface of the capillary endothelium (En).

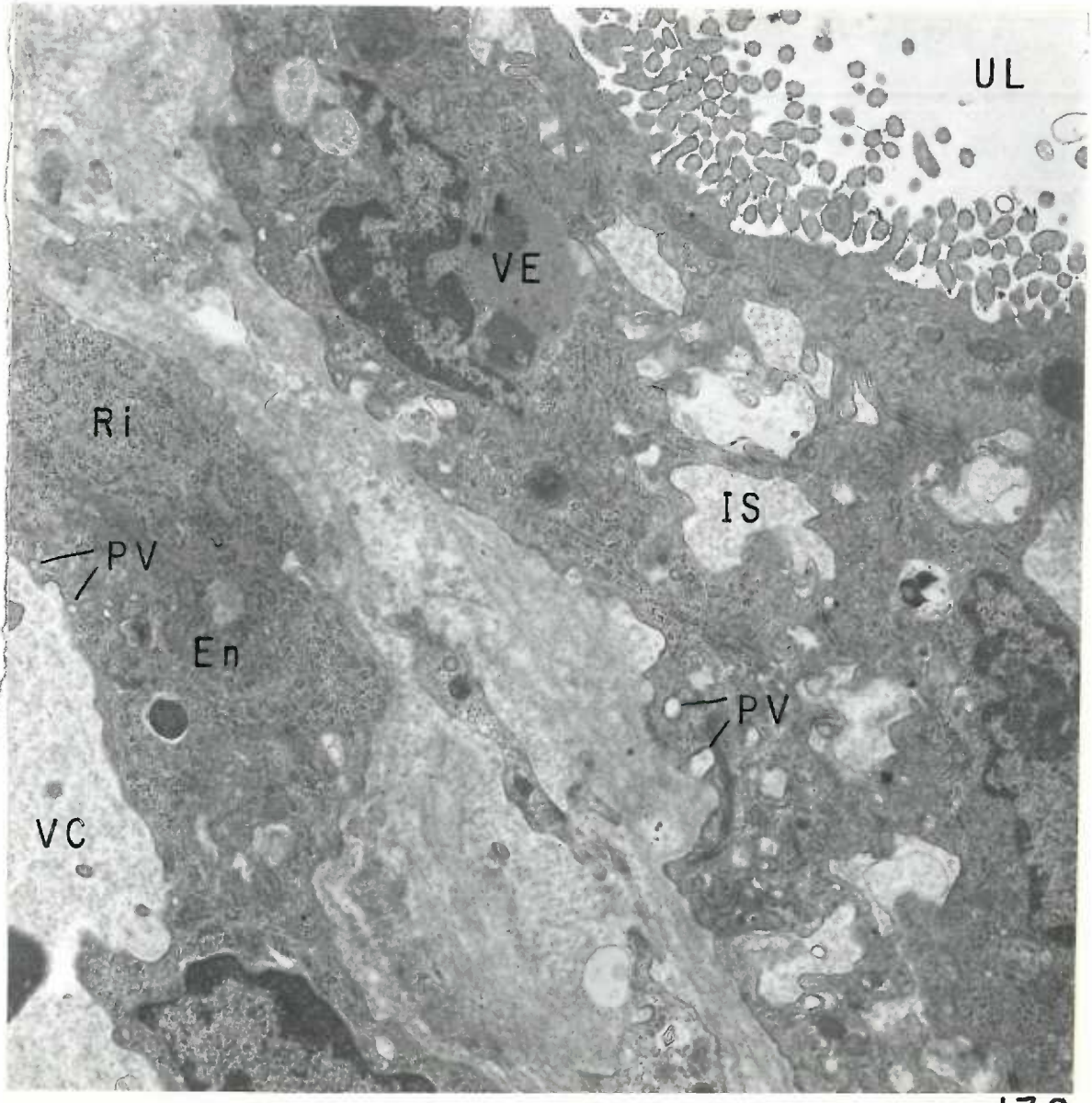

130

FIGURE 131

Twenty-five day visceral yolk sac incubated with ADP as substrate. Magnification 12,900 X. Final reaction product is deposited as dense precipitates at the free surface of the visceral epithelium. The lateral plasma membranes (arrows) of the endodermal cells in the middle of the figure are closely apposed and exhibit few irregularities along their course toward the visceral basement membrane. Large lipid droplets (Li) are evident in the endodermal cytoplasm.

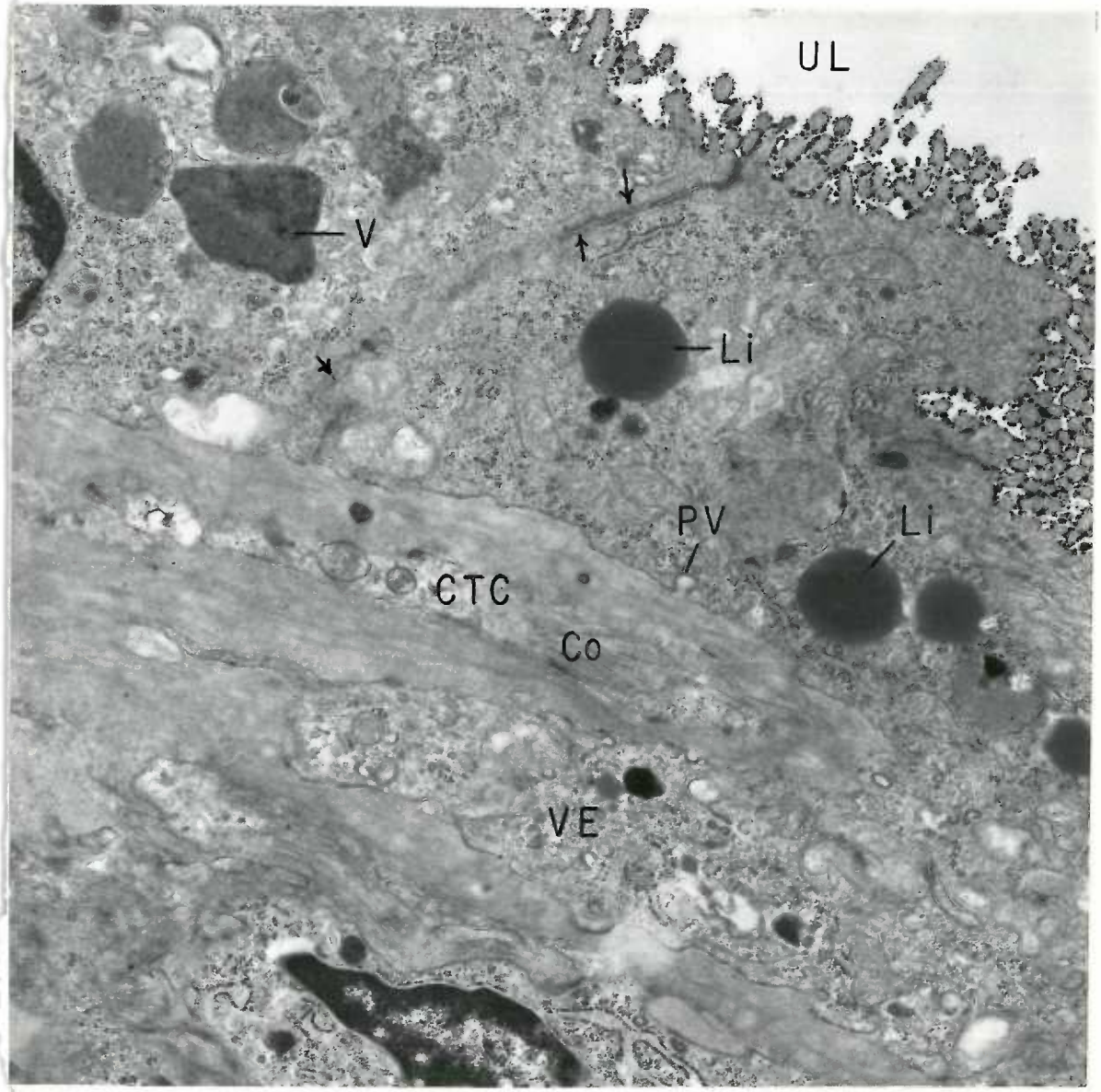

131

FIGURE 132

Twenty-five day visceral yolk sac incubated with AMP as substrate. Magnification 18,600 X. Sparse deposits of final reaction product occur at the free surface of the visceral epithelium. Note the complex system of lateral plications between adjacent endodermal cells. The serosal basal lamina (SBM) is well developed and appears to merge with the dense mat of fibrils (Co) within the connective tissue space as does the thickened visceral basal lamina (VBM).

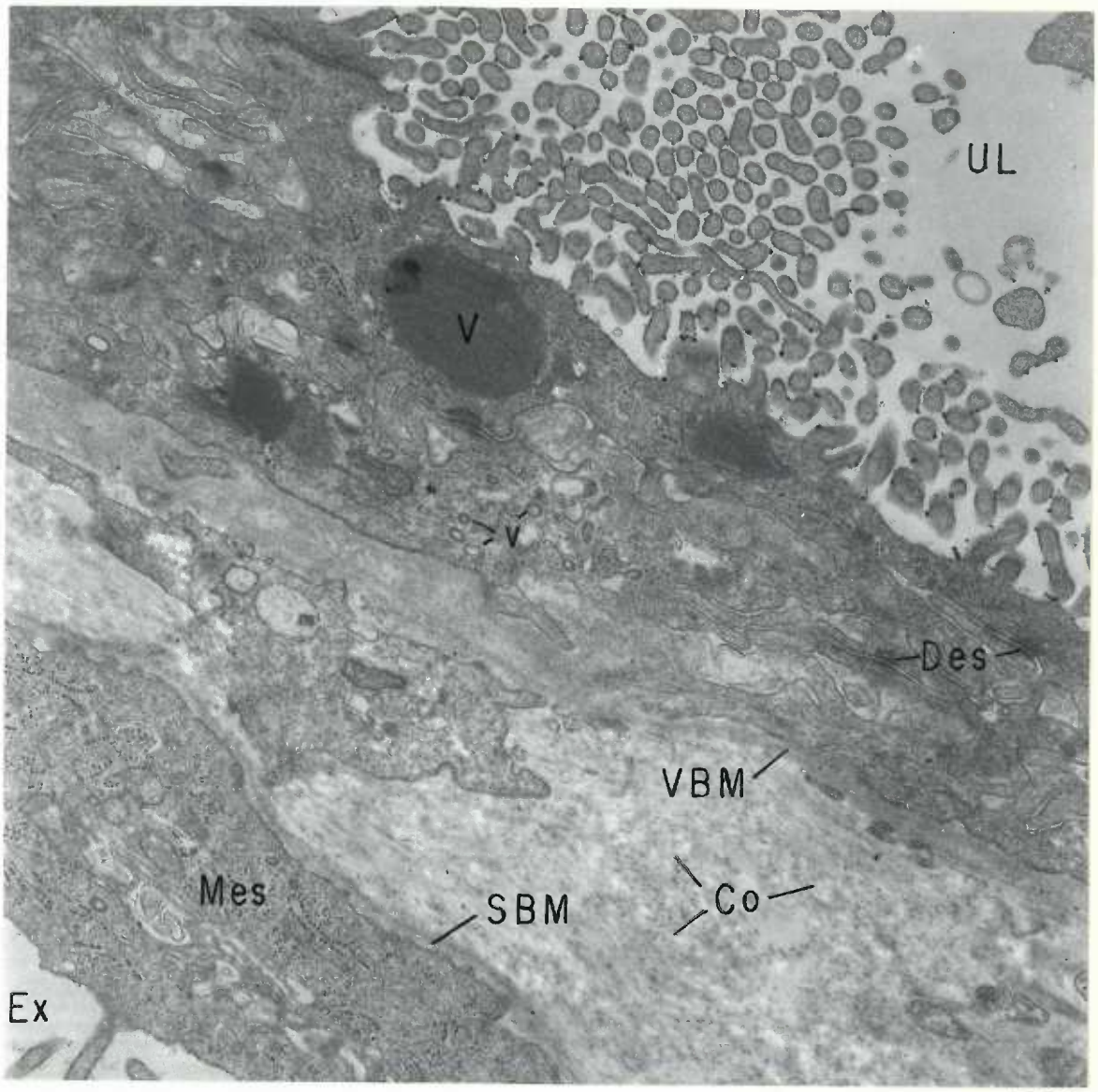

132

FIGURE 133

Cross section of the 25 day mesothelium incubated with AMP as substrate. Magnification 12,900 X. Sparse deposits of final reaction product are seen on the surface of microvilli which project into the exocoelom (Ex). In addition to polyribosomes and granular endoplasmic reticulum, the mesothelial cytoplasm is richly provided with branching bundles of fine fibrils (Fi). Disrupted mitochondria (arrows) and vacuoles (V) with varying contents of granular material and myelin figures are also seen. Evidence of pinocytotic activity (PV) occurs on both inner and outer cell surfaces.

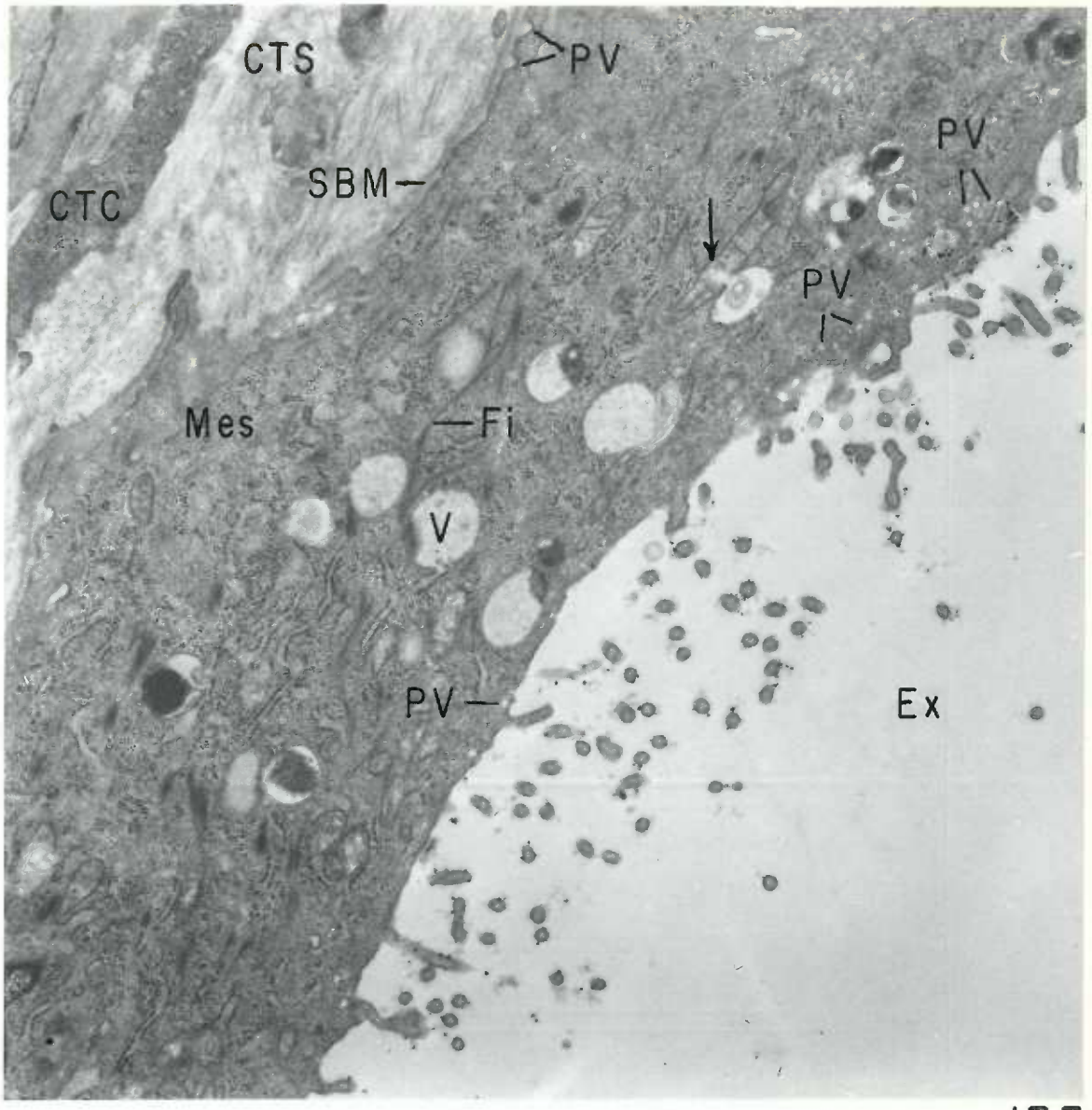

133

FIGURE 134

Cross sectional view of the 25 day mesothelium incubated with ATP as substrate. Magnification 12,900 X. Moderate deposits of final reaction product are present along the free surface and its microvillous projections. As seen in Figure 133, the cytoplasm is richly provided with branching bundles of fibrils (Fi) and ribosome-studded profiles of endoplasmic reticulum (ER) whose cisternae are distended by accumulations of a fine granular material.

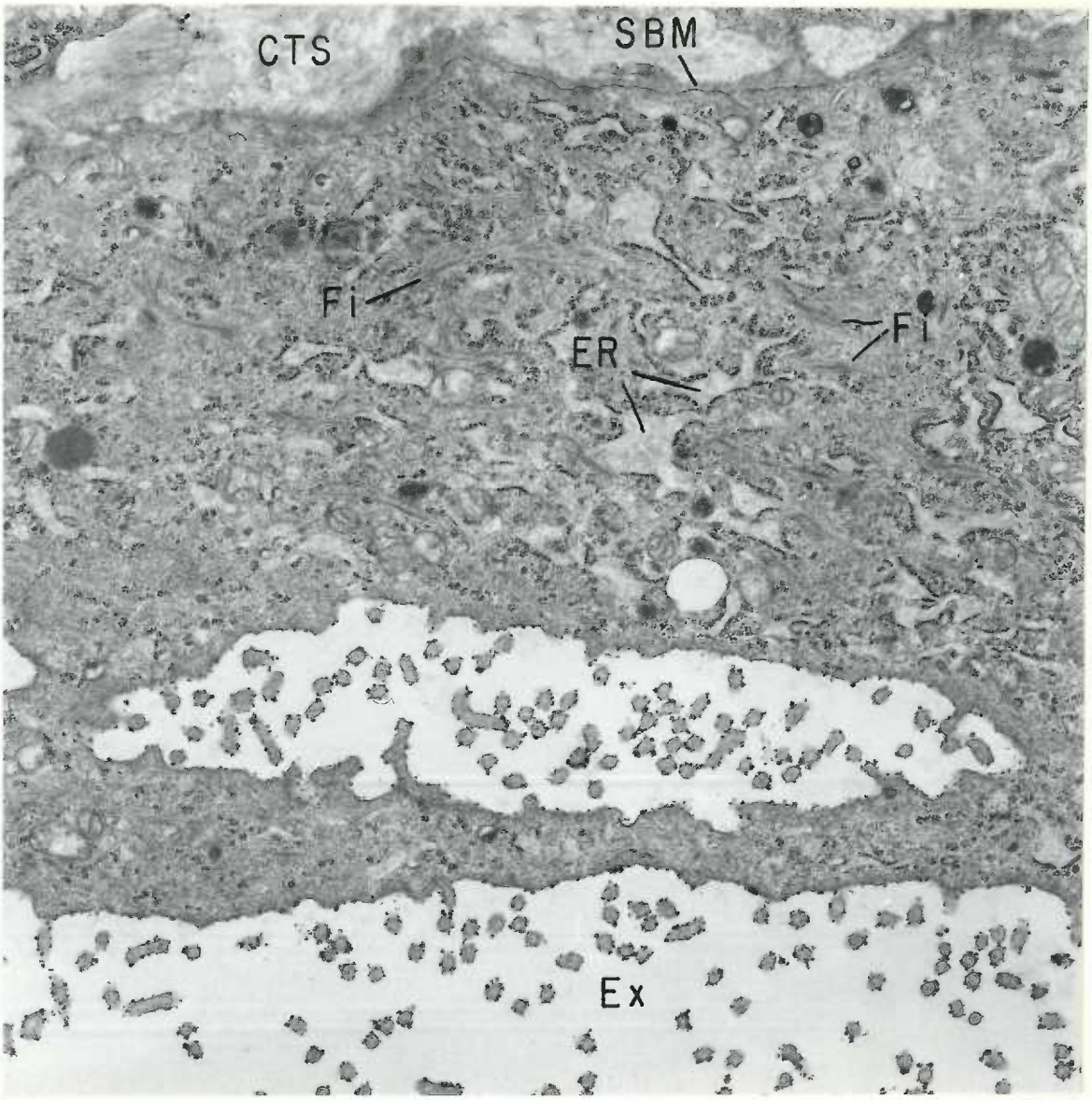

134